frontiers | Research Topics

Thymoma and thymic carcinoma: Diagnostic imaging, pathological assessment, and treatment options

Edited by
Cesar Moran, Mylene Truong and Patrick Loehrer

Published in
Frontiers in Oncology
Frontiers in Surgery

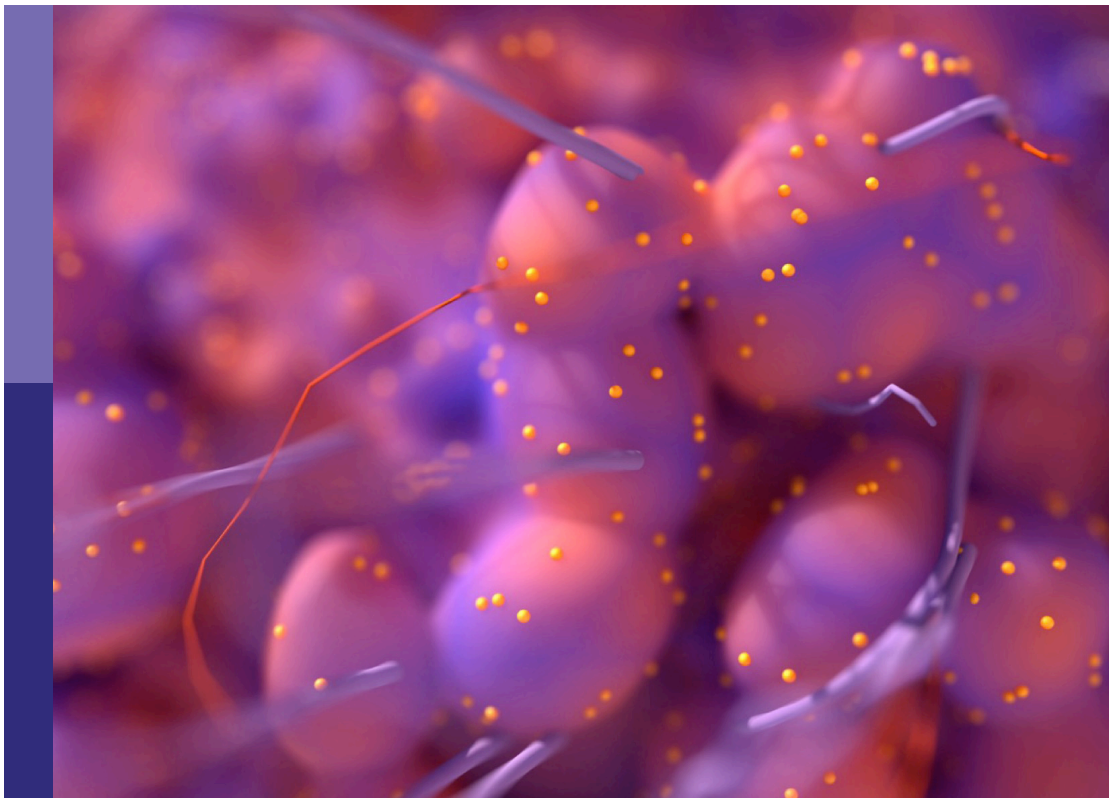

FRONTIERS EBOOK COPYRIGHT STATEMENT

The copyright in the text of individual articles in this ebook is the property of their respective authors or their respective institutions or funders. The copyright in graphics and images within each article may be subject to copyright of other parties. In both cases this is subject to a license granted to Frontiers.

The compilation of articles constituting this ebook is the property of Frontiers.

Each article within this ebook, and the ebook itself, are published under the most recent version of the Creative Commons CC-BY licence. The version current at the date of publication of this ebook is CC-BY 4.0. If the CC-BY licence is updated, the licence granted by Frontiers is automatically updated to the new version.

When exercising any right under the CC-BY licence, Frontiers must be attributed as the original publisher of the article or ebook, as applicable.

Authors have the responsibility of ensuring that any graphics or other materials which are the property of others may be included in the CC-BY licence, but this should be checked before relying on the CC-BY licence to reproduce those materials. Any copyright notices relating to those materials must be complied with.

Copyright and source acknowledgement notices may not be removed and must be displayed in any copy, derivative work or partial copy which includes the elements in question.

All copyright, and all rights therein, are protected by national and international copyright laws. The above represents a summary only. For further information please read Frontiers' Conditions for Website Use and Copyright Statement, and the applicable CC-BY licence.

ISSN 1664-8714
ISBN 978-2-83251-125-1
DOI 10.3389/978-2-83251-125-1

About Frontiers

Frontiers is more than just an open access publisher of scholarly articles: it is a pioneering approach to the world of academia, radically improving the way scholarly research is managed. The grand vision of Frontiers is a world where all people have an equal opportunity to seek, share and generate knowledge. Frontiers provides immediate and permanent online open access to all its publications, but this alone is not enough to realize our grand goals.

Frontiers journal series

The Frontiers journal series is a multi-tier and interdisciplinary set of open-access, online journals, promising a paradigm shift from the current review, selection and dissemination processes in academic publishing. All Frontiers journals are driven by researchers for researchers; therefore, they constitute a service to the scholarly community. At the same time, the *Frontiers journal series* operates on a revolutionary invention, the tiered publishing system, initially addressing specific communities of scholars, and gradually climbing up to broader public understanding, thus serving the interests of the lay society, too.

Dedication to quality

Each Frontiers article is a landmark of the highest quality, thanks to genuinely collaborative interactions between authors and review editors, who include some of the world's best academicians. Research must be certified by peers before entering a stream of knowledge that may eventually reach the public - and shape society; therefore, Frontiers only applies the most rigorous and unbiased reviews. Frontiers revolutionizes research publishing by freely delivering the most outstanding research, evaluated with no bias from both the academic and social point of view. By applying the most advanced information technologies, Frontiers is catapulting scholarly publishing into a new generation.

What are Frontiers Research Topics?

Frontiers Research Topics are very popular trademarks of the *Frontiers journals series*: they are collections of at least ten articles, all centered on a particular subject. With their unique mix of varied contributions from Original Research to Review Articles, Frontiers Research Topics unify the most influential researchers, the latest key findings and historical advances in a hot research area.

Find out more on how to host your own Frontiers Research Topic or contribute to one as an author by contacting the Frontiers editorial office: frontiersin.org/about/contact

Thymoma and thymic carcinoma: Diagnostic imaging, pathological assessment, and treatment options

Topic editors

Cesar Moran — University of Texas MD Anderson Cancer Center, United States
Mylene Truong — University of Texas MD Anderson Cancer Center, United States
Patrick Loehrer — Indiana University Bloomington, United States

Citation

Moran, C., Truong, M., Loehrer, P., eds. (2023). *Thymoma and thymic carcinoma: Diagnostic imaging, pathological assessment, and treatment options*. Lausanne: Frontiers Media SA. doi: 10.3389/978-2-83251-125-1

Table of contents

frontiers in Oncology

ORIGINAL RESEARCH
published: 27 November 2020
doi: 10.3389/fonc.2020.583489

Myasthenia Gravis Is Not an Independent Prognostic Factor of Thymoma: Results of a Propensity Score Matching Trial of 470 Patients

Yirui Zhai[1†], Yong Wei[2,3†], Zhouguang Hui[1,4], Yushun Gao[5], Yang Luo[6], Zongmei Zhou[1], Qinfu Feng[1] and Yuemin Li[2*]*

[1] Department of Radiation Oncology, National Cancer Center/National Clinical Research Center for Cancer/Cancer Hospital, Chinese Academy of Medical Sciences & Peking Union Medical College, Beijing, China, [2] Department of Radiation Oncology, The 8th Medical Center of Chinese PLA General Hospital, Beijing, China, [3] Graduate School, Hebei North University, Zhangjiakou, China, [4] Department of VIP Medical Services, National Cancer Center/National Clinical Research Center for Cancer/Cancer Hospital, Chinese Academy of Medical Sciences & Peking Union Medical College, Beijing, China, [5] Department of Thoracic Surgery, National Cancer Center/National Clinical Research Center for Cancer/Cancer Hospital, Chinese Academy of Medical Sciences & Peking Union Medical College, Beijing, China, [6] Department of Medical Oncology, National Cancer Center/National Clinical Research Center for Cancer/Cancer Hospital, Chinese Academy of Medical Sciences & Peking Union Medical College, Beijing, China

OPEN ACCESS

Edited by:
Iacopo Petrini, University of Pisa, Italy

Reviewed by:
Margaret Ottaviano, University of Naples Federico II, Italy
Tommaso Martino De Pas, European Institute of Oncology (IEO), Italy

***Correspondence:**
Qinfu Feng
qinfufeng19@163.com
Yuemin Li
liyuemin224@sina.com

[†]These authors have contributed equally to this work

Specialty section:
This article was submitted to Thoracic Oncology, a section of the journal Frontiers in Oncology

Received: *15 July 2020*
Accepted: *29 October 2020*
Published: *27 November 2020*

Citation:
Zhai Y, Wei Y, Hui Z, Gao Y, Luo Y, Zhou Z, Feng Q and Li Y (2020) Myasthenia Gravis Is Not an Independent Prognostic Factor of Thymoma: Results of a Propensity Score Matching Trial of 470 Patients. Front. Oncol. 10:583489. doi: 10.3389/fonc.2020.583489

Objective: The association between the prognosis of thymoma and MG remains controversial. Differences in clinical characteristics and treatments between patients with and without MG may affect the findings of those studies. We designed this propensity score matching trial to investigate whether MG is an independent prognostic predictor in thymoma.

Methods: Patients with pathologically diagnosed thymoma and MG were enrolled in the MG group. Moreover, the propensity score matching method was used to select patients who were diagnosed with thymoma without MG from the database of two participating centers. Matched factors included sex, age, Masaoka stage, pathological subtypes, and treatments. Matched patients were enrolled in the non-MG group. Chi-squared test was used to compare the characteristics of the two groups. Overall survival, local-regional relapse-free survival, distant metastasis-free survival, progression-free survival, and cancer-specific survival were calculated from the diagnosis of thymoma using the Kaplan–Meier method.

Results: Between April 1992 and October 2018, 235 patients each were enrolled in the MG and non-MG groups (1:1 ratio). The median ages of patients in the MG and non-MG groups were 46 years old. The World Health Organization pathological subtypes were well balanced between the two groups (B2 + B3: MG vs. non-MG group, 63.0 vs. 63.4%, p = 0.924). Most patients in both groups had Masaoka stages I–III (MG vs. non-MG group, 90.2 vs. 91.5%, p = 0.631). R0 resections were performed in 86.8 and 90.2% of the MG and non-MG groups, respectively (p = 0.247). The median follow-up time of the two

groups was 70.00 months (MG vs. non-MG group, 73.63 months vs. 68.00 months). Five-year overall survivals were 92.5 and 90.3%, 8-year overall survivals were 84.2 and 84.2%, and 10-year overall survivals were 80.2 and 81.4% (p = 0.632) in the MG and non-MG groups, respectively. No differences were found in the progression-free survival, distant metastasis-free survival, and local-regional relapse-free survival between the two groups.

Conclusion: MG is not an independent or direct prognostic factor of thymoma, although it might be helpful in diagnosis thymoma at an early stage, leading indirectly to better prognosis.

Keywords: myasthenia gravis, thymoma, propensity score matching, survival, prognosis

INTRODUCTION

Thymic epithelia neoplasm, including thymoma and thymic carcinoma, accounts for 0.2–1.5% of malignancies and is a rare disease with an incidence of 0.013–1.5 per million people (1, 2). Thymic carcinoma is typically characterized by more extensive local invasion, more frequent metastases, and a worse prognosis compared with thymoma. Paraneoplastic syndrome is relatively common in patients with thymoma. Although a wide range of such syndromes have been reported, including pure red blood cell aplasia, Good's syndrome, and myasthenia gravis (MG), caused by impaired neuromuscular transmission resulting from the presence of antibodies at the neuromuscular junction is the most common paraneoplastic disease (3). Occurring in approximately 30–50% of patients with thymoma, MG is deemed a special characteristic (3, 4). Oppositely, the occurrence of MG is much lower in thymic carcinoma, at only 0–30%, probably because of the lack of thymus-like features compared with thymoma (5, 6). In patients with MG, thymoma has been found in approximately 8.5–15% of cases (7, 8). Thymoma is considered to be a negative prognostic factor of MG, (7) although whether MG is a prognostic factor of thymoma is still controversial (9–17). Differences in clinical characteristics and treatments between patients with and without MG may have affected the findings of previous studies (11, 12, 15, 17). From a clinical point of view, this controversy is important. Therefore, we designed this trial to investigate whether MG is an independent prognostic predictor in thymoma and used the propensity score matching method to eliminate the bias from other variables.

MATERIALS AND METHODS

Ethics

The Institutional Ethics Committees of National Cancer Center/National Clinical Research Center for Cancer/Cancer Hospital, Chinese Academy of Medical Sciences & Peking Union Medical College and the 8th Medical Center of Chinese PLA General Hospital gave approval for the trial protocol, and informed written consent including the therapeutic regimens and possible data collections for the future academic analysis was obtained from patients before the treatment.

Patient Selection

We searched for patients with pathologically diagnosed thymoma at the two medical centers between January 1992 and December 2018. Patients with pathologic diagnosis of thymoma and complete clinical information and follow-up data were identified. Thymic carcinoma was excluded. Data on sex, age, Masaoka stage, World Health Organization histological type, MG status, therapeutic regimens, and follow-up records were collected. Next, patients in the database were divided into two groups: MG and non-MG, according to their MG status. Then, propensity score matching (PSM) was used to achieve balance in clinicopathological characteristics.

Statistical Analysis

In PSM, the matching ratio was 1:1 ratio, and the caliper is 0.05. Matched factors included sex, age, Masaoka stage, TNM stage (American Joint Committee on Cancer, 8th Edition), pathological subtypes, and treatments included surgery, radiotherapy, and chemotherapy. The chi-square test was used to compare characteristics of the two groups. Overall survival (OS), local-regional relapse-free survival (LRFS) distant metastasis-free survival (DMFS), progression-free survival (PFS), and cancer-specific survival (CSS) were calculated for based on the diagnosis of thymoma. OS was calculated from the time to death. LRFS was calculated as the time to local progression, which defined the mediastinal recurrence and supraclavicular lymph node relapse. DMFS was calculated as the time to distant metastasis. PFS was calculated as the time to documented clinical progression or to the patient's death. CSS was calculated as the time to death from thymoma. All the survivals' calculation utilized the Kaplan–Meier method. Univariate analysis was performed using the log-rank test. A p-value of <0.05 was considered statistically significant. PSM and other statistical analyses were performed using SAS software (Cary, NC, USA) and the SPSS statistical software package version 24.0 (SPSS Inc., Chicago, IL, USA), respectively.

RESULTS

Patients' Characteristics and Treatment

Overall, 927 patients were eligible to be enrolled in the database. Among them, 243 patients had MG. After PSM, 235 patients

were enrolled into each group. There were 135 and 141 men in the non-MG and MG groups, respectively (p = 0.926). The median age was 46 years in both groups. The World Health Organization pathological subtypes were well balanced between the two groups (B2 + B3: non-MG vs. MG group, 63.4 vs. 63.0%, p = 0.924). Most patients in both groups had Masaoka stages I–II and TNM stages I–III (non-MG vs. MG group, 91.5 vs. 90.2%, p = 0.631).

R0 resections were performed in 212 and 204 patients in the non-MG and MG groups, respectively. Ninety-two and 42 patients in the non-MG group received radiotherapy and chemotherapy, respectively. The corresponding numbers of patients in the MG group were 102 and 29, respectively. The median radiation doses in the non-MG and MG groups were 50 Gy (40–60 Gy) and 50 Gy (20–60 Gy), respectively. The median chemotherapy cycles in the non-MG and MG groups were 2 (1–10) and 2 (1–6), respectively.

The clinicopathological variables were well balanced. Details are shown in **Table 1**.

TABLE 1 | Patients' Characteristics.

Number of patients (%)	Non-MG	MG	p-value
Number	235	235	
Age (years)	46 (17–84)	46 (16–78)	0.563
≤50	149 (63.4)	155 (66.0)	
>50	86 (36.6)	80 (34.0)	
Sex			0.574
Male	135 (57.4)	141 (60.0)	
Female	100 (42.6)	94 (40.0)	
Masaoka stage			0.631
I	119 (50.6)	103 (43.8)	
II	72 (30.6)	70 (29.8)	
III	24 (10.2)	39 (16.6)	
IV	20 (8.5)	23 (9.8)	
Histology			0.924
A	17 (7.2)	10 (4.3)	
AB	37 (15.7)	41 (17.4)	
B1	32 (13.6)	36 (15.3)	
B2	90 (38.3)	77 (32.7)	
B3	47 (20.0)	54 (23.0)	
Mixed B2 and B3	12 (5.1)	17 (7.2)	
T stage			0.385
T1	192 (81.7)	176 (74.9)	
T2	5 (2.1)	10 (4.3)	
T3	29 (12.3)	38 (16.2)	
T4	9 (3.8)	11 (4.7)	
N stage			0.890
N0	225 (95.7)	226 (96.2)	
N1	6 (2.6)	5 (2.1)	
N2	4 (1.7)	4 (1.7)	
M stage			0.945
M0	217(92.3)	216 (91.9)	
M1a	14 (6.0)	14 (6.0)	
M1b	4 (1.7)	5 (2.1)	
TNM stage			0.631
I	190 (80.6)	174 (74.0)	
II	5(2.1)	6 (2.6)	
III	20 (8.5)	32 (13.6)	
IV	20(8.5)	23 (9.8)	
R0 resection			0.247
Yes	212 (90.2)	204 (86.8)	
No	23 (9.8)	31 (13.2)	
Radiation			0.349
Yes	92 (39.1)	102 (43.4)	
No	143 (60.9)	133 (56.6)	
Chemotherapy			0.094
Yes	42 (17.9)	29 (12.3)	
No	193 (82.1)	206 (87.7)	

MG, myasthenia gravis; TNM, tumor, node, and metastasis.
Statistical significance is defined as p-value <0.05.
Values are presented as numbers (percentages).

MG

In the MG group, MG symptoms were classified according to the Osserman classification. The number of patients with Types I, II, III, and IV were 85 (36.2%), 125 (55.2%), 16 (6.8%), and 9 (3.8%), respectively.

Survival

The median follow-up time of the two groups was 70.00 months (MG vs. non-MG group, 73.63 months vs. 68.00 months). At the last follow-up, 28 patients had died in each group. Five patients died of myasthenic crisis without progression of thymoma. Local-regional recurrences were observed in 15 and 16 patients in the MG and non-MG groups, respectively. Distant metastasis was observed in 39 patients in each group. The 5-year OS rates were 90.3 and 92.5%, 8-year OS rates were 84.2 and 84.2%, and 10-year OS rates were 81.4 and 80.2% (p = 0.632) in the non-MG and MG groups, respectively. The respective PFS rates were 79.8 and 79.3%, 71.7 and 73.7%, and 67.9 and 65.4% (p = 0.832) in the non-MG and MG groups. The two groups also had similar 5-year (93.9 vs. 96.1%), 8-year (90.2 vs. 93.4%), and 10-year LRFS rates (87.7 vs. 87.8%, p = 0.613). Additionally, the 5-, 8-, and 10-year DMFS rates in the non-MG group were almost equal to those in the MG group (84.1 vs. 83.8%, 77.1 vs. 81.0%, 77.1 vs. 77.5%, p = 0.884). There were no significant differences in the 5-, 8-, and 10-year CSS rates between the two groups (91.8 vs. 94.0%, 84.4 vs. 87.2%, 84.4 vs. 85.6%, p = 0.441). The survival curves are plotted in **Figures 1**–**5**.

Subgroup Analyses

Subgroup analysis according to Masaoka stage and TNM stage did not show any significant differences in OS, LRFS, DMFS, CSS, or PFS between patients with or without MG. However, patients with stage IV (both TNM and Masaoka) in the MG group had somewhat better OS than those in the non-MG group. Details are shown in **Table 2**.

DISCUSSION

Thymoma, which accounts for 20% of mediastinal neoplasm, is the most frequent primary malignancy. MG is deemed as a special characteristic of thymoma compared with other thoracic malignancies (1, 4, 8). In previous reports, 5- and 10-year OS rates were 63.9–90.0% and 70.9–82.0%, for patients without MG, respectively. Five- and 10-year OS rates were 76.0–93.6% and 62.0–83.0% for patients without MG (7, 9, 10, 12–17). The results in our study are consistent with those in previous studies.

Whether MG influences the prognosis of thymomas has long been controversial. In the 1970s, MG was identified as a negative

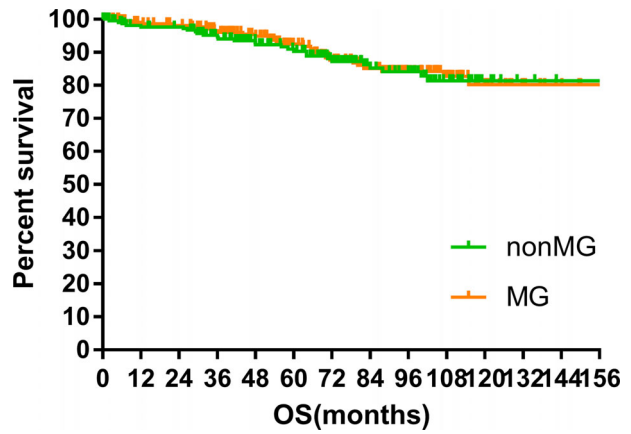

FIGURE 1 | Overall survival.

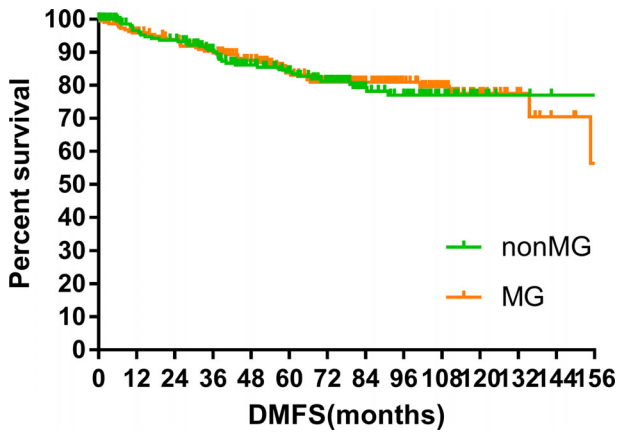

FIGURE 4 | Distant metastasis free survival.

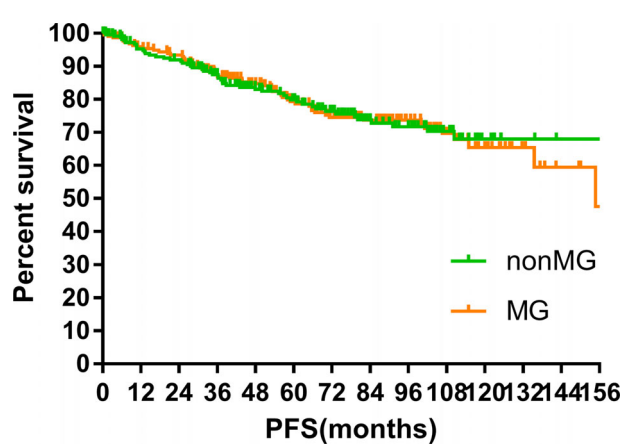

FIGURE 2 | Progression-free survival.

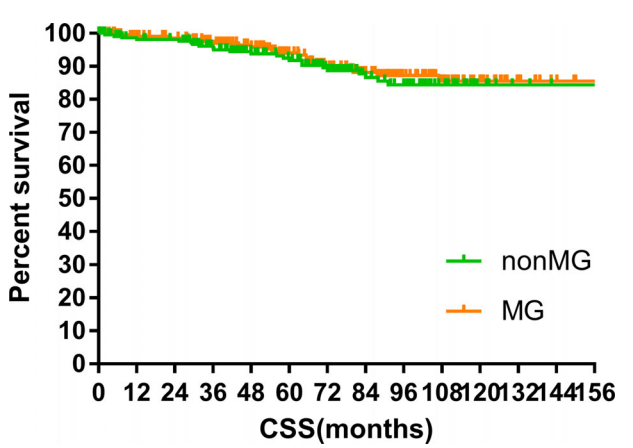

FIGURE 5 | Cancer specific survival.

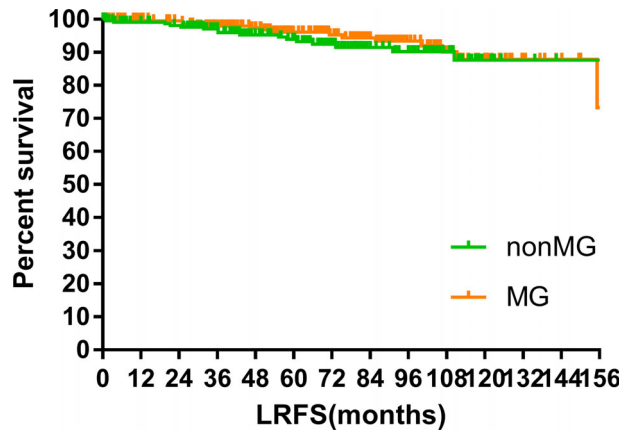

FIGURE 3 | Local-regional relapse free survival.

prognostic factor of thymoma according to the poor experience and therapeutic regimens with MG and MG-related postoperative complications (18). Once the therapeutic technologies for MG progressed, the role of MG in the prognosis of thymoma took a favorable turn. Recently, only one study identified MG as a negative indicator of prognosis, and that study had a severe bias of radiation delivery between the two groups (17). Other studies came to the opposite conclusion. Recent studies are listed in **Table 3**. A study by Wang et al. showed that patients with MG had higher OS than those without MG in univariate analysis. However, this advantage disappeared in multi-variate analysis (15). Another study by Ruffini et al. showed similar results as that in Wang et al.'s (13). Two other studies by Filosso et al. and Kondo et al. did not show statistically significant differences in OS between patients with and without MG, although patients with MG had better OS (11, 12). Interestingly, the slight difference in OS disappeared at the 10th year in the study by Filosso et al. (11). Results from the other four studies showed no significant differences (9, 10, 14, 16).

TABLE 2 | Subgroup Analyses.

Survival	Masaoka stage	Non-MG%	MG%	p-value	TNMstage	Non-MG%	MG%	p-value
5y OS	I	94.8	93.7	0.299	I	93.8	94.1	0.625
	II	91.7	94.7	0.630	II	100.0	100.0	–*
	III	89.4	93.9	0.820	III	87.4	92.5	0.949
	IV	57.5	76.4	0.069	IV	57.5	76.4	0.069
5y PFS	I	95.0	89.9	0.125	I	89.5	91.0	0.815
	II	79.4	92.4	0.166	II	66.7	88.3	0.127
	III	46.4	57.1	0.105	III	43.2	50.9	0.217
	IV	33.7	33.5	0.875	IV	33.7	33.5	0.875
5y LRFS	I	98.0	98.9	0.850	I	95.4	99.3	0.732
	II	90.6	100.0	0.461	II	100.0	100.0	–*
	III	94.1	87.6	0.388	III	92.9	84.5	0.504
	IV	77.0	88.2	0.593	IV	77.0	88.2	0.593
5y DMFS	I	96.7	95.1	0.782	I	92.4	94.7	0.343
	II	84.5	94.0	0.088	II	66.7	88.3	0.127
	III	46.4	63.3	0.190	III	43.2	58.3	0.313
	IV	52.1	38.7	0.731	IV	52.1	38.7	0.731
5y CSS	I	95.7	96.2	0.609	I	94.9	95.6	0.929
	II	93.2	94.7	0.631	II	100.0	100.0	–*
	III	89.4	96.6	0.628	III	87.4	95.7	0.751
	IV	63.9	76.4	0.133	IV	63.9	76.4	0.133

**P value is not defined because of limited number of patients in each group. MG, myasthenia gravis; OS, overall survival; PFS, progression-free survival; LRFS, local-regional relapse-free survival; DMFS, distant metastasis-free survival; CSS, cancer-specific survival.*
Statistical significance is defined as p-value <0.05.
Values are presented as percentages.

TABLE 3 | Survival Measures in Previous Studies.

	Year	Number of patients Non-MG vs. MG	Imbalanced characteristics	OS Non-MG vs. MG	p-value
Cacho-Díaz et al. (10)	2018	46 vs. 18	WHO stage	MST 120.6 m vs. NR	0.606
Zhang et al. (17)	2016	66 vs. 38	Age, histology, Masaoka stage, radiotherapy	5y 89.1 vs. 76.0%	0.026
Wang et al. (15)	2016	1429 vs. 421	Sex, age, histology, R0 resection, chemotherapy, radiotherapy.	5y 88 vs. 93% 10y 81 vs. 83%	0.034[a] 0.967[b]
Aydemir (9)	2016	34 vs. 24	histology	5y 82.4 vs. 87.5%	0.311
Filosso et al. (11)	2015	422 vs. 375	Sex, stage, histology, induction therapy.	5y 84.9 vs. 93.6% 10y 70.9 vs. 77.2%	0.058[a] 0.956[b]
Yu et al. (16)	2012	103 vs. 125	Histology	5y 90 vs. 89.3% 10y 78.9 vs. 81.2%	0.886[b]
Vachlas et al. (14)	2012	40 vs. 39	Histology	MST 15.7y vs. 14.5y	0.681
Ruffini et al. (13)	2011	150 vs. 105	Masaoka stage, histology	10y 62 vs. 82%	0.001[a] 0.88[b]
Kondo et al. (12)	2005	770 vs. 259	Age, histology, resection,	5y 89.3 vs. 85.7%[c] 5y 63.9 vs. 85.1%[d]	>0.05[c] 0.052[d]

[a]univariate analysis, [b]multivariate analysis, [c]stage III, [d]stage IV.
MG, myasthenia gravis; MST, median survival time; NR, not reached; OS, overall survival; WHO, World Health Organization; y, year.
Statistical significance is defined as p-value <0.05.
Values are presented as numbers (percentages).

We analyzed the characteristics of the patients enrolled in previous studies and found that in none of the characteristics of the patients were well balanced. In a study by Ruffini et al., there is an obvious correspondence between MG and other features that might contribute to the effect on prognosis (13). Generally, patients in the MG group always had a higher proportion of favorable prognostic factors, including Masaoka stages I–II, AB/B1 classification, and R0 resection (12, 15, 17). The study designed by Wang et al., which showed the most significant differences in survival measures, also showed the most imbalances in the characteristics of the patients (15). Additionally, we found that more the imbalances, more likely was the study to show differences in survival. For example, imbalances existed in six aspects (sex, age, histology, R0 resection, chemotherapy, and radiotherapy) in the study by Wang et al. (15). Previous studies showed that these factors obviously influence survival. The studies by Filosso et al. and Kondo et al. showed four and three imbalanced factors, respectively. There was only one imbalanced factor in the other studies, which showed no significant differences in survival (9, 10, 14, 16). In an attempt to reduce the imbalances, four of the studies had conducted multivariate analysis, and none of them demonstrated the effect of MG on survival (11, 13, 15, 16). Our study, utilizing the PSM method, also tried to balance other substantially influencing factors, and we found no difference in

survival measures between patients with and without MG. From the historical studies and our study, one can reach a conclusion that once the other influencing factors were well balanced, MG appeared not to be an independent positive indicator in thymoma. The positive prognostic effect of MG in previous studies is probably the result of patients with MG being more eager for precise diagnosis at an earlier stage, with the disease histologically expressed as less invasive.

Several studies insisted that the effect of MG on survival was according to the Masaoka stage. The views of the effect of MG on prognosis differed quite dramatically among studies. In the study by Ruffini et al., difference in OS was observed only in patients with Masaoka stage I (10-year OS in nonMG and MG groups: 80 vs.100%, p = 0.02) (13). Wang et al. showed that the survival rate was significantly higher in the non-MG group than in the MG group when the Masaoka staging was I (p = 0.000), equal when the Masaoka staging was II (p = 0.484), and significantly lower when the Masaoka staging was III/IV (P = 0.003) (15). The study by Kondo et al. clarified that although MG was not associated with survival in patients with stage III, OS tended to be better in patients with stage IV with MG than in those without MG (12). The results of subgroup analysis in our study were consistent with those of Kondo et al. The reason for this might be that thymoma is a disease with relatively better prognosis than other common thoracic malignancies and the causes of deaths in patients with thymoma are very complex. In long-term follow-up, patients might have other diseases or accidents. Therefore, CSS is a more representative measure to evaluate survival. However, few studies have focused on CSS, and our study did not show that MG is associated with CSS in any Masaoka stage.

Very few studies focused on MG as a prognostic factor of disease progression including local relapse and distant metastasis. A study from Italy evaluated whether MG is an indicator of the cumulative incidence of recurrence. It showed that 5- and 10-year progression rates were 10.7 and 14.7% in MG patients and 11.1 and 15.7% in non-MG patients (11). The recurrence rate in our study was consistent with this study. The study by Kondo et al. showed no recurrent difference between patients with and without MG (6.4 vs. 8.3%) (12). However, the frequency of recurrence in the non-MG group was higher than that in the MG group in stage IV (12). The study by Wang et al. showed higher recurrence rate in the non-MG group, although again, we cannot overlook the severe imbalances of other factors in that study (15). After using PSM to stabilize other factors, our study showed similar local recurrence, distant metastasis, and progression rates between the two groups.

Because this is the first study using PSM to investigate the relationship of MG and survivals of thymomas, our study has several strengths. First, because it is difficult to propose a prospective study in a rare disease, PSM is a stable substitutive method. The other influencing factors were reduced by using PSM, and it helped us to clearly see the effect of MG on prognosis of thymoma. Second, the number of patients was relatively large although thymoma is a rare disease. Third, the enrolled patients were all from two high-volume institutions, and the data are reliable. Last, the results are consistent with those of previous studies in which other clinical features were statistically analyzed using multivariate Cox regression models.

There are also some limitations to our study. First, because this was a retrospective study, treatments for thymoma and MG were not always the same. Second, the two participating centers have different academic advantages. One is a cancer center and the other is famous for treatments for MG. Inevitably, the treatment details are not totally consistent. Third, we made an effort to shrink the imbalances using PSM, although it is not realistic to achieve a perfect balance because the proportions of clinical features had their own peculiarity in the database before PSM, and there were minor differences in delivery of chemotherapy between the two groups.

In conclusion, MG is not an independent or direct prognostic factor of thymoma, although it might be helpful to get the diagnosis at an early stage, indirectly leading to better prognosis.

DATA AVAILABILITY STATEMENT

The raw data supporting the conclusions of this article will be made available by the authors, without undue reservation.

ETHICS STATEMENT

The studies involving human participants were reviewed and approved by The Ethics Committees of National Cancer Center and the 8th Medical Center of Chinese PLA General Hospital. The patients/participants provided their written informed consent to participate in this study.

AUTHOR CONTRIBUTIONS

YZ, YW, YLi, and QF designed the study and wrote and reviewed the manuscript. YZ and YW collected the data, finished statistical analysis, and wrote the manuscript. ZH, YG, YLu and ZZ enrolled patients, collected the data, finished data interpretation and manuscript editing. All authors contributed to the article and approved the submitted version.

FUNDING

This work was supported by PUMC FUND of the Funds for the Central Universities (No. 3332018075), CAMS Innovation Fund for Medical Sciences (No. 2019-I2M-2-003), and the National Key Projects of Research and Development of China (2016YFC 0904600).

ACKNOWLEDGMENTS

We would like to thank Editage (www.editage.cn) for English language editing.

REFERENCES

1. Detterbeck FC, Parsons AM. Thymic tumors. *Ann Thorac Surg* (2004) 77 (5):1860–9. doi: 10.1016/j.athoracsur.2003.10.001
2. Venuta F, Anile M, Diso D, Vitolo D, Rendina EA, De Giacomo T, et al. Thymoma and thymic carcinoma. *Eur J Cardiothorac Surg* (2010) 37(1):13–25. doi: 10.1016/j.ejcts.2009.05.038
3. Evoli A, Lancaster E. Paraneoplastic disorders in thymoma patients. *J Thorac Oncol* (2014) 9(9 Suppl 2):S143–7. doi: 10.1097/JTO.0000000000000300
4. Scorsetti M, Leo F, Trama A, D'Angelillo R, Serpico D, Macerelli M, et al. Thymoma and thymic carcinomas. *Crit Rev Oncol Hematol* (2016) 99:332–50. doi: 10.1016/j.critrevonc.2016.01.012
5. Zhai Y, Hui Z, Ji W, Wang X, Liang J, Mao Y, et al. A Single-Center Analysis of the Treatment and Prognosis of Patients With Thymic Carcinoma. *Ann Thorac Surg* (2017) 104(5):1718–24. doi: 10.1016/j.athoracsur.2017.06.025
6. Ahmad U, Yao X, Detterbeck F, Huang J, Antonicelli A, Filosso PL, et al. Thymic carcinoma outcomes and prognosis: results of an international analysis. *J Thorac Cardiovasc Surg* (2015) 149(1):95–100101 e1–2. doi: 10.1016/j.jtcvs.2014.09.124
7. de Perrot M, Liu J, Bril V, McRae K, Bezjak A, Keshavjee SH. Prognostic significance of thymomas in patients with myasthenia gravis. *Ann Thorac Surg* (2002) 74(5):1658–62. doi: 10.1016/s0003-4975(02)04083-3
8. Thomas CR, Wright CD, Loehrer PJ. Thymoma: state of the art. *J Clin Oncol* (1999) 17(7):2280–9. doi: 10.1200/JCO.1999.17.7.2280
9. Aydemir B. The effect of myasthenia gravis as a prognostic factor in thymoma treatment. *North Clin Istanb* (2016) 3(3):194–200. doi: 10.14744/nci.2016.60352
10. Cacho-Diaz B, Salmeron-Moreno K, Lorenzana-Mendoza NA, Texcocano J, Arrieta O. Myasthenia gravis as a prognostic marker in patients with thymoma. *J Thorac Dis* (2018) 10(5):2842–8. doi: 10.21037/jtd.2018.04.95
11. Filosso PL, Evangelista A, Ruffini E, Rendina EA, Margaritora S, Novellis P, et al. Does myasthenia gravis influence overall survival and cumulative incidence of recurrence in thymoma patients? A Retrospective clinicopathological multicentre analysis on 797 patients. *Lung Cancer* (2015) 88(3):338–43. doi: 10.1016/j.lungcan.2015.03.007
12. Kondo K, Monden Y. Thymoma and myasthenia gravis: a clinical study of 1,089 patients from Japan. *Ann Thorac Surg* (2005) 79(1):219–24. doi: 10.1016/j.athoracsur.2004.06.090
13. Ruffini E, Filosso PL, Mossetti C, Bruna MC, Novero D, Lista P, et al. Thymoma: inter-relationships among World Health Organization histology, Masaoka staging and myasthenia gravis and their independent prognostic significance: a single-centre experience. *Eur J Cardiothorac Surg* (2011) 40 (1):146–53. doi: 10.1016/j.ejcts.2010.09.042
14. Vachlas K, Zisis C, Rontogianni D, Tavernarakis A, Psevdi A, Bellenis I. Thymoma and myasthenia gravis: clinical aspects and prognosis. *Asian Cardiovasc Thorac Ann* (2012) 20(1):48–52. doi: 10.1177/0218492311433189
15. Wang F, Pang L, Fu J, Shen Y, Wei Y, Tan L, et al. Postoperative survival for patients with thymoma complicating myasthenia gravis-preliminary retrospective results of the ChART database. *J Thorac Dis* (2016) 8(4):711–7. doi: 10.21037/jtd.2016.02.07
16. Yu L, Zhang XJ, Ma S, Jing Y, Li F, Krasna MJ. Different characteristics of thymomas with and without myasthenia gravis. *Ann Surg Oncol* (2012) 19 (1):94–8. doi: 10.1245/s10434-011-1896-8
17. Zhang Z, Cui Y, Jia R, Xue L, Liang H. Myasthenia gravis in patients with thymoma affects survival rate following extended thymectomy. *Oncol Lett* (2016) 11(6):4177–82. doi: 10.3892/ol.2016.4528
18. Salyer WR, Eggleston JC. Thymoma: a clinical and pathological study of 65 cases. *Cancer* (1976) 37(1):229–49. doi: 10.1002/1097-0142(197601)37:1<229::aid-cncr2820370133>3.0.co;2-2

Conflict of Interest: The authors declare that the research was conducted in the absence of any commercial or financial relationships that could be construed as a potential conflict of interest.

Copyright © 2020 Zhai, Wei, Hui, Gao, Luo, Zhou, Feng and Li. This is an open-access article distributed under the terms of the Creative Commons Attribution License (CC BY). The use, distribution or reproduction in other forums is permitted, provided the original author(s) and the copyright owner(s) are credited and that the original publication in this journal is cited, in accordance with accepted academic practice. No use, distribution or reproduction is permitted which does not comply with these terms.

frontiers in Oncology

ORIGINAL RESEARCH
published: 26 February 2021
doi: 10.3389/fonc.2021.628534

CT-Based Radiomics Signatures for Predicting the Risk Categorization of Thymic Epithelial Tumors

Jin Liu[1†], *Ping Yin*[1†], *Sicong Wang*[2], *Tao Liu*[1], *Chao Sun*[1] *and Nan Hong*[1*]

[1] Department of Radiology, Peking University People's Hospital, Beijing, China, [2] Pharmaceutical Diagnostic Team, GE Healthcare, Shanghai, China

OPEN ACCESS

Edited by:
Chuanming Li,
Chongqing Medical University, China

Reviewed by:
Chen Liu,
Army Medical University, China
Jie Chen,
Soochow University, China
Carol Wu,
University of Texas MD Anderson Cancer Center, United States

***Correspondence:**
Nan Hong
hongnan1968@163.com

[†]These authors have contributed equally to this work

Specialty section:
This article was submitted to Cancer Imaging and Image-directed Interventions, a section of the journal Frontiers in Oncology

Received: 12 November 2020
Accepted: 13 January 2021
Published: 26 February 2021

Citation:
Liu J, Yin P, Wang S, Liu T, Sun C and Hong N (2021) CT-Based Radiomics Signatures for Predicting the Risk Categorization of Thymic Epithelial Tumors. Front. Oncol. 11:628534. doi: 10.3389/fonc.2021.628534

Objectives: This study aims to assess the performance of radiomics approaches based on 3D computed tomography (CT), clinical and semantic features in predicting the pathological classification of thymic epithelial tumors (TETs).

Methods: A total of 190 patients who underwent surgical resection and had pathologically confirmed TETs were enrolled in this retrospective study. All patients underwent non-contrast-enhanced CT (NECT) scans and contrast-enhanced CT (CECT) scans before treatment. A total of 396 hand-crafted radiomics features of each patient were extracted from the volume of interest in NECT and CECT images. We compared three clinical features and six semantic features (observed radiological traits) between patients with TETs. Two triple-classification radiomics models (RMs), two corresponding clinical RMs, and two corresponding clinical-semantic RMs were built to identify the types of the TETs. The area under the receiver operating characteristic curve (AUC) and accuracy (ACC) were useful to evaluate the different models.

Results: Of the 190 patients, 83 had low-risk thymoma, 58 had high-risk thymoma, and 49 had thymic carcinoma. Clinical features (Age) and semantic features (mediastinal fat infiltration, mediastinal lymph node enlargement, and pleural effusion) were significantly different among the groups($P < 0.001$). In the validation set, the NECT-based clinical RM (AUC = 0.770 for low-risk thymoma, 0.689 for high-risk thymoma, and 0.783 for thymic carcinoma; ACC = 0.569) performed better than the CECT-based clinical-semantic RM (AUC = 0.785 for low-risk thymoma, 0.576 for high-risk thymoma, and 0.774 for thymic carcinoma; ACC = 0.483).

Conclusions: NECT-based and CECT-based RMs may provide a non-invasive method to distinguish low-risk thymoma, high-risk thymoma, and thymic carcinoma, and NECT-based RMs performed better.

Advances in Knowledge: Radiomics models may be used for the preoperative prediction of the pathological classification of TETs.

Keywords: radiomics, thymic epithelial tumors, pathologic classification, computed tomography, machine learning

INTRODUCTION

Thymic epithelial tumors (TETs) originate from thymic epithelial cells and are the most common tumors in the anterior mediastinum, accounting for 47% of mediastinal neoplasms (1). The most common age of patients is 35–70 years, with no significant difference in sex. Approximately one-third of patients have myasthenia gravis (2).

The World Health Organization (WHO) histological classification of TETs is complex. Before 1980, TET classification was based on the morphological features of tumor cells and was divided into spindle cell, lymphocyte dominant, epithelial cell, and lymphoepithelial types. In 1999, the WHO revised the classification by tissue origin and function and adopted the classification proposed by the German pathologist Muller–Hermelink. Then, TETs were divided into types A, AB, B1, B2, and B3 and thymic cancer. Based on the consensus of the international thymic malignancy interest group on thymic tumors, the 2015 WHO classification of TETs modified the view of thymoma as a benign tumor, except for nodule-type thymoma and micro thymoma with lymphoid stroma. Moreover, other thymomas are considered malignant tumors (3). Therefore, the main treatment for TETs is surgical excision. Previous studies have found that type B2 and B3 thymomas are less likely to be completely removed than type A, AB, or B1 thymomas because of their more aggressive behavior (4). Moreover, patients with types B2 and B3 thymomas had higher tumor recurrence rates and mortality rates than those with other types (5). According to clinical needs, Jeong et al. (6) simplified the TET classification into low-risk thymoma (A, AB, and B1), high-risk thymoma (B2 and B3), and thymic cancer. Recently, some scholars found that there was a significant correlation between the new tumor nodes metastasis (TNM) staging system and the WHO histological grade (7). The potential for complete resection and the overall and disease-free survival outcomes were closely related to the thymoma stage. Furthermore, both the histotype and stage correlated with disease-free survival. Therefore, accurate preoperative classification can help develop individualized treatment methods for TET patients and improve prognosis (8, 9).

CT is the most important imaging method in the diagnosis of TETs. The CT features of non-invasive TETS are as follows: round or oval mass, usually located on one side of the anterior superior mediastinum; intact capsule, uniform density, clear surrounding fat space; and homogeneous light to moderate enhancement on the enhanced scan. The CT signs of invasive TETS are as follows: irregular mass with unclear margin; an incomplete capsule, peritumoral fat deposition; visible calcification; obvious uneven enhancement on enhanced scans; pleural effusion; pericardial effusion; and displacement and compression of cardiac vessels (9). The differential diagnosis includes mainly the following: 1) anterior mediastinal lymphoma, mediastinal lymphoma with the nodular fusion of multiple lymph nodes, the uneven density of lesions, rare calcification, swelling of adjacent lymph nodes and displacement of adjacent vessels; showing mild to moderate enhancement on enhanced scans; and 2) teratoma, mostly located in the middle of the anterior mediastinum and containing fat, bone, calcification, and soft tissue components; showing heterogeneous enhancement.

Radiomics models (RMs) have been widely used to predict tumor type and stage, lymph node metastasis, and prognosis (10–19), specifically in lung, breast, and colorectal cancer. Previous studies have shown that texture analysis based on CT images can distinguish high-risk thymoma from low-risk thymoma (20). However, thymic cancer has not been included. Because identifying thymic cancer *via* conventional imaging is difficult and accurate preoperative identification facilitates the development of individualized treatment approaches, a simple non-invasive method of identification would be of great clinical benefit.

Different high-dimensional quantitative radiomics features can be combined into predictive RMs to quantify tumor heterogeneity and show underlying malignant features (21, 22). Moreover, previous studies have shown that low-risk thymoma, high-risk thymoma, and thymic carcinoma are associated with variations in the morphology of epithelial cells, the ratio of lymphocytes to epithelial cells, invasiveness, and gene expression (3, 23, 24). Overexpression of specific genes is common in thymic carcinoma but rare in thymoma, and the expression levels of these genes are related to the degree of malignancy, biological characteristics, and prognosis of the patient. Therefore, we hypothesized that CT-based radiomics signatures can distinguish among low-risk thymoma, high-risk thymoma, and thymoma. The purpose of this study was to assess the performance of radiomics approaches based on CT, clinical and semantic features for predicting the pathological classification of TETs.

MATERIALS AND METHODS

Patients

This study was approved by the local ethics committee of our hospital, and the requirement for informed consent was waived. A total of 285 patients who underwent surgical resection and were pathologically confirmed as having TETs in our hospital between July 2012 and December 2019 were retrospectively analyzed. The inclusion criteria were as follows: (1) surgical resection and pathological diagnosis of TET; (2) CECT scan performed within 1 month before surgery; (3) no treatment before CT scan; and (4) available medical and surgical records. The exclusion criteria were as follows: (1) poor image quality due to artefacts or other causes and (2) absence of a CECT scan. Finally, a total of 190 patients were included in our study, and 95 patients were excluded (**Figure 1**). The WHO histologic classification of TETs was determined by surgical conditions and pathological examinations. The clinical features assessed included the following: age, sex, and symptoms (absence of symptoms, chest pain, cough or dyspnoea, myasthenia gravis, weakness, and others).

Image Acquisition

All patients underwent chest NECT and CECT scans. The scanning equipments were Philips 256 slice iCT of Holland and GE Lightspeed VCT 64 layers of USA. The scanning parameters were as follows: (1) Philips iCT: tube voltage 120 kV, automatic tube current, layer thickness 5 mm, pitch 0.980, reconstruction layer thickness 1 mm; (2) GE Lightspeed VCT: tube voltage 120 kV, tube current 150 mA, slice thickness 5 mm, pitch 0.516, reconstruction layer thickness 0.625 mm. All patients were examined in a supine position, arms up, deep inspiration and scanning. The contrast

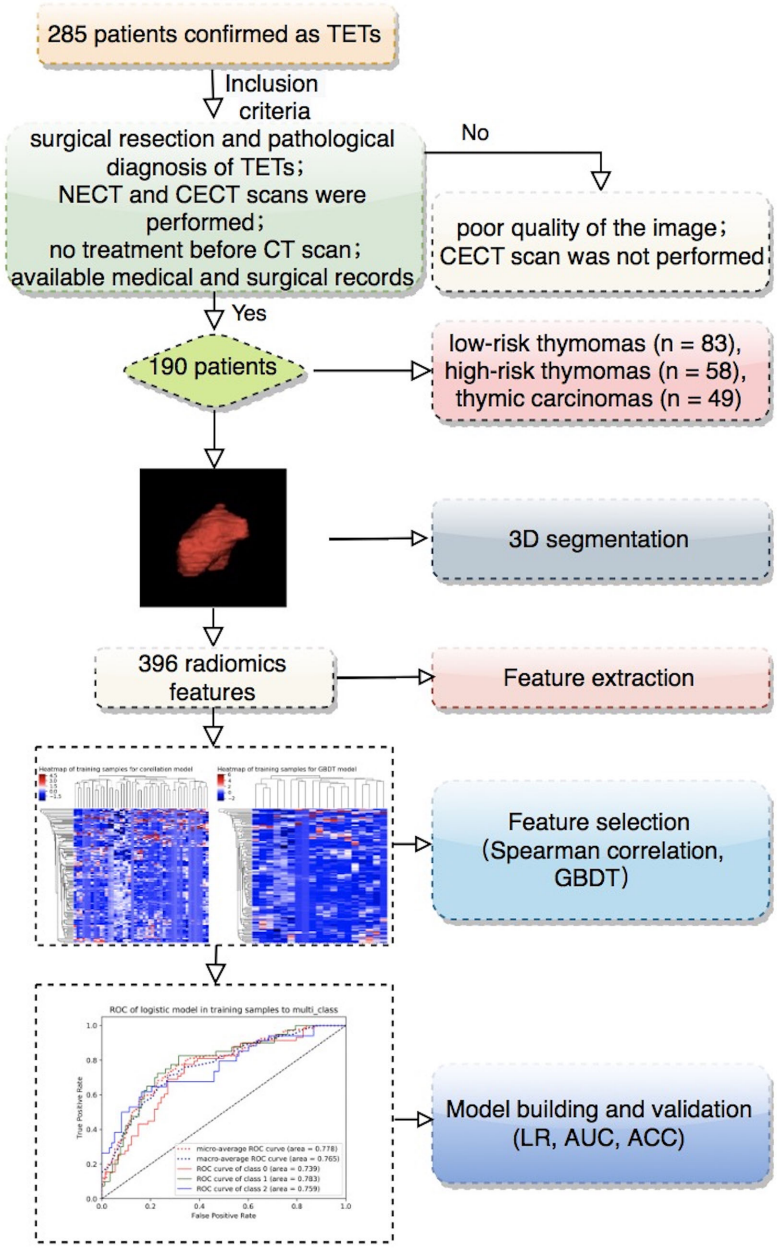

FIGURE 1 | The workflow of this study.

medium was injected rapidly through the forearm vein using a high-pressure syringe. The contrast agents included iopromide and iohexol. The enhancement phase was delayed for 60 s. The CT images were reconstructed with a standard kernel.

Tumor Segmentation

All NECT and CECT Digital Imaging and Communications in Medicine images were exported from the picture archiving and communication system (PACS) of our hospital. ITK-SNAP software version 3.6.0 (www.itksnap.org) was used for manual segmentation. All regions of interest were handcrafted on NECT and CECT images on each slice by a thoracic radiologist with 10 years of experience and validated by a senior thoracic radiologist with 20 years of experience, as shown in **Figure 2**.

Feature Extraction and Selection

For each patient, a total of 396 radiomics features, including 42 first-order histogram features, 334 second-order texture features, 9 morphological features, and 11 gray-level size zone matrix features, were extracted from all the NECT and CECT images based on Artificial Intelligence Kit software version 3.3.0 (GE Healthcare, China).

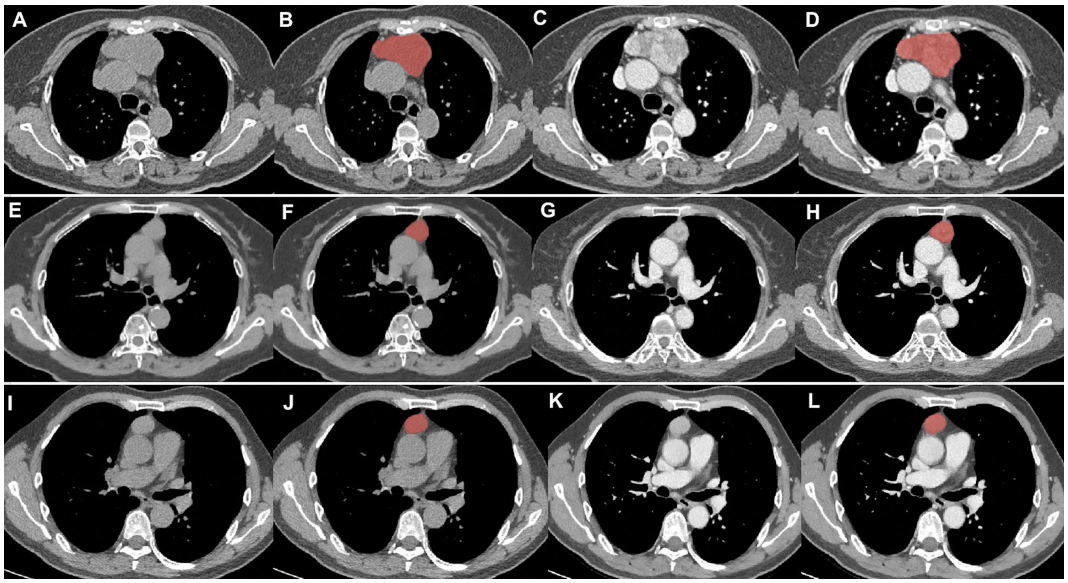

FIGURE 2 | Tumor segmentation. **(A–D)** thymic carcinomas; **(E–H)** high-risk thymomas; **(I–L)**, low-risk thymomas. Columns 1 and 2 were the NECT scan, columns 3 and 4 were the CECT scan. Columns 2 and 4 showed the delineation of different lesions (red areas).

We preprocessed the data and normalized the extracted features. When the data value exceeded the range of the mean value and standard deviation, the median of a specific variance vector was used to replace the outliers. In addition, the data were standardized in specific intervals.

In terms of the feature selection method, the Spearman correlation coefficients with a threshold of 0.7 was first used to exclude redundant features. Then, the gradient boosting decision tree (GBDT) algorithm, which has good generalization ability, was used to optimize the subset of features. After the number of features was determined, the most predictive radiomics features were used to construct the final model.

The consistency of features from different machines was evaluated by using intra- and interclass correlation coefficients (ICC). An ICC greater than 0.75 was considered as a good agreement.

Semantic Features

All images were reviewed by two radiologists, each of whom had more than 10 years of experience in chest CT study interpretation. The two radiologists were blinded to the histologic classification and clinical information. If there was variation in the results, they reviewed the CT images together, and any discrepancies were resolved by discussion until consensus was reached. The semantic features assessed included the following: the maximum diameter of the tumor (measured as the largest cross-section of the mass), cystic degeneration, calcification, mediastinal fat infiltration, mediastinal lymph node enlargement (short diameter >1 cm), and pleural effusion.

Model Construction and Validation

First, we constructed two triple-classification radiomics classifiers, namely, NECT- and CECT-based RMs, using a logistic regression model. Subsequently, the variables of the clinical features with a P value <0.05 were added to the NECT- and CECT-based clinical RMs. Finally, the variables of semantic features with a P value <0.05 were added to the NECT- and CECT-based clinical-semantic RMs.

All patients were randomly divided into the training and validation sets at a ratio of 7:3. All three models were trained on the training set by using the repeated five-fold cross-validation method, and the estimation performance of the models was evaluated with the validation set. The performance of different models was assessed using the area under the receiver operating characteristic curve (AUC) and accuracy (ACC).

Statistical Analysis

All statistical analyses were performed with R (version 3.5.1) and Python (version 3.5.6). Kruskal–Wallis H test was performed to compare continuous variables, whereas the chi-squared test or Fisher's exact was used for categorical variables amongst groups. All statistical tests were two-sided, and Bonferroni-corrected P value was used to identify the feature significance of multiple comparisons.

RESULTS

Patient Characteristics

A total of 190 patients (108 males, 82 females; mean age of 51.86 ± 13.09 years, range 24–83 years) were included in this study. Of the patients, 165 underwent thoracoscopic surgery (80 low-risk thymomas, 51 high-risk thymomas, 32 thymic carcinomas) and 25 underwent thoracotomy (3 low-risk thymomas, 7 high-risk thymomas, 17 thymic carcinomas), with a significant difference among the groups (P < 0.001). The histopathological results indicated that 83 patients (16 type A, 49 type AB, and 18 type B1) had low-risk thymoma (43 males, 40 females; mean age of 51.25 ±

12.29 years, range 24–79 years), 58 patients (38 type B2 and 20 type B3) had high-risk thymoma (33 males, 25 females; mean age of 47.98 ± 14.04 years, range 24–81 years), and 49 patients (49 type C) had thymic carcinoma (31 males, 18 females; mean age of 57.47 ± 11.46 years, range 31–83 years). The age was significantly different among the groups ($Z = 7.637$, $P < 0.01$). The average age of patients with thymic carcinoma was higher than that of patients in the other two groups. In this study, 101 patients presented no symptoms at tumor diagnosis. For symptomatic patients, the most common symptom in 38 patients was chest discomfort or pain, followed by cough or dyspnea in 18 patients, myasthenia gravis in 14 patients, weakness in 14 patients, and other symptoms in 5 patients. No significant differences were found in sex or symptoms among the three groups ($P > 0.05$; **Table 1**).

Semantic Features

The reproducibility of the radiomics features by the different machines was satisfactory (ICC, ranged from 0.771 to 0.905).

In total, six CT image descriptors were developed to characterize the TETs as follows: 1) the mean ± standard deviation of the maximum diameter of the tumor: low-risk thymoma (5.186 ± 2.662 cm), high-risk thymoma (4.857 ± 2.273 cm), thymic carcinoma (5.335 ± 1.914 cm); 2) cystic degeneration (18 low-risk thymomas, 6 high-risk thymomas, 5 thymic carcinomas); 3) calcification (11 low-risk thymomas, 14 high-risk thymomas, 6 thymic carcinomas); 4) mediastinal fat infiltration (7 low-risk thymomas, 13 high-risk thymomas, 30 thymic carcinomas); 5) mediastinal lymph node enlargement (1 low-risk thymoma, 5 high-risk thymomas, 18 thymic carcinomas); and 6) pleural effusion (2 low-risk thymomas, 11 high-risk thymomas, 5 thymic carcinomas). Mediastinal fat infiltration, mediastinal lymph node enlargement, and pleural effusion were significantly different among the groups ($P < 0.001$).

Radiologic Diagnosis

The radiologists diagnosed 91 low-risk thymomas, 63 high-risk thymomas, and 36 thymic carcinomas. The ACCs of the radiologists' diagnoses are shown in **Tables 2** and **3**.

Performance of the Different Models

No significant differences were observed in clinical or semantic features between the training and validation groups ($P > 0.05$). After feature selection, 19 NECT features and 19 CECT features remained to construct the RMs (see **Supplementary Material**).

In the training set, the NECT-based RM achieved AUCs of 0.739 (for low-risk thymoma), 0.783 (for high-risk thymoma), and 0.759 (for thymic carcinoma) and an ACC of 0.644 (**Table 2**, **Figure 3**). In contrast, the CECT-based RM achieved AUCs of 0.679 (for low-risk thymoma), 0.688 (for high-risk thymoma), and 0.721 (for thymic carcinoma) and an ACC of 0.576. In the validation set, similar results were found, where the NECT-based RM achieved AUCs of 0.686 (for low-risk thymoma), 0.601 (for high-risk thymoma), and 0.632 (for thymic carcinoma) and an ACC of 0.483 (**Table 3**). In contrast, the CECT-based RM achieved AUCs of 0.611 (for low-risk thymoma), 0.574 (for high-risk thymoma), and 0.626 (for thymic carcinoma) and an ACC of 0.448.

When combined with the significantly different clinical features, the clinical RMs performed better than the individual RMs. In the training set, the NECT-based clinical RM exhibited AUCs of 0.746 (for low-risk thymoma), 0.808 (for high-risk thymoma), and 0.813 (for thymic carcinoma) and an ACC of 0.659. Moreover, the CECT-based clinical RM exhibited AUCs of 0.690 (for low-risk thymoma), 0.717 (for high-risk thymoma), and 0.768 (for thymic carcinoma) and an ACC of 0.553. Similarly, in the validation set, the NECT-based clinical RM exhibited AUCs of 0.687 (for low-risk thymoma), 0.699 (for high-risk thymoma), and 0.689 (for thymic carcinoma) and an ACC of 0.483. The CECT-based clinical RM exhibited AUCs of 0.538 (for low-risk thymoma), 0.644 (for high-risk thymoma), and 0.679 (for thymic carcinoma) and an ACC of 0.448.

Finally, when the clinical and semantic features with significant differences were combined, the analysis results showed that the clinical-semantic RMs had the best performance among the three models. In the training set, the NECT-based clinical-semantic RM exhibited AUCs of 0.880 (for low-risk thymoma), 0.850 (for high-risk thymoma), and 0.939 (for thymic carcinoma) and an ACC of 0.750. Moreover, the

TABLE 1 | Clinical characteristic of patients.

Variable	Training set					Validation set				
	Low-risk thymoma	High-risk thymoma	Thymic carcinoma	Statistics	*P* value	Low-risk thymoma	High-risk thymoma	Thymic carcinoma	Statistics	*P* value
N	58	40	34			25	18	15		
Age	50.40 ± 11.70	49.85 ± 14.23	57.79 ± 10.76	4.87	0.009	53.24 ± 13.61	43.83 ± 13.04	56.73 ± 13.29	4.316	0.018
Female	28 (48.28%)	17 (42.50%)	14 (41.18%)	0.549	0.76	11 (44.00%)	8 (44.44%)	4 (26.67%)	1.427	0.49
Male	30 (51.72%)	23 (57.50%)	20 (58.82%)			14 (56.00%)	10 (55.56%)	11 (73.33%)		
Symptom				–	0.054				–	0.508
No symptom	37 (63.79%)	23 (57.50%)	14 (41.18%)			11 (44.00%)	8 (44.44%)	8 (53.33%)		
Chest pain	9 (15.52%)	7 (17.50%)	11 (32.35%)			6 (24.00%)	3 (16.67%)	2 (13.33%)		
Cough/ dyspnea	3 (5.17%)	3 (7.50%)	4 (11.76%)			4 (16.00%)	1 (5.56%)	3 (20.00%)		
Weakness	6 (10.34%)	3 (7.50%)	0 (0.00%)			3 (12.00%)	1 (5.56%)	1 (6.67%)		
Myasthenia gravis	3 (5.17%)	4 (10.00%)	2 (5.88%)			1 (4.00%)	4 (22.22%)	0 (0.00%)		
Others	0 (0.00%)	0 (0.00%)	3 (8.82%)			0 (0.00%)	1 (5.56%)	1 (6.67%)		

TABLE 2 | Performance of three-class models in training set.

	AUC	ACC	Precision	Recall	F1-score
NECT-based RM					
Low-risk thymoma	0.739	0.644	0.618	0.810	0.701
High-risk thymoma	0.783	0.644	0.639	0.575	0.605
Thymic carcinoma	0.759	0.644	0.750	0.441	0.556
CECT-based RM					
Low-risk thymoma	0.679	0.576	0.566	0.810	0.667
High-risk thymoma	0.688	0.576	0.536	0.375	0.441
Thymic carcinoma	0.721	0.576	0.667	0.412	0.509
NECT-based clinical-RM					
Low-risk thymoma	0.746	0.659	0.647	0.759	0.698
High-risk thymoma	0.808	0.659	0.676	0.625	0.649
Thymic carcinoma	0.813	0.659	0.667	0.529	0.590
CECT-based clinical-RM					
Low-risk thymoma	0.690	0.553	0.569	0.707	0.631
High-risk thymoma	0.717	0.553	0.500	0.375	0.429
Thymic carcinoma	0.768	0.553	0.567	0.500	0.531
NECT-based clinical-sematic-RM					
Low-risk thymoma	0.880	0.750	0.731	0.845	0.784
High-risk thymoma	0.850	0.750	0.706	0.600	0.649
Thymic carcinoma	0.939	0.750	0.839	0.765	0.800
CECT-based clinical-sematic-RM					
Low-risk thymoma	0.835	0.705	0.672	0.776	0.720
High-risk thymoma	0.813	0.705	0.731	0.475	0.576
Thymic carcinoma	0.946	0.705	0.744	0.853	0.795
Radiologist diagnosis					
Low-risk thymoma	-	0.455	0.551	0.655	0.599
High-risk thymoma	-	0.455	0.225	0.225	0.225
Thymic carcinoma	-	0.455	0.565	0.382	0.456

AUC, area under curve; ACC, accuracy.

TABLE 3 | Performance of three-class models in validation set.

	AUC	ACC	Precision	Recall	F1-score
NECT-based RM					
Low-risk thymoma	0.686	0.483	0.571	0.640	0.604
High-risk thymoma	0.601	0.483	0.350	0.389	0.368
Thymic carcinoma	0.632	0.483	0.500	0.333	0.400
CECT-based RM					
Low-risk thymoma	0.611	0.448	0.514	0.720	0.600
High-risk thymoma	0.574	0.448	0.222	0.111	0.148
Thymic carcinoma	0.626	0.448	0.429	0.400	0.414
NECT-based clinical-RM					
Low-risk thymoma	0.687	0.483	0.500	0.560	0.528
High-risk thymoma	0.699	0.483	0.500	0.444	0.471
Thymic carcinoma	0.689	0.483	0.429	0.400	0.414
CECT-based clinical-RM					
Low-risk thymoma	0.538	0.448	0.486	0.680	0.567
High-risk thymoma	0.644	0.448	0.143	0.056	0.080
Thymic carcinoma	0.679	0.448	0.500	0.533	0.516
NECT-based clinical-sematic-RM					
Low-risk thymoma	0.770	0.569	0.636	0.840	0.724
High-risk thymoma	0.689	0.569	0.500	0.333	0.400
Thymic carcinoma	0.783	0.569	0.462	0.400	0.429
CECT-based clinical-sematic-RM					
Low-risk thymoma	0.785	0.483	0.640	0.640	0.640
High-risk thymoma	0.576	0.483	0.250	0.111	0.154
Thymic carcinoma	0.774	0.483	0.400	0.667	0.500
Radiologist diagnosis					
Low-risk thymoma	-	0.448	0.636	0.583	0.609
High-risk thymoma	-	0.448	0.261	0.316	0.286
Thymic carcinoma	-	0.448	0.462	0.400	0.429

AUC, area under curve; ACC, accuracy.

CECT-based clinical-semantic RM exhibited AUCs of 0.835 (for low-risk thymoma), 0.813 (for high-risk thymoma), and 0.946 (for thymic carcinoma) and an ACC of 0.705. Similarly, in the validation set, the NECT-based clinical-semantic RM exhibited AUCs of 0.770 (for low-risk thymoma), 0.689 (for high-risk thymoma), and 0.783 (for thymic carcinoma) and an ACC of 0.569. The CECT-based clinical-semantic RM exhibited AUCs of 0.785 (for low-risk thymoma), 0.576 (for high-risk thymoma), and 0.774 (for thymic carcinoma) and an ACC of 0.483.

DISCUSSION

In this study, we found that NECT-based and CECT-based three-class RMs performed well in predicting low-risk thymoma, high-risk thymoma, and thymic cancer, although NECT-based RMs performed better. When combined with clinical data (age only), the clinical RMs performed better than the individual RMs. When the clinical and semantic features with significant differences were combined, the analysis results showed that the clinical-semantic RMs had the best performance among the three models.

In this study, we compared age, sex, and symptoms among the patients with low-risk thymoma, high-risk thymoma, and thymic carcinoma. However, we found a significant difference only in age among the groups, with thymic carcinomas tending to occur at an older average age. Males accounted for slightly more TET cases than females, but there was no difference in the sex composition among the three groups, consistent with previous results (2). Myasthenia gravis is the most important clinical symptom of TETs. Approximately one-third of patients have myasthenia gravis (2). In our study, the incidence of myasthenia gravis was low (less than one-tenth), which may be related to the fact that chest CT has gradually become a routine examination. Most patients were identified through physical examination, while some patients had a cough, usually without symptoms related to myasthenia gravis.

Previous studies have attempted to differentiate low-risk thymoma, high-risk thymoma and thymic carcinoma with conventional CT imaging signs. Some scholars (25) found significant differences in tumor size, contour, adjacent mediastinal fat infiltration, invasion of large vessels, etc. amongst low-risk thymoma, high-risk thymoma, and thymic carcinoma. However, there may be some overlap and lack of specificity in these signs, and the diagnosis is highly dependent on the doctor's experience. In clinical practice, accurately distinguishing among low-risk thymoma, high-risk thymoma, and thymic carcinoma is still difficult (25). In our study, we compared the maximum tumor diameter, cystic degeneration, calcification, mediastinal fat infiltration, mediastinal lymph node enlargement, and pleural effusion among the low-risk thymoma, high-risk thymoma, and thymic carcinoma groups. The results showed that mediastinal fat infiltration, mediastinal lymph node enlargement, and pleural effusion were significantly different among the groups ($P <$ 0.001. We also compared the performance of radiologists in classification *via* RMs. The results showed that the accuracy of

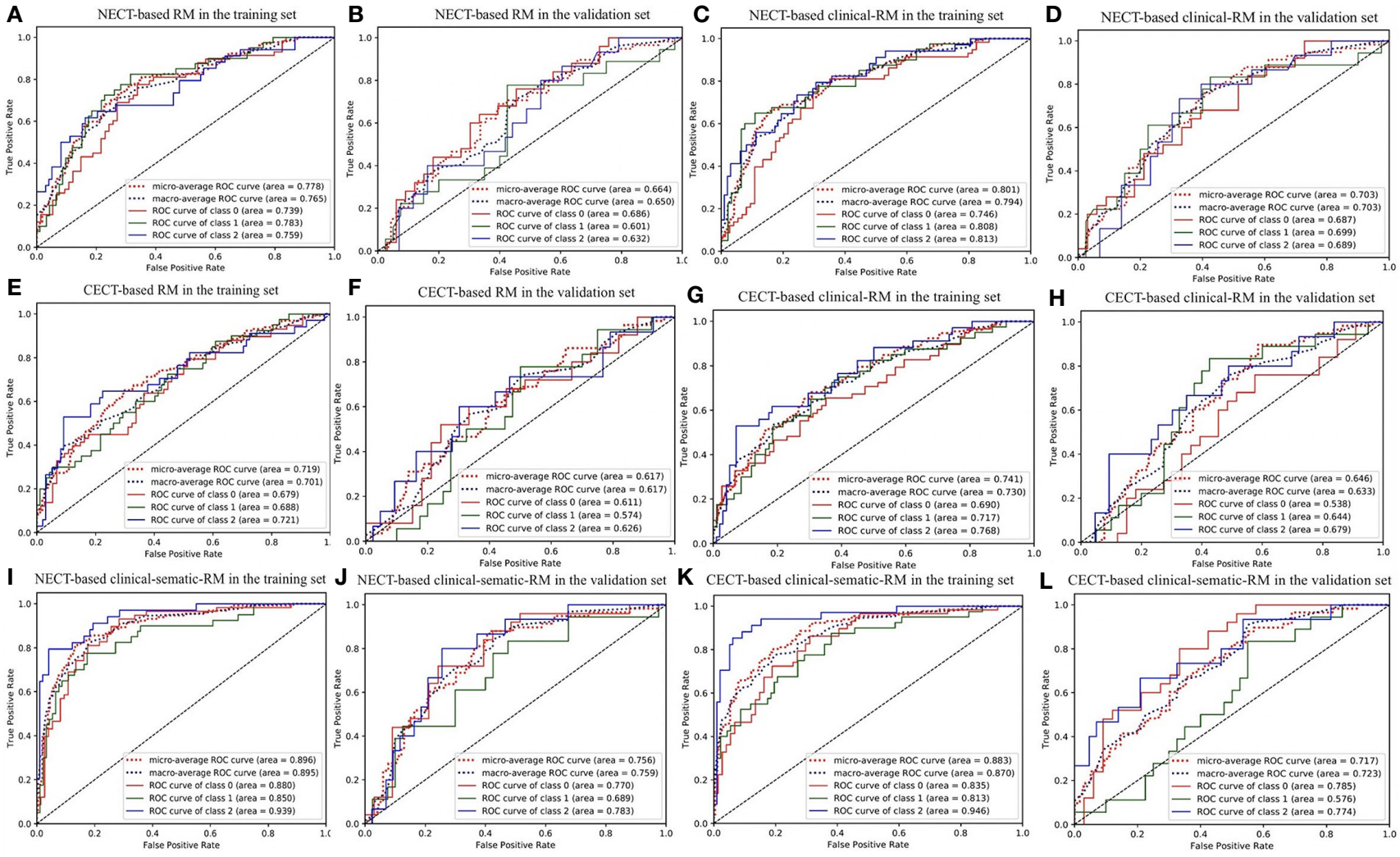

FIGURE 3 | The ROC curve of three-class models. **(A, B)** NECT-based RM in the training and validation sets; **(C, D)** NECT-based clinical-RM in the training and validation sets; **(E, F)** CECT-based RM in the training and validation sets; **(G, H)** CECT-based clinical-RM in the training and validation sets; **(I, J)** NECT-based clinical-sematic-RM in the training and validation sets; **(K, L)** CECT-based clinical-sematic-RM in the training and validation sets. Class 0, low-risk thymoma; class 1, high-risk thymoma; class 2, thymic carcinoma.

the radiologists was lower than that of the RMs. Therefore, identifying quantitative imaging parameters for the histological typing of TETs is essential.

Based on the heterogeneity of tumors, radiomics can non-invasively and quantitatively analyze the characteristics of tumors and monitor the occurrence, development and treatment response of tumors to assist physicians in making clinical decisions (26–28). Previously, some scholars have aimed to distinguish the histological types of TETs through radiomics. Yasaka et al. (29) analyzed the CT images of 39 patients with thymomas and used logistic regression analysis to establish an RM, which exhibited high diagnostic ability. However, the small sample size of the study based on 2D texture analysis did not include thymic carcinoma. Wang et al. (22) analyzed the 3D CT images of 199 patients with thymomas and established an RM by logistic regression analysis. Similarly, thymic carcinoma was not included in that study, and the clinical and semantic features of thymic epithelial neoplasms were not included. Xiao et al. (30) developed a radiological nomogram for predicting TET tissue type by combining a RM, conventional MRI imaging signs and clinical features in multivariable logistic regression analysis and drew a good conclusion.

In our study, we established two triple-classification radiomics classifiers based on the 3D NECT images and CECT images of 190 patients with TETs and analyzed three clinical features and six semantic features. The results showed that the clinical RMs performed better than the individual RMs and that the clinical-semantic RMs had the best performance among the models. However, the AUCs of the radiomics signatures in our study were lower than those in a previous study. We believe that these differences were caused mainly by the different radiomics features extracted from 2D or 3D texture analysis, the different classification methods and different inspection methods. Several studies have shown that compared with 2D texture analysis, 3D texture analysis can improve the classification accuracy (19, 31). Our previous study showed that the results of three classifications are lower than those of two classifications (32). Furthermore, we included both NECT and CECT images and found that NECT-based RMs performed better than CECT-based RMs in predicting low-risk thymoma, high-risk thymoma, and thymic cancer, which we considered to be reasonable. The diagnostic ability of the enhanced image was found to be better than that of the non-enhanced image. However, the enhanced image was observed together with the non-enhanced image rather than separately. In the radiomics approach in our study, the non-enhanced image and the enhanced image were analyzed separately. Moreover, the features extracted from the enhanced and non-enhanced images were different. Therefore, it was possible that the performance of the NECT-based RMs might have been better than that of the CECT-based RMs. A similar situation also arose in our previous studies (33). In clinical practice, NECT-based RMs can provide more diagnostic information in patients who are unsuitable for contrast-enhanced examination.

Our study has several limitations. First, the number of patients was not large. We aimed to reduce false discovery by using training and test cohorts. Despite this approach, we also recognize that TET radiomics data of a larger cohort is necessarily beneficial to validate the model in future studies. Second, multimodal data, such as magnetic resonance (MR) data, may be needed to provide additional useful information for the identification of lesions. Third, in clinical practice, an anterior mediastinal mass that is recommended for surgery may not be a TET. We plan to include more types of anterior mediastinal masses, such as lymphomas and genitourinary tumors, in a later study.

Our study shows that NECT-based and CECT-based RMs may provide a non-invasive method to distinguish low-risk thymoma, high-risk thymoma, and thymic carcinoma. As a quantitative method, radiomics signature analysis can provide complementary diagnostic information, facilitate the development of individualized treatment methods for TET patients, and improve prognosis.

DATA AVAILABILITY STATEMENT

The original contributions presented in the study are included in the article/**Supplementary Material**. Further inquiries can be directed to the corresponding author.

ETHICS STATEMENT

The studies involving human participants were reviewed and approved by the Peking University People's Hospital Ethics Review Committee and waived the informed consent. Written informed consent from the participants' legal guardian/next of kin was not required to participate in this study in accordance with the national legislation and the institutional requirements. Written informed consent was not obtained from the individual(s), nor the minor(s)' legal guardian/next of kin, for the publication of any potentially identifiable images or data included in this article.

AUTHOR CONTRIBUTIONS

1. Guarantor of integrity of the entire study: NH. 2. Study concepts: JL and PY. 3. Study design: JL, PY, and NH. 4. Definition of intellectual content: JL and PY. 5. Literature research: JL, PY, TL, and CS. 6. Clinical studies: JL and PY. 7. Experimental studies: JL and PY. 8. Data acquisition: JL, PY, TL, and CS. 9. Data analysis: PY and SW. 10. Statistical analysis: SW and PY. 11. Manuscript preparation: JL and PY. 12. Manuscript editing: JL and PY. 13. Manuscript review: NH. All authors contributed to the article and approved the submitted version.

FUNDING

This work was supported by National Key Research and Development Program of China (No. 2017YFC0109003).

SUPPLEMENTARY MATERIAL

The Supplementary Material for this article can be found online at: https://www.frontiersin.org/articles/10.3389/fonc.2021.628534/full#supplementary-material

REFERENCES

1. Fujii Y. Published guidelines for management of thymoma. *Thorac Surg Clin* (2011) 21(1):125–viii. doi: 10.1016/j.thorsurg.2010.08.002
2. Yuan D, Gu Z, Liang G, Fang W, Li Y. Chinese Alliance for Research of Thymoma Database. Clinical Study on the Prognosis of Patients with Thymoma with Myasthenia Gravis]. *Zhongguo Fei Ai Za Zhi.* (2018) 21 (1):1–7. doi: 10.3779/j.issn.1009-3419.2018.01.01
3. Meurgey A, Girard N, Merveilleux du Vignaux C, Maury JM, Tronc F, Thivolet-Bejui F, et al. Assessment of the ITMIG Statement on the WHO Histological Classification and of the Eighth TNM Staging of Thymic Epithelial Tumors of a Series of 188 Thymic Epithelial Tumors. *J Thorac Oncol* (2017) 12(10):1571–81. doi: 10.1016/j.jtho.2017.06.072
4. Miller Q, Moulton MJ, Pratt J. Surgical treatment of thymoma. *Curr Surg* (2002) 59(1):101–5. doi: 10.1016/s0149-7944(01)00629-8
5. Chen G, Marx A, Chen WH, Yong J, Puppe B, Stroebel P, et al. New WHO histologic classification predicts prognosis of thymic epithelial tumors: a clinicopathologic study of 200 thymoma cases from China. *Cancer* (2002) 95 (2):420–9. doi: 10.1002/cncr.10665
6. Jeong YJ, Lee KS, Kim J, Shim YM, Han J, Kwon OJ. Does CT of thymic epithelial tumors enable us to differentiate histologic subtypes and predict prognosis? *AJR Am J Roentgenol* (2004) 183(2):283–9. doi: 10.2214/ajr.183.2.1830283
7. Tamburini N, Maniscalco P, Migliorelli A, Nigim F, Quarantotto F, Maietti E, et al. Thymic Epithelial Tumors: Prognostic Significance and Relationship between Histology and the New TNM Staging System. *Thorac Cardiovasc Surg* (2020) 68(5):433–9. doi: 10.1055/s-0039-1678612
8. Banna GL, Sheel A, Sheel V, Bille A, Routledge T, Fernando S, et al. Treatment and prognostic factors of patients with thymic epithelial tumors at first recurrence or progression. *Future Oncol* (2017) 13(27):2429–39. doi: 10.2217/fon-2017-0236
9. Kaba E, Ozkan B, Erus S, Duman S, Cimenoglu B, Toker A. Role of Surgery in the Treatment of Masaoka Stage IVa Thymoma. *Ann Thorac Cardiovasc Surg* (2018) 24(1):6–12. doi: 10.5761/atcs.oa.17-00108
10. Xu X, Zhang X, Tian Q, Wang H, Cui L, Li S, et al. Quantitative Identification of Nonmuscle-Invasive and Muscle-Invasive Bladder Carcinomas: A Multiparametric MRI Radiomics Analysis. *J Magn Reson Imaging* (2019) 49 (5):1489–98. doi: 10.1002/jmri.26327
11. Huang YQ, Liang CH, He L, Tian J, Liang CS, Chen X, et al. Development and Validation of a Radiomics Nomogram for Preoperative Prediction of Lymph Node Metastasis in Colorectal Cancer published correction appears in J Clin Oncol. 2016 Jul 10;34(20):2436]. *J Clin Oncol* (2016) 34(18):2157–64. doi: 10.1200/JCO.2015.65.9128
12. Bianconi F, Fravolini ML, Bello-Cerezo R, Minestrini M, Scialpi M, Palumbo B. Evaluation of Shape and Textural Features from CT as Prognostic Biomarkers in Non-small Cell Lung Cancer. *Anticancer Res* (2018) 38(4):2155–60. doi: 10.21873/anticanres.12456
13. Corino VDA, Montin E, Messina A, Casali PG, Gronchi A, Marchianò A, et al. Radiomic analysis of soft tissues sarcomas can distinguish intermediate from high-grade lesions. *J Magn Reson Imaging* (2018) 47(3):829–40. doi: 10.1002/jmri.25791
14. Ferreira Junior JR, Koenigkam-Santos M, Cipriano FEG, Fabro AT, Azevedo-Marques PM. Radiomics-based features for pattern recognition of lung cancer histopathology and metastases. *Comput Methods Programs Biomed* (2018) 159:23–30. doi: 10.1016/j.cmpb.2018.02.015
15. Wang G, He L, Yuan C, Huang Y, Liu Z, Liang C. Pretreatment MR imaging radiomics signatures for response prediction to induction chemotherapy in patients with nasopharyngeal carcinoma. *Eur J Radiol* (2018) 98:100–6. doi: 10.1016/j.ejrad.2017.11.007
16. Suh HB, Choi YS, Bae S, Ahn SS, Chang JH, Kang SG, et al. Primary central nervous system lymphoma and atypical glioblastoma: Differentiation using radiomics approach. *Eur Radiol* (2018) 28(9):3832–9. doi: 10.1007/s00330-018-5368-4
17. Ortiz-Ramón R, Larroza A, Ruiz-España S, Arana E, Moratal D. Classifying brain metastases by their primary site of origin using a radiomics approach based on texture analysis: a feasibility study. *Eur Radiol* (2018) 28(11):4514–23. doi: 10.1007/s00330-018-5463-6
18. Coroller TP, Agrawal V, Huynh E, Narayan V, Lee SW, Mak RH, et al. Radiomic-Based Pathological Response Prediction from Primary Tumors and Lymph Nodes in NSCLC. *J Thorac Oncol* (2017) 12(3):467–76. doi: 10.1016/j.jtho.2016.11.2226
19. Fan TW, Malhi H, Varghese B, Cen S, Hwang D, Aron M, et al. Computed tomography-based texture analysis of bladder cancer: differentiating urothelial carcinoma from micropapillary carcinoma. *Abdom Radiol (NY)* (2019) 44(1):201–8. doi: 10.1007/s00261-018-1694-x
20. Wang X, Sun W, Liang H, Mao X, Lu Z. Radiomics Signatures of Computed Tomography Imaging for Predicting Risk Categorization and Clinical Stage of Thymomas. *BioMed Res Int* (2019) 2019:3616852. doi: 10.1155/2019/3616852
21. Ganeshan B, Miles KA. Quantifying tumour heterogeneity with CT. *Cancer Imaging* (2013) 13(1):140–9. doi: 10.1102/1470-7330.2013.0015
22. Miles KA, Ganeshan B, Hayball MP. CT texture analysis using the filtration-histogram method: what do the measurements mean? *Cancer Imaging* (2013) 13(3):400–6. doi: 10.1102/1470-7330.2013.9045
23. Kim BS, Kim JK, Kang CH, Kim YT, Jung KC, Won JK. An immunohistochemical panel consisting of EZH2, C-KIT, and CD205 is useful for distinguishing thymic squamous cell carcinoma from type B3 thymoma. *Pathol Res Pract* (2018) 214(3):343–9. doi: 10.1016/j.prp.2018.01.009
24. Aydiner A, Toker A, Sen F, Bicakci E, Saglam EK, Erus S, et al. Association of clinical and pathological variables with survival in thymoma. *Med Oncol* (2012) 29(3):2221–8. doi: 10.1007/s12032-011-0101-z
25. Liu GB, Qu YJ, Liao MY, Hu HJ, Yang GF, Zhou SJ. Relationship between computed tomography manifestations of thymic epithelial tumors and the WHO pathological classification. *Asian Pac J Cancer Prev* (2012) 13 (11):5581–5. doi: 10.7314/apjcp.2012.13.11.5581
26. Yin P, Mao N, Liu X, Sun C, Wang S, Chen L, et al. Can clinical radiomics nomogram based on 3D multiparametric MRI features and clinical characteristics estimate early recurrence of pelvic chondrosarcoma? *J Magn Reson Imaging* (2020) 51(2):435–45. doi: 10.1002/jmri.26834
27. Mao N, Yin P, Wang Q, Liu M, Dong J, Zhang X, et al. Added Value of Radiomics on Mammography for Breast Cancer Diagnosis: A Feasibility Study. *J Am Coll Radiol* (2019) 16(4 Pt A):485–91. doi: 10.1016/j.jacr.2018.09.041
28. Sun Q, Lin X, Zhao Y, Li L, Yan K, Liang D, et al. Deep Learning vs. Radiomics for Predicting Axillary Lymph Node Metastasis of Breast Cancer Using Ultrasound Images: Don't Forget the Peritumoral Region. *Front Oncol* (2020) 10:53. doi: 10.3389/fonc.2020.00053
29. Yasaka K, Akai H, Nojima M, Shinozaki-Ushiku A, Fukayama M, Nakajima J, et al. Quantitative computed tomography texture analysis for estimating histological subtypes of thymic epithelial tumors. *Eur J Radiol* (2017) 92:84–92. doi: 10.1016/j.ejrad.2017.04.017
30. Xiao G, Rong WC, Hu YC, Shi ZQ, Yang Y, Ren JL, et al. MRI Radiomics Analysis for Predicting the Pathologic Classification and TNM Staging of Thymic Epithelial Tumors: A Pilot Study. *AJR Am J Roentgenol* (2020) 214 (2):328–40. doi: 10.2214/AJR.19.21696
31. Fetit AE, Novak J, Peet AC, Arvanitits TN. Three-dimensional textural features of conventional MRI improve diagnostic classification of childhood brain tumours. *NMR Biomed* (2015) 28(9):1174–84. doi: 10.1002/nbm.3353
32. Yin P, Mao N, Zhao C, Wu J, Chen L, Hong N. A Triple-Classification Radiomics Model for the Differentiation of Primary Chordoma, Giant Cell Tumor, and Metastatic Tumor of Sacrum Based on T2-Weighted and Contrast-Enhanced T1-Weighted MRI. *J Magn Reson Imaging* (2019) 49 (3):752–9. doi: 10.1002/jmri.26238
33. Yin P, Mao N, Wang S, Sun C, Hong N. Clinical-radiomics nomograms for pre-operative differentiation of sacral chordoma and sacral giant cell tumor based on 3D computed tomography and multiparametric magnetic resonance imaging. *Br J Radiol* (2019) 92(1101):20190155. doi: 10.1259/bjr.20190155

Conflict of Interest: Author SW was employed by the company GE Healthcare.

The remaining authors declare that the research was conducted in the absence of any commercial or financial relationships that could be construed as a potential conflict of interest.

Copyright © 2021 Liu, Yin, Wang, Liu, Sun and Hong. This is an open-access article distributed under the terms of the Creative Commons Attribution License (CC BY). The use, distribution or reproduction in other forums is permitted, provided the original author(s) and the copyright owner(s) are credited and that the original publication in this journal is cited, in accordance with accepted academic practice. No use, distribution or reproduction is permitted which does not comply with these terms.

frontiers in Oncology

REVIEW
published: 22 July 2021
doi: 10.3389/fonc.2021.704220

Induction Strategy for Locally Advanced Thymoma

Yang Zhang[1†], Zongjuan Li[1†], Yixing Chen[1], Lijie Tan[2], Zhaochong Zeng[1], Jianyong Ding[2] and Shisuo Du[1*]*

[1] Department of Radiation Oncology, Zhongshan Hospital, Fudan University, Shanghai, China, [2] Department of Thoracic Surgery, Zhongshan Hospital, Fudan University, Shanghai, China

Surgery remains cornerstone for the management of thymoma. Complete surgical resection (R0), is recognized as the constant and significant factor for prognosis. However, in locally advanced (Masaoka-Koga stages III-IVa) thymomas, achieving R0 resection remains challenging due to local-regional invasion of the disease. Induction treatment, with the aim of reducing bulky tumor mass, offers new strategy to facilitate totally surgical resection. Herein, we reviewed recent progress and provided a comprehensive overview of induction strategy in locally advance thymoma.

Keywords: locally advanced, thymoma, induction therapy, neoadjuvant, R0 resection

OPEN ACCESS

Edited by:
Marco Lucchi,
University of Pisa, Italy

Reviewed by:
Paola Ciriaco,
San Raffaele Scientific Institute (IRCCS), Italy
Dragana Jovanovic,
University of Belgrade, Serbia

****Correspondence:***
Jianyong Ding
ding.jianyong@zs-hospital.sh.cn
Shisuo Du
du.shisuo@zs-hospital.sh.cn

[†]These authors have contributed equally to this work and share first authorship

Specialty section:
This article was submitted to Thoracic Oncology, a section of the journal Frontiers in Oncology

Received: *02 May 2021*
Accepted: *12 July 2021*
Published: *22 July 2021*

Citation:
Zhang Y, Li Z, Chen Y, Tan L, Zeng Z, Ding J and Du S (2021) Induction Strategy for Locally Advanced Thymoma. Front. Oncol. 11:704220. doi: 10.3389/fonc.2021.704220

INTRODUCTION

Thymic epithelial neoplasms, commonly comprising thymoma and thymic carcinoma, are rare tumors with a broad spectrum of biological behavior. Unlike thymic carcinomas, thymomas are relatively indolent. Once they are completely resected (R0), long-term survival may be easily achieved (1–3). Thereby, only thymomas were considered for this review.

According to published data, approximately 30% thymomas are staged as Masaoka-Koga III-IVa, and for these patients, performing R0 resection is not easy, due to locoregional extent of the disease (4, 5). Given the prognostic benefits of R0 resection, induction strategies, including chemotherapy, radiotherapy and even targeted drugs, have been explored, and some reviews have also been published during last decade (6, 7). However, in recent years, chemo regimens and radiotherapy technologies are rapidly evolving, immunotherapy and targeted drugs are fast-growing. Knowledge regarding induction strategy in thymoma, requires updating. So, we conducted this narrative review, discuss the current progress and future directions in the setting of induction treatment of locally advanced thymoma.

INDUCTION CHEMOTHERAPY: THEORETICAL ADVANTAGES AND CLINICAL PRACTICES

Induction chemotherapy is a priority criteria for initially unresectable thymomas. Firstly, this is because thymoma is revealed as chemo-sensitive (8, 9); Secondly, chemotherapy is easily to perform and with limited toxicity. Theoretically, induction chemotherapy presents several advantages. Foremost, induction chemotherapy can result in tumor shrinkage, which then improves the probability of R0 resection. Further, the systematic micro-metastasis of the neoplasm may be

inhibited at an early stage. Patients show a better tolerance to induction therapy compared with adjuvant chemotherapy. Ultimately, the objective response to induction treatment may provide information to help guide post-operative chemotherapy (10–12). However, to transform theory into reality, the following questions must be answered.

What Is the Exact Role of Induction Chemotherapy in Clinical Practice?

The exact role of induction chemotherapy in locally advanced thymoma patients still remains controversial. Given the rarity of the tumor, there have been no randomized controlled trials conducted to date. Nonetheless, some studies may provide insight into the effects of induction chemotherapy treatment.

Yamada et al. (13) using a Japanese Nationwide Database retrospectively explored the role of induction chemotherapy in stage III thymoma, surprisingly the authors determined that induction chemotherapy was an adverse prognostic factor. The authors proposed that induction treatment in their study was correlated to larger radiological tumor size, a higher number of involved sites, and invasion into the phrenic nerve. Thus, induction therapy itself did not worsen prognosis but acted as a selection bias. In addition, the small sample size may have represented another reason for this phenomenon.

Most recently, Khorfan et al. (3) retrospectively analyzed the management of advanced thymoma in the United States, a total of 160 patients (128 patients received induction chemotherapy) were administered induction treatment. As in the study by Yamada et al., patients with more advanced unresectable disease were more likely to be chosen for induction treatment. However, R0 resection rates in the induction group, were similar to those of patients receiving surgical intervention (57.2% *vs.* 54.2%), which may indicate the role of induction chemotherapy in facilitating R0 resection.

To eliminate the influence of confounding biases, a propensity score-matched analysis was performed. Thymoma patients receiving induction chemotherapy followed by surgery and patients receiving surgery alone had similar resectability, overall survival, and recurrence-free survival rates (14). In addition, Cardillo et al. (12) conducted a study to evaluate the prognostic factors in locally advanced thymoma and thymic carcinoma. In their study, 30 patients received immediate surgery, 31 patients ineligible for surgery at presentation underwent induction chemotherapy followed by surgery. Patient characteristics in these two groups were well-balanced. The results showed that the 10-year survival rates in the induction group were better than those for the immediate surgery group (57.9% *vs.* 38.1%, p=0.03).

Bretti et al. (15) performed a study in Masaoka-Koga stages III-IVa malignant thymoma patients. Thirty patients received surgical treatment, while 25 cases, ineligible for radical surgery, received induction chemotherapy before surgical reassessment. Following induction chemotherapy, 14 patients (56%) underwent surgery, and 11 cases (78.6%) achieved a complete resection. The study revealed that the overall survival of individuals who initially performed R0 resection was better than those failing to achieve R0 resection. Furthermore, the survival outcomes in the R0 resection subgroup after induction chemotherapy approximated that of direct R0 resection patients.

Despite the paucity of clinical data confirming the importance of induction chemotherapy, the existing evidence strongly suggests that induction chemotherapy is a preferred choice for initially unresectable thymoma patients.

Which Scheme Is Commonly Recommended for Induction Chemotherapy?

Currently, the optimal chemotherapy regimen remains controversial. Apart from induction therapy, patient prognosis can be influenced by surgical intervention, the adjuvant treatment strategy, and several other confounding factors. Thus, this review will place a greater focus on treatment response and the R0 resection rate to compare different chemotherapeutic regimens.

Cisplatin and Etoposide-Based Treatment Regimens

Hassan et al. (16) performed a study including 9 patients with unresectable (III and IVa) thymic tumors. Patients underwent induction chemotherapy with 3 courses of cisplatin and etoposide (EP). One (11%) patient achieved a complete remission (CR), 6 (66%) a partial remission (PR), and the remaining 2 (22%) patients, achieved only a minor remission. After induction therapy, 1 patient refused surgery and 5 (62.5%) of the other 8 achieved a R0 resection.

Macchiarini et al. (9) incorporated epirubicin into a cisplatin and etoposide regimen (PAE). Nine clinically staged IIIa invasive thymoma patients were enrolled in the analysis. After 3 cycles of treatment, all patients (100%) achieved a PR and 4 of the 7 (57.1%) patients were subjected to R0 resection. Lucchi et al. (17) also explored the role of PAE regimen as an induction scheme, in his study, treatment response and R0 resection rates were 73.3% and 76.7% respectively.

Platinum and Anthracycline-Based Treatment Regimens

The platinum and anthracycline-based scheme is most widely prescribed in clinical practice, and the following combinations were included: cisplatin+doxorubicin+cyclophosphamide (PAC), cisplatin+doxorubicin+cyclophosphamide+prednisone (PACE), cisplatin+adriamycin +cyclophosphamide+vincristine (ADOC), and cisplatin+doxorubicin+methylprednisolone (CAMP).

Shin et al. (18) conducted a prospective study which included 12 unresectable III-IVa thymoma patients, in which all of them received 3 courses of PACE. Three patients (25%) achieved a complete tumor response and a partial response was obtained in 8 patients (67%). One patient refused the subsequent surgical intervention, while for the remaining 11 patients, R0 resection was achieved in 9 (81.8%) patients. Kim et al. (19) also explored the role of PACE in III-IVb invasive thymoma. All patients included in the study received 3 courses of chemotherapy, and major responses were observed in 17 (77%) of the 22 patients, including 3 (14%) CRs and 14 (63%) PRs. After induction treatment, 1 patient refused surgery, but the remaining 21 patients were treated surgically, and of these, 16 (76%) achieved a R0 resection.

Sixteen clinically staged III-IVa invasive thymoma were enrolled in a study from January 1985 to November 1991, all patients were treated with the ADOC scheme. The response rates for ADOC induction therapy were 100% (7 CRs and 9 PRs). Subsequently, all

the patients underwent surgery and 11 patients (68.8%) achieved a complete resection (20). Another clinical trial including 16 consecutive patients with stage III and IVa invasive thymoma, also evaluated the effects of ADOC induction chemotherapy, 13 (81.3%) patients responded well to the regimen. All 13 patients responding well were directed to surgery, and for 9 (69.2%) patients, tumors were radically resected (21).

CAMP is also widely used in clinical trials. In a study conducted by Kohei et al. (22), the CAMP regimen was administered in the neoadjuvant setting in 14 invasive III-IVb stage thymoma patients. All patients except 1 (92.9%) showed a good response to this scheme. Finally, surgical treatment was performed in 9 patients and 2 (22.2%) achieved a R0 resection.

Other Combinations

Park et al. (23) explored the role of induction chemotherapy using docetaxel and cisplatin (TP). In their study, 9 (1 stage III and 8 stage IVa stage) thymoma patients were enrolled. After receiving induction chemotherapy, 5 (55.6%) patients achieve a PR and 4 patients responded stably to the scheme. Following reassessment, 7 patients became eligible for surgery and all (100%) ultimately achieved a R0 resection. Detailed information about induction chemotherapy regimens is listed in detail in **Table 1**.

INCORPORATING RADIATION INTO INDUCTION CHEMOTHERAPY

Induction radiotherapy alone is rarely used as initial therapy in thymoma patients (**Table 2**). After screening of National Cancer Database, the largest cancer registry in the whole world, a total of 160 advanced stage thymoma patients received neoadjuvant therapy, however, only 5.7% underwent induction radiation alone (3). According to Chinese Alliance for Research in Thymomas Database, among induction therapy patients, only 13.2% received radiotherapy (31).

Currently, chemotherapy remains the mainstream induction strategy, meanwhile, in some cases, chemotherapy alone is not sufficiently effective, especially in heavily invasive diseases. Under such circumstances, the potential synergism of combining chemotherapy with radiotherapy, may further potentiate induction response rates and facilitate R0 resection (**Table 3**). Similar to induction chemotherapy, deep consideration should also be given to the following questions.

What Is the Exact Role of Induction Chemoradiotherapy?

A study conducted by Chu et al., compared radiological response of chemotherapy alone with the combination of chemotherapy and radiotherapy in the management of locally advanced or advanced thymic epithelial tumors (including thymoma and other thymic tumors). An increased average radiological response was observed in the combination treatment group compared with chemotherapy alone (volume: reduction of 47.0 cm^3 or more, $P < 0.001$; diameter: a reduction of 0.8 cm or more, $P = 0.03$), and for patients receiving chemotherapy, further tumor shrinkage was observed in 33% patients when additional radiotherapy or chemoradiotherapy was administered (median volume: 42.3% reduction, $P = 0.03$; diameter: 3.0% reduction, $P = 0.049$ (35).

Another study performed by Wright et al., explored the function of induction concurrent chemoradiotherapy in 10 initially unresectable locally advanced thymic tumors (including 7 stage B3 thymomas and 1 thymic carcinoma). The treatment scheme consisted of 2 cycles of EP combined with concurrent radiotherapy (33 to 49 Gy) before surgery. Adjuvant chemotherapy (EP) was administered to incomplete resection patients and for those with

TABLE 1 | Induction chemotherapy for locally advanced thymoma.

Author	Sample size	Stage	Pathology	Chemo regimen	Response rate % (CR+PR)	No. of R0/No. of surgery (%)
Macchiarini et al. (9)	7	IIIa	thymic tumor*	PAE	100%	4/7 (57.1%)
Lucchi et al. (17)	30	III-IVa	thymoma	PAE	73.3%	23/30 (76.7%)
Hassan and Seoud (16)	9	III-IVa	thymoma	EP	77%	5/8 (62.5%)
Kunitoh et al. (24)	21	III	thymoma	PAE+vincristine	62%	9/13 (69.2%)
Berruti et al. (8)	6	III-IVa	thymoma	ADOC	83.3%	-/5 (-%)
Rea et al. (20)	16	III-IVa	thymoma	ADOC	100%	11/16 (68.8%)
Berruti et al. (21)	16	III-IVa	thymoma	ADOC	81.3%	9/13 (69.2%)
Tan et al. (25)	14	III-IVa	thymoma	ADOC	100%	9/14 (64.3%)
Bretti et al. (15)	25	III-IVa	thymic tumor*	ADOC、EP	72%	11/14 (78.6%)
Leuzzi et al. (26)	11	III-IV	thymic tumor*	PAC	81.8%	9/11 (81.8%)
Shin et al. (18)	12	III-IVa	thymoma	PACE	91.7%	9/11 (81.8%)
Kim et al. (19)	22	III-IV	thymoma	PACE	77%	16/21 (76.2%)
Cardillo et al. (12)	41	III-IVa	thymic tumor*	PACE	75.6% at least a minimal response	–
Yokoi et al. (22)	14	III-IV	thymoma	CAMP	92.9%	2/9 (22.2%)
Ishikawa et al. (27)	11	IVa-IVb	thymoma	CAMP	75%	4/7 (57.1%)
Nakamura et al. (11)	19	IV	thymoma	CAMP	78.9%	–
Park et al. (23)	9	III-IV	thymoma	TP	55.6%	7/7 (100%)

**including thymoma and thymic carcinoma.*

EP, cisplatin+etoposide; PAE, cisplatin+etoposide+ epirubicin; ADOC, cisplatin +adriamycin +cyclophosphamide +vincristine; PAC, cisplatin +doxorubicin +cyclophosphamide; PACE, cisplatin +doxorubicin +cyclophosphamide +prednisone; CAMP, cisplatin +doxorubicin +methylprednisolone; TP, docetaxol+cisplatin; CR, complete remission; PR, partial remission; R0, complete resection.

TABLE 2 | Induction radiotherapy for locally advanced thymoma.

Author	Sample size	Stage	Pathology	RT dose	Response rate % (CR+PR)	No. of R0/No. of surgery (%)
Bretti et al. (15)	8	III-IVa	malignant thymoma*	30 Gy	37.5%	1/3 (33.3%)
Akaogi et al. (28)	12	III-IVb	thymoma	12-21 Gy	91.7%	9/12 (75%)
Yagi et al. (29)	11	III-IV	thymoma	20-66 Gy	–	–
Ohara et al. (30)	6	III-IV	thymoma	12-20 Gy	83.3%	3/6 (50%)

**Detailed information was not shown.*
RT, radiotherapy; CR, complete remission; PR, partial remission.

TABLE 3 | Induction chemoradiotherapy for locally advanced thymoma.

Author	Sample size	Stage	Pathology	Chemo regimen	RT dose	Response rate % (CR+PR)	No. of R0/No. of surgery (%)
Wright et al. (32)	10	III-IVa	thymic tumor*	EP	40-45Gy	40%	8/10 (80%)
Korst et al. (33)	21	–	thymic tumor*	EP	40-45Gy	47.6%	17/21 (77%)
Wang et al. (34)	33	III	thymic tumor*	TP	40Gy	78.8%	85.7%

**including thymoma and thymic carcinoma.*
RT, radiotherapy; EP, cisplatin+etoposide; TP, docetaxol+cisplatin; CR, complete remission; PR, partial remission.

high risk of recurrence. After completion of induction treatment, 4 (40%) patients achieved a PR while the remaining 6 patients presented no changes. After reassessment, all 10 patients were directed towards surgery, and an impressive R0 resection was achieved in 8 (80%) patients. After examination of the resected specimens, substantial (>90%) necrosis was observed in 4 (40%) patients. No postoperative deaths were observed and the 5-year estimated survival was 69% (32).

In view of the encouraging results achieved following induction chemoradiotherapy, especially the high pathological response rate, a phase II multi-center study was prospectively conducted. A total of 21 thymic tumor patients (13 thymomas, 7 thymic carcinomas and 1 metaplastic tumor) who met the specific computed tomograph criteria were enrolled. The induction protocol consisted of 2 cycles of the EP scheme and concurrent radiation 40-45 Gy. Ten (47.6%) patients achieved a PR on radiographic assessment, while the remaining 11 showed no response. All patients received surgical treatment, and 17 (77%) of them underwent R0 resection (33).

A study conducted in China examined the induction role of concurrent chemoradiotherapy with a different chemotherapy scheme. In total, 33 patients (10 thymomas, 21 thymic carcinomas and 2 thymic carcinoids) were included. All patients received docetaxel and cisplatin concurrently accompanied by 40 Gy radiation treatment before surgery. After reassessment, the response rate was 78.8% (1 CR, 25 PR, and 7 stable disease [SD] cases). Among the 10 thymoma patients, an 80% response rate was achieved. Finally, 21 patients were recognized as responsive to the surgical procedure, and 18 (85.7%) achieved R0 resection (34).

Due to the differences in the inclusion criteria, the definition of an "unresectable tumor", and chemotherapy scheme, treatment outcomes in different clinical trials cannot be fully compared. However, a roughly higher rate of R0 resection can still be observed in the induction chemoradiotherapy groups. It may be not appropriate for all thymoma patients to receive induction chemoradiotherapy. Some patients may achieve favorable responses with chemotherapy alone, and furthermore, increased treatment toxicity and the potential risks induced by radiotherapy should not be ignored. Thus, eligible patients should be carefully selected.

Who Will Benefit Most From Induction Chemoradiotherapy?

Patients Presenting Invasion of Great Vessels

Yamada et al. extracted and analyzed data relative to a total of 310 stage III thymoma patients from the Japanese National Database. Among these 310 patients, 126 had great vessel invasion. These cases had significantly lower R0 resection rates compared with patients with no vessel invasion (73.8% *vs.* 83.7%, p= 0.011) (13). Hassan et al. (16) conducted a study to explore the function of induction chemotherapy in locally advanced thymoma patients, 3 cycles of EP were administered before surgery. Of these, only 3 patients presented great vessel invasion before induction chemotherapy, and unfortunately an extensive full-thickness tumor invasion of the vessels was still evident at the time of surgical intervention. Ultimately, all 3 patients achieved an incomplete resection. Thereby, for thymoma with great vessel invasion, chemotherapy alone may be not sufficient, while combining chemotherapy with radiotherapy may enhance the antitumor activity and the possibility of totally resection.

Patients With More Invasive Histological Subtype

Onuki et al. (36) performed a study to assess the pathological radioresponse to preoperatively irradiated thymoma. The authors found that type B1 or B2 group had higher reduction ratios than the type B3 group (mean value of 39.7%, 31.8%, and 21.0%, respectively, $P < 0.01$). One explanation for this phenomenon was that type B1 or B2 presents a larger percentage of radiosensitive lymphocytes compared with B3 tumors. Furthermore, high response rates can also be achieved in type A-B2 thymoma patients who have received either chemotherapy or corticosteroid treatment alone (37). Furthermore, in the study conducted by Korst et al., 21 thymic tumor patients were enrolled to assess the treatment response of induction chemoradiotherapy, and 5 patients ultimately showed near complete pathologic response, and intriguingly, 80% of them were thymic carcinomas (33). Thereby, we may ponder whether

preoperative chemotherapy is sufficient for type A-B2 tumors, and for more invasive histological subtypes like B3 thymoma or even thymic carcinoma, induction chemoradiotherapy may represent a better choice.

Patients Refractory to the First-Line Induction Chemotherapy

In a study performed by Robert et al., 8 thymic epithelial tumor patients received additional radiotherapy or chemoradiotherapy after the initial chemotherapy. Subsequent radiotherapy further decreased the median tumor volume by 39.9 cm^3 (P = 0.03) and median tumor diameter by 1.0 cm (P = 0.049) compared to post-chemotherapy measurements (35). Thus, in clinical practice, thymoma patients who are still not amenable to surgery after the first-line induction chemotherapy, additional induction radiotherapy may be a good choice, as it may lead to further tumor shrinkage and facilitate R0 resection. Our institute is performing a prospective clinical trial to further confirm this therapeutic schedule.

What's the Role of Radiation Technology Advances in Thymoma?

A major concern about radiotherapy is the undesired dose deposition to the surrounding tissues. In thymoma radiation, this concern is even more pronounced, because surrounding organs, including heart, lungs and esophagus, can not avoid being irradiated. Thymomas patients commonly have long-term survival, and the tumor mass of thymomas requiring induction radiation, is relatively bulky. The above characteristics, provide a strong rational for conducting advanced radiation technology to reduce toxicity. Radiation therapy has made significant technological strides over the past decades. More and more innovative techniques have been applied to the treatment of thymoma, like adaptive radiation therapy (ART), tomotherapy and particle radiotherapy (proton radiotherapy and carbon ion radiotherapy). By the implication of cutting-edge radiation technology, the final goal is to provide a culmination of innovation advances to maximize the therapeutic ratio, and improve R0 resection rate, while minimizing radiation-related toxicity.

The application of ART, or modifying the physical plan during the radiotherapy process, is becoming increasingly available in clinical practice. ART provides powerful potential for minimizing radiation-related injury while escalating or de-escalating target doses based on the dose to organs at risk (38). ART is worthwhile especially in tumors that shrink rapidly during radiation therapy. As reported in the literature, tumor mass of thymoma could be reduced by 40%-78% within the first two weeks of radiation (28, 39). So, ART may have potential role in thymoma treatment. In a pre-clinical study, the dosimetric benefit of ART in neoadjuvant setting of canine and feline thymoma was explored. The research demonstrated that rapid tumor-shrinkage was observed within 1 week of radiation, with a mean shrinkage of 31.0% ± 15.2%, which surly will exert huge adverse impact on normal tissues around the target. After mid-therapy replanning, the dose to organs at risk was significantly reduced, with −18.2% in the mean heart dose and −27.9% in the V20 lung dose (40). Although being promising, the usage of this technology faces the dilemma of lacking enough patients. After screen of papers, only a case report was found. The case showed that induction chemoradiotherapy with ART appears to be powerful weapons for locally advanced intact thymoma (41).

Tomotherapy is the delivery of intensity modulated radiation therapy using rotational delivery of a fan beam in the manner of a computed tomograph scanner (42). To the best of our knowledge, no clinical trial using tomotherapy has been conducted in the field of thymoma. Based on the experiences of our center, tomotherapy will be considered under the following two conditions: 1) complex-shaped thymoma: 3-dimentional radiation therapy or intensity modulated radiation therapy can not achieve satisfactory target volume coverage, or at the sacrifice of organs at risk; 2) multiple tumor lesions: treatment protocol can not be accomplished with single radiotherapy plan. In our institution, tomo is widely used in Masaoka-Koga IVa patients with pleural dissemination. In addition to radiotherapy to the primary site which is not eligible for surgery at initial evaluation, radiation is also delivered to the pleural area. For localized pleural disease, local radiation will be conducted. However, for patients with relative extensive pleural metastases, besides local treatment, prophylactic radiation of ipsilateral entire pleural will also be considered. As we know, most of the recurrence of thymoma occur on the pleural surface (43, 44). So, the aim of the above treatment strategy possesses two purposes: Improve R0 resection rate and reduce the risk of pleural dissemination during operation.

Particle radiotherapy possesses the theoretical dosimetric advantage over photon techniques by the production of "Bragg Peak", which provides a sharp increase in dose at a given depth in tissue that can be modulated by the treating physician (45). Several studies of lung cancer and Hodgkin lymphoma, have well demonstrated that particle radiotherapy could maintain target dose coverage while minimizing the dose of organs at risk (46, 47). In the field of thymoma, Haefner et al. conducted dosimetric comparison between photon and particle radiotherapy in the postoperative management of thymoma. The results revealed that particle radiotherapy showed superior organs at risk sparing and optimal target volume coverage (48). However, up to now, no data were reported about the implementation of particle radiation in induction radiation of thymoma.

ADDING IMMUNOTHERAPY TO INDUCTION TREATMENT

Immunotherapy is currently a revolution, as is thymoma. The most commonly used predictor for Programmed Cell Death-1/Programmed Cell Death- Ligand 1 (PD-1/PD-L1) immune therapy is the expression of PD-L1 (49, 50). As reported, high expression of PD-L1, being statistically associated with more aggressive histological types, higher Masaoka-Koga stages and even worse prognosis (51–54), was observed in 23%-92% thymoma patients (52, 55–61). In addition, tumor-infiltrating lymphocytes, which are required for adequate activation of immune system, were diffusely and abundantly distributed in

thymoma cases (60, 62). Taken together, high PD-L1 expression on tumor cells and abundant tumor-infiltrating lymphocytes in the microenvironment, provide a strong rational for implementing PD-1/PD-L1 therapy for thymomas to overcome the poor outcome results. Several trials have tentatively explored the efficacy and safety of immunotherapy in relapsed or advanced thymomas.

Cho et al. (63) performed a prospective phase II study to evaluate the role of pembrolizumab in thymoma patients who are refractory to initial standard platinum-based chemotherapy. A total of 7 thymoma patients were enrolled in the study and 2 of them (28.6%) achieved a partial response. Rajan et al. conducted a phase I trial with anti- PD-L1 antibody (Avelumab) in 7 advanced thymomas. Similar to the prior research, nearly 30% of the patients had an objective response (64). Due to the preliminarily promising results, a series of trials are on going to explore the role of immune therapy in relapsed or advanced thymomas (NCT03076554, NCT03134118, NCT03295227, NCT03463460, NCT02364076). In addition to efficacy, treatment toxicities are also important considerations. In the study of Cho et al., 5 (71.4%) of the 7 patients developed grade ≥ 3 immune-related adverse events, including 4 hepatitis and 3 myocarditis events. And in the research of Rajan et al., all of these patients that had tumor shrinkage developed immune related adverse events. Meanwhile, another article revealed that the administration of anti-PD1 immune check point inhibitor resulted in a storm of immune related adverse events (including myositis, myocarditis and myasthenia gravis and death) after administration of the first treatment cycle (65). Taken these limited data together, it looks that thymoma patients were at higher risk of developing immune-related side effects, so special caution is required for the usage of these agents in thymomas.

The exact role of induction immunotherapy in thymoma must be answered by clinical trials. To date, only two ongoing studies registered in the Chinese Clinical Trial Registry (ChiCTR2000036033) and clinicaltrials.gov (NCT03858582) are currently underway. All patients in the above two clinical trials will receive induction immunotherapy combined with chemotherapy. We hope these clinical trials will provide a conclusive answer to this question.

ADDITION OF TARGETED DRUGS TO PREOPERATIVE TREATMENT

Similar to immunotherapy, evidence supporting targeted treatment in the neoadjuvant setting for thymoma is limited. We searched the database of Chinese Clinical Trial Registry and ClinicalTrials.gov and only one clinical trial was found. This ongoing phase II study (NCT01025089) is exploring the effects of the combination of cetuximab with traditional PAC scheme as neoadjuvant therapy for locally advanced thymoma. Patients will initially receive cetuximab weekly for up to 4 weeks to assess tumor response to cetuximab alone. Then, they will continue to receive weekly cetuximab along with concurrent CAP for 4 cycles before surgical treatment. The primary endpoint of the study is the frequency of a complete pathological response. The secondary endpoints include toxicity, treatment response, and R0 resection.

With the advances in the understanding of molecular biology, unique genetic aberrations associated with thymoma have been identified. All these specific biological markers involving KIT, EGFR, IGF-1R, and VEGF pathways, will facilitate the use of new targeted drugs in the future (66). Targeted drugs may be an option in clinical practice for heavily pretreated thymoma patients. Like immune therapy, targeted drugs alone cannot exert a sufficient impact on thymoma shrinkage in the setting of induction treatment. However, different from immunotherapy, the side effects of targeted drugs in thymoma may be well tolerated, based on current evidence and some agents have shown promising effects (67). Thus, the benefits of incorporating these targeted drugs into preoperative chemotherapy deserve further study.

DISCUSSION

This narrative review is presenting updated knowledge regarding induction strategy in initially unresectable thymomas. Based on current evidence, induction chemotherapy is still the mainstay in the induction setting.

The actual role of various chemo regimens needs to be answered in randomized clinical trial. However, under the circumstance of lacking enough patients, systematic review using the principle of evidence-based medicine may be an alternative way. Berghmans et al. evaluated the effectiveness of the different systemic therapies in the systemic treatments for thymoma. It revealed that cisplatin-anthracycline (PAC or ADOC) combinations were the most popular and active regimens (68). Similarly, the Italian Collaborative Group for Thymic Malignancies also recommends PAC scheme given the high rate of tumor shrinkage (69). Though, some differences may exist between induction and systemic chemotherapy, the results of the above systematic review, can also shed light onto the the choice of induction chemotherapy. Towards data shown in **Table 1**, the common type of induction chemo was platinum-anthracycline-based followed by platinum-etoposide-based schedules. Similar response rate, approximately 62%-100%, could be achieved by the two regimens. As for another chemo regimen (TP), the response rate was only 55.6%. Consequently, platinum-anthracycline-based or platinum-etoposide-based schedules should be proposed as front-line therapy.

In addition to efficacy, clinicians should also pay close attention to potential side effects, particularly cardiac toxicity. The risk of cardiotoxicity in patients with thymoma is very high due to a number of factors. Firstly, the tumor itself can invade the adjacent heart and great vessels. Secondly, the surgical procedure and radiotherapy can also exert a harmful impact on the heart (70, 71). Thirdly, cardiotoxicity can be caused by anthracycline treatment (72). Thus, for patients with old age, heart disease, and concomitant radiotherapy, great caution should be given to potential cardiotoxicity. Chemotherapeutic regimens without

anthracycline, such as EP-based schemes, should be considered preferentially.

Although effective, chemotherapy alone sometimes is not powerful enough to make tumor remission. In these cases, additional radiotherapy, or chemoradiotherapy can present as salvage treatment modalities. Collectively, we propose the following strategies deserve to be tested in future studies. For patients with highly invasive features, such as great blood vessel invasion or B3 subtype, concurrent chemoradiotherapy may be a better induction strategy compared with chemotherapy alone (not in bulky tumors where radiation fields include a large proportion of the lung). For patients without such features, induction chemotherapy is preferred, and once tumors being refractory to chemotherapy, subsequent induction radiation should be considered.

Immunotherapy alone or in combination with chemotherapy is currently a revolution in the neoadjuvant treatment of non-small cell lung cancer (73–75). As for thymoma patients, will immunotherapy exert similar encouraging effects? From the available data, therapeutic prospects may be not very optimistic, because of limited activity of tumor control and high incidence of sever immune-induced toxicity. In our center, induction immunotherapy is only considered in thymomas, especially B3 subtype, refractory to induction chemotherapy or additional radiotherapy. So, the role of immunotherapy in induction treatment still requires confirmation.

Next generation sequencing and other advances in molecular biology have opened a new era for molecularly targeted therapies. From current data, targeted therapies in thymoma exhibited limited value and are only recommended to heavily pretreated advanced thymoma patients (67). However, different from immune or chemo therapy, the treatment-related toxicity of such agents is well tolerable in almost all reported cases. Thus, the benefits of incorporating these targeted drugs into preoperative chemotherapy deserve further study.

In general, given the rarity of the tumor, high-level clinical trials are difficult to perform. Thereby, in the future, collaborative efforts involving different organizations that specially focus on thymomas, such as the International Thymic Malignancy Interest Group (ITMIG) and Chinese Alliance for Research in Thymomas (ChART), should be promoted to encourage multicenter cooperation in clinical studies. Only in this way can we obtain enough sample sizes which will allow definitive conclusions about optimal treatment modalities.

AUTHOR CONTRIBUTIONS

Conception and design: SD and JD. Literature review and analysis: SD, JD, YZ, and ZL. Drafting of the manuscript: YZ, ZL, and YC. Supervision: LT and ZZ. All authors contributed to the article and approved the submitted version.

FUNDING

This work was supported by the National Nature Science Foundation of China (82073479) and Scientific Research Project of Shanghai Science and Technology Commission (20ZR1410600).

REFERENCES

1. Moser B, Scharitzer M, Hacker S, Ankersmit J, Matilla JR, Lang G, et al. Thymomas and Thymic Carcinomas: Prognostic Factors and Multimodal Management. *Thorac Cardiovasc Surg* (2014) 62:153–60. doi: 10.1055/s-0032-1322611
2. Roden AC, Yi ES, Jenkins SM, Edwards KK, Donovan JL, Cassivi SD, et al. Modified Masaoka Stage and Size Are Independent Prognostic Predictors in Thymoma and Modified Masaoka Stage Is Superior to Histopathologic Classifications. *J Thorac Oncol* (2015) 10:691–700. doi: 10.1097/JTO.0000000000000482
3. Khorfan R, Bharat A, Odell DD. Management and Long-Term Outcomes of Advanced Stage Thymoma in the United States. *Ann Thorac Surg* (2020) 111:223–30. doi: 10.1016/j.athoracsur.2020.05.088
4. Detterbeck FC, Parsons AM. Thymic Tumors. *Ann Thorac Surg* (2004) 77:1860–9. doi: 10.1016/j.athoracsur.2003.10.001
5. Huang J, Ahmad U, Antonicelli A, Catlin AC, Fang W, Gomez D, et al. Development of the International Thymic Malignancy Interest Group International Database: An Unprecedented Resource for the Study of a Rare Group of Tumors. *J Thorac Oncol* (2014) 9:1573–8. doi: 10.1097/JTO.0000000000000269
6. Riely GJ, Huang J. Induction Therapy for Locally Advanced Thymoma. *J Thorac Oncol* (2010) 5:S323–6. doi: 10.1097/JTO.0b013e3181f20e90
7. Ahmad U, Huang J. Induction Therapy for Thymoma. *Thorac Surg Clin* (2016) 26:325–32. doi: 10.1016/j.thorsurg.2016.04.011
8. Berruti A, Borasio P, Roncari A, Gorzegno G, Mossetti C, Dogliotti L. Neoadjuvant Chemotherapy With Adriamycin, Cisplatin, Vincristine and Cyclophosphamide (ADOC) in Invasive Thymomas: Results in Six Patients. *Ann Oncol* (1993) 4:429–31. doi: 10.1093/oxfordjournals.annonc.a058527
9. Macchiarini P, Chella A, Ducci F, Rossi B, Testi C, Bevilacqua G, et al. Neoadjuvant Chemotherapy, Surgery, and Postoperative Radiation Therapy for Invasive Thymoma. *Cancer* (1991) 68:706–13. doi: 10.1002/1097-0142(19910815)68:4<706::aid-cncr2820680407>3.0.co;2-h
10. Kanzaki R, Kanou T, Ose N, Funaki S, Shintani Y, Minami M, et al. Long-Term Outcomes of Advanced Thymoma in Patients Undergoing Preoperative Chemotherapy or Chemoradiotherapy Followed by Surgery: A 20-Year Experience. *Interact Cardiovasc Thorac Surg* (2019) 28:360–7. doi: 10.1093/icvts/ivy276
11. Nakamura S, Kawaguchi K, Fukui T, Hakiri S, Ozeki N, Mori S, et al. Multimodality Therapy for Thymoma Patients With Pleural Dissemination. *Gen Thorac Cardiovasc Surg* (2019) 67:524–9. doi: 10.1007/s11748-018-01054-7
12. Cardillo G, Carleo F, Giunti R, Lopergolo MG, Salvadori L, De Massimi AR, et al. Predictors of Survival in Patients With Locally Advanced Thymoma and Thymic Carcinoma (Masaoka Stages III and IVa). *Eur J Cardiothorac Surg* (2010) 37:819–23. doi: 10.1016/j.ejcts.2009.11.001
13. Yamada Y, Yoshino I, Nakajima J, Miyoshi S, Ohnuki T, Suzuki M, et al. Surgical Outcomes of Patients With Stage III Thymoma in the Japanese Nationwide Database. *Ann Thorac Surg* (2015) 100:961–7. doi: 10.1016/j.athoracsur.2015.04.059
14. Park S, Park IK, Kim YT, Lee GD, Kim DK, Cho JH, et al. Comparison of Neoadjuvant Chemotherapy Followed by Surgery to Upfront Surgery for Thymic Malignancy. *Ann Thorac Surg* (2019) 107:355–62. doi: 10.1016/j.athoracsur.2018.08.055
15. Bretti S, Berruti A, Loddo C, Sperone P, Casadio C, Tessa M, et al. Multimodal Management of Stages III-IVa Malignant Thymoma. *Lung Cancer* (2004) 44:69–77. doi: 10.1016/j.lungcan.2003.09.022
16. Hassan M, Seoud DE. Multimodality Treatments in Locally Advanced Stage Thymomas. *Hematol Oncol Stem Cell Ther* (2009) 2:340–4. doi: 10.1016/s1658-3876(09)50022-2

17. Lucchi M, Melfi F, Dini P, Basolo F, Viti A, Givigliano F, et al. Neoadjuvant Chemotherapy for Stage III and IVA Thymomas: A Single-Institution Experience With a Long Follow-Up. *J Thorac Oncol* (2006) 1:308–13. doi: 10.1097/01243894-200605000-00007
18. Shin DM, Walsh GL, Komaki R, Putnam JB, Nesbitt J, Ro JY, et al. A Multidisciplinary Approach to Therapy for Unresectable Malignant Thymoma. *Ann Intern Med* (1998) 129:100–4. doi: 10.7326/0003-4819-129-2-199807150-00006
19. Kim ES, Putnam JB, Komaki R, Walsh GL, Ro JY, Shin HJ, et al. Phase II Study of a Multidisciplinary Approach With Induction Chemotherapy, Followed by Surgical Resection, Radiation Therapy, and Consolidation Chemotherapy for Unresectable Malignant Thymomas: Final Report. *Lung Cancer* (2004) 44:369–79. doi: 10.1016/j.lungcan.2003.12.010
20. Rea F, Sartori F, Loy M, Calabro F, Fornasiero A, Daniele O, et al. Chemotherapy and Operation for Invasive Thymoma. *J Thorac Cardiovasc Surg* (1993) 106:543–9. doi: 10.1016/S0022-5223(19)34092-9
21. Berruti A, Borasio P, Gerbino A, Gorzegno G, Moschini T, Tampellini M, et al. Primary Chemotherapy With Adriamycin, Cisplatin, Vincristine and Cyclophosphamide in Locally Advanced Thymomas: A Single Institution Experience. *Br J Cancer* (1999) 81:841–5. doi: 10.1038/sj.bjc.6690773
22. Yokoi K, Matsuguma H, Nakahara R, Kondo T, Kamiyama Y, Mori K, et al. Multidisciplinary Treatment for Advanced Invasive Thymoma With Cisplatin, Doxorubicin, and Methylprednisolone. *J Thorac Oncol* (2007) 2:73–8. doi: 10.1097/JTO.0b013e31802bafc8
23. Park S, Ahn MJ, Ahn JS, Sun JM, Shim YM, Kim J, et al. A Prospective Phase II Trial of Induction Chemotherapy With Docetaxel/Cisplatin for Masaoka Stage III/IV Thymic Epithelial Tumors. *J Thorac Oncol* (2013) 8:959–66. doi: 10.1097/JTO.0b013e318292c41e
24. Kunitoh H, Tamura T, Shibata T, Takeda K, Katakami N, Nakagawa K, et al. A Phase II Trial of Dose-Dense Chemotherapy, Followed by Surgical Resection and/or Thoracic Radiotherapy, in Locally Advanced Thymoma: Report of a Japan Clinical Oncology Group Trial (JCOG 9606). *Br J Cancer* (2010) 103:6–11. doi: 10.1038/sj.bjc.6605731
25. Tan L, Qiu D, Wang Q. Preoperative Chemotherapy and Operation for Invasive Masaoke Stage III and IV a Thymoma. *Zhonghua Zhong Liu Za Zhi* (2000) 22:327–9.
26. Leuzzi G, Alessandrini G, Sperduti I, Forcella D, Marino M, Ceribelli A, et al. Induction Therapy Versus Initial Surgery in Advanced Thymic Tumors: Perioperative and Oncological Outcome. *Thorac Cardiovasc Surg* (2017) 65:234–43. doi: 10.1055/s-0035-1564890
27. Ishikawa Y, Matsuguma H, Nakahara R, Suzuki H, Ui A, Kondo T, et al. Multimodality Therapy for Patients With Invasive Thymoma Disseminated Into the Pleural Cavity: The Potential Role of Extrapleural Pneumonectomy. *Ann Thorac Surg* (2009) 88:952–7. doi: 10.1016/j.athoracsur.2009.05.019
28. Akaogi E, Ohara K, Mitsui K, Onizuka M, Ishikawa S, Mitsui T, et al. Preoperative Radiotherapy and Surgery for Advanced Thymoma With Invasion to the Great Vessels. *J Surg Oncol* (1996) 63:17–22. doi: 10.1002/(SICI)1096-9098(199609)63:1<17::AID-JSO4>3.0.CO;2-T
29. Yagi K, Hirata T, Fukuse T, Yokomise H, Inui K, Ike O, et al. Surgical Treatment for Invasive Thymoma, Especially When the Superior Vena Cava Is Invaded. *Ann Thorac Surg* (1996) 61:521–4. doi: 10.1016/0003-4975(95)00983-3
30. Ohara K, Okumura T, Sugahara S, Akisada M, Yokose T, Ogata T, et al. The Role of Preoperative Radiotherapy for Invasive Thymoma. *Acta Oncol* (1990) 29:425–9. doi: 10.3109/02841869009090025
31. Wei Y, Gu Z, Shen Y, Fu J, Tan L, Zhang P, et al. Preoperative Induction Therapy for Locally Advanced Thymic Tumors: A Retrospective Analysis Using the ChART Database. *J Thorac Dis* (2016) 8:665–72. doi: 10.21037/jtd.2016.03.02
32. Wright CD, Choi NC, Wain JC, Mathisen DJ, Lynch TJ, Fidias P. Induction Chemoradiotherapy Followed by Resection for Locally Advanced Masaoka Stage III and IVA Thymic Tumors. *Ann Thorac Surg* (2008) 85:385–9. doi: 10.1016/j.athoracsur.2007.08.051
33. Korst RJ, Bezjak A, Blackmon S, Choi N, Fidias P, Liu G, et al. Neoadjuvant Chemoradiotherapy for Locally Advanced Thymic Tumors: A Phase II, Multi-Institutional Clinical Trial. *J Thorac Cardiovasc Surg* (2014) 147:36–46.e1. doi: 10.1016/j.jtcvs.2013.08.061
34. Wang C, Lv C, Gao L, Liu J, Guo J, Fang W, et al. Surgical Resection After Neoadjuvant Concurrent Chemoradiotherapy for Stage III Invasive Thymic Tumor: A Phase II Prospective Clinical Trial. *Tumor* (2015) 35:190–6.
35. Chu RF, Hussien A, Li QK, Wang J, Friedes C, Ferro A, et al. Radiologic Response of Chemotherapy Alone Versus Radiation and Chemotherapy in the Treatment of Locally-Advanced or Advanced Thymic Epithelial Tumors. *Thorac Cancer* (2020) 11:2924–31. doi: 10.1111/1759-7714.13635
36. Onuki T, Ishikawa S, Yamamoto T, Ito H, Sakai M, Onizuka M, et al. Pathologic Radioresponse of Preoperatively Irradiated Invasive Thymomas. *J Thorac Oncol* (2008) 3:270–6. doi: 10.1097/JTO.0b013e3181653c8c
37. Fujii Y. Published Guidelines for Management of Thymoma. *Thorac Surg Clin* (2011) 21:125–9, viii. doi: 10.1016/j.thorsurg.2010.08.002
38. Glide-Hurst CK, Lee P, Yock AD, Olsen JR, Cao M, Siddiqui F, et al. Adaptive Radiation Therapy (ART) Strategies and Technical Considerations: A State of the ART Review From NRG Oncology. *Int J Radiat Oncol Biol Phys* (2021) 109:1054–75. doi: 10.1016/j.ijrobp.2020.10.021
39. Ohara K, Tatsuzaki H, Fuji H, Sugahara S, Okumura T, Akaogi E, et al. Radioresponse of Thymomas Verified With Histologic Response. *Acta Oncol* (1998) 37:471–4. doi: 10.1080/028418698430421
40. Rohrer Bley C, Meier V, Schneider U. Dosimetric Benefit of Adaptive Radiotherapy in the Neoadjuvant Management of Canine and Feline Thymoma-An Exploratory Case Series. *Vet Comp Oncol* (2018) 16:324–9. doi: 10.1111/vco.12382
41. Chevli N, Bland RE, Farach AM, Pino R, Mathews T, Okoye EI, et al. Adaptive Radiation Therapy for Intact Thymoma: An Illustrative Report. *Anticancer Res* (2021) 41:2467–71. doi: 10.21873/anticanres.15022
42. Mackie TR. History of Tomotherapy. *Phys Med Biol* (2006) 51:R427–53. doi: 10.1088/0031-9155/51/13/R24
43. Xu C, Feng QF, Fan CC, Zhai YR, Chen YD, Zhang HX, et al. Patterns and Predictors of Recurrence After Radical Resection of Thymoma. *Radiother Oncol* (2015) 115:30–4. doi: 10.1016/j.radonc.2015.03.001
44. Rimner A, Gomez DR, Wu AJ, Shi W, Yorke ED, Moreira AL, et al. Failure Patterns Relative to Radiation Treatment Fields for Stage II-IV Thymoma. *J Thorac Oncol* (2014) 9:403–9. doi: 10.1097/JTO.0000000000000099
45. Gomez D, Komaki R. Technical Advances of Radiation Therapy for Thymic Malignancies. *J Thorac Oncol* (2010) 5:S336–43. doi: 10.1097/JTO.0b013e3181f20ea2
46. Chang JY, Zhang X, Wang X, Kang Y, Riley B, Bilton S, et al. Significant Reduction of Normal Tissue Dose by Proton Radiotherapy Compared With Three-Dimensional Conformal or Intensity-Modulated Radiation Therapy in Stage I or Stage III Non-Small-Cell Lung Cancer. *Int J Radiat Oncol Biol Phys* (2006) 65:1087–96. doi: 10.1016/j.ijrobp.2006.01.052
47. Chera BS, Rodriguez C, Morris CG, Louis D, Yeung D, Li Z, et al. Dosimetric Comparison of Three Different Involved Nodal Irradiation Techniques for Stage II Hodgkin's Lymphoma Patients: Conventional Radiotherapy, Intensity-Modulated Radiotherapy, and Three-Dimensional Proton Radiotherapy. *Int J Radiat Oncol Biol Phys* (2009) 75:1173–80. doi: 10.1016/j.ijrobp.2008.12.048
48. Haefner MF, Verma V, Bougatf N, Mielke T, Tonndorf-Martini E, Konig L, et al. Dosimetric Comparison of Advanced Radiotherapy Approaches Using Photon Techniques and Particle Therapy in the Postoperative Management of Thymoma. *Acta Oncol* (2018) 57:1713–20. doi: 10.1080/0284186X.2018.1502467
49. Herbst RS, Soria JC, Kowanetz M, Fine GD, Hamid O, Gordon MS, et al. Predictive Correlates of Response to the Anti-PD-L1 Antibody MPDL3280A in Cancer Patients. *Nature* (2014) 515:563–7. doi: 10.1038/nature14011
50. Reck M, Rodriguez-Abreu D, Robinson AG, Hui R, Csoszi T, Fulop A, et al. Pembrolizumab Versus Chemotherapy for PD-L1-Positive Non-Small-Cell Lung Cancer. *N Engl J Med* (2016) 375:1823–33. doi: 10.1056/NEJMoa1606774
51. Song JS, Kim D, Kwon JH, Kim HR, Choi CM, Jang SJ. Clinicopathologic Significance and Immunogenomic Analysis of Programmed Death-Ligand 1 (PD-L1) and Programmed Death 1 (PD-1) Expression in Thymic Epithelial Tumors. *Front Oncol* (2019) 9:1055. doi: 10.3389/fonc.2019.01055
52. Yokoyama S, Miyoshi H, Nishi T, Hashiguchi T, Mitsuoka M, Takamori S, et al. Clinicopathologic and Prognostic Implications of Programmed Death Ligand 1 Expression in Thymoma. *Ann Thorac Surg* (2016) 101:1361–9. doi: 10.1016/j.athoracsur.2015.10.044
53. Ishihara S, Okada S, Ogi H, Kodama Y, Shimomura M, Tsunezuka H, et al. Programmed Death-Ligand 1 Expression Profiling in Thymic Epithelial Cell Tumors: Clinicopathological Features and Quantitative Digital Image Analyses. *Lung Cancer* (2020) 145:40–7. doi: 10.1016/j.lungcan.2020.04.038
54. Hakiri S, Fukui T, Mori S, Kawaguchi K, Nakamura S, Ozeki N, et al. Clinicopathologic Features of Thymoma With the Expression of

Programmed Death Ligand 1. *Ann Thorac Surg* (2019) 107:418–24. doi: 10.1016/j.athoracsur.2018.08.037
55. Padda SK, Riess JW, Schwartz EJ, Tian L, Kohrt HE, Neal JW, et al. Diffuse High Intensity PD-L1 Staining in Thymic Epithelial Tumors. *J Thorac Oncol* (2015) 10:500–8. doi: 10.1097/JTO.0000000000000429
56. Katsuya Y, Fujita Y, Horinouchi H, Ohe Y, Watanabe S, Tsuta K. Immunohistochemical Status of PD-L1 in Thymoma and Thymic Carcinoma. *Lung Cancer* (2015) 88:154–9. doi: 10.1016/j.lungcan.2015.03.003
57. Yokoyama S, Miyoshi H, Nakashima K, Shimono J, Hashiguchi T, Mitsuoka M, et al. Prognostic Value of Programmed Death Ligand 1 and Programmed Death 1 Expression in Thymic Carcinoma. *Clin Cancer Res* (2016) 22:4727–34. doi: 10.1158/1078-0432.CCR-16-0434
58. Marchevsky AM, Walts AE. PD-L1, PD-1, CD4, and CD8 Expression in Neoplastic and Nonneoplastic Thymus. *Hum Pathol* (2017) 60:16–23. doi: 10.1016/j.humpath.2016.09.023
59. Weissferdt A, Fujimoto J, Kalhor N, Rodriguez J, Bassett R, Wistuba II, et al. Expression of PD-1 and PD-L1 in Thymic Epithelial Neoplasms. *Mod Pathol* (2017) 30:826–33. doi: 10.1038/modpathol.2017.6
60. Higuchi R, Goto T, Hirotsu Y, Nakagomi T, Yokoyama Y, Otake S, et al. PD-L1 Expression and Tumor-Infiltrating Lymphocytes in Thymic Epithelial Neoplasms. *J Clin Med* (2019) 8:1833. doi: 10.3390/jcm8111833
61. Owen D, Chu B, Lehman AM, Annamalai L, Yearley JH, Shilo K, et al. Expression Patterns, Prognostic Value, and Intratumoral Heterogeneity of PD-L1 and PD-1 in Thymoma and Thymic Carcinoma. *J Thorac Oncol* (2018) 13:1204–12. doi: 10.1016/j.jtho.2018.04.013
62. Galon J, Costes A, Sanchez-Cabo F, Kirilovsky A, Mlecnik B, Lagorce-Pages C, et al. Type, Density, and Location of Immune Cells Within Human Colorectal Tumors Predict Clinical Outcome. *Science* (2006) 313:1960–4. doi: 10.1126/science.1129139
63. Cho J, Kim HS, Ku BM, Choi YL, Cristescu R, Han J, et al. Pembrolizumab for Patients With Refractory or Relapsed Thymic Epithelial Tumor: An Open-Label Phase II Trial. *J Clin Oncol* (2019) 37:2162–70. doi: 10.1200/JCO.2017.77.3184
64. Rajan A, Heery CR, Thomas A, Mammen AL, Perry S, O'Sullivan Coyne G, et al. Efficacy and Tolerability of Anti-Programmed Death-Ligand 1 (PD-L1) Antibody (Avelumab) Treatment in Advanced Thymoma. *J Immunother Cancer* (2019) 7:269. doi: 10.1186/s40425-019-0723-9
65. Konstantina T, Konstantinos R, Anastasios K, Anastasia M, Eleni L, Ioannis S, et al. Fatal Adverse Events in Two Thymoma Patients Treated With Anti-PD-1 Immune Check Point Inhibitor and Literature Review. *Lung Cancer* (2019) 135:29–32. doi: 10.1016/j.lungcan.2019.06.015
66. Lamarca A, Moreno V, Feliu J. Thymoma and Thymic Carcinoma in the Target Therapies Era. *Cancer Treat Rev* (2013) 39:413–20. doi: 10.1016/j.ctrv.2012.11.005
67. Hu B, Rong H, Han Y, Li Q. Do Thymic Malignancies Respond to Target Therapies? *Interact Cardiovasc Thorac Surg* (2015) 20:855–9. doi: 10.1093/icvts/ivv040
68. Berghmans T, Durieux V, Holbrechts S, Jungels C, Lafitte JJ, Meert AP, et al. Systemic Treatments for Thymoma and Thymic Carcinoma: A Systematic Review. *Lung Cancer* (2018) 126:25–31. doi: 10.1016/j.lungcan.2018.10.018
69. Imbimbo M, Ottaviano M, Vitali M, Fabbri A, Leuzzi G, Fiore M, et al. Best Practices for the Management of Thymic Epithelial Tumors: A Position Paper by the Italian Collaborative Group for ThYmic MalignanciEs (TYME). *Cancer Treat Rev* (2018) 71:76–87. doi: 10.1016/j.ctrv.2018.10.001
70. Darby SC, McGale P, Taylor CW, Peto R. Long-Term Mortality From Heart Disease and Lung Cancer After Radiotherapy for Early Breast Cancer: Prospective Cohort Study of About 300,000 Women in US SEER Cancer Registries. *Lancet Oncol* (2005) 6:557–65. doi: 10.1016/S1470-2045(05)70251-5
71. Atkins KM, Chaunzwa TL, Lamba N, Bitterman DS, Rawal B, Bredfeldt J, et al. Association of Left Anterior Descending Coronary Artery Radiation Dose With Major Adverse Cardiac Events and Mortality in Patients With Non-Small Cell Lung Cancer. *JAMA Oncol* (2021) 7:206–19. doi: 10.1001/jamaoncol.2020.6332
72. Minotti G, Menna P, Salvatorelli E, Cairo G, Gianni L. Anthracyclines: Molecular Advances and Pharmacologic Developments in Antitumor Activity and Cardiotoxicity. *Pharmacol Rev* (2004) 56:185–229. doi: 10.1124/pr.56.2.6
73. Forde PM, Chaft JE, Smith KN, Anagnostou V, Cottrell TR, Hellmann MD, et al. Neoadjuvant PD-1 Blockade in Resectable Lung Cancer. *N Engl J Med* (2018) 378:1976–86. doi: 10.1056/NEJMoa1716078
74. Yeh J, Marrone KA, Forde PM. Neoadjuvant and Consolidation Immuno-Oncology Therapy in Stage III Non-Small Cell Lung Cancer. *J Thorac Dis* (2018) 10:S451–S9. doi: 10.21037/jtd.2018.01.109
75. Shu CA, Gainor JF, Awad MM, Chiuzan C, Grigg CM, Pabani A, et al. Neoadjuvant Atezolizumab and Chemotherapy in Patients With Resectable Non-Small-Cell Lung Cancer: An Open-Label, Multicentre, Single-Arm, Phase 2 Trial. *Lancet Oncol* (2020) 21:786–95. doi: 10.1016/S1470-2045(20)30140-6

Conflict of Interest: The authors declare that the research was conducted in the absence of any commercial or financial relationships that could be construed as a potential conflict of interest.

Copyright © 2021 Zhang, Li, Chen, Tan, Zeng, Ding and Du. This is an open-access article distributed under the terms of the Creative Commons Attribution License (CC BY). The use, distribution or reproduction in other forums is permitted, provided the original author(s) and the copyright owner(s) are credited and that the original publication in this journal is cited, in accordance with accepted academic practice. No use, distribution or reproduction is permitted which does not comply with these terms.

frontiers in Oncology

ORIGINAL RESEARCH
published: 08 September 2021
doi: 10.3389/fonc.2021.647512

Transcriptomic and Mutational Analysis Discovering Distinct Molecular Characteristics Among Chinese Thymic Epithelial Tumor Patients

Naixin Liang[1†], Lei Liu[1†], Cheng Huang[1], Hongsheng Liu[1], Chao Guo[1], Ji Li[2], Weiwei Wang[1], Nan Li[3], Rui Lin[3], Tao Wang[3], Lieming Ding[4], Li Mao[4] and Shanqing Li[1*]*

[1] Department of Thoracic Surgery, Peking Union Medical College Hospital, Chinese Academy of Medical Sciences, Beijing, China, [2] Department of Pathology, Peking Union Medical College Hospital, Chinese Academy of Medical Sciences, Beijing, China, [3] Department of R&D, Hangzhou Repugene Technology Co., Ltd., Hangzhou, China, [4] Department of Medical, Betta Pharmaceuticals Co., Ltd., Hangzhou, China

Introduction: Thymic epithelial tumors (TETs) are malignancies arising from the epithelium of the thymic gland, rare but with relatively favorable prognosis. TETs have different pathological subtypes: thymomas and thymic carcinoma, and they show different clinical characteristics regarding prognosis, pathology, and molecular profiles, etc. Although some studies have investigated the pathogenesis of TETs, more molecular data is still needed to further understand the underlying mechanisms among different TETs subtypes and populations.

Methods: In this study, we performed targeted gene panel sequencing and whole transcriptome sequencing on the tumor tissues from 27 Chinese TET patients, including 24 thymomas (A, AB, and B subtypes) and 3 thymic squamous cell carcinomas. We analyzed the genetic variations and differentially expressed genes among multiple TET subtypes. Moreover, we compared our data with the published The Cancer Genome Atlas (TCGA) TET data on both the genetic and transcriptomic levels.

Results: Compared with the TCGA TET genomic data, we found that *NF1* and *ATM* were the most frequently mutated genes (each with a frequency of 11%, 3/27). These mutations were not mutually exclusive, since one B1 thymoma showed mutations of both genes. The *GTF2I* mutation was mainly enriched in subtype A and AB thymomas, consistent with the previous reports. RNA-seq results unveiled that the genes related to thymus development (*FGF7*, *FGF10* and *CLDN4*) were highly expressed in certain TET subtypes, implicating that the developmental process of thymus might be linked to the tumorigenesis of these subtypes. We found high expression of *CD274* (PD-L1) in B2 and B3 thymoma samples, and validated its expression using immunohistochemistry (IHC). Based on the expression profiles, we further established a machine learning model to

OPEN ACCESS

Edited by:
Iacopo Petrini, University of Pisa, Italy

Reviewed by:
Alexander Marx, Heidelberg University, Germany
Mirella Marino, Regina Elena National Cancer Institute (IRCCS), Italy
Francesco Facciolo, Regina Elena National Cancer Institute (IRCCS), Italy
Giovannella Palmieri, Federico II University Hospital, Italy

***Correspondence:**
Shanqing Li
lishanqing@pumch.cn
Li Mao
li.mao@bettapharma.com

†These authors have contributed equally to this work

Specialty section:
This article was submitted to Thoracic Oncology, a section of the journal Frontiers in Oncology

Received: *30 December 2020*
Accepted: *24 May 2021*
Published: *08 September 2021*

Citation:
Liang N, Liu L, Huang C, Liu H, Guo C, Li J, Wang W, Li N, Lin R, Wang T, Ding L, Mao L and Li S (2021) Transcriptomic and Mutational Analysis Discovering Distinct Molecular Characteristics Among Chinese Thymic Epithelial Tumor Patients. Front. Oncol. 11:647512. doi: 10.3389/fonc.2021.647512

predict the myasthenia gravis status of TET patients and achieved 90% sensitivity and 70.6% specificity in the testing cohort.

Conclusion: This study provides the first genomic and transcriptomic analysis of a Chinese TET cohort. The high expression of genes involved in thymus developmental processes suggests the potential association between tumorigenesis of TETs and dysregulation of developmental pathways. The high expression of PD-L1 in B2 and B3 thymomas support the potential application of immunotherapy on certain thymoma subtypes.

Keywords: thymic epithelial tumor, thymoma, next-generation sequencing, PD-L1, RNA-seq

1 INTRODUCTION

Thymoma and thymic carcinoma (TC) are thymic epithelial tumors (TETs) with low occurrence rate, roughly 1-5 cases per million population per year (1, 2). Pathologically, thymomas can be stratified into A, AB, B1, B2 and B3 subtypes depending on the morphology and the proportion of cancer cells and lymphocytes (3). A and AB thymomas are generally considered to be low malignancy, whereas B and TC subtypes are associated with moderate and high malignancy, respectively (1, 2). Auto-immune disorders, such as myasthenia gravis (MG), are the most frequent syndrome co-occurring with thymomas (4). A few studies have focused on characterizing genomic variations and expression of certain genes in thymomas and TCs (5–9), which provide new insights to decipher mechanisms of tumorigenesis and develop novel therapeutic strategies for clinical practice. However, more molecular data is still needed to deeply understand the TET etiology among different subtypes and populations.

Mutations and aberrant expression levels of several genes have been identified in thymoma and TC. *EGFR* is highly expressed in some thymoma and TC samples, but only a few mutations have been identified within *EGFR* in thymoma samples (10). Mutations and overexpression of *ERBB2*, *KRAS*, and *TP53* are found in TC samples (5). The high expression of *KIT* has also been confirmed in TCs (10, 11). However, mutations have been rarely found in *KIT* in either TCs or thymomas (12). A leucine to histidine substitution (L383H, L404H) of *GTF2I* was recently identified to be one of the most frequent mutations in A and AB thymomas (13). *In vitro* experiments showed the mutations were associated with the tumorigenesis of thymomas (13). Radovich et al. also demonstrated the high prevalence of GTF2I L424H mutation in A and AB subtypes (6).

The application of next-generation sequencing (NGS) has greatly broadened the mutational landscape of thymomas and TCs. Wang et al. identified mutations of several genes related to epigenetic regulation in both thymomas and TCs, including *BAP1*, *SETD2*, *ASXL1*, *SMARCA4*, *DNMT3A*, *TET2*, and *WT1* (8). Mutations of the RAS family genes, including *HRAS* and *NRAS*, were also identified by a 50-gene panel on A, B3, and TC subtypes (7). Another study identified recurrent somatic mutations of *TET2*, *CYLD*, *SETD2*, *TP53*, *FBXW7*, *HRAS*, and *RB1*genes on TC samples by whole exome sequencing (WES) (9). These studies provide a more thorough understanding of the mutational landscapes of TET, although mechanistic insight is still needed to understand the relationship between different subtypes and to provide new clues for development of therapeutic strategies.

The TCGA TET study represents the most systematic investigation on molecular profiles of thymomas and TCs so far (6). In the study, 117 samples from various thymoma subtypes and TCs were analyzed by WES, RNA-seq, miRNA-seq, DNA methylation and RPPA arrays. Unsupervised clustering resulted in four clusters which were consistent with the pathologic classifications. The auto-immune MG was linked to somatic copy number variations and the intratumor over-expression of auto-antigen related genes, such as *CHRNA1*, *NEFM*, and *RYR3* (6). *GTF2I* mutated samples had higher expression in several pathways related to cancer and cell signaling. Meanwhile, the TCGA TET study still leaves the interpretation of expression differences between subtypes as an open question. Importantly, it was worth noting that more than 80% of people in the TCGA cohort were Caucasian, and the Asian population was under-represented. More molecular studies on TET patients of other ethnicities are still needed.

In this pilot study, we present a comprehensive analysis on genomic and transcriptomic data of a Chinese TET cohort of 27 patients. To unveil the specific mechanisms involved in TET tumorigenesis of Asians, we made a thorough comparison between our cohort and the TCGA TET cohort on both the genomic variation and expression profiles of each subtypes.

2 MATERIALS AND METHODS

2.1 Patients and Sample Collection

Twenty-seven TET patients, including 24 thymomas and 3 thymic squamous cell carcinomas, were enrolled in this study (**Table 1** and **Supplementary Tables 1**, **2**). All patients were Chinese and were treated in Peking Union Medical College Hospital. Clinical characteristic information regarding age, gender, race, histological classification, and clinical stage (Masaoka and TNM staging) were collected. Fresh frozen tumor tissue and white blood cells were collected from each patient during surgery or biopsy with informed consent forms and approval from the Ethics Committee of the Peking Union Medical College Hospital. Part of fresh tissue sampled from

TABLE 1 | Clinical characteristics of the 27 thymic epithelial tumor (TET) patients.

Characteristic	All (n=27)
Age	
Median	53
Range	25-70
Sex	
Male	12 (44%)
Female	15 (56%)
Race	
Asian	27 (100%)
Histologic Type	
A	2 (7.4%)
AB	6 (22.2%)
B1	4 (14.8%)
B2	7 (25.9%)
B3	5 (18.5%)
TC	3 (11.1%)
Masaoka Stage	
I	13 (48.2%)
II	5 (18.5%)
III	9 (33.3%)
TNM Stage	
I	13 (48.2%)
II	5 (18.5%)
IIIA	8 (29.6%)
IIIB	1 (3.7%)

multiple distinct regions of the resected tumor tissue was made to one or several formalin-fixed, paraffin-embedded blocks in the pathology department of the hospital. The histologic subtypes for the 27 patients were examined following the 2015 World Health Organization (WHO) classification of tumors of the thymus (4th edition) (14). The CT images and immunohistochemistry (IHC) results were provided in the **Supplementary Tables 1**, **2**. Typical hematoxylin and eosin (H&E) result of each histological subtype (A, AB, B1, B2, B3 and TC) was also obtained (**Supplementary Figure 1**). The remained fresh tissue was frozen by liquid nitrogen and transported to the molecular lab for DNA panel and RNA-seq analysis.

2.2 Sample Processing

Before DNA and RNA extraction, a frozen tissue section for each sample was cut by a cryostat (Leica CM 1950, Leica Biosystems, Wetzlar, Germany), then fixed on glass slide and stained by Hematoxylin and Eosin (H&E) to examine the tumor percentage of the tissue sample. The tumor cell proportions are confirmed to be above 20%. DNA and total RNA were extracted from fresh frozen tissue using the DNeasy Blood&Tissue Kit (Qiagen, Valencia, CA, USA) and RNeasy Mini Kit (Qiagen), respectively, following the manufacturer's protocols. Genomic DNA was extracted from peripheral blood using the QIAamp DNA Mini and Blood Mini Kit (Qiagen) per manufacturer's protocol. The Qubit 3.0 Fluorometer and Qubit dsDNA HS Assay kit (Life Technologies, Carlsbad, CA) were used to quantify DNA following the manufacturer's recommended protocol. The quality and quantity of extracted RNA were evaluated with NanoDrop 2000 (ThermoFisher, Pittsburgh, PA, USA) and Agilent 2100 Bioanalyzer (Agilent Technologies, Santa Clara, CA, USA).

2.3 DNA Sequencing

NGS library preparation was performed to the DNA samples using KAPA Hyper Prep kit (Kapa Biosystems, Wilmington, MA, USA) according to the manufacturer's instruction and hybridized with probes targeting to the whole exons of 474 cancer-related genes using SureSelectXT Target Enrichment System (Agilent Technologies, Santa Clara, CA, USA). The libraries were sequenced using the HiSeq-X10 platform (Illumina, San Diego, CA, USA).

FASTQ files of raw sequencing reads were generated using bcl2fastq Conversion Software (Illumina, Version: 2.17.1.14). Low quality reads were filtered out and short reads were aligned to hg38 genome using bwa-0.7.15 (15). PCR duplicates were removed using GATK Picard. Indel realignment and base recalibration were performed by GATK to improve indel detection sensitivity and correct bias of base quality scores (16). MuTect2 and GATK were used for single nucleotide variation (SNV) and indel calling, respectively. All variants were annotated with HGVS using snpEff-2.3.7 (17). Only coding region variants (SNV and INDEL) with mutation allele frequencies (MAF) ≥ 5% were retained for further analysis. The tumor mutation burden (TMB) was calculated by counting the non-synonymous somatic mutations in coding regions and normalized by the panel size as previously described (18).

2.4 RNA Sequencing

The RNA-seq library was constructed using NEBNext Ultra Directional RNA Library Prep Kit (New England Biolabs, Ipswich, MA, USA) according to the manufacturer's instructions, and qualified using Qubit 3.0 Fluorometer (Life Technologies, Carlsbad, CA, USA) and 2100 Bioanalyzer (Agilent Technologies, Santa Clara, CA, USA). Libraries were sequenced on HiSeq-X10 platform (Illumina, San Diego, CA, USA).

After FASTQ was generated, low quality reads were filtered out and short reads were mapped to hg38 reference genome and ensemble 93 genome annotation using STAR (19). Gene expression quantification was performed using RSEM (20) to obtain the fragment per kilo exon per million reads (FPKM) value of each gene. Coefficient of variation (CV) was calculated for each gene. Three thousand genes with the largest CV were selected for clustering. All samples were clustered by hierarchical clustering with ward D2 method. Cluster heat maps were generated using pheatmap. The sample and gene cluster numbers were determined using ConsensusCluster (21). Genes with median FPKM larger than 4 were considered as highly expressed in each cluster. STRING web tools was used to perform pathway enrichment analysis of highly expressed genes (22). The differential gene expression analysis among clusters was performed using DESeq2 (23).

2.5 Protein-Protein Interaction Network Analysis

PPI network analysis was performed to investigate the potential effects of somatic mutations on cellular functional networks. Mutations in genes were first filtered by the gene expression

levels based on the FPKM (fragment per kilo exon per million reads) values (> 4). These highly expressed genes were then mapped to the PPI network from STRING database, and further subjected to gene clustering using the Markov clustering (MCL) method provided on STRING website.

2.6 Immunohistochemistry for PD-L1

Before PD-L1 immunohistochemistry (IHC), we first estimated the tumor cell percentage (TCP) of FFPE tissue using hematoxylin and eosin (H&E). FFPE samples with more than 100 tumor cells were further examined by IHC using PD-L1 IHC 22C3 pharmDx (Agilent Technologies, Santa Clara, CA, USA) according to the manufacturer's instructions. PD-L1 expression in TET tumor tissue is determined by the tumor proportion score (TPS). TPS is the percentage of viable tumor cells showing partial or complete membrane staining at any intensity (≥ 1+) relative to all viable tumor cells present in the sample, which is defined accordingly:

$$\mathrm{TPS}\,(\%) = \frac{No.\ of\ PD-L1\ staining\ cells\ (tumor\ cells)}{Total\ No.\ of\ viable\ tumor\ cells} \times 100$$

Based on the TPS, the expression level of PD-L1 protein is defined as 'High expression' (TPS ≥ 50%), 'Positive' (1% ≤ TPS < 50%) and 'Negative' (TPS < 1%).

2.7 Prediction on Myasthenia Gravis Using SVM

LIB-SVM 3.25 was used for construction of support vector machine (SVM) model in this study (24). Gene expression profiles of the TCGA cohort and our cohort were normalized using the median absolute deviation (MAD) method (6). The prediction power of each gene in the top variable gene list was evaluated using the single gene SVM model by the area under the curve (AUC) from the Receiver Operating Characteristics (ROC) analysis. The forward selection was then used to construct a gene set for prediction. SVM hyper parameters were selected using the top three gene sets. The top three gene set models were used on the validation cohort to evaluate the generalization error performance.

3 RESULTS

3.1 Clinical Characteristics

Twenty-seven patients with clinical diagnoses of thymoma or TC (thymic squamous cell carcinoma) were enrolled in this study (**Table 1** and **Supplementary Tables 1**, **2**). The median age of all the patients was 53, ranging between 25 and 70 years, and there were 12 male and 15 female patients. The histologic types for the 27 patients were determined by pathological examination following the 2015 World Health Organization (WHO) classification of tumors of the thymus (4th edition) (14), which were classified into A type (n = 2), AB type (n = 6), B1 type (n = 4), B2 type (n = 7), B3 type (n = 5), and TC (n = 3) (**Supplementary Figure 1**). All the three TC samples were histologically diagnosed as thymic squamous cell carcinomas with CD5+ and CD117+. Most of the patients were in Masaoka stage I (n = 13), with the remained patients distributed in stage II (n = 5), and stage III (n = 9). For TNM staging, there were also 13, 5, and 9 patients distributed in stage I, II, and III, respectively.

3.2 Genome Variation of Subtypes in TETs

DNA samples from the paired tissue and white blood cells for each patient were sequenced using a 476-gene panel (**Supplementary Table 3**). In total, 27 tissue samples from thymoma or TC were sequenced. We used MAF ≥ 5% as the cutoff for variant filtering. Fifty-eight genomic variations from 47 genes were identified (**Figure 1**). The average TMB of the 27 samples was as low as 0.82 mut/MB, which was consistent with the low mutation burden discovered in the TCGA TET study (6). Ten samples possess a TMB of 0 mut/MB. Four of the six samples with TMB > 1 mut/MB were found in the B subtypes. One A subtype and two B subtypes had exceptionally high TMB > 5 muts/MB. Of the three TC samples, only the sample with MSH6 mutation had a TMB of 0.95 mut/MB and the other two was 0 mut/MB. Consistently, the two carcinomas from Asian patients in the TCGA cohort also had a low mutational burden (0.13 and 0.66 mut/MB).

Among the 47 genes carrying at least one mutation, *NF1* and *ATM* were the most frequently mutated genes (11%, 3/27) in all samples. The predicted pathogenicity of the identified mutations was also retrieved from NCBI ClinVar database (25). Three *NF1* mutations were detected in one B1 (G1090*, nonsense mutation, unknown), one B2 (D1067V, missense mutation, likely benign) and one B3 (P1087L, missense mutation, unknown) subtypes. Three *ATM* mutations were identified in one A (P424H, missense mutation, uncertain significance), one B1 (R493G, missense mutation, unknown) and one B3 (S169F, missense mutation, uncertain significance) subtypes. These mutations were not mutually exclusive, since the B1 thymoma showed mutations of both genes. One AB subtype had a *KRAS* A59del mutation, and another AB subtype had an *NRAS* Q61K mutation. Only one TC sample were identified to have somatic mutations, which are MSH6 I927M (missense mutation, uncertain significance) and TERT R972S (missense mutation, unknown). IHC result didn't show loss of MSH6 protein expression and thus didn't imply microsatellite instable status. MSH6 I927M is predicted to be uncertain significance as also supported by the finding that the respective TC sample did not exhibit a high TMB as would be expected in a microsatellite instable tumor. The TC samples in our study had fewer somatic mutations than thymoma samples, which might implicate that somatic mutation related tumorigenesis differs in thymomas and TCs. We found significant enrichment of mutated genes in both the RAS (q=7E-8) and PI3K-Akt signaling pathways (q=2E-7), including *AKT3*, *CSF1R*, *FGFR4*, *KRAS*, *NRAS*, *PIK3CA*, and *PIK3CB* (**Figure 1** and **Supplementary Table 4**), and those mutated genes were mainly enriched in thymoma samples, suggesting that RAS and PI3K-Akt signaling pathways may involve in the tumor development of thymoma. In summary, the two most frequently mutated genes in our cohort, *NF1* and *ATM*, could be

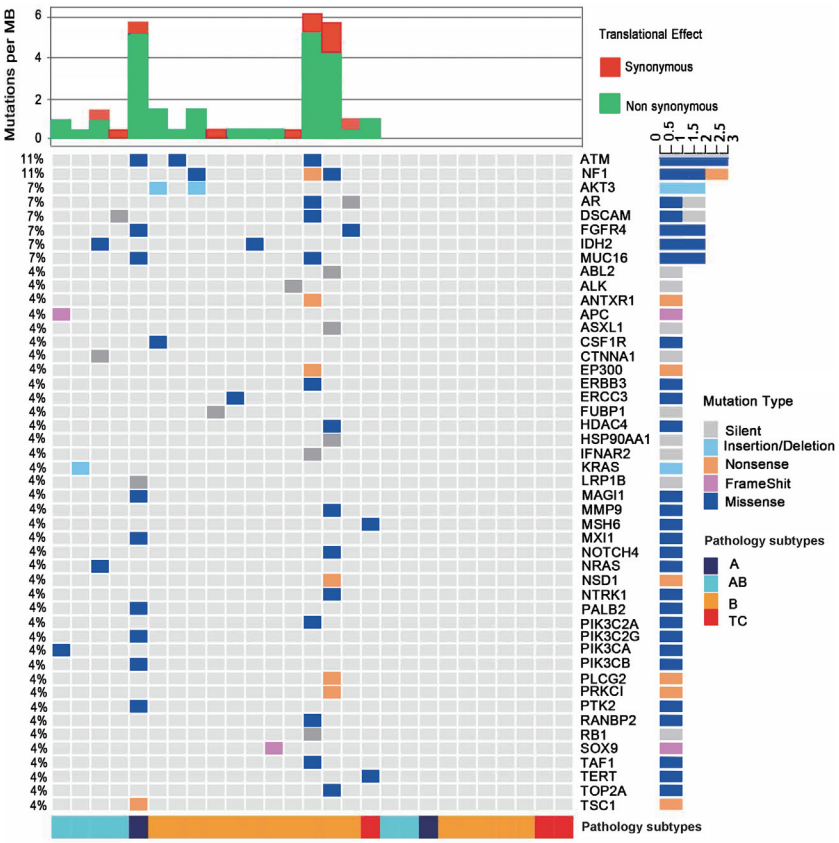

FIGURE 1 | Mutational landscape of the 27 patients with thymoma or thymic carcinoma. The percentages in the left showing the frequency of each gene mutated in the cohort. The bottom of the figure shows pathological types of each sample. Type B contains all B subtypes, including B1, B2 and B3. The top of the figure shows mutational burden for each sample, red for synonymous mutations and blue for non-synonymous mutations.

somatic mutations specific to Chinese TET patients, as no *NF1* or *ATM* mutations were found in the TCGA TET cohort.

3.3 Perturbation of Somatic Mutations on Protein-Protein Interactions

The functions of somatic mutations in our TET cohort were further explored for their potential perturbation on cellular PPI network. Twenty-eight highly expressed genes harboring 37 non-synonymous mutations were used for perturbation analysis on the PPI network (**Figure S2A**). Another twenty-two genes were also included in the network if they had at least one interaction with one of the 28 highly expressed genes. Clustering analysis of the 28 genes resulted in 6 clusters on the PPI network. The largest cluster had 9 genes, primarily belonging to the RAS signaling pathway. Other clusters were much smaller and showed no significant function enrichment. Furthermore, we performed the same analysis using the mutational landscape of each subtype separately. Different subtypes showed significantly different network topologies. The largest cluster of A and AB type (**Figures S2B, C**) contained genes in the RAS and PI3K-Akt signaling pathways, but no overlap was observed between the two subtypes. The largest cluster of B subtypes contained four genes that did not show significant enrichment in any pathways (**Figure S2D**). The results from the pathway analyses and PPI network clustering analysis were largely consistent, and suggested that the functional consequences of mutated genes in thymoma were closely related to key signaling pathways in cancer, which may contribute to the tumorigenesis of TET.

3.4 *GTF2I* Mutation in Thymoma Samples

The *GTF2I* L424H mutation was a newly identified recurrent genomic variation in A and AB subtypes of thymomas (13) Since the gene was not covered by our gene panel, we analyzed the RNA-seq data for the mutation status of *GTF2I* in our cohort (**Supplementary Table 5**). Eleven samples showed the *GTF2I* L424H mutation, including all the six patients in the AB subtype and one patient in A subtype, which was consistent with the observation in the TCGA-TET study that the *GTF2I* mutation mainly occurred in the A and AB subtypes (6). Besides that, we also detected *GTF2I* L424H mutation in two B2 and two B3

subtypes. The frequency of *GTF2I* mutation in subtype B of our cohort was 25% (4/16), which was roughly equal to the frequency reported by Petrini et al. (24%, 29/122), and higher than that in TCGA cohort (11%, 6/55) (P=0.024). To further validate the *GTF2I* mutation status, we performed Sanger sequencing on three representative samples [i.e., P1 (A), P21 (B3) and P24 (B3)] (**Figure S3**). The Sanger results were consistent with the RNA-seq data, which further confirmed the occurrence of *GTF2I* mutation in thymoma samples.

3.5 Hierarchical Clustering on Expression Profiles of Thymomas and Thymic Carcinomas

RNA-seq data from 26 samples passed the quality control and were used for the hierarchical clustering analysis. Based on the distinct expression patterns, 5 clusters (C1-C5) were generated which were closely related to the pathogenic subtypes of thymomas and TCs (**Figure 2A**). Cluster 1 (C1) contains three samples, including one A and two B3 subtypes. Cluster 2 (C2) is an AB dominant cluster that includes five AB and two B2 subtypes. Except for one A subtype, all the other C3 samples are TC subtypes. Clusters C4 and C5 are dominated by B subtypes. Among them, C4 has three B2 and two B3 samples, and C5 includes four B1, two B2 and one AB subtypes. Overall, the expression profiling based clusters was generally consistent with histologic classifications.

We also performed an integrative clustering analysis using a combination of the RNA-seq data from TCGA and our cohort to validate the consistency of the clusters and histologic subtypes. The combined clustering results showed that all C1 members were clustered with either A or AB samples in the TCGA data set. The A subtype that clustered together with TC subtypes, was

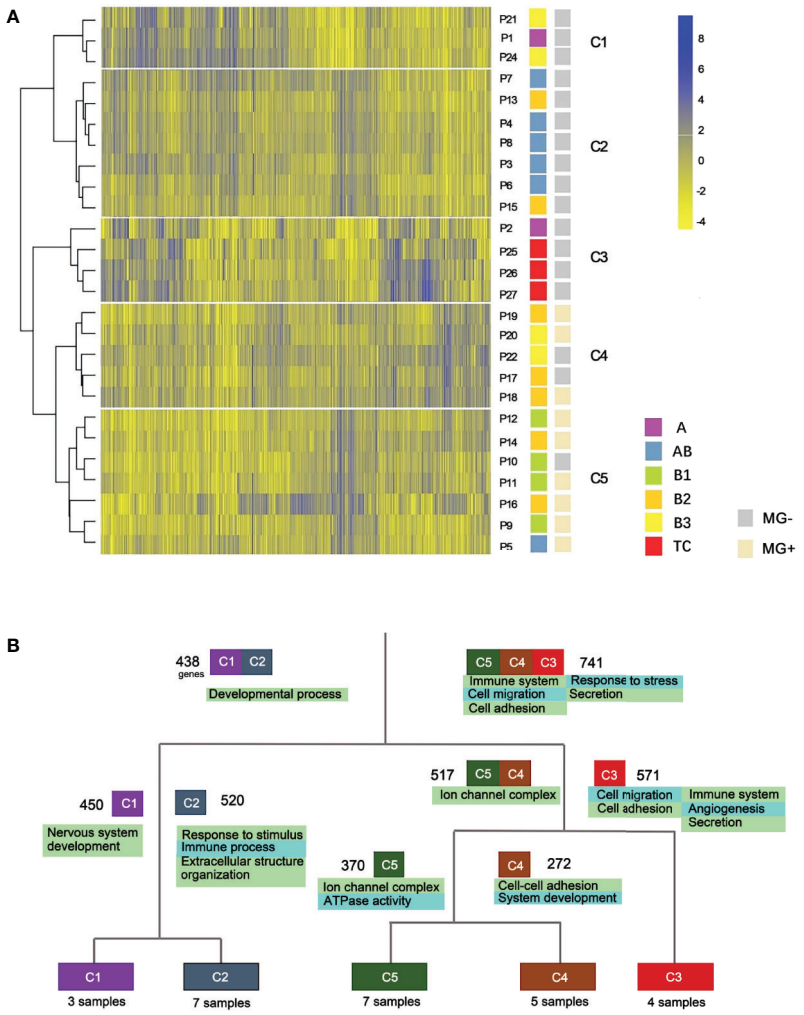

FIGURE 2 | Expression profile clustering of thymoma and thymic carcinoma. **(A)** Five clusters were established. C1-C5, different clusters; P, patient; MG, myasthenia gravis. **(B)** Gene function differences between thymic epithelial tumor types. Cluster-based differential expression analysis was performed. Four splits were used to separate the five clusters. Numbers besides the cluster boxes represent numbers of highly expressed genes.

confirmed to be an outlier in the integrative analysis of TCGA data and our data (**Figure S4**). It is worth noting that the samples from Asian patients of the two cohorts were evenly distributed among non-Asian clusters. No ethnics-specific gene expression profiles were discovered in this analysis.

3.6 Expression Differences Among Thymic Epithelial Tumor Subtypes

We next performed cluster-based differential expression analysis to explore the gene functional differences among different TET subtypes. Differential expression analysis was performed within the five clusters of the hierarchical clustering. Differentially expressed genes (DEGs) from each cluster were then analyzed for functional pathways enrichment (**Figure 2B**). We observed that subtypes of TET (C3, C4 and C5) tended to enrich in the pathways related to immune system and cell adhesion/migration, whereas the subtypes of C1 and C2 were enriched in the pathways related to developmental processes and cellular components. In the sub-branches of C1 and C2, the enriched genes functions of the C2 cluster were immune processes, whereas the C1 was related to nervous system development. Those results showed that the differentially expressed genes were more enriched in immune system and cell adhesion/migration pathways in the more malignant subtypes than that in the less malignant subtypes.

We further sought to identify genes that were specifically expressed in each cluster and analyze their biological functions (**Figure 3A**). Transcription factor *EHF* was highly expressed in C1 (**Figures 3A** and **S5A**). The high expression of *EHF* has been related to the progression of gastric cancer and to the elevation of HER family proteins *ERBB3* and *ERBB4* (26). In our study, C1 samples had higher expression levels of *ERBB3* and *ERBB4* (**Figures S6A, B**), which together with *EHF*, suggested possible implication of the C1 cluster to the development of epithelial malignancies (27–29). Two thymus development related genes, *CLDN4* (**Figures 3B** and **S5B**) and *TNFRSF11A* (**Figure S7B**), were also highly expressed in C1 samples. RANK (coded by *TNFRSF11A*) is highly expressed in medullary progenitor cells and also an important regulator in medullary formation by promoting the generation of AIRE+ mature medullary epithelial cells (30) Claudin-4, which is encoded by *CLDN4*, is a highly expressed gene marker for medullary epithelial stem cells (31). These findings may implicate that the tumorigenesis of A subtype is associated with the deregulation of gene expression and reconstitution of stem cell like properties of medullary epithelial cells.

E2F8 gene, which involves in cell proliferation and cancer development, was found to be highly expressed in C2, C4 and C5 clusters (**Figures 3C** and **S5C**). E2F8 gene was previously reported highly expressed in several different cancers compared to their normal tissues (32, 33). To investigate whether high expression of E2F8 gene was associated with epithelial cells and immature T cells, we calculated the correlation coefficient between E2F8 and TdT gene expressions using RNA-seq data for all the C2, C4 and C5 samples. The result showed a low R-squared value of 0.36 which indicated E2F8 expression was not highly correlated with TdT expression from immature T cells, and thus implied high expression of E2F8 possibly originate from both the immature T cells and epithelial cells. Compared to C1 cluster, we did not find any expression of genes related to development of either medullary or cortex epithelial cells in C2 cluster, which might indicate a difference in tumorigenesis for the AB subtype of thymoma.

C3 contains mostly TC subtypes. *KIT* was highly expressed in all TC subtypes in our cohort (**Figure S8A**), consistent with the previous research (12) We also found that the cell surface receptor *PDGFRA* was highly expressed in the TC subtypes (**Figure S8B**). Although no statistical significance was observed for either *KIT* or *PDGFRA* due to the small size of TC samples, the trend was observed for the median expression level. Several

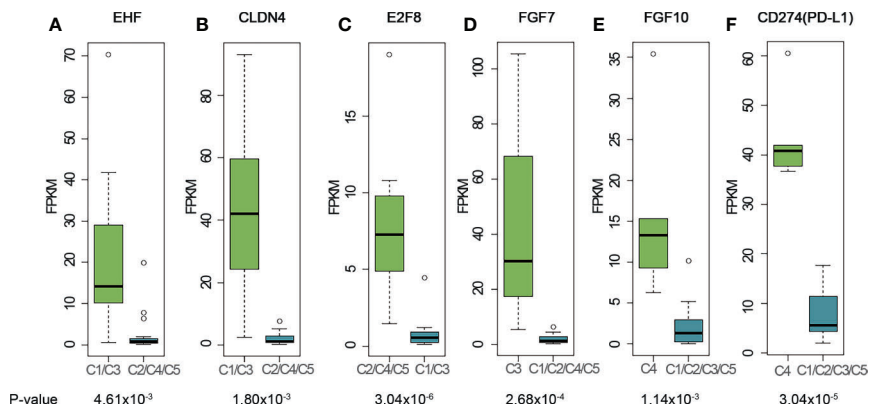

FIGURE 3 | Representative genes highly expressed in different clusters. **(A)** EHF; **(B)** CLDN4; **(C)** E2F8; **(D)** FGF7; **(E)** FGF10; **(F)** CD274 (PD-L1). The cluster name on X-axis uses the histologic type corresponding to the expression profiling cluster. The matches of dominant pathological subtype and RNA-seq clusters are: A, B3 subtypes - C1, AB subtypes - C2, TC subtypes - C3, B2, B3 subtypes - C4, and B1, B2 subtypes - C5. P-values were calculated using Mann-Whitney-Wilcoxon test. FPKM stands for fragment per kilo exon per million reads.

FGF family genes, like *FGF1*, *FGF7* and *FGF11* were also highly expressed in the TC group (*FGF7*, **Figures 3D** and **S5D**; *FGF1*, **Figure S6C**; *FGF11*, **Figure S6D**). In the cortex, mesenchymal cells produce *FGF7* that promotes the proliferation of epithelial cells (34). The high expression of *FGF7* in TC subtypes supports this mechanism of self-maintenance of epithelial proliferation in TC subtypes.

C4 consisted of five B2 or B3 subtypes. *FGF10*, a regulator of cortex epithelial cell proliferation, was highly expressed in C4 cluster (**Figures 3E** and **S5E**), which may be related to the mechanism of self-maintenance of proliferation of B2 and B3 subtypes. Importantly, *CD274* (PD-L1, **Figures 3F** and **S5F**) and *PDCD1LG2* (PD-L2, **Figure S7A**), encoding PD-1 ligand, were highly expressed in this cluster. We further performed PD-L1 IHC and the results showed the patients with B2 or B3 thymomas in the cluster C4 had high PD-L1 expressions (**Figure 4**), which suggested patients with B2 and B3 thymomas could potentially benefit from immunotherapy (35–37). The biological roles for the highly expressed genes in C5 remain to be further investigated.

Expression profiling and pathway analysis showed the differences of highly expressed genes in each cluster. These data showed that histologic subtypes and molecular clustering patterns were mostly consistent, which was also supported by the TCGA analysis. For low-risk subtypes (A and AB), the molecular function was associated with tissue development and cell proliferation. The absence of transcription factors, such as *EHF* and *E2F8*, may represent the initial steps of gene dysregulation. For the more malignant types (B2 and B3, and TC), more cancer progression related genes were highly expressed. Several important genes associated with thymus development, such as *CLDN4*, *FGF7* and *FGF10*, showed high expression in certain thymoma subtypes and TCs, suggesting their potential role in the development of TETs.

3.7 Myasthenia Gravis Related Gene Analysis on Thymic Epithelial Cancer

Thymoma is often associated with an autoimmune thymus disease MG. We found 149 genes with differential expression between MG+ and MG- groups (**Supplementary Table 6**). Nonetheless, these DEGs did not contain genes involved in immunity or auto-antigens. Among the auto-antigen related DEGs between MG+ and MG- reported in TCGA, *NEFM* was highly expressed in the MG+ group in our cohort, but there was no statistically significant difference in comparison with the MG- group (**Figure S9**).

To investigate whether the MG status can be inferred from the gene expression profiles of TET patients, we constructed a machine learning model using SVM, in which the TCGA-TET samples (n = 104) were used as the training set to select the gene features, and 22 samples in our cohort were used as a validation set to verify the prediction performance of the model. We found that a three-gene model had optimal prediction performance between the TCGA cohort and our cohort (**Figure S10**). The AUC of the training and validation set was comparable (0.840 vs 0.841), with 93.8% sensitivity and 64.0% specificity for the training set, and 90% sensitivity and 70.6% specificity in the testing cohort. The three genes used in this model were *PPARGC1A*, *GABRA5*, and *NEFM*, in which *NEFM* was related to MG according to the previous reports and the TCGA TET study (6).

4 DISCUSSION

The rare occurrence of TETs hinders clinical research and biomarker discovery. The recent integrative multi-omics study extended the knowledge of molecular signatures to the clinical characteristics of thymic epithelial tumors (6). In this pilot study,

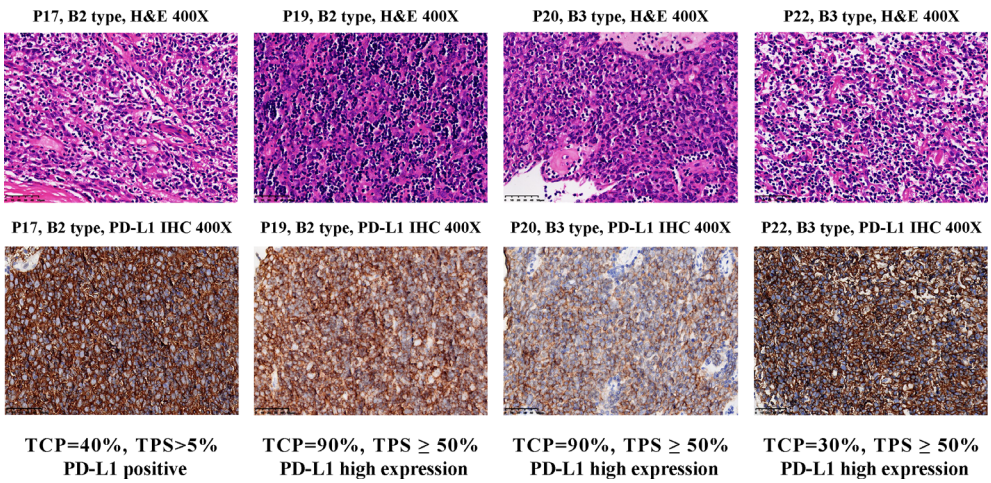

FIGURE 4 | PD-L1 IHC staining for B2 and B3 samples in the cluster C4. Top, hematoxylin and eosin (H&E) staining of the tissues. Bottom, IHC staining of PD-L1 in the cells using antibody 22C3 (Dako). Brown cells are PD-L1 staining cells. The H&E staining was used to estimate the tumor cell percentage (TCP). The expression level of PD-L1 protein is determined by the tumor proportion score (TPS), which is further divided into three types: 'High expression' (TPS ≥ 50%), 'Positive' (1% ≤ TPS < 50%) and 'Negative' (TPS < 1%).

we performed genomic and transcriptomic analysis to explore the underlying molecular characteristics and mechanisms of a Chinese TET cohort. To the best of our knowledge, this is the first multi-omics study reported on a Chinese TET population.

The mutational landscape of our cohort showed several key differences from the TCGA dataset. First, the top mutated genes in our cohort did not match those in the TCGA cohort. Prevalent mutations in *NF1* and *ATM* suggest potential difference of the mutational landscape in the Chinese TET population. Though our sample size was small, the difference in the mutation frequency of *GTF2I* L424H on the B subtypes still can provide preliminary evidence that the Chinese TET population may have different mutational landscape compared with the TCGA dataset. Another example of different mutational profiles between Chinese and Caucasians is different prevalence of driver mutations in lung adenocarcinoma (LUAD) (38). While east Asian LUAD patients are frequently mutated on *EGFR* L858R and 19del (40-55%) and less occurrence of *KRAS* mutations (8-12%), the Caucasians have a lower incidence of *EGFR* mutations (15-25%) and higher incidence of *KRAS* mutations (20-30%). The etiology of the Chinese TET patient could be possibly different from Caucasian population represented in TCGA. However, the expression profiles showed no obvious differences between different population groups, and the myasthenia gravis prediction model worked well for both cohorts. These results suggest that mutational landscape, which may involve in tumorigenesis, differs in populations, but with overall consistent expression patterns among them.

Consistent with the TCGA's findings, expression profiling clusters was largely consistent with the pathological subtypes. We further demonstrated that the less malignant TETs had more gene expression of developmental processes and cellular components whereas the more malignant TETs had more genes with altered expression that associated with immune system and cell adhesion/migration. It was interesting to point out that several genes related to thymus medullary and cortex development such as *CLDN4*, *FGF7*, and *FGF10* were linked to TETs. Such relationships unveil possible links between tumorigenesis and dysregulation of regulatory networks that can lead to an insightful understanding of the etiology of the disease. Targeting those genes might provide potential therapeutic clues with further cellular mechanism and clinical studies.

The expression profiling analysis also identified high expression of PD-L1 for most of the B2 and B3 subtypes in our cohort, suggesting immunotherapy opportunity for those patients. This is consistent with the previous studies which reported high PD-L1 expression in TET patients with more malignant subtypes, such as type B2 and B3 thymomas, and thymic carcinomas (39, 40). Moreover, we proposed here the first machine learning model to predict myasthenia gravis status for TET patients, which provides new perspectives for tackling the problem and could probably help high risk myasthenia gravis patients in advance.

The limitation of this study is the relatively small number of cases in view of the heterogeneity of histological subtypes in TET patients. The size of the sample was largely restricted by the low incidence of TET and the sample availability from TET patients. Another limitation is that we applied targeted gene panel rather than whole exome or whole-genome sequencing. Though the panel is relatively large and contains 476 closely cancer related genes, the resulting mutation profiles may still be limited and possibly miss novel somatic mutations associated with Chinese TET patients. Future studies should expand the sample size to further validate both the molecular profiles and the MG prediction model in Chinese TET patients and clinical applications.

DATA AVAILABILITY STATEMENT

The original contributions presented in the study are included in the article/**Supplementary Material**. Further inquiries can be directed to the corresponding authors.

ETHICS STATEMENT

The studies involving human participants were reviewed and approved by Ethics Committee of the Peking Union Medical College Hospital. The patients/participants provided their written informed consent to participate in this study.

AUTHOR CONTRIBUTIONS

All authors contributed to the article and approved the submitted version. Tissue experiments were performed by NLiang, LL, JL, CH, HL, CG, WW, and RL. Pathological diagnosis was conducted by JL. Data analysis were performed by NLi, and TW. The article was written by NLiang, NLi, RL, TW, LM, and SL. Funding was acquired by NLiang and SL.

FUNDING

This work was supported by the Foundation for Key Program of Ministry of Education, China (Grant No. 311037), CAMS Innovation Fund for Medical Sciences (2017-12M-1-009), and Beijing Natural Science Foundation (7182132).

ACKNOWLEDGMENTS

We thank Zheng Li, Jingyu Yuan, Xiang Zheng for technical assistance.

SUPPLEMENTARY MATERIAL

The Supplementary Material for this article can be found online at: https://www.frontiersin.org/articles/10.3389/fonc.2021.647512/full#supplementary-material

REFERENCES

1. Engels EA. Epidemiology of Thymoma and Associated Malignancies. *J Thorac Oncol* (2010) 5(10, Supplement 4):S260–5. doi: 10.1097/JTO.0b013e3181f1f62d
2. de Jong WK, Blaauwgeers JL, Schaapveld M, Timens W, Klinkenberg TJ, Groen HJ. Thymic Epithelial Tumours: A Population-Based Study of the Incidence, Diagnostic Procedures and Therapy. *Eur J Cancer* (2008) 44 (1):123–30. doi: 10.1016/j.ejca.2007.11.004
3. Marx A, Strobel P, Badve SS, Chalabreysse L, Chan JK, Chen G, et al. ITMIG Consensus Statement on the Use of the WHO Histological Classification of Thymoma and Thymic Carcinoma: Refined Definitions, Histological Criteria, and Reporting. *J Thorac Oncol* (2014) 9(5):596–611. doi: 10.1097/JTO.0000000000000154
4. Shelly S, Agmon-Levin N, Altman A, Shoenfeld Y. Thymoma and Autoimmunity. *Cell Mol Immunol* (2011) 8(3):199–202. doi: 10.1038/cmi.2010.74
5. Weissferdt A, Wistuba II, Moran CA. Molecular Aspects of Thymic Carcinoma. *Lung Cancer* (2012) 78(2):127–32. doi: 10.1016/j.lungcan.2012.08.002
6. Radovich M, Pickering CR, Felau I, Ha G, Zhang H, Jo H, et al. The Integrated Genomic Landscape of Thymic Epithelial Tumors. *Cancer Cell* (2018) 33 (2):244–58.e10. doi: 10.1016/j.ccell.2018.01.003
7. Enkner F, Pichlhofer B, Zaharie AT, Krunic M, Holper TM, Janik S, et al. Molecular Profiling of Thymoma and Thymic Carcinoma: Genetic Differences and Potential Novel Therapeutic Targets. *Pathol Oncol Res* (2017) 23(3):551–64. doi: 10.1007/s12253-016-0144-8
8. Wang Y, Thomas A, Lau C, Rajan A, Zhu Y, Killian JK, et al. Mutations of Epigenetic Regulatory Genes Are Common in Thymic Carcinomas. *Sci Rep* (2014) 4:7336. doi: 10.1038/srep07336
9. Saito M, Fujiwara Y, Asao T, Honda T, Shimada Y, Kanai Y, et al. The Genomic and Epigenomic Landscape in Thymic Carcinoma. *Carcinogenesis* (2017) 38(11):1084–91. doi: 10.1093/carcin/bgx094
10. Yoh K, Nishiwaki Y, Ishii G, Goto K, Kubota K, Ohmatsu H, et al. Mutational Status of EGFR and KIT in Thymoma and Thymic Carcinoma. *Lung Cancer* (2008) 62(3):316–20. doi: 10.1016/j.lungcan.2008.03.013
11. Tsuchida M, Umezu H, Hashimoto T, Shinohara H, Koike T, Hosaka Y, et al. Absence of Gene Mutations in KIT-Positive Thymic Epithelial Tumors. *Lung Cancer* (2008) 62(3):321–5. doi: 10.1016/j.lungcan.2008.03.035
12. Petrini I, Zucali PA, Lee HS, Pineda MA, Meltzer PS, Walter-Rodriguez B, et al. Expression and Mutational Status of C-Kit in Thymic Epithelial Tumors. *J Thorac Oncol* (2010) 5(9):1447–53. doi: 10.1097/JTO.0b013e3181e96e30
13. Petrini I, Meltzer PS, Kim IK, Lucchi M, Park KS, Fontanini G, et al. A Specific Missense Mutation in GTF2I Occurs at High Frequency in Thymic Epithelial Tumors. *Nat Genet* (2014) 46(8):844–9. doi: 10.1038/ng.3016
14. Travis WD, Brambilla E, Burke AP, Marx A, Nicholson A. *WHO Classification of Tumours of the Lung, Pleura, Thymus and Heart. 4th ed.* Vol. 7. IARC Lyon: WHO Classification of Tumours (2015).
15. Li H, Durbin R. Fast and Accurate Long-Read Alignment With Burrows-Wheeler Transform. *Bioinformatics* (2010) 26(5):589–95. doi: 10.1093/bioinformatics/btp698
16. DePristo MA, Banks E, Poplin R, Garimella KV, Maguire JR, Hartl C, et al. A Framework for Variation Discovery and Genotyping Using Next-Generation DNA Sequencing Data. *Nat Genet* (2011) 43(5):491–8. doi: 10.1038/ng.806
17. Cingolani P, Platts A, Wang le L, Coon M, Nguyen T, Wang L, et al. A Program for Annotating and Predicting the Effects of Single Nucleotide Polymorphisms, SnpEff: SNPs in the Genome of Drosophila Melanogaster Strain W1118; Iso-2; Iso-3. *Fly (Austin)* (2012) 6(2):80–92. doi: 10.4161/fly.19695
18. Gandara DR, Paul SM, Kowanetz M, Schleifman E, Zou W, Li Y, et al. Blood-Based Tumor Mutational Burden as a Predictor of Clinical Benefit in Non-Small-Cell Lung Cancer Patients Treated With Atezolizumab. *Nat Med* (2018) 24(9):1441–8. doi: 10.1038/s41591-018-0134-3
19. Dobin A, Davis CA, Schlesinger F, Drenkow J, Zaleski C, Jha S, et al. STAR: Ultrafast Universal RNA-Seq Aligner. *Bioinformatics* (2013) 29(1):15–21. doi: 10.1093/bioinformatics/bts635
20. Li B, Dewey CN. RSEM: Accurate Transcript Quantification From RNA-Seq Data With or Without a Reference Genome. *BMC Bioinf* (2011) 12:323. doi: 10.1186/1471-2105-12-323
21. Wilkerson MD, Hayes DN. ConsensusClusterPlus: A Class Discovery Tool With Confidence Assessments and Item Tracking. *Bioinformatics* (2010) 26 (12):1572–3. doi: 10.1093/bioinformatics/btq170
22. Szklarczyk D, Franceschini A, Wyder S, Forslund K, Heller D, Huerta-Cepas J, et al. STRING V10: Protein-Protein Interaction Networks, Integrated Over the Tree of Life. *Nucleic Acids Res* (2015) 43(Database issue):D447–52. doi: 10.1093/nar/gku1003
23. Love MI, Huber W, Anders S. Moderated Estimation of Fold Change and Dispersion for RNA-Seq Data With Deseq2. *Genome Biol* (2014) 15(12):550. doi: 10.1186/s13059-014-0550-8
24. Chang C-CL, Chih-Jen. LIBSVM: A Library for Support Vector Machines. *ACM Trans Intelligent Syst Technol* (2011) 2(3):27:1–27:27. doi: 10.1145/1961189.1961199
25. Landrum MJ, Chitipiralla S, Brown GR, Chen C, Gu B, Hart J, et al. ClinVar: Improvements to Accessing Data. *Nucleic Acids Res* (2019) 48(D1):D835–44. doi: 10.1093/nar/gkz972
26. Shi J, Qu Y, Li X, Sui F, Yao D, Yang Q, et al. Increased Expression of EHF via Gene Amplification Contributes to the Activation of HER Family Signaling and Associates With Poor Survival in Gastric Cancer. *Cell Death Dis* (2016) 7 (10):e2442. doi: 10.1038/cddis.2016.346
27. Amsellem-Ouazana D, Bieche I, Tozlu S, Botto H, Debre B, Lidereau R. Gene Expression Profiling of ERBB Receptors and Ligands in Human Transitional Cell Carcinoma of the Bladder. *J Urol* (2006) 175(3 Pt 1):1127–32. doi: 10.1016/S0022-5347(05)00317-4
28. Lv Y, Sui F, Ma J, Ren X, Yang Q, Zhang Y, et al. Increased Expression of EHF Contributes to Thyroid Tumorigenesis Through Transcriptionally Regulating HER2 and HER3. *Oncotarget* (2016) 7(36):57978–90. doi: 10.18632/oncotarget.11154
29. Jaiswal BS, Kljavin NM, Stawiski EW, Chan E, Parikh C, Durinck S, et al. Oncogenic ERBB3 Mutations in Human Cancers. *Cancer Cell* (2013) 23 (5):603–17. doi: 10.1016/j.ccr.2013.04.012
30. Akiyama N, Takizawa N, Miyauchi M, Yanai H, Tateishi R, Shinzawa M, et al. Identification of Embryonic Precursor Cells That Differentiate Into Thymic Epithelial Cells Expressing Autoimmune Regulator. *J Exp Med* (2016) 213 (8):1441–58. doi: 10.1084/jem.20151780
31. Sekai M, Hamazaki Y, Minato N. Medullary Thymic Epithelial Stem Cells Maintain a Functional Thymus to Ensure Lifelong Central T Cell Tolerance. *Immunity* (2014) 41(5):753–61. doi: 10.1016/j.immuni.2014.10.011
32. Park SA, Platt J, Lee JW, Lopez-Giraldez F, Herbst RS, Koo JS. E2F8 as a Novel Therapeutic Target for Lung Cancer. *J Natl Cancer Inst* (2015) 107(9):djv151. doi: 10.1093/jnci/djv151
33. Ye L, Guo L, He Z, Wang X, Lin C, Zhang X, et al. Upregulation of E2F8 Promotes Cell Proliferation and Tumorigenicity in Breast Cancer by Modulating G1/S Phase Transition. *Oncotarget* (2016) 7(17):23757–71. doi: 10.18632/oncotarget.8121
34. Ohigashi I, Kozai M, Takahama Y. Development and Developmental Potential of Cortical Thymic Epithelial Cells. *Immunol Rev* (2016) 271 (1):10–22. doi: 10.1111/imr.12404
35. Duan J, Liu X, Chen H, Sun Y, Liu Y, Bai H, et al. Impact of PD-L1, Transforming Growth Factor-Beta Expression and Tumor-Infiltrating CD8 (+) T Cells on Clinical Outcome of Patients With Advanced Thymic Epithelial Tumors. *Thorac Cancer* (2018) 9(11):1341–53. doi: 10.1111/1759-7714.12826
36. Owen D, Chu B, Lehman AM, Annamalai L, Yearley JH, Shilo K, et al. Expression Patterns, Prognostic Value, and Intratumoral Heterogeneity of PD-L1 and PD-1 in Thymoma and Thymic Carcinoma. *J Thorac Oncol* (2018) 13(8):1204–12. doi: 10.1016/j.jtho.2018.04.013
37. Hakiri S, Fukui T, Mori S, Kawaguchi K, Nakamura S, Ozeki N, et al. Clinicopathologic Features of Thymoma With the Expression of Programmed Death Ligand 1. *Ann Thorac Surg* (2019) 107(2):418–24. doi: 10.1016/j.athoracsur.2018.08.037
38. Yang CY, Yang JC, Yang PC. Precision Management of Advanced Non-Small Cell Lung Cancer. *Annu Rev Med* (2020) 71:117–36. doi: 10.1146/annurev-med-051718-013524

39. Chen HF, Wu LX, Li XF, Zhu YC, Pan WW, Wang WX, et al. PD-L1 Expression Level in Different Thymoma Stages and Thymic Carcinoma: A Meta-Analysis. *Tumori* (2020) 106(4):306–11. doi: 10.1177/0300891620915788
40. Yokoyama S, Miyoshi H. Comparison of PD-L1 Immunohistochemical Assays and the Significance of PD-L1 Expression in Thymoma. *J Thorac Dis* (2020) 12(12):7553–60. doi: 10.21037/jtd-19-3703

Conflict of Interest: NLi, RL, and TW are employees at Repugene Technology. LD and LM are employees and shareholders at Betta Pharmaceuticals.

The remaining authors declare that the research was conducted in the absence of any commercial or financial relationships that could be construed as a potential conflict of interest.

Publisher's Note: All claims expressed in this article are solely those of the authors and do not necessarily represent those of their affiliated organizations, or those of the publisher, the editors and the reviewers. Any product that may be evaluated in this article, or claim that may be made by its manufacturer, is not guaranteed or endorsed by the publisher.

Copyright © 2021 Liang, Liu, Huang, Liu, Guo, Li, Wang, Li, Lin, Wang, Ding, Mao and Li. This is an open-access article distributed under the terms of the Creative Commons Attribution License (CC BY). The use, distribution or reproduction in other forums is permitted, provided the original author(s) and the copyright owner(s) are credited and that the original publication in this journal is cited, in accordance with accepted academic practice. No use, distribution or reproduction is permitted which does not comply with these terms.

frontiers in Oncology

MINI REVIEW
published: 11 October 2021
doi: 10.3389/fonc.2021.738320

Hadrontherapy for Thymic Epithelial Tumors: Implementation in Clinical Practice

Pierre Loap[1,2], Viviana Vitolo[2], Amelia Barcellini[2], Ludovic De Marzi[1,3], Alfredo Mirandola[2], Maria Rosaria Fiore[2], Barbara Vischioni[2], Barbara Alicja Jereczek-Fossa[4,5], Nicolas Girard[6,7,8], Youlia Kirova[1†] and Ester Orlandi[2†]*

[1] Department of Radiation Oncology, Institut Curie, Paris, France, [2] Radiation Oncology Clinical Department, National Center for Oncological Hadrontherapy (CNAO), Pavia, Italy, [3] Institut Curie, Paris Sciences & Lettres (PSL) Research University, University Paris Saclay, laboratoire d'Imagerie Translationnelle en Oncologie, Institut National de la Santé et de la Recherche Médicale (INSERM LITO), Orsay, France, [4] Department of Oncology and Hemato-oncology, University of Milan, Milan, Italy, [5] Division of Radiotherapy, Istituto Europeo di Oncologia (IEO) European Institute of Oncology Istituti di Ricovero e Cura a Carattere Scientifico (IRCCS), Milan, Italy, [6] Institut du Thorax Curie Montsouris, Paris, France, [7] Department of Medical Oncology, Institut Curie, Paris, France, [8] University Paris Saint-Quentin, Versailles, France

Radiation therapy is part of recommendations in the adjuvant settings for advanced stage or as exclusive treatment in unresectable thymic epithelial tumors (TETs). However, first-generation techniques delivered substantial radiation doses to critical organs at risk (OARs), such as the heart or the lungs, resulting in noticeable radiation-induced toxicity. Treatment techniques have significantly evolved for TET irradiation, and modern techniques efficiently spare normal surrounding tissues without negative impact on tumor coverage and consequently local control or patient survival. Considering its dosimetric advantages, hadrontherapy (which includes proton therapy and carbon ion therapy) has proved to be worthwhile for TET irradiation in particular for challenging clinical situations such as cardiac tumoral involvement. However, clinical experience for hadrontherapy is still limited and mainly relies on small-size proton therapy studies. This critical review aims to analyze the current status of hadrontherapy for TET irradiation to implement it at a larger scale.

Keywords: thymoma, thymic carcinoma, proton therapy, carbon ion therapy, hadrontherapy

OPEN ACCESS

Edited by:
Cesar Moran, University of Texas MD Anderson Cancer Center, United States

Reviewed by:
Xabier Mielgo Rubio, Hospital Universitario Fundación Alcorcón, Spain
Yong Chan Ahn, Samsung Medical Center, South Korea

****Correspondence:***
Pierre Loap
pierre.loap@gmail.com

†These authors have contributed equally to this work and share last authorship

Specialty section:
This article was submitted to Thoracic Oncology, a section of the journal Frontiers in Oncology

Received: *08 July 2021*
Accepted: *21 September 2021*
Published: *11 October 2021*

Citation:
Loap P, Vitolo V, Barcellini A, De Marzi L, Mirandola A, Fiore MR, Vischioni B, Jereczek-Fossa BA, Girard N, Kirova Y and Orlandi E (2021) Hadrontherapy for Thymic Epithelial Tumors: Implementation in Clinical Practice. Front. Oncol. 11:738320. doi: 10.3389/fonc.2021.738320

1 INTRODUCTION

Thymic epithelial tumors (TETs) represent a noticeable heterogeneous group of rare thoracic malignancies, including thymomas and thymic carcinomas, with an estimated incidence of 1.3 and 3.2 cases per million person-years (1). When feasible, surgery is the gold standard, but radiation therapy (RT) plays an important role in radical and adjuvant settings. In particular, RT is part of the

Abbreviations: CIRT, carbon ion radiation therapy; DIBH, deep-inspiration breath hold; DS, double scattering; IMRT, intensity-modulated radiation therapy; IMPT, intensity-modulated proton therapy; OAR, organ at risk; MCE, major cardiac event; MHD, mean heart dose; MLD, mean lung dose; NTCP, normal tissue complication probability; PBS, pencil beam scanning; PBT, proton beam therapy; TET, thymic epithelial tumor; VMAT, volumetric modulated arc therapy.

recommendations for locally advanced (stage III–IV) TETs after surgery, especially in cases of thymic carcinomas or positive margins, or as a radical treatment for unresectable patients. For R0-resected localized TETs, adjuvant RT is recommended in cases of thymic carcinoma histology, since it significantly increases recurrence-free survival and overall survival; the clinical benefit or RT seems however inexistent for completely resected stage I thymomas and is debatable in other stages (2). First-generation RT techniques relied on two-dimensional (2-D) planning, which exposed critical organs at risk (OARs) to substantial doses (such as the heart or the lungs) and was consequently associated with significant toxicity (3). The technical evolution of RT allows to better spare OARs without altering the tumor coverage and consequently the local control. Such breakthroughs included intensity-modulated RT (IMRT) and respiratory control techniques such as respiratory gating and deep-inspiration breath hold (DIBH). Nevertheless, despite these advances, some clinical situations (i.e., pericardial or myocardial tumoral involvement) are still challenging even with highly conformal IMRT. Particle beams of protons or carbon ions are able to deliver most of their energy towards the end of the particle range resulting from an increased linear energy transfer (LET) before particle rest, in the well-known Bragg peak (4). Consequently, distant-to-target dose deposition is substantially reduced compared with conventional photon RT technique. Proton RT has been recently considered for TET irradiation in patients with significant baseline cardiac risk factors or with cardiac tumoral involvement. However, clinical experience of hadrontherapy for TET irradiation is still limited. The purpose of this review is to provide a contextualized analysis of the status of hadrontherapy in TET management.

2 EXPECTATIONS ON HADRONTHERAPY FOR THYMIC EPITHELIAL TUMORS

2.1 Clinical Considerations

2.1.1 Cardiotoxicity Risk Reduction

The cause-specific mortality analysis on a retrospective series of the SEER database reported no significant difference ($p = 0.68$) in cardiac mortality rate between the TET patients who had received RT (14.3%) and those who had not (12.9%), with a non-statistically significant difference in terms of cardiac death incidence between the two groups (3.4% vs. 5.9% at 6 years and 17.4% vs. 11.8% at 24 years for irradiated and non-irradiated patients, $p = 0.85$) (5). This delayed increase of cardiac death might be related to the late toxicity, for which long-term follow-up is needed. The potential benefit of hadrontherapy for late cardiac adverse event reduction is based on the improved cardiac sparing capacity of particle beams, compared with photon RT techniques. In the *in silico* study by Vogel et al., proton beam plans delivered in a cohort of 22 TET patients were reoptimized with an IMRT approach showing a significant reduction in dose to the heart and left ventricle (6). Based on a linear relationship between MCE and mean heart dose (MHD) (7), major cardiac event (MCE) risk was significantly lower with proton beam therapy (PBT) compared with IMRT (74% vs. 135%, $p = 0.04$) (6). Using a linear relationship between MCE and MHD developed for Hodgkin's lymphoma (8), Franceschini et al. (9) evidenced that PBT would significantly reduce congestive heart failure incidence when compared with volumetric modulated arc therapy (VMAT) in an adjuvant setting, with a relative risk (RR) of 1.3 for PBT and of 1.6 for VMAT.

2.1.2 Pulmonary Toxicity Risk Reduction

Moiseenko et al. (3) proposed a normal tissue complication probability (NTCP) model, based on the Lyman formalism, from a cohort of 55 thymoma patients treated with photon RT. In this study, the mean lung dose (MLD) significantly correlated with symptomatic acute pneumonitis and late lung fibrosis. It should be stressed that patients included in this study were treated with outdated techniques, including ^{60}Co 2-D irradiation. Whether this NTCP model is valid for IMRT and hadrontherapy is an open question but justifies lowering as much as possible MLD during TET irradiation. Expectedly, Swisher-McClure et al. (10) demonstrated in a limited-size dosimetric study that PBT was associated with a significant dosimetric reduction of lung dosimetric parameters (including MLD, V20, and V5) in an adjuvant setting. In addition, using NTCP models, Lidestahl et al. (11) demonstrated that the risk of pneumonitis would be significantly lower with PBT than IMRT or 3D-RT (respectively, 2.5%, 10.8%, and 9.1%).

2.1.3 Toxicity to Other Organs at Risk

PBT has proved to be worthwhile in decrease radiation-induced esophagitis (4.3% with PBT vs. 5.8% with IMRT) and myelopathy (0% with PBT vs. 0.4% with 3D-RT) (11); however, these reductions were of limited clinical amplitude. In the mono-institutional *in silico* experience by Haefner et al. (12), particle therapy (carbon ion radiation therapy (CIRT) and PBT) gives lower doses to the heart, lungs, breast, esophagus, and spinal cord, than did the conventional RT approach (VMAT, helical tomotherapy (HT), and 3D-RT). Moreover, among photon beam RT, HT was associated with substantial low-dose exposure to the lungs, breasts, and heart. While the effects of low-dose exposure on carcinogenesis are subject to notable debate, lowering cumulative radiation dose to OARs may result in fewer secondary cancers (13). Franceschini et al. (9) found a substantial risk reduction of secondary cancer induction with PBT compared with VMAT based on the Schneider model (14): notable decreases in excess absolute risk (EAR) of esophagus cancer (EAR of 3.6 vs. 1.0–1.2/10,000 patient-years), breast cancer (EAR of 17.4 vs. 5.7–6.1/10,000 patient-years), and lung cancer (EAR of 24.8 vs. 8.1–8.7/10,000 patient-years) were observed. Similarly, Vogel et al. (15) estimated that five excess secondary malignancies per 100 patients would be avoided by treating TET patients with PBT instead of IMRT.

2.2 Biological Considerations

2.2.1 Immunomodulation of the Tumor Microenvironment

TETs are associated with one of the lowest tumor mutation burden (TMB) among all adult cancers as well as a notable intratumoral heterogeneity concerning PD-L1 and PD-1 expression (16). Indeed,

high PD-1 expression is associated with a lower tumor grade, contrary to PD-L1 expression, which does not correlate with tumor grade, since PD-L1 expression is constitutive of TETs (16). TET patients present a notable increase in extrathymic cancers (17), and there has been increased suspicion of immune disturbance leading to defective cancer immunosurveillance. An additional argument for immune disturbance is the frequency of autoimmune diseases, such as myasthenia gravis. Abscopal effects after RT for TETs have been reported, suggesting possible RT immunomodulation in the microenvironment (18, 19). Notably, one abscopal case report followed the use of CyberKnife stereotactic radiotherapy (20). In this context, heavy-ion RT is of particular interest. Spina et al. (21) and Simoniello et al. (22) unambiguously demonstrated that CIRT could efficiently induce pro-inflammatory cytokines, while sparing circulating lymphocytes, which could polarize the tumor microenvironment into an antitumor one. For their physical selectivity, fewer chromosomal aberrations were described in patients treated with CIRT than with photon beam RT (23–25), leading to a higher number of available immune cells that might be recruited for the immune response after cancer (26). Moreover, the radiobiological hallmarks of CIRT can lead to a production of double-stranded DNA (dsDNA) scraps that have been proved to enhance the immune response (26). Even the above results are promising but still inconclusive; several strategies are under study to induce an abscopal effect; and considering their characteristics, TET might be a suitable study target.

2.2.2 Hypoxia

In addition, TET represents a highly heterogeneous cancer group at the molecular level. Thymomas are associated with a homogeneous ^{18}F-FDG uptake, and more aggressive thymic carcinomas are characterized by a heterogeneous one (27). Kaira et al. (28) reported a ^{18}F-FDG uptake correlation with the upregulation of hypoxia-inducible factor (HIF)-1α, a transcription factor that plays a key role in hypoxic adaptation of neoplastic cells. Overexpression of HIF-1α is related to aggressiveness and scant prognosis (29). High expression level of hypoxia-related genes was reported in TET (30). In particular, carbonic anhydrase 9 (CA9) level was associated with Masaoka stage, World Health Organization classification, and relapse-free survival in the adjuvant setting (30). CA9 was found to be expressed in 81% of thymic carcinomas and 21% of all TETs (30). In addition, preclinical data on mice models demonstrated the existence of quiescent radioresistant epithelial progenitors (31), which might exist as well in humans. In this context, hadrontherapy might be beneficial in cases of such heterogeneous hypoxic tumors, due to the reduced effect of tissue oxygenation on antitumor efficacy of particle beams.

3 CURRENT EXPERIENCE OF HADRONTHERAPY FOR THYMIC EPITHELIAL TUMORS

While particle beam therapy demonstrated a theoretical dosimetric benefit for TET irradiation, the rarity of this tumor as well as the smaller number of available particle facilities might explain the paucity of available clinical data. Most of the evidence relies on PBT.

3.1 Clinical Evidence

Current clinical experience of hadrontherapy for TETs is summarized in **Table 1**.

3.1.1 Hadrontherapy

The first case report of PBT for TETs has been reported by Figura et al. (32) in an adjuvant context: a 23-year-old female patient was treated for a stage III thymoma with initial surgery with positive margins; considering her young age and due to the risk of long-term complication of thoracic RT based on the initial IMRT plan evaluation, it was ultimately decided to deliver adjuvant RT with PBT to a total dose of 50.4 Gy. No tolerance data were reported in this first case report. Parikh et al. (34) demonstrated on four patients treated in an adjuvant context an excellent toxicity profile without any grade ≥3 adverse events. Vogel et al. (35) described the efficacy outcomes of PBT on a cohort of 27 TET patients (85% thymoma and 15% of thymic carcinomas) treated for 63% in an adjuvant context, for 22% in a definitive context, and 15% in recurrent disease. The 2-year local control was 100%; 3-year regional control was 96%, 3-year distant control was 74%, and 3-year overall survival was 94%. PBT was well-tolerated without grade ≥3 toxicity. Zhu et al. (36) described similar outcomes on a small cohort of six patients in terms of toxicities (no grade 3) and local control (after a median follow-up of 2.6 years, two out-of-field recurrences were observed). Compared with IMRT, MHD was reduced by 36.5%, MLD by 33.5%, and mean dose to the esophagus by 60%. Mercado et al. (38) confirmed on a cohort of 22 patients the good tolerance profile of PBT for TETs where the most frequent adverse event was a grade 2 dermatitis, occurring in 37% of patients. With a median follow-up of 13 months, there were five relapses, including one local. Finally, McGunigal et al. (41) evaluated recent Monte Carlo dose calculation algorithms for pencil beam scanning (PBS)-PBT on a cohort of seven patients in an adjuvant setting with no relapse after 21 months. Considering the above reported results, with all their limitations (small simple size, retrospective data, and lack of data on follow-up), PBT for TET irradiation seems to be well tolerated, without any grade ≥3 toxicity reported to date and is associated with a promising local control. Longer follow-up and a prospective series are however necessary to confirm these preliminary results in terms of tolerance and efficacy. The ongoing PROTHYM single-arm phase-2 trial (NCT04822077) intends to recruit 40 patients to precise cardiac and pulmonary toxicities and 5-year local control with PBT for TET irradiation.

CIRT has been seldomly used for TET irradiation. In the series of Hayashi et al. (37), one of the 95 patients treated with CIRT for lung metastases has a TET lung localization. The patient underwent up to a total dose of 52.8 Gy of relative biological effectiveness (RBE) in 12 fractions without concurrent chemotherapy. No further specific data are available.

TABLE 1 | Current experience on hadrontherapy for thymic epithelial tumors.

Study	Size	Particle	Technique	Radiation therapy setting	Dose (RBE)	Follow-up	Efficacy	Tolerance
Figura et al. (32)	1 pt.	Proton	*NA*	Adjuvant	50.4 + 10.8 Gy	*NA*	*NA*	*NA*
Sugawara et al. (33)	1 pt.	Proton	DS. Respiratory gating	Definitive (cardiac invasion)	74 Gy	*NA*	*NA*	*NA*
Parikh et al. (34)	4 pts.	Proton	US	Adjuvant	57 Gy [50.4–66.6 Gy]	5.5 months	No relapse	One grade 2 dermatitis. No grade ≥3 toxicity
Vogel et al. (35)	27 pts.	Proton	DS. Respiratory gating	Adjuvant (63%), definitive (22%) and relapse (15%)	61.2 Gy [50.4–70.2 Gy]	2.0 years	2-year local control: 100%. 3-year regional control: 96%. 3-year distant control: 74%. 3-year overall survival: 94%	Grade 2 dermatitis (37%), esophagitis (7%), and pneumonitis (4%). No grade ≥3 toxicity
Zhu et al. (36)	6 pts.	Proton	DS. Respiratory gating	Adjuvant (83%), definitive (17%)	60 Gy [54–74 Gy]	2.6 years	Local control at 2.6 years: 100%. 2 out-of-field recurrences	Grade 2 dermatitis (83%), grade 2 esophagitis (17%). No grade ≥3 toxicity
Hayashi et al. (37)	1 pt.	Carbon ion	Respiratory gating	Metastatic (lung)	52.8 Gy (12 fractions)	*NA*	*NA*	*NA*
Mercado et al. (38)	22 pts.	Proton	DS, US, and PBS. Respiratory gating	Adjuvant (91%), definitive (9%)	54 Gy [45–70 Gy]	13 months	5 relapses (including 1 local relapse)	Grade 2 dermatitis (37%), cough (13%) and esophagitis (10%). No grade ≥3 toxicity
Fukai et al. (39)	1 pt.	Proton	*NA*	Definitive (progressive residual intramyocardial lesion)	50 Gy	*NA*	*NA*	*NA*
Loap et al. (40)	1 pt.	Proton	DS. DIBH	Definitive (primitive lesion + pericardial nodules)	60 Gy	*NA*	*NA*	*NA*
McGunigal et al. (41)	7 pts	Proton	PBS. Respiratory gating	Adjuvant	54 Gy	21 months	No relapse	Grade 2 dermatitis (29%). No grade ≥3 toxicity)

DS, double scattering; PBS, pencil beam scanning; US, uniform scanning; NA, non-assessable; Pt, patient; Gy, Gray.

3.1.2 Specific Clinical Situations

The tumoral involvement of cardiac substructures in advanced-stage TETs is a challenge for radiation oncologist considering the significant cardiotoxicity risk. Hadrontherapy might be of interest to limit radiation exposure to unaffected cardiac substructure as described also in non-oncological settings (42). With regards non-metastatic TETs, Sugawara et al. (33) reported the use of PBT to treat a large cardiac-invading TET in a definitive setting, Loap et al. (40) described the PBT treatment of anterior pericardial nodules of a stage IVB TET, and Fukai et al. (39) irradiated an evolutive intramyocardial post-surgery residue. These challenging situations, where planned target volumes include part of the heart, might be associated with a limited control (40) and pose specific technical challenges. While respiratory motion control strategies relying on gating or DIBH techniques are widespread, cardiac movement is challenging to take simultaneously into account. To this end, dual ECG-respiratory gating techniques have been proposed (43).

3.2 Treatment Considerations

3.2.1 Proton Therapy Technique

The optimal respiratory control technique for TET PBT is still undefined yet. Most clinical experience on PBT used 4D-CT gating systems (35, 36, 41), which is particularly convenient for patients that may have limited breathing capacities resulting from advanced-stage disease. DIBH, possibly controlled with spirometers, is an alternative that may limit range uncertainty and reduce target volumes (40). Dosimetric comparison studies between DIBH and FB with respiratory gating are equivocal. Rechner et al. (44) found on seven TET patients that DIBH would be associated with a dose reduction to the heart and to the lungs; on the other hand, Fracchiolla et al. (45), focusing on PBS-PBT with respiratory gating, did not find any significant interplay effect due to breathing on TET plans. In addition, a comparison between the two main PBT delivery modalities, PBS and double scattering (DS), has not been conducted yet. Loap et al. (40) estimated that PBS would lower skin dose compared with DS. However, in daily practice, PBS tends to become the only delivery modality available in new particle treatment centers, partly due to its increased conformity characteristics. It should be kept in mind, however, that PBS may have a greater interplay effect than DS, which could justify rescanning or tracking techniques (46), and a larger lateral penumbra (47). The lateral penumbra corresponds to the lateral dose fall-off, depends on the PBT system design and on setup parameters, and is an important point to consider for the dosimetric sparing of the OARs adjacent to the proton beams.

3.2.2 Treatment Planning

There are small variations in published treatment volumes for TET PBT. Zhu et al. (36) defined gross target volume (GTV) as

radiological disease at diagnosis, including ^{18}F-FDG imagery modality. Clinical target volume (CTV) was defined as the GTV (in case of adjuvant PBT) or as the postoperative bed (in case of definitive PBT) with a margin of 5 mm. An internal target volume (ITV) was defined on the 10 phases of a 4D-CT simulation scanner. Planning target volume (PTV) was defined as ITV with a margin of 5 mm. On the other hand, Vogel et al. (35) contoured the GTV on multiple phases of a 4D-CT scan; an ITV was defined as the fusion of the GTV with a margin of 8 mm. PTV was defined as ITV and a margin of 5 mm. In addition, treatment planning algorithms are also evolving for TET PBT: evaluation of robust optimization planning algorithms has been evaluated for TET proton therapy by Franceschini et al. (9), while McGunigal et al. (41) demonstrated that Monte Carlo algorithms might lead to more realist dose calculations compared with standard pencil beam calculation algorithms.

3.2.3 Practical Recommendations for Thymic Epithelial Tumor Hadrontherapy

Practical propositions for modern hadrontherapy for TETs are summarized in **Table 2** and in **Figure 1**. Hadrontherapy may be proposed for selected TET patients, in both postoperative or definitive settings, in case of significant cardiotoxicity risk, such as cardiac tumoral involvement or patient-specific clinical considerations (cardiovascular history and risk factors, and baseline lung disease). A ^{18}F-FDG PET may be realized to

TABLE 2 | Practical propositions for hadron therapy for thymic epithelial tumor irradiation.

Treatment planning phase	Proposition	Remark
Initial imaging	^{18}F-FDG PET	Target delineation. Radiomic prognosis.
Patient simulation	4D-CT scans or DIBH	DIBH may be spirometer-controlled
Delineation and dose	According to guidelines for photon RT	CTV = GTV (or tumor bed) + 5–8 mm. Thymic loge, tumor expansion, and anterior upper-middle mediastina to be included in the CTV according to ESMO guidelines. ITV to be delineated if 4D-CT acquisition. PTV margins according to local referential (usually, +5 mm) Dose: 45–50 Gy (R0 surgery). 50–54 (R1 surgery). 60 Gy (R2 surgery or definitive)
Particle	Proton therapy should be preferred	Limited experience for CIRT (metastatic sites only)
Particle delivery modality	For proton therapy: PBS. DS possible when PBS is not available	For CIRT: PBS
Fractionation	For proton therapy: 1.8-2.0 Gy/fraction	For CIRT (metastatic site): 4.4 Gy/fraction, 12 fractions
Dose calculation	Monte Carlo algorithms	
Planning	Robust planning algorithms	

^{18}F-PET, fluorodeoxyglucose F18 positron emission tomography; CIRT, carbon ion radiation therapy; DIBH, deep-inspiration breath hold; CT, computed tomography; PBS, pencil beam scanning; DS, double scattering; GTV, gross target volume; ITV, internal target volume; CTV, clinical target volume.

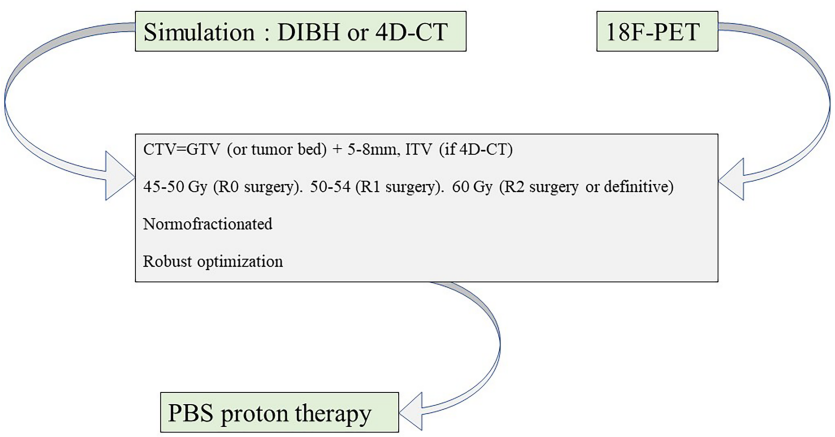

FIGURE 1 | Proton therapy planning for thymic epithelial tumor irradiation. CT, computed tomography; ^{18}F-PET, fluorodeoxyglucose F18 positron emission tomography; DIBH, deep-inspiration breath hold; PBS, pencil beam scanning; GTV, gross target volume; ITV, internal target volume; CTV, clinical target volume.

better define GTV, in addition to the radiomic value of this imagery modality (27). Patient simulation should take into account the range uncertainties of particle beams, and a respiratory control should be included, either 4D-CT or DIBH. DIBH could be spirometer-controlled, when possible (48). The volume definition and contouring rely on published guidelines. Most publications on TET PBT defined CTV as the GTV or the postoperative bed with a margin of 5–8 mm; in addition, according to European Society for Medical Oncology (ESMO) guidelines (2), the whole thymic space, the tumor and its extension, and the anterior and superior-middle mediastina should be included in the CTV. An ITV is necessary in case of 4D-CT acquisition but not in case of DIBH. Several studies are ongoing to further define reproducible target volumes, such as the ongoing RADIORYTHMIC trial (NCT04731610) (49). For PBT, the prescribed dose should be the same as for photon RT, following published guidelines. ESMO guidelines recommend 45–50 Gy after R0 resection, 50–54 Gy after R1 resection, and 60 Gy after R2 resection or in a definitive setting. PBS might be preferred over DS due to its increased conformity. Rescanning should be considered to mitigate interplay effect in case of 4D-CT planning. Robust optimization should be recommended. ECG gating, when possible, should be considered in case of target volumes next to the heart or in case of cardiac tumoral involvement. 4D-MRI and four-dimensional restricted robust optimization should be considered especially for CIRT treatment (50).

4 DISCUSSION

Hadrontherapy has been proposed for TET treatment based on dosimetric considerations from which a reduction in late adverse events is expected (in particular, for cardiac and lung toxicities). Short-term follow-up of current studies demonstrates an excellent tolerance profile to this date. However, the frequency of autoimmune diseases in patients with TETs should be kept in mind. It might be explained by the release of immature auto-reactive T cells that have not undergone negative selection, a physiologic function of the thymus (51). The pro-inflammatory signals induced by particle beam (especially in case of CIRT) may lead to an immunological activation of auto-reactive T-lymphocyte clones. Jakopovic et al. (52) demonstrated that TETs were associated with increased activation of auto-reactive T-lymphocyte clones under immunotherapy treatment compared with other cancer types. Lymphocytes are particularly sensitive to ionizing radiations and die off at a low dose level. Multiple studies have demonstrated a significant sparing of circulating lymphocytes with hadrontherapy compared with photon RT (53, 54), which is one of its theoretical advantages. However, the impact on antitumor immunity and on clinical outcome is still to be precisely evaluated.

A significant proportion of myocarditis-type adverse events were reported in TET patients undergoing immunotherapy treatment, compared with other cancer types (55). Future trials potentially evaluating a potential combination of immunotherapy and hadrontherapy should be consequently done cautiously. Similarly, a potential immune-activating abscopal effect on auto-reactive T-lymphocyte clones against cardiac antigens might act synergically with direct radiation-induced damage on cardiac substructures: the localization of critical cardiac substructures, such as the left anterior descending coronary artery (LADCA), the right coronary artery, or the left ventricle is localized close or at the contact of the target volumes. In this situation, these OARs are localized in a zone where the RBE value is uncertain and where the classic RBE value of 1.1 might not be valid. Variable RBE planning algorithms might consequently be considered (56). In addition, cardiac movement is usually not taken into account during treatment planning since ECG-gated treatments are not generalized yet. However, proton beams are extremely sensitive to range uncertainties, and cardiac intrinsic movement might consequently lead to over-dosing on coronary arteries. Use of planned OAR volumes for the LADCA (57) or specific surrogate OAR (58), associated with robust planning algorithms, might reduce this potential cardiotoxicity risk.

To this date, RT is recommended for inoperable patients, in the adjuvant setting after surgery in cases of R1–R2 residue and possibly after R0 surgery (depending on stage and histology); RT can be combined with chemotherapy (2). Surgical techniques are rapidly evolving (59), and the indications for adjuvant RT might consequently evolve. In addition, clear selection criteria for TET hadrontherapy (over photon RT) are still to be precisely defined, but Glimelius et al. (60) grossly estimated that 50% of TET patients could benefit from proton therapy to reduce acute and long-term side effects. The location of the target volumes in relation to the OARs is the prime determinant of radiation-induced toxicities. It should be noted that in the adjuvant setting, the target volumes are usually located above most cardiac substructures (including the coronary arteries); consequently, the dosimetric benefit of hadrontherapy may not be clinically significant in this situation, since high doses to cardiac substructures should theoretically be limited regardless of the RT technique. However, in the definitive setting, when R0 tumor resection is unrealistic due to an extensive disease extent or when the tumor abuts the heart, hadrontherapy is expected to substantially spare cardiac substructures compared with photon RT.

There is an unequal access to hadrontherapy facilities around the world. In Europe, the European Particle Therapy Network has been created to ease international cooperation and to enhance clinical research on hadrontherapy (61), which is of prime importance for rare tumors like TETs. The development of large registries can increase the evidence level of hadrontherapy. Nevertheless, reimbursement issues exist for tumor types with low evidence levels for hadrontherapy such as TETs, which is currently not widely recognized as a hadrontherapy indication (62). No cost-effectiveness analyses or NTCP-model-based evaluations (63) have been conducted to this date. Finally, adjuvant irradiation, which represents most of TET hadrontherapy indication, might not be prioritized over definitive treatment of aggressive or in-place tumors at the

level of a given typical hadrontherapy center with limited treatment resources (64).

In conclusion, hadrontherapy for TET irradiation has the potential to significantly reduce radiation exposure to several OARs, including cardiac substructures, which should substantially reduce late radiation-induced toxicities and secondary cancer risk. While hadrontherapy could be useful in the case of complex clinical presentation with cardiac tumoral involvement, its implementation in clinical practice is facing technical and societal challenges, and its clinical benefit is difficult to evaluate in practice due to limited available data and short follow-up. Large registries might help to increase the evidence of hadrontherapy in this indication.

AUTHOR CONTRIBUTIONS

Conceptualization: PL, YK, and EO. Methodology: PL, YK, and EO. Writing: PL. Review and editing: PL, LM, BJ-F, AM, AB, VV, NG, MF, BV, YK, and EO. Supervision: YK and EO. YK and EO contributed equally to the work. All authors contributed to the article and approved the submitted version.

REFERENCES

1. de Jong WK, Blaauwgeers JLG, Schaapveld M, Timens W, Klinkenberg TJ, Groen HJM. Thymic Epithelial Tumours: A Population-Based Study of the Incidence, Diagnostic Procedures and Therapy. *Eur J Cancer* (2008) 44 (1):123–30. doi: 10.1016/j.ejca.2007.11.004
2. Girard N, Ruffini E, Marx A, Faivre-Finn C, Peters SESMO Guidelines Committee. Thymic Epithelial Tumours: ESMO Clinical Practice Guidelines for Diagnosis, Treatment and Follow-Up. *Ann Oncol* (2015) 26 Suppl 5:v40–55. doi: 10.1093/annonc/mdv277
3. Moiseenko V, Craig T, Bezjak A, Van Dyk J. Dose-Volume Analysis of Lung Complications in the Radiation Treatment of Malignant Thymoma: A Retrospective Review. *Radiother Oncol* (2003) 67(3):265–74. doi: 10.1016/S0167-8140(03)00003-3
4. Tinganelli W, Durante M. Carbon Ion Radiobiology. *Cancers (Basel)* (2020) 12(10):E3022. doi: 10.3390/cancers12103022
5. Fernandes AT, Shinohara ET, Guo M, Mitra N, Wilson LD, Rengan R, et al. The Role of Radiation Therapy in Malignant Thymoma: A Surveillance, Epidemiology, and End Results Database Analysis. *J Thorac Oncol* (2010) 5 (9):1454–60. doi: 10.1097/JTO.0b013e3181e8f345
6. Vogel J, Lin L, Simone CB, Berman AT. Risk of Major Cardiac Events Following Adjuvant Proton Versus Photon Radiation Therapy for Patients With Thymic Malignancies. *Acta Oncol* (2017) 56(8):1060–4. doi: 10.1080/0284186X.2017.1302097
7. Darby SC, Ewertz M, McGale P, Bennet AM, Blom-Goldman U, Brønnum D, et al. Risk of Ischemic Heart Disease in Women After Radiotherapy for Breast Cancer. *N Engl J Med* (2013) 368(11):987–98. doi: 10.1056/NEJMoa1209825
8. van Nimwegen FA, Schaapveld M, Cutter DJ, Janus CPM, Krol ADG, Hauptmann M, et al. Radiation Dose-Response Relationship for Risk of Coronary Heart Disease in Survivors of Hodgkin Lymphoma. *J Clin Oncol* (2016) 34(3):235–43. doi: 10.1200/JCO.2015.63.4444
9. Franceschini D, Cozzi L, Loi M, Franzese C, Reggiori G, Mancosu P, et al. Volumetric Modulated Arc Therapy Versus Intensity-Modulated Proton Therapy in the Postoperative Irradiation of Thymoma. *J Cancer Res Clin Oncol* (2020) 146(9):2267–76. doi: 10.1007/s00432-020-03281-z
10. Swisher-McClure SD, Wang K, Hahn SM, James P, Tochner ZA, Both S. Adjuvant Radiotherapy (RT) for Thymoma: A Dosimetric Comparison of Photon and Proton Based Treatment Techniques. *Int J Radiat Oncol Biol Physics* (2011) 81(2):S881–2. doi: 10.1016/j.ijrobp.2011.06.1576
11. Lideståhl A, Mondlane G, Gubanski M, Lind PA, Siegbahn A. An in Silico Planning Study Comparing Doses and Estimated Risk of Toxicity in 3D-CRT, IMRT and Proton Beam Therapy of Patients With Thymic Tumours. *Phys Med* (2019) 60:120–6. doi: 10.1016/j.ejmp.2019.03.028
12. Haefner MF, Verma V, Bougatf N, Mielke T, Tonndorf-Martini E, König L, et al. Dosimetric Comparison of Advanced Radiotherapy Approaches Using Photon Techniques and Particle Therapy in the Postoperative Management of Thymoma. *Acta Oncol* (2018) 57(12):1713–20. doi: 10.1080/0284186X.2018.1502467
13. Facoetti A, Barcellini A, Valvo F, Pullia M. The Role of Particle Therapy in the Risk of Radio-Induced Second Tumors: A Review of the Literature. *Anticancer Res* (2019) 39(9):4613–7. doi: 10.21873/anticanres.13641
14. Schneider U, Sumila M, Robotka J. Site-Specific Dose-Response Relationships for Cancer Induction From the Combined Japanese A-Bomb and Hodgkin Cohorts for Doses Relevant to Radiotherapy. *Theor Biol Med Model* (2011) 8:27. doi: 10.1186/1742-4682-8-27
15. Vogel J, Lin L, Litzky LA, Berman AT, Simone CB. Predicted Rate of Secondary Malignancies Following Adjuvant Proton Versus Photon Radiation Therapy for Thymoma. *Int J Radiat Oncol Biol Phys* (2017) 99 (2):427–33. doi: 10.1016/j.ijrobp.2017.04.022
16. Owen D, Chu B, Lehman AM, Annamalai L, Yearley JH, Shilo K, et al. Expression Patterns, Prognostic Value, and Intratumoral Heterogeneity of PD-L1 and PD-1 in Thymoma and Thymic Carcinoma. *J Thorac Oncol* (2018) 13(8):1204–12. doi: 10.1016/j.jtho.2018.04.013
17. Yen Y-T, Lai W-W, Wu M-H, Lin M-Y, Chang J-M, Hsu I-L, et al. Thymic Neuroendocrine Carcinoma and Thymoma Are Both Associated With Increased Risk of Extrathymic Malignancy: A 20-Year Review of a Single Institution. *Ann Thorac Surg* (2011) 91(1):219–25. doi: 10.1016/j.athoracsur.2010.09.025
18. Lesueur P, Chevalier F, Stefan D, Habrand J-L, Lerouge D, Gervais R. Review of the Mechanisms Involved in the Abscopal Effect and Future Directions With a Focus on Thymic Carcinoma. *Tumori* (2017) 103(3):217–22. doi: 10.5301/tj.5000616
19. Guan S, Wang H, Qi X-H, Guo Q, Zhang H-Y, Liu H, et al. Abscopal Effect of Local Irradiation Treatment for Thymoma: A Case Report. *Am J Transl Res* (2020) 12(5):2234–40.
20. Xu C, Sun J, Zhang W, Yuan Z, Wang J. The Safety and Efficacy of Cyberknife® for Thymic Malignancy. *Cancer/Radiothérapie* (2021) 25 (2):119–25. doi: 10.1016/j.canrad.2020.06.026
21. Spina CS, Tsuruoka C, Mao W, Sunaoshi MM, Chaimowitz M, Shang Y, et al. Differential Immune Modulation With Carbon-Ion Versus Photon Therapy. *Int J Radiat Oncol Biol Physics* (2021) 109(3):813–8. doi: 10.1016/j.ijrobp.2020.09.053
22. Simoniello P, Wiedemann J, Zink J, Thoennes E, Stange M, Layer PG, et al. Exposure to Carbon Ions Triggers Proinflammatory Signals and Changes in Homeostasis and Epidermal Tissue Organization to a Similar Extent as Photons. *Front Oncol* (2015) 5:294. doi: 10.3389/fonc.2015.00294
23. Durante M, Yamada S, Ando K, Furusawa Y, Kawata T, Majima H, et al. X-Rays vs. Carbon-Ion Tumor Therapy: Cytogenetic Damage in Lymphocytes. *Int J Radiat Oncol Biol Phys* (2000) 47(3):793–8. doi: 10.1016/s0360-3016(00)00455-7
24. Hartel C, Nikoghosyan A, Durante M, Sommer S, Nasonova E, Fournier C, et al. Chromosomal Aberrations in Peripheral Blood Lymphocytes of Prostate Cancer Patients Treated With IMRT and Carbon Ions. *Radiother Oncol* (2010) 95(1):73–8. doi: 10.1016/j.radonc.2009.08.031
25. Pignalosa D, Lee R, Hartel C, Sommer S, Nikoghosyan A, Debus J, et al. Chromosome Inversions in Lymphocytes of Prostate Cancer Patients Treated With X-Rays and Carbon Ions. *Radiother Oncol* (2013) 109(2):256–61. doi: 10.1016/j.radonc.2013.09.021
26. Durante M, Formenti S. Harnessing Radiation to Improve Immunotherapy: Better With Particles? *Br J Radiol* (2020) 93(1107):20190224. doi: 10.1259/bjr.20190224
27. Kim JY, Kim HO, Kim JS, Moon DH, Kim YH, Kim DK, et al. 18f-FDG PET/CT Is Useful for Pretreatment Assessment of the Histopathologic Type of

Thymic Epithelial Tumors. *Nucl Med Mol Imaging* (2010) 44(3):177–84. doi: 10.1007/s13139-010-0036-x
28. Kaira K, Endo M, Abe M, Nakagawa K, Ohde Y, Okumura T, et al. Biologic Correlation of 2-[18F]-Fluoro-2-Deoxy-D-Glucose Uptake on Positron Emission Tomography in Thymic Epithelial Tumors. *J Clin Oncol* (2010) 28 (23):3746–53. doi: 10.1200/JCO.2009.27.4662
29. Surov A, Schmidt SA, Prasad V, Beer AJ, Wienke A. FDG PET Correlates Weakly With HIF-1α Expression in Solid Tumors: A Meta-Analysis. *Acta Radiol* (2021) 62(4):557–64. doi: 10.1177/0284185120932378
30. Ohtaki Y, Shimizu K, Kawabata-Iwakawa R, Gombodorj N, Altan B, Rokudai S, et al. Carbonic Anhydrase 9 Expression is Associated With Poor Prognosis, Tumor Proliferation, and Radiosensitivity of Thymic Carcinomas. *Oncotarget* (2019) 10(13):1306–19. doi: 10.18632/oncotarget.26657
31. Dumont-Lagacé M, Daouda T, Depoërs L, Zumer J, Benslimane Y, Brochu S, et al. Qualitative Changes in Cortical Thymic Epithelial Cells Drive Postpartum Thymic Regeneration. *Front Immunol* (2020) 10:3118. doi: 10.3389/fimmu.2019.03118/full
32. Figura N, Hoppe BS, Flampouri S, Su Z, Osian O, Monroe A, et al. Postoperative Proton Therapy in the Management of Stage III Thymoma. *J Thorac Oncol* (2013) 8(5):e38–40. doi: 10.1097/JTO.0b013e31827a8911
33. Sugawara K, Mizumoto M, Numajiri H, Ohno T, Ohnishi K, Ishikawa H, et al. Proton Beam Therapy for a Patient With a Giant Thymic Carcinoid Tumor and Severe Superior Vena Cava Syndrome. *Rare Tumors* (2014) 6(2):5177. doi: 10.4081/rt.2014.5177
34. Parikh RR, Rhome R, Hug E, Tsai H, Cahlon O, Chon B, et al. Adjuvant Proton Beam Therapy in the Management of Thymoma: A Dosimetric Comparison and Acute Toxicities. *Clin Lung Cancer* (2016) 17(5):362–6. doi: 10.1016/j.cllc.2016.05.019
35. Vogel J, Berman AT, Lin L, Pechet TT, Levin WP, Gabriel P, et al. Prospective Study of Proton Beam Radiation Therapy for Adjuvant and Definitive Treatment of Thymoma and Thymic Carcinoma: Early Response and Toxicity Assessment. *Radiother Oncol* (2016) 118(3):504–9. doi: 10.1016/j.radonc.2016.02.003
36. Zhu HJ, Hoppe BS, Flampouri S, Louis D, Pirris J, Nichols RC, et al. Rationale and Early Outcomes for the Management of Thymoma With Proton Therapy. *Transl Lung Cancer Res* (2018) 7(2):106–13. doi: 10.21037/tlcr.2018.04.06
37. Hayashi K, Yamamoto N, Karube M, Nakajima M, Tsuji H, Ogawa K, et al. Feasibility of Carbon-Ion Radiotherapy for Re-Irradiation of Locoregionally Recurrent, Metastatic, or Secondary Lung Tumors. *Cancer Sci* (2018) 109 (5):1562–9. doi: 10.1111/cas.13555
38. Mercado CE, Hartsell WF, Simone CB, Tsai HK, Vargas CE, Zhu HJ, et al. Proton Therapy for Thymic Malignancies: Multi-Institutional Patterns-of-Care and Early Clinical Outcomes From the Proton Collaborative Group and the University of Florida Prospective Registries. *Acta Oncol* (2019) 58 (7):1036–40. doi: 10.1080/0284186X.2019.1575981
39. Fukai R, Irie Y, Akimoto T, Akasaka K, Nakano K. Survival for Ten Years After Aggressive Surgery for Pericardial Recurrent Thymoma With Proton-Beam Radiation Therapy for An Unresectable Intramyocardial Lesion: A Case Report. *Arch Clin Med Case Rep* (2020) 4(5):940–5. doi: 10.26502/acmcr.96550283
40. Loap P, Scher N, Goudjil F, Kirova Y, Girard N, Cao KI. Proton Beam Therapy for Thymic Carcinoma With Pericardial Involvement. *Int J Part Ther* (2021) 7 (3):65–70. doi: 10.14338/IJPT-20-00023.1
41. McGunigal M, Margolis M, Forsthoefel M, Singh T, Amarell K, Deblois D, et al. Thymic Malignancies Treated With Active Scanning Proton Beam Radiation and Monte Carlo Planning: Early Clinical Experience. *Acta Oncol* (2021) 60(5):649–52. doi: 10.1080/0284186X.2021.1887516
42. Dusi V, Vitolo V, Frigerio L, Totaro R, Valentini A, Barcellini A, et al. First-In-Man Case of non-Invasive Proton Radiotherapy for the Treatment of Refractory Ventricular Tachycardia in Advanced Heart Failure. *Eur J Heart Fail* (2021) 23(1):195–6. doi: 10.1002/ejhf.2056
43. Reynolds T, Shieh C-C, Keall PJ, O'Brien RT. Dual Cardiac and Respiratory Gated Thoracic Imaging *via* Adaptive Gantry Velocity and Projection Rate Modulation on a Linear Accelerator: A Proof-Of-Concept Simulation Study. *Med Phys* (2019) 46(9):4116–26. doi: 10.1002/mp.13670
44. Rechner LA, af Rosenschöld PM, Bäck A, Stagaard Johansen T, Schut DA, Aznar M, et al. Proton Therapy and Deep Inspiration Breath Hold for Optimal Radiotherapy for Patients With Thymoma. *Int J Particle Ther* (2019) 6(4). doi: 10.26226/morressier.5cb72190ae0a09001583093e
45. Fracchiolla F, Dionisi F, Giacomelli I, Hild S, Esposito PG, Lorentini S, et al. Implementation of Proton Therapy Treatments With Pencil Beam Scanning of Targets With Limited Intrafraction Motion. *Phys Med* (2019) 57:215–20. doi: 10.1016/j.ejmp.2019.01.007
46. Mastella E, Molinelli S, Pella A, Vai A, Maestri D, Vitolo V, et al. 4D Strategies for Lung Tumors Treated With Hypofractionated Scanning Proton Beam Therapy: Dosimetric Impact and Robustness to Interplay Effects. *Radiother Oncol* (2020) 146:213–20. doi: 10.1016/j.radonc.2020.02.025
47. Safai S, Bortfeld T, Engelsman M. Comparison Between the Lateral Penumbra of a Collimated Double-Scattered Beam and Uncollimated Scanning Beam in Proton Radiotherapy. *Phys Med Biol* (2008) 53(6):1729–50. doi: 10.1088/0031-9155/53/6/016
48. Loap P, Goudjil F, Dendale R, Kirova Y. Clinical and Technical Considerations for Mediastinal Hodgkin Lymphoma Protontherapy Based on a Single-Center Early Experience. *Cancer Radiother* (2021). doi: 10.1016/j.canrad.2021.06.016
49. Basse C, Botticella A, Molina TJ, Falcoz PE, Oulkhouir Y, Kerjouan M, et al. RADIORYTHMIC: Phase III, Opened, Randomized Study of Postoperative Radiotherapy Versus Surveillance in Stage IIb/III of Masaoka Koga Thymoma After Complete Surgical Resection. *Clin Lung Cancer* (2021) 22(5):469–72. doi: 10.1016/j.annonc.2021.08.1986
50. Meschini G, Paganelli C, Vai A, Fontana G, Molinelli S, Pella A, et al. An MRI Framework for Respiratory Motion Modelling Validation. *J Med Imaging Radiat Oncol* (2021) 65(3):337–44. doi: 10.1111/1754-9485.13175
51. Weksler B, Lu B. Alterations of the Immune System in Thymic Malignancies. *J Thorac Oncol* (2014) 9(9):S137–42. doi: 10.1097/JTO.0000000000000299
52. Jakopovic M, Bitar L, Seiwerth F, Marusic A, Krpina K, Samarzija M. Immunotherapy for Thymoma. *J Thorac Dis* (2020) 12(12):7635–41. doi: 10.21037/jtd-2019-thym-12
53. Fang P, Shiraishi Y, Verma V, Jiang W, Song J, Hobbs BP, et al. Lymphocyte-Sparing Effect of Proton Therapy in Patients With Esophageal Cancer Treated With Definitive Chemoradiation. *Int J Part Ther* (2018) 4(3):23–32. doi: 10.14338/IJPT-17-00033.1
54. Routman DM, Garant A, Lester SC, Day CN, Harmsen WS, Sanheuza CT, et al. A Comparison of Grade 4 Lymphopenia With Proton Versus Photon Radiation Therapy for Esophageal Cancer. *Adv Radiat Oncol* (2019) 4(1):63–9. doi: 10.1016/j.adro.2018.09.004
55. Zhao C, Rajan A. Immune Checkpoint Inhibitors for Treatment of Thymic Epithelial Tumors: How to Maximize Benefit and Optimize Risk? *Mediastinum* (2019) 3:35. doi: 10.21037/med.2019.08.02
56. Giovannini G, Böhlen T, Cabal G, Bauer J, Tessonnier T, Frey K, et al. Variable RBE in Proton Therapy: Comparison of Different Model Predictions and Their Influence on Clinical-Like Scenarios. *Radiat Oncol* (2016) 11(1):68. doi: 10.1186/s13014-016-0642-6
57. Nicolas E, Khalifa N, Laporte C, Kirova Y. Safety Margins for the Delineation of the Left Anterior Descending Artery in Patients Treated for Breast Cancer. *Int J Radiat Oncol Biol Physics* (2020) 109(1):267–72. doi: 10.1016/j.ijrobp.2020.08.051
58. Loap P, Tkatchenko N, Nicolas E, Fourquet A, Kirova Y. Optimization and Auto-Segmentation of a High Risk Cardiac Zone for Heart Sparing in Breast Cancer Radiotherapy. *Radiother Oncol* (2020) 153:146–54. doi: 10.1016/j.radonc.2020.09.044
59. Billè A, Bilkhu R, Benedetti G, Lucchese G. Improving Outcomes of Surgery in Advanced Infiltrative Thymic Tumours: The Benefits of Multidisciplinary Approach. *Tumori* (2021). doi: 10.1177/03008916211023154
60. Glimelius B, Ask A, Bjelkengren G, Björk-Eriksson T, Blomquist E, Johansson B, et al. Number of Patients Potentially Eligible for Proton Therapy. *Acta Oncol* (2005) 44(8):836–49. doi: 10.1080/02841860500361049
61. Weber DC, Langendijk JA, Grau C, Thariat J. Proton Therapy and the European Particle Therapy Network: The Past, Present and Future. *Cancer Radiother* (2020) 24(6):687–90. doi: 10.1016/j.canrad.2020.05.002
62. Minsat M, Ferrari C, Viguier J, Samb A, Le bihan-benjamin C, Bousquet P-J, et al. La Protonthérapie, Indications Et Capacité De Traitement, Juin 2016, Appui À La Décision, INCa. (2016). Available at: https://www.e-cancer.fr/Expertises-et-publications/Catalogue-des-publications/Protontherapie-indications-et-capacite-de-traitement-Juin-2016.
63. Langendijk JA, Lambin P, De Ruysscher D, Widder J, Bos M, Verheij M. Selection of Patients for Radiotherapy With Protons Aiming at Reduction of Side Effects: The Model-Based Approach. *Radiother Oncol* (2013) 107(3):267–73. doi: 10.1016/j.radonc.2013.05.007

64. Loap P, Beddok A, Cao KI, Goudjil F, Fourquet A, Dendale R, et al. Clinical Practice of Breast Cancer Protontherapy: A Single-Centre Experience From Selection to Treatment. *Cancer Radiother* (2021) 25(4):358–65. doi: 10.1016/j.canrad.2021.01.005

Conflict of Interest: The authors declare that the research was conducted in the absence of any commercial or financial relationships that could be construed as a potential conflict of interest.

Publisher's Note: All claims expressed in this article are solely those of the authors and do not necessarily represent those of their affiliated organizations, or those of the publisher, the editors and the reviewers. Any product that may be evaluated in this article, or claim that may be made by its manufacturer, is not guaranteed or endorsed by the publisher.

Copyright © 2021 Loap, Vitolo, Barcellini, De Marzi, Mirandola, Fiore, Vischioni, Jereczek-Fossa, Girard, Kirova and Orlandi. This is an open-access article distributed under the terms of the Creative Commons Attribution License (CC BY). The use, distribution or reproduction in other forums is permitted, provided the original author(s) and the copyright owner(s) are credited and that the original publication in this journal is cited, in accordance with accepted academic practice. No use, distribution or reproduction is permitted which does not comply with these terms.

frontiers in Oncology

ORIGINAL RESEARCH
published: 10 December 2021
doi: 10.3389/fonc.2021.744021

CT-Based Radiomics Nomogram for Differentiation of Anterior Mediastinal Thymic Cyst From Thymic Epithelial Tumor

Chengzhou Zhang[1†], Qinglin Yang[1†], Fan Lin[1,2], Heng Ma[1], Haicheng Zhang[1], Ran Zhang[3], Ping Wang[1] and Ning Mao[1*]*

[1] Department of Radiology, Yantai Yuhuangding Hospital, Affiliated Hospital of Qingdao University, Yantai, China, [2] School of Medical Imaging, Binzhou Medical University, Yantai, China, [3] Collaboration Department, Huiying Medical Technology, Beijing, China

OPEN ACCESS

Edited by:
Mylene Truong, University of Texas MD Anderson Cancer Center, United States

Reviewed by:
Alberto Traverso, Maastro Clinic, Netherlands
Chang Hyun Kang, Seoul National University, South Korea

****Correspondence:***
Ping Wang
p_wang8485@163.com
Ning Mao
maoning@pku.edu.cn

[†]These authors have contributed equally to this work

Specialty section:
This article was submitted to Thoracic Oncology, a section of the journal Frontiers in Oncology

Received: *19 July 2021*
Accepted: *18 November 2021*
Published: *10 December 2021*

Citation:
Zhang C, Yang Q, Lin F, Ma H, Zhang H, Zhang R, Wang P and Mao N (2021) CT-Based Radiomics Nomogram for Differentiation of Anterior Mediastinal Thymic Cyst From Thymic Epithelial Tumor. Front. Oncol. 11:744021. doi: 10.3389/fonc.2021.744021

Objectives: This study aimed to distinguish preoperatively anterior mediastinal thymic cysts from thymic epithelial tumors *via* a computed tomography (CT)-based radiomics nomogram.

Methods: This study analyzed 74 samples of thymic cysts and 116 samples of thymic epithelial tumors as confirmed by pathology examination that were collected from January 2014 to December 2020. Among the patients, 151 cases (scanned at CT 1) were selected as the training cohort, and 39 cases (scanned at CT 2 and 3) served as the validation cohort. Radiomics features were extracted from pre-contrast CT images. Key features were selected by SelectKBest and least absolute shrinkage and selection operator and then used to build a radiomics signature (Rad-score). The radiomics nomogram developed herein *via* multivariate logistic regression analysis incorporated clinical factors, conventional CT findings, and Rad-score. Its performance in distinguishing the samples of thymic cysts from those of thymic epithelial tumors was assessed *via* discrimination, calibration curve, and decision curve analysis (DCA).

Results: The radiomics nomogram, which incorporated 16 radiomics features and 3 conventional CT findings, including lesion edge, lobulation, and CT value, performed better than Rad-score, conventional CT model, and the clinical judgment by radiologists in distinguishing thymic cysts from thymic epithelial tumors. The area under the receiver operating characteristic (ROC) curve of the nomogram was 0.980 [95% confidence interval (CI), 0.963–0.993] in the training cohort and 0.992 (95% CI, 0.969–1.000) in the validation cohort. The calibration curve and the results of DCA indicated that the nomogram has good consistency and valuable clinical utility.

Conclusion: The CT-based radiomics nomogram presented herein may serve as an effective and convenient tool for differentiating thymic cysts from thymic epithelial tumors. Thus, it may aid in clinical decision-making.

Keywords: radiomics, nomogram, computed tomography, thymic epithelial tumor, cyst

INTRODUCTION

An increasing number of anterior mediastinal lesions has been incidentally found with the widespread application of computed tomography (CT) screening (1). Thymoma and thymic cysts are the most common lesions of anterior mediastinum (2, 3). Nam et al. (2) found that thymoma and thymic cysts account for 34.2% and 26.7%, respectively, of surgically resected anterior mediastinal lesions. The clinical treatment of thymic cysts and thymoma differs. In general, asymptomatic thymic cysts can be treated without surgical treatment, but early surgical resection is highly recommended if thymoma is definitively identified (4–6). Therefore, the correct preoperative diagnosis of thymic cysts and thymoma is important.

CT is the first choice of preoperative diagnosis of anterior mediastinal masses because of its high-density resolution and convenience for clinical use (7–9). However, discriminating thymic cysts from thymoma is often difficult, and many cysts had been misdiagnosed as thymoma that led to unnecessary surgery (2, 10–13). The primary reason attributed to misdiagnoses of thymoma is that thymic cysts with a high density (>20 Hu) are difficult to distinguish from non-invasive thymoma *via* unenhanced CT (11, 12). Even by contrast-enhanced CT, some small thymic cysts may be misdiagnosed as thymoma because of pseudo-enhancement, which is caused by their proximity to the aorta, and some non-invasive thymomas with low enhancement may be misdiagnosed as cysts (2, 14). Thus, new diagnostic methods must be developed to improve the performance in distinguishing these two types of lesions.

Radiomics, which extracts large quantitative features from medical images, can be used to evaluate the heterogeneity of lesions objectively and quantitatively, thereby overcoming the limitation of subjective visual image interpretation (15, 16). Radiomics methods are widely applied in the field of medicine to assist in disease diagnosis and prognosis (17, 18). Radiomics methods have been recently utilized in predicting histological subtype classification and staging of thymic epithelial tumors (19–22). However, studies that employ radiomics methods to differentiate thymic cysts from thymic epithelial tumors are limited. Yasaka et al. (23) used radiomics method to differentiate solid mediastinal masses from cysts. However, the number of their quantitative features and their sample size were relatively small, and they did not perform any type of validation. The current study aimed to develop a CT-based radiomics nomogram that incorporates radiomics features, clinical factors, and conventional CT findings to improve the accuracy of preoperative diagnosis of thymic cysts and thymic epithelial tumors.

MATERIALS AND METHODS

Patients

This retrospective study was approved by the Institutional Ethics Committee. From January 2014 to December 2020, 240 patients who had anterior mediastinal lesions underwent contrast-enhanced CT examination and pathological examination after surgical resection at our hospital. The patient inclusion and exclusion criteria are presented in **Figure 1**. Ultimately, 190 eligible patients were included in this study. Among these patients, 151 cases (scanned at CT 1) were selected as the training cohort, and 39 cases (scanned at CT 2 and 3) served as the validation cohort.

Various clinical factors, including gender, age, and myasthenia gravis, were recorded at baseline.

CT Protocols

The pieces of CT equipment used in this study were Philips iCT 256, GE Light Speed 64, and Philips Brilliance 64. The CT parameters were as follows: voltage was 120 kV, tube current was 120–250 mA, matrix was 512 × 512, layer thickness was 5 mm, reconstruction thickness was 1.25 or 1 mm, lung window width/level was 1,500/550, and mediastinum window width/level was 350/40. Plain and contrast-enhanced CT scans (Ultravist 370 with a dose of 1.5 ml/kg; bolus injection through the antecubital vein using a high-pressure syringe at a rate of 3–3.5 ml/s; three-phase scanning time windows of 30, 60, and 90 s after the injection of the contrast agent) were performed.

Analysis of Conventional CT Findings

The CT images were independently reviewed by two radiologists with over 10 years of experience in thoracic radiology. The radiologists were blinded to the clinical history of the patients or the final histopathology diagnosis. Consensus was reached through discussion.

The conventional CT findings included 1. location (right, left, or midline), which was determined according to the relationship between the lesion and the sternum; 2. size (average size of the maximum long axis, short axis, and coronal height); 3. lesion edge (smooth or rough); 4. shape (round, oval, or plaque)—when the ratio of the dimension of the long axis to the short axis dimension was <1.5, ≥1.5 and <3, and ≥3, it was considered round, oval, and plaque, respectively (24); 5. conformation to the shape of the adjacent mediastinum—the standard was the lesion was abutted to the adjacent mediastinal pleura with no protrusion toward the adjacent lung parenchyma; 6. lobulation (absent or present)—a lobulation margin was defined when the lesion's surface showed convex contours with adjacent notches between lesion lobules (25); 7. calcification (absent or present); 8. CT value—the region of interest (ROI) was placed in the maximum uniform density area of the lesion on the pre-contrast CT at three different levels, and the average of the three values was calculated as the CT value; and 9. homogeneity—not counting calcification, if the density of the lesion was uniform on the pre-contrast CT, then it was defined as homogeneous; otherwise, it was defined as inhomogeneous.

Interobserver agreement of the conventional CT findings was measured by Kappa statistics and intraclass correlation coefficients (ICCs).

Image Segmentation, Feature Selection, and Radiomics Signature Construction

The radiomics workflow is presented in **Figure 2**. Lesion segmentation and feature extraction were performed on the RadCloud platform (Huiying Medical Technology Co., Ltd., http://radcloud.cn/). The RadCloud platform used the

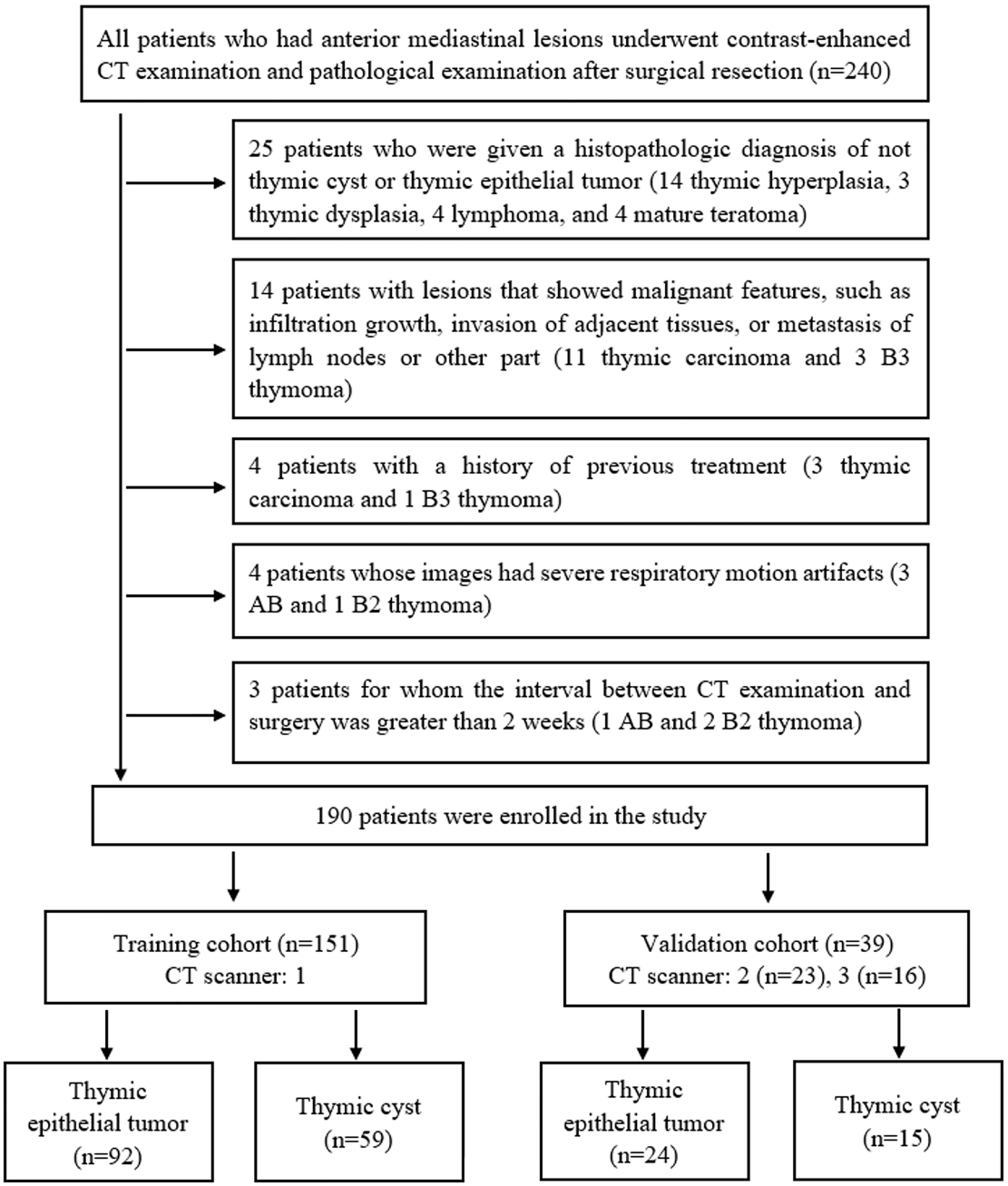

FIGURE 1 | Flow chart of patients' enrolment.

Pyradiomics v.2.1.2 package (https://pyradiomics.readthedocs.io/en/latest/) for feature extraction following the recommendations of the Image Biomarker Standardization Initiative. The volume of interest was segmented on the basis of transverse axial pre-contrast CT images. The CT images of 40 patients were randomly selected for ROI delineation and feature extraction to ensure intra- and interobserver reproducibility. The ROIs were manually delineated by the two radiologists mentioned above independently. The processes were repeated a month later by a junior radiologist. Agreement on feature extraction in the intra- and interobserver reproducibility was evaluated by ICCs, and features that had ICC values of >0.75 were used for further analysis. The remaining ROIs were completed by the junior radiologist, and all ROIs completed by the junior radiologist were selected for further feature extraction and analysis.

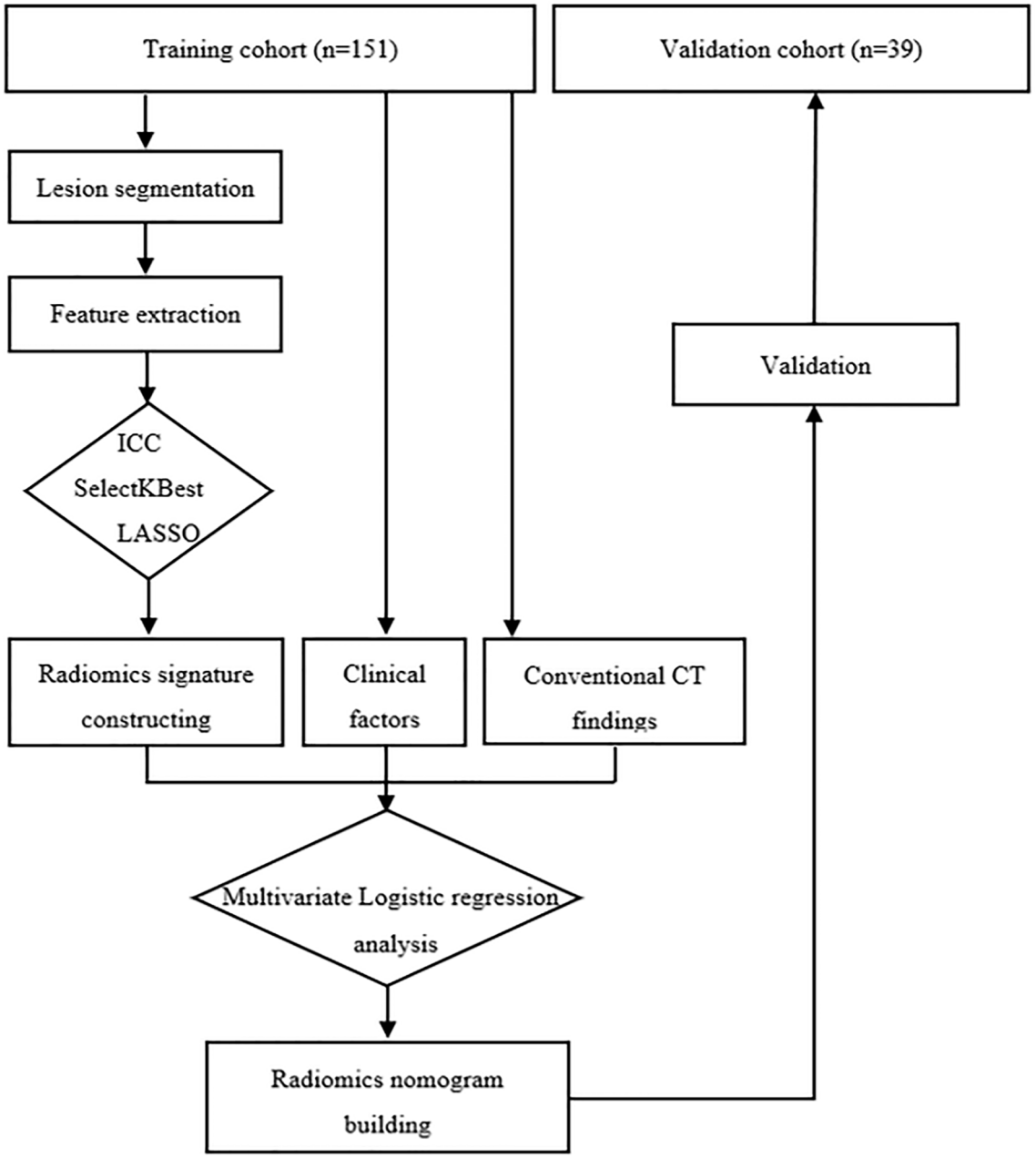

FIGURE 2 | Radiomics workflow of the study.

The optimal diagnostic-related features were selected by SelectKBest and the least absolute shrinkage and selection operator (LASSO). The radiomics signature (i.e., Rad-score) was computed for each lesion by a linear combination of the selected features as weighted by their respective quotient.

Radiomics Nomogram Building and Validation

The variables of clinical factors, conventional CT findings, and Rad-score between the samples of thymic cysts and epithelial tumors with significant differences were analyzed *via* multivariate logistic regression to build the radiomics nomogram. The nomogram's performance was evaluated by plotting receiver operating characteristic curves. The classification accuracy between the predicted probability and the observed results was evaluated by calibration curves. Decision curve analysis (DCA) was performed to evaluate the clinical utility of the nomogram. The boundary was set to 2 and 3 cm, and the stratification performance of the nomogram in the validation cohort was further verified according to the size.

For comparison, the Rad-score and conventional CT model were also built and evaluated. The radiologists' judgments were also recorded. The same radiologists mentioned above independently reviewed the pre-contrast and contrast-enhanced CT images with clinical information. They reached the final diagnosis by consensus.

Statistical Analysis

Statistical analysis was performed using the R software (version 3.4.1) and the SPSS software (Version 23.0). Quantitative variables are shown as mean ± SD. Categorical variables were assessed by χ^2 or Fisher's exact test, whereas differences in continuous variables were assessed by t-test or Mann–Whitney U test. The area under the receiver operating characteristic (ROC) curves (AUCs) of the nomogram, Rad-score, and conventional CT model were compared *via* DeLong test. Statistical significance was set at $p < 0.05$.

RESULTS

Patients' Characteristics and Conventional CT Findings

A total of 190 patients, namely, 74 patients with pathologically confirmed thymic cysts (4 of which were thymic bronchogenic cysts) and 116 patients with thymic epithelial tumors, were involved in this study. The specific pathological types of the 116 thymic epithelial tumors were as follows: type A (n = 13), type AB (n = 35), type B1 (n = 16), type B2 (n = 33), type B3 (n = 6), and thymic carcinoma (n = 13). The patients' characteristics and their conventional CT findings are summarized in **Table 1**. No significant difference was observed in the ratio of the dimension of the thymic cysts to the thymic epithelial tumors between the training and validation cohorts (p = 0.944).

The interobserver agreement of the two radiologists in their analysis of the conventional CT findings was good (κ = 0.774–0.957, ICC = 0.851–0.988).

Radiomics Feature Selection and Radiomics Signature Construction

A total of 1,409 features were extracted using the RadCloud platform, including first-order statistics, shape- and size-based features, texture features, and higher order statistics features.

After assessing intra- and interobserver reproducibility, 1,358 robust features with ICCs >0.75 were retained. After SelectKBest analysis, 605 features were retained, and after LASSO feature selection, 16 features were retained (**Supplementary Figure S1** and **Table 2**). The Rad-scores, which were calculated by the 16 features, were statistically different ($p < 0.001$) between the samples of thymic cysts and epithelial tumors, and the optimal cutoff value was 0.705.

Radiomics Nomogram Building

The variables of clinical factors, conventional CT findings, and Rad-score between the samples of thymic cysts and epithelial tumors with significant differences were analyzed *via* multivariate logistic regression. Among them, three conventional CT findings (including lesion edge, lobulation, and CT value) and the Rad-score were identified as independent predictors for differentiating thymic cysts from thymic epithelial tumors. A radiomics nomogram was constructed using the selected variables to provide a visualized outcome measure (**Figure 3**).

TABLE 1 | The patients' characteristics and conventional CT findings of the two cohorts.

Characteristics	Training cohort			Validation cohort		
	Thymic cyst (n = 59)	Thymic epithelial tumor (n = 92)	p	Thymic cyst (n = 15)	Thymic epithelial tumor (n = 24)	p
Gender (%)						
Male	24/59	34/92	0.646	6/15	7/24	0.508
Female	35/59	58/92		9/15	17/24	
Age (year)	52.75 ± 10.87	54.75 ± 11.86	0.297	55.67 ± 9.27	54.46 ± 9.04	0.292
Myasthenia gravis (%)	4/59	17/92	0.043	0/15	6/24	0.065
Location (%)						
Right	13/59	29/92	0.026	3/15	11/24	0.106
Left	18/59	39/92		5/15	9/24	
Midline	28/59	24/92		7/15	4/24	
Size (cm)	2.73 ± 1.41	3.84 ± 1.79	0.000	2.46 ± 0.68	3.41 ± 1.44	0.023
Lesion edge (%)						
Smooth	51/59	67/92	0.048	10/15	20/24	0.266
Rough	8/59	25/92		5/15	4/24	
Lesion shape (%)						
Round	26/59	38/92	0.158	4/15	10/24	0.041
Oval	25/59	49/92		7/15	14/24	
Plaque	8/59	5/92		4/15	0/24	
Lobulation (%)	7/59	60/92	0.000	1/15	12/24	0.006
Conformal to the shape of adjacent mediastinum (%)	14/59	2/92	0.000	6/15	2/24	0.037
Calcification (%)	11/59	27/92	0.139	1/15	8/24	0.115
Homogeneous (%)	56/59	67/92	0.001	14/15	16/24	0.115
CT value (HU)	28.16 ± 17.64	47.25 ± 9.55	0.000	24.60 ± 17.34	46.67 ± 12.87	0.000

TABLE 2 | Least absolute shrinkage and selection operator (LASSO) coefficient profiles of the 16 features.

Radiomics Features	Coefficients
wavelet-LLH_firstorder_Minimum	–0.06640596
wavelet-HLL_glcm_Autocorrelation	0.087935231
wavelet-LLH_glrlm_RunEntropy	0.017874634
original_shape_Maximum2DDiameterSlice	0.009097243
original_shape_Elongation	0.103026944
wavelet-HHL_glszm_ZoneEntropy	0.043976985
wavelet-HHL_glcm_Autocorrelation	–0.007486597
wavelet-HHL_gldm_GrayLevelVariance	–0.004601087
wavelet-HHL_firstorder_Entropy	–0.000113446
wavelet-HHL_glszm_GrayLevelVariance	0.017546166
wavelet-HHL_glszm_GrayLevelNonUniformityNormalized	–1.51E-08
logarithm_firstorder_Range	0.058735878
exponential_firstorder_Minimum	–0.044695771
square_firstorder_Minimum	–0.034266806
square_firstorder_Kurtosis	–0.034990685
squareroot_firstorder_RobustMeanAbsoluteDeviation	0.006370002

glcm, gray level co-occurrence matrix; glrlm, gray level run length matrix; glszm, gray level size zone matrix; gldm, gray level dependence matrix.

Performance of Conventional CT Model, Rad-Score, and Radiomics Nomogram

The AUCs of conventional CT model, Rad-score, and radiomics nomogram were 0.917, 0.909, and 0.980 in the training cohort, respectively, and 0.868, 0.953, and 0.992 in the validation cohort, respectively. Compared with conventional CT model and Rad-score, the radiomics nomogram had the best performance in the training cohort ($p < 0.01$). In the validation cohort, the radiomics nomogram performed better than the conventional CT model ($p = 0.02$), but its performance was not statistically different from that of Rad-score ($p = 0.17$). The AUC values diagnosed by the radiologists were lower than those in the conventional CT model, Rad-score, and the radiomics nomogram (**Figure 4**). The radiomics nomogram had a higher accuracy than Rad-score, conventional CT model, and the clinical judgment by the radiologists (**Table 3**). The diagnostic efficiency of the radiomics nomogram was excellent in the stratification verification according to the size in the validation cohort. The AUCs, sensitivity, specificity, and accuracy were 1.000, 0.800, 1.000, and 0.875 for the group of ≤2 cm, respectively; 1.000, 0.800, 1.000, and 0.933 for the group of 2–3 cm, respectively; and 1.000, 0.929, 1.000, and 0.938 for the group of >3 cm, respectively (**Figure 5** and **Table 4**).

The calibration curves demonstrated good diagnostic consistency between the radiomics nomogram's predictions and the actual observations of the samples of thymic cysts and thymic epithelial tumors (**Figure 6**). DCA revealed that the radiomics nomogram provided the greatest net benefit compared with "no treatment" or "all treatment" (**Figure 7**).

DISCUSSION

This study used a CT-based radiomics nomogram to distinguish anterior mediastinal thymic cysts from thymic epithelial tumors. In both the training and validation cohorts, the radiomics nomogram performed better with a larger AUC value and a higher accuracy than Rad-score, conventional CT model, and the clinical judgment of the radiologists. The calibration curves and DCA demonstrated the clinical utility of the radiomics nomogram developed herein.

Thymoma is the most common lesion of the anterior mediastinum, followed by thymic cyst (2, 3). Among the lesions included in this study, 58.8% were thymic epithelial tumors, and 30.8% were thymic cysts. The remaining 25 lesions, including 14 thymic hyperplasia, 3 thymic dysplasia, 4

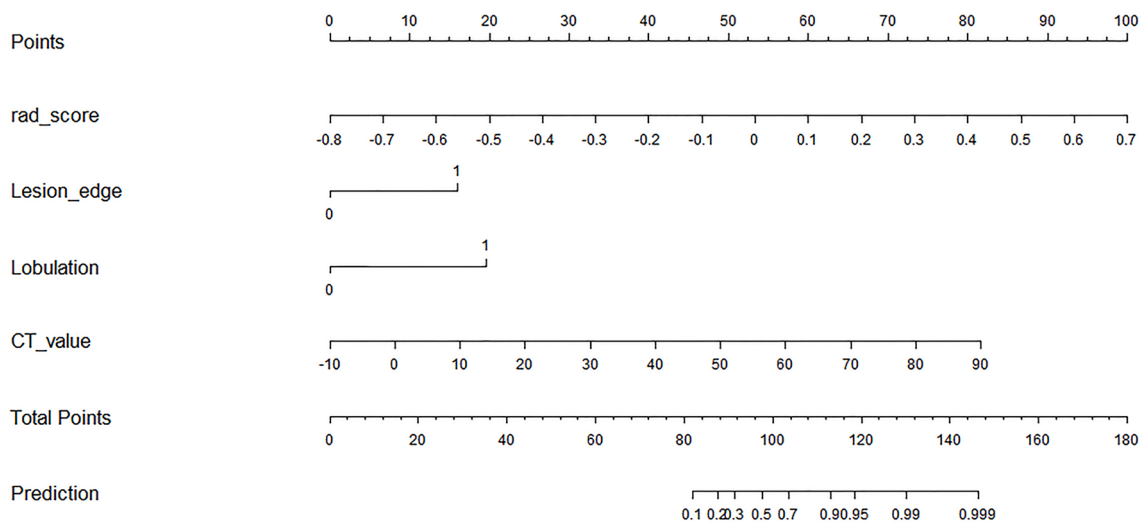

FIGURE 3 | Radiomics nomogram with Rad-score and three conventional CT findings, including lesion edge, lobulation, and CT value.

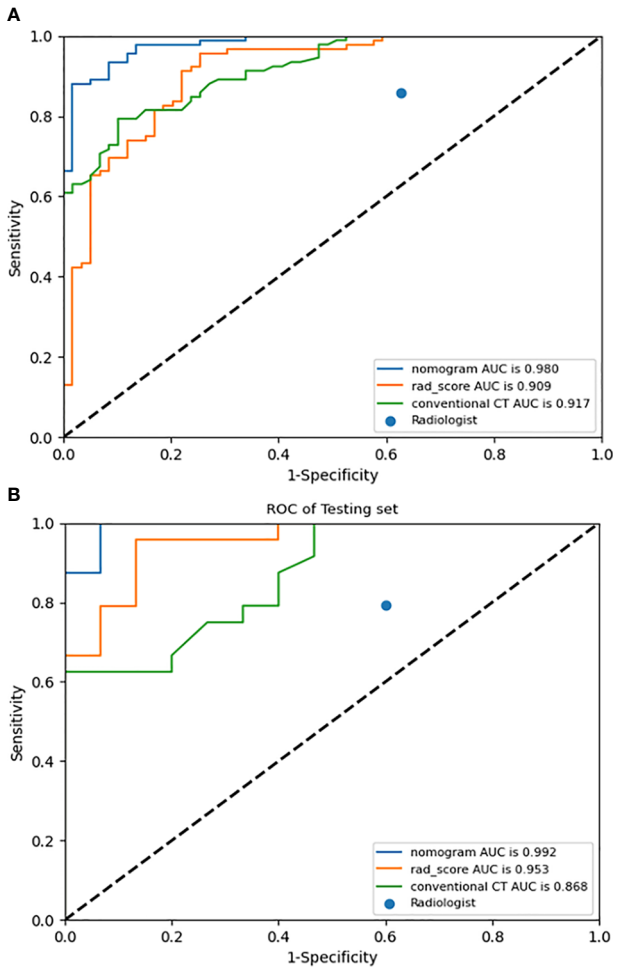

FIGURE 4 | ROC curves of radiomics nomogram, Rad-score, conventional CT model, and judgment by radiologists in the training **(A)** and validation **(B)** cohorts.

lymphomas, and 4 mature teratomas, accounted for only 10.4%. Given the high incidence of thymic epithelial tumors and cysts in the anterior mediastinum, their correct preoperative diagnosis is important. Among our case series, all four mature teratomas were found to contain fat density, and they were all correctly diagnosed by CT. Malignant features were found in all four cases of lymphoma, which were easily differentiated from thymic cysts. CT images with a triangular or a quadrilateral shape with a convex, concave, or straight margin may be helpful in diagnosing thymus hyperplasia/thymus degeneration, but they are often misdiagnosed as thymoma and not cysts (26).

CT is widely used in the preoperative diagnosis of thymic cysts and thymic epithelial tumors. The typical CT features of thymic cysts are well-circumscribed anterior mediastinal mass with a homogeneous water attenuation and a thin or imperceptible wall (12, 27). However, CT attenuation increases when hemorrhage or inflammation occurs in the cysts as a complication, which presents as a soft tissue density (27, 28). Partial thymoma, especially non-invasive thymoma, usually shows homogeneous attenuation and has a smooth contour (7, 13, 29). Thus, distinguishing thymic cysts from thymoma is difficult in some cases, especially when dealing with high-density cysts. Xun et al. (11) reported that the CT value of >20 Hu is an independent factor of misdiagnosis of thymic cysts. Previous studies found thymic cysts with CT values of >20 Hu in 62.5%–83% of patients (2, 12, 13). The accuracy of CT in diagnosing anterior mediastinal lesions was 90.1% for thymoma and only 42.3% for thymic cysts. Among the misdiagnosed thymic cysts, 80.5% were misdiagnosed as thymoma (2). Xun et al. (11) correctly diagnosed thymic cysts *via* CT in 54.6% of the patients only. In the present study, the sensitivity, specificity, and accuracy of the diagnosis of the radiologists were 0.859, 0.373, and 0.669, respectively, for the training cohort and 0.792, 0.400, and 0.641, respectively, for the validation cohort. The specificity and accuracy were low, especially specificity. A probable reason was that many thymic cysts had been misdiagnosed as thymomas as in previous studies. Another possible reason was that the subjects with thymic epithelial tumors that showed malignant features on CT were excluded. Thus, distinguishing thymic cysts from thymic epithelial tumors *via* CT was more difficult in the present study than in previous works.

Jung et al. (7) used a nomogram based on conventional contrast-enhanced CT findings that included the degree of enhancement (HU) and lobulated contour to differentiate thymic cysts from thymoma. In the training cohort, their

TABLE 3 | Predictive performances of radiomics nomogram, Rad-score, conventional CT model, and judgment by radiologists in the training and validation cohorts.

Model	Training cohort				Validation cohort			
	AUC (95% CI)	Sensitivity (95% CI)	Specificity (95% CI)	Accuracy	AUC (95% CI)	Sensitivity (95% CI)	Specificity (95% CI)	Accuracy
Radiomics nomogram	0.980 (0.963–0.993)	0.870 (0.779–0.928)	0.983 (0.897–0.999)	0.914	0.992 (0.969–1.000)	0.958 (0.769–0.998)	0.933 (0.660–0.997)	0.949
Rad-score	0.909 (0.864–0.948)	0.946 (0.872–0.980)	0.746 (0.613–0.846)	0.868	0.953 (0.893–0.997)	0.917 (0.715–0.985)	0.867 (0.584–0.977)	0.897
Conventional CT	0.917 (0.882–0.949)	0.783 (0.682–0.859)	0.898 (0.785–0.958)	0.828	0.868 (0.759–0.944)	0.583 (0.369–0.772)	1.000 (0.747–1.000)	0.744
Radiologist	NA	0.859 (0.767–0.920)	0.373 (0.253–0.509)	0.669	NA	0.792 (0.573–0.921)	0.400 (0.175–0.671)	0.641

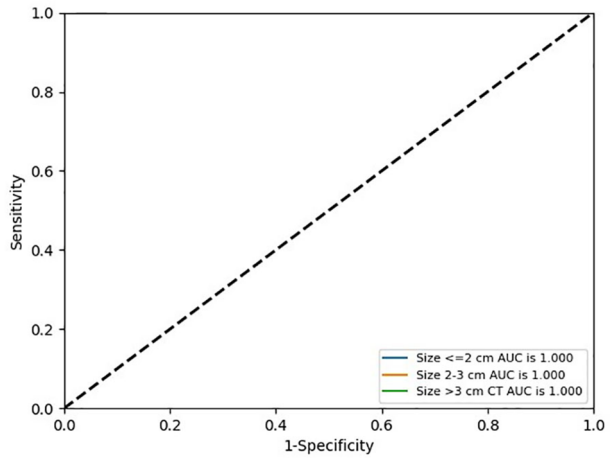

FIGURE 5 | ROC curves of radiomics nomogram in the stratification verification according to the size in the validation cohort.

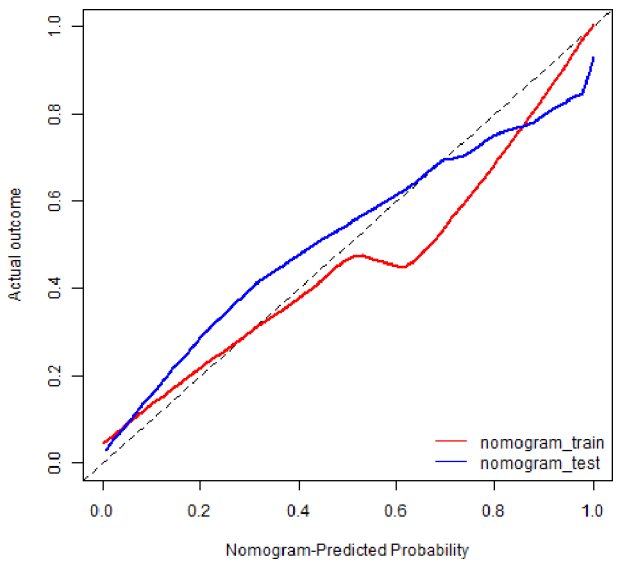

FIGURE 6 | Calibration curves of radiomics nomogram. The diagonal line represented the perfect prediction of the radiomics nomogram. The red and blue solid line represented the calibration curve of nomogram in the training and validation cohorts, separately. The calibration curves were close to the diagonal line, which indicated good prediction performance of the nomogram.

nomogram had an AUC of 0.929, sensitivity of 0.824, and specificity of 0.889. In the validation cohort, their nomogram correctly predicted 95% (19/20) of the thymomas. Radiomics methods have recently gained increased attention from radiologists. Yasaka et al. (23) used a radiomics method to differentiate solid mediastinal masses from cysts. Through logistic regression analyses, they found that their nomogram had an AUC of 0.869 for unenhanced CT and 0.997 for contrast-enhanced CT. However, they only selected texture features, their sample size was small, and they lacked any type of validation. In the present study, 1,409 features were extracted, including 1. first-order statistics, such as minimum, entropy, and range, which described the distribution of voxel intensity; 2. shape- and size-based features, such as elongation and maximum 2D diameter slice, which reflected the shape and size of the ROIs; 3. texture features, such as gray level co-occurrence matrix, gray level run length matrix, and gray level size zone matrix, which quantified regional heterogeneity differences; and 4. higher order statistics features, which were obtained by filter transformation of the original image. The filters used in this study were wavelet, logarithm, exponential, square, square root, gradient, and Ibp-2D. After feature selection *via* SelectKBest and LASSO, 16 features were retained. The majority of the features were found to have originated from digital filtering of the original images plus only two shape features. These results indicated that the higher order statistics features more accurately reflected the image features, making them more valuable for differentiating thymic cysts from thymic epithelial tumors than the other features. The radiomics nomogram that incorporated Rad-score and three conventional CT findings (including lesion edge, lobulation, and CT value) achieved a good diagnostic efficiency. The AUC, sensitivity, specificity, and accuracy of this radiomics nomogram were 0.980, 0.870, 0.983, and 0.914, respectively, for the training cohort and 0.992, 0.958, 0.933, and 0.949, respectively, for the validation cohort. Accurate diagnosis of small thymic nodules is very challenging in clinical settings. On the basis of the characteristics of cases included herein, 2 and 3 cm were set as the boundary, and the stratification performance of the radiomics nomogram was further verified according to the size. Its diagnostic efficiency was excellent in the stratification verification. Its AUC, sensitivity, specificity, and accuracy were 1.000, 0.800, 1.000, and 0.875 for the group of ≤2 cm, respectively; 1.000, 0.800, 1.000, and 0.933 for the groups of 2–3 cm,

TABLE 4 | Predictive performance of radiomics nomogram in the stratification verification according to the size in the validation cohort.

Size (cm)	Predictive performance			
	AUC (95% CI)	Sensitivity (95% CI)	Specificity (95% CI)	Accuracy
≤2	1.000 (1.000–1.000)	0.800 (0.299–0.989)	1.000 (0.310–1.000)	0.875
2–3	1.000 (1.000–1.000)	0.800 (0.299–0.989)	1.000 (0.655–1.000)	0.933
>3	1.000 (1.000–1.000)	0.929 (0.769–0.998)	1.000 (0.660–0.997)	0.938

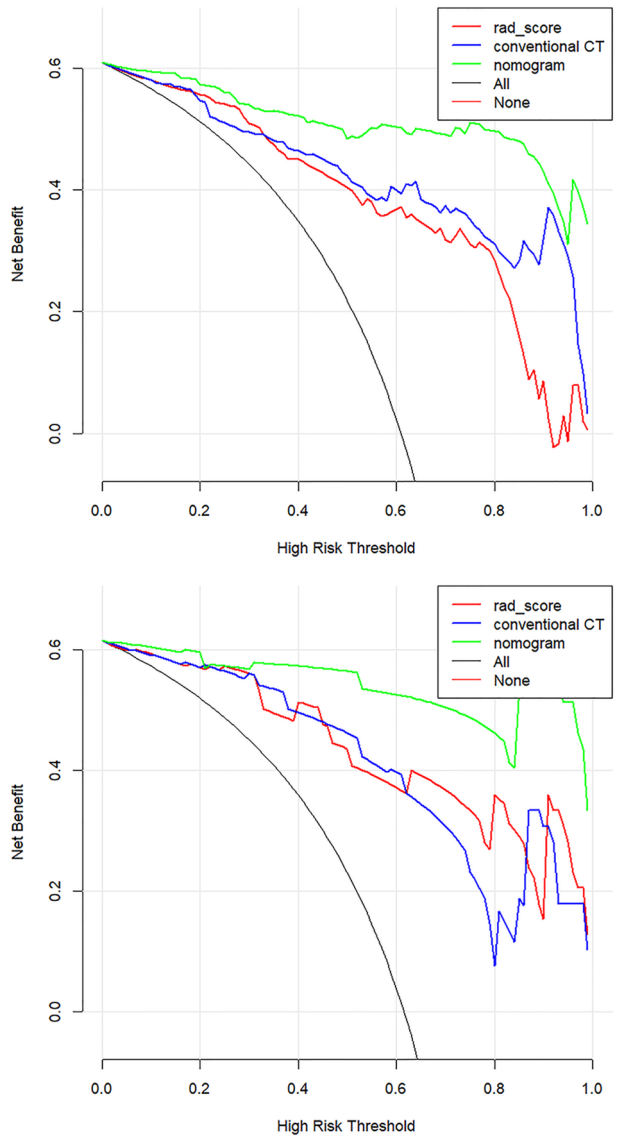

FIGURE 7 | Decision curve analysis (DCA) for the three models. The net benefit *versus* the threshold probability was plotted. The x-axis represents the threshold probability, while the y-axis represents the net benefits. The sensitivity and specificity of the model are calculated at each threshold to determine the net benefit. The DCAs showed that the net benefits of the nomogram model (green line) were superior to the benefits of the conventional CT model (blue line) and the Rad-score based model (red line) with the threshold probability range from 0 to 1.

respectively; and 1.000, 0.929, 1.000, and 0.938 for the group of >3 cm, respectively.

The radiomics nomogram presented herein was developed on the basis of unenhanced CT, which can reduce a patient's exposure to radiation and risk of allergy to the contrast media compared with multiphasic enhanced CT. Moreover, unenhanced CT is routinely scanned in clinical work. Thus, radiomics features based on unenhanced CT images can be easily obtained. In this study, three CT scanners were used. Thus, another advantage of the radiomics nomogram developed herein was that it performed well in both the training and validation cohorts, indicating that it was robust.

This study has several limitations. First, a selection bias may exist because of the retrospective nature of the study. Second, a multicenter study with more sample size is needed to achieve a more robust external validation. Finally, the ROIs were segmented manually, a process that is vulnerable to subjective factors and is time consuming. Semiautomatic or automatic segmentation methods should be applied in further works.

In conclusion, the CT-based radiomics nomogram developed herein that integrates Rad-score and conventional CT findings may serve as an effective tool for differentiating thymic cysts from thymic epithelial tumors. Thus, it can aid in clinical decision-making. Accordingly, patients can receive a reasonable intervention and treatment.

DATA AVAILABILITY STATEMENT

The raw data supporting the conclusions of this article will be made available by the authors, without undue reservation.

ETHICS STATEMENT

The studies involving human participants were reviewed and approved by Yantai Yuhuangding Hospital, Affiliated Hospital of Qingdao University. Written informed consent from the participants' legal guardian/next of kin was not required to participate in this study in accordance with the national legislation and the institutional requirements.

AUTHOR CONTRIBUTIONS

PW and NM: study design. CZ and FL: data collection. QY, HM, HZ, and RZ: data processing. CZ and QY: manuscript writing. PW and NM: manuscript revision. All authors contributed to the article and approved the submitted version.

ACKNOWLEDGMENTS

We thank Huiying Medical Technology for technical support.

SUPPLEMENTARY MATERIAL

The Supplementary Material for this article can be found online at: https://www.frontiersin.org/articles/10.3389/fonc.2021.744021/full#supplementary-material

Supplementary Figure 1 | Least absolute shrinkage and selection operator (LASSO) regression algorithm for identifying features with the best correlation and reproducibility. **(A)**16 features that correspond to the optimal alpha value were selected (5-fold cross-validation, alpha [the optimal value of the LASSO tuning parameter] = 1.7). **(B)** Mean squared error (MSE) path (5-fold cross-validation).

REFERENCES

1. Yoon SH, Choi SH, Kang CH, Goo JM. Incidental Anterior Mediastinal Nodular Lesions on Chest CT in Asymptomatic Subjects. *J Thorac Oncol* (2018) 13(3):359–66. doi: 10.1016/j.jtho.2017.11.124
2. Nam JG, Goo JM, Park CM, Lee HJ, Lee CH, Yoon SH. Age- and Gender-Specific Disease Distribution and the Diagnostic Accuracy of CT for Resected Anterior Mediastinal Lesions. *Thorac Cancer* (2019) 10(6):1378–87. doi: 10.1111/1759-7714.13081
3. Roden AC, Fang WT, Shen Y, Carter BW, White DB, Jenkins SM, et al. Distribution of Mediastinal Lesions Across Multi-Institutional, International, Radiology Databases. *J Thorac Oncol* (2020) 15(4):568–79. doi: 10.1016/j.jtho.2019.12.108
4. Turna A, Sarbay İ. Multimodality Approach in Treatment of Thymic Tumors. *J Thorac Dis* (2020) 12(12):7626–34. doi: 10.21037/jtd-20-818
5. Khorfan R, Bharat A, Odell DD. Management and Long-Term Outcomes of Advanced Stage Thymoma in the United States. *Ann Thorac Surg* (2021) 111 (1):223–30. doi: 10.1016/j.athoracsur.2020.05.088
6. Kamata S, Ishida I, Suzuki Y, Oura H. Single-Center Evaluation of Prognostic Factors for Thymoma Treated by Surgery: A Retrospective Study. *J Cardiothorac Surg* (2021) 16(1):8. doi: 10.1186/s13019-020-01386-7
7. Jung W, Cho S, Yum S, Lee YK, Kim K, Jheon S. Differentiating Thymoma From Thymic Cyst in Anterior Mediastinal Abnormalities Smaller Than 3 Cm. *J Thorac Dis* (2020) 12(4):1357–65. doi: 10.21037/jtd.2020.02.14
8. Jin ZG, Wu YJ, Wang YF, Pu ZT, Wang J, Li DS, et al. Multislice Computed Tomography Performance in Differential Diagnosis of High-Density Thymic Cyst and Thymoma in Lesions Less Than 3 Cm. *Thorac Cancer* (2018) 9 (10):1300–04. doi: 10.1111/1759-7714.12840
9. Li X, Han XP, Sun W, Wang M, Jing GH, Zhang X. Preoperative Misdiagnosis Analysis and Accurate Distinguish Intrathymic Cyst From Small Thymoma on Computed Tomography. *J Thorac Dis* (2016) 8(8):2086–92. doi: 10.21037/jtd.2016.07.83
10. Tomiyama N, Honda O, Tsubamoto M, Inoue A, Sumikawa H, Kuriyama K, et al. Anterior Mediastinal Tumors: Diagnostic Accuracy of CT and MRI. *Eur J Radiol* (2009) 69(2):280–8. doi: 10.1016/j.ejrad.2007.10.002
11. Wang X, Chen K, Li X, Li Y, Yang F, Li J, et al. Clinical Features, Diagnosis and Thoracoscopic Surgical Treatment of Thymic Cysts. *J Thorac Dis* (2017) 9 (12):5203–11. doi: 10.21037/jtd.2017.10.148
12. Araki T, Sholl LM, Gerbaudo VH, Hatabu H, Nishino M. Intrathymic Cyst: Clinical and Radiological Features in Surgically Resected Cases. *Clin Radiol* (2014) 69(7):732–8. doi: 10.1016/j.crad.2014.03.002
13. Ackman JB, Verzosa S, Kovach AE, Louissaint A Jr, Lanuti M, Wright CD, et al. High Rate of Unnecessary Thymectomy and Its Cause. Can Computed Tomography Distinguish Thymoma, Lymphoma, Thymic Hyperplasia, and Thymic Cysts? *Eur J Radiol* (2015) 84(3):524–33. doi: 10.1016/j.ejrad.2014.11.042
14. Lee SH, Yoon SH, Nam JG, Kim HJ, Ahn SY, Kim HK, et al. Distinguishing Between Thymic Epithelial Tumors and_Benign Cysts *via* Computed Tomography. *Korean J Radiol* (2019) 20(4):671–82. doi: 10.3348/kjr.2018.0400
15. Kumar V, Gu Y, Basu S, Berglund A, Eschrich SA, Schabath MB, et al. Radiomics: The Process and the Challenges. *Magn Reson Imaging* (2012) 30 (9):1234–48. doi: 10.1016/j.mri.2012.06.010
16. Lambin P, Rios-Velazquez E, Leijenaar R, Carvalho S, van Stiphout RG, Granton P, et al. Radiomics: Extracting More Information From Medical Images Using Advanced Feature Analysis. *Eur J Cancer* (2012) 48(4):441–6. doi: 10.1016/j.ejca.2011.11.036
17. Liu JK, Xu H, Qing HM, Li Y, Yang X, He CJ, et al. Comparison of Radiomic Models Based on Low-Dose and Standard Dose CT for Prediction of Adenocarcinomas and Benign Lesions in Solid Pulmonary Nodules. *Front Oncol* (2021) 10:634298. doi: 10.3389/fonc.2020.634298
18. Yang LF, Yang JB, Zhou XB, Huang LY, Zhao WL, Wang T, et al. Development of a Radiomics Nomogram Based on the 2D and 3D CT Features to Predict the Survival of non-Small Cell Lung Cancer Patients. *Eur Radiol* (2019) 29(5):2196–206. doi: 10.1007/s00330-018-5770-y
19. Shen QJ, Shan YN, Xu W, Hu GZ, Chen WH, Feng Z, et al. Risk Stratification of Thymic Epithelial Tumors by Using a Nomogram Combined With Radiomic Features and TNM Staging. *Eur Radiol* (2021) 31(1):423–35. doi: 10.1007/s00330-020-07100-4
20. Xiao G, Rong WC, Hu YC, Shi ZQ, Yang Y, Ren JL, et al. MRI Radiomics Analysis for Predicting the Pathologic Classification and TNM Staging of Thymic Epithelial Tumors: A Pilot Study. *AJR Am J Roentgenol* (2020) 214 (2):328–40. doi: 10.2214/AJR.19.21696
21. Liu J, Yin P, Wang SC, Liu T, Sun C, Hong N. CT-Based Radiomics Signatures for Predicting the Risk Categorization of Thymic Epithelial Tumors. *Front Oncol* (2021) 11:628534. doi: 10.3389/fonc.2021.628534
22. Hu JP, Zhao YJ, Li MC, Liu Y, Wang F, Weng Q, et al. Machine-Learning-Based Computed Tomography Radiomic Analysis for Histologic Subtype Classification of Thymic Epithelial Tumours. *Eur J Radiol* (2020) 126:108929. doi: 10.1016/j.ejrad.2020.108929
23. Yasaka K, Akai H, Abe O, Ohtomo K, Kiryu S. Quantitative Computed Tomography Texture Analyses for Anterior Mediastinal Masses: Differentiation Between Solid Masses and Cysts. *Eur J Radiol* (2018) 100:85–91. doi: 10.1016/j.ejrad.2018.01.017
24. Jeong YJ, Lee KS, Kim J, Shim YM, Han J, Kwon OJ. Does CT of Thymic Epithelial Tumors Enable Us to Differentiate Histologic Subtypes and Predict Prognosis? *AJR Am J Roentgenol* (2004) 183(2):283–9. doi: 10.2214/ajr.183.2.1830283
25. Marom EM, Rosado-de-Christenson ML, Bruzzi JF, Hara M, Sonett JR, Ketai L. Standard Report Terms for Chest Computed Tomography Reports of Anterior Mediastinal Masses Suspicious for Thymoma. *J Thorac Oncol* (2011) 7 Suppl 3):S1717–23. doi: 10.1097/JTO.0b013e31821e8cd6
26. Priola AM, Priola SM, Gned D, Giraudo MT, Fornari A, Veltri A. Comparison of CT and Chemical-Shift MRI for Differentiating Thymoma From non-Thymomatous Conditions in Myasthenia Gravis: Value of Qualitative and Quantitative Assessment. *Clin Radiol* (2016) 71(3):e157–69. doi: 10.1016/j.crad.2015.12.009
27. Jeung MY, Gasser B, Gangi A, Bogorin A, Charneau D, Wihlm JM, et al. Imaging of Cystic Masses of the Mediastinum. *Radiographics* (2002) 22 Spec No:S79–93. doi: 10.1148/radiographics.22.suppl_1.g02oc09s79
28. Choi YW, McAdams HP, Jeon SC, Hong EK, Kim YH, Im JG, et al. Idiopathic Multilocular Thymic Cyst: CT Features With Clinical and Histopathologic Correlation. *AJR Am J Roentgenol* (2001) 177(4):881–5. doi: 10.2214/ajr.177.4.1770881
29. Tomiyama N, Müller NL, Ellis SJ, Cleverley JR, Okumura M, Miyoshi S, et al. Invasive and Noninvasive Thymoma: Distinctive CT Features. *J Comput Assist Tomogr* (2001) 25(3):388–93. doi: 10.1097/00004728-200105000-00010

Conflict of Interest: Author RZ was employed by Huiying Medical Technology.

The remaining authors declare that the research was conducted in the absence of any commercial or financial relationships that could be construed as a potential conflict of interest.

Publisher's Note: All claims expressed in this article are solely those of the authors and do not necessarily represent those of their affiliated organizations, or those of the publisher, the editors and the reviewers. Any product that may be evaluated in this article, or claim that may be made by its manufacturer, is not guaranteed or endorsed by the publisher.

Copyright © 2021 Zhang, Yang, Lin, Ma, Zhang, Zhang, Wang and Mao. This is an open-access article distributed under the terms of the Creative Commons Attribution License (CC BY). The use, distribution or reproduction in other forums is permitted, provided the original author(s) and the copyright owner(s) are credited and that the original publication in this journal is cited, in accordance with accepted academic practice. No use, distribution or reproduction is permitted which does not comply with these terms.

frontiers in Oncology

REVIEW
published: 03 January 2022
doi: 10.3389/fonc.2021.810419

Imaging Evaluation of Thymoma and Thymic Carcinoma

Chad D. Strange[1], Jitesh Ahuja[1], Girish S. Shroff[1], Mylene T. Truong[1] and Edith M. Marom[2]*

[1] Department of Thoracic Imaging, University of Texas MD Anderson Cancer Center, Houston, TX, United States, [2] Department of Diagnostic Radiology, Chaim Sheba Medical Center, Tel Aviv University, Tel Aviv, Israel

Imaging is integral in the management of patients with thymoma and thymic carcinoma. At initial diagnosis and staging, imaging provides the clinical extent of local invasion as well as distant metastases to stratify patients for therapy and to determine prognosis. Following various modalities of therapy, imaging serves to assess treatment response and detect recurrent disease. While imaging findings overlap, a variety of CT, MRI, and PET/CT characteristics can help differentiate thymoma and thymic carcinoma, with new CT and MRI techniques currently under evaluation showing potential.

Keywords: thymoma, thymic carcinoma, CT, MRI, PET/CT

OPEN ACCESS

Edited by:
Marco Lucchi,
University of Pisa, Italy

Reviewed by:
Chul Kim,
Georgetown University, United States
Meinoshin Okumura,
Toneyama National Hospital (NHO), Japan

****Correspondence:***
Chad D. Strange
CDStrange@mdanderson.org

Specialty section:
This article was submitted to Thoracic Oncology, a section of the journal Frontiers in Oncology

Received: *06 November 2021*
Accepted: *09 December 2021*
Published: *03 January 2022*

Citation:
Strange CD, Ahuja J, Shroff GS, Truong MT and Marom EM (2022) Imaging Evaluation of Thymoma and Thymic Carcinoma. Front. Oncol. 11:810419. doi: 10.3389/fonc.2021.810419

INTRODUCTION

Imaging plays several roles in the management of patients with thymoma and thymic carcinoma. Imaging is integral in the initial diagnosis and staging of patients, emphasizing the detection of locally invasive disease and distant metastases, to properly stratify patients for therapy, and to establish prognosis. Following various modalities of treatment, imaging serves to assess therapy response and to identify recurrent disease. This is particularly important in that patients with resected recurrent disease have similar outcomes as patients without recurrence (1).

ROUTINE IMAGING MODALITIES

Chest radiographs are the most commonly performed imaging examination and can be the first modality to suggest a thymic mass. Larger thymic tumors can result in extra soft tissue projecting over normal anatomic structures. Radiographically, thickening of the anterior junction line can signal a thymic tumor in the prevascular space. Additionally, the "silhouette sign" is another useful radiographic sign. In patients with a normal chest radiograph, the air in the lungs delineates the structures that abut the lung, such as the heart or the mediastinum. When a mass is present, clear delineation of anatomic structures is limited given that the mass now abuts the normal structure instead of air. As the mass and normal mediastinal structures are of similar densities, thus cannot be distinguished one from another, this results in the obscuration of structures or loss of their silhouette, designated the "silhouette sign." The lateral radiograph can help confirm the presence of thymic tumors in the prevascular space. The prevascular space is readily seen on the lateral radiograph behind the sternum and is normally lucent. When a mass is present in this space, it is dense and has a sharp border if the lung abuts it (**Figure 1**). It should be noted, however, that smaller

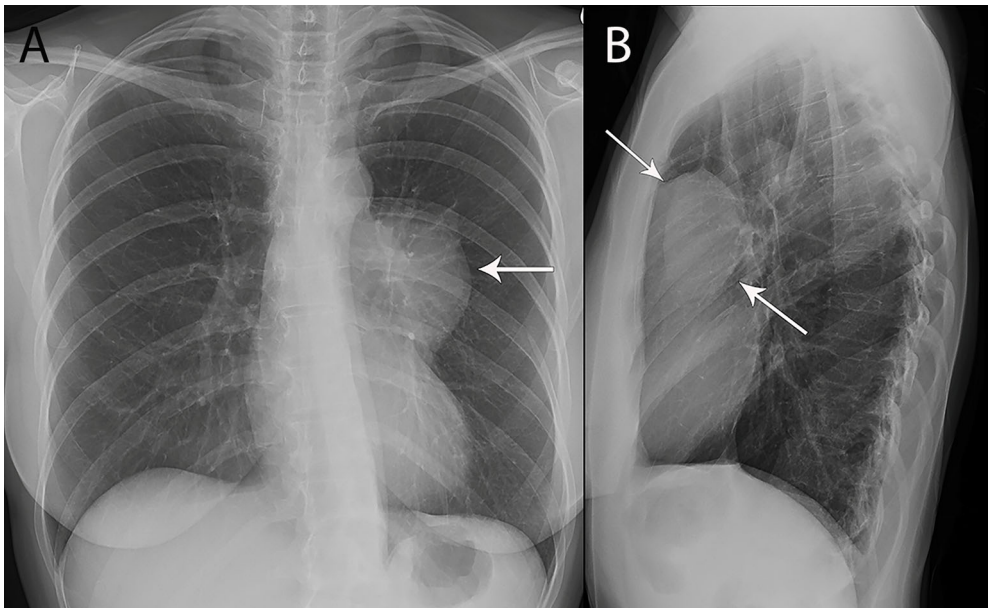

FIGURE 1 | 53 year old woman with thymoma. **(A, B)** Frontal chest radiograph **(A)** shows left mediastinal contour abnormality (arrow) that results in loss of the silhouette of the upper left heart border. **(B)** The lesion is localized to the prevascular mediastinum in the retrosternal space (arrows) on the lateral chest radiograph **(B)**.

prevascular lesions are often not radiographically apparent. Low sensitivity and specificity of routine radiographs in prevascular tumor detection offsets the advantages of low cost and low radiation exposure; therefore, cross-sectional imaging is invariably utilized.

Contrast enhanced computed tomography (CT) is the imaging modality of choice for imaging thymic tumors due to its high spatial and temporal resolution, ease of access, and convenience (2). CT can discern location, morphology, shape, margins, size, density, enhancement, and relationship to, or invasion of, adjacent structures (3) (**Figure 2**). Overall, CT has been found to be equal or superior to magnetic resonance imaging (MRI) in the evaluation of mediastinal masses with the exception of cysts or cystic components of tumors (4) (**Figure 3**).

While MRI is not routinely used in the evaluation of thymic tumors, there are certain scenarios where it is uniquely helpful, such as to distinguish solid from cystic lesions when CT is

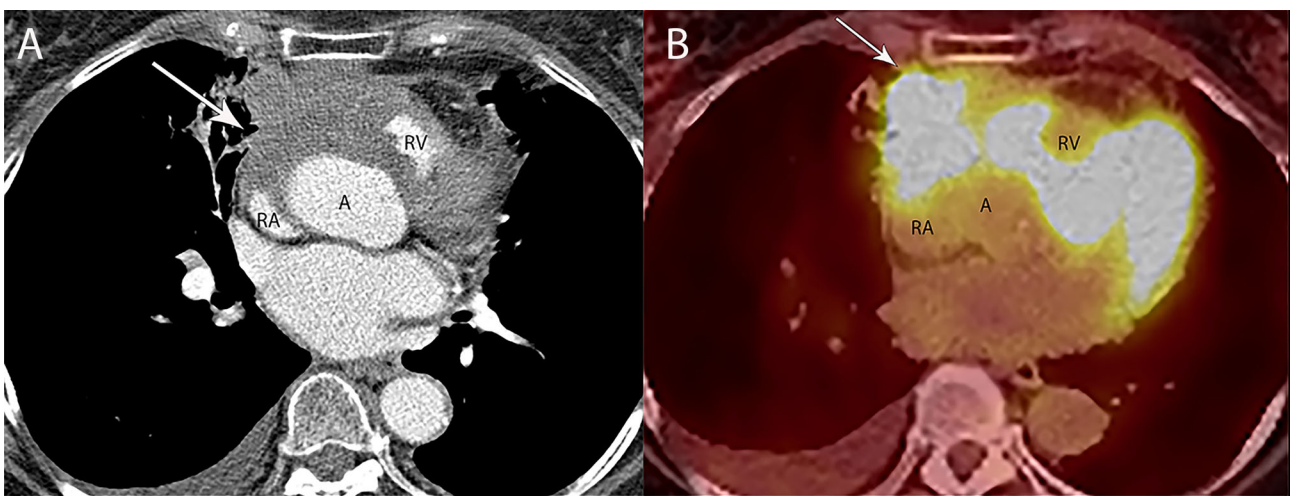

FIGURE 2 | 80 year old woman with adenosquamous thymic carcinoma. **(A)** Contrast-enhanced CT shows right prevascular mediastinal tumor (arrow) invading the pericardium between the right atrium (RA), ascending aorta **(A)** and right ventricle (RV). **(B)** PET/CT shows the tumor is markedly FDG avid.

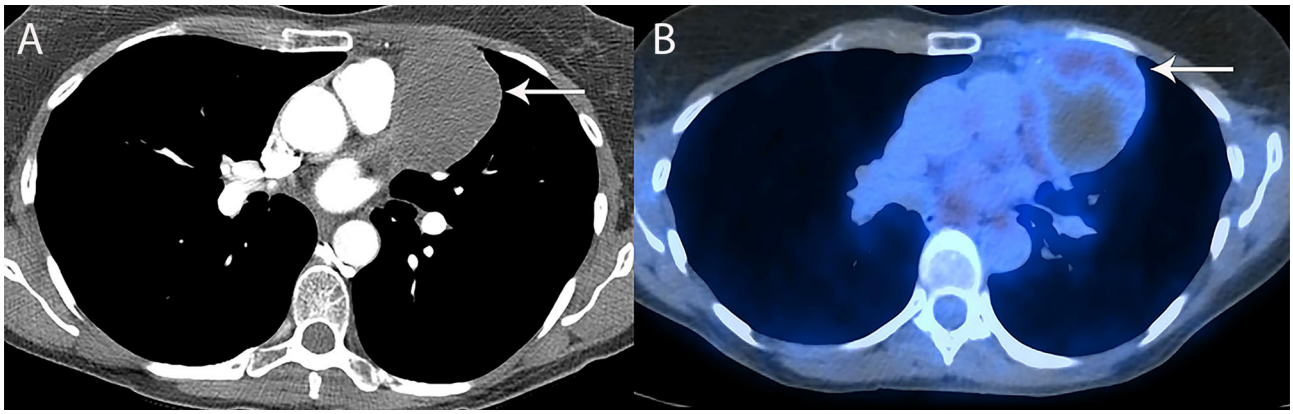

FIGURE 3 | 53 year old woman with thymoma. **(A)** CT shows the left prevascular mediastinal mass (arrow) is mostly homogenous, with low attenuation measuring 10 Hounsfield Units suggesting a cystic component, yet has a denser component of 48 Hounsfield Units along the anterior peripheral aspect suggesting some solid component. **(B)** PET/CT shows FDG uptake with SUVmax of 3.4 along the anterior peripheral aspect of the mass (arrow). At resection, pathology showed thymoma with cystic component and no invasion of the pericardium or lung.

equivocal, to evaluate cystic or necrotic components of a mass, to evaluate for enhancing septae within cystic lesions, and to evaluate for areas of subtle local invasion (**Figures 4**, **5**). Additionally, chemical shift imaging can be utilized to detect microscopic or intravoxel fat, which can help differentiate thymic neoplasm from benign thymic hyperplasia (5–7). MRI can be performed when limiting radiation exposure is of concern, such as in younger patients. Finally, unenhanced MRI can be performed in patients who cannot receive iodinated CT contrast due to contrast allergy or poor renal function.

Fluorodeoxyglucose (FDG) positron emission tomography (PET)/computed tomography (CT) has a complicated and incompletely defined role in the evaluation of thymic masses. Some of the confounding variables related to FDG PET/CT usage include false-positive results, meaning FDG uptake within a non-neoplastic mass, which can be seen in infection, thymic hyperplasia, fibrosing mediastinitis, and other non-neoplastic processes. On the other hand, lack of increased FDG uptake is seen in some histological types of thymic malignancy, and there is lack of standardization in techniques which can result in quantitative variability between studies (8). Other neoplasms found in the prevascular mediastinum are also FDG avid, such as lymphoma or malignant germ cell tumors. Thus the presence of FDG uptake in a prevascular mass cannot distinguish between a thymic epithelial tumor and other tumors which commonly occupy this anatomical area. FDG uptake has been studied to predict tumor invasiveness and prognosis. Some studies reported FDG PET/CT as useful in differentiating low-grade from high-grade thymic malignancies, while other studies reported these observations as controversial owing to overlap in imaging findings and FDG uptake between low-grade and high-grade thymic tumors (9). The role of PET/CT is more clear in aggressive tumors, such as thymic carcinoma, due to higher overall tumor metabolism, with studies indicating that a maximum standard uptake value (SUVmax) of 6 possibly serving as a cutoff to separate thymic carcinoma from lower grade thymic tumors (10) (**Figures 2**, **3**). Finally, PET/CT has a role in the detection of occult metastasis when the tumor is FDG avid.

STAGING

While fifteen different staging systems have been proposed over the years, thymic tumors have predominately been staged using the Masaoka-Koga staging system as it has been shown to correlate with survival (11–13). Masaoka-Koga staging is based on gross and microscopic tumor properties with Stage 1 tumors being completely encapsulated; Stage II tumors demonstrating microscopic invasion through the capsule (IIa) or macroscopic invasion into surrounding fat (IIb); Stage III tumors invading into adjacent structures such as lung, great vessels, or pericardium; and Stage IV tumors demonstrating pleural or pericardial dissemination (IVa) or lymphatic-hematogenous metastasis (IVb) (1). Issues with this staging scheme were that it relied on a small series, of 96 patients from one institution, and was difficult to implement. A capsule was not always present or complete making implementation of the stage II problematic at pathology and impossible to see with imaging at clinical staging.

Given the need to more accurately stage patients prior to treatment (clinical staging) and the need to find a staging system with greater consistency at pathologic examination, as well as proven as a prognostic determinant on a large patient population from multiple institutions, the International Association for the Study of Lung Cancer (IASLC), the International Thymic Malignancies Interest Group (ITMIG), the European Society of Thoracic Surgeons, the Chinese Alliance for Research on Thymomas, and the Japanese Association of Research on Thymus partnered together to develop a TNM staging system for thymic tumors. While the Masaoka-Koga staging system was derived from retrospective series of only 96 patients, the retrospective database of thymic tumors included nearly 10,000

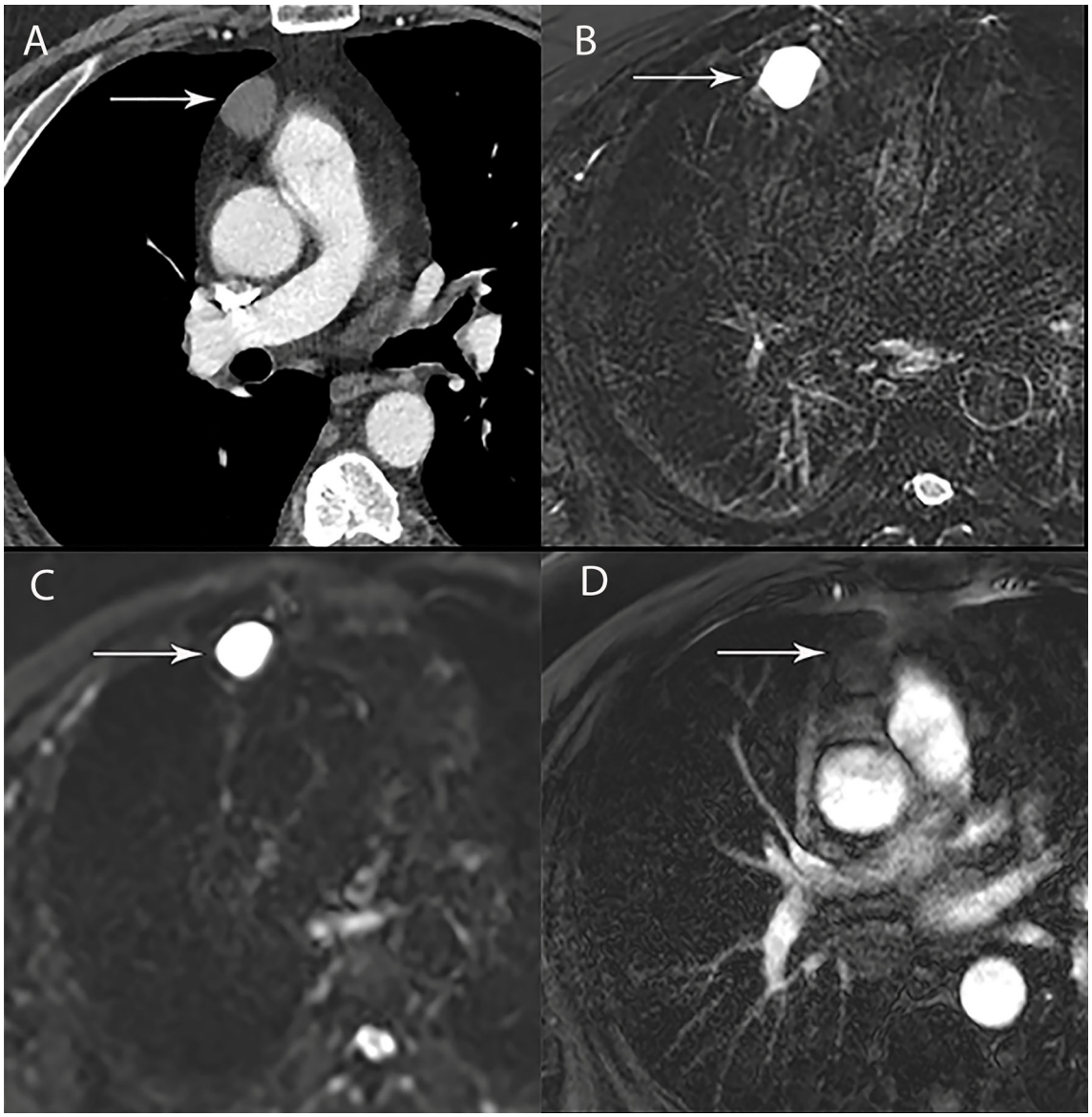

FIGURE 4 | 67 year old man with right thymic cyst. **(A)** Contrast-enhanced CT shows a right prevascular mediastinal 2.2 cm lesion (arrow) with 34 Hounsfield units, which can represent solid or cystic lesion with proteinaceous material or hemorrhage. **(B–D)** MRI is useful to determine that this is a simple thymic cyst (arrow) with high signal intensity on T2 weighted **(B)** and short tau inversion recovery (STIR) **(C)** and no enhancement on the post contrast images **(D)**.

cases (14, 15). These cases were collected for the eighth edition of TNM classification for malignant tumors which has now been adopted by the American Joint Committee on Cancer and the Union for International Cancer Control (16).

In the new TNM classification system for thymic tumors, the T descriptor describes local invasion, and not size of tumor, as size was not found to be a prognostic factor, with T1 tumors demonstrating invasion into the mediastinal fat (T1a) or mediastinal pleura (T1b), T2 tumors demonstrating invasion into the pericardium, T3 tumors demonstrating invasion into the lung, brachiocephalic vein, superior vena cava, chest wall, or phrenic nerve, and T4 tumors demonstrating invasion into the aorta, intrapericardial pulmonary artery, myocardium, trachea, or esophagus. The N descriptor distinguishes anterior/perithymic lymph nodes as N1 and deep intrathoracic or cervical lymph nodes as N2. Pleural and pericardial nodules represent M1a disease and distant organ metastasis represent M1b disease (17–19). While the ultimate assigned stage may be the same with the TNM and Masaoka-Koga staging systems, TNM allows for a more detailed breakdown and reporting of the extent of disease (16). A few highlighted differences help contrast the two staging systems. In TNM, capsular and mediastinal pleural invasion are T1 disease, and in the absence of nodal disease, stage I, compared with stage II disease in Masaoka-Koga.

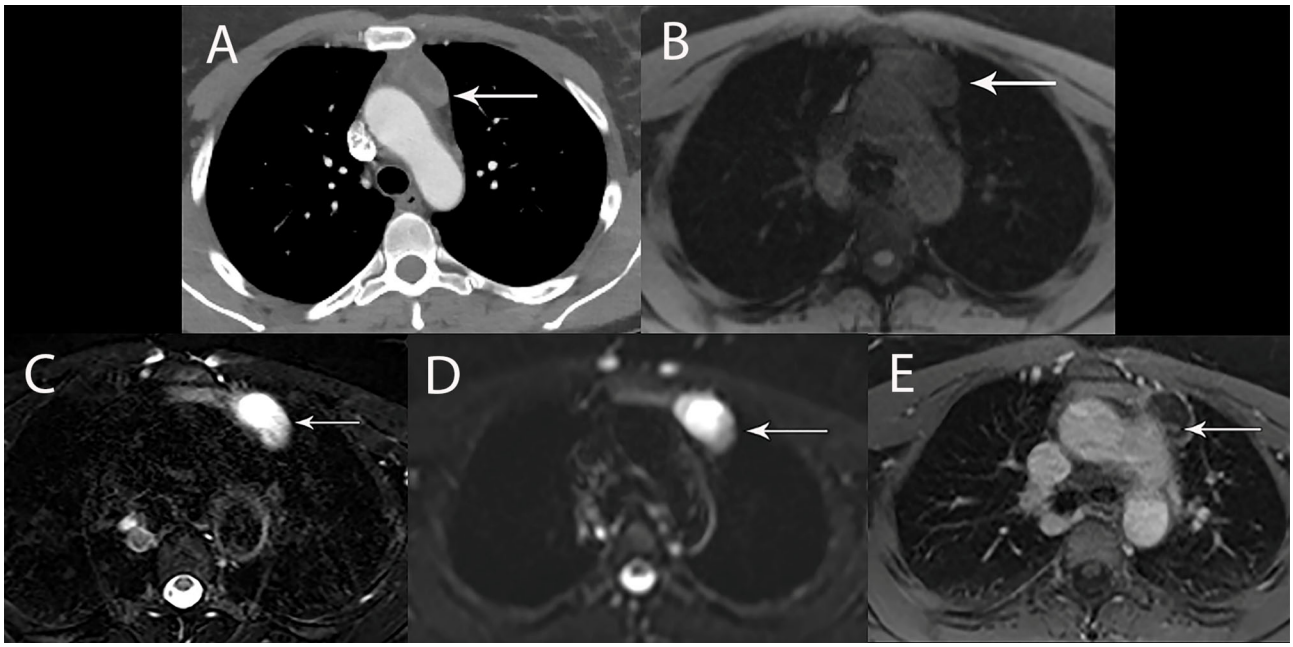

FIGURE 5 | 44 year old woman with cystic thymoma. **(A)** Contrast enhanced CT shows solid component along the posterior aspect. MRI showed intermediate signal intensity on T1 weighted **(B)**, high signal intensity on T2 weighted images **(C)** and DWI **(D)** consistent with cystic component. The small solid component (arrow) shows enhancement on post contrast T1 weighted images **(E)**.

Pericardial invasion is TNM T2/stage II instead of Masaoka-Koga stage III. Anterior/perithymic nodal involvement has been downgraded from Masaoka-Koga stage IVb to TNM stage IVa.

Ried et al. studied 76 patients to compare the Masaoka-Koga staging system with the recently proposed TNM staging system. They found that a number of Masaoka-Koga stage IIa and IIb tumors were reclassified as TNM stage I. Additionally, they reported the TNM system more accurately characterized the more heterogeneous Masaoka-Koga stage III disease to determine which patients were better surgical candidates. They concluded that the TNM staging system was overall clinically useful and applicable as compared with the Masaoka-Koga staging system (20).

A few limitations of the new TNM staging system for thymic tumors have been discussed, however. The number of patients who had nonsurgical treatment was small which could hinder staging predictive ability with higher stage disease. The nodal map was derived from Japanese practice patterns which are more empirically based with more consideration on feasibility of surgical sampling. Finally, due to the limited data available, differentiation between parenchymal nodules (M1b) and pleural/pericardial nodules (M1a) was made empirically, not statistically (16).

ASSESSMENT OF TREATMENT RESPONSE

The most commonly utilized method to assess response to treatment is the Response Evaluation Criteria in Solid Tumors (RECIST) version 1.1. ITMIG does, however, recommend certain modifications and caveats to the use of RECIST version 1.1 in thymic tumors due to unique patterns of spread (8). First, ITMIG recommends pretreatment and posttreatment image interpretation be done by the same experienced radiologist to decrease interobserver variability when assessing the often large irregular tumors, vague borders, and local infiltration (21, 22). Second, because thymic epithelial tumors tend to spread along the pleura, ITMIG recommends using a modification of RECIST similar to that used for malignant pleural mesothelioma (MPM) (8, 12).

A summary of RECIST version 1.1, using the modification for MPM, would involve measuring up to a maximum of two lesions per organ and five lesions in total, representing all involved organs, as target lesions at baseline. Longest diameter measurements are used, with the exception of pleura and lymph nodes which are measured in short axis. When the pleura is used as a target organ, short axis (or perpendicular to the pleura) measurements are taken at two locations at three separate CT levels separated by at least 1 cm. The sum of these pleural measurements, up to a maximum of 6, is the overall pleural measurement, which is then added to non-pleural target lesions up to a total of five (8, 23).

The National Comprehensive Cancer Network (NCCN) recommends a surveillance regimen of CT of the thorax every six months for two years, then annually for ten years in thymoma and annually for five years in thymic carcinoma. Alternatively, ITMIG recommends surveillance frequency for patients after resection of any thymic tumor as annual CT of the thorax for five

years following resection. From years six to eleven alternating yearly CT and chest radiograph is performed, and then yearly chest radiographs thereafter. For resected stage III or IVa thymoma, thymic carcinoma, incomplete resection, or other high-risk tumors, additional CT of the thorax is recommended every six months for the first three years with consideration of CT one to three months after surgery to obtain a new baseline after post-surgical inflammation has resolved (12, 24).

CT is the recommended modality of choice for tumor reassessment given that it is the most reproducible (25). In younger patients and in those who cannot be given CT contrast due to allergy or renal function, MRI can be utilized for tumor reassessment. Kerpel et al. evaluated 22 of 187 patients who underwent resection for thymic epithelial tumors to assess the accuracy of MRI compared with CT for follow-up assessment. They concluded that MRI was an adequate alternative to CT for reassessment with the caveat that in patients with sternotomy wires alternating CT with MRI was recommended given associated artifact (24).

In patients with R0 resection (microscopically margin negative resection) or in patients who demonstrate complete radiologic response to therapy, local recurrence in the prevascular mediastinum is defined as tumor in the thymic bed, pericardial, pleural, or pulmonary parenchymal tumor that is immediately adjacent to the thymic bed, lymph nodes immediately adjacent to thymic bed, or in the site of previous noncontiguous metastasis. Regional recurrence is defined as intrathoracic recurrence that is not contiguous with the thymic bed such as parietal pleural nodules, pericardial nodules, visceral pleural nodules, and lymph nodes not contiguous with the thymic bed. Distal recurrence is defined as extrathoracic recurrence or intraprenchymal pulmonary nodules that are not contiguous with the thymic bed (12).

ROUTINE IMAGING CHARACTERISTICS OF THYMIC TUMORS

The thymus normally appears as a triangular shaped structure in the prevascular space; however, a variety of normal morphological shapes may be seen. Benign and malignant pathologic processes can alter the size and shape of the thymus with considerable overlap which can pose a diagnostic dilemma. Generally, a variety of benign processes can be easily distinguished based on imaging characteristics. A brief review of benign entities will serve as a comparison to the more difficult to distinguish malignant thymic tumors.

BENIGN

Thymic Cysts

Congenital thymic cysts arise from remnants of the thymopharyngeal duct which can occur anywhere along the course of the thymic descent, but most often occur in the prevascular mediastinal space (26). Acquired thymic cysts are more common and are often multi-locular, complex, associated with neoplasm (such as thymoma, lymphoma, or germ cell tumors), radiation therapy, Sjogren syndrome, aplastic anemia, systemic lupus erythematosus, myasthenia gravis, acquired immune deficiency syndrome (AIDS) in children, and can occur after tumor resection (26, 27). In general, on CT, thymic cysts present as well circumscribed round or oval lesions in the prevascular space with fluid density Hounsfield units (HU) under 20, with no thickened, irregular, or enhancing walls. If HU are indeterminate, or if there is a question of enhancement, MRI can be helpful for further evaluation. On MRI, thymic cysts demonstrate increased T2 signal, variable T1 signal depending on protein content, and no appreciable wall or nodular enhancement (**Figure 4**).

Thymic Hyperplasia

True thymic hyperplasia, often referred to as "rebound" hyperplasia, is present when the thymic volume is increased by more than 50%, and is commonly seen after infection, surgery, burns, chemotherapy, radiation therapy, or steroid therapy (**Figure 6**). Lymphoid/follicular hyperplasia is present when there is an increase in the number of lymphoid follicles which is commonly associated with autoimmune diseases, myasthenia gravis (**Figure 7**), and human immunodeficiency virus infection (27–30). In thymic hyperplasia, there is generally symmetric thymic enlargement with smooth contour and margins; however, nodular or bulky appearance can be seen which cannot be readily distinguished from malignancy. In equivocal cases, MRI utilizing in-phase and out-of-phase gradient-echo sequences is performed to identify thymic hyperplasia. Loss of thymic signal during out-of-phase imaging corresponds with microscopic or intravoxel fat, which confirms thymic hyperplasia instead of thymic mass (31) (**Figure 7**).

Thymolipoma

Thymolipoma is a benign, often large, slow growing tumor that arises from the thymus gland. Thymolipomas are composed mainly of adipose tissue with scattered soft tissue/thymic tissue interposed (32, 33). The classic CT appearance of a thymolipoma is a very large predominantly fat density mass in a cardiophrenic angle (**Figure 8**). Occasional symptoms related to compression or displacement of adjacent structures and association with Graves' disease, myasthenia gravis, and hematological disorders may be seen (3, 30).

Malignant

Thymic Epithelial Tumors

Thymic epithelial neoplasms, including thymoma, thymic neuroendocrine tumor/carcinoid, and thymic carcinoma are predominantly prevascular mediastinal masses which can have a myriad of imaging findings, including homogeneous or heterogeneous, solid or solid/cystic, and well-circumscribed or irregular borders. While there is significant imaging overlap between various grades of thymoma and between thymoma and thymic carcinoma, there are clinical and imaging patterns that emerge that aid in differentiation. Malignant thymic tumors have a median age at presentation in the six decade, while more

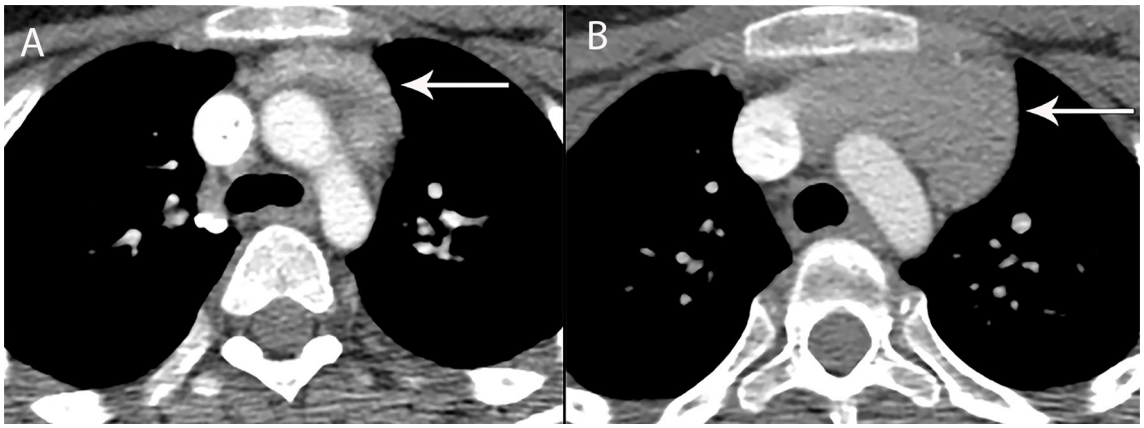

FIGURE 6 | 13 year old boy with chondroblastic osteosarcoma of the femur, treated with methotrexate, doxorubicin, cisplatin **(A)** CT shows the normal thymus (arrow) at baseline. **(B)** CT 4 months later shows increase in size of the thymus consistent with rebound hyperplasia (arrow). Enlargement of the thymus gland due to hyperplasia during the recovery phase from physical stress such as after chemotherapy or recovering from burns, does not displace or change the contour of vessels surrounding it. In the appropriate clinical context of thymic hyperplasia, CT is adequate for diagnosis and MRI is not needed for confirmation.

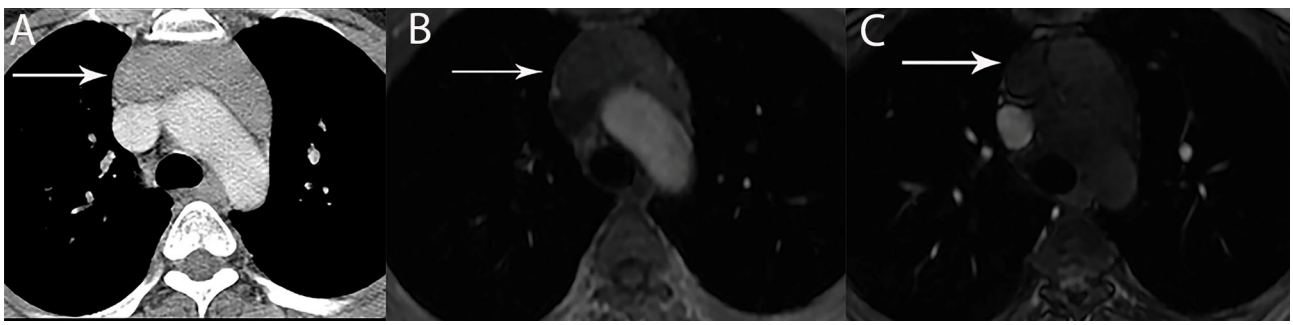

FIGURE 7 | 42 year old woman with Grave's disease and lymphoid thymic hyperplasia. **(A)** Contrast-enhanced CT shows mass-like thymic enlargement (arrow). With such an appearance, thymic hyperplasia, a thymic epithelial neoplasm or lymphoma involvement of the thymus cannot be distinguished one from another. **(B, C)** MRI with in and out of phase imaging shows drop in signal intensity consistent with thymic hyperplasia (arrow), obviating the need for further investigation or biopsy.

benign processes have a median age in the fourth to fifth decades (34–36). Clinical symptoms such as pain or shortness of breath are more common in higher grade and malignant tumors (36). Finally, benign tumors more often demonstrate intralesional fat, are midline, and retain normal thymic triangular shape, while malignant tumors are often larger and are more likely to be locally invasive (37–39). Imaging generalizations will be reviewed, followed by techniques being utilized and studied to more accurately differentiate various thymic tumors.

Thymoma

Thymoma typically presents on CT as a smooth or lobular mass involving one lobe of the thymus, with bilateral involvement more rarely occurring (40). The majority of thymomas demonstrate homogeneous contrast enhancement, however, approximately one third are more heterogeneous due to areas of hemorrhage, necrosis, or cystic change with punctate, linear capsular, or coarse intratumoral calcifications possible (1) (**Figures 9**, **10**). CT characteristics of thymoma can vary according to lesion grade, with vascular invasion, pleural and pericardial involvement more common with higher-grade lesions (**Figure 2**). While imaging overlap is present, higher grade tumors tend to be larger, have lobular or irregular contour, areas of cystic or necrotic change, areas of calcification, and evidence of infiltration of surrounding fat (41–43) (**Figure 11**).

On MRI, thymomas present as prevascular masses with low to intermediate signal intensity on T1 weighted images and high signal intensity on T2 weighted images with areas of cystic change or necrosis presenting as decreased T1 signal intensity and increased T2 signal intensity. Fat suppression imaging can be utilized to better delineate thymomas from surrounding mediastinal fat which facilitates more exact measurements and evaluation of enhancement. When compared to CT, MRI is more limited in the detection of areas of calcification. However, MRI excels in identifying nodules, thickened septae, and/or thickened capsule seen in cystic thymoma and differentiating this from a

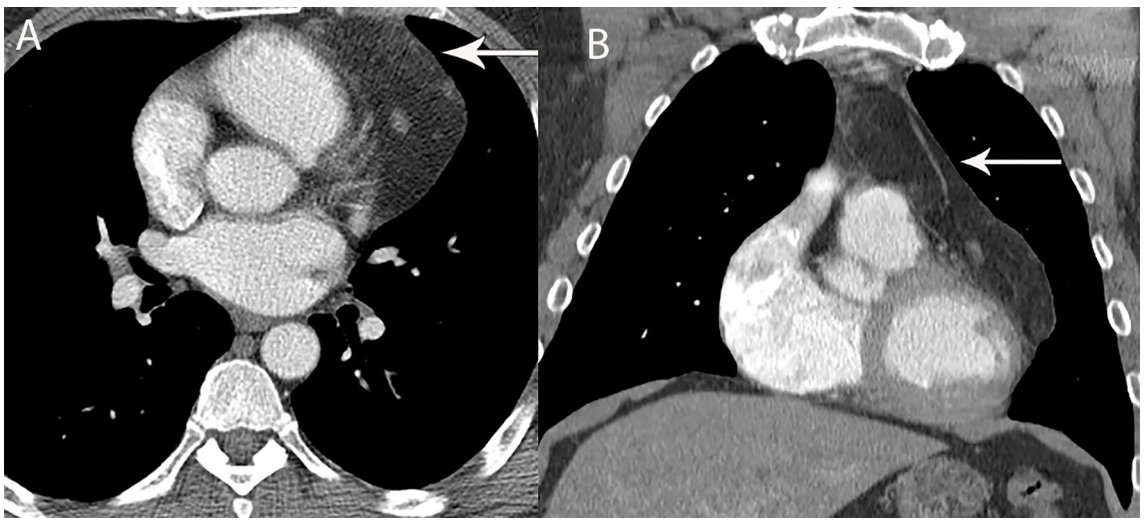

FIGURE 8 | 49 year old man with thymolipoma. **(A, B)** Axial and coronal contrast-enhanced CT shows large left prevascular mediastinal lesion with fat attenuation (arrow).

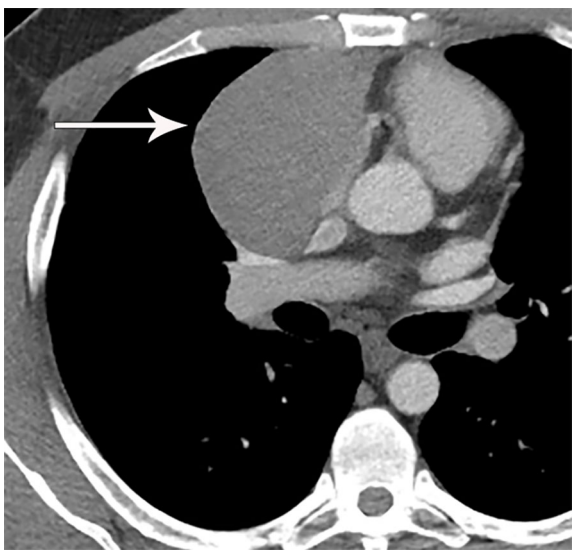

FIGURE 9 | 32 year old man with thymoma and myasthenia gravis. Contrast-enhanced CT shows right prevascular mediastinal mass (arrow).

benign prevascular cyst. MRI also excels in identifying direct cardiac involvement due to its improved contrast resolution as compared to CT (44).

The role of PET/CT in thymoma imaging is limited by the presence of FDG uptake in the normal and hyperplastic thymus, especially in younger adults and children. Physiologic uptake in the thymus has been reported in 28% of patients under 40 years of age and up to 73% in children less than 13 years of age (45). While studies are small, PET/CT has not been demonstrated to reliably differentiate various grades of thymic tumors, although, higher grade tumors do tend towards higher FDG activity (46, 47) (**Figures 2**, **3**). Indium-^{111} octreotide nuclear medicine scans, previously used to demonstrate which tumors may respond to octreotide, which is a second or third line therapy after chemotherapy failure (48), have now been replaced by ^{68}Ga-labeled somatostatin analogues. This is because these ^{68}Ga-labeled somatostatin analogues, such as ^{68}Ga-DOTATATE, are used to image with a PET/CT scanner providing better resolution.

THYMIC CARCINOMA AND NEUROENDOCRINE TUMOR/CARCINOID

Thymic carcinoma and thymic neuroendocrine tumors have similar imaging characteristics that can overlap with higher-grade thymomas, and are thus described together. Thymic carcinomas present as large prevascular masses with irregular poorly marginated borders, demonstrate a greater degree of necrosis, cystic change, and hemorrhage, with greater local invasion when compared to thymomas (1) (**Figures 2**, **12**). Evidence of pleural or pericardial nodules, pleural effusion, or distant metastasis suggests thymic carcinoma or thymic neuroendocrine tumor as compared to thymoma (**Figures 13**, **14**).

In particular, aggressive thymic epithelial tumors can commonly invade or extrinsically compress the superior vena cava (SVC) resulting in SVC syndrome, which is a clinical syndrome marked by swelling of the neck, face, and upper extremities, cough, headache, and shortness of breath.

MRI imaging findings of thymic carcinoma and thymic neuroendocrine tumors are similar as described with thymomas. Thymic carcinomas, however, tend to have a more irregular contour, greater heterogeneity related to hemorrhage, necrosis, and cystic change, greater degree of local vascular and mediastinal invasion, and lymphadenopathy (44, 49, 50).

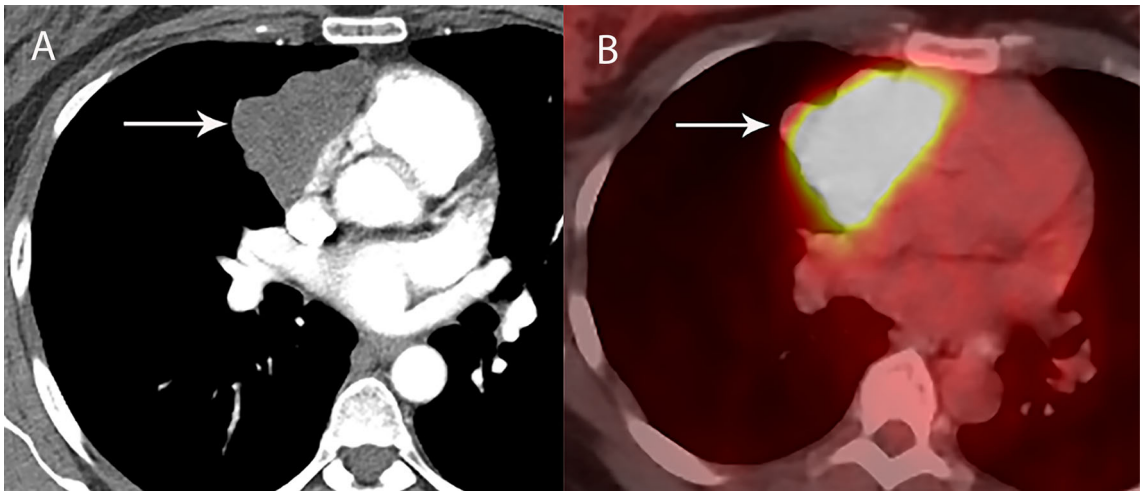

FIGURE 10 | 43 year old woman with thymoma. **(A)** Contrast-enhanced CT shows right prevascular mediastinal mass (arrow). **(B)** FDG PET/CT shows FDG avid thymoma (arrow) with SUV of 16. Presence of intense FDG uptake suggests more aggressive type thymoma or thymic carcinoma.

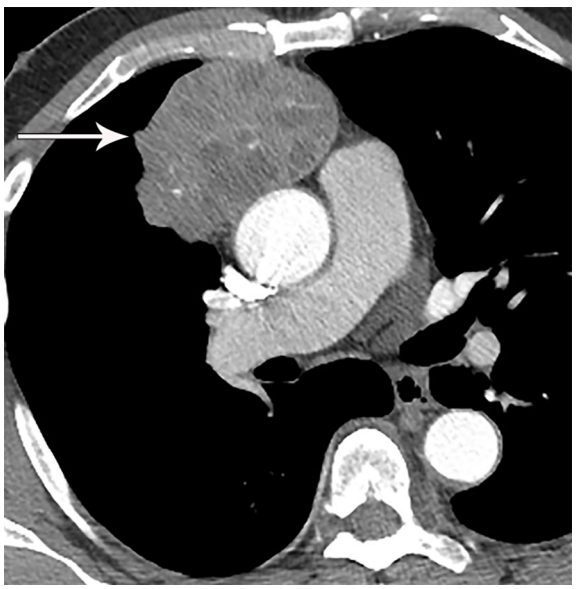

FIGURE 11 | 70 year old man with WHO type B3 thymoma. Contrast-enhanced CT shows right prevascular mediastinal mass with heterogeneous attenuation and areas of necrosis (arrow), consistent with more aggressive WHO subtype identified pathologically.

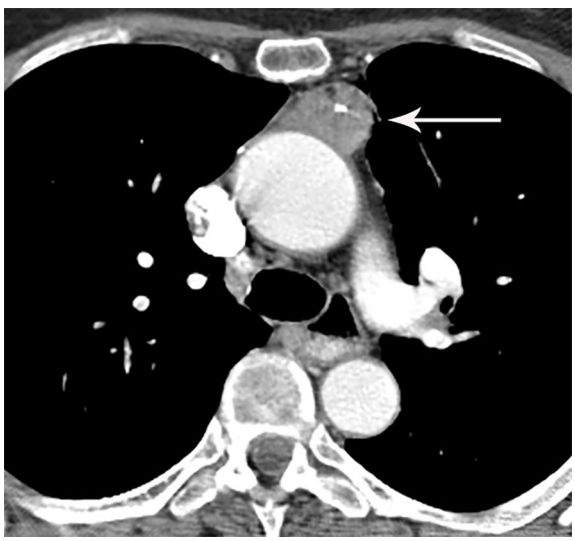

FIGURE 12 | 69 year old woman with thymic carcinoma. Contrast-enhanced CT shows left prevascular mediastinal mass (arrow) with small calcific focus.

While FDG PET/CT does not reliably differentiate various grades of thymoma, several studies of up to 112 patients suggest that PET/CT can be utilized to differentiate thymoma from thymic carcinoma using various cutoffs of SUV max ranging between 4.6 and 6.3 (51, 52). Given increased levels of FDG uptake in higher grade tumors, FDG PET/CT can be useful in the assessment and follow-up of thymic carcinoma (53). Thymic neuroendocrine tumors can also be evaluated with ^{68}Ga-DOTATATE PET/CT which may demonstrate improved sensitivity for lesion detection compared with FDG PET/CT and can additionally identify tumors that are candidates for peptide receptor radiotherapy (PRRT) with ^{177}Lutetium (53) (**Figure 14**).

PRIMARY THYMIC SALIVARY GLAND TUMORS

Primary salivary gland tumors of the thymus are quite rare and must be differentiated from metastasis by detailed radiographic

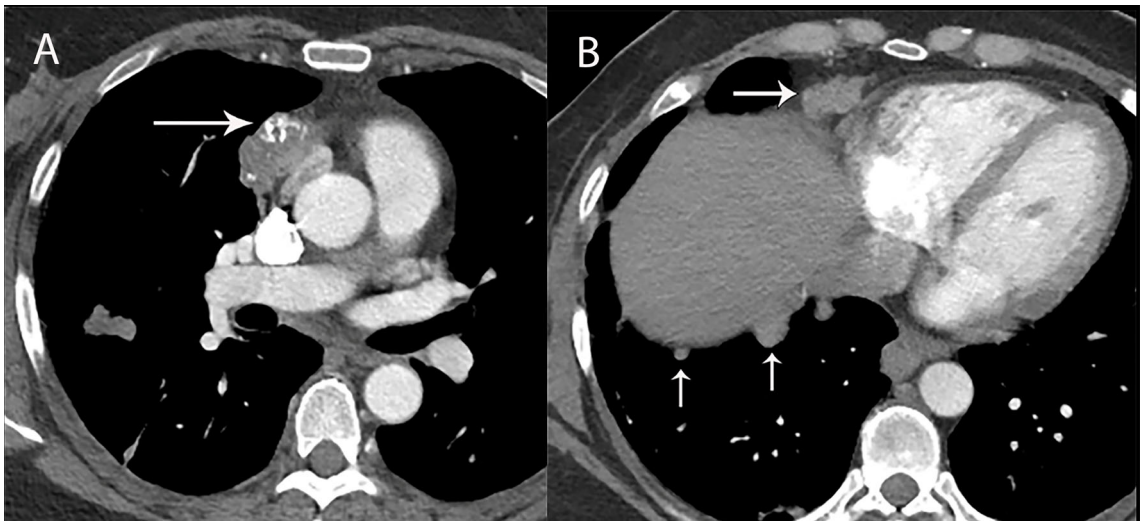

FIGURE 13 | 46 year old woman with thymic carcinoma with pleural metastases. **(A)** Contrast-enhanced CT shows right prevascular mediastinal mass (arrow) with heterogeneous attenuation and calcifications. **(B)** CT shows nodular right diaphragmatic pleural metastases (vertical arrows) and right anterior diaphragmatic nodal metastasis (horizontal arrow).

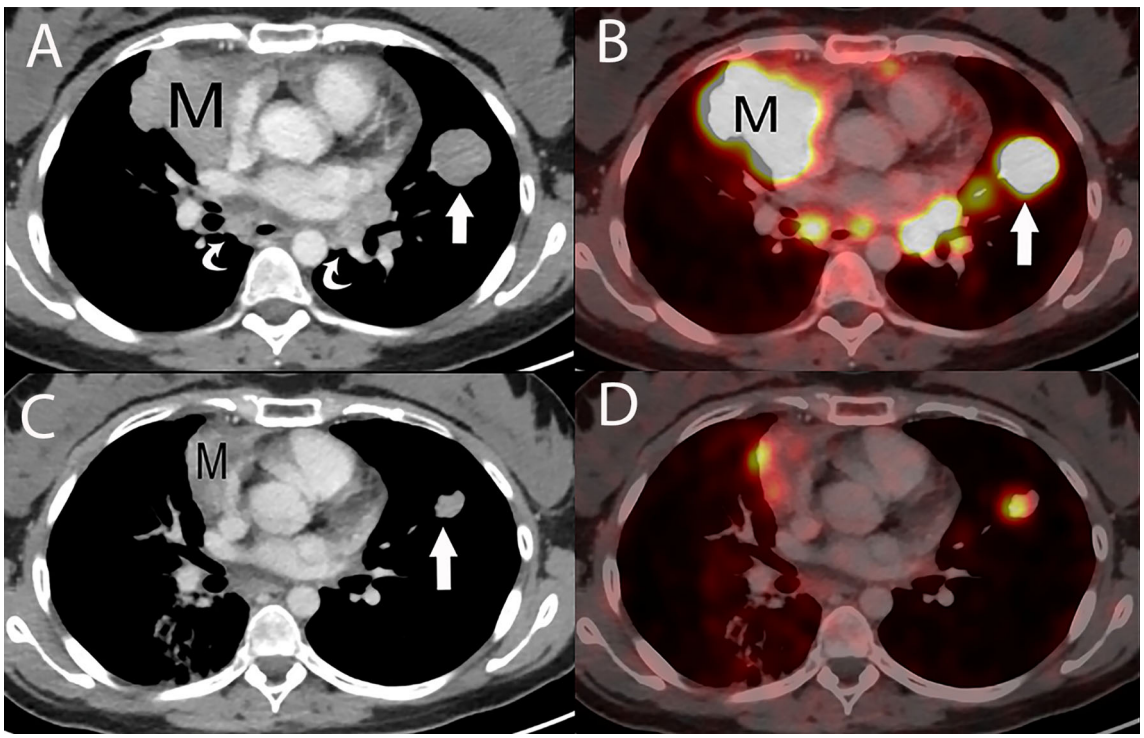

FIGURE 14 | 29 year old woman with metastatic thymic carcinoma treated with peptide receptor radiotherapy (PRRT) with ^{177}Lutetium. **(A)** Baseline contrast enhanced chest CT prior to PRRT treatment shows the primary prevascular mass (M), lung metastasis (straight arrow) and metastatic mediastinal lymphadenopathy (curved arrows). **(B)** Axial fused PET/CT scan at the same level as A, using a somatostatin analogue, Ga ^{68}-DOTATATE, reveals DOTATATE uptake in the primary mass (M), lung metastasis (straight arrow) and mediastinal lymphadenopathy. **(C)** Contrast enhanced chest CT, following two peptide receptor radiotherapy (PRRT) with ^{177}Lutetium sessions show an impressive partial response with a decrease in size of the primary mass (M) and of the lung metastasis (straight arrow), with resolution of the mediastinal lymphadenopathy. **(D)** Axial fused Ga ^{68}-DOTATATE PET/CT scan at the same level as C, shows a corresponding marked decrease in DOTATATE uptake consistent with an impressive metabolic partial response.

and clinical evaluation (54). Only a few dozen cases of primary thymic adenoid cystic carcinoma and mucoepidermoid carcinoma have been reported (55–57). Primary thymic salivary gland tumors have similar imaging characteristics as other thymic epithelial neoplasms with final diagnosis depending on histochemical evaluation.

OTHER PREVASCULAR MEDIASTINAL MASSES

Other prevascular mediastinal masses can have overlapping imaging features with thymic epithelial tumors. Hodgkin and non-Hodgkin lymphomas can be seen in the prevascular space. In distinction from higher grade thymic epithelial tumors, however, lymphoma generally presents as a homogeneous smooth or lobulated soft tissue mass that may surround, but rarely invades, adjacent structures. Calcifications are rare in untreated lymphoma.

Additionally, a variety of germ-cell tumors including benign mature teratoma and malignant embryonal carcinoma, yolk sac tumor, choriocarcinoma, and mixed germ cell tumor can be seen in the prevascular space. Heterogeneously enhancing masses with areas of cystic change, necrosis, and calcification have overlapping imaging features with thymic epithelial tumors.

ADVANCED IMAGING OPTIONS

CT

A variety of CT techniques are being evaluated to better distinguish various prevascular mediastinal masses. CT perfusion, a functional imaging technique, provides quantitative data on tissue perfusion by acquiring specific graphs for tissue blood flow (BF), blood volume (BV), and permeability surface (PS) which can be used to evaluate tumor angiogenesis, tumor infiltration, and response to therapy (58). Bakan et al. found that while CT perfusion values were not significantly different between thymoma and thymic hyperplasia, there were significant differences in BF and BV values between thymomas and malignant prevascular lesions, such as thymic carcinoma, demonstrating the role of CT perfusion imaging to aid in differentiation between thymoma and thymic carcinoma (59).

Dual-energy computed tomography (DECT) has been evaluated to differentiate prevascular masses with malignant tumors revealing higher iodine concentrations (IC) as compared to benign tumors (60). Testing this on 37 patients, Chang et al. found that iodine related Hounsfield units (IHU) and IC were different among low-risk thymomas, high-risk thymomas, and thymic carcinomas, with lower values noted in higher grade tumors, presumably due to the presence of necrosis (61). They concluded that DECT, using iodine concentration measurement derived quantitative analysis, could help differentiate between low-risk thymoma, high-risk thymoma, and thymic carcinoma.

MRI

It has been noted that routine contrast enhanced MRI cannot reliably differentiate low-risk from high-risk thymic epithelial tumors (50). Diffusion-weighted imaging (DWI) and apparent diffusion coefficient (ADC) values, which are generated using DWI data, are non-invasive functional MRI techniques that allow for quantitative evaluation of thymic epithelial tumors. Razek et al. demonstrated in a group of 30 patients with thymic epithelial tumor, that an ADC cutoff value of 1.22 x 10^3 mm2/sec could be used to differentiate low-risk thymoma from high-risk thymoma and thymic carcinoma with an 87% sensitivity, 85% specificity, and 86% accuracy (62). Generally, hot-spot regions of interest (ROI) are utilized for DWI/ADC measurements because of ease of use. However, given concern for errors in sampling, studies have shown that histogram analysis of ADC maps can be utilized for more accurate evaluation and continued ability to aid in differentiation between low-risk thymomas, high-risk thymomas, and thymic carcinomas (63, 64).

Dynamic contrast enhanced (DCE) MRI has also been studied in relation to prevascular mediastinal tumors. In a study comparing thymic epithelial tumors, lymphoma, and malignant germ cell tumors, Yabuuchi et al. found that only thymic epithelial tumors demonstrated a washout pattern on DCE-MRI, possibly due to high tumor cellularity and limited stroma, as compared to other tumor types (65, 66). Similarly, in a study evaluating the ability of DCE-MRI to differentiate thymic carcinoma from thymic lymphoma in 29 patients, Shen et al. reported that reflux rate constant from the extracellular extravascular space (EES) to the blood plasma (k_{ep}) was lower in thymic carcinoma and that the volume fraction of the EES (v_e) was higher in thymic carcinoma as compared to thymic lymphoma (67). While these results are interesting and promising, further research is needed to clarify if DCE-MRI can be utilized to differentiate between various grades of thymoma and between thymoma and thymic carcinoma. Finally, early work reveals that quantitative features derived from MRI images are related to biologic behavior and radiomics models (advanced mathematical analysis of existing data) could help facilitate predictions of pathologic classification and staging of thymic epithelial tumors (68).

CONCLUSION

Imaging plays an integral role in the management of patients with thymoma and thymic carcinoma. Imaging is used in the initial diagnosis and staging of patients, particularly in the detection of locally invasive disease and distant metastasis, to stratify patients for therapy, and to determine prognosis. Following various modalities of therapy, imaging serves to assess treatment response and to detect recurrent disease. While imaging findings overlap, a variety of CT, MRI, and PET/CT characteristics can help differentiate thymoma and thymic carcinoma, with new CT and MRI techniques currently under evaluation showing potential.

AUTHOR CONTRIBUTIONS

CS wrote the first draft of the manuscript. All authors contributed to obtaining images, manuscript revision, read, and approved the submitted version.

REFERENCES

1. Benveniste MF, Rosado-de-Christenson ML, Sabloff BS, Moran CA, Swisher SG, Marom EM. Role of Imaging in the Diagnosis, Staging, and Treatment of Thymoma. *Radiographics* (2011) 31(7):1847–61; discussion 61-3. doi: 10.1148/rg.317115505
2. Li HR, Gao J, Jin C, Jiang JH, Ding JY. Comparison Between CT and MRI in the Diagnostic Accuracy of Thymic Masses. *J Cancer* (2019) 10(14):3208–13. doi: 10.7150/jca.30240
3. Carter BW, Okumura M, Detterbeck FC, Marom EM. Approaching the Patient With an Anterior Mediastinal Mass: A Guide for Radiologists. *J Thorac Oncol* (2014) 9(9 Suppl 2):S110–8. doi: 10.1097/JTO.0000000000000295
4. Tomiyama N, Honda O, Tsubamoto M, Inoue A, Sumikawa H, Kuriyama K, et al. Anterior Mediastinal Tumors: Diagnostic Accuracy of CT and MRI. *Eur J Radiol* (2009) 69(2):280–8. doi: 10.1016/j.ejrad.2007.10.002
5. Ackman JB. MR Imaging of Mediastinal Masses. *Magn Reson Imaging Clin N Am* (2015) 23(2):141–64. doi: 10.1016/j.mric.2015.01.002
6. Ackman JB, Wu CC. MRI of the Thymus. *AJR Am J Roentgenol* (2011) 197(1): W15–20. doi: 10.2214/AJR.10.4703
7. Daye D, Ackman JB. Characterization of Mediastinal Masses by MRI: Techniques and Applications. *Appl Radiol* (2017) 46(7):10–22.
8. Benveniste MF, Korst RJ, Rajan A, Detterbeck FC, Marom EMInternational Thymic Malignancy Interest G. A Practical Guide From the International Thymic Malignancy Interest Group (ITMIG) Regarding the Radiographic Assessment of Treatment Response of Thymic Epithelial Tumors Using Modified RECIST Criteria. *J Thorac Oncol* (2014) 9(9 Suppl 2):S119–24. doi: 10.1097/JTO.0000000000000296
9. Lococo F, Cesario A, Okami J, Cardillo G, Cavuto S, Tokunaga T, et al. Role of Combined 18F-FDG-PET/CT for Predicting the WHO Malignancy Grade of Thymic Epithelial Tumors: A Multicenter Analysis. *Lung Cancer* (2013) 82 (2):245–51. doi: 10.1016/j.lungcan.2013.08.003
10. Benveniste MF, Moran CA, Mawlawi O, Fox PS, Swisher SG, Munden RF, et al. FDG PET-CT Aids in the Preoperative Assessment of Patients With Newly Diagnosed Thymic Epithelial Malignancies. *J Thorac Oncol* (2013) 8 (4):502–10. doi: 10.1097/JTO.0b013e3182835549
11. Falkson CB, Bezjak A, Darling G, Gregg R, Malthaner R, Maziak DE, et al. The Management of Thymoma: A Systematic Review and Practice Guideline. *J Thorac Oncol* (2009) 4(7):911–9. doi: 10.1097/JTO.0b013e3181a4b8e0
12. Huang J, Detterbeck FC, Wang Z, Loehrer PJC. Standard Outcome Measures for Thymic Malignancies. *J Thorac Oncol* (2010) 5(12):2017–23. doi: 10.1097/JTO.0b013e3181f13682
13. Filosso PL, Ruffini E, Lausi PO, Lucchi M, Oliaro A, Detterbeck F. Historical Perspectives: The Evolution of the Thymic Epithelial Tumors Staging System. *Lung Cancer* (2014) 83(2):126–32. doi: 10.1016/j.lungcan.2013.09.013
14. Huang J, Ahmad U, Antonicelli A, Catlin AC, Fang W, Gomez D, et al. Development of the International Thymic Malignancy Interest Group International Database: An Unprecedented Resource for the Study of a Rare Group of Tumors. *J Thorac Oncol* (2014) 9(10):1573–8. doi: 10.1097/JTO.0000000000000269
15. Masaoka A, Monden Y, Nakahara K, Tanioka T. Follow-Up Study of Thymomas With Special Reference to Their Clinical Stages. *Cancer* (1981) 48(11):2485–92. doi: 10.1002/1097-0142(19811201)48:11<2485::AID-CNCR2820481123>3.0.CO;2-R
16. Ahmad U. The Eighth Edition TNM Stage Classification for Thymic Tumors: What do I Need to Know? *J Thorac Cardiovasc Surg* (2021) 161(4):1524–9. doi: 10.1016/j.jtcvs.2020.10.131
17. Bhora FY, Chen DJ, Detterbeck FC, Asamura H, Falkson C, Filosso PL, et al. The ITMIG/IASLC Thymic Epithelial Tumors Staging Project: A Proposed Lymph Node Map for Thymic Epithelial Tumors in the Forthcoming 8th Edition of the TNM Classification of Malignant Tumors. *J Thorac Oncol* (2014) 9(9):S88–96. doi: 10.1097/JTO.0000000000000293
18. Kondo K, Van Schil P, Detterbeck FC, Okumura M, Stratton K, Giroux D, et al. The IASLC/ITMIG Thymic Epithelial Tumors Staging Project: Proposals for the N and M Components for the Forthcoming (8th) Edition of the TNM Classification of Malignant Tumors. *J Thorac Oncol* (2014) 9(9 Suppl 2):S81–7. doi: 10.1097/JTO.0000000000000291
19. Nicholson AG, Detterbeck FC, Marino M, Kim J, Stratton K, Giroux D, et al. The IASLC/ITMIG Thymic Epithelial Tumors Staging Project: Proposals for the T Component for the Forthcoming (8th) Edition of the TNM Classification of Malignant Tumors. *J Thorac Oncol* (2014) 9(9):S73–80. doi: 10.1097/JTO.0000000000000303
20. Ried M, Eicher MM, Neu R, Sziklavari Z, Hofmann HS. Evaluation of the New TNM-Staging System for Thymic Malignancies: Impact on Indication and Survival. *World J Surg Oncol* (2017) 15(1):214. doi: 10.1186/s12957-017-1283-4
21. Erasmus JJ, Gladish GW, Broemeling L, Sabloff BS, Truong MT, Herbst RS, et al. Interobserver and Intraobserver Variability in Measurement of non-Small-Cell Carcinoma Lung Lesions: Implications for Assessment of Tumor Response. *J Clin Oncol* (2003) 21(13):2574–82. doi: 10.1200/JCO.2003.01.144
22. Schwartz LH, Ginsberg MS, DeCorato D, Rothenberg LN, Einstein S, Kijewski P, et al. Evaluation of Tumor Measurements in Oncology: Use of Film-Based and Electronic Techniques. *J Clin Oncol* (2000) 18(10):2179–84. doi: 10.1200/JCO.2000.18.10.2179
23. Byrne MJ, Nowak AK. Modified RECIST Criteria for Assessment of Response in Malignant Pleural Mesothelioma. *Ann Oncol* (2004) 15(2):257–60. doi: 10.1093/annonc/mdh059
24. Kerpel A, Beytelman A, Ofek E, Marom EM. Magnetic Resonance Imaging for the Follow-Up of Treated Thymic Epithelial Malignancies. *J Thorac Imaging* (2019) 34(6):345–50. doi: 10.1097/RTI.0000000000000444
25. Eisenhauer EA, Therasse P, Bogaerts J, Schwartz LH, Sargent D , Ford R, et al. New Response Evaluation Criteria in Solid Tumours: Revised RECIST Guideline (Version 1.1). *Eur J Cancer* (2009) 45(2):228–47. doi: 10.1016/j.ejca.2008.10.026
26. Quint LE. Imaging of Anterior Mediastinal Masses. *Cancer Imaging* (2007) 7 Spec No A:S56–62. doi: 10.1102/1470-7330.2007.9014
27. Shahrzad M, Le TS, Silva M, Bankier AA, Eisenberg RL. Anterior Mediastinal Masses. *AJR Am J Roentgenol* (2014) 203(2):W128–38. doi: 10.2214/AJR.13.11998
28. Juanpere S, Canete N, Ortuno P, Martinez S, Sanchez G, Bernado L. A Diagnostic Approach to the Mediastinal Masses. *Insights Imaging* (2013) 4 (1):29–52. doi: 10.1007/s13244-012-0201-0
29. Nasseri F, Eftekhari F. Clinical and Radiologic Review of the Normal and Abnormal Thymus: Pearls and Pitfalls. *Radiographics* (2010) 30(2):413–28. doi: 10.1148/rg.302095131
30. Nishino M, Ashiku SK, Kocher ON, Thurer RL, Boiselle PM, Hatabu H. The Thymus: A Comprehensive Review. *Radiographics* (2006) 26(2):335–48. doi: 10.1148/rg.262045213
31. Inaoka T, Takahashi K, Mineta M, Yamada T, Shuke N, Okizaki A, et al. Thymic Hyperplasia and Thymus Gland Tumors: Differentiation With Chemical Shift MR Imaging. *Radiology* (2007) 243(3):869–76. doi: 10.1148/radiol.2433060797
32. Gaerte SC, Meyer CA, Winer-Muram HT, Tarver RD, Conces DJJr. Fat-Containing Lesions of the Chest. *Radiographics* (2002) 22 Spec No:S61–78. doi: 10.1148/radiographics.22.suppl_1.g02oc08s61
33. Molinari F, Bankier AA, Eisenberg RL. Fat-Containing Lesions in Adult Thoracic Imaging. *AJR Am J Roentgenol* (2011) 197(5):W795–813. doi: 10.2214/AJR.11.6932
34. de Jong WK, Blaauwgeers JL, Schaapveld M, Timens W, Klinkenberg TJ, Groen HJ. Thymic Epithelial Tumours: A Population-Based Study of the Incidence, Diagnostic Procedures and Therapy. *Eur J Cancer* (2008) 44 (1):123–30. doi: 10.1016/j.ejca.2007.11.004
35. Engels EA, Pfeiffer RM. Malignant Thymoma in the United States: Demographic Patterns in Incidence and Associations With Subsequent Malignancies. *Int J Cancer* (2003) 105(4):546–51. doi: 10.1002/ijc.11099
36. McErlean A, Huang J, Zabor EC, Moskowitz CS, Ginsberg MS. Distinguishing Benign Thymic Lesions From Early-Stage Thymic Malignancies on Computed Tomography. *J Thorac Oncol* (2013) 8(7):967–73. doi: 10.1097/JTO.0b013e3182904bc2
37. Jeong YJ, Lee KS, Kim J, Shim YM, Han J, Kwon OJ. Does CT of Thymic Epithelial Tumors Enable Us to Differentiate Histologic Subtypes and Predict Prognosis? *AJR Am J Roentgenol* (2004) 183(2):283–9. doi: 10.2214/ajr.183.2.1830283
38. Jung KJ, Lee KS, Han J, Kim J, Kim TS, Kim EA. Malignant Thymic Epithelial Tumors: CT-Pathologic Correlation. *AJR Am J Roentgenol* (2001) 176(2):433–9. doi: 10.2214/ajr.176.2.1760433
39. Rosado-de-Christenson ML, Templeton PA, Moran CA. From the Archives of the AFIP. Mediastinal Germ Cell Tumors: Radiologic and Pathologic Correlation. *Radiographics* (1992) 12(5):1013–30. doi: 10.1148

40. Rosado-de-Christenson ML, Strollo DC, Marom EM. Imaging of Thymic Epithelial Neoplasms. *Hematol Oncol Clin North Am* (2008) 22(3):409–31. doi: 10.1016/j.hoc.2008.03.011
41. Priola AM, Priola SM, Di Franco M, Cataldi A, Durando S, Fava C. Computed Tomography and Thymoma: Distinctive Findings in Invasive and Noninvasive Thymoma and Predictive Features of Recurrence. *Radiol Med* (2010) 115(1):1–21. doi: 10.1007/s11547-009-0478-3
42. Tomiyama N, Muller NL, Ellis SJ, Cleverley JR, Okumura M, Miyoshi S, et al. Invasive and Noninvasive Thymoma: Distinctive CT Features. *J Comput Assist Tomogr* (2001) 25(3):388–93. doi: 10.1097/00004728-200105000-00010
43. Marom EM, Milito MA, Moran CA, Liu P, Correa AM, Kim ES, et al. Computed Tomography Findings Predicting Invasiveness of Thymoma. *J Thorac Oncol* (2011) 6(7):1274–81. doi: 10.1097/JTO.0b013e31821c4203
44. Sadohara J, Fujimoto K, Muller NL, Kato S, Takamori S, Ohkuma K, et al. Thymic Epithelial Tumors: Comparison of CT and MR Imaging Findings of Low-Risk Thymomas, High-Risk Thymomas, and Thymic Carcinomas. *Eur J Radiol* (2006) 60(1):70–9. doi: 10.1016/j.ejrad.2006.05.003
45. Jerushalmi J, Frenkel A, Bar-Shalom R, Khoury J, Israel O. Physiologic Thymic Uptake of 18F-FDG in Children and Young Adults: A PET/CT Evaluation of Incidence, Patterns, and Relationship to Treatment. *J Nucl Med* (2009) 50(6):849–53. doi: 10.2967/jnumed.108.058586
46. Endo M, Nakagawa K, Ohde Y, Okumura T, Kondo H, Igawa S, et al. Utility of 18FDG-PET for Differentiating the Grade of Malignancy in Thymic Epithelial Tumors. *Lung Cancer* (2008) 61(3):350–5. doi: 10.1016/j.lungcan.2008.01.003
47. Sung YM, Lee KS, Kim BT, Choi JY, Shim YM, Yi CA. 18f-FDG PET/CT of Thymic Epithelial Tumors: Usefulness for Distinguishing and Staging Tumor Subgroups. *J Nucl Med* (2006) 47(10):1628–34.
48. Loehrer PJ, Wang W, Johnson DH, Aisner SC, Ettinger DSEastern Cooperative Oncology Group Phase IIT. Octreotide Alone or With Prednisone in Patients With Advanced Thymoma and Thymic Carcinoma: An Eastern Cooperative Oncology Group Phase II Trial. *J Clin Oncol* (2004) 22(2):293–9. doi: 10.1200/JCO.2004.02.047
49. Han J, Lee KS, Yi CA, Kim TS, Shim YM, Kim J, et al. Thymic Epithelial Tumors Classified According to a Newly Established WHO Scheme: CT and MR Findings. *Korean J Radiol* (2003) 4(1):46–53. doi: 10.3348/kjr.2003.4.1.46
50. Inoue A, Tomiyama N, Fujimoto K, Sadohara J, Nakamichi I, Tomita Y, et al. MR Imaging of Thymic Epithelial Tumors: Correlation With World Health Organization Classification. *Radiat Med* (2006) 24(3):171–81. doi: 10.1007/s11604-005-1530-4
51. Nakagawa K, Takahashi S, Endo M, Ohde Y, Kurihara H, Terauchi T. Can (18)F-FDG PET Predict the Grade of Malignancy in Thymic Epithelial Tumors? An Evaluation of Only Resected Tumors. *Cancer Manag Res* (2017) 9:761–8. doi: 10.2147/CMAR.S146522
52. Shibata H, Nomori H, Uno K, Sakaguchi K, Nakashima R, Iyama K, et al. 18F-Fluorodeoxyglucose and 11C-Acetate Positron Emission Tomography are Useful Modalities for Diagnosing the Histologic Type of Thymoma. *Cancer* (2009) 115(11):2531–8. doi: 10.1002/cncr.24278
53. Hephzibah J, Shanthly N, Oommen R. Diagnostic Utility of PET CT in Thymic Tumours With Emphasis on 68Ga-DOTATATE PET CT in Thymic Neuroendocrine Tumour - Experience at a Tertiary Level Hospital in India. *J Clin Diagn Res* (2014) 8(9):QC01–3. doi: 10.7860/JCDR/2014/10499.4840
54. Woo WL, Panagiotopoulos N, Gvinianidze L, Proctor I, Lawrence D. Primary Mucoepidermoid Carcinoma of the Thymus Presenting With Myasthenia Gravis. *J Thorac Dis* (2014) 6(10):E223–5. doi: 10.3978/j.issn.2072-1439.2014.09.19
55. Nonaka D, Klimstra D, Rosai J. Thymic Mucoepidermoid Carcinomas: A Clinicopathologic Study of 10 Cases and Review of the Literature. *Am J Surg Pathol* (2004) 28(11):1526–31. doi: 10.1097/01.pas.0000137999.23780.2a
56. Wu SG, Li Y, Li B, Tian XY, Li Z. Unusual Combined Thymic Mucoepidermoid Carcinoma and Thymoma: A Case Report and Review of Literature. *Diagn Pathol* (2014) 9:8. doi: 10.1186/1746-1596-9-8
57. Yasuda M, Yasukawa T, Ozaki D, Yusa T. Mucoepidermoid Carcinoma of the Thymus. *Jpn J Thorac Cardiovasc Surg* (2006) 54(1):23–6. doi: 10.1007/BF02743780
58. Trojanowska A, Trojanowski P, Bisdas S, Staskiewicz G, Drop A, Klatka J, et al. Squamous Cell Cancer of Hypopharynx and Larynx - Evaluation of Metastatic Nodal Disease Based on Computed Tomography Perfusion Studies. *Eur J Radiol* (2012) 81(5):1034–9. doi: 10.1016/j.ejrad.2011.01.084
59. Bakan S, Kandemirli SG, Dikici AS, Ersen E, Yildirim O, Samanci C, et al. Evaluation of Anterior Mediastinal Solid Tumors by CT Perfusion: A Preliminary Study. *Diagn Interv Radiol* (2017) 23(1):10–4. doi: 10.5152/dir.2016.16093
60. Lee SH, Hur J, Kim YJ, Lee HJ, Hong YJ, Choi BW. Additional Value of Dual-Energy CT to Differentiate Between Benign and Malignant Mediastinal Tumors: An Initial Experience. *Eur J Radiol* (2013) 82(11):2043–9. doi: 10.1016/j.ejrad.2013.05.040
61. Chang S, Hur J, Im DJ, Suh YJ, Hong YJ, Lee HJ, et al. Volume-Based Quantification Using Dual-Energy Computed Tomography in the Differentiation of Thymic Epithelial Tumours: An Initial Experience. *Eur Radiol* (2017) 27(5):1992–2001. doi: 10.1007/s00330-016-4542-9
62. Abdel Razek AA, Khairy M, Nada N. Diffusion-Weighted MR Imaging in Thymic Epithelial Tumors: Correlation With World Health Organization Classification and Clinical Staging. *Radiology* (2014) 273(1):268–75. doi: 10.1148/radiol.14131643
63. Guo Y, Kong QC, Zhu YQ, Liu ZZ, Peng LR, Tang WJ, et al. Whole-Lesion Histogram Analysis of the Apparent Diffusion Coefficient: Evaluation of the Correlation With Subtypes of Mucinous Breast Carcinoma. *J Magn Reson Imaging* (2018) 47(2):391–400. doi: 10.1002/jmri.25794
64. Zhang W, Zhou Y, Xu XQ, Kong LY, Xu H, Yu TF, et al. A Whole-Tumor Histogram Analysis of Apparent Diffusion Coefficient Maps for Differentiating Thymic Carcinoma From Lymphoma. *Korean J Radiol* (2018) 19(2):358–65. doi: 10.3348/kjr.2018.19.2.358
65. Moran CA, Weissferdt A, Kalhor N, Solis LM, Behrens C, Wistuba II, et al. Thymomas I: A Clinicopathologic Correlation of 250 Cases With Emphasis on the World Health Organization Schema. *Am J Clin Pathol* (2012) 137(3):444–50. doi: 10.1309/AJCP76KEGWQKWOKA
66. Yabuuchi H, Matsuo Y, Abe K, Baba S, Sunami S, Kamitani T, et al. Anterior Mediastinal Solid Tumours in Adults: Characterisation Using Dynamic Contrast-Enhanced MRI, Diffusion-Weighted MRI, and FDG-PET/Ct. *Clin Radiol* (2015) 70(11):1289–98. doi: 10.1016/j.crad.2015.07.004
67. Shen J, Xue L, Zhong Y, Wu YL, Zhang W, Yu TF. Feasibility of Using Dynamic Contrast-Enhanced MRI for Differentiating Thymic Carcinoma From Thymic Lymphoma Based on Semi-Quantitative and Quantitative Models. *Clin Radiol* (2020) 75(7):560 e19– e25. doi: 10.1016/j.crad.2020.02.010
68. Xiao G, Rong WC, Hu YC, Shi ZQ, Yang Y, Ren JL, et al. MRI Radiomics Analysis for Predicting the Pathologic Classification and TNM Staging of Thymic Epithelial Tumors: A Pilot Study. *AJR Am J Roentgenol* (2020) 214(2):328–40. doi: 10.2214/AJR.19.21696

Conflict of Interest: EM received hononaria from Merck Sharp & Dohme and Boehringer Ingelheim for giving lectures.

The remaining authors declare that the research was conducted in the absence of any commercial or financial relationships that could be construed as a potential conflict of interest.

Publisher's Note: All claims expressed in this article are solely those of the authors and do not necessarily represent those of their affiliated organizations, or those of the publisher, the editors and the reviewers. Any product that may be evaluated in this article, or claim that may be made by its manufacturer, is not guaranteed or endorsed by the publisher.

Copyright © 2022 Strange, Ahuja, Shroff, Truong and Marom. This is an open-access article distributed under the terms of the Creative Commons Attribution License (CC BY). The use, distribution or reproduction in other forums is permitted, provided the original author(s) and the copyright owner(s) are credited and that the original publication in this journal is cited, in accordance with accepted academic practice. No use, distribution or reproduction is permitted which does not comply with these terms.

frontiers in Oncology

ORIGINAL RESEARCH
published: 05 January 2022
doi: 10.3389/fonc.2021.791647

Induction Therapy Followed by Surgery for Unresectable Thymic Epithelial Tumours

Shuai Wang[1†], Jiahao Jiang[1†], Jian Gao[1], Gang Chen[2], Yue Fan[3], Bei Xu[4], Jihong Dong[5], Shisuo Du[6], Junzhen Liu[7] and Jianyong Ding[1]*

[1] Department of Thoracic Surgery, Zhongshan Hospital, Fudan University, Shanghai, China, [2] Department of Pathology, Zhongshan Hospital, Fudan University, Shanghai, China, [3] Department of Integrated Traditional Chinese Medicine (TCM) & Western Medicine, Zhongshan Hospital, Fudan University, Shanghai, China, [4] Department of Medical Oncology, Zhongshan Hospital, Fudan University, Shanghai, China, [5] Department of Neurology, Zhongshan Hospital, Fudan University, Shanghai, China, [6] Department of Radiotherapy, Zhongshan Hospital, Fudan University, Shanghai, China, [7] Department of Radiology, Zhongshan Hospital, Fudan University, Shanghai, China

OPEN ACCESS

Edited by:
Patrick Loehrer, Sr., Indiana University Bloomington, United States

Reviewed by:
Agathe Seguin-Givelet, L'Institut Mutualiste Montsouris, France
Angelo Carretta, Vita-Salute San Raffaele University, Italy

***Correspondence:**
Jianyong Ding
DoctorDingVIP@126.com

[†]These authors have contributed equally to this work

Specialty section:
This article was submitted to Thoracic Oncology, a section of the journal Frontiers in Oncology

Received: *08 October 2021*
Accepted: *13 December 2021*
Published: *05 January 2022*

Citation:
Wang S, Jiang J, Gao J, Chen G, Fan Y, Xu B, Dong J, Du S, Liu J and Ding J (2022) Induction Therapy Followed by Surgery for Unresectable Thymic Epithelial Tumours. Front. Oncol. 11:791647. doi: 10.3389/fonc.2021.791647

Background and Objectives: The treatment of unresectable thymic epithelial tumours (TETs) remains controversial. Here, we present the efficacy and safety of induction therapy followed by surgery for unresectable TET.

Methods: Eighty-one patients with unresectable TETs treated with induction therapy followed by surgery were selected from a retrospective review of consecutive TETs from January 2005 to January 2021. Clinicopathological data were analyzed to assess tumour responses, resectability, adverse events, progression-free survival (PFS) and overall survival (OS).

Results: Induction therapy produced a major tumour response rate of 69.1%, a tumour response grade (TRG) 1-3 rate of 84.0% and an R0 resection rate of 74.1%. The most common toxic effects were all-grade neutropenia (35.8%) and anaemia (34.6%). The 10-year OS and PFS rates were 45.7% and 35.2%. Multivariate analysis showed that ypTNM stage, ypMasaoka stage, complete resection, and TRG were significant independent prognostic factors. Exploratory research revealed that different induction modalities and downstaging of T, N, M, TNM, or Masaoka classifications did not significantly alter the pooled hazard ratio for survival.

Conclusions: Induction therapy followed by surgery is well tolerated in patients with unresectable TETs, with encouraging R0 resection rates. Multimodality management provides good control of tumors for unresectable TET patients.

Keywords: thymic epithelial tumors, survival, induction therapy, complete resection, stage

HIGHLIGHTS

- Induction therapy followed by surgery had encouraging tumor response and complete resection rate for initially unresectable thymic epithelial tumors.
- ypTNM stage, ypMasaoka stage, complete resection, and tumor response grade (TRG) were all independent significant prognostic factors.
- Induction therapy followed by surgery provides good control of tumor for unresectable TETs patients.

INTRODUCTION

Thymic epithelial tumours (TETs), comprised of thymoma and thymic carcinoma, are the most common tumours in the anterior mediastinum (1). However, a notable proportion of patients with TETs present at advanced stages based on the International Thymic Malignancy Interest Group (2). Until now, TETs have generally been considered surgical diseases, and complete resection remains the mainstay of treatment. However, complete resection is challenging and unavailable for advanced lesions due to invasion of the mediastinal structures or diffuse pleural implants. Successful treatment of unresectable TETs involves multidisciplinary evaluation. A variety of chemotherapy regimens for TET have been reported. A majority of patients with TETs in the reported studies were able to proceed to resection with clinical response rates of 62%-100% and complete resection rates of 22%-92% (3, 4). Preoperative radiation has been used in locally advanced malignancies, and this strategy has also been examined in TETs. However, there was no survival difference between patients who underwent preoperative radiation and those who did not based on retrospective studies (5). Loehrer PJ Sr. et al. (6) reported that preoperative chemoradiation had encouraging clinical responses and potentially high pathological response rates. The opportunity to achieve complete resection after induction therapy followed by surgery has led to interest in pursuing this strategy in unresectable TETs.

In general, previous studies on induction therapy mainly comprised small retrospective case series. Investigators were unable to draw firm conclusions about the outcomes of induction treatment. Because of the rarity of TETs and their natural behaviour, it is difficult to reach definite conclusions with small samples. Currently, the standard management of unresectable TETs remains controversial. We performed a study with multimodal treatments to improve the resectability and responses of unresectable TETs. The objective of the present study was to retrospectively evaluate the tumour responses and prognosis of patients with unresectable TETs treated with induction therapy followed by surgery.

METHODS

Patients Selection

From January 2005 to January 2021, we selected patients with TETs who underwent induction therapy followed by surgery. Approval was obtained from the Research Ethics Committee of Zhongshan Hospital, Fudan University. Informed consent was obtained, and this study was compliant with the Helsinki Declaration. The inclusion criteria were as follows: (a) primary mediastinal TETs were confirmed by pathological examination according to the World Health Organization classification (7). (b) Patients received multidisciplinary consultation for mediastinal tumours, and unresectable advanced TET patients were treated with induction therapy followed by resection. Patients were deemed to have primary unresectable TETs as judged by a joint consensus of a multimodality oncology team (thoracic surgeon, medical oncologist, radiation oncologist, radiologist, and pathologist). Patients were judged to be unresectable with radiographic findings of extensive invasion, large tumors with indistinct borders, or great vessel invasion. Deep intrathoracic or cervical nodal involvement, pleural or pericardial nodules, and pulmonary intraparenchymal nodule or distant organ metastasis were also defined as poorly resectable. (c) Tumours were dimensionally measurable lesions according to the Response Evaluation Criteria in Solid Tumours (RECIST) criteria. We excluded patients with (a) incomplete information regarding pathological variables and clinical data, (b) noncurative resection (i.e., biopsy only), and (c) surgical resection for recurrence after primary treatment. Tumour stage was determined using the Masaoka staging system and the 8th edition TNM classification of TETs (8, 9). Medical records and laboratory data were collected in accordance with the recommendation of the International Thymic Malignancy Interest Group (ITMIG) standard definitions and policies (10).

Treatment and Evaluation

Patients with inoperable disease were treated with induction therapy, as judged by joint consensus of a multidisciplinary mediastinal oncology team (thoracic surgery, medical oncology, pathology, neurology and radiology). All patients had an initial biopsy that confirmed the suspected TETs before induction therapy. Induction therapies were quite heterogeneous and individualized depending on each patient's status, including chemotherapy, radiotherapy or sequential/concurrent chemoradiation. Chemotherapies included different cycles of chemotherapy using cisplatin-based regimens of CAP (cyclophosphamide, doxorubicin, cisplatin), TP (paclitaxel, carboplatin/cisplatin), DP (docetaxel, cisplatin), VP (etoposide, cisplatin) or GP (gemcitabine, cisplatin). Radiotherapy was performed with involved fields that covered the primary and metastatic tumours with margins of approximately 1–2 cm. Three-dimensional conformal or intensity-modulated radiation with a total dose of 60–70 Gy was administered for radiation alone, and lower doses of 40–50 Gy were administered for sequential/concurrent chemoradiation. After completion of induction therapy, TETs were reevaluated and restaged by CT, MRI or PET scan. The tumour response to induction therapy was evaluated as progressive disease (PD), stable disease (SD), partial response (PR) or complete response (CR). Specimens were evaluated by independent senior pathologists. All postoperative specimens were reviewed for tumour response grade (TRG) based on the percent necrosis and viable tumour on the entire tumour

bed as following: TRG1: no viable tumor; TRG2: rare residual viable tumor cells scattered through fibrosis; TRG3: increase in number of residual tumor cells, fibrosis predominant; TRG4: residual viable tumor outgrowing fibrosis; TRG5: no regressive changes (11). The Common Terminology Criteria for Adverse Events (CTCAE 3.0) was used to grade the severity of adverse events (AEs). Total thymectomy was performed with the goal of complete removal of the tumour and all attached structures. The operation procedure was reported partially in our previous study (12). Complete surgical resection (R0) was defined as en bloc resection of the tumour without macroscopic (R2) or microscopic (R1) residuals.

Statistical Analysis

The chi-square test and Fisher's exact test were used to compare categorical variables, and Student's t-test was used to compare continuous variables. Overall survival (OS) was defined as the period from the date of treatment initiation to the date of death from any cause or the final follow-up. Progression-free survival (PFS) was defined as the time from surgery to the date of the first recurrence or metastasis. Clinicopathologic variables were entered in the univariate logistic regression analysis. Only variables with a P-value <0.1 were entered into the multivariable logistic regression analysis. Statistical analyses were performed using SPSS 22 software. A 2-sided P<0.05 was considered to be statistically significant.

RESULTS

Patient Characteristics

From January 2005 to January 2021, 3191 patients were diagnosed with primary TETs and treated with surgery at Zhongshan Hospital, Fudan University. We excluded patients with incomplete information (153 patients) and those who underwent surgical resection for recurrence (377 patients). A total of 2,561 TET patients remained, and only 81 (2.5%, 81/3191) patients with unresectable TETs received induction therapies followed by surgery. The patient characteristics are presented in **Supplemental Table 1**.

The patients included 45 men and 36 women. At the time of presentation, 52 patients (64.2%) had one or more symptoms, including 19 with chest distress or pain (23.8%), 17 (21.0%) with myasthenia gravis (MG), 9 with cough (11.1%), 4 with fatigue (4.8%), 7 with superior vena cava syndrome (8.6%), and 2 with pure red cell aplastic anaemia (3.2%). The interval time from diagnosis to initial treatment ranged from 0.07 to 24 months (median 1.5). Radiologically, the diameters of TETs ranged from 4.0 cm to 19.0 cm (**Supplemental Figure 1**). The pathological subtypes are shown in **Supplemental Table 1**.

Treatment Modalities

Treatment strategies of induction therapy were individualized for each patient. The treatment modalities were shown in **Table 1** and **Supplemental Table 2**. Induction therapies consisted of chemotherapy (41 patients, 50.6%), radiotherapy (12 patients, 14.8%), chemoradiotherapy (26 patients, 32.1%), and chemoimmunotherapy (2 patients, 2.5%). When the tumor was considered likely to be incompletely resected, the patients were treated with chemotherapy first. Of the 67 patients receiving chemotherapy, the most commonly used regimen was TP (29 patients, 43.3%). Other cisplatin-based regimens included CAP (15 cases, 22.4%), DP (6 cases, 9.0%), and VP or GP regimens (17 cases, 25.4%). Two patients received chemotherapy (one patient received CAP and one patient received TP) in combination with immunotherapy using camrelizumab. Similar to other malignancies, the addition of radiation to

TABLE 1 | Tumor responses and resectability according to induction therapy modalities.

Variables		Cases	Percentage (%)	
Radiotherapy (12 cases)	CR	5	41.7	ORR: 83.3
	PR	5	41.7	
	SD	2	16.7	
	R0	10	83.3	R0: 83.3
	R1	1	8.3	
	R2	1	8.3	
Chemotherapy (41 cases)	CR	1	2.4	ORR: 70.7
	PR	28	68.3	
	SD	9	22.0	
	PD	3	7.3	
	R0	32	78.0	R0: 78.0
	R1	6	14.6	
	R2	3	7.3	
Chemo-radiotherapy (26 cases)	CR	3	11.5	ORR: 61.5
	PR	13	50.0	
	SD	9	34.6	
	PD	1	3.8	
	R0	16	61.5	R0: 61.5
	R1	2	7.7	
	R2	8	30.8	
Chemo-immunotherapy (2 case)	PR	1	–	–
	SD	1	–	
	R0	2	–	–

induction chemotherapy has been administered in unresectable TETs with deep intrathoracic or cervical nodal involvement, pleural or pericardial nodules, and pulmonary intraparenchymal nodule or distant organ metastasis. In this study, there were 26 (32.1%) patients received chemo-radiotherapy. Radiation therapy applied as a sole therapeutical induction therapy modality was not routinely suggested in our study. Of these 12 patients receiving induction radiotherapy alone, 8 patients who had huge tumor with pleural, pulmonary or pericardial invasion, but without great vessels invasion, extrathoracic nor intrathoracic metastasis, were deemed not to be a margin-negative surgical resection candidate. Induction radiotherapy was applied for another 4 patients, because they could not tolerate to chemotherapy or were allergic to cytotoxic drug. Induction therapy produced major responses in 56 patients, including 9 (11.1%) complete responses and 47 (58.0%) partial responses with a disease control rate of 95.1%. Pathological R0 resection was performed in 60 patients (74.1%), and 21 patients (25.9%) had incomplete resection. Postoperative pathology revealed that most TETs had improved TRG, with a TRG 1–3 rate of 84.0% (**Supplemental Table 2**).

After patients were evaluated to have recovered from induction therapy (4 to 8 weeks), they underwent surgical resection including the tumor, thymus, mediastinal fat, and all attached structures. However, debulking surgery were considered for thirteen patients to relieve symptoms or reduce tumor burden. Systematic mediastinal lymph node dissection was performed in 23 patients who presented with enlarged lymph nodes, otherwise, only the anterior mediastinal lymph node was resected en bloc with the tumor. Briefly, three different techniques have been suggested to achieve complete resection by reconstruction of the great vessels, including tangential resection and direct suture repair (10 cases), localized resection and repair with pericardial patch (3 cases), and circumferential resection with replacement by polytetrafluoroethylene (PTFE) graft (23 cases). Fifteen patient required pleurectomy for confluent pleural disease. Nine patients received partial sternal resection and chest wall reconstruction. Other structures resected included lung (42 cases), pericardium (32 cases), phrenic nerve (23 cases), brachiocephalic vein (18 cases), diaphragm (10 cases). Twenty-one patients had an incomplete resection, owing to extensive or multi-site infiltration of chest wall (5 cases), main pulmonary artery (2 cases), aorta or arch vessels (7 cases), myocardium (4 cases), trachea (2 cases) or pleural metastasis (13 cases). Nine patients had all gross tumor resected and were thought to be pathological R1 resection and twelve patients had R2 resection.

The decision to use postoperative chemotherapy and/or radiotherapy was individualized for each patient. Briefly, for patients with incomplete resection, adjuvant chemotherapy and/or radiotherapy was performed routinely for a limited time. For those with a close margin or at high risk for recurrence, adjuvant treatment was performed routinely, even if the tumor was completely resected. Postoperative adjuvant treatment was not recommended for patients had complete response and pathological TRG1 with complete resection. Both physiological and psychological conditions of the individual patient were fully taken into account. Adjuvant treatment was not planned for patients receiving induction therapies with maximum tolerated dose of chemotherapy and radiotherapy. Close follow-up without postoperative treatment was also acceptable for patients with intolerance, anaphylaxis or refusing treatment. In this study, thirty-seven patients (45.7%) did not receive postoperative therapy, including 9 cases of TRG1 with R0, 19 cases of maximum tolerated dose of induction chemotherapy and radiotherapy, 4 cases of intolerance or anaphylaxis, and 5 cases of refusing treatment. While, 44 patients (54.3%) underwent postoperative treatment. Detailed information on postoperative treatment is described in **Supplemental Table 2**. Adjuvant therapy was performed in 9 cases of chemotherapy, 23 cases of radiotherapy, 9 cases of chemo-radiotherapy. One patient received postoperative chemotherapy with sintilimab, while two patients received postoperative tyrosine kinase inhibitor (TKI) therapy with surufatinib or anlotinib.

AEs From Induction Therapy

The common AEs are summarized in **Supplemental Table 3**. The major toxic effects were all-grade haematologic AEs, including anaemia (34.6%) and neutropenia (35.8%). Thirty patients (37.0%) experienced grade ≥ 3 haematologic AEs. The most common all-grade nonhaematologic side effects were weight loss (13.6%) and fatigue (12.3%). Major grade ≥ 3 nonhaematologic toxicities included vomiting (3.7%) and oesophagitis or stomatitis (3.7%). None of the patients had myocardial toxicity or ototoxicity, and no mortalities occurred. The AEs from induction therapy were modest and well tolerated.

Postoperative Complications and Survival

There were no perioperative deaths in this study. The postoperative length of hospital stay was between 3 and 61 days, with an average of 9.4 ± 7.5 days. There were twelve cases (14.8%) of postoperative complications, including four cases of bleeding, five cases of hydrothorax, two cases of atelectasis and one case of unhealing wounds.

The OS rate was 88.2% at 3 years and 77.8% at 5 years. As shown in **Supplemental Table 4**, univariate analysis revealed that cM stage (P=0.036), cTNM stage (P=0.076), cMasaoka stage (P=0.026), pathological type (P=0.048), ypT stage (P=0.047), ypN stage (P<0.001), ypM stage (P=0.045), ypTNM stage (P<0.001), ypMasaoka stage (P=0.018), complete resection (P=0.001), and TRG (P=0.012) were significant prognostic factors. To rule out confounding factors, we performed multivariate analysis using the Cox proportional hazards model (**Supplemental Table 5**). Multivariate analysis revealed that ypTNM stage (P=0.025), ypMasaoka stage (P=0.031), complete resection (P=0.001), and TRG (P=0.007) were significant independent prognostic factors of OS (**Figure 1**).

The 3- and 5-year PFS rates were 58.6% and 46.2%. Univariate analysis revealed that cM stage (P=0.015), cMasaoka stage (P=0.004), pathological type (P=0.033), ypT stage (P<0.001), ypN stage (P<0.001), ypM stage (P<0.001), ypTNM stage (P<0.001), ypMasaoka stage (P=0.004), complete

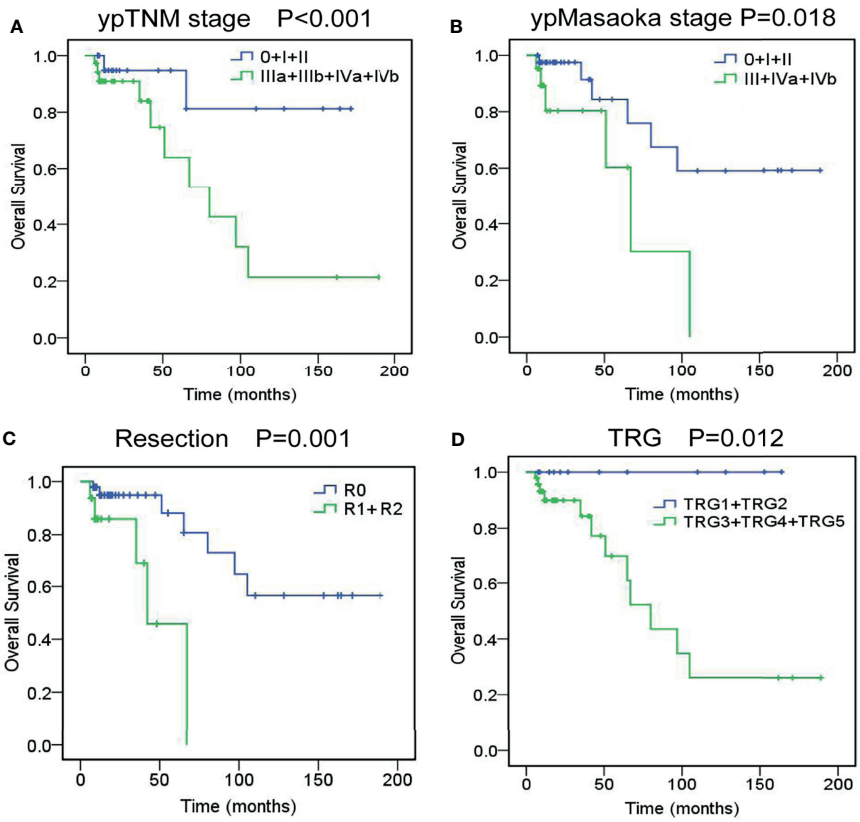

FIGURE 1 | Overall survival curves of unresectable TETs treated with induction therapy followed by surgery, according to ypTNM stage **(A)**, ypMasaoka stage **(B)**, complete resection **(C)**, and tumor response grade **(D)**.

resection (P<0.001), TRG (P=0.001) and postoperative radiotherapy (P=0.018) were significant prognostic factors of PFS. Multivariate analysis showed that ypTNM stage (P=0.001), ypMasaoka stage (P=0.022), complete resection (P<0.001), and TRG (P<0.001) were significant independent prognostic factors of PFS (**Figure 2**).

Survival analyses indicated patients received radical thymectomy with extended resections had similar OS (P=0.065) and PFS (P=0.071) compared to those without extended resection. We also found resected structures were not significant prognostic factors for OS (P=0.136) and PFS (P=0.086), including pericardium, lung, phrenic nerve, chest wall, innomate vein, vena cava, aorta, main pulmonary artery or myocardium.

Subgroup Analyses of Induction Therapy

In this cohort study, radiotherapy produced the highest objective response rate (ORR) (83.3%) and complete resection rate (83.3%) compared with chemotherapy (ORR: 70.7%, R0: 78.0%) and chemoradiotherapy (ORR: 61.5%, R0: 61.5%) (**Table 1**). Of the 67 patients receiving chemotherapy, the CAP regimen produced the highest ORR (86.7%) and complete resection rate (80.0%) compared with the TP (ORR: 58.6%, R0: 75.9%), DP (ORR: 50.0%, R0: 50.0%), and VP or GP regimens (ORR: 64.7%, R0: 64.7%) (**Table 2**). Patients with thymoma had a better ORR (69.4%) and complete resection rate (75.5%) than those with thymic carcinoma (ORR: 68.9%, R0: 71.9%) (**Table 3**). Induction chemotherapy (P=0.592 for OS, P=0.237 for PFS), induction radiotherapy (P=0.714 for OS, P=0.784 for PFS) and different induction modalities (P=0.645 for OS, P=0.303 for PFS) were not prognostic variables. For the 67 patients receiving chemotherapy, different chemotherapy regimens did not significantly alter the pooled hazard ratio for OS (P=0.887) or PFS (P=0.656) (**Supplemental Table 4**).

The Values of Clinical and Pathological Downstaging After Induction Therapy

The preinduction treatment clinical (c) stages, postinduction treatment clinical (yc) stages and postoperative pathological (yp) stages are shown in **Figure 3**. Based on the Masaoka stage, clinical downstaging of TETs occurred in 20 patients (24.7%), and pathological downstaging occurred in 35 patients (43.2%). For the TNM staging system, 38 patients (46.9%) had clinical downstaging of disease and 48 patients (59.3%) had pathological downstaging of disease. Exploration research revealed that pathological downstaging of T, N, and M classifications occurred in 42 patients, 18 patients, and 6 patients, respectively. Pathological upstaging was found in 5 patients

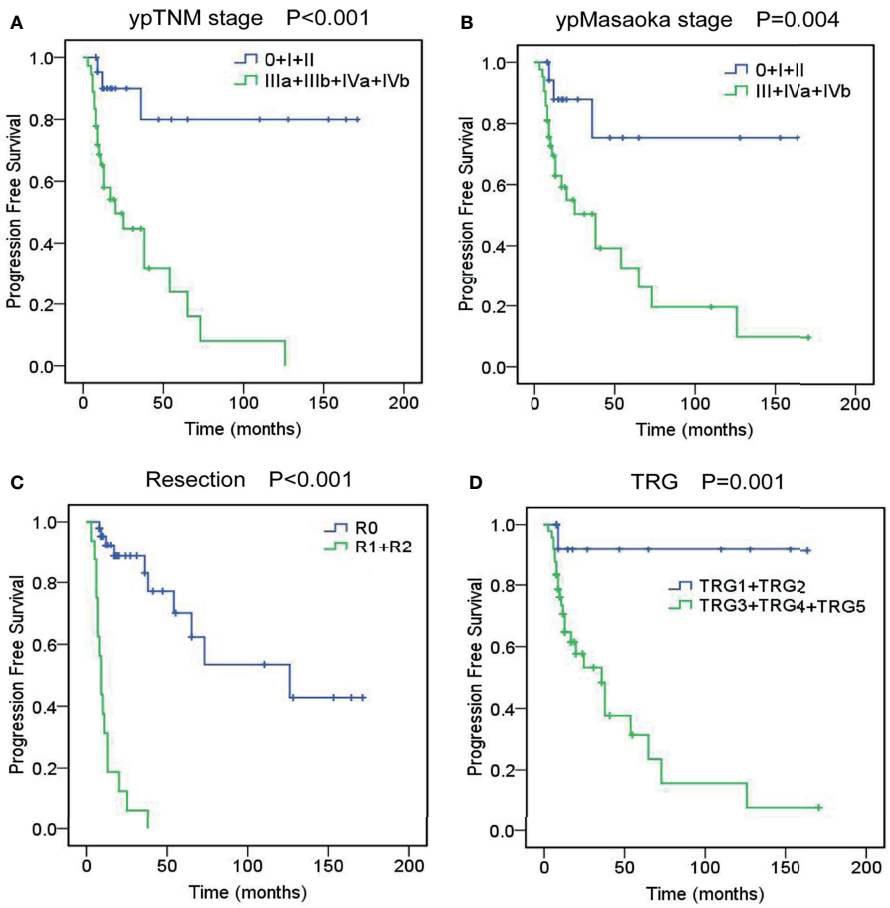

FIGURE 2 | Progression-free survival curves of unresectable TETs treated with induction therapy followed by surgery, according to ypTNM stage **(A)**, ypMasaoka stage **(B)**, complete resection **(C)**, and tumor response grade (TRG) **(D)**.

(6.2%) because of tumour progression or pleural dissemination. Survival analyses indicated that clinical downstaging of the T, N, M, TNM, and Masaoka classifications was not a prognostic factor. Pathological downstaging of the T (P=0.046 for OS, P<0.001 for PFS), N (P=0.003 for OS, P=0.035 for PFS), M (P=0.040 for OS, P=0.048 for PFS), TNM (P=0.018 for OS, P<0.001 for PFS), and Masaoka (P=0.031 for OS, P=0.022 for PFS) classifications had prognostic significance (**Supplemental Table 4**). However, pathological downstaging of neither the TNM classification (P=0.409 for OS, P=0.630 for PFS) nor the Masaoka classification (P=0.708 for OS, P=0.784 for PFS) were independent prognostic variables.

DISCUSSION

Complete resection is frequently unfeasible in patients with advanced-stage TETs. Induction therapy has been shown to be effective for advanced TETs due to four distinct advantages: (1) producing objective clinical responses and shrinking tumours to relieve symptoms; (2) downstaging tumours and converting unresectable tumours to resectable tumours; (3) improving early local and systemic disease control; and (4) providing evidence of the feasibility and efficacy of drugs or therapies. However, until now, standard induction therapeutic modalities have not been established. Our study further recognizes the clinicopathological features of unresectable TETs and promotes the development of treatment standards and options.

This study was the largest retrospective report to date with favorable long-term outcomes at a single centre. With the use of induction therapies, the R0 rate was 74.1%, with an ORR of 69.1%. These results are in accordance with those of previous studies. In the literature, the range of the ORR in the large series was wide: 62% (13), 73% (14), and 100% (15). The R0 rate reported was also a wide range depending on the study: 22% (16), 43% (13), 69% (15), and 77% (14). The difference among studies might result from the selection of patients, treatment modality, race, and limited number of cases. To date, the recognized results of chemotherapy for TETs have been obtained from the ADOC (doxorubicin, cisplatin, vincristine, cyclophosphamide) regimen, with a 92% ORR and a 43% R0 rate (17). However, which regimens are the best for TETs is unclear thus far. Even worse,

TABLE 2 | Tumor responses and resectability according to induction chemotherapy regimens.

Variables		Cases	Percentage (%)	
CAP (15 cases)	PR	13	86.7	ORR: 86.7
	SD	2	13.3	
	R0	12	80.0	R0: 80.0
	R1	2	13.3	
	R2	1	6.6	
TP (29 cases)	CR	2	6.9	ORR: 58.6
	PR	15	51.7	
	SD	9	31.0	
	PD	3	10.3	R0: 75.9
	R0	22	75.9	
	R1	2	6.9	
	R2	5	17.2	
DP (6 cases)	PR	3	50.0	ORR: 50.0
	SD	2	33.3	
	PD	1	16.7	
	R0	3	50.0	R0: 50.0
	R1	2	33.3	
	R2	1	16.7	
Other (VP or GP, 17 case)	CR	2	11.8	ORR: 64.7
	PR	9	52.9	
	SD	6	35.3	
	R0	11	64.7	R0: 64.7
	R1	2	11.8	
	R2	4	23.5	

direct comparisons between regimens are difficult because of the scarcity of cases and heterogeneity of pathology. Our exploration results showed that the CAP regimen had the highest ORR (86.7%) and R0 rate (80.0%), while the DP regimen had the lowest ORR (50.0%) and R0 rate (50.0%). Although the number of cases was limited, differences in tumour responses and resection among regimens were obvious. The CAP regimen might facilitate complete surgical resection, resulting in a higher cure rate. Discouragingly, our data revealed that the CAP regimen had no survival benefit compared with the other regimens, and different induction chemotherapy regimens did not produce survival differences. Consequently, although this study demonstrated that induction chemotherapy was active against unresectable TETs, we did not definitively draw a conclusion about which regimens offer significant survival advantages.

Based on the European Society of Thoracic Surgeons database, only 1% of TET patients receive radiation alone (18). Induction radiotherapy is an attempt to enhance radical complete resection, but induction radiation has only been reported in small retrospective series. A few studies reported that TET patients treated with preoperative radiation had variable outcomes, with R0 rates ranging from 50% to 75% (5, 18, 19). In this study, 12 of 81 (14.8%) patients received induction radiotherapy alone. We found that induction radiotherapy had a slightly better ORR (83.3%) and R0 rate (83.3%) than chemotherapy. Induction radiation allows more precise radiation planning than postoperative radiation because the initial tumour volume is undisturbed and natural tumour margins can be dimensioned without disturbance. Our data implied that radiation had an important role in the local

TABLE 3 | Tumor responses and resectability according to pathological types.

Variables		Cases	Percentage (%)	
Thymoma (49 cases)	CR	4	8.2	ORR: 69.4
	PR	30	61.2	
	SD	13	26.5	
	PD	2	4.1	
	R0	37	75.5	R0:75.5
	R1	4	8.2	
	R2	8	16.3	
Thymic carcinoma (32 cases)	CR	5	15.6	ORR: 68.9
	PR	17	53.1	
	SD	8	25.0	
	PD	2	6.3	
	R0	23	71.9	R0: 71.9
	R1	6	18.8	
	R2	3	9.4	

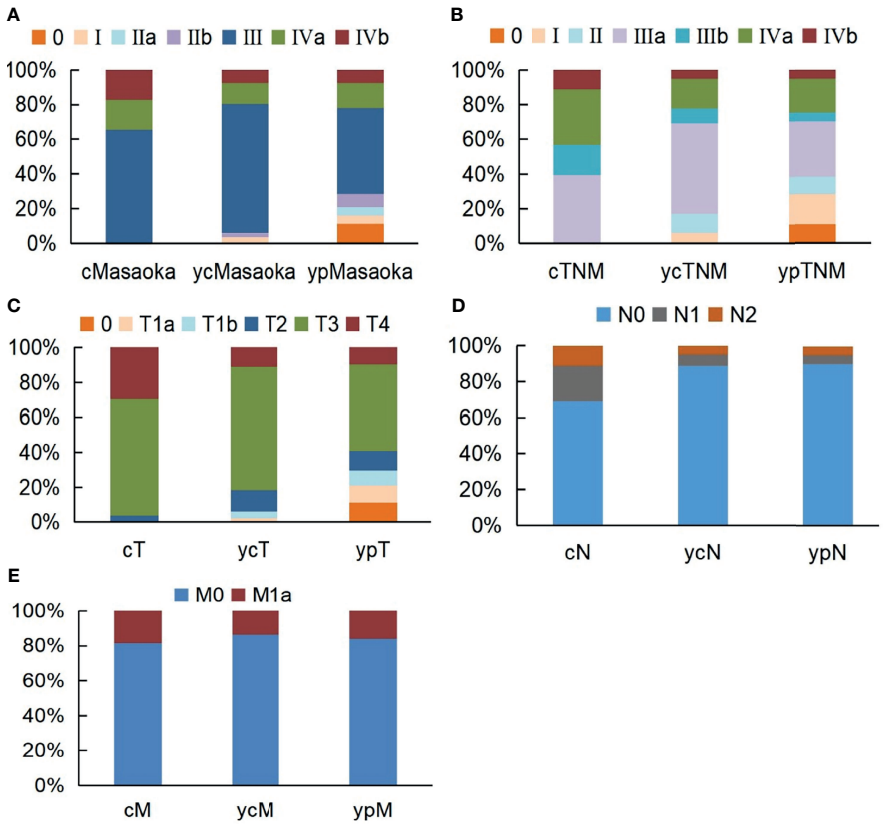

FIGURE 3 | Stage alternations of unresectable TETs treated with induction therapy followed by surgery according to Masaoka **(A)**, TNM **(B)**, T **(C)**, N **(D)**, M **(E)** classifications.

control of TETs. However, there were no differences in OS and PFS between patients who received induction radiation and those who did not. Our data shed light on the rationale for induction radiotherapy in unresectable TET patients.

The combination of induction radiation and chemotherapy has been used in TETs, with a wide range of ORRs (40%-70%) and R0 rates (60%-80%) (4, 6, 20). All patients with unresectable TETs received multidisciplinary consultation for mediastinal tumours in our centre. In this series, 26 patients (32.1%) received chemoradiotherapy, with an ORR of 61.5% and an R0 rate of 61.5%. This retrospective study demonstrated that chemoradiotherapy did not achieve better tumour control and surgical resection rates than chemotherapy or radiotherapy alone. Unsurprisingly, we also found that chemoradiotherapy did not offer a survival benefit compared with chemotherapy or radiotherapy alone. Induction therapy facilitates tumour control and surgical removal. However, induction strategies need further research to achieve successful treatment of unresectable TETs. The tricky problem of induction therapy is the toxicity of induction. In the current study, our results demonstrated that AEs from induction therapy were modest and well tolerated. The efficacy and safety of induction therapy should be established by randomized trials to essentially decide optimal treatment.

Theoretically, the potential benefit of induction therapy is the downstaging of bulky tumours. In fact, clinical Masaoka downstaging only occurred in 24.7% of patients, and 46.9% of patients had clinical TNM downstaging. Our results seemed to be in line with the low clinical downstaging rate in a previous report by Park et al. (21) Moreover, we found that patients who were clinically downstaged after induction therapy had similar clinical outcomes compared with those who were not. Most importantly, many variations make it difficult to evaluate clinical stage alterations, such as research subjectivity, observation of lymph node metastasis, and measurement bias of tumour size. We analyzed T, N, M and TNM classifications to provide granularity of tumour stages. Our data showed that clinical and pathological downstaging of the Masaoka, TNM, T, N, or M classifications were not independent prognostic variables. Pathological examination is the gold standard to assess tumour downstaging from induction therapy. Consequently, clinical downstaging could be underestimated and has no clear survival implications for unresectable TETs.

Only a few studies have reviewed the histologic response of TETs to induction treatment (11). We classified a reproducible five-tier TRG system for TET specimens after induction treatment. Previous studies reported the percentage of viable

tumours after preoperative therapy for both resectable and unresectable TETs. The results were quite variable, with 0% to 100% viable tumour cells (11, 13, 15, 20). The cause for pathological response differences is not entirely clear but could be due to diverse induction treatment modalities. In this study, we found that the morphological response to induction treatment correlated with TRG. All patients with TRG 1 had a complete radiologic response, whereas those with TRG 5 did not show any radiologic response but had tumour progression. Moreover, patients with radiologic PR had a better TRG and a lower percentage of viable tumours than those with SD. Given the close correlation of radiologic response and TRG, we selected TRG as a prognostic variable in survival analyses. TRG was not only a prognostic factor but also a significant independent prognostic factor for OS and PFS by multivariate analyses. The completeness of resection significantly increases the survival time, even for primary unresectable TETs. Among various clinical factors, R0 resection was the most important independent prognostic factor of OS and PFS for unresectable TETs. However, tumour regression does not guarantee the achievement of R0 resection. In our study, the incomplete resection rate was 25.9%, although only 13 patients (16.0%) had TRG 4–5. The success of R0 resection depends on whether involved structures can be removed or reconstructed. R0 resection is our primary goal, and every effort should be made to achieve resectability.

There were considerable challenges in this study. First, the data were retrospectively reviewed from a single centre. Thus, there was inevitable selection bias. Second, a wide variety of induction therapies were used in our patients. Chemotherapy regimens were not the uniform protocol owing to heterogeneous histological subtypes. Third, although this study gave a rough indication of distinct responses to different induction therapies, direct comparisons between regimens were limited. Given the rarity of the tumour, enrolling a large number of patients with complete survival data will unavoidably take many years. To establish a more effective formula for induction therapy, multicentre randomized controlled trials with the best supportive care are necessary.

CONCLUSION

In this study, we retrieved 81 patients with unresectable TETs received induction therapy followed by surgery. We found induction therapy produced major tumor responses of 69.1% and tumor response grade (TRG) 1-3 of 84.0%. Moreover, R0 resection rate was 74.1% with the 10-year OS of 45.7% and 10-year PFS of 35.2%. We also found ypTNM stage, ypMasaoka stage, complete resection, and TRG were all independent significant prognostic factors. Exploratory research revealed different induction modalities and different chemotherapy regimens had no significant survival difference. Neither clinical nor pathological downstaging of T, N, M, TNM, Masaoka classifications were independent prognostic variables. Therefore, induction therapy followed by surgery provides good control of tumor for unresectable TETs patients.

DATA AVAILABILITY STATEMENT

The raw data supporting the conclusions of this article will be made available by the authors, without undue reservation.

ETHICS STATEMENT

Approval was obtained from the Research Ethics Committee of Zhongshan Hospital, Fudan University (Y2019-187).

AUTHOR CONTRIBUTIONS

SW and JIAD conceived and supervised the research. SW, JJ, GC, YF, BX, JIAD, SD, JL, and JIHD contributed to the design of the project and discussions. JJ, SW, and JIAD contributed to data analyses; SW, JJ, GC, YF, BX, JIHD, SD, JL, and JIAD contributed to materials or clinical data; SW, JJ, and JIAD wrote the manuscript. All authors contributed to the article and approved the submitted version.

FUNDING

This work was supported by grants from the National Natural Science Foundation of China (81972168).

ACKNOWLEDGMENTS

We thank doctors at Department of Pathology, Zhongshan Hospital, Fudan University for kindly providing pathological data.

SUPPLEMENTARY MATERIAL

The Supplementary Material for this article can be found online at: https://www.frontiersin.org/articles/10.3389/fonc.2021.791647/full#supplementary-material

REFERENCES

1. Engels EA. Epidemiology of Thymoma and Associated Malignancies. *J Thorac Oncol* (2010) 5:S260–5. doi: 10.1097/JTO.0b013e3181f1f62d
2. Huang J, Ahmad U, Antonicelli A, Catlin AC, Fang W, Gomez D, et al. Development of the International Thymic Malignancy Interest Group International Database: An Unprecedented Resource for the Study of a Rare Group of Tumors. *J Thorac Oncol* (2014) 9:1573–8. doi: 10.1097/JTO.0000000000000408
3. Riely GJ, Huang J. Induction Therapy for Locally Advanced Thymoma. *J Thorac Oncol* (2010) 5:S323–6. doi: 10.1097/JTO.0b013e3181f20e90
4. Wright CD, Choi NC, Wain JC, Mathisen DJ, Lynch TJ, Fidias P. Induction Chemoradiotherapy Followed by Resection for Locally Advanced Masaoka

Stage III and IVA Thymic Tumors. *Ann Thorac Surg* (2008) 85:385–9. doi: 10.1016/j.athoracsur.2007.08.051
5. Yagi K, Hirata T, Fukuse T, Yokomise H, Inui K, Ike O, et al. Surgical Treatment for Invasive Thymoma, Especially When the Superior Vena Cava Is Invaded. *Ann Thorac Surg* (1996) 61:521–4. doi: 10.1016/0003-4975(95)00983-3
6. Loehrer PJ Sr, Chen M, Kim K, Aisner SC, Einhorn LH, Livingston R, et al. Cisplatin, Doxorubicin, and Cyclophosphamide Plus Thoracic Radiation Therapy for Limited-Stage Unresectable Thymoma: An Intergroup Trial. *J Clin Oncol* (1997) 15:3093–9. doi: 10.1200/JCO.1997.15.9.3093
7. Marx A, Chan JK, Coindre JM, Detterbeck F, Girard N, Harris NL, et al. The 2015 World Health Organization Classification of Tumors of the Thymus: Continuity and Changes. *J Thorac Oncol* (2015) 10:1383–95. doi: 10.1097/JTO.0000000000000654
8. Masaoka A. Staging System of Thymoma. *J Thorac Oncol* (2010) 5:S304–12. doi: 10.1097/JTO.0b013e3181f20c05
9. Detterbeck FC, Stratton K, Giroux D, Asamura H, Crowley J, Falkson C, et al. The IASLC/ITMIG Thymic Epithelial Tumors Staging Project: Proposal for an Evidence-Based Stage Classification System for the Forthcoming (8th) Edition of the TNM Classification of Malignant Tumors. *J Thorac Oncol* (2014) 9:S65–72. doi: 10.1097/JTO.0000000000000290
10. ITMIG. Definitions and Policies. *J Thorac Oncol* (2011) 6:S1689–90. doi: 10.1097/JTO.0b013e3181f13682
11. Johnson GB, Aubry MC, Yi ES, Koo CW, Jenkins SM, Garces YI, et al. Radiologic Response to Neoadjuvant Treatment Predicts Histologic Response in Thymic Epithelial Tumors. *J Thorac Oncol* (2017) 12:354–67. doi: 10.1016/j.jtho.2016.09.118
12. Jiang JH, Gao J, Zhang Y, Wang H, Tan LJ, Ding JY. Modified Subxiphoid Thoracoscopic Thymectomy for Locally Invasive Thymoma. *Ann Thorac Surg* (2020) S0003-4975:32009–9. doi: 10.1016/j.athoracsur.2020.10.032
13. Kunitoh H, Tamura T, Shibata T. Et Al, JCOG Lung Cancer Study Group. A Phase II Trial of Dosedense Chemotherapy, Followed by Surgical Resection and/or Thoracic Radiotherapy, in Locally Advanced Thymoma: Report of a Japan Clinical Oncology Group Trial (JCOG 9606). *Br J Cancer* (2010) 103:6–11. doi: 10.1038/sj.bjc.6605731
14. Lucchi M, Melfi F, Dini P, Basolo F, Viti A, Givigliano F, et al. Neoadjuvant Chemotherapy for Stage III and IVA Thymomas: A Singleinstitution Experience With a Long Follow-Up. *J Thorac Oncol* (2006) 1:308–13. doi: 10.1097/01243894-200605000-00007
15. Rea F, Sartori F, Loy M, Calabrò F, Fornasiero A, Daniele O, et al. Chemotherapy and Operation for Invasive Thymoma. *J Thorac Cardiovasc Surg* (1993) 106:543–9. doi: 10.1016/S0022-5223(19)34092-9
16. Yokoi K, Matsuguma H, Nakahara R, Kondo T, Kamiyama Y, Mori K, et al. Multidisciplinary Treatment for Advanced Invasive Thymoma With Cisplatin, Doxorubicin, and Methylprednisolone. *J Thorac Oncol* (2007) 2:73–8. doi: 10.1097/JTO.0b013e31802bafc8
17. Fornasiero A, Daniele O, Ghiotto C, Piazza M, Fiore-Donati L, Calabró F, et al. Chemotherapy for Invasive Thymoma. A 13-Year Experience. *Cancer* (1991) 68:30–3. gdoi: 10.1002/1097-0142(19910701)68:1<30::AID-CNCR2820680106>3.0.CO;2-4
18. Ruffini E, Detterbeck F, Van Raemdonck D, Rocco G, Thomas P, Weder W, et al. European Association of Thoracic Surgeons (ESTS) Thymic Working Group. Tumours of the Thymus: A Cohort Study of Prognostic Factors From the European Society of Thoracic Surgeons Database. *Eur J Cardiothorac Surg* (2014) 46:361–8. doi: 10.1093/ejcts/ezt649
19. Akaogi E, Ohara K, Mitsui K, Onizuka M, Ishikawa S, Mitsui T, et al. Preoperative Radiotherapy and Surgery for Advanced Thymoma With Invasion to the Great Vessels. *J Surg Oncol* (1996) 63:17–22. doi: 10.1002/(SICI)1096-9098(199609)63:1<17::AID-JSO4>3.0.CO;2-T
20. Korst RJ, Bezjak A, Blackmon S, Choi N, Fidias P, Liu G, et al. Neoadjuvant Chemoradiotherapy for Locally Advanced Thymic Tumors: A Phase II, Multi-Institutional Clinical Trial. *J Thorac Cardiovasc Surg* (2014) 147:36–44. doi: 10.1016/j.jtcvs.2013.08.061
21. Park S, Park IK, Kim YT, Lee GD, Kim DK, Cho JH, et al. Comparison of Neoadjuvant Chemotherapy Followed by Surgery to Upfront Surgery for Thymic Malignancy. *Ann Thorac Surg* (2019) 107:355–62. doi: 10.1016/j.athoracsur.2018.08.055

Conflict of Interest: The authors declare that the research was conducted in the absence of any commercial or financial relationships that could be construed as a potential conflict of interest.

Publisher's Note: All claims expressed in this article are solely those of the authors and do not necessarily represent those of their affiliated organizations, or those of the publisher, the editors and the reviewers. Any product that may be evaluated in this article, or claim that may be made by its manufacturer, is not guaranteed or endorsed by the publisher.

Copyright © 2022 Wang, Jiang, Gao, Chen, Fan, Xu, Dong, Du, Liu and Ding. This is an open-access article distributed under the terms of the Creative Commons Attribution License (CC BY). The use, distribution or reproduction in other forums is permitted, provided the original author(s) and the copyright owner(s) are credited and that the original publication in this journal is cited, in accordance with accepted academic practice. No use, distribution or reproduction is permitted which does not comply with these terms.

frontiers in Oncology

ORIGINAL RESEARCH
published: 07 January 2022
doi: 10.3389/fonc.2021.746304

Clinical and Genetic Characteristics of Thymoma Patients With Autoimmune Hepatitis and Myocarditis

Xin-tao Yu, Lei Yu, Xin Du, Zhen Yu, Xing-guo Yang and Yu-xuan Jiang*

Department of Thoracic Surgery, Beijing Tongren Hospital, Capital Medical University, Beijing, China

Background: Our study investigated a special series of thymoma with autoimmune hepatitis and myocarditis and tried to reveal the gene expression profiles of this series of thymoma.

Methods: From 2011 to 2019, a total of 13 special thymoma patients presented with autoimmune hepatitis and myocarditis, accounting for about 1.26% of thymoma patients undergoing surgery in Beijing TongRen Hospital. Clinical data were retrospectively collected. All samples were harvested during surgical procedures, and analyzed to identify changes in gene expression using the CapitalBio mRNA microarray analysis, the Whole exome sequencing analysis (WES), qPCR and immunohistochemistry (IHC) tools.

Results: After surgery, patient symptoms were relieved gradually. Levels of lactate dehydrogenase (LDH), creatine kinase MB (CK-MB), aspartate transaminase (AST), and alanine amiotransferase (ALT) increased to some extent within 1 to 3 months after surgery, and fluctuated, and then, gradually decreased close to normal within 6 months after surgery. Enrichment analysis of Kyoto Genome and Genome Encyclopedia (KEGG) pathway was performed and enrichment results were visualized. It indicated that gene expression of 5 signaling pathways, including cell cycle and p53 signaling pathway, were generally abnormal. P53 expression was up-regulated in all tumor tissues. However, IHC and qPCR analysis showed that there was no significant difference in p21 expression between normal and tumor tissue. Results of WES showed that only one driver gene-*MDM4* amplified 4 fold in 53.2% thymoma cells. Further qPCR and IHC analysis confirmed the up-regulation of the expression of p53 and mdm4 in 13 thymoma patients with autoimmune hepatitis and myocarditis.

Conclusion: Our study reveals the clinical and genetic characteristics of thymoma patients with autoimmune hepatitis and myocarditis. For this special category of thymoma, the up-regulation of p53 and mdm4 plays an important role in the occurrence of thymoma and autoimmune hepatitis/myocarditis.

Keywords: autoimmune hepatitis, myocarditis, mdm4, p53, thymoma

OPEN ACCESS

Edited by:
Patrick Loehrer Sr., Indiana University Bloomington, United States

Reviewed by:
Min Li, Sun Yat-sen University Cancer Center (SYSUCC), China
Paul Emile Van Schil, Antwerp University Hospital, Belgium

****Correspondence:***
Lei Yu
yulei1118@sohu.com

Specialty section:
This article was submitted to Thoracic Oncology, a section of the journal Frontiers in Oncology

Received: *23 July 2021*
Accepted: *17 December 2021*
Published: *07 January 2022*

Citation:
Yu X-t, Yu L, Du X, Yu Z, Yang X-g and Jiang Y-x (2022) Clinical and Genetic Characteristics of Thymoma Patients With Autoimmune Hepatitis and Myocarditis. Front. Oncol. 11:746304. doi: 10.3389/fonc.2021.746304

INTRODUCTION

Thymoma is the most common type of neoplasms of the anterior mediastinum. It's often associated with a variety of autoimmune diseases (1). The most common autoimmune diseases is the myasthenia gravis (MG), which is characterized by weakness and fatigability of skeletal and extraocular muscles (2). Other thymoma-related autoimmune diseases include Good's syndrome, dermatomyositis, Addison's disease, rheumatoid arthritis, and so on (3–6). Autoimmune hepatitis and myocarditis are uncommon presentations of thymoma. The association between thymoma and autoimmune hepatitis/myocarditis has been found in very few cases. Extended thymectomy is an effective way to treat these patients (7). However, the mechanism underlying the development of autoimmune hepatitis/myocarditis in patients with thymoma is unclear. Here, we report a special series of 13 thymoma patients with autoimmune hepatitis and myocarditis, and investigate their clinical and genetic characteristics.

MATERIALS AND METHODS

Clinical data were retrospectively collected from the department of thoracic surgery of Beijing TongRen Hospital. From 2011 to 2019, there were 1030 thymoma patients who underwent surgery at Beijing TongRen Hospital. Among these patients, a total of 13 special thymoma patients presented with autoimmune hepatitis and myocarditis, accounting for about 1.26% of thymoma patients undergoing surgery in our department. The diagnostic criteria was according to NCCN Clinical Practice Guidelines in Oncology, American Heart Association and American Association for the Study of Liver Diseases. Diagnostic criteria remained the same in this study. Among the 13 patients, 8 (61.5%) were male and 5 (38.5%) females with an overall median age of 47 years (range 22-72). The patients underwent thymoma resection. Primary thymomas were classified according to the World Health Organization (WHO) criteria as follows: type AB, B1, B2, and B3 (8). The modified Masaoka's classification was used to stage for these primary thymic tumors.

Laboratory test parameters, such as routine biochemistry and lymphocyte count, were obtained from the Clinical laboratory of Beijing Tongren Hospital. All thymoma samples were harvested during surgical procedures from Beijing Tongren Hospital. Normal thymus tissue and adjacent tumor tissue were used as the control groups. The specimens were immediately frozen in liquid nitrogen and stored at −80°C until use. The protocol for sample collection was approved by the Institutional Review Board of Beijing Tongren Hospital, China. Informed written consent was obtained from each patient before sample collection. All study procedures were conducted in line with the approved protocol.

Sample Collection and Determination of Lymphocyte Subsets

Fasting venous blood (1-2ml) was collected from thymoma patients before and after operation. 50μl heparin and 20μl of six color fluorescent monoclonal antibodies were added to the blood and mixed at room temperature in the dark for 15 minutes. 450μl hemolysin was added to each tube and BD FACS Lysing was used to dilute it. Samples were mixed at room temperature for 10 minutes and then analyzed by flow cytometry and lymphocyte subsets analysis software. T lymphocyte surface markers were CD3+, CD4+, CD8+, and NK cells markers were CD16+ and CD56+.

RNA Extraction, Labeling, and Hybridization

Total RNA, containing small RNA, was extracted from thymoma and paraneoplastic thymic carcinoma tissues using the Trizol reagent (Invitrogen) and purified using mirVana miRNA Isolation Kit (Ambion, Austin, TX, USA) following the manufacturer's instructions. Next, the purity and integrity of RNA were determined using gel electrophoresis whereas RNA concentration was determined spectrophotometrically. Only total RNA samples with RNA integrity number (RIN) values >6 was selected for subsequent analysis.

Microarray Imaging and Data Analysis

Data from mRNA array was used to analyze data summarization, normalization, and quality control using the GeneSpring software V13.0 (Agilent). Differentially expressed genes were selected if the change of threshold values was ≥2 or ≤−2-folds and if the Benjamini-Hochberg corrected p-values were 0.05.

KEGG Analysis

The differentially expressed genes obtained from the above analyzes were imported into DAVID 6.8 database (https://david.ncifcrf.gov/) to further examine the differentially expressed pathways. By entering the name list of target genes and selecting species as "Homo Sapiens", the official names of all target genes were identified. Enrichment analysis of Kyoto Genome and Genome Encyclopedia (KEGG) pathway was performed and enrichment results were visualized.

RNA Isolation, cDNA Synthesis, and Quantitative PCR Analysis

Tissue samples were homogenized in 1 ml of TRIzol reagent (Invitrogen) using a PowerGen tissue homogenizer. Then, total RNA was isolated from all samples according to the manufacturer's recommendations. Subsequently, complementary DNA (cDNA) was synthesized from 1μg total RNA using the MMLV Reverse Transcriptase cDNA kit (TAKARA) following the manufacturer's instructions. Next, quantitative PCR (qPCR) was performed in a 96-well reaction plate using SYBR premix Ex Taq (TAKARA) on a Bio-RadCFX96 real-time PCR detection system (Bio-Rad). The comparative Ct (ΔΔCt) method was used to analyze relative mRNA expression.

Histologic and Immunohistochemical (IHC) Testing

Immunohistochemical (IHC) staining was performed on 4-μm-thick slides with anti-p53 (ab26, Abcam), anti-p21 (ab109520,

Abcam) and anti-mdm4 (ab49993, Abcam) using an automated immunostainer (BenchMark XT, Ventana Medical Systems, Tucson, AZ, USA) following the manufacturer's protocol. The p53, p21 and mdm4 IHC were interpreted in three tiers: strong nuclear staining in more than 10% of the tumor cells was considered strong positive staining, samples without any nuclear staining of tumor cells (complete absence) were interpreted as negative staining, and cases exhibiting weak, scattered, or patchy positivity were regarded as weak positive staining. Representative images for each category are shown in **Figures 6**, **8**.

Statistical Analysis

The expression level of p53 in tumor tissues, normal tissues, and tissues adjacent to the tumor was determine using the SPSS 23.0 (IBM, Armonk, NY, USA) and statistical analyses were conducted using Graphpad prism 8 software (Graphpad Software Inc., San Diego, CA, USA). Significance level and misjudgment rate of each KEGG term were estimated by Fisher's exact and chi-squared ($\chi 2$) tests. Measurement data with normal distribution were expressed as mean ± standard deviation, and groups were compared using *t*-tests. For measurement data that did not conform to the normal distribution, rank sum test was used for comparison between groups. Differences were considered statistically significant at a *p*-value of <0.05.

RESULTS

Abnormal Symptoms and Auxiliary Examination Results Were Observed in All Patients

Clinical and demographic data of the study population are summarized in **Table 1**. The common clinical characteristic identified in these thymoma patients was that all of them had autoimmune hepatitis and myocarditis. Some patients also presented with other autoimmune diseases, such as autoimmune enteritis, dermatomyositis, Graves' disease and rheumatoid arthritis. The patients experienced symptoms, such as diarrhea, shortness of breath and fatigue without any known precipitating factors.

Ultrasonic cardiogram revealed that most patients had an ejection fraction (EF) of 70%, with a slightly enlarged left atrium, aortic sinus expansion, and aortic valve regurgitation. However, the echocardiography results of several patients demonstrated a diffuse myocardial wall hypokinesis with reduced left ventricular ejection fraction (LVEF) of less than 35%.

Laboratory examination showed that all patients who received preoperative examination had multiple autoantibody-positive statuses for antinuclear antibody (ANA), anticardiolipin antibody (ACA), antimitochondrial antibody (AMA), Ro52, etc. Their serological tests showed abnormally elevated levels of myocardial enzymes like LDH, AST, ALT, and CK-MB before surgery. Immunophenotyping tests on lymphocyte subsets identified some abnormal cells, such as CD3+CD4+ helper T cells (TH), CD3+CD8+ suppressor T cells (TS).

Extended Resection of Thymoma Relieved Symptoms of Autoimmune Diseases and Reduced Hepatic and Cardiac Injury

All patients underwent extended resection of thymoma. After surgery, abnormal symptoms disappeared gradually. It was observed that levels of LDH, CK-MB, AST, and ALT increased to some extent within 1 to 3 months after surgery, and fluctuated, and then, gradually decreased close to normal within 6 months after surgery (**Figure 1**). As shown in **Table 2**, the same trend was observed in the percentages of total CD3+ T cells and CD4+/CD8+ T cells ratio.

mRNA Profiles Differing Between Thymoma and Controls

To further investigate molecular mechanisms, mRNA samples from 13 thymoma patients and 13 normal thymus tissue controls were analyzed using the Agilent Whole Human Genome Microarray. A scatter plot revealed notable differences between the two groups as illustrated in **Figure 2**.

Disease Analysis

KEGG analysis was conducted for the significantly differential expression genes. Significantly altered mRNAs were analyzed from our microarray datasets. Results showed that the top 30 diseases included immune system diseases (**Figure 3**), which is consistent with the basic information of the 13 patients.

Several Pathways Had a Close Relation With the 13 Patients

Pathway's analysis revealed top 5 abnormal signaling pathways in thymoma tissues. Among the pathways, cell cycle pathway has been shown to play a vital role in the formation of thymoma tumor cells (**Figure 4**).

P53 and p21 Gene Which Mainly Regulate Cell Cycle Pathway Were Tested in Thymoma Tumor Cells

The expression of p53 and p21 in thymoma tissues of 13 patients was determined using qPCR and IHC assays.

Firstly, the expression of p53 and p21 at the RNA level was explored using real-time qPCR. The results indicated that p53 expression was up-regulated in all tumor tissues from the patients. However, there was no significant difference in p21 expression between normal and all tumor tissues (**Figure 5**).

P53-positive cells were observed in the frozen sections of the tumor tissues with autoimmune hepatitis/myocarditis and the tumor tissues without autoimmune disease based on immunohistochemistry. As shown in **Figure 6**, p53-positive cell was not detected in some epithelial-like cells located in the medulla for normal thymus tissues, whereas for thymoma tissues, p53-positive cells were detected in medulla regions. On the contrary, there weren't p21-positive cells in both normal and tumor tissues (**Figure 6**).

TABLE 1 | Patients' information.

Autoimmune disease	Radiotherapy or Chemotherapy (Y/N)	Symptom	Antibody (+)	WHO histology	Masaoka stage	TNM stage	Genetic mutation	Invasion of adjacent mediastinal structures (Y/N)	Autoimmune disease occurs after thymoma (Y/N)
Autoimmune hepatitis	N	dyspnea fatigue	ANA	B1	II	I	p53	N	Y
Myocarditis			AMA				mdm4		
Autoimmune hepatitis	N	dyspnea	ANA	B2	II	I	p53	Y	Y
Myocarditis		fatigue	AMA				mdm4	(lung)	
Autoimmune enteritis		tenesmus	GAB Ro52						
Autoimmune hepatitis	N	fatigue	ANA	B2	II	I	p53	Y	Y
Myocarditis		dizzy	AMA				mdm4	(chest wall)	
Autoimmune hepatitis	N	nausea	ANA	B1	II	I	p53	N	Y
Myocarditis		jaundice	AMA				mdm4		
Autoimmune hepatitis	N	dyspnea	ANA	AB	I	I	p53	N	Y
Myocarditis		fatigue	AMA				mdm4		
Dermatomyositis		erythra							
Autoimmune hepatitis	Y	dyspnea	ANA	B3	I	I	p53	Y	Y
Myocarditis		fatigue	AMA				mdm4	(pericardium)	
Autoimmune hepatitis	Y	fatigue	ANA	B1	II	I	p53	N	Y
Myocarditis		arthrodynia	AMA				mdm4		
Rheumatoid arthritis		fever	SSA CCP						
Autoimmune hepatitis	N	dyspnea fatigue	ANA	B2	I	I	p53	N	Y
Myocarditis			AMA				mdm4		
Autoimmune hepatitis	Y	dyspnea fatigue	ANA	B1	II	I	p53	Y	Y
Myocarditis			AMA				mdm4	(phrenic nerve)	
Autoimmune hepatitis	Y	dyspnea fatigue	ANA	B2	II	I	p53	Y	Y
Myocarditis		chromatosis hypotension	AMA ACA				mdm4	(left innominate vein)	
Graves' disease									
Autoimmune hepatitis	N	dyspnea fatigue	ANA	AB	II	I	p53	N	Y
Myocarditis			AMA				mdm4		
Autoimmune hepatitis	N	dyspnea fatigue	ANA	B3	III	II	p53	Y	Y
Myocarditis			AMA				mdm4	(lung)	
Autoimmune hepatitis	N	dyspnea fatigue	ANA	B3	III	II	p53	Y	Y
Myocarditis		diminution of vision	AMA SSA Ro52 Jo-1				mdm4	(pericardium)	

ANA, anti-nuclear antibody; AMA, anti-mitochondrial antibody; ACA, anti-cardiolipin antibody; CCP, cyclic citrullinated peptide.

Mdm4 Expression Was Up-Regulated in Tumor Tissue With Autoimmune Hepatitis and Myocarditis

The expression of mdm4 was explored at the RNA level using qPCR. The result indicated that the level of mdm4 was up-regulated in tumor tissues with autoimmune hepatitis and myocarditis comparing to the normal thymus tissue and tumor tissues without autoimmune disease (**Figure 7**).

Using IHC, mdm4 staining was negative in epithelial-like cells located in the medulla for the normal thymus tissue and tumor tissues without autoimmune disease. In contrast, more mdm4-positive cells were found in medulla regions for tumor tissues with autoimmune hepatitis and myocarditis (**Figure 8**).

DISCUSSION

Thymoma, a mediastinal malignant tumor, has often been associated with autoimmune diseases. Previous studies have shown that many autoimmune diseases, such as Hashimoto's

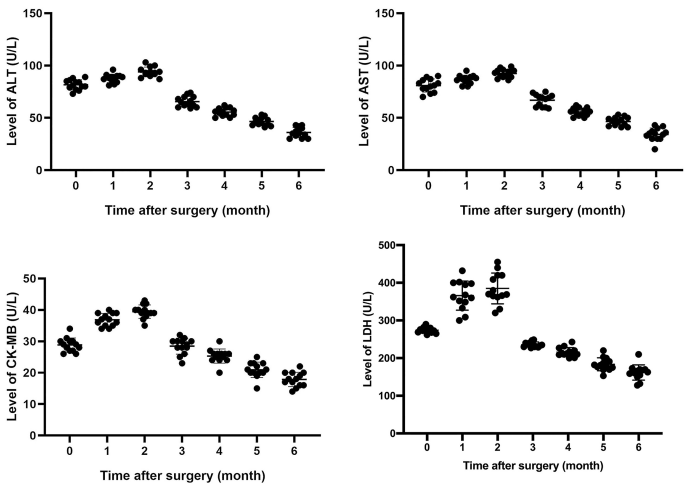

FIGURE 1 | Changes of different enzymes' levels after surgery.

TABLE 2 | T lymphocyte subsets analysis of 13 patients ($\bar{x} \pm s$).

	preoperative%	postoperative% (6 months)	*t* value	*p* value
Total T-lymphocytes (CD3+)	91.92 ± 5.30	80.23 ± 2.56	8.77	<0.01
TH (CD3+CD8+	51.10 ± 1.24	33.6 ± 2.32	28.27	<0.01
TS (CD3+CD4+	28.20 ± 3.87	59.01 ± 12.25	-7.34	<0.01
CD4+/CD8+T-lymphocytes ratio	0.55 ± 0.08	1.75 ± 0.34	-10.96	<0.01
Treg (CD4+CD25+foxp3+)	6.98 ± 1.31	6.85 ± 1.36	0.23	0.822
NK (CD3-CD16+56+	9.76 ± 2.95	8.81 ± 2.04	1.86	0.088

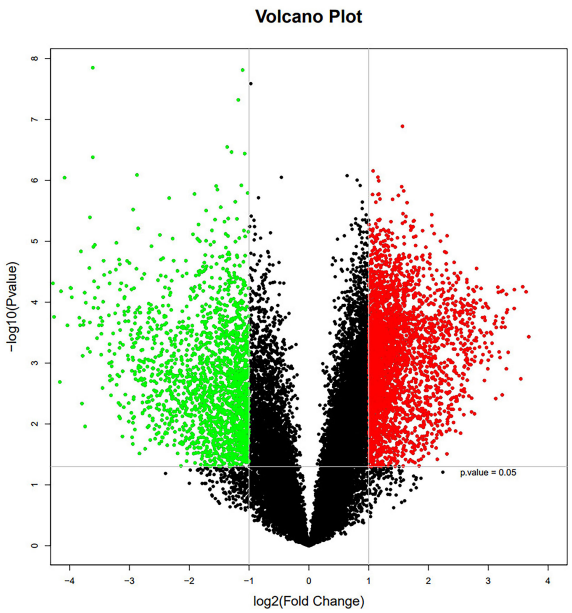

FIGURE 2 | The mRNA expression profile in thymoma patients and normal thymic tissue controls. Red and green dots stand for up-regulated and down-regulated genes, respectively.

thyroiditis, Isaac's syndrome, and Morvan syndrome were caused by thymoma (9). Sometimes, surgical treatment might result in good prognosis of thymoma combined with non-myasthenia gravis autoimmune diseases (10–13). Here, we report the clinical and genetic characteristics of 13 special thymoma patients with autoimmune hepatitis and myocarditis.

Before surgery, these 13 patients had abnormal assay index of LDH, CK-MB, AST, ALT and lymphocyte subsets, which might be attributed to thymoma, autoimmune hepatitis and myocarditis. We continued to trace on the change of these enzymes' levels for 6 months after extended resection for thymoma. The follow-up results indicated that levels of LDH, CK-MB, AST, and ALT rose to some extent within 1 to 3 months after surgery, and then, gradually decreased close to normal. It provided evidence that there exists a link between thymoma and autoimmune hepatitis/myocarditis.

To interpret the results at the genetic level, we conducted microarray analysis to examine differential gene expression profiles of human mRNAs in patients with thymoma and autoimmune hepatitis/myocarditis. And then, we took the differential genes a step further.

As a transcriptional factor, p53 is activated in response to cell stress and regulates many genes involved in cell cycle control, apoptosis, angiogenesis, and cell senescence (14). P53 was reported to be one of the most significantly mutated gene in thymic carcinoma and thymoma (15). Our study revealed that

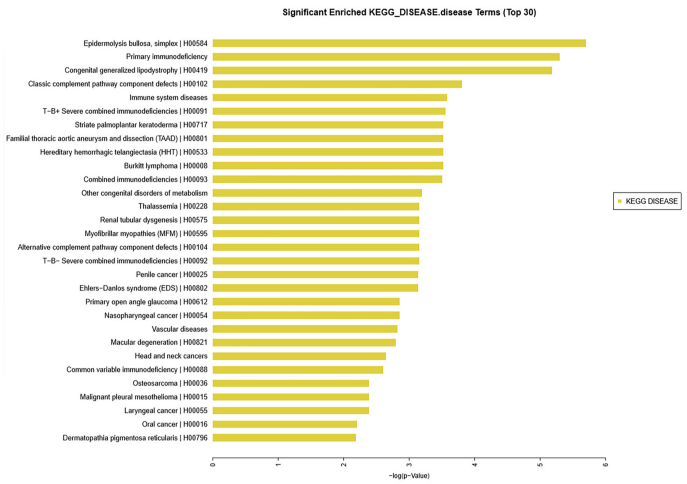

FIGURE 3 | KEGG database analysis identified the top 30 diseases in 13 patients with thymoma unlike control patients. Among such diseases were epidermolysis bullosa, primary immunodeficiency, congenital generalized lipodystrophy, classic complement pathway component defects, and immune system diseases.

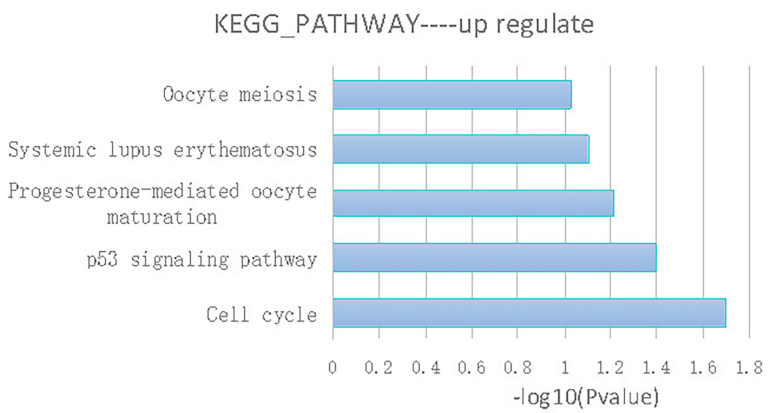

FIGURE 4 | KEGG database analysis indicated that gene expression of 5 signaling pathways including cell cycle, p53 signaling pathway, progesterone mediated oocyte maturation, systemic lupus erythematosus and oocyte meiosis were generally abnormal.

p53 was highly expressed in thymoma patients with autoimmune hepatitis/myocarditis. Results of KEGG database analysis also indicated that cell cycle, p53 signaling pathway and so on were abnormal, similar to our previous study.

Next step, we selected the downstream gene of p53 pathway, p21, to try further revealing the mechanism between thymoma and autoimmune hepatitis/myocarditis. The p21 gene is located on the short arm of chromosome 6 downstream of the p53 pathway. Usually, an abnormal expression of its protein affects the regulation of Cyclin, CDK, and kinase activity, thus affecting cell proliferation and differentiation (16). Previously, some researchers proved that this gene was up-regulated in dermatomyositis (17). But in our study, there was no obvious difference of p21's expression between thymoma and normal tissue.

Meanwhile, the whole exome sequencing analysis (WES) result indicated that the MDM4 amplifiied in this thymoma cells (18). Mdm2 and mdm4 proteins form heterodimers that are much more effective in regulating p53 (19). We ever tested that mdm4/mdm2 heterodimers were down-regulated in thymoma patients without autoimmune hepatitis/myocarditis. However, we used the qPCR assay and IHC test to measure mdm4 levels in these 13 thymoma patients with autoimmune hepatitis/myocarditis, and discovered that mdm4 level was up-regulated. Jonathan P. McNallya's research group found that potentiation of p53 (via inhibition of mdm2) led to the selective elimination of activated and pathological T cells *in vivo*, which had an impact on the immune system (20). It has also been reported that the *mdm4/mdm2* heterodimers are upregulated not only in the brain and nerve tumor tissues, breast cancer, soft tissue sarcomas, type

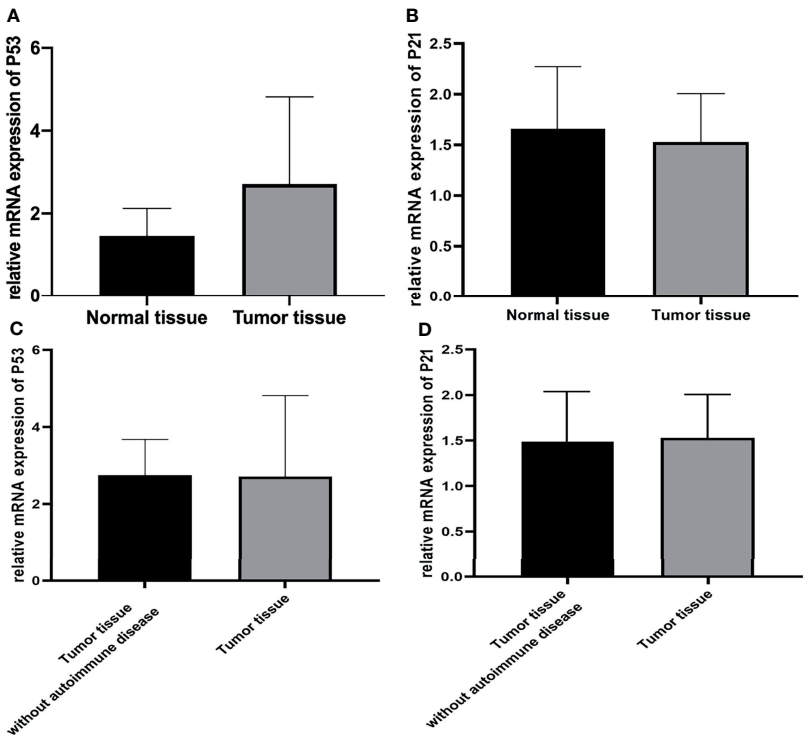

FIGURE 5 | **(A, C)** The expression of p53 was higher in all tumor tissues than in normal tissues. ($p<0.05$), but it was similar between tumor tissue with autoimmune hepatitis and myocarditis and tumor tissue without autoimmune disease. ($p>0.05$) **(B, D)** The expression of p21 was similar between normal and all tumor tissues. ($p>0.05$).

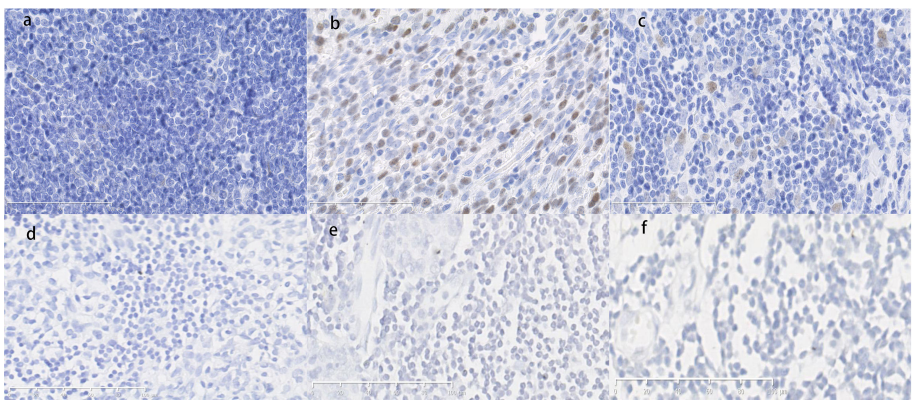

FIGURE 6 | **(A)** Normal thymus tissue immunostained with p53 antibodies. Score=0, low expression. **(B)** Thymoma tissue with hepatitis/myocarditis immunostained with p53 antibodies. The p53-positive cells are presented in the field. Score=9, high expression. **(C)** Tumor tissue without autoimmune disease immunostained with p53 antibodies. Score=2, low expression. **(D)** Normal thymus tissue immunostained with p21 antibodies. Score=0, low expression. **(E)** Thymoma tissue with hepatitis/myocarditis immunostained with p21 antibodies. Score=0, low expression. **(F)** Tumor tissues without autoimmune disease immunostained with p21 antibodies. Score=0, low expression. (×400).

1 diabetes, and systemic lupus erythematosus (21–23), but also in the parathyroid glands of patients with renal secondary hyperparathyroidism (24). Therefore, we think that there was a strong association between the up-regulation of p53 and mdm4 and thymoma, as well as autoimmune hepatitis/myocarditis. We can also infer that abnormal p53-mdm4 pathway may promote the occurrence and development of thymoma, which further cause autoimmune hepatitis and myocarditis.

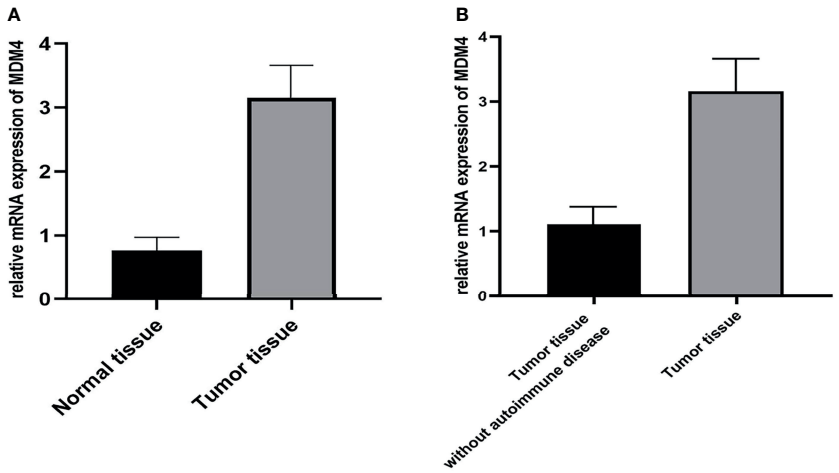

FIGURE 7 | **(A, B)** Results of qPCR showed that mdm4 was up-regulated in tumor tissues comparing with normal tissue and tumor tissue without autoimmune disease. ($p<0.05$).

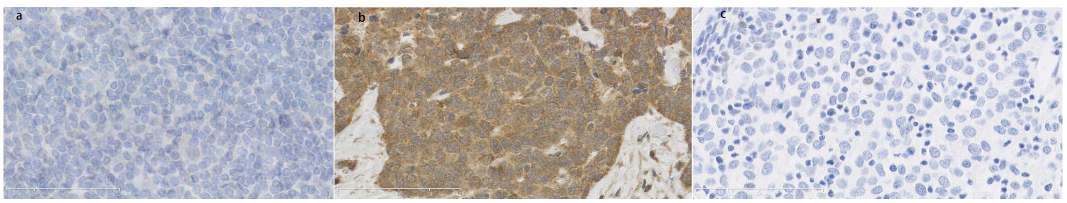

FIGURE 8 | **(A)** Normal thymus tissue immunostained with mdm4 antibodies. Score=0, low expression. **(B)** Thymoma tissue with hepatitis/myocarditis immunostained with mdm4 antibodies. Mdm4-positive cells were shown in the field. Score=12, high expression. **(C)** Tumor tissues without autoimmune disease immunostained with p21 antibodies. Score=0, low expression. (×400).

CONCLUSION

Our study reveals the clinical and genetic characteristics of thymoma patients with autoimmune hepatitis and myocarditis. For this special category of thymoma, the up-regulation of p53 and mdm4 plays an important role in the occurrence of thymoma and autoimmune hepatitis/myocarditis.

DATA AVAILABILITY STATEMENT

The datasets presented in this study can be found in online repositories. The names of the repository/repositories and accession number(s) can be found in the article/supplementary material.

ETHICS STATEMENT

Because all patients in this study signed consent forms and were enrolled, informed consent was obtained from all participants. The study was approved by the Human Research Ethics Board of Beijing Tongren Hospital, Capital Medical University, and all experiments were performed in accordance with relevant guidelines and regulations.

AUTHOR CONTRIBUTIONS

X-tY and LY: Conceptualization, Methodology, Software. X-tY: Data curation, Writing- Original draft preparation. XD: Visualization, Investigation. ZY: Supervision. X-gY: Software, Validation. Y-xJ: Writing- Reviewing and Editing. All authors contributed to the article and approved the submitted version.

FUNDING

This study was supported by the Clinical Technology Innovation Project of Beijing Hospital Authority (XMLX201839) and the National Natural Science Foundation of China (Grant Number: 81550004).

ACKNOWLEDGMENTS

We thank Mr. Xiang Gao for helpful discussions in the preparation of the manuscript. We are grateful to all the current and former members of our laboratories for their excellent contributions to the research projects that were cited in this article.

REFERENCES

1. Tomita M, Atsuzaki Y, Edagawa M, Maeda M, Shimizu T, Hara T, et al. Correlation Between Tumor Angiogenesis and Invasiveness in Thymic Epithelial Tumors. *J Thorac Cardiovasc Surg* (2002) 124(3):493–8. doi: 10.1067/mtc.2002.124389
2. Gilhus NE. Autoimmune Myasthenia Gravis. *Expert Rev Neurother* (2009) 9 (3):351–8. doi: 10.1586/14737175.9.3.351
3. Zaman M, Huissoon A, Buckland M, Patel S, Alachkar H, Edgar JD, et al. Clinical and Laboratory Features of Seventy-Eight UK Patients With Good's Syndrome (Thymoma and Hypogammaglobulinaemia). *Clin Exp Immunol* (2019) 195(1):132–8. doi: 10.1111/cei.13216
4. Agmon-Levin N, Altman A, Shoenfeld Y. Thymoma and Autoimmunity. *Cell Mol Immunol* (2011) 8(3):199–202. doi: 10.1038/cmi.2010.74
5. Seker M, Gozu HI, Oven Ustaalioğlu BB, Sonmez B, Erkal FY, Kocak M, et al. Myasthenia Gravis and Autoimmune Addison Disease in a Patient With Thymoma. *Clin Lung Cancer* (2009) 10(5):367–70. doi: 10.3816/CLC.2009.n.051
6. Tsuchiya T, Sano A, Kawashima M. Paraneoplastic Dermatomyositis as a Potential Precursor to Thymic Carcinoma. *Ann Thorac Surg* (2020) 109(4): e247–9. doi: 10.1016/j.athoracsur.2019.07.039
7. Mendogni P, Rosso L, Tosi D, Palleschi A, Righi I, Minonzio F, et al. Autoimmune Hepatitis: An Uncommon Presentation of Thymoma. *Tumori* (2016) 102(Suppl. 2):40–42. doi: 10.5301/tj.5000505
8. Marx A, Chan JK, Coindre JM, Detterbeck F, Girard N, Harris NL, et al. The 2015 World Health Organization Classification of Tumors of the Thymus: Continuity and Changes. *J Thorac Oncol* (2015) 10(10):1383–95. doi: 10.1097/JTO.0000000000000654
9. Bernard C, Frih H, Pasquet F, Kerever S, Jamilloux Y, Tronc F, et al. Thymoma Associated With Autoimmune Diseases: 85 Cases and Literature Review. *Autoimmun Rev* (2016) 15(1):82–92. doi: 10.1016/j.autrev.2015.09.005
10. Liu L, Zhang J, Wang G, Guo C, Chen Y, Huang C, et al. Surgical Treatment is Effective in Treating Thymoma Accompanied With Non-Myasthenia Gravis Autoimmune Diseases: A Single-Center Clinical Experience. *Scand J Surg* (2021) 110(3):420–6. doi: 177/1457496920964337
11. Fukushima A, Ichimura Y, Obata S, Kinoshita-Ise M, Fujio Y, Takeno M, et al. Thymoma-Associated Multi-Organ Autoimmunity: A Case of Graft-Versus-Host Disease-Like Erythroderma Complicated by Good Syndrome Successfully Treated by Thymectomy. *J Dermatol* (2017) 44(7):830–5. doi: 10.1111/1346-8138.13777
12. Solimani F, Maglie R, Pollmann R, Schmidt T, Schmidt A, Ishii N, et al. Thymoma-Associated Paraneoplastic Autoimmune Multiorgan Syndrome-From Pemphigus to Lichenoid Dermatitis. *Front Immunol* (2019) 10:1413. doi: 10.3389/fimmu.2019.01413
13. Vogrig A, Pauletto G, Belgrado E, Pegolo E, Di Loreto C, Rogemond V, et al. Effect of Thymectomy on Refractory Autoimmune Status Epilepticus. *J Neuroimmunol* (2018) 317:90–4. doi: 10.1016/j.jneuroim.2018.01.009
14. Klein C, Vassilev LT. Targeting the P53-MDM2 Interaction to Treat Cancer. *Br J Cancer* (2004) 91(8):1415–9. doi: 10.1038/sj.bjc.6602164
15. Moreira AL, Won HH, McMillan R, Huang J, Riely GJ, Ladanyi M, et al. Massively Parallel Sequencing Identifies Recurrent Mutations in TP53 in Thymic Carcinoma Associated With Poor Prognosis. *J Thorac Oncol* (2015) 10(2):373–80. doi: 10.1097/JTO.0000000000000397
16. Kobayashi S, Fujimori T, Mitomi H, Tomita S, Ichikawa K, Imura J, et al. Immunohistochemical Assessment of a Unique Basal Pattern of P53 Expression in Ulcerative-Colitis-Associated Neoplasia Using Computer-Assisted Cytometry. *Diagn Pathol* (2014) 9:99. doi: 10.1186/1746-1596-9-99
17. Gallardo E, de Andres I, Illa I. Cathepsins are Upregulated by IFN-Gamma/STAT1 in Human Muscle Culture: A Possible Active Factor in Dermatomyositis. *J Neuropathol Exp Neurol* (2001) 60(9):847–55. doi: 10.1093/jnen/60.9.847
18. Du X, Yu L, Li F, Yu Z, Yang XG, Jiang YX, et al. Case Report: MDM4 Amplified in a Thymoma Patient With Autoimmune Enteropathy and Myocarditis. *Front Endocrinol (Lausanne)* (2021) 12:661316. doi: 10.3389/fendo.2021.661316
19. Moscetti I, Teveroni E, Moretti F, Bizzarri AR, Cannistraro S. MDM2-MDM4 Molecular Interaction Investigated by Atomic Force Spectroscopy and Surface Plasmon Resonance. *Int J Nanomed* (2016) 11:4221–9. doi: 10.2147/IJN.S114705
20. McNally JP, Millen SH, Chaturvedi V, Lakes N, Terrell CE, Elfers EE, et al. Manipulating DNA Damage-Response Signaling for the Treatment of Immune-Mediated Diseases. *Proc Natl Acad Sci USA* (2017) 114(24): E4782–91. doi: 10.1073/pnas.1703683114
21. Shvarts A, Steegenga WT, Riteco N, van Laar T, Dekker P, Bazuine M, et al. MDMX: A Novel P53-Binding Protein With Some Functional Properties of MDM2. *EMBO J* (1996) 15(19):5349–57. doi: 10.1002/j.1460-2075.1996.tb00919.x
22. Liu Y, Dai L, Liu W, Shi G, Zhang J. Autoantibody to MDM2: A Potential Serological Marker of Systemic Lupus Erythematosus. *J Immunol Res* (2015) 2015:963568. doi: 10.1155/2015/963568
23. Pellegrino M, Traversi G, Arena A, Cappa M, Rosado MM, Andreani M, et al. Effect of P53 Activation Through Targeting MDM2/MDM4 Heterodimer on T Regulatory and Effector Cells in the Peripheral Blood of Type 1 Diabetes Patients. *PloS One* (2020) 15(1):e0228296. doi: 10.1371/journal.pone.0228296
24. Alcázar JA, Polo JR, Tardío JC, Anguita J, Martínez-Montero JC, Jofré R, et al. Comparative Study of the Expression of Proteins Involved in the Cell Cycle in Renal Secondary Hyperparathyroidism. *Kidney Int Suppl* (2003) (85):S28–31. doi: 10.1046/j.1523-1755.63.s85.8.x

Conflict of Interest: The authors declare that the research was conducted in the absence of any commercial or financial relationships that could be construed as a potential conflict of interest.

Publisher's Note: All claims expressed in this article are solely those of the authors and do not necessarily represent those of their affiliated organizations, or those of the publisher, the editors and the reviewers. Any product that may be evaluated in this article, or claim that may be made by its manufacturer, is not guaranteed or endorsed by the publisher.

Copyright © 2022 Yu, Yu, Du, Yu, Yang and Jiang. This is an open-access article distributed under the terms of the Creative Commons Attribution License (CC BY). The use, distribution or reproduction in other forums is permitted, provided the original author(s) and the copyright owner(s) are credited and that the original publication in this journal is cited, in accordance with accepted academic practice. No use, distribution or reproduction is permitted which does not comply with these terms.

frontiers in Oncology

ORIGINAL RESEARCH
published: 14 January 2022
doi: 10.3389/fonc.2021.779700

Cisplatin and Irinotecan as First-Line Chemotherapy for Previously Untreated Metastatic Thymic Carcinoma: Updated Analysis

Akito Fukuda[1,2], *Yusuke Okuma*[1,2*], *Taiki Hakozaki*[1], *Kie Mirokuji*[1], *Makiko Yomota*[1], *Tsunekazu Hishima*[3] *and Yukio Hosomi*[1]

[1] Department of Thoracic Oncology and Respiratory Medicine, Tokyo Metropolitan Cancer and Infectious Diseases Center Komagome Hospital, Tokyo, Japan, [2] Department of Thoracic Oncology, National Cancer Center Hospital, Tokyo, Japan, [3] Department of Pathology, Tokyo Metropolitan Cancer and Infectious diseases Center Komagome Hospital, Tokyo, Japan

Platinum-based chemotherapy is the *de facto* standard treatment for metastatic or unresectable thymic carcinoma. The optimal chemotherapy regimen has not yet been determined, including whether this should be combined with a second- or third-generation anti-cancer agent. We retrospectively evaluated the data of patients with metastatic or unresectable thymic carcinoma who were treated with a combination of cisplatin and irinotecan as first-line chemotherapy between 2002 and 2021 (trial registration UMIN000012175). The primary endpoint was response rate according to the RECIST criteria version 1.1. Secondary endpoints were disease control rate, progression-free survival (PFS), overall survival (OS), and toxicity (adverse events). Some patients analyzed in this study were also included in the previous trial, which was terminated early. For this analysis, we included 18 patients with a median age of 56 years and an Eastern Cooperative Oncology Group performance status of 0 or 1. All patients had clinical stage IVa or IVb thymic carcinoma according to the Masaoka-Koga staging system. The response rate was 44% and the disease control rate was 89%. The median PFS was 8.4 months (95% confidence interval (CI): 2.7–11.6 months) and the median OS was 45.6 months (95% CI: 15.7–69.1 months). Grade 3 or worse hematological toxicity was observed in 5 patients and grade 3 or worse non-hematological toxicity was observed in 3 patients. None of the patients developed febrile neutropenia, and no treatment-related deaths occurred. Thus, the combination of cisplatin and irinotecan as first-line chemotherapy for metastatic thymic carcinoma showed efficacy and acceptable toxicity.

Keywords: thymic carcinoma, cisplatin, irinotecan, first-line chemotherapy, metastasis

OPEN ACCESS

Edited by:
Mylene Truong, University of Texas MD Anderson Cancer Center, United States

Reviewed by:
Jun-Ling Li, Chinese Academy of Medical Sciences and Peking Union Medical College, China
Lothar Bergmann, University Hospital Frankfurt, Germany

***Correspondence:**
Yusuke Okuma
yokuma@ncc.go.jp
orcid.org/0000-0002-3225-4879

Specialty section:
This article was submitted to Thoracic Oncology, a section of the journal Frontiers in Oncology

Received: *19 September 2021*
Accepted: *24 December 2021*
Published: *14 January 2022*

Citation:
Fukuda A, Okuma Y, Hakozaki T, Mirokuji K, Yomota M, Hishima T and Hosomi Y (2022) Cisplatin and Irinotecan as First-Line Chemotherapy for Previously Untreated Metastatic Thymic Carcinoma: Updated Analysis. Front. Oncol. 11:779700. doi: 10.3389/fonc.2021.779700

INTRODUCTION

Thymic carcinoma is a rare cancer arising from the mediastinum originating from thymic epithelial cells, accounting for approximately 5% of all thymic epithelial tumors (1). Thymic carcinoma tends to metastasize with invasive growth, but without associated immunological symptoms such as type B thymoma; therefore, it is often diagnosed at an advanced stage and has a poor prognosis (2).

The standard of care for metastatic thymic carcinoma is palliative chemotherapy. The key drugs for treating thymic malignancies include platinum and doxorubicin containing chemotherapy used in the Einhorn protocol (3) including CAP (cisplatin, doxorubicin, cyclophosphamide, and prednisone) (4), CODE (cisplatin, vincristine, doxorubicin, and etoposide) (5), ADOC (cisplatin, doxorubicin, vincristine, and cyclophosphamide) (6), and VIP (etoposide, ifosfamide, and cisplatin) regimens (7, 8). Doxorubicin does not tend to be beneficial in the treatment of thymic carcinoma; therefore, a combination of carboplatin and paclitaxel is now commonly used owing to its satisfactory response rate, time-to-event data, and toxicity profile (9–11). However, given the rarity of this cancer, data are only available from phase II or retrospective studies with small sample sizes. There is minimal evidence of the effectiveness of first- or later-line chemotherapy for thymic malignancies. With respect to later lines of chemotherapy, recent phase II trials have shown an increase in the clinical effectiveness of cytotoxic chemotherapy, molecular-targeted agents, and immune checkpoint inhibitors. The key drugs or optimal strategy for the treatment of thymic carcinoma are gradually being revealed, but there is still ample room for development.

Our cancer center previously reported a retrospective single-center analysis that demonstrated the efficacy and mild hematological toxicity of combination treatment with cisplatin and irinotecan as the first-line chemotherapy for patients with metastatic/unresectable thymic carcinoma (12). We performed a phase II clinical trial of irinotecan and cisplatin for thymic carcinoma. Although the clinical trial was interrupted because of late accrual (UMIN000012175), we reported all treated patients with irinotecan and cisplatin for thymic carcinoma. The purpose of the current study was to evaluate the efficacy and toxicity of this combination therapy as first-line chemotherapy for irinotecan and cisplatin for metastatic/unresectable thymic carcinoma by including additional cases over a longer follow-up time.

PATIENTS AND METHODS

Study Cohort and Data Acquisition

This retrospective observational study included patients with metastatic/unresectable thymic carcinoma who received a combination of cisplatin and irinotecan as first-line chemotherapy between January 2002 and December 2021 at Tokyo Metropolitan Cancer and Infectious Disease Center Komagome Hospital. All patients had histologically confirmed stage IVa or IVb thymic carcinoma based on the Masaoka-Koga staging system (13). The inclusion criteria were as follows: <75 years of age, Eastern Cooperative Oncology Group Performance Scale status (ECOG PS) of 0 or 1, adequate organ function for chemotherapy, neutrophil count of 1500 cells/mm^3 or higher, hemoglobin concentration of 9.0 g/dL or higher, platelet count of $10.0 \times 10^4/mm^3$ or more, and adequate renal and liver function. Patients with resectable tumors and those who had previously undergone treatment were excluded. The Institutional Review Board of Komagome Hospital approved the present study (IRB number 2415), and the study protocol adhered to the principles of the Declaration of Helsinki.

Between October 30, 2013 and March 22, 2019, our cancer center performed a prospective phase II trial of cisplatin and irinotecan for patients with previously untreated thymic carcinoma; however, the trial had to be terminated because of late accrual. For the current analysis, further patients were enrolled in the trial (UMIN000012175) who were treated with cisplatin and irinotecan, thereby enabling data collection according to the same study protocol. This prospective study has also been approved by the Institutional Review Board of Komagome Hospital (IRB number 1306).

Treatment Procedure

The included patients were treated with combination chemotherapy of cisplatin (60 mg/m^2 or 80 mg/m^2) on day 1 and irinotecan (60 mg/m^2) on days 1, 8, and 15 every 4 weeks for up to 6 cycles if the patients did not exhibit unacceptable toxicities or disease progression. The dose of cisplatin was reduced from 80 mg/m^2 to 60 mg/m^2 at the physician's discretion.

Evaluation and Statistical Analysis

The primary endpoint of this study was response rate based on the Response Evaluation Criteria in Solid Tumors (RECIST) version 1.1 (14). Objective response was defined as a complete response plus partial response, and disease control was defined as an objective response plus stable disease. The secondary endpoints were progression-free survival (PFS), overall survival (OS), and disease control rate (DCR) to assess the efficacy and toxicity of this regimen. PFS was assessed from the date of the first chemotherapy cycle until the date of progressive disease first detected by the investigators' assessments or loss to follow-up. OS was assessed from the date of the first cycle of chemotherapy until death or loss to follow-up. Disease assessment was evaluated by computed tomography after every two cycles of chemotherapy. After the last chemotherapy cycle, computed tomography was performed once every two to three months until the disease progressed.

Safety was assessed according to the Common Terminology Criteria for Adverse Events version 4.0 (CTCAE v4.0). We also collected and evaluated data on second- and later-line chemotherapy.

All statistical analyses were performed using the JMP 14.3.0 statistical software for Windows (SAS Institute, Cary, NC) with a two-sided α value set at 0.05.

RESULTS

Patient Characteristics

Eighteen patients with previously untreated metastatic/unresectable thymic carcinoma were treated with irinotecan and cisplatin. One of eighteen patient has been enrolled in the prospective analysis (trial registration UMIN000012175). Clinical characteristics of the patients are summarized in **Table 1**.

TABLE 1 | Patient characteristics.

Patient characteristics	Value (N = 18)
Age (years), median (range)	56 (44–73)
Sex, n (%)	
Male	11 (61)
Female	7 (39)
ECOG	
0	7 (39)
1	11 (61)
2-4	0 (0)
Masaoka-Koga staging system	
IVa	3 (17)
IVb	15 (83)
Metastatic sites at diagnosis	
LUNG	7
HEP	4
LYM	6
BRA	2
OSS	5
PLE	8
Histology	
Squamous cell carcinoma	14 (77)
Undifferentiated carcinoma	3 (17)
Large cell neuroendocrine carcinoma	1 (6)
Smoking history	
Never-smoker	5 (28)
Previously/current smoker	13 (72)
Paraneoplastic syndrome	0

Data are presented as n (%) unless otherwise stated. ECOG, Eastern Cooperative Oncology Group; HEP, liver; LYM, lymph nodes; BRA, brain; OSS, bone; PLE, pleura.

TABLE 2 | Delivery methods of first- and later-line chemotherapy and response to cisplatin and irinotecan combination therapy.

Patient characteristics	Value (N = 18)
Cisplatin dose	
80 mg/m^2	3 (17)
60 mg/m^2	15 (83)
Average number of cycles	3.6 (1–6)
Response to cisplatin and irinotecan	
Complete response	0 (0)
Partial response	8 (44)
Stable disease	8 (44)
Progressive disease	2 (12)
Discontinuation of first-line regimen	6 (33)
Reason for discontinuation	
Progressive disease	2
Adverse event	3
Other	1
Later chemotherapy line	
Average of later chemotherapy line (range)	2.8 (0–8)
Number of later chemotherapy line	1
8	1
6	1
5	3
4	3
3	3
2	4
1	2
0	

Data are presented as n (%) unless otherwise stated.

There were 7 patients (39%) with an ECOG PS of 0 and 11 (61%) with an ECOG PS of 1. Three patients (17%) had Masaoka-Koga stage IVa and fifteen (83%) had stage IVb disease. The most common metastatic site was the lungs. With respect to the pathological diagnosis, 14 patients (77%) had squamous cell carcinoma, 3 (17%) had undifferentiated carcinoma, and 1 (6%) had large cell neuroendocrine carcinoma. There were no instances of paraneoplastic syndrome or immunological complications, including myasthenia gravis, pure red cell anemia, or Good syndrome.

Treatment Delivery

The delivery mode for the irinotecan and cisplatin treatment is summarized in **Table 2**. Cisplatin was administered at a dose of 80 mg/m^2 in 3 patients (17%) and 60 mg/m^2 in 15 (83%). The average number of cycles of cisplatin and irinotecan combination therapy was 3.6 (range, 1–6). Two patients discontinued chemotherapy due to progressive disease, and three patients discontinued chemotherapy because of adverse events. The average number of later lines of chemotherapy was 2.8. S-1, carboplatin, and paclitaxel combination therapies were commonly used in the second-line setting (**Figure 1A**). One patient received nivolumab as part of an investigation with the PREMIER (15) study and one patient received lenvatinib through the REMORA study (16).

Treatment Efficacy

Among the 18 patients, 8 (44%) had a partial response and 8 (44%) had stable disease. The objective response and disease control rates were 44% and 89%, respectively. Progressive disease was observed in only two patients (**Table 2**). The best response and change in tumor size for each patient are shown in **Figure 1B**. Only 2 of the 18 patients exhibited tumor growth based on baseline measurements. Eight patients showed a tumor reduction rate of 30% or more. The median follow-up time was 29.5 months. The median PFS was 8.4 months [95% confidence interval (CI): 2.7–11.6 months] (**Figure 2A**). The median OS was 45.6 months (95% CI: 15.7–69.1 months) (**Figure 2B**).

A Swimmer plot is shown in **Figure 1A**. Fifteen patients received S-1 as the second- or later-line regimen, with a response rate of 33% and median PFS of 8.1 months (95% CI: 0.7–10.3 months) (**Table 3**). Eight patients received carboplatin and paclitaxel as the second- or the later-line regimen, with a response rate of 38% and median PFS of 4.1 months (95% CI: 0.9–7.7 months). One patient (number 17) was treated with nivolumab as third-line chemotherapy, with a PFS of 25 months. One patient (number 14) received lenvatinib as the fifth-line chemotherapy with a PFS of 3.4 months.

Toxicities

The toxicity results are shown in **Table 4**. Grade 3 hematological toxicity was observed in six patients. The major treatment-related adverse events were nausea (73%), neutropenia (72%), and leukocytopenia (45%). Three patients showed grade 3 neutropenia; however, none of the patients developed febrile neutropenia. Grade 3 non-hematological adverse events were observed in five patients and grade 3 diarrhea was observed in one patient. No patient exhibited Grade 4 adverse events and

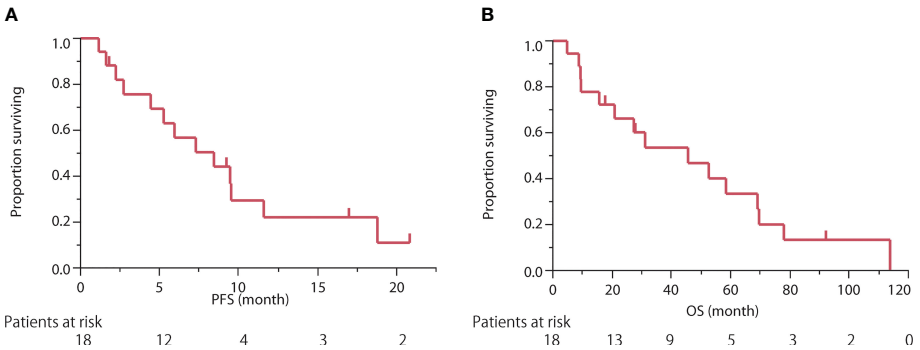

FIGURE 1 | **(A)** Swimmer's plot of progression-free survival in individual patients at each chemotherapeutic line. **(B)** Change in tumor size from baseline (%) in thymic carcinoma patients treated with the cisplatin and irinotecan combination regimen as the first-line chemotherapy. TC, carboplatin and paclitaxel; GV, gemcitabine and vinorelbine; DOC, docetaxel; AMR, amrubicin; CPT-11, irinotecan; PEM, pemetrexed; ADOC, cisplatin, doxorubicin, vincristine, and cyclophosphamide; GEM, gemcitabine; CBG, carboplatin and gemcitabine; CA, cisplatin and adriamycin; PE, cisplatin and etoposide.

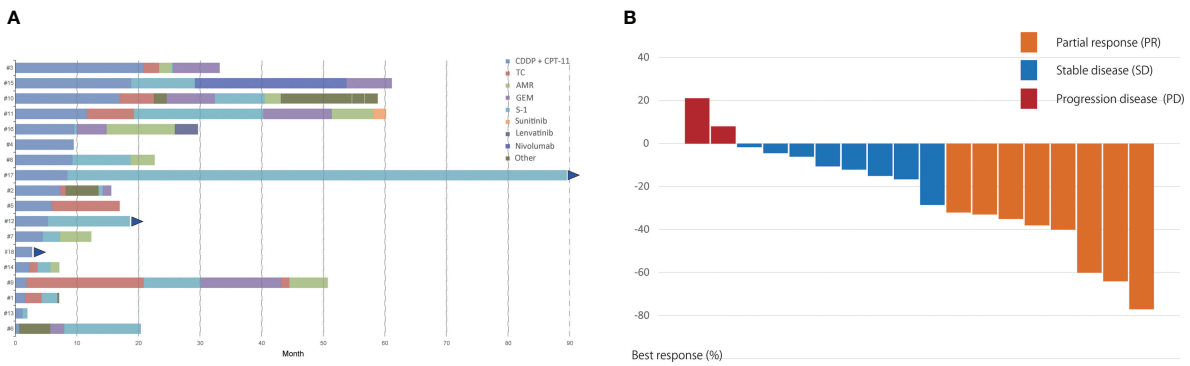

FIGURE 2 | **(A)** Progression-free survival and **(B)** overall survival for 18 patients with unresectable thymic carcinoma who received cisplatin and irinotecan combination therapy.

there were no treatment-related deaths. Three patients discontinued the cisplatin and irinotecan regimens because of gastrointestinal adverse events.

DISCUSSION

In the current analysis, our long-term experience with cisplatin and irinotecan combination chemotherapy for unresectable or metastatic thymic carcinoma demonstrated clinical effectiveness and tolerability, which is in line with previous studies (**Table 5**). It is worth noting that the 5-year survival rate for patients with metastatic or recurrent thymic carcinoma in this trial was 26.8%, and the 1-year PFS rate was 22.1%.

The National Comprehensive Cancer Network (NCCN) Clinical Practice Guidelines in Oncology (17) lists platinum-containing agents (including carboplatin, paclitaxel, ADOC, VIP, and CAP) as the recommended first-line chemotherapy options for thymic carcinoma. The guideline also suggests carboplatin and paclitaxel combination therapy as a *de facto* standard first-line chemotherapy, owing to its mild toxicity but similar efficacy. The present study also showed that cisplatin and irinotecan combination therapy had good efficacy and mild toxicity; moreover, the rate of grade 3 or 4 toxicities was 33% in the present study. However, it was more than 40% in the other regimens (**Table 5**). This combination appears to have lower toxicity than the carboplatin and paclitaxel combination regimen given the lack of peripheral neuropathy and that the patients can survive for more than 5 years. Thus, fewer adverse events could be a reason for choosing a cisplatin-based regimen. In terms of efficacy, cisplatin irinotecan therapy, as the first-line regimen, showed positive activity for thymic carcinoma. The ORR and PFS were 44% and 8.4 months, respectively. Xue et al. reported the efficacy of gemcitabine and platinum regimen as a first-line chemotherapy for stage IV thymic carcinoma (11). The PFS was 12.0 months, which seems long; however, 64.5% of patients treated with gemcitabine and platinum regimens received radiotherapy after chemotherapy. Furthermore, the ORR of the gemcitabine and platinum regimens was 29%. Therefore, it is not possible to conclude that the gemcitabine and platinum regimens are better

TABLE 3 | Efficacy of second- or later-line regimen.

Chemotherapy	N	PR	SD	PD	RR (%)	Median PFS, months (95% confidence interval)
S-1	15	5	5	5	33%	8.1 (0.7–10.3)
CBDCA+ PTX	8*	3	1	3	38%	4.1 (0.9–7.7)

PFS, progression-free survival; PR, partial response; SD, stable disease; PD, progressive disease; RR, response rate; CBDCA, carboplatin; PTX, paclitaxel.
**The outcome of one patient was not evaluated.*

TABLE 4 | Treatment-related hematological and non-hematological adverse events.

Adverse events	Grade 1 or 2, n (%)	Grade 3, n (%)	Grade 4, n (%)
Hematological			
Leukocytopenia	7 (39)	1 (6)	0
Neutropenia	9 (50)	3 (17)	0
Anemia	6 (33)	2 (11)	0
Thrombocytopenia	3 (16)	0	0
Febrile neutropenia	–	0	0
Non-hematological			
Nausea	12 (67)	1 (6)	0
Vomiting	5 (27)	0 (0)	0
Anorexia	4 (22)	3 (17)	0
Diarrhea	5 (29)	1 (6)	0

TABLE 5 | Previously reported platinum-combination chemotherapy for unresectable/metastatic thymic carcinoma.

Study	Chemotherapy	N	RR (%)	PFS, months (median)	OS, months (median)	Toxicities (Grade ≥ 3)	
						Hematological (%)	FN (%)
Agatsuma et al. (6)	ADOC	34	50	–	21.3	71	12
Magois et al. (8)	VIP	9	44	–	20	–	–
Igawa et al. (9)	CBDCA+PTX	11	36	7.9	22.7	45	0
Hirai et al. (10)	CBDCA+PTX	39	36	7.5	–	44	5
Current study	CDDP+CPT-11	18	44	8.4	45.6	33	0

PFS, progression-free survival; RR, response rate; OS, overall survival; FN, febrile neutropenia; ADOC, cisplatin + doxorubicin + vincristine + cyclophosphamide; VIP, cisplatin + etoposide + cyclophosphamide; CBDCA, carboplatin; PTX, paclitaxel; CDDP, cisplatin; CPT-11, irinotecan.

than cisplatin and irinotecan regimens. Additionally, we also believe that irinotecan is a key drug for treating thymic malignancies. Antibody-drug conjugates with topoisomerase I inhibitor (irinotecan) payload are potentially going to be active agents for thymic malignancies. Moreover, cisplatin and irinotecan combination therapy showed therapeutic activity as a second-line regimen, with a response rate of 29% and mild toxicity (18). These results suggest that irinotecan and cisplatin combination therapy may be a useful regimen for advanced thymic carcinoma.

Based on the results of a randomized controlled phase 3 trial performed in Japanese patients (JCOG9511) (19), cisplatin and irinotecan combination therapy had been widely used as a first-line regimen for extensive-disease small-cell lung cancer (ED-SCLC) in Japan until the era of oncoimmunotherapy. In the JCOG9511 trial, the cisplatin and irinotecan regimen resulted in longer survival and milder hematological toxicity than the cisplatin and etoposide regimen for ED-SCLC. After the results of the JCOG9511 trial were published, a randomized controlled trial (SWOG S0124) in North American patients (20) failed to show the superiority of cisplatin and irinotecan chemotherapy for ED-SCLC over cisplatin and etoposide, as both exhibited comparable efficacy. The toxicity profiles, including diarrhea, differed in the cisplatin and irinotecan regimen arms in the SWOG S0124 and JCOG9511 trials, but there were no significant differences in treatment delivery between the two arms. Therefore, cisplatin and irinotecan combination therapy is not suggested as a suitable treatment option for North American patients with small-cell lung cancer, whereas it is feasible in Japanese patients in terms of tolerability.

In the present study, the response rate, PFS, and OS of cisplatin and irinotecan chemotherapy for thymic carcinoma were 44%, 8.4 months, and 45.6 months, respectively. In the previous study on carboplatin and paclitaxel, the response rate, PFS, and OS were 36%, 7.9 months, and 22.7 months, respectively (9). We did not conduct a comparative study; therefore, this was only compared with published data, the PFS in the present study was similar to that in the study on carboplatin and paclitaxel regimen. In contrast, the response was higher, and the median OS was longer than as compared to the that in the study on carboplatin and paclitaxel. With regard to platinum-based treatments, it is controversial whether cisplatin- or carboplatin-based chemotherapy treatment is

preferred for patients with thymic malignances (21, 22). These studies showed that a cisplatin-based regimen was superior to a carboplatin-based regimen with respect to the response rate and OS. However, carboplatin tended to be used in elderly patients and in patients with low performance status, and there has been no comparative trial or clear survival data. We speculate that the reason for the longer OS observed in this study was the inclusion of post-treatment regimens and the ability of patients to register in other clinical trials, such as carboplatin and paclitaxel combination therapy, S-1 (23), lenvatinib (16), and nivolumab (15). In particular, 15 patients who received S-1 showed a longer PFS (8.1 months), and 3 of these 15 patients had a long-term response of over 10 months. A recent phase II trial of S-1 as a second- or later line-regimen for 23 patients with thymic carcinoma demonstrated moderate activity, resulting in a 30.8% response rate (90% CI, 18.3–46.9), an 80.8% disease control rate (90% CI, 65.4–90.3), a median PFS of 4.3 months (95% CI, 2.3–10.3 months), and a median OS of 27.4 months (95% CI, 16.6–34.3) (23). The present study also supports the effectiveness of S-1 as a second- or later-line chemotherapy.

In the current era of molecular-targeted drugs and immuno-oncology, focusing only on a cytotoxic chemotherapy regimen is no longer necessary. Lenvatinib, a multi-kinase inhibitor that inhibits receptor tyrosine kinases such as VEGFR1 (FLT1), VEGFR2 (KDR), VEGFR (FLT4), FGFR, PDGFR, KIT, and RET FGR1, showed an objective response of 38% and a disease control rate of 95% (16). Sunitinib, a multitargeted kinase inhibitor that inhibits certain receptor tyrosine kinases, has been reported to have a moderate effect on thymic carcinoma (24). Pembrolizumab demonstrated a mild objective response (23%) with several long responders (25). Currently, chemoimmunotherapy is considered to be the optimal strategy for non-small cell lung cancer (26–30) and small-cell lung cancer (31, 32). The biological plausibility of targeted drugs for thymic carcinoma is currently unknown because there is no known biomarker for thymic carcinoma. It is important to identify the oncogenic drivers for lenvatinib and a biomarker for selecting patients that would benefit from pembrolizumab and to reduce the immunological toxicities of immunotherapy. The present milestone of chemotherapy is based on single agents for second-line chemotherapy and platinum-containing cytotoxic chemotherapy for first-line chemotherapy. In the future, finding the best combination regimen with key drugs in first-line therapy is crucial, even in rare cancers. In fact, the paradigm of immunochemotherapy focuses on the combination of other agents, including lenvatinib, in non-squamous non-small cell lung cancer (MK-7902-006/E7080-G000-315/LEAP-006) [NCT04716933]. Irinotecan and cisplatin could be considered as key drugs in combination therapy with immunotherapy or molecular-targeted drugs based on the present and previous studies.

The present study had several limitations. First, this study was a retrospective analysis of phase 2 trial data obtained from a single center. Second, we evaluated only a small number of patients. The broad range of 95% confidence interval was due to the small sample size. However, this is an unavoidable limitation as thymic carcinoma is a rare disease; therefore, the sample sizes for such studies are generally small. Moreover, given the current direction of the field with an increasing focus on immuno-chemotherapy, a detailed discussion of conventional chemotherapy for thymic malignancies is no longer be relevant. Thymic carcinoma is characterized by high expression of PD-L1; thus, immune checkpoint inhibitors may also be a key drug for this malignancy. Combination therapies including lenvatinib, pembrolizumab, or sunitinib for patients previously treated with chemotherapy for thymic carcinoma are currently being investigated, and chemoimmunotherapy is expected to become the first-line treatment in the future. However, further biological investigations to identify the origins of thymic carcinoma and potential actionable targets must continue to conquer this disease.

In summary, the combined use of cisplatin and irinotecan as first-line chemotherapy for metastatic or recurrent thymic carcinoma revealed efficacy and acceptable toxicity. Therefore, we propose that this combination chemotherapy is a feasible option as first-line chemotherapy for thymic carcinoma. However, it is important to further investigate combination chemotherapies and immunotherapies for thymic malignancies.

DATA AVAILABILITY STATEMENT

The raw data supporting the conclusions of this article will be made available by the authors, without undue reservation.

ETHICS STATEMENT

The Institutional Review Board of Komagome Hospital approved the present study (IRB number 2415). Written informed consent from the participants' legal guardian/next of kin was not required to participate in this study in accordance with the national legislation and the institutional requirements.

AUTHOR CONTRIBUTIONS

AF: Writing Original Draft, Data Curation, Formal analysis. YO: Conceptualization, Methodology, Data Curation and Writing and Editing Draft. THa: Writing- Reviewing and Editing, Data Curation, Investigation. KM Writing- Reviewing and Editing, Data Curation, Invetsitgation. MY: Writing- Reviewing and Editing, Investigation. THi: Writing- Reviewing and Editing, Investigation. YH: Writing- Reviewing and Editing, Investigation. All authors contributed to the article and approved the submitted version.

ACKNOWLEDGMENTS

English native-checked from the fund of Department of Thoracic Oncology, National Cancer Center Hospital. We thank Enago (https://www.enago.or.jp/) for the English language review.

REFERENCES

1. Lemma GL, Lee JW, Aisner SC, Langer CJ, Tester WJ, Johnson DH, et al. Phase II Study of Carboplatin and Paclitaxel in Advanced Thymoma and Thymic Carcinoma. *J Clin Oncol* (2011) 29(15):2060–5. doi: 10.1200/JCO.2010.32.9607
2. Eng TY, Fuller CD, Jagirdar J, Bains Y, Thomas CRJr. Thymic Carcinoma: State of the Art Review. *Int J Radiat Oncol Biol Phys* (2004) 59(3):654–64. doi: 10.1016/j.ijrobp.2003.11.021
3. Loehrer PJSr., Perez CA, Roth LM, Greco A, Livingston RB, Einhorn LH. Chemotherapy for Advanced Thymoma. Preliminary Results of an Intergroup Study. *Ann Intern Med* (1990) 113(7):520–4. doi: 10.7326/0003-4819-113-7-520
4. Kim ES, Putnam JB, Komaki R, Walsh GL, Ro JY, Shin HJ, et al. Phase II Study of a Multidisciplinary Approach With Induction Chemotherapy, Followed by Surgical Resection, Radiation Therapy, and Consolidation Chemotherapy for Unresectable Malignant Thymomas: Final Report. *Lung Cancer* (2004) 44(3):369–79. doi: 10.1016/j.lungcan.2003.12.010
5. Yoh K, Goto K, Ishii G, Niho S, Ohmatsu H, Kubota K, et al. Non-Small Cell Lung Cancer. *NCCN* (2003) 98(5):926–31.
6. Agatsuma T, Koizumi T, Kanda S, Ito M, Urushihata K, Yamamoto H, et al. Weekly Chemotherapy With Cisplatin, Vincristine, Doxorubicin, and Etoposide Is an Effective Treatment for Advanced Thymic Carcinoma. *Cancer* (2013) 98(5):926–31. doi: 10.1002/cncr.11606
7. Loehrer PJ Sr, Jiroutek M, Aisner S, Aisner J, Green M, Thomas CR Jr, et al. Combined Etoposide, Ifosfamide, and Cisplatin in the Treatment of Patients With Advanced Thymoma and Thymic Carcinoma: An Intergroup Trial. *Cancer* (2001) 91(11):2010–5. doi: 10.1002/1097-0142(20010601)91:11<2010::AID-CNCR1226>3.0.CO;2-2
8. Magois E, Guigay J, Blancard PS, Margery J, Milleron B, Lher P, et al. Multimodal Treatment of Thymic Carcinoma: Report of Nine Cases. *Lung Cancer* (2008) 59(1):126–32. doi: 10.1016/j.lungcan.2007.05.016
9. Igawa S, Murakami H, Takahashi T, Nakamura Y, Tsuya A, Naito T, et al. Efficacy of Chemotherapy With Carboplatin and Paclitaxel for Unresectable Thymic Carcinoma. *Lung Cancer* (2010) 67(2):194–7. doi: 10.1016/j.lungcan.2009.03.031
10. Hirai F, Yamanaka T, Taguchi K, Daga H, Ono A, Tanaka K, et al. A Multicenter Phase II Study of Carboplatin and Paclitaxel for Advanced Thymic Carcinoma: WJOG4207L. *Ann Oncol* (2015) 26(2):363–8. doi: 10.1093/annonc/mdu541
11. Yang X, Zhuo M, Shi A, Yang S, Wang Z, Wu M, et al. Optimal First-Line Treatment for Advanced Thymic Carcinoma. *Thorac Cancer* (2019) 10(11):2081–7. doi: 10.1111/1759-7714.13181
12. Okuma Y, Hosomi Y, Takagi Y, Iguchi M, Okamura T, Shibuya M. Cisplatin and Irinotecan Combination Chemotherapy for Advanced Thymic Carcinoma: Evaluation of Efficacy and Toxicity. *Lung Cancer* (2011) 74(3):492–6. doi: 10.1016/j.lungcan.2011.05.013
13. Koga K, Matsuno Y, Noguchi M, Mukai K, Asamura H, Goya T, et al. A Review of 79 Thymomas: Modification of Staging System and Reappraisal of Conventional Division Into Invasive and non-Invasive Thymoma. *Pathol Int* (1994) 44(5):359–67. doi: 10.1111/j.1440-1827.1994.tb02936.x
14. Eisenhauer EA, Therasse P, Bogaerts J, Schwartz LH, Sargent D, Ford R, et al. New Response Evaluation Criteria in Solid Tumours: Revised RECIST Guideline (Version 1.1). *Eur J Cancer* (2009) 45(2):228–47. doi: 10.1016/j.ejca.2008.10.026
15. Katsuya Y, Horinouchi H, Seto T, Umemura S, Hosomi Y, Satouchi M, et al. Single-Arm, Multicentre, Phase II Trial of Nivolumab for Unresectable or Recurrent Thymic Carcinoma: PRIMER Study. *Eur J Cancer* (2019) 113:78–86. doi: 10.1016/j.ejca.2019.03.012
16. Sato J, Satouchi M, Itoh S, Okuma Y, Niho S, Mizugaki H, et al. Lenvatinib in Patients With Advanced or Metastatic Thymic Carcinoma (REMORA): A Multicentre, Phase 2 Trial. *Lancet Oncol* (2020) 21(6):843–50. doi: 10.1016/S1470-2045(20)30162-5
17. De Montpréville VT. National Comprehensive Cancer Network (NCCN) Guidelines for Thymomas and Thymic Carcinomas. (2010) p:1281–7. Available at: https://www.nccn.org/guidelines/guidelines-detail?category=1&id=1469.
18. Kanda S, Koizumi T, Komatsu Y, Yoshikawa S, Okada M, Hatayama O, et al. Second-Line Chemotherapy of Platinum Compound Plus CPT-11 Following ADOC Chemotherapy in Advanced Thymic Carcinoma: Analysis of Seven Cases. *Anticancer Res* (2007) 27(4c):3005–8.
19. Noda K, Nishiwaki Y, Kawahara M, Negoro S, Sugiura T, Yokoyama A, et al. Irinotecan Plus Cisplatin Compared With Etoposide Plus Cisplatin for Extensive Small-Cell Lung Cancer. *N Engl J Med* (2002) 346(2):85–91. doi: 10.1056/NEJMoa003034
20. Lara PNJr., Natale R, Crowley J, Lenz HJ, Redman MW, Carleton JE, et al. Phase III Trial of Irinotecan/Cisplatin Compared With Etoposide/Cisplatin in Extensive-Stage Small-Cell Lung Cancer: Clinical and Pharmacogenomic Results From SWOG S0124. *J Clin Oncol* (2009) 27(15):2530–5. doi: 10.1200/JCO.2008.20.1061
21. Smit E, Moro-Sibilot D, Carpeño J, Lesniewski-Kmak K, Aerts J, Villatoro R, et al. Cisplatin and Carboplatin-Based Chemotherapy in the First-Line Treatment of non-Small Cell Lung Cancer: Analysis From the European FRAME Study. *Lung Cancer* (2016) 92:35–40. doi: 10.1016/j.lungcan.2015.11.022
22. Okuma Y, Saito M, Hosomi Y, Sakuyama T, Okamura T. Key Components of Chemotherapy for Thymic Malignancies: A Systematic Review and Pooled Analysis for Anthracycline-, Carboplatin- or Cisplatin-Based Chemotherapy. *J Cancer Res Clin Oncol* (2014) 141(2):323–31. doi: 10.1007/s00432-014-1800-6
23. Okuma Y, Goto Y, Ohyanagi F, Sunami K, Nakahara Y, Kitazono S, et al. Phase II Trial of S-1 Treatment as Palliative-Intent Chemotherapy for Previously Treated Advanced Thymic Carcinoma. *Cancer Med* (2020) 9(20):7418–27. doi: 10.1002/cam4.3385
24. Thomas A, Rajan A, Berman A, Tomita Y, Brzezniak C, Lee S, et al. Sunitinib in Patients With Chemotherapy-Refractory Thymoma and Thymic Carcinoma:an Open-Label Phase 2 Trial. *Lancet Oncol* (2016) 16(2):177–86. doi: 10.1016/S1470-2045(14)71181-7
25. Giaccone G, Kim C, Thompson J, McGuire C, Kallakury B, Chahine JJ, et al. Pembrolizumab in Patients With Thymic Carcinoma: A Single-Arm, Single-Centre, Phase 2 Study. *Lancet Oncol* (2018) 19(3):347–55. doi: 10.1016/S1470-2045(18)30062-7
26. Gadgeel S, Rodriguez-Abreu D, Speranza G, Esteban E, Felip E, Domine M, et al. Updated Analysis From KEYNOTE-189: Pembrolizumab or Placebo Plus Pemetrexed and Platinum for Previously Untreated Metastatic Nonsquamous Non-Small-Cell Lung Cancer. *J Clin Oncol* (2020) 38(14):1505–17. doi: 10.1200/JCO.19.03136
27. Paz-Ares L, Vicente D, Tafreshi A, Robinson A, Soto Parra H, Mazieres J, et al. A Randomized, Placebo-Controlled Trial of Pembrolizumab Plus Chemotherapy in Patients With Metastatic Squamous NSCLC: Protocol-Specified Final Analysis of KEYNOTE-407. *J Thorac Oncol* (2020) 15(10):1657–69. doi: 10.1016/j.jtho.2020.06.015
28. Socinski MA, Nishio M, Jotte RM, Cappuzzo F, Orlandi F, Stroyakovskiy D, et al. IMpower150 Final Overall Survival Analyses for Atezolizumab Plus Bevacizumab and Chemotherapy in First-Line Metastatic Nonsquamous NSCLC. *J Thorac Oncol* (2021) 16(11):1909–24. doi: 10.1016/j.jtho.2021.07.009
29. Paz-Ares L, Ciuleanu TE, Cobo M, Schenker M, Zurawski B, Menezes J, et al. First-Line Nivolumab Plus Ipilimumab Combined With Two Cycles of Chemotherapy in Patients With Non-Small-Cell Lung Cancer (CheckMate 9LA): An International, Randomised, Open-Label, Phase 3 Trial. *Lancet Oncol* (2021) 22(2):198–211. doi: 10.1016/S1470-2045(20)30641-0
30. West H, McCleod M, Hussein M, Morabito A, Rittmeyer A, Conter HJ, et al. Atezolizumab in Combination With Carboplatin Plus Nab-Paclitaxel Chemotherapy Compared With Chemotherapy Alone as First-Line Treatment for Metastatic Non-Squamous Non-Small-Cell Lung Cancer (IMpower130): A Multicentre, Randomised, Open-Label, Phase 3 Trial. *Lancet Oncol* (2019) 20(7):924–37. doi: 10.1016/S1470-2045(19)30167-6
31. Horn L, Mansfield AS, Szczesna A, Havel L, Krzakowski M, Hochmair MJ, et al. First-Line Atezolizumab Plus Chemotherapy in Extensive-Stage Small-Cell Lung Cancer. *N Engl J Med* (2018) 379(23):2220–9. doi: 10.1056/NEJMoa1809064
32. Paz-Ares L, Dvorkin M, Chen Y, Reinmuth N, Hotta K, Trukhin D, et al. Durvalumab Plus Platinum-Etoposide Versus Platinum-Etoposide in First-Line Treatment of Extensive-Stage Small-Cell Lung Cancer (CASPIAN): A Randomised, Controlled, Open-Label, Phase 3 Trial. *Lancet* (2019) 394(10212):1929–39. doi: 10.1016/S0140-6736(19)32222-6

Conflict of Interest: The authors declare that the research was conducted in the absence of any commercial or financial relationships that could be construed as a potential conflict of interest.

Publisher's Note: All claims expressed in this article are solely those of the authors and do not necessarily represent those of their affiliated organizations, or those of the publisher, the editors and the reviewers. Any product that may be evaluated in

this article, or claim that may be made by its manufacturer, is not guaranteed or endorsed by the publisher.

Copyright © 2022 Fukuda, Okuma, Hakozaki, Mirokuji, Yomota, Hishima and Hosomi. This is an open-access article distributed under the terms of the Creative Commons Attribution License (CC BY). The use, distribution or reproduction in other forums is permitted, provided the original author(s) and the copyright owner(s) are credited and that the original publication in this journal is cited, in accordance with accepted academic practice. No use, distribution or reproduction is permitted which does not comply with these terms.

frontiers in Oncology

CASE REPORT
published: 20 January 2022
doi: 10.3389/fonc.2021.814544

Pembrolizumab Plus Chemotherapy in Metastatic Thymic Carcinoma: A Case Report

Quentin Dominique Thomas[1,2*], *Clémence Basse*[3], *Marie Luporsi*[4] *and Nicolas Girard*[3]

[1] Department of Medical Oncology, Montpellier Cancer institute (ICM), Montpellier, France, [2] Oncogenic Pathways in Lung Cancer, Montpellier Cancer Research Institute (IRCM), University of Montpellier (UM), Montpellier, France, [3] Department of Medical Oncology, Curie Montsouris Thorax Institute, Institut Curie, Paris, France, [4] Department of Nuclear Medicine, Institut Curie, Paris, France

Metastatic thymic carcinomas have a poor prognosis. Pembrolizumab, an anti-PD-1 antibody, has recently been evaluated for patients with metastatic thymic carcinomas progressing after at least one line of platinum-based chemotherapy. The antitumor activity of immunotherapy appears to be promising for these patients and pembrolizumab in monotherapy is actually a treatment option in second metastatic line. To the best of our knowledge, we report the first case of a patient treated for metastatic thymic adenocarcinoma with a combination of chemotherapy–immunotherapy. The patient is a 46-year-old man with metastatic thymic adenocarcinoma treated in third metastatic line with a combination of pembrolizumab plus platinum-based chemotherapy with a very good metabolic tumor response. He had a progression-free survival of 7.9 months and did not experience any severe side effects related to pembrolizumab. The association of immunotherapy and chemotherapy, as in non-small cell and small cell lung cancers, could be of interest for future therapeutic trials evaluating the survival of patients with metastatic thymic carcinoma.

Keywords: immunotherapy, immune checkpoint inhibitor (ICI), thoracic malignancies, thymic epithelial tumor (TET), therapeutic option, case report

OPEN ACCESS

Edited by:
Maen Abdelrahim, Houston Methodist Research Institute, United States

Reviewed by:
Xabier Mielgo Rubio, Hospital Universitario Fundación Alcorcón, Spain
Alessandro Morabito, G. Pascale National Cancer Institute Foundation (IRCCS), Italy

****Correspondence:***
Quentin Dominique Thomas
quentin.thomas@icm.unicancer.fr

Specialty section:
This article was submitted to Pharmacology of Anti-Cancer Drugs, a section of the journal Frontiers in Oncology

Received: *13 November 2021*
Accepted: *20 December 2021*
Published: *20 January 2022*

Citation:
Thomas QD, Basse C, Luporsi M and Girard N (2022) Pembrolizumab Plus Chemotherapy in Metastatic Thymic Carcinoma: A Case Report. Front. Oncol. 11:814544. doi: 10.3389/fonc.2021.814544

INTRODUCTION

Thymic carcinomas are a rare and heterogeneous subgroup of thymic tumors registered according to the 2015 World Health Organization (WHO) classification (1). For unresectable metastatic or recurrent tumors, exclusive chemotherapy is recommended. Standards of first metastatic line chemotherapy regimens are carboplatin area under curve (AUC) 6 + paclitaxel 200 mg/m^2 (2, 3) or CAP [cisplatin (50 mg/m^2), Adriamycin (50 mg/m^2), cyclophosphamide (500 mg/m^2)] both administered every 3 weeks intravenously (4). In a cohort of 54 patients treated by chemotherapy in first line for a metastatic thymoma or thymic carcinoma, the objective response rate was 37% for thymic carcinoma with a median progression-free survival (PFS) of 6.2 months (5).

Pembrolizumab is a humanized monoclonal antibody blocking the interaction of programmed cell death 1 (PD-1) with its ligand (PD-L1). It has been tested in two phase 2 trials for patients with thymic epithelial tumors (TETs) progressing after a first line of platinum-based chemotherapy. The median PFS was 6.1 months on a cohort of 33 patients (26 thymic carcinomas and 7 thymomas) and 4.2 months on a cohort of 40 thymic carcinomas (6, 7). These trials show encouraging results and

pembrolizumab is actually a treatment option in monotherapy proposed for patient in second metastatic line with thymic carcinoma according to the National Comprehensive Cancer Network (NCCN) guidelines. There are actually no recommendations for the concomitant administration of platinum-based chemotherapy with PD-1 or PD-L1 immune checkpoint inhibitor.

We report to the best of our knowledge the first case of a patient treated in third metastatic line by chemotherapy combined with immunotherapy for a thymic carcinoma.

CASE REPORT

The patient, a 46-year-old man, was referred in December 2019 in our institute for a mucinous thymic adenocarcinoma with enteric flexion and neuroendocrine differentiation revealed by a painful metastasis of the right humerus. He had no significant medical history and never smoked. The Eastern Cooperative Oncology Group performance status was classified as 1. The clinical examination only revealed a functional impotence of the right shoulder due to pain, requiring morphine titration. He had no paraneoplastic manifestations of his TET, especially no myasthenia gravis and no other autoimmune disorder at baseline.

His disease was classified as stage IVb according to the eighth edition of the TNM classification proposed by the International Association for the Study of Lung Cancer (IASLC) and the International Thymic Malignancies Interest Group (ITMIG) (8). Immunohistochemistry analysis showed CK-20-positive expression. TTF1, CD-5, and CD-117 expressions were negative. CD-56 and synaptophysin were positive indicating neuroendocrine differentiation. All markers suggesting a tumor of the digestive tract or urothelial tract or germ cell tumors were negative. PD-L1 expression was 2% according to the tumor proportion score (TPS). The next-generation sequencing (NGS) panel performed on the tumor sample found a BRAF V600E mutation. The imaging assessment concluded to an oligometastatic disease with three bones sites involved. Endoscopic digestive explorations did not reveal any suspicious lesions which may suggest a primary to the digestive tract.

The patient received five cycles of carboplatin–paclitaxel in the first line until April 2020 associated with analgesic irradiations of metastatic bone lesions. Given a good response to chemotherapy and the oligometastatic status, the patient benefited from radiotherapy by proton therapy delivering 60 Gy to the primary tumor after induction chemotherapy. He did not experience any side effects related to these treatments.

A second line was initiated on bone progression in August 2020 with sunitinib 37.5 mg/day, showing poor efficacy with rapid metastatic progression on bone, pleura, and adrenal gland as detected by positron emission tomography (PET/CT) in November 2020.

A third line associating carboplatin AUC 6, pemetrexed 500 mg/m^2, and pembrolizumab 200 mg was then initiated intravenously every 3 weeks. After two cycles, we observed a significant reduction of pain related to bone involvement allowing morphine withdrawal. This clinical benefit was associated to a very good partial metabolic response on PET/CT from the second cycle of chemo-immunotherapy onwards. He was treated with four induction cycles of chemotherapy–immunotherapy until February 2021. Afterwards, he received a double maintenance treatment with pembrolizumab and pemetrexed every 3 weeks, with a total of 8 cycles administered every 3 weeks until August 2021 (**Figure 1**). Unfortunately, the PET/CT performed at this time showed a dissociated response with a multimetastatic progression (on the left pleura, right adrenal gland, retroperitoneum, and various bone sites) despite the stability of the antero-superior mediastinal mass (**Figure 2**). The PFS under chemo-immunotherapy was 7.9 months. The

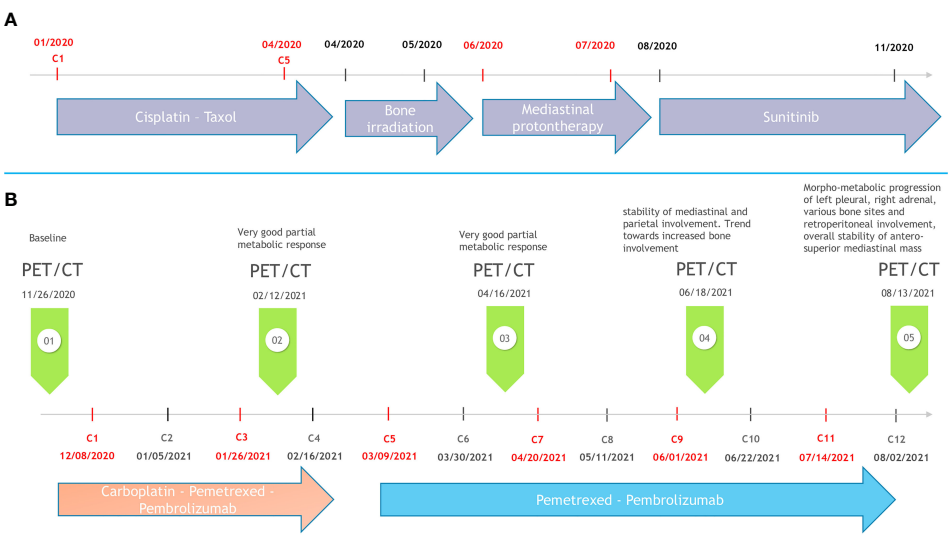

FIGURE 1 | Timeline of the disease course. **(A)** Previous treatment modalities. **(B)** Third metastatic line regimen with pembrolizumab plus chemotherapy.

maintenance treatment was therefore discontinued and the patient was switched to a fourth line with lenvatinib.

DISCUSSION

Our patient presented a PFS of 7.9 months in the third metastatic line for a thymic carcinoma treated by a combination of chemo-immunotherapy by carboplatin AUC 6, pemetrexed 500 mg/m^2, and pembrolizumab 200 mg intravenously every 3 weeks followed by double maintenance with pemetrexed–pembrolizumab. There is currently no recommendation to propose a combination of immunotherapy and chemotherapy for metastatic TETs. Our decision was based on the aggressiveness of the disease, the fact that this combination is a standard of care for metastatic lung adenocarcinoma, and the preexisting data on the individual efficacy of chemotherapy and anti-PD-1 therapy for thymic carcinomas. This decision was also based on manageable safety profile of this combination based on trials evaluating metastatic non-small cell lung cancer (NSCLC) (9). Our patient did not experiment any severe side effects related to chemotherapy or immunotherapy. This result is encouraging compared with patients treated in first metastatic line by chemotherapy with a median PFS of 6.2 months on the RYTHMIC prospective cohort (5).

Giaccone et al. studied 40 patients treated with pembrolizumab in monotherapy after at least one previous chemotherapy regimen. In this cohort, progression-free survival was longer in patients with high PD-L1 expression (>50% of tumor cells) than those with low or no expression (median 24 months, 95% CI 5.8–42.3 versus 2.9 months, 95% CI 1.7–4.1) (7). For metastatic NSCLC, the benefit of the combination of chemotherapy and immunotherapy is found in patients with PD-L1 >50% and also with lower PD-L1 expression (9, 10). These results should be evaluated for TETs in dedicated trials to select the population benefiting from chemo-immunotherapy in this type of tumor. The benefit obtained by our patient with a PD-L1 of 2% seems to suggest that the benefit of chemo-immunotherapy is not limited to patients with a PD-L1 >50% for metastatic thymic carcinomas.

BRAF mutation is known as an oncogenic addiction with significant immunogenicity in patients with NSCLC (11). This is

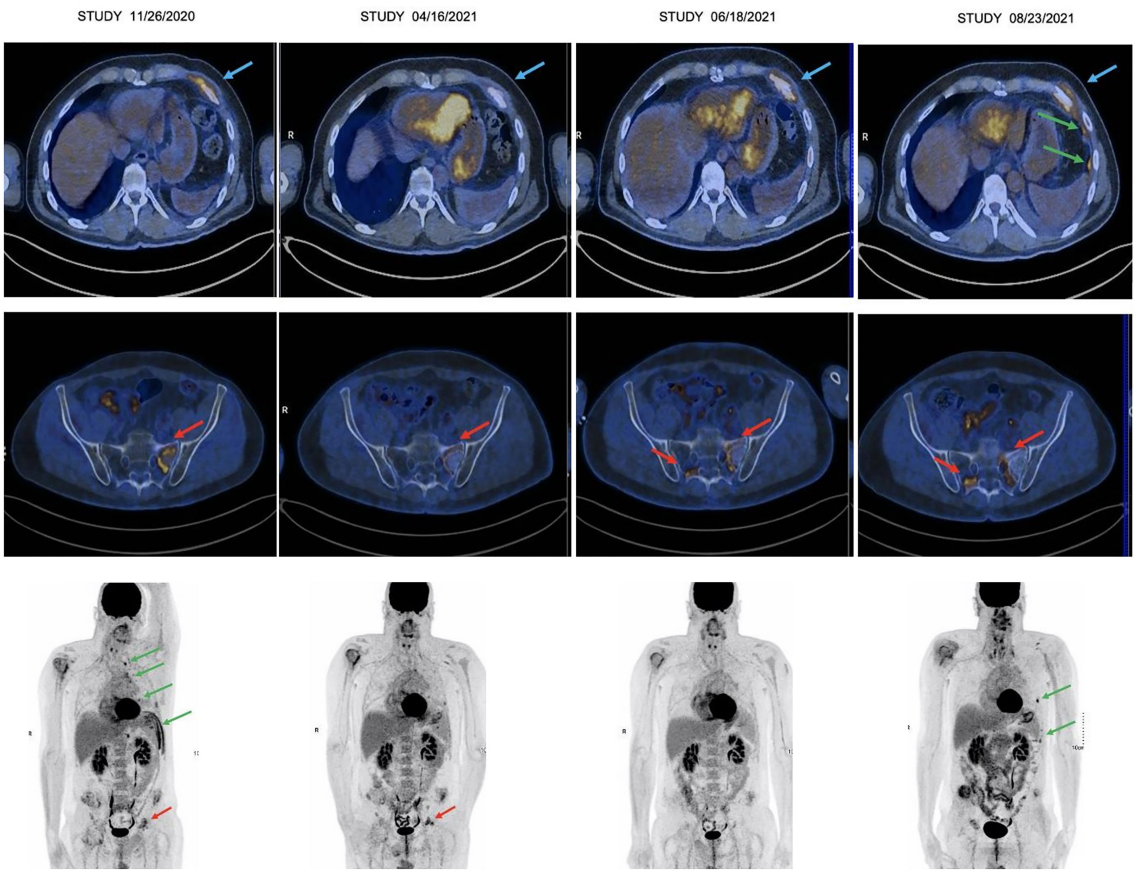

FIGURE 2 | Thoracic (top) and pelvic (middle) transaxial images and whole-body PET/CT (bottom) illustrating the morphometabolic evolution. From left to right on each image: PET/CT 11/26/2020: baseline; PET/CT 04/16/2020: partial response; PET/CT 06/18/2020: maintenance of partial response with very discrete bone progression; PET/CT 08/23/2020: left pleural, soft tissues and bone morphometabolic progression. Blue arrows: soft tissue involvement; greens arrows: pleura involvement; red arrows: bone involvement.

TABLE 1 | Completed and ongoing trials evaluating immunotherapy in thymic epithelial tumors.

Drug regimens	Tumor type	ClinicalTrials.gov	Therapeutic line	Development stage	Patients included	Clinical outcomes
Published clinical trials						
Pembrolizumab IV (anti-PD-1)	Thymic carcinoma	–	After at least one previous chemotherapy regimen	Single arm phase 2	40	ORR: 22.5% (95% CI 10.8–38.5)
Pembrolizumab IV (anti-PD-1)	– Thymoma (21.2%) – Thymic carcinoma (78.2%)	–	After at least one previous platinum-based chemotherapy regimen	Single arm phase 2	33	– Global ORR: 21.2% (95% CI 10.7–37.8) – Thymoma ORR: 28.6% (95% CI 8.2–61.4) – Thymic carcinoma ORR: 19.2% (95% CI 8.5–37.9)
Nivolumab IV (anti-PD-1)	– Thymic carcinoma	–	After at least one chemo(radio) therapy	Single arm phase 2	15	ORR: 0% (95% CI 0–21.8)
Avelumab IV (anti-PD-L1)	– Thymoma (87.5%) – Thymic carcinoma (12.5%)	–	After at least one prior standard therapy (systemic therapy, thymectomy, chest radiation therapy)	Phase 1 dose escalation	8	ORR: 25%
Ongoing clinical trials						
Pembrolizumab IV (anti-PD-1) + Epacadostat PO (IDO1 inhibitor)	Thymic carcinoma	NCT02364076	After at least one previous chemotherapy regimen	– Single arm phase 2 – Active, not recruiting	40	ORR
Nivolumab IV (anti-PD-1) + Vorolanib PO (VEGFR/PDGFR dual kinase inhibitor)	– Thymic carcinoma – NSCLC – Refractory thoracic tumors – SCLC	NCT03583086	After any number of prior lines (no prior anti-PD-1; PD-L1 or VEGF TKI allowed)	– Phase 1/2 dose escalation and dose expansion study – Recruiting	177	– Phase 1: safety and tolerability of nivolumab and vorolanib – Phase 2: ORR/PFS/DOR
Nivolumab IV (anti-PD-1)	– Thymic carcinoma – Thymoma B3	NCT03134118	After a first platinum-based chemotherapy	– Single arm phase 2 – Recruiting	55	PFS rate at 6 months
Pembrolizumab IV (anti-PD-1) + Lenvatinib PO (multi-TKI)	– Thymic carcinoma – Thymoma B3	NCT04710628	After a first platinum-based chemotherapy	– Single arm phase 2 – Not yet recruiting	43	PFS rate at 5 months
Pembrolizumab IV (anti-PD-1) + Carboplatin–paclitaxel/nab-paclitaxel	– Thymic carcinoma – Thymoma	NCT04554524	First systemic line for locally advanced or metastatic unresectable disease	– Single arm phase 4 – Recruiting	40	ORR
Pembrolizumab IV (anti-PD-1) + Sunitinib PO (multi-TKI)	Thymic carcinoma	NCT03463460	After at least one previous regimen of platinum-based chemotherapy	– Single arm phase 2 – Recruiting	40	ORR
Pembrolizumab IV (anti-PD-1) + Cisplatin – docetaxel IV (chemotherapy)	– Thymic carcinoma – Thymoma	NCT03858582	Neoadjuvant chemo-immunotherapy for patients with unresectable thymic epithelial tumors (Masaoka stages III, IVA) followed by surgery and pembrolizumab consolidation therapy with or without radiation	– Single arm phase 2 – Recruiting	40	Percentage of major pathologic response rate defined by ≤10% of tumor composed of viable tumor
KN046 IV (bispecific PD-L1/CTLA-4 inhibitor)	– Thymic carcinoma	NCT04925947	After prior platinum-based chemotherapy and at least one immune checkpoint blockade therapy targeting PD-1, PD-L1, or CTLA-4 for locally advanced unresectable or metastatic disease	– Single arm phase 2 – Recruiting	29	Disease response rate

CTLA-4, cytotoxic T-lymphocyte antigen 4; DOR, duration of response; IDO1, indoleamine 2,3-dioxygenase 1; IV, intravenously; NSCLC, non-small cell lung cancer; ORR, partial response + complete response; PD-1, programmed death-1; PD-L1, programmed death ligand-1; PO, per os; PFS, progression-free survival; SCLC, small cell lung cancer; TKI, tyrosine kinase inhibitor; VEGF, vascular endothelial growth factor.

considered to be more significant for non-V600E BRAF mutations. Indeed, in the IMMUNOTARGET database, non-V600E mutations tended to be associated with better response rates and PFS than V600E mutations, likely due to its epidemiologic association with tobacco use compared with V600E patients (12). Our patient had a BRAF V600E mutation which may have been a factor influencing the good therapeutic response observed.

There are currently several published or ongoing trials evaluating the use of immunotherapy in the management of TETs. Published trials evaluate immunotherapy as monotherapy after at least one line of systemic treatment. Ongoing trials are evaluating doublets of immunotherapy or combinations of immunotherapy with antiangiogenic agent or chemotherapy (**Table 1**). The benefits of immunotherapy in the management of TETs seem promising, and in the coming years, it could have an important place in the management of first-line metastatic and even non-metastatic patients.

Particular attention should be taken for patients with metastatic TETs with frequent autoimmune myasthenia gravis associated with the diagnosis of their disease. A pre-immunotherapy autoimmune checkup should be carried out systematically, and treatment by immunotherapy should probably not be introduced in case of myasthenia gravis requiring specific treatment.

The combination of anti-PD-1 plus platinum-based chemotherapy appears to be an interesting therapeutic option which should be evaluated for metastatic thymic carcinoma in dedicated prospective trials.

DATA AVAILABILITY STATEMENT

The original contributions presented in the study are included in the article/supplementary material. Further inquiries can be directed to the corresponding author.

ETHICS STATEMENT

Written informed consent was obtained from the individual(s) for the publication of any potentially identifiable images or data included in this article.

AUTHOR CONTRIBUTIONS

QT: conceptualization, writing—original draft, and visualization. CB: resources, writing—review and editing, and supervision. ML: resources, writing—review and editing, and visualization. NG: conceptualization, writing—review and editing, and supervision. All authors contributed to the article and approved the submitted version.

REFERENCES

1. Marx A, Chan JKC, Coindre J-M, Detterbeck F, Girard N, Harris NL, et al. The 2015 World Health Organization Classification of Tumors of the Thymus: Continuity and Changes. *J Thorac Oncol Off Publ Int Assoc Study Lung Cancer* (2015) 10(10):1383–95. doi: 10.1097/JTO.0000000000000654
2. Lemma GL, Lee J-W, Aisner SC, Langer CJ, Tester WJ, Johnson DH, et al. Phase II Study of Carboplatin and Paclitaxel in Advanced Thymoma and Thymic Carcinoma. *J Clin Oncol Off J Am Soc Clin Oncol* (2011) 29(15):2060–5. doi: 10.1200/JCO.2010.32.9607
3. Hirai F, Yamanaka T, Taguchi K, Daga H, Ono A, Tanaka K, et al. A Multicenter Phase II Study of Carboplatin and Paclitaxel for Advanced Thymic Carcinoma: WJOG4207L. *Ann Oncol Off J Eur Soc Med Oncol* (2015) 26(2):363–8. doi: 10.1093/annonc/mdu541
4. Loehrer PJ, Kim K, Aisner SC, Livingston R, Einhorn LH, Johnson D, et al. Cisplatin Plus Doxorubicin Plus Cyclophosphamide in Metastatic or Recurrent Thymoma: Final Results of an Intergroup Trial. The Eastern Cooperative Oncology Group, Southwest Oncology Group, and Southeastern Cancer Study Group. *J Clin Oncol Off J Am Soc Clin Oncol* (1994) 12(6):1164–8. doi: 10.1200/JCO.1994.12.6.1164
5. Merveilleux du Vignaux C, Dansin E, Mhanna L, Greillier L, Pichon E, Kerjouan M, et al. Systemic Therapy in Advanced Thymic Epithelial Tumors: Insights From the RYTHMIC Prospective Cohort. *J Thorac Oncol Off Publ Int Assoc Study Lung Cancer* (2018) 13(11):1762–70. doi: 10.1016/j.jtho.2018.08.005
6. Cho J, Kim HS, Ku BM, Choi Y-L, Cristescu R, Han J, et al. Pembrolizumab for Patients With Refractory or Relapsed Thymic Epithelial Tumor: An Open-Label Phase II Trial. *J Clin Oncol Off J Am Soc Clin Oncol* (2019) 37(24):2162–70. doi: 10.1200/JCO.2017.77.3184
7. Giaccone G, Kim C, Thompson J, McGuire C, Kallakury B, Chahine JJ, et al. Pembrolizumab in Patients With Thymic Carcinoma: A Single-Arm, Single-Centre, Phase 2 Study. *Lancet Oncol* (2018) 19(3):347–55. doi: 10.1016/S1470-2045(18)30062-7
8. Detterbeck FC, Stratton K, Giroux D, Asamura H, Crowley J, Falkson C, et al. The IASLC/ITMIG Thymic Epithelial Tumors Staging Project: Proposal for an Evidence-Based Stage Classification System for the Forthcoming (8th) Edition of the TNM Classification of Malignant Tumors. *J Thorac Oncol Off Publ Int Assoc Study Lung Cancer* (2014) 9(9 Suppl 2):S65–72. doi: 10.1097/JTO.0000000000000290
9. Gandhi L, Rodríguez-Abreu D, Gadgeel S, Esteban E, Felip E, De Angelis F, et al. Pembrolizumab Plus Chemotherapy in Metastatic Non-Small-Cell Lung Cancer. *N Engl J Med* (2018) 378(22):2078–92. doi: 10.1056/NEJMoa1801005
10. Paz-Ares L, Luft A, Vicente D, Tafreshi A, Gümüş M, Mazières J, et al. Pembrolizumab Plus Chemotherapy for Squamous Non-Small-Cell Lung Cancer. *N Engl J Med* (2018) 379(21):2040–51. doi: 10.1056/NEJMoa1810865
11. Mhanna L, Guibert N, Milia J, Mazieres J. When to Consider Immune Checkpoint Inhibitors in Oncogene-Driven Non-Small Cell Lung Cancer? *Curr Treat Options Oncol* (2019) 20(7):60. doi: 10.1007/s11864-019-0652-3
12. Mazieres J, Drilon A, Lusque A, Mhanna L, Cortot AB, Mezquita L, et al. Immune Checkpoint Inhibitors for Patients With Advanced Lung Cancer and Oncogenic Driver Alterations: Results From the IMMUNOTARGET Registry. *Ann Oncol Off J Eur Soc Med Oncol* (2019) 30(8):1321–8. doi: 10.1093/annonc/mdz167

Conflict of Interest: The authors declare that the research was conducted in the absence of any commercial or financial relationships that could be construed as a potential conflict of interest.

Publisher's Note: All claims expressed in this article are solely those of the authors and do not necessarily represent those of their affiliated organizations, or those of the publisher, the editors and the reviewers. Any product that may be evaluated in this article, or claim that may be made by its manufacturer, is not guaranteed or endorsed by the publisher.

Copyright © 2022 Thomas, Basse, Luporsi and Girard. This is an open-access article distributed under the terms of the Creative Commons Attribution License (CC BY). The use, distribution or reproduction in other forums is permitted, provided the original author(s) and the copyright owner(s) are credited and that the original publication in this journal is cited, in accordance with accepted academic practice. No use, distribution or reproduction is permitted which does not comply with these terms.

frontiers in Oncology

ORIGINAL RESEARCH
published: 25 January 2022
doi: 10.3389/fonc.2021.808396

CD70 in Thymic Squamous Cell Carcinoma: Potential Diagnostic Markers and Immunotherapeutic Targets

Jumpei Kashima[1,2], Tsunekazu Hishima[1], Yusuke Okuma[3], Hirotoshi Horio[4], Masumi Ogawa[1], Yukiko Hayashi[1], Shin-ichiro Horiguchi[1], Toru Motoi[1], Tetsuo Ushiku[2] and Masashi Fukayama[2]*

[1] Department of Pathology, Tokyo Metropolitan Cancer and Infectious diseases Center Komagome Hospital, Tokyo, Japan, [2] Department of Pathology, Graduate School of Medicine, The University of Tokyo, Tokyo, Japan, [3] Department of Thoracic Oncology and Respiratory Medicine, National Cancer Center, Tokyo, Japan, [4] Department of Thoracic Surgery, Tokyo Metropolitan Cancer and Infectious diseases Center Komagome Hospital, Tokyo, Japan

OPEN ACCESS

Edited by:
Mylene Truong, University of Texas MD Anderson Cancer Center, United States

Reviewed by:
Jelena Stojsic, Clinical Center of Serbia, University of Belgrade, Serbia
Giulia Mazzaschi, University Hospital of Parma, Italy

***Correspondence:**
Tsunekazu Hishima
hishima@cick.jp

Specialty section:
This article was submitted to Thoracic Oncology, a section of the journal Frontiers in Oncology

Received: *03 November 2021*
Accepted: *29 December 2021*
Published: *25 January 2022*

Citation:
Kashima J, Hishima T, Okuma Y, Horio H, Ogawa M, Hayashi Y, Horiguchi S-i, Motoi T, Ushiku T and Fukayama M (2022) CD70 in Thymic Squamous Cell Carcinoma: Potential Diagnostic Markers and Immunotherapeutic Targets. Front. Oncol. 11:808396. doi: 10.3389/fonc.2021.808396

CD70 – a ligand protein of CD27 on lymphocytes – is expressed in a large spectrum of malignancies. It is an attractive target for antibody-based therapy and several clinical trials are currently being conducted. However, there is no evidence regarding the expression of CD70 and its relationship with expression of programmed death ligand-1 (PD-L1) and CD27+ tumor-infiltrating lymphocytes (TIL) in formalin-fixed paraffin-embedded (FFPE) tissues of thymic tumors. FFPE tissues of thymic squamous cell carcinoma (TSCC) (operative specimens, n = 31; biopsy specimens, n = 11), thymoma (n = 60), thymic carcinoid (n = 3), and lung squamous cell carcinoma (LSCC) (n = 30) were analyzed immunohistochemically. Immunoreactivity for CD70 was semi-quantitatively scored according to the proportion of positive tumor cells. Moreover, the densities of CD27-positive intratumoral TIL (iTIL) and stromal TIL of TSCC were assessed and survival was compared. Most TSCC cases (87%; 27/31) were CD70-positive. In contrast, all thymoma and thymic carcinoid cases were CD70-negative. In LSCC cases, CD70-positivity was significantly lower than TSCC cases (20%; 6/30). Biopsy and resected specimens obtained from the same patients demonstrated a consistent staining pattern (6/6 patients). The proportion of CD70-positive TSCC was comparable with those of CD5 (87%) and CD117 (90%). Correlation between CD70 and PD-L1 expression score was observed. There was no significant difference in survival between the CD70-high and CD70-low expression groups. Meanwhile, patients with CD27-positive iTIL-high tumors exhibited better survival than those with iTIL-low tumors. This tendency was weaker in the CD70-high subset. CD70 immunohistochemistry is useful in diagnosing TSCC. CD70 may prevent anti-tumor immunity *via* CD27. Immunotherapy targeting the CD70–CD27 axis may be a promising option for the treatment of TSCC.

Keywords: thymic carcinoma, CD70, CD27, immunohistochemistry, tumor-infiltrating lymphocyte

INTRODUCTION

CD70 belongs to the tumor necrosis factor family of proteins and acts as a ligand of CD27. Thymic epithelium and activated T-cells and B-cells are known to express CD70 (1), which promotes differentiation to effector or memory T-cells by expressing CD27 on lymphocytes (2). CD70–CD27 pathway is demonstrated to promote survival of FOXP3-positive regulatory T-cells (3). Hematological malignancies and solid tumors have also been shown to express CD70, leading to the development of antibodies against CD70 as therapeutic agents (4–6).

Thymic carcinoma is a rare disease, accounting for 14% of thymic epithelial tumors according to the International Thymic Malignancy Interest Group database (7). Thymic squamous cell carcinoma (TSCC), which accounts for the majority of thymic carcinoma cases, has some histological mimickers, such as type B3 thymoma and lung squamous cell carcinoma (LSCC). Immunohistochemical (IHC) analysis of CD5, CD117 (KIT), GLUT-1, and MUC1 is useful in differentiating TSCC from type B3 thymoma (8–19). In addition, CD5 and CD117 are helpful in distinguishing TSCC from LSCC (13, 14, 18).

Using IHC analysis in a limited number of frozen TSCC sections, we previously demonstrated that positive staining for CD70 was observed frequently in neoplastic epithelial cells of TSCC, unlike in those of thymoma and LSCC (20). Recently, an anti-CD70 antibody for formalin-fixed, paraffin-embedded (FFPE) tissues became commercially available; however, the diagnostic value of this antibody in TSCC is currently not well documented.

Programmed death ligand-1 (PD-L1) interacts programmed death-1 (PD-1) and inhibits antitumor immunity by T-cells. PD-L1 and PD-1 have become established targets of immunotherapy for various types of cancer. Several clinical trials of immune checkpoint inhibitors targeting PD-1/PD-L1 axis for thymic epithelial tumors have been conducted (21–23). These reagents seemed effective especially in thymic tumor with high-PD-L1 expression (21, 22).

Tumor-infiltrating lymphocytes (TIL) have been associated with favorable prognosis in various types of solid tumors (24–30). CD27-positive TIL are indicated to correlate with activated T-cell response in non-small cell lung cancer and renal cell carcinoma, both of which are known as CD70-expressing tumors (6, 31–33). However, currently, no studies examine the CD27+ TIL status in thymic carcinoma.

In the present study, we performed an IHC analysis for CD70 in TSCC and compared the results with those obtained in thymoma and LSCC. We also assessed the correlation between CD70 and PD-L1 expression in TSCC tissue. In addition, the correlation of the CD70-positivity of tumor cells and CD27-positive TIL on survival was analyzed.

Abbreviations: FFPE, formalin-fixed, paraffin-embedded; RT-PCR, reverse transcriptase polymerase chain reaction; IHC, immunohistochemical; ITMIG, International Thymic Malignancy Interest Group; TIL, tumor-infiltrating lymphocytes; iTIL, intratumoral tumor-infiltrating lymphocytes; sTIL, stromal tumor-infiltrating lymphocytes, PD-L1, Programmed death ligand-1; HE, hematoxylin and eosin.

MATERIALS AND METHODS

Tissue Preparation and Patient Characteristics

TSCC (n = 31), thymoma (type A: n = 5, type AB: n = 20, type B1: n = 9, type B2: n = 9, type B3: n = 17), thymic carcinoid (n = 3), and LSCC (n = 30) resected at a single institution between 1987 and 2017 were analyzed retrospectively. Metastatic squamous cell carcinoma is excluded with clinical information. Biopsy specimens of TSCC (n = 11) and LSCC (n=12) were also analyzed. The diagnosis was based on hematoxylin and eosin staining of FFPE tissues. In addition, the diagnosis was reviewed and confirmed by two pathologists (J.K. and T.H.) according to the 4th Edition of the World Health Organization Classification of Tumours of the Lung, Pleura, Thymus & Heart. The clinical characteristics of the patients were retrospectively obtained from the electronic medical records. Written informed consent was acquired from the patients. This study was approved by the Institutional Review Board of the Tokyo Metropolitan Cancer and Infectious Diseases Center Komagome Hospital (approval number: 2120).

IHC Evaluation

FFPE tissues were subjected to IHC analysis. Sections (3.5 μm in thickness) were cut and stained with the avidin–biotin–peroxidase complex method using the ABC Elite Kit (Vector, Burlingame, CA, USA). The antibodies used in this study were CD70 (clone 301731, R&D Systems, Minneapolis, MN, USA; 1:50 dilution), CD5 (4C7, Leica Biosystems, Wetzlar, Germany; 1:70 dilution), CD117 (YR145, Epitomics, Burlingame, CA, USA; 1:2,000 dilution), PD-L1 (E1L3N, Cell Signaling, Danvers, MA, USA; 1:100 dilution), CD8(C8/144B, Nichirei, Tokyo, Japan; 1:100 dilution), FOXP3 (236A/E7, Abcam, Cambridge, UK; 1:150 dilution), and CD27 (HPA038936, Sigma-Aldrich, St. Louis, MO, USA; 1:50 dilution). To evaluate the positivity of each marker, the proportion of positive cells in random spots was estimated and graded as follows: CD70: score 0 (<1% positivity), score 1 (1–25% positivity), score 2 (26–50% positivity), score 3 (51–75% positivity), or score 4 (76–100% positivity); PD-L1: score 0 (<1% positivity), score 1 (1–49% positivity), or score 2 (50–100% positivity). Intratumoral TIL (iTIL) and stromal TIL (sTIL) were defined as infiltrating lymphocytes within tumor nests and tumor stroma, respectively. The average counts (cells per mm^2) of CD8-, FOXP3-, and CD27-positive iTIL and stromal sTIL in triplicate high-magnification images obtained with Nikon DS-Ri2 (Nikon, Tokyo, Japan) and counted with NIS-Elements D Imaging Software (Nikon, Tokyo, Japan).

Gene Expression Analysis

Analysis of gene expression was performed with real-time quantitative reverse transcriptase polymerase chain reaction (RT-PCR) using first-strand cDNA derived from RNA isolated from frozen tissues of TSCC (n = 12) and thymoma with few non-neoplastic lymphocytes (type A: n = 4, type B3: n = 5), as described previously (30). SYBR green sequence detection reagents (Applied Biosystems, Foster City, CA, USA) and sense and anti-sense primers were used. All reactions were performed

in duplicate. The CD70 primers used were as follows: F, gctgctttggtcccattggtcg (exon 1); R, gaggtcctgtgtgattcagctg (exon 2/3 junction; 141-bp product). Reaction products were assayed on a LightCycler 480 Real-Time PCR Instrument (Roche Diagnostics, Rotkreuz, Switzerland) and the PCR product was measured in real time as the increase in SYBR green fluorescence. Data were analyzed using the LightCycler 480 Software version 1.5 (Roche Diagnostics). The CD70 copy number was standardized against the β-actin copy number in each sample.

Survival Analysis

Survival was defined as the period from tissue acquisition of TSCC to death by any cause. We adopted only overall survival to see the prognostic value of CD70 and other immune-related factors in limited number of patients for two reasons. First, more than 40% of the patients enrolled in this study had stage IVa or IVb diseases, and many of them received palliative-intent surgery. Moreover, our study also enrolled patients with thymic carcinoma resected almost 30 years ago, when the following-up frequency after surgery and available images were heterogenous, which might have biased progression free survival. One case was excluded from survival analysis due to the lack of data. We compared the survival of patients with TSCC between two groups defined according to the CD70 IHC score (CD70-low: IHC score 0 or 1; CD70-high: score 2, 3, or 4), the number of CD27-positive iTIL (iTIL-low: iTIL<median; iTIL-high: iTIL≥median), and the number of CD27-positive sTIL (sTIL-low: sTIL<median; sTIL-high: sTIL≥median).

Statistical Analysis

Tumor positivity, revealed by IHC (i.e., the proportion of tumors with a CD70 IHC score ≥1), was compared between TSCC and LSCC using Fisher's exact test. Relation between CD70 and PD-L1 positivity score, and between CD8, FOXP3 and CD27-positive TIL were assessed using Spearman's rank correlation test. Quantitative comparison of CD70 expression determined by RT-PCR between thymoma and TSCC, and comparison of TIL levels between CD70-high and low TSCC were performed using the Mann–Whitney U-test. Survival curves were generated using the Kaplan–Meier method. The univariate Cox proportional hazards regression model was employed to assess the hazards ratio according to age, while the log-rank test was used for categorical values (Masaoka–Koga staging, CD70-low/high, CD27-positive iTIL-low/high, and sTIL-low/high). Factors with $p < 0.10$ were included in the multivariate analysis. Subsequently, a multivariate Cox proportional hazards regression model was employed to estimate the relationship between variables and survival. A p-value < 0.05 denoted statistical significance. All calculations were performed using the R version 3.3.3 (Vienna, Austria).

RESULTS

Patient Characteristics

The characteristics of patients with TSCC and thymoma are summarized in **Table 1**. A total of 31 patients with TSCC underwent surgical tumor resection. Of those, six patients also underwent biopsies prior to surgery. Notably, five patients with advanced disease underwent only biopsy. The cases with notable lymphocyte infiltration underwent Epstein-Barr virus encoded small RNA *in situ* hybridization to confirm the diagnosis of TSCC. None of the patients received immune checkpoint blockade after surgery.

TABLE 1 | Patient characteristics.

	TSCC	Thymoma
Male/female	17/14	21/39
Age, years (median, range)	65.5, 41–83	58, 34–84
Masaoka–Koga staging	n (%)	n (%)
I	1 (3)	15 (25)
II	7 (23)	33 (55)
III	10 (32)	4 (7)
IVa	3 (10)	3 (5)
IVb	10 (32)	4 (7)
Histological subtype		(%)
A		5 (8)
AB		20 (33)
B1		9 (15)
B2		9 (15)
B3		17 (28)
Neoadjuvant chemotherapy and/or radiotherapy		
Yes	6 (19)	2 (3)
No	25 (81)	58 (97)

TSCC, thymic squamous cell carcinoma.

IHC Analysis of CD70, CD5 and CD117

CD70 in the Healthy Thymus

The immunoactivity of CD70 was detected as coarse-granular staining in scattered medullary epithelial cells or dendritic cells, which are indistinguishable from each other morphologically, of the adult thymus (**Figures 1A, B**). In contrast, thymocyte and epithelial cells in the cortex or subcortex did not show CD70 staining.

IHC Analysis in TSCC, Thymoma, and LSCC

The immunostaining of CD70 in TSCC is shown in **Figure 1C**. Most TSCC (87%, 27/31) showed a score ≥1 for positivity: score 1: 12 cases (39%); score 2: four cases (13%); score 3: eight cases (26%); and score 4: three cases (10%) (**Table 2** and **Figure 1C**). The majority of CD70-positive TSCC revealed a coarse-granular pattern similar to that observed in the normal thymus. A minority of TSCC showed both granular and membranous staining patterns. CD5- and CD117-positive cases accounted for 87% (27/31 patients) and 90% (28/31 patients) of TSCC, respectively (**Figures 1D, E**). Twenty-nine cases (94%) were positive for at least two of the markers.

On the other hand, all cases of thymoma and thymic carcinoid were negative for CD70. Six of 30 LSCC were CD70-positive; however, the score was ≤2 and the staining pattern showed intratumoral heterogeneity (**Figure 1F**).

In addition, the diagnostic utility of CD70 IHC analysis in small biopsy specimens were assessed, because score 1 positivity was observed in as many as 39% of operative specimens. A large proportion of TSCC was immunoreactive for CD70 (81%), CD5 (91%), and CD117 (100%). Six patients underwent both biopsy

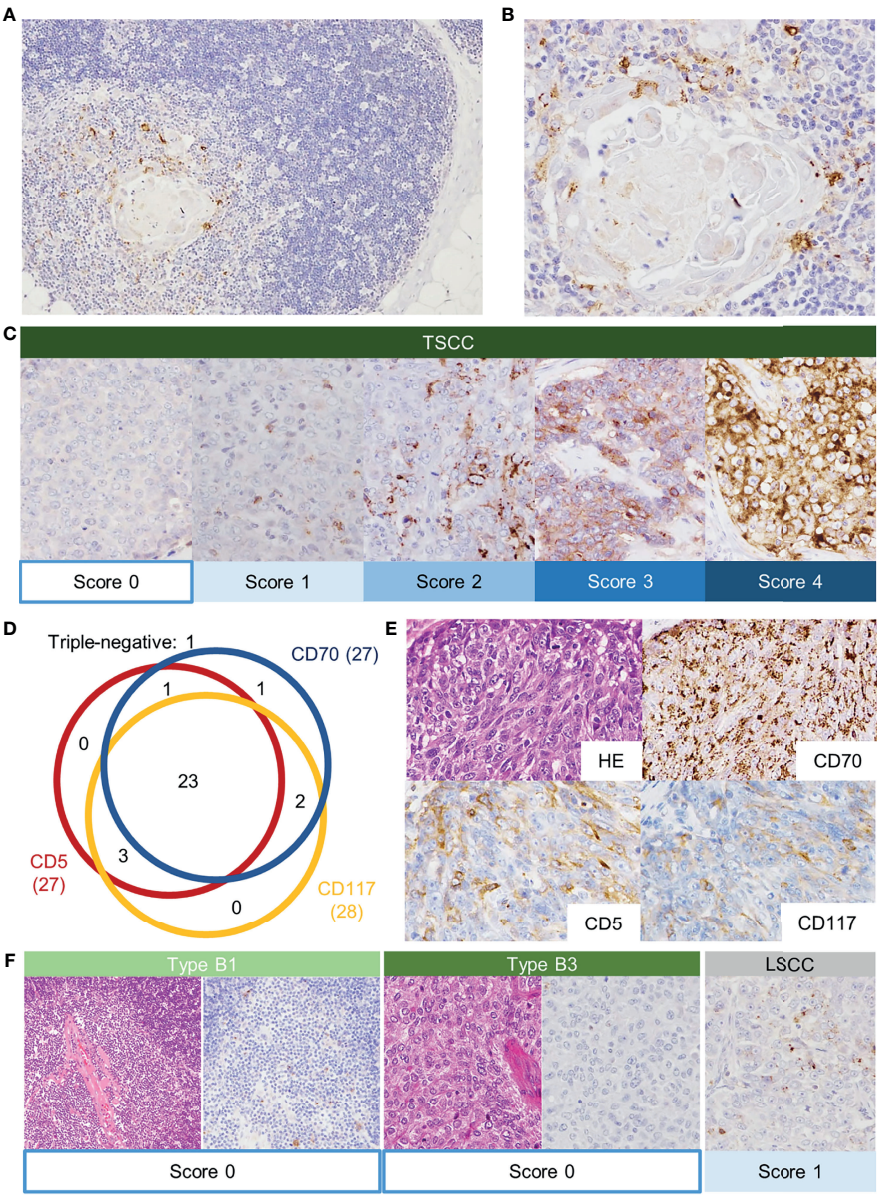

FIGURE 1 | Normal adult thymus tissue stained with anti-CD70 antibody. Thymic medullary epithelial cells or dendritic cells were positive for CD70 **(A, B)**. Immunostaining of CD70 in thymic squamous cell carcinoma (TSCC) **(C)**. CD70-positivity was scored according to the proportion of positive tumor cells (score 0: <1%; score 1: 1–24%; score 2: 25–49%; score 3: 50–74%; score 4: 75–100%). Schematic summary of immunohistochemical analysis (D).The numbers indicate the positive cases of each staining. The numbers in the parentheses are the total number of the positive cases. Immunostaining of CD70 (score 4), CD5 and CD117 in TSCC **(E)**. In contrast, thymoma showed the absence of CD70 expression **(F)**. The CD70 score in lung squamous cell carcinoma was relatively low.

and resection of TSCC, and all specimens (biopsy and resection) were CD70-positive (**Table 3**). On the other hand, only one biopsy specimen of LSCC was positive for CD70 (8.3%), and the positivity was significantly lower compared to TSCC ($p < 0.001$).

Gene Expression Analysis of CD70 by RT-PCR

The mRNA extracted from frozen tissues of TSCC (n = 12) and thymoma (type A: n = 4; type B3: n = 5) was quantified using RT-PCR for CD70 (**Figure 2**). The expression levels of CD70 in TSCC were significantly higher than those observed in thymoma ($p < 0.001$). This finding was consistent with the IHC score.

Association Between Tumor CD70/PD-L1 Expression and FOXP3/ CD27-Positive Lymphocytes

PD-L1 was positive (≥1%) in 74% of TSCC (**Supplementary Table 1**). Tumors with high PD-L1 score tended to have high

TABLE 2 | Immunohistochemical analysis of CD70 in surgical specimens.

	TSCC (n = 31)	Thymoma (n = 60)	Thymic carcinoid (n = 3)	LSCC (n = 30)
CD70-positivity	27 (87%)	0/60 (0%)	0/3 (0%)	6/30 (20%)*
Score 0	4 (13%)	60 (100%)	3 (100%)	24 (80%)
Score 1	12 (39%)	0 (0%)	0 (0%)	4 (13%)
Score 2	4 (13%)	0 (0%)	0 (0%)	2 (7%)
Score 3	8 (26%)	0 (0%)	0 (0%)	0 (0%)
Score 4	3 (10%)	0 (0%)	0 (0%)	0 (0%)

TSCC, thymic squamous cell carcinoma; LSCC, lung squamous cell carcinoma.
**The proportion of CD70-positive cases in LSCC was significantly lower than that observed in TSCC (p<0.0001).*

TABLE 3 | CD70, CD5, and CD117 immunostaining concordance between surgical and biopsy specimens.

	CD70 (%)	CD5 (%)	CD117 (%)
Positivity in biopsy specimens of TSCC	9/11 (81)	10/11 (91)	11/11 (100)
Concordance between surgical and biopsy specimens from the same patient	6/6 (100)	6/6 (100)	6/6 (100)

TSCC, thymic squamous cell carcinoma.

CD70 score (p = 0.013). Some tumors were diffusely positive for both PD-L1 and CD70; however, distribution of PD-L1 positive cells and that of CD70 positive cells did not seem correlated.

CD27 was scantly stained in a small proportion of lymphocytes infiltrating the thymoma. In contrast, in TSCC, CD27-positive lymphocytes were observed in tumor nests and rather prominent in the fibrous stroma (**Figure 3A**). Correlation between the number of CD8-positive TIL and that of CD27-positive TIL, and correlation between the number of FOXP3-positive TIL and that of CD27-positive TIL were observed (**Supplementary Table 2**). Neither the number of CD8, FOXP3, nor CD27-positive TIL showed difference between CD70-high and low tumor, whereas the number of FOXP3-positive iTIL in CD70-high TSCC was slightly higher than CD70-low (p = 0.07, **Supplementary Table 3**). On the other hand, significant correlation was observed between PD-L1 score and the level of CD27-positive iTIL (**Table 4**).

Survival Analysis of Patients With TSCC

We compared the postoperative survival of patients with TSCC between the CD70-high and CD70-low groups. Patient characteristics are shown in **Supplementary Table 4**. The median survival time in the CD70-high and CD70-low groups was 74 and 101 months, respectively. There was no significant difference in survival observed between the two groups (p = 0.53, **Figure 3B**).

On the other hand, patients with CD27-positive iTIL-high tumors were associated with longer survival than those with iTIL-low tumors (p = 0.024, **Figure 3C**). Moreover, the CD27+ sTIL-high and -low groups showed a slight, non-statistically significant difference in the survival curve (p = 0.096, **Figure 3D**).

PD-L1 expressional score neither showed potential for stratification of survival in the cohort (median overall survival: 74.0 months in score 0, 68.5 months in score 1, and 89.7 months in score 2, p=0.97).

The univariate Cox proportional hazard model for all clinicopathological variables revealed that the Masaoka–Koga stage IV, FOXP3-positive sTIL and CD27-positive iTIL status showed p-value <0.10 (p = 0.022, p = 0.008 and p = 0.033, respectively) (**Supplementary Table 5**), while high PD-L1 expression (≥50%) did not show significant correlation with survival (p = 0.88). Neither Masaoka–Koga stage IV, FOXP3-positive sTIL or CD27-positive iTIL status was shown to be statistically significant in the multivariate analysis (p = 0.24, p = 0.36 and p = 0.73, respectively) (**Supplementary Table 6**).

Preferable survival of iTIL-high tumor seemed more obvious in the CD70-low group than in the CD70-high group. However, the difference observed between these two subsets was not statistically significant (p = 0.12 and p = 0.15, respectively) (**Figures 3E, F**).

TABLE 4 | Correlation between CD27-positive TIL and PD-L1 expression.

	CD27+ iTIL			CD27+ sTIL		
	low	high	p-value	low	high	p-value
PD-L1			0.033			0.719
Score 0	7	1		4	4	
Score 1	7	9		9	7	
Score 2	1	5		2	4	

iTIL, intratumoral tumor-infiltrating lymphocytes; sTIL, stromal tumor-infiltrating lymphocytes; PD-L1, programmed death ligand-1.

DISCUSSION

In this study, using IHC analysis of FFPE tissues, we showed that CD70 was expressed in 87% of TSCC. The percentage of TSCC with >50% (score 3 and 4, 36%) was consistent with a recent study by Flieswasser et al., whereas the sample size of our study is six times as large (34). In contrast, all cases of thymoma were negative for CD70. We also demonstrated good agreement with IHC score and mRNA expression levels of CD70 by quantitative RT-PCR in TSCC and thymoma. These results indicate that CD70 can be utilized as a specific marker discriminating TSCC from thymoma.

The IHC analysis revealed the characteristic staining pattern (coarse-granular or membranous) observed in CD70 (**Figure 1**). Notably, CD70 has been shown to be expressed in the thymic medulla (3, 20). The current study showed a consistent expression of CD70 in the normal thymic medulla adjacent to the tumor, which was also retained in <1% of tumor cells observed in the medullary island of type B1 thymoma. Thus, CD70 is one of the specific markers of medullary differentiation, along with CD40 and claudin-4 (35).

Diagnostic Potential of CD70 IHC

Positivity for CD5 and CD117 was similar to that observed for CD70. The present findings are consistent with those reported in our previous study involving IHC analysis of CD70 in frozen sections (20). All cases of thymoma were negative for CD70.

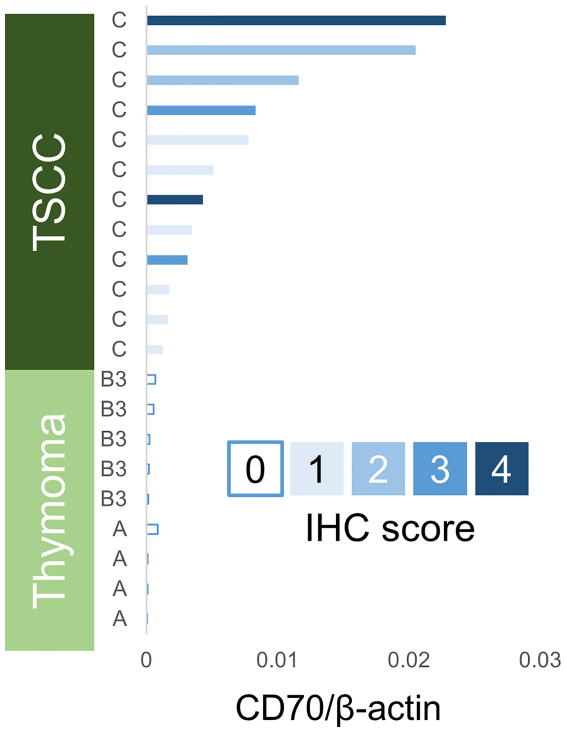

FIGURE 2 | CD70 expression analysis using real-time reverse transcriptase polymerase chain reaction (RT-PCR). A, type A thymoma; B3, type B3 thymoma; C, thymic squamous cell carcinoma; TSCC, thymic squamous cell carcinoma.

Previous studies showed that 0–7% and 0–18% of thymoma were positive for CD5 and CD117, respectively (9, 10, 12, 13, 16, 18, 36). Although the percentage of CD70 positive cells in each case was rather small, the sensitivity and specificity of CD70 in distinguishing TSCC from thymoma are comparable with those of CD5 and CD117.

In the present study, 20% of LSCC cases were positive for CD70. This percentage is similar to that reported in a previous study of LSCC (27%) (6). CD5 and CD117 are utilized as diagnostic markers of TSCC; however, LSCC occasionally expresses CD5 (0–15%) or CD117 (6.2–20%) (18, 37). In the present study, we observed one CD70-positive and CD5/CD117-negative case. These findings indicate that each marker does not independently enable complete discrimination between TSCC and LSCC. Combining IHC analyses of CD70, CD5, and CD117 might enhance the diagnostic ability, while it needs larger scale studies to confirm.

Morphological analysis using biopsy specimens is sometimes limited due to the amount of tissue. In this study, all six biopsy specimens from the patients whose surgical specimens was CD70-positive were also positive for CD70. In addition, the CD70-positivity in biopsy specimens of LSCC was significantly lower than that of TSCC. Although the sample size was small, these results may imply that adding CD70 to the IHC panel has a potential to improve the specificity and sensitivity of TSCC diagnosis, especially when biopsy is the only source of tumor tissue.

Biological Meaning of CD70 and CD27 Expression in TSCC Tissue

The CD27-positive iTIL-high group exhibited significantly longer overall survival than the CD27-positive iTIL-low group. The sTIL-high and -low groups also showed a similar difference. These results are consistent with those of previous studies showing a favorable prognosis in solid tumors, including thymic carcinoma, with high numbers of TIL (24–30, 38). The number of CD8-positive TIL, on the other hand, was not significant prognostic factor in the univariate analysis. The effector T-cell response associated with CD27-positive TIL might partially explain the phenomenon as previously discussed (31). We also showed that the survival curves of the CD27-positive iTIL-high and -low groups became closer in the CD70-high subset. This trend suggests that CD70 expressed in tumor tissue represses anti-tumor immunity *via* CD27. In the meantime, CD27 is known to be cleaved off when interacted by CD70 (32). Therefore, another possible explanation for the trend and for the irrelevance between CD70 score and CD27+TIL is that CD27-positive iTIL-low subset of CD70-high cases may be a mixture of those with TIL-low cases and with activated CD27-CD70 axis.

Previous studies revealed the aberrant expression of CD70 in several hematological malignancies and solid malignant tumors, including lung cancer, renal cell carcinoma, glioblastoma osteosarcoma, nasopharyngeal carcinoma and ovarian carcinoma (6, 39–44),. The role of the CD70–CD27 axis in anti-tumor

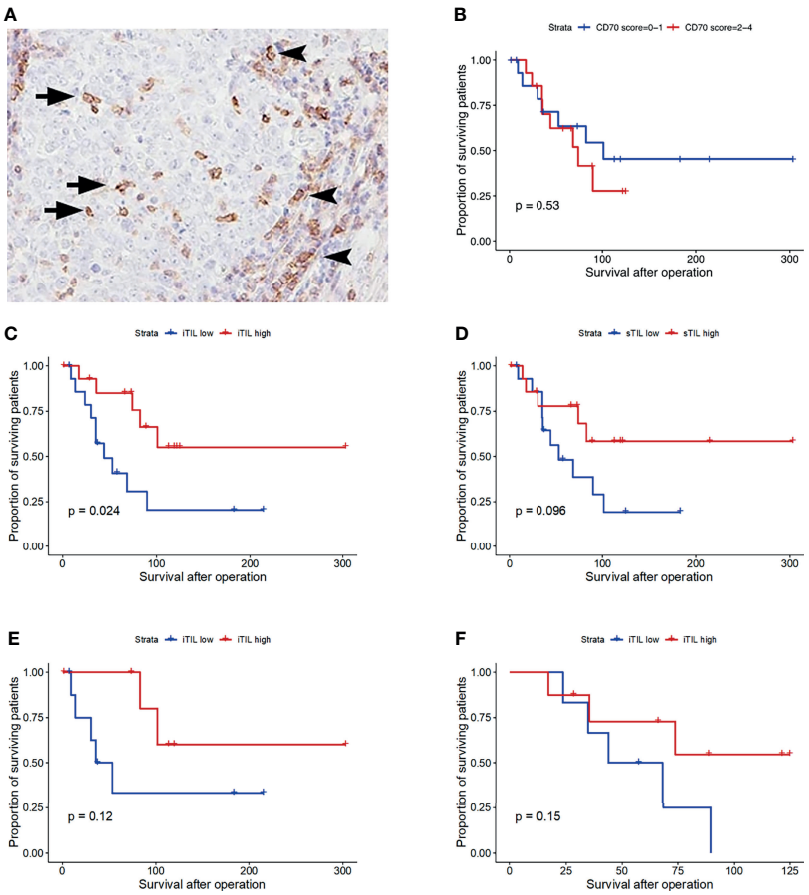

FIGURE 3 | CD27 staining of thymic squamous cell carcinoma **(A)**. CD27-positive intratumoral tumor-infiltrating lymphocytes (iTIL, arrow) and stromal TIL (sTIL, arrowhead). Overall survival of patients with thymic carcinoma according to the CD70 expression status **(B)**, the number of CD27-positive iTIL **(C)** and sTIL **(D)**. Stratified survival curve in the CD70-low group **(E)** and CD70-high group **(F)**. x-axis: days.

immunity is controversial. In physiological conditions, CD70 is expressed transiently in lymphocytes and dendritic cells and affects its receptor, CD27, leading to differentiation into effector or memory T-cells (2). On the other hand, the constitutive expression of CD70 observed in chronic viral infection and lymphoma leads to immune exhaustion (45, 46). Moreover, the expression of CD70 in renal carcinoma cell lines induces apoptosis of lymphocytes (47). We could not detect the significant difference between CD70-high and -low tumor in the levels of CD8-positive TIL or FOXP3-positive TIL; however, the number of FOXP3-positive iTIL in CD70-high TSCC was marginally larger than CD70-low TSCC. This result may reflect activation of CD70–CD27 axis and subsequent maintenance of regulatory T-cells. The impact of the amount of such TILs in TSCC to patient survival is still unclear. We suspect that CD70-expressing tumor induces immune suppressed state *via* CD70–CD27 pathway, which warrants further studies to confirm.

CD70 as Immunotherapeutic Target

Some anti-CD70 reagents have been developed for cancer. For example, SGN-CD70A underwent phase I trial in CD70-positive renal cell carcinoma patients (48). In addition, CD70 expression on malignant pleural mesothelioma and lower CD27–positive TIL accumulation are reported to correlate with poor prognosis (49). The present study showed that the survival curves of the CD27-positive iTIL-high and -low groups became closer in the CD70-high subset. This implies that CD70-targeted reagent may be beneficial for TSCC patients.

PD-L1 expression levels in thymic epithelial tumors and the correlation between survival have been examined in some studies but the results varied (50–53). Our study demonstrated no evident correlation between PD-L1 score and survival. It may be derived from small sample size, while PD-L1 expression alone might not be prognostic factor in thymic carcinoma patients who did not receive immunotherapy.

Patients with thymoma/thymic carcinoma have been shown that those with high-PD-L1 expression (>50% of tumor cells) appeared to have responded better to pembrolizumab (an anti-PD-L1 reagent), compared to those with low-PD-L1 expression (21, 22). Our result showed that CD70 and PD-L1 expression is correlated in TSCC. Therefore, combination of anti-CD70 and anti-PD-L1 reagents may be beneficial for many of the TSCC patients with high-PD-L1 expression. In addition, low-PD-L1

expression TSCC tended to have lower CD70 score and lower number of CD27-positive iTIL. In such cases, CD27-agonsitic treatment which is expected to facilitate immunity may be beneficial.

Chimeric antigen receptor (CAR) T cell therapy has achieved great success in the treatment of several hematologic malignancies. Recent evidence revealed that CAR T cells targeting CD70 could inhibit the growth of glioma (54), head and neck squamous cell carcinoma (55), and multiple solid tumors (56) as well as hematologic malignancies (57) *in vitro* and *in vivo*. CD70-targeting CAR T cell therapy may also be a new candidate for immunotherapy in thymic carcinoma.

Limitations

There were some limitations to our study. First, TSCC is a rare type of cancer; thus, the number of analyzed patients was small. Additional replication and collaboration studies are required. The multivariate analysis failed to show an independent survival effect of TIL or Masaoka–Koga staging, which also might partially be due to the small number of patients. Studies involving larger numbers of cases are warranted to assess the prognostic value of TIL. Second, sampling bias could not be excluded because we performed only IHC analysis in the representative specimens of each tumor. We confirmed the concordance between the staining pattern of CD70 in TSCC and expression using quantitative RT-PCR. Therefore, we suppose that a small amount of TSCC tissue may be sufficient to evaluate the expression of CD70.

CONCLUSION

CD70 was specifically positive in TSCC versus thymoma. In addition, in TSCC, a significantly higher positivity was observed than in LSCC. The CD70–CD27 axis is a potentially useful diagnostic marker and a promising therapeutic target.

DATA AVAILABILITY STATEMENT

The raw data supporting the conclusions of this article will be made available by the authors, without undue reservation.

ETHICS STATEMENT

This study was approved by the Institutional Review Board of the Tokyo Metropolitan Cancer and Infectious Diseases Center Komagome Hospital (approval number: 2120). Written informed consent for participation was not required for this study in accordance with the national legislation and the institutional requirements.

AUTHOR CONTRIBUTIONS

JK and TH drafted the manuscript. JK, TH, MO, YH, SH, TM, TU, and MF contributed to histopathological and immunohistochemical analysis. JK, YO, and HH contributed to the analysis of clinicopathological features. All authors contributed to the article and approved the submitted version.

ACKNOWLEDGMENTS

The authors would like to thank Enago (www.enago.jp) for the English language review.

SUPPLEMENTARY MATERIAL

The Supplementary Material for this article can be found online at: https://www.frontiersin.org/articles/10.3389/fonc.2021.808396/full#supplementary-material

REFERENCES

1. Hintzen RQ, Lens SMA, Koopman G, Pals ST, Spits H, van Lier RA. CD70 Represents the Human Ligand for CD27. *Int Immunol* (1994) 6:477–80. doi: 10.1093/intimm/6.3.477
2. van de Ven K, Borst J. Targeting the T-Cell Co-Stimulatory CD27/CD70 Pathway in Cancer Immunotherapy: Rationale and Potential. *Immunotherapy* (2015) 7:655–67. doi: 10.2217/imt.15.32
3. Coquet JM, Ribot JC, Babała N, Middendorp S, Van der Horst G, Xiao Y, et al. Epithelial and Dendritic Cells in the Thymic Medulla Promote CD4+Foxp3+ Regulatory T Cell Development *via* the CD27-CD70 Pathway. *J Exp Med* (2013) 210:715–28. doi: 10.1084/jem.20112061
4. McEarchern JA, Oflazoglu E, Francisco L, McDonagh CF, Gordon KA, Stone I, et al. Engineered Anti-CD70 Antibody With Multiple Effector Functions Exhibits *In Vitro* and *In Vivo* Antitumor Activities. *Blood* (2007) 109:1185–92. doi: 10.1182/blood-2006-07-034017
5. McEarchern JA, Smith LM, McDonagh CF, Klussman K, Gordon KA, Morris-Tilden CA, et al. Preclinical Characterization of SGN-70, a Humanized Antibody Directed Against CD70. *Clin Cancer Res* (2008) 14:7763–72. doi: 10.1158/1078-0432.CCR-08-0493
6. Jacobs J, Zwaenepoel K, Rolfo C, Van den Bossche J, Deben C, Silence K, et al. Unlocking the Potential of CD70 as a Novel Immunotherapeutic Target for non-Small Cell Lung Cancer. *Oncotarget* (2015) 6:13462–75. doi: 10.18632/oncotarget.3880
7. Huang J, Ahmad U, Antonicelli A, Catlin AC, Fang W, Gomez D, et al. International Thymic Malignancy Interest Group International Database Committee and Contributors. Development of the International Thymic Malignancy Interest Group International Database: An Unprecedented Resource for the Study of a Rare Group of Tumors. *J Thorac Oncol* (2014) 9:1573–8. doi: 10.1097/JTO.0000000000000269
8. Dorfman DM, Shahsafaei A, Chan JKC. Thymic Carcinomas, But Not Thymomas and Carcinomas of Other Sites, Show CD5 Immunoreactivity. *Am J Surg Pathol* (1997) 21:936–40. doi: 10.1097/00000478-199708000-00008
9. Pan CC, Chen PC-H, Chiang H. KIT (CD117) is Frequently Overexpressed in Thymic Carcinomas But is Absent in Thymomas. *J Pathol* (2004) 202:375–81. doi: 10.1002/path.1514
10. Kojika M, Ishii G, Yoshida J, Nishimura M, Hishida T, Ota S, et al. Immunohistochemical Differential Diagnosis Between Thymic Carcinoma and Type B3 Thymoma: Diagnostic Utility of Hypoxic Marker, GLUT-1, in Thymic Epithelial Neoplasms. *Mod Pathol* (2009) 22:1341–50. doi: 10.1038/modpathol.2009.105
11. Kaira K, Murakami H, Serizawa M, Koh Y, Abe M, Ohde Y, et al. MUC1 Expression in Thymic Epithelial Tumors: MUC1 may be Useful Marker as

Differential Diagnosis Between Type B3 Thymoma and Thymic Carcinoma. *Virchows Arch* (2011) 458:615–20. doi: 10.1007/s00428-011-1041-x
12. Khoury T, Chandrasekhar R, Wilding G, Tan D, Cheney RT. Tumour Eosinophilia Combined With an Immunohistochemistry Panel is Useful in the Differentiation of Type B3 Thymoma From Thymic Carcinoma. *Int J Exp Pathol* (2011) 92:87–96. doi: 10.1111/j.1365-2613.2010.00745.x
13. Pomplun S, Wotherspoon AC, Shah G, Goldstraw P, Ladas G, Nicholson AG. Immunohistochemical Markers in the Differentiation of Thymic and Pulmonary Neoplasms. *Histopathology* (2002) 40:152–8. doi: 10.1046/j.1365-2559.2002.01328.x
14. Hishima T, Fukayama M, Fujisawa M, Hayashi Y, Arai K, Funata N, et al. CD5 Expression in Thymic Carcinoma. *Am J Pathol* (1994) 145:268–75.
15. Kornstein MJ, Rosai J. CD5 Labeling of Thymic Carcinomas and Other Nonlymphoid Neoplasms. *Am J Clin Pathol* (1998) 109:722–6. doi: 10.1093/ajcp/109.6.722
16. Song N, Chen G, Zhang P, Liu M, He WX, Jiang GN. Diagnostic and Clinical Significance of KIT(CD117) Expression in Thymic Epithelial Tumors in China. *Asian Pac J Cancer Prev* (2012) 13:2745–8. doi: 10.7314/APJCP.2012.13.6.2745
17. Thomas de Montpréville V, Ghigna MR, Lacroix L, Besse B, Broet P, Dartevelle P, et al. Thymic Carcinomas: Clinicopathologic Study of 37 Cases From a Single Institution. *Virchows Arch* (2013) 462:307–13. doi: 10.1007/s00428-013-1371-y
18. Nakagawa K, Matsuno Y, Kunitoh H, Maeshima A, Asamura H, Tsuchiya R. Immunohistochemical KIT (CD117) Expression in Thymic Epithelial Tumors. *Chest* (2005) 128:140–4. doi: 10.1378/chest.128.1.140
19. Petrini I, Zucali PA, Lee HS, Pineda MA, Meltzer PS, Walter-Rodriguez B, et al. Expression and Mutational Status of C-Kit in Thymic Epithelial Tumors. *J Thorac Oncol* (2010) 5:1447–53. doi: 10.1097/JTO.0b013e3181e96e30
20. Hishima T, Fukayama M, Hayashi Y, Fujii T, Ooba T, Funata N, et al. CD70 Expression in Thymic Carcinoma. *Am J Surg Pathol* (2000) 24:742–6. doi: 10.1097/00000478-200005000-00014
21. Cho J, Kim H, Ku B, Choi YL, Cristescu R, Han J, et al. Pembrolizumab for Patients With Refractory or Relapsed Thymic Epithelial Tumor: An Open-Label Phase II Trial. *J Clin Oncol* (2019) 37:2162–70. doi: 10.1200/JCO.2017.77.3184
22. Giaccone G, Kim C, Thompson J, McGuire C, Kallakury B, Chahine JJ, et al. Pembrolizumab in Patients With Thymic Carcinoma: A Single-Arm, Single-Centre, Phase 2 Study. *Lancet Oncol* (2018) 19:347–55. doi: 10.1016/S1470-2045(18)30062-7
23. Katsuya Y, Horinouchi H, Seto T, Umemura S, Hosomi Y, Satouchi M, et al. Single-Arm, Multicentre, Phase II Trial of Nivolumab for Unresectable or Recurrent Thymic Carcinoma: PRIMER Study. *Eur J Cancer* (2019) 113:78–86. doi: 10.1016/j.ejca.2019.03.012
24. Galon J, Costes A, Sanchez-Cabo F, Kirilovsky A, Mlecnik B, Lagorce-Pagès C, et al. Type, Density, and Location of Immune Cells Within Human Colorectal Tumors Predict Clinical Outcome. *Science* (2006) 313:1960–4. doi: 10.1126/science.1129139
25. Sharma P, Shen Y, Wen S, Yamada S, Jungbluth AA, Gnjatic S, et al. CD8 Tumor-Infiltrating Lymphocytes are Predictive of Survival in Muscle-Invasive Urothelial Carcinoma. *Proc Natl Acad Sci U S A* (2007) 104:3967–72. doi: 10.1073/pnas.0611618104
26. Azimi F, Scolyer RA, Rumcheva P, Moncrieff M, Murali R, McCarthy SW, et al. Tumor-Infiltrating Lymphocyte Grade is an Independent Predictor of Sentinel Lymph Node Status and Survival in Patients With Cutaneous Melanoma. *J Clin Oncol* (2012) 30:2678–83. doi: 10.1200/JCO.2011.37.8539
27. Zhang L, Conejo-Garcia JR, Katsaros D, Gimotty PA, Massobrio M, Regnani G, et al. Intratumoral T Cells, Recurrence, and Survival in Epithelial Ovarian Cancer. *N Engl J Med* (2003) 348:203–13. doi: 10.1056/NEJMoa020177
28. Clemente CG, Mihm MC, Bufalino R, Zurrida S, Collini P, Cascinelli N. Prognostic Value of Tumor Infiltrating Lymphocytes in the Vertical Growth Phase of Primary Cutaneous Melanoma. *Cancer* (1996) 77:1303–10. doi: 10.1002/(SICI)1097-0142(19960401)77:7<1303::AID-CNCR12>3.0.CO;2-5
29. Mahmoud SMA, Paish EC, Powe DG, Macmillan RD, Grainge MJ, Lee AHS, et al. Tumor-Infiltrating CD8+ Lymphocytes Predict Clinical Outcome in Breast Cancer. *J Clin Oncol* (2011) 29:1949–55. doi: 10.1200/JCO.2010.30.5037
30. Al-Shibli KI, Donnem T, Al-Saad S, Persson M, Bremnes RM, Busund LT. Prognostic Effect of Epithelial and Stromal Lymphocyte Infiltration in non-Small Cell Lung Cancer. *Clin Cancer Res* (2008) 14:5220–7. doi: 10.1158/1078-0432.CCR-08-0133
31. Bruno TC, Ebner PJ, Moore BL, Squalls OG, Waugh KA, Eruslanov EB, et al. Antigen-Presenting Intratumoral B Cells Affect CD4+ TIL Phenotypes in non-Small Cell Lung Cancer Patients. *Cancer Immunol Res* (2017) 5:898–907. doi: 10.1158/2326-6066.CIR-17-0075
32. Ruf M, Mittmann C, Nowicka AM, Hartmann A, Hermanns T, Poyet C, et al. pVHL/HIF-Regulated CD70 Expression is Associated With Infiltration of CD27+ Lymphocytes and Increased Serum Levels of Soluble CD27 in Clear Cell Renal Cell Carcinoma. *Clin Cancer Res* (2015) 21:889–98. doi: 10.1158/1078-0432.CCR-14-1425
33. Adam PJ, Terrett JA, Steers G, Stockwin L, Loader JA, Fletcher GC, et al. CD70 (TNFSF7) is Expressed at High Prevalence in Renal Cell Carcinomas and is Rapidly Internalised on Antibody Binding. *Br J Cancer* (2006) 95:298–306. doi: 10.1038/sj.bjc.6603222
34. Flieswasser T, Camara-Clayette V, Danu A, Bosq J, Ribrag V, Zabrocki P, et al. Screening a Broad Range of Solid and Haematological Tumour Types for CD70 Expression Using a Uniform IHC Methodology as Potential Patient Stratification Method. *Cancers* (2019) 11:1611. doi: 10.3390/cancers11101611
35. Ströbel P, Hartmann E, Rosenwald A, Kalla J, Ott G, Friedel G, et al. Corticomedullary Differentiation and Maturational Arrest in Thymomas. *Histopathology* (2014) 64:557–66. doi: 10.1111/his.12279
36. Hayashi A, Fumon T, Miki Y, Sato H, Yoshino T, Takahashi K. The Evaluation of Immunohistochemical Markers and Thymic Cortical Microenvironmental Cells in Distinguishing Thymic Carcinoma From Type B3 Thymoma or Lung Squamous Cell Carcinoma. *J Clin Exp Hematop* (2013) 53:9–19. doi: 10.3960/jslrt.53.9
37. Kriegsmann M, Muley T, Harms A, Tavernar L, Goldmann T, Dienemann H, et al. Differential Diagnostic Value of CD5 and CD117 Expression in Thoracic Tumors: A Large Scale Study of 1465 non-Small Cell Lung Cancer Cases. *Diagn Pathol* (2015) 10:210. doi: 10.1186/s13000-015-0441-7
38. Shim HS, Byun CS, Bae MK, Lee CY, Park IK, Kim DJ, et al. Prognostic Effect of Stromal Lymphocyte Infiltration in Thrymic Carcinoma. *Lung Cancer* (2011) 74:338–43. doi: 10.1016/j.lungcan.2011.03.008
39. Law CL, Gordon KA, Toki BE, Yamane AK, Hering MA, Cerveny CG, et al. Lymphocyte Activation Antigen CD70 Expressed by Renal Cell Carcinoma is a Potential Therapeutic Target for Anti-CD70 Antibody-Drug Conjugates. *Cancer Res* (2006) 66:2328–37. doi: 10.1158/0008-5472.CAN-05-2883
40. Yang ZZ, Novak AJ, Ziesmer SC, Witzig TE, Ansell SM. CD70(+) non-Hodgkin Lymphoma B Cells Induce Foxp3 Expression and Regulatory Function in Intratumoral CD4(+)CD25(–) T Cells. *Blood* (2007) 110:2537–44. doi: 10.1182/blood-2007-03-082578
41. Wischhusen J, Jung G, Radovanovic I, Beier C, Steinbach JP, Rimner A, et al. Identification of CD70-Mediated Apoptosis of Immune Effector Cells as a Novel Immune Escape Pathway of Human Glioblastoma. *Cancer Res* (2002) 62:2592–9.
42. Pahl JHW, Santos SJ, Kuijjer ML, Boerman GH, Sand LGL, Szuhai K, et al. Expression of the Immune Regulation Antigen CD70 in Osteosarcoma. *Cancer Cell Int* (2015) 15:31. doi: 10.1186/s12935-015-0181-5
43. Agathanggelou A, Niedobitek G, Chen R, Nicholls J, Yin W, Young LS. Expression of Immune Regulatory Molecules in Epstein-Barr Virus-Associated Nasopharyngeal Carcinomas With Prominent Lymphoid Stroma. Evidence for a Functional Interaction Between Epithelial Tumor Cells and Infiltrating Lymphoid Cells. *Am J Pathol* (1995) 147:1152–60.
44. Liu N, Sheng X, Liu Y, Zhang X, Yu J. Increased CD70 Expression is Associated With Clinical Resistance to Cisplatin-Based Chemotherapy and Poor Survival in Advanced Ovarian Carcinomas. *Onco Targets Ther* (2013) 6:615–9. doi: 10.2147/OTT.S44445
45. Penaloza-MacMaster P, Ur Rasheed A, Iyer SS, Yagita H, Blazar BR, Ahmed R. Opposing Effects of CD70 Costimulation During Acute and Chronic Lymphocytic Choriomeningitis Virus Infection of Mice. *J Virol* (2011) 85:6168–74. doi: 10.1128/JVI.02205-10
46. Yang ZZ, Grote DM, Xiu B, Ziesmer SC, Price-Troska TL, Hodge LS, et al. TGF-β Upregulates CD70 Expression and Induces Exhaustion of Effector Memory T Cells in B-Cell non-Hodgkin's Lymphoma. *Leukemia* (2014) 28:1872–84. doi: 10.1038/leu.2014.84
47. Diegmann J, Junker K, Loncarevic IF, Michel S, Schimmel B, von Eggeling F. Immune Escape for Renal Cell Carcinoma: CD70 Mediates Apoptosis in Lymphocytes. *Neoplasia* (2006) 8:933–8. doi: 10.1593/neo.06451
48. Pal SK, Forero-Torres A, Thompson JA, Morris JC, Chhabra S, Hoimes CJ, et al. A Phase 1 Trial of SGN-CD70A in Patients With CD70-Positive, Metastatic Renal Cell Carcinoma. *Cancer* (2019) 125:1124–32. doi: 10.1002/cncr.31912

49. Inaguma S, Lasota J, Czapiewski P, Langfort R, Rys J, Szpor J, et al. CD70 Expression Correlates With a Worse Prognosis in Malignant Pleural Mesothelioma Patients via Immune Evasion and Enhanced Invasiveness. *J Pathol* (2019) 250:205–16. doi: 10.1002/path.5361
50. Katsuya Y, Fujita Y, Horinouchi H, Ohe Y, Watanabe SI, Tsuta K, et al. Immunohistochemical Status of PD-L1 in Thymoma and Thymic Carcinoma. *Lung Cancer* (2015) 88:154–9. doi: 10.1016/j.lungcan.2015.03.003
51. Yokoyama S, Miyoshi H, Nakashima K, Shimono J, Hashiguchi T, Mitsuoka M, et al. Prognostic Value of Pro-Grammed Death Ligand 1 and Programmed Death 1 Expression in Thymic Carcinoma. *Clin Cancer Res* (2016) 22:4727–34. doi: 10.1158/1078-0432.CCR-16-0434
52. Weissferdt A, Fujimoto J, Kalhor N, Rodriguez J, Bassett R, Wistuba II, et al. Expression of PD-1 and PD-L1 in Thymic Epithelial Neoplasms. *Mod Pathol* (2017) 30:826–33. doi: 10.1038/modpathol.2017.6
53. Arbour KC, Naidoo J, Steele KE, Ni A, Moreira AL, Rekhtman N, et al. Expression of PD-L1 and Other Immunotherapeutic Targets in Thymic Epithelial Tumors. *PloS One* (2017) 12:e0182665. doi: 10.1371/journal.pone.0182665
54. Jin L, Ge H, Long Y, Yang C, Chang YE, Mu L, et al. CD70, a Novel Target of CAR T-Cell Therapy for Gliomas. *J Neuro Oncol* (2018) 20:55–65. doi: 10.1093/neuonc/nox116
55. Park YP, Jin L, Bennett KB, Wang D, Fredenburg KM, Tseng JE, et al. CD70 as a Target for Chimeric Antigen Receptor T Cells in Head and Neck Squamous Cell Carcinoma. *Oral Oncol* (2018) 78:145–50. doi: 10.1016/j.oraloncology.2018.01.024
56. Yang M, Tang X, Zhang Z, Gu L, et al. Tandem CAR-T Cells Targeting CD70 and B7-H3 Exhibit Potent Preclinical Activity Against Multiple Solid Tumors. *Theranostics* (2020) 10:7622–34. doi: 10.7150/thno.43991
57. Sauer T, Parikh K, Sharma S, et al. CD70-Specific CAR T Cells Have Potent Activity Against Acute Myeloid Leukemia Without HSC Toxicity. *Blood* (2021) 138:318–30. doi: 10.1182/blood.2020008221

Conflict of Interest: The authors declare that the research was conducted in the absence of any commercial or financial relationships that could be construed as a potential conflict of interest.

Publisher's Note: All claims expressed in this article are solely those of the authors and do not necessarily represent those of their affiliated organizations, or those of the publisher, the editors and the reviewers. Any product that may be evaluated in this article, or claim that may be made by its manufacturer, is not guaranteed or endorsed by the publisher.

Copyright © 2022 Kashima, Hishima, Okuma, Horio, Ogawa, Hayashi, Horiguchi, Motoi, Ushiku and Fukayama. This is an open-access article distributed under the terms of the Creative Commons Attribution License (CC BY). The use, distribution or reproduction in other forums is permitted, provided the original author(s) and the copyright owner(s) are credited and that the original publication in this journal is cited, in accordance with accepted academic practice. No use, distribution or reproduction is permitted which does not comply with these terms.

frontiers in Oncology

ORIGINAL RESEARCH
published: 07 February 2022
doi: 10.3389/fonc.2022.823667

Correlation of Somatostatin Receptor 2 Expression, 68Ga-DOTATATE PET Scan and Octreotide Treatment in Thymic Epithelial Tumors

Anja C. Roden[1], Sagar Rakshit[2], Geoffrey B. Johnson[3,4], Sarah M. Jenkins[5] and Aaron S. Mansfield[2]*

[1] Department of Laboratory Medicine and Pathology, Mayo Clinic, Rochester, MN, United States, [2] Division of Medical Oncology, Mayo Clinic, Rochester, MN, United States, [3] Department of Radiology, Mayo Clinic, Rochester, MN, United States, [4] Department of Immunology, Mayo Clinic, Rochester, MN, United States, [5] Division of Clinical Trials and Biostatistics, Mayo Clinic, Rochester, MN, United States

OPEN ACCESS

Edited by:
Cesar Moran, University of Texas MD Anderson Cancer Center, United States

Reviewed by:
Paul Emile Van Schil, Antwerp University Hospital, Belgium
Jelena Stojsic, University of Belgrade, Serbia

***Correspondence:**
Anja C. Roden
roden.anja@mayo.edu

Specialty section:
This article was submitted to Thoracic Oncology, a section of the journal Frontiers in Oncology

Received: *27 November 2021*
Accepted: *10 January 2022*
Published: *07 February 2022*

Citation:
Roden AC, Rakshit S, Johnson GB, Jenkins SM and Mansfield AS (2022) Correlation of Somatostatin Receptor 2 Expression, 68Ga-DOTATATE PET Scan and Octreotide Treatment in Thymic Epithelial Tumors. Front. Oncol. 12:823667. doi: 10.3389/fonc.2022.823667

Somatostatin receptor 2 (SSTR2) has been shown to be expressed in a subset of neuroendocrine tumors and carcinomas and plays a role in imaging studies and guiding therapy. Patients with tumors expressing SSTR2 may be successfully treated with somatostatin inhibitors or radiolabeled somatostatin analogues. We studied SSTR2 expression in TET and correlated it with 68Ga-DOTATATE PET/CT or 68Ga-DOTATATE PET/MR results and treatment outcome. An institutional database of TET was searched for thymoma, thymic carcinoma, and thymic neuroendocrine tumor (TNET) with available resection specimens. Cases were subtyped (2021 WHO classification) and staged (8th AJCC/UICC staging). A section was stained with anti-SSTR2 antibody (clone UMB1). Percent tumor cells with membranous staining was recorded if present in ≥1% of tumor cells. Medical records were searched for 68Ga-DOTATATE PET scans and treatment. Statistical analysis was performed. Eighty patients (1969-2021) with a median age of 61.3 years (range, 19.1-87.3) (37 males, 46.3%) had thymic carcinoma (N=33), TNET (N=7), or thymoma (N=40). SSTR2 expression was identified in 29 (of 80, 36.3%) TET including 2/2 (100%) small cell carcinomas, 2/5 (40.0%) atypical carcinoid tumors, 16/23 (69.6%) squamous cell carcinomas, 2/2 (100%) lymphoepithelial carcinomas, 1/1 (100%) adenosquamous carcinoma, and 6/40 (15.0%) thymomas. SSTR2 expression in ≥50% of tumor cells (vs 1-49%) was associated with younger age (p=0.023) and shorter recurrence/metastasis-free survival (p=0.007). 68Ga-DOTATATE PET scans (N=9) revealed a Krenning score of 3 in patients with atypical carcinoid tumor, small cell carcinoma, and squamous cell carcinoma (N=1 each) with SSTR2 expression in 95, 100, and 5% of tumor cells, respectively. Scans with Krenning scores of ≤2 (N=5) were seen in tumors with no SSTR2 expression in 80% of cases and a single atypical carcinoid tumor with SSTR2 expression in 10% of tumor cells. One scan resulted as "increased uptake" was in a patient with no SSTR2 expression. In conclusion, 68Ga-DOTATATE PET

scans correlated with SSTR2 expression in TET in most patients and appeared to be useful to identify patients with TET who may be amenable to treatment with somatostatin analogues. Larger studies including more patients with 68Ga-DOTATATE PET scans are necessary to independently and prospectively validate our findings.

Keywords: somatostatin receptor 2, SSTR2, DOTATATE scan, octreotide treatment, thymoma, thymic carcinoma, atypical carcinoid tumor, thymic neuroendocrine tumor

INTRODUCTION

Thymic epithelial tumors (TET) including thymomas, thymic carcinomas, and thymic neuroendocrine tumors (TNET) are malignant neoplasms. Although these tumors are rare, they together represent the most common solitary lesions in the prevascular mediastinum (1). Specifically thymic carcinomas and TNETs are often diagnosed at high stage and their large size and infiltration of vital organs commonly prevents complete resection. For instance, 71 to 79% of patients with thymic carcinoma present at stages III or IV and complete resection is reported in only 46 to 69% of patients with 5-year overall survival rates of 52 to 64% and disease-free survival of 41% (2–6). In TNET, the outcome depends on the histologic subtype with 5-year overall survivals of 50 to 70% for typical and atypical carcinoid tumors, 30 to 66% for large cell neuroendocrine carcinomas, and 0% with a median survival of 13-26 months for small cell carcinomas (7).

Predictive biomarkers are scarce in TET and therefore options for targetable therapy are currently very limited. Thymomas and thymic carcinomas have very low tumor mutational burdens with 0.48 mutations and 1.2 mutations/Mb, respectively with a rare thymic carcinoma reported to harbor 21.3 mutations/Mb (8–10). *GTF2I* mutation is the most common molecular alteration in TET, specifically in type A and AB thymomas where it occurs in 70 to 100% of cases. In contrast to thymomas, *GTF2I* mutation is only identified in 0 to 8% of thymic carcinomas, and has not been described in TNETs (8, 10, 11). Moreover, no therapies are currently available to target *GTF2I*. *KIT* mutations occur in 6 to 20% of thymic carcinomas although only a few tumors harbor an activating *KIT* mutation and therefore only some patients may benefit from receptor tyrosine kinase inhibitors (12–14). Other mutations in thymic carcinomas include *TP53*, *CDKN2A*, *cyclin D1*, *FGFR3*, and *ALK* among others, some of which may potentially be targetable (8, 12, 13, 15, 16). While PD-L1 expression has been identified in 27 to 80% of thymic carcinomas and 23 to 54% of thymomas, given the unique immune status of the thymic gland, immune checkpoint inhibitor treatment requires further investigation (9, 17–20). Taken together, predictive biomarkers are still strongly sought to predict tumor responsiveness of TET to targeted therapy.

Somatostatin receptor 2 (SSTR2) is a G protein-coupled cell surface receptor in the family of somatostatin receptors that has multiple roles *via* adenylate cyclase, calcium influx, and has effects on cell cycling angiogenesis, apoptosis, and growth factor signalling (21, 22). The activation of the receptor by extracellular ligands has been shown to lead to inhibition of cell proliferation (23). In contrast, in a study of small cell lung carcinomas in which 48% of tumors expressed SSTR2, high SSTR2 expression (defined in that study as SSTR2 expression in tumor tissue 1+ or greater or immunohistochemical score ≥ 1) was associated with worse 2-year survival when compared to low expression of SSTR2 (21). These results were largely attributed to limited stage disease and not seen in patients with extensive stage disease. The authors concluded that SSTR2 signaling in small cell lung cancer may support tumor growth and maintenance. Indeed, that study further showed that downregulation of SSTR2 leads to increased apoptosis and decreased tumor growth in small cell lung carcinoma (21).

SSTR2 has also been recognized as an imaging and treatment target in various neoplasms including neuroendocrine tumors such as paragangliomas and small cell lung carcinomas, but also other malignancies such as thyroid carcinomas, and EBV-driven and non-EBV-driven nasopharyngeal carcinomas (22, 24–26). There are two primary mechanisms by which treatment may be delivered including 1) SSTR2 analogues that rely on SSTR2 signaling-induced changes and 2) the use of SSTR2 as a targeting molecule to deliver a cytotoxic or radioactive payload in form of an antibody-drug conjugate (22). For instance, DOTATATE and DOTA-Tyr-octreotide (DOTA-TOC) are clinically available somatostatin analogues that bind to SSTR2 (26). Patients with tumors expressing SSTR2 have been shown to be successfully treated with peptide somatostatin inhibitors such as octreotide or DOTATATE (27). These agents can be linked to radionuclides like 68-gallium (68Ga) and 177-lutetium (177Lu) for both imaging and therapeutic applications respectively. For instance, Thakur et al. found that SSTR2 is higher expressed in thyroid carcinomas and medullary carcinomas than in normal thyroid tissue and most patients with metastatic thyroid cancer showed positive 68Ga-DOTATATE uptake indicating that SSTR2 is expressed by these tumors (28). Treatment of mice with 177Lu DOTATATE resulted in tumor growth reduction (28). Furthermore, in a randomized, placebo-controlled study of the somatostatin analogue lanreotide in patients with SSTR-positive (by scintigraphy) grade 1 or 2 neuroendocrine tumors with a Ki-67 proliferative index of <10% originating in the pancreas, midgut, or hindgut or of unknown origin lanreotide treatment was associated with significantly prolonged progression-free survival of 65% at 24 months when compared to 33% for the placebo group (29).

Although DOTATATE PET scans are part of the clinical workup of some TET, specifically TNETs and octreotide treatment has been used in a subset of TET including

thymomas, thymic carcinomas, and TNETs, SSTR2 expression has only been studied in small case series or case reports (30–32). Furthermore, the correlation between SSTR2 expression and results of 68Ga-DOTATATE PET scans in TET is largely unknown. Therefore, we studied the expression of SSTR2 in TET and its correlation with results of DOTATATE PET scans and treatment outcome.

METHODS

Patients

In this retrospective study, an institutional database of TET (1941-2021) was searched for thymoma, thymic carcinoma, and TNET from patients who underwent surgery. All cases were reviewed by a thoracic pathologist (ACR) to confirm the diagnosis. TETs were subtyped according to the 2021 WHO classification (33) and staged using the 8th AJCC/UICC staging manual (34). To avoid possible misinterpretation of SSTR2-expression on tumor cells due to potentially high numbers of SSTR2-expressing thymocytes only type A and B3 thymomas, micronodular thymomas with lymphoid stroma, thymic carcinomas, and TNETs were included in the study. Patient demographics and outcomes were recorded from medical records. Medical records were also searched for 68Ga-DOTATATE PET scans and treatment. The study was approved by the Mayo Clinic Rochester Institutional Review Board (#10-003525).

Immunohistochemistry

Formalin-fixed paraffin-embedded tissue blocks were cut at 4µm and stained with anti-SSTR2 antibody (clone UMB1, Abcam, Boston, MA). Percent tumor cells with membranous staining was recorded if present in ≥ 1% of tumor cells. The staining evaluation was modified from the evaluation used by Volante et al. (35) Similar to the evaluation system by Volante et al. no expression or focal or diffuse cytoplasmic expression of SSTR2 were regarded as negative. Membranous SSTR2 staining in 1 to 49% of tumor cells and 50 to 100% of tumor cells were considered positive. Staining intensity was noted as negative, weak, moderate, or strong.

68Ga-DOTATATE PET Scans

Available 68Ga-DOTATATE PET/CT and PET/MR scans were reviewed by a nuclear medicine physician and radiologist (GBJ) and a Krenning score was applied. Briefly, Krenning score is a qualitative measure of relative uptake of 68Ga-DOTATATE in tumors versus the physiologic uptake in the internal organs of the liver and spleen, with a Krenning score of 1 being negative and tumor activity far below liver activity, a Krenning score of 2 being mildly positive with activity slightly less than liver, a Krenning score of 3 being positive with activity higher than liver, and a Krenning score of 4 being very positive with activity above spleen. Scans were performed on GE Discovery 710, GE Discovery MI and Siemens Vision 600 PET/CT or GE Signa PET/MR scanners. Uptake was 60 minutes plus or minus 5 minutes in all patients, and the injected dose was 5.2 mCi 68Ga-DOTATATE IV +/- 10% IV.

Statistical Analysis

Continuous and ordinal characteristics were compared between SSTR2 expression groups with Wilcoxon rank-sum tests, and categorical characteristics were compared with Fisher's exact tests. The WHO type was compared using the following compressed categories: thymoma, thymic carcinoma, and thymic neuroendocrine tumors (including small cell carcinomas and atypical carcinoid tumors). Recurrence/metastasis-free survival (RFS) and overall survival (OS) were compared between groups with likelihood ratio tests from Cox proportional-hazards regression models. Five-year RFS and OS were summarized using the Kaplan-Meier method along with 95% confidence intervals (CI). P-values less than 0.05 were considered statistically significant. All analyses were performed using SAS version 9.4 (SAS Institute Inc., Cary, NC).

RESULTS

Patient Characteristics and Tumor Histology

Eighty patients surgically treated between 1969 and 2021 were included in the study. Demographics of the study population are summarized in **Table 1**. These 80 patients carried thymomas (N=40, 50%), thymic carcinomas (N=33, 41.3%), and TNETs (N=7, 8.8%). Tumor histology is detailed in **Table 2**.

The median age of the study population was 61.3 years with a slight female predominance (53.7%). Patients with thymoma were significantly older at time of surgery than patients with thymic carcinoma (median age [range], 64.6 years [28.1-87.3] vs 52.8 [19.1-79.6], respectively) (p=0.02) and patients with TNET (median age [range], 64.6 years [28.1-87.3] vs 44.1 [29.7-61.4], respectively) (p=0.004). There was no difference in age between patients with thymic carcinoma and patients with TNET (p=0.11). Most patients (85%) underwent complete resection. The median tumor size of resected tumors was 5.0 cm. Most tumors (52.8%) were of stage I. Additional neoadjuvant and/or adjuvant therapy was given in 42.9% of patients; 3 patients also received octreotide.

Follow up was available in 78 patients for a median of 3.1 years (range, 0.1-19.6). The outcome of patients is detailed in **Table 1**. Twenty-three patients had a metastasis and/or recurrence within 0.2 to 4.5 years after resection of the primary tumor (5-year rate of metastasis/recurrence, 41.3%, 95% CI: 27.4%-55.2%). Most patients (43 of 78) were alive without disease at the time of last follow-up. Ten (of 78) died due to TET. All patients who died due to disease had either thymic carcinoma or TNET. The 5-year overall survival was 68.1% (95% CI: 55.5%-80.7%).

SSTR2 Expression of Tumors

SSTR2 expression (1-100%) was identified in 29 (of 80, 36.3%) TET. Results of SSTR2 expression are detailed in **Table 2**. SSTR2 expression was more common among thymic carcinomas

TABLE 1 | Demographics, treatment, and outcome of study population.

Feature	Results
Study population, N	80
Male sex, N (%)	37 (46.3)
Age, years, median (range)	61.3 (19.1-87.3)
Surgical treatment, N (%)	
Complete resection	68 (85.0)
Incomplete resection	7 (8.8)
Biopsy	3 (3.8)
Recurrence/metastasis[a]	2 (2.5)
Tumor size in cm, median (range)[b]	5.0 (0.5-23.0)
pT stage, N (%)[c]	
T1a	50 (66.7)
T2	1 (1.3)
T3	23 (30.7)
T4	1 (1.3)
pN stage [c]	
N0	36 (72.0)
N1	13 (26.0)
N2	1 (2.0)
NX	25
pM stage [c]	
M0	68 (90.7)
M1a	3 (4.0)
M1b	4 (5.3)
TNM Stage	
I	28 (52.8)
II	1 (1.9)
IIIA	4 (7.5)
IVA	15 (28.3)
IVB	5 (9.4)
N/A	27
Additional Therapies, N (%)	34 (42.5)
Octreotide[d]	3
Adjuvant radiation	10
Adjuvant chemoradiation	9
Neoadjuvant & adjuvant chemotherapy & adjuvant radiation	3
Adjuvant chemotherapy	2
Neoadjuvant chemotherapy	2
Neoadjuvant radiation	2
Neoadjuvant chemotherapy	2
Neoadjuvant chemotherapy & adjuvant radiation	2
Neoadjuvant chemoradiation	1
Neoadjuvant & adjuvant radiation	1
Unknown	3
Outcome	
Follow up available, N	78
Follow up time in years, median (range)	3.1 (0.1-19.6)
Metastasis and/or recurrence, N (5-year estimate, %)[c,e]	23 (41.3 [95% CI: 27.4%-55.2%])
Ongoing disease after incomplete resection, N	1
Alive, N (5-year estimate, %)	53 (68.1 [95%CI: 55.5%-80.7%])
Alive without disease, N	43
Alive with disease, N	10
Death, N (5-year estimate, %)	25 (32.9 [95% CI: 19.3%-45.5%])
Died due to disease, N	10
Died due to other cause, N	5
Died due to unknown cause, N	10

[a]*In these 2 patients the specimen at time of recurrence/metastasis was tested for SSTR2 expression; date of resection of primary tumor was used for outcome analysis;*
[b]*Only including completely resected primary tumors;*
[c]*Only including resected tumors;*
[d]*All 3 patients received octreotide in addition to other additional treatment;*
[e]*Data available in 75 patients; N/A, not available.*

(57.6%) and TNET (57.1%) as compared to thymomas (15.0%, p<0.001) (**Table 2**). Furthermore, among those expressing SSTR2, there was a trend of higher expression of SSTR2 (≥ 50%) in thymic carcinomas (10 of 19, 52.6%) and TNETs (2 of 4, 50%) than in thymomas (0 of 6) (p=0.07) (**Table 2**).

SSTR2 expression was strong in 19 (of 29, 65.5%), moderate in 7 (24.1%), and weak in 3 (10.3%) TET. Weak expression was seen in 2 thymomas with 1% of tumor cells expressing SSTR2 and in an adenosquamous carcinoma with 5% of tumor cells expressing SSTR2.

TABLE 2 | Histopathologic features and expression of SSTR2 in thymic epithelial tumors.

Tumor Histology	Number of Cases (%)	Number of SSTR2-negative Cases (%)	Number of Total Cases Expressing SSTR2 in 1-100% of Tumor Cells (%) (median % SSTR-positive tumor cells, range)	Number of Cases Expressing SSTR2 in 1-49% of Tumor Cells (%) (median % SSTR-positive tumor cells, range)	Number of Cases Expressing SSTR2 in ≥ 50% of Tumor Cells (%) (median % SSTR-positive tumor cells, range)	P-Value [Pos vs Neg[a], 1-49% vs ≥50%[b]]
Total number of cases, N (%)	80	51 (63.7)	29 (36.3)	17 (21.3)	12 (15.0)	
Age in years, median (range)	61.3 (19.1-87.3)	63.9 (28.1-83.9)	56.3 (19.1-87.3)	61.6 (29.7-87.3)	49.4 (19.1-65.6)	0.09, 0.023
Thymoma	40 (50.0)	34 (85)	6 (15.0) (1.5; 1-5)	6 (15.0) (1.5; 1-5)	0	<0.001,
Type A	24	21 (87.5)	3 (12.5) (1;1-5)	3 (12.5) (1;1-5)	0	0.07
Type B3	9	8 (88.9)	1 (11.1) (1)	1 (11.1) (1)	0	
Micronodular thymoma with lymphoid stroma	7	5 (71.4)	2 (28.6) (3.5,2-5)	2 (28.6) (3.5,2-5)	0	
Thymic carcinoma	33 (41.3)	14 (42.4)	19 (57.6) (50; 1-100)	9 (27.3) (10; 1-30)	10 (30.3) (85; 50-100)	
Squamous cell carcinoma	23	7 (30.4)	16 (69.6) (40;1-100)	8 (34.8) (10;1-30)	8 (34.8) (90;50-100)	
Adenocarcinoma	4	4 (100.0)	0	0	0	
Mucoepidermoid carcinoma	2	2 (100.0)	0	0	0	
Lymphoepithelial carcinoma	2	0 (0.0)	2 (100.0) (70; 70 each)	0	2 (100.0) (70; 70 each)	
Adenosquamous carcinoma	1	0 (0.0)	1 (100.0) (5)	1 (100.0) (5)	0	
Undifferentiated carcinoma	1	1 (100.0)	0	0	0	
Thymic neuroendocrine tumor	7 (8.8)	3 (42.9)	4 (57.1) (52.5; 2-100)	2 (28.6) (6.0; 2-10)	2 (28.6) (97.5; 95-100)	
Atypical carcinoid tumor	5	3 (60.0)	2 (40.0) (52.5;10-95)	1 (20.0) (10)	1 (20.0) (95)	
Small cell carcinoma	2	0 (0.0)	2 (100.0) (51;2-100)	1 (50.0) (2)	1 (50.0) (100)	
TNM Stage						0.10, 0.22
I	28 (52.8)	20 (71.4)	8 (28.6) (3.5; 1-70)	7 (25.0) (2; 1-10)	1 (3.6) (70)	
II	1 (1.9)	1 (100.0)	0	0	0	
IIIA	4 (7.5)	1 (25.0)	3 (75.0) (90; 10-95)	1 (25.0) (10)	2 (50.0) (92.5; 90-95)	
IVA	15 (28.3)	8 (53.3)	7 (46.7) (90.0; 1-100)	3 (20.0) (10.0; 1-30)	4 (26.7) (95.0; 90-100)	
IVB	5 (9.4)	2 (40.0)	3 (60.0) (5.0; 5-70)	2 (40.0) (5 each)	1 (20.0) (70)	
N/A	27	19 (70.4)	8 (29.6) (37.5; 1-100)	4 (14.8) (7.5; 1-25)	4 (14.8) (75.0; 50-100)	

[a]*P-value for comparison of positive vs negative SSTR2 expression (1-100% vs <1%) between thymoma, thymic carcinoma, and thymic neuroendocrine tumor.*

[b]*P-value for comparison of SSTR2 expression (1-49% vs ≥50%) between thymoma, thymic carcinoma and thymic neuroendocrine tumor (excluding those with <1% expression).*

N/A, not available.

As compared to those with lower SSTR2 expression (1-49% of tumor cells), those with ≥ 50% tumor cells expression were younger in age (p=0.023). Also, SSTR2 expression in ≥ 50% of tumor cells trended to be more common in thymic carcinomas when compared to TNET and thymoma (p=0.056). SSTR2 expression (1-100%) was more commonly seen in TET of patients with high stage (stages IIIA-IVB; 13 of 24, 54.2%) compared to patients with low stage (stage I; 8 of 28, 28.6%) tumors although that was not statistically significant (p=0.10). The distribution of tumor stage in relationship to the subtype of TET is summarized in **Table 3**.

SSTR2 expression in ≥ 50% of tumor cells was associated with worse RFS with an estimated 5-year RFS of 11.4% (95% CI: 0%-32.5%) vs 72.7% (95% CI: 46.4%-99.0%) in patients with 1-49% of tumor cells expressing SSTR2 (p=0.007). The estimated 5-year RFS among patients with <1% SSTR2 expression was 67.8% (95% CI: 51.3%-84.3%; p=0.10 for <1% vs 1-100% SSTR2 expression). SSTR2 expression was not associated with 5-year OS (estimated 66.3% [95% CI: 34.4%-98.2%], 67.9% [95% CI: 41.7%-94.1%], 69.2% [53.5%-84.9%] for patients with ≥ 50%, 1-49%, <1% tumor cells expressing SSTR2, respectively; p=0.71 for <1% vs 1-100% SSTR2 expression; p=0.96 for ≥ 50% vs 1-49% SSTR2 expression).

Results of 68Ga-DOTATATE Scans and Correlation With Clinicopathologic Features and SSTR2 Expression

68Ga-DOTATATE PET scans were available in 9 patients. The results of the scans are presented in **Table 4**. Scans were available

TABLE 3 | Stage distribution of thymic epithelial tumors of the study population (N=53)[a].

Stage	Thymoma Type (N)	Thymic Carcinoma	Thymic Neuroendocrine Tumor
I	A (16) B3 (5) Micronodular thymoma with lymphoid stroma (3)	Squamous cell carcinoma (2) Adenocarcinoma (1)	Small cell carcinoma (1)
II		Squamous cell carcinoma (1)	
IIIA	Micronodular thymoma with lymphoid stroma (1)	Squamous cell carcinoma (3)	
IVA	B3 (1)	Squamous cell carcinoma (8) Adenocarcinoma (2)	Atypical carcinoid tumor (4)
IVB		Squamous cell carcinoma (1) Adenosquamous carcinoma (1) Lymphoepithelial carcinoma (1) Undifferentiated carcinoma (1)	Atypical carcinoid tumor (1)

[a]*Only includes patients with primary tumors and available staging.*

from 6 patients with TNET including 5 patients with atypical carcinoid tumor and 1 patient with small cell carcinoma. In addition, scans were available from 2 patients with squamous cell carcinoma and one patient with type B3 thymoma. In 3 patients the scan was performed at some time after resection of the primary tumor. Krenning score 3 was identified in cases of atypical carcinoid tumor, small cell carcinoma, and squamous cell carcinoma (N=1, each). The small cell carcinoma also showed strong expression of SSTR2 in 100% of the tumor cells (**Figure 1**), the atypical carcinoid tumor showed moderate SSTR2 expression in 95% of tumor cells and the squamous cell carcinoma exhibited strong SSTR2 expression in 5% of tumor cells. "Increased uptake" was reported in an additional squamous cell carcinoma which had 0% of tumor cell staining with SSTR2. However, that scan was not available for re-review. Krenning score 2 was identified in 2 atypical carcinoid tumors, score 1 in an atypical carcinoid tumor (**Figure 2**), and no uptake was seen in an atypical carcinoid tumor and the type B3 thymoma. Interestingly, while all tumors with scans showing Krenning scores 1 or 2 or no uptake had no expression of SSTR2, the atypical carcinoid tumor with no uptake on 68Ga-DOTATATE PET scan did show strong SSTR2 expression in 10% of the tumor cells. However, that scan was also not available for review.

All 3 patients with Krenning score 3 were treated with octreotide; none of the other patients received a somatostatin analogue treatment. One of these 3 patients who were treated with octreotide and had an atypical carcinoid tumor was metastasis and recurrence-free for 3.3 years after neoadjuvant chemotherapy, complete resection, adjuvant radiation, and adjuvant octreotide. Another patient was treated with octreotide when the thymic squamous cell carcinoma recurred. However, the patient was only treated for 3 months at which time a breast carcinoma was diagnosed and the treatment regimen was altered accordingly. Whether her disease progressed or regressed during those 3 months is unknown. The patient with small cell carcinoma was treated with octreotide for 3 months after bone metastases had developed; however, her disease progressed and therefore she underwent chemoradiation therapy 3 months later. All 3 patients were alive with disease at last follow up. None of the patients who did not undergo a 68Ga-DOTATATE PET scan were treated with octreotide.

Both lymphoepithelial carcinomas which were EBV-associated showed strong and diffuse expression of SSTR2. A poorly differentiated squamous cell carcinoma with marked tumor infiltrating lymphocytes, morphologically reminiscent of a lymphoepithelial carcinoma but without EBV association also showed expression of SSTR2 in 90% of tumor cells. These cases are detailed in **Table 4**. Results of DOTATATE PET scans are also detailed in **Table 4**.

DISCUSSION

Our study of 80 retrospectively collected TET including 33 thymic carcinomas and 7 TNETs revealed expression of SSTR2 in all thymic small cell carcinomas, lymphoepithelial carcinomas, and the single adenosquamous carcinoma, three-fourths of thymic squamous cell carcinomas, and 40% of atypical carcinoid tumors. Indeed, significantly more thymic carcinomas and TNETs expressed SSTR2 than thymomas. In slightly more than half of thymic carcinomas and TNETs SSTR2 was expressed in 50% or more tumor cells. In contrast, SSTR2 was only expressed in 15% of type A and B3 thymomas and micronodular thymomas with lymphoid stroma with expression in 5% or less of tumor cells. We also found that in all patients in whom a 68Ga-DOTATATE PET scan was available and the Krenning score was 3, the TET also expressed SSTR2 while in almost all cases of 68Ga-DOTATATE PET scan Krenning score 1 or 2 the tumor was negative for SSTR2 expression. Our results indicate that 68Ga-DOTATATE PET scan may serve as a screening tool for SSTR2 expression in TET although confirmation of SSTR2 expression in a resection specimen may reveal an occasional TET that is negative on 68Ga-DOTATATE PET scan. Our results suggest that at least a subset of thymic carcinomas and TNETs may be responsive to somatostatin analogue treatment or SSTR2 antibody-drug conjugates while type A and B3 thymomas and micronodular thymomas with lymphoid stroma are less likely to express SSTR2 and may not respond to such treatments.

Despite our findings of low SSTR2 expression in thymomas, literature has suggested that thymomas may show response to treatment with octreotide. For instance, in a study of 15 patients with unresectable or locally recurrent thymoma and 2 patients

TABLE 4 | Summary of patients with available DOTATATE scan.

Case	WHO Type	pTNM	% (Intensity) SSTR2-positive Tumor Cells	Krenning Score/ Description of Scan	Treatment with Octreotide/ somatostatin analogue	Treatment & Outcome
1	Squamous cell carcinoma	T3N1M0	0	Increased uptake	No	Incomplete resection, adjuvant radiation No recurrent disease Died 4 yrs after resection of unknown cause
2	Atypical carcinoid tumor	T3N1M0	10 (moderate)	No uptake	No	Complete resection of 3.2 cm tumor; adjuvant radiation First metastasis at 15 months after resection Metastases/recurrence to lymph nodes, bone, pleura, mediastinum, lung, brain DOD 3.5 years after resection
3	Atypical carcinoid tumor	T3N1M0	95 (moderate)	3	Yes	MEN1 syndrome Neoadjuvant chemotherapy Complete resection of 12.5 cm tumor, adjuvant radiation, octreotide acetate (Sandostatin) First metastasis 3.3 years after resection Metastasis to pleura AWD 11.2 years after resection
4	Atypical carcinoid tumor (**Figure 2**)	T3N1M0	0	1	No	Complete resection of 4.4 cm tumor; adjuvant radiation First metastases/recurrence 3.2 years after resection Metastases to hilar lymph nodes, lung, mediastinum AWD 5.2 years after resection
5	Atypical carcinoid tumor	T1N1M0	0	2	No	Complete resection of 3.7 cm tumor; adjuvant chemotherapy and steroids First metastasis 0.3 years after resection Metastasis to breast AWD 2.8 years after resection
6	WHO type B3 thymoma, recurrent	N/A	0	Performed 4 months after resection Negative	No	Resection of recurrence 6 years after initial incomplete resection, adjuvant chemoradiation Alive without disease 11.7 years after resection of primary tumor.
7	Squamous cell carcinoma	T3NXM1b	5 (strong)	Performed at time of recurrence/ metastasis 3	Yes	Neoadjuvant chemotherapy Complete resection of 5 cm tumor; metastases to lung and liver at time of initial diagnosis First metastasis at 1.4 years after resection Metastasis to lung 4.5 years after resection metastases to lymph nodes, pleura, pericardium, lung - at that time Ga68-DOTATATE scan; treatment with Octreotide for 3 months until diagnosed with breast carcinoma AWD 7.9 years after resection of primary tumor
8	Small cell carcinoma (**Figure 1**)	T1NXM0	100 (strong)	3 Multiple postoperative scans with scores 3 or 4	Yes	Complete resection of 2.7 cm tumor; adjuvant chemoradiation, First metastasis 1 year after resection Metastases to bone; treatment with octreotide (Sandostatin) for 3 months; follow up Ga68-DOTATATE showed progressive disease; chemoradiation AWD 1.6 years after resection of primary tumor
9	Atypical carcinoid tumor	T3N2M0	0	Multiple postoperative scans with score 2	No	Complete resection of 18.3 cm tumor; neoadjuvant & adjuvant chemotherapy & adjuvant radiation First metastasis/recurrence 0.8 years after resection Metastases to lung, pleura, mediastinal and abdominal lymph nodes AWD 0.9 years after resection of primary tumor

DOD, died of disease; AWD, alive with disease; N/A, not applicable.

with thymic carcinoma at Masaoka stage III who had a positive octreotide scan and who were treated with octreotide and prednisone, a treatment response was found in 15 (88%) patients with a median reduction of tumor volume of 51% after 12 weeks of treatment; subsequent complete surgical resection was achieved in 9 (52%) patients (30). No response was observed in one of the carcinomas and a single AB thymoma. However, it is not clear whether the observed response in that study was indeed due to octreotide, a combined effect of prednisone and octreotide or a prednisone-only effect as studies have shown that prednisone by itself may lead to reduction in tumor volume of thymomas (36). In a similar study of 16 patients with advanced thymoma (N=10), thymic carcinoma (N=3), and thymic small cell carcinoma (N=3) unresponsive to conventional chemotherapy and positive octreotide scan, treatment with octreotide and prednisone resulted in a response rate of 37% with 1 complete response, 5 partial responses and 6 stable diseases (31). In a third clinical trial

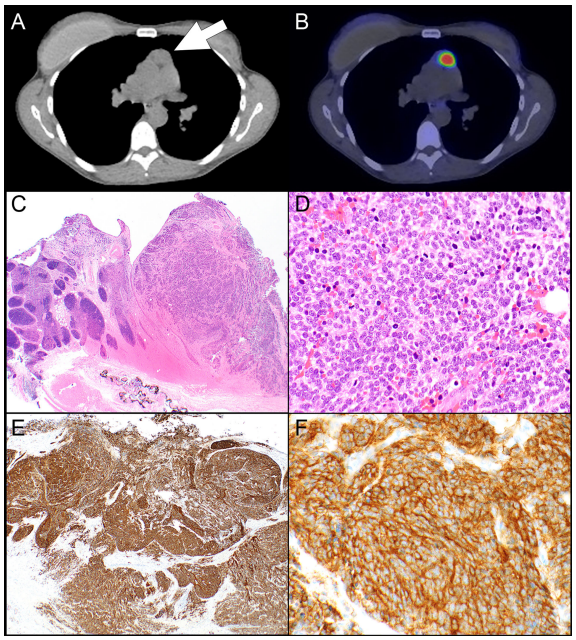

FIGURE 1 | Patient #8. **(A)** A computed tomography scan shows a prevascular mediastinal lesion (arrow) that takes up 68Ga on a DOTATATE PET scan which was interpreted as Krenning score 3 **(B)**. **(C)** The resection specimen shows sheets and nests of neoplastic cells (right side) in a background of thymic gland (left side). **(D)** The neoplastic cells are round with high nuclear-to-cytoplasmic ratio and high mitotic activity. The neoplastic cells are positive for keratin CAM5.2 (focal), synaptophysin, chromogranin (focal), and TTF-1 and negative for p63; Ki-67 shows a high proliferative index (stains not shown). **(E)** SSTR2 expression is diffuse and strong in virtually all tumor cells in a membranous and cytoplasmic expression pattern **(F)**. Magnification, H&E x 20 **(C)**, x 400 **(D)**, SSTR2 x 40 **(E)**, x 400 **(F)**.

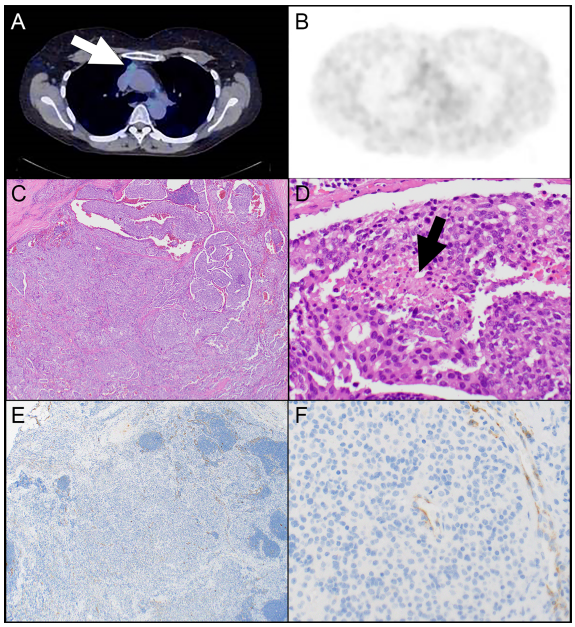

FIGURE 2 | Patient #4. **(A)** A computed tomography scan shows a prevascular mediastinal lesion (arrow) that shows 68Ga take up on a DOTATATE PET scan that is much lower than liver (interpreted as Krenning score 1) **(B)**. **(C)** A nested neoplasm is comprised of round to oval cells with a small amount of cytoplasm and associated with focal necrosis (**D**, arrow). **(E)** There is no expression of SSTR2 in tumor cells. **(F)** Note SSTR2 expression in endothelial cells serving as internal control. Magnification, H&E x 40 **(C)**, x 400 **(D)**, SSTR2 x 40 **(E)**, x 400 **(F)**.

including patients with invasive, recurrent, or metastatic thymoma (N=32), thymic carcinoma (N=5), and thymic carcinoid tumor (N=1) not amenable to curative therapy and positive octreotide scan, all patients were treated with octreotide for 2 cycles (32). Patients with complete or partial response would continue to be treated with octreotide, patients with stable disease received prednisone and octreotide and patients with progressive disease were removed from the study. Two (5.3%) patients had complete response and 10 (25%) had partial response with an overall response rate of 30.3%. Fourteen (36.8%) patients had stable disease. Of 38 patients treated with octreotide alone, only 4 (10.5%) had a partial response. In 21 patients in whom prednisone was added there were 2 complete and 6 partial responses. All responses occurred in patients with thymoma. While these studies did not investigate the expression of SSTR2 in the tumor tissue, conceivably thymomas did express SSTR2 given the positive octreotide scans and the response to octreotide treatment in a small subset of patients. However, since tissue was not examined for SSTR2 expression in these thymomas it remains unclear whether SSTR2 was expressed in thymocytes, tumor cells or both. That may be one of the reasons for the discrepancy with our findings as we only included thymomas that were rich in neoplastic cells and either lacked or contained very few thymocytes. Furthermore, because none of the studies disclosed how many patients had undergone octreotide scan before patients were selected for these trials the incidence of SSTR2 expression in thymomas could not be estimated.

Both of our lymphoepithelial carcinomas, which were associated with EBV, showed strong and diffuse expression of SSTR2. This finding is consistent with a recent study by Lechner et al. that showed that in EBV-driven nasopharyngeal carcinomas the expression of SSTR2 is induced by EBV latent membrane protein 1 *via* the NF-κB pathway (23). Indeed in that study 252 of 311 (81%) nasopharyngeal carcinomas expressed SSTR2 and SSTR2 expression was enriched in EBV-positive and in non-keratinizing nasopharyngeal carcinomas. Similarly, Viswanathan et al. in a study of primary, recurrent, and/or undifferentiated nasopharyngeal carcinomas, showed multifocal to diffuse strong SSTR2 expression in 90% of tumors including 8 of 9 EBV-associated and one EBV-negative nasopharyngeal carcinoma (37). While one HPV-positive sinonasal carcinoma also showed patchy SSTR2 staining, the remaining HPV-positive sinonasal carcinomas, HPV-positive oropharyngeal squamous cell carcinomas, or oral cavity head and neck squamous cell carcinomas did not reveal any significant SSTR2 staining. Similarly, SSTR2 expression and 68Ga-DOTATATE uptake

were observed in pulmonary lymphoepithelial carcinomas which also were associated with EBV (23, 38). However, not all carcinomas and TNETs that expressed SSTR2 in our and other studies were EBV-related and therefore other pathways for expression of SSTR2 must exist in these tumors. Interestingly, one of our study cases, a poorly differentiated thymic squamous cell carcinoma with marked lymphocytic tumor infiltrate at least suggestive of lymphoepithelial carcinoma but without EBV expression also showed strong and diffuse expression of SSTR2.

SSTR2 has been shown to be expressed in a subset of neuroendocrine tumors. A study by Popa et al. suggested that SSTR2 expression may be more common in low grade than in high grade neuroendocrine tumors (39). That study showed that 96% of G1, 71% of G2 and only 23% of G3 tumors expressed SSTR2. In addition, only 33% of neuroendocrine carcinomas were SSTR2 positive which was significantly lower than in well differentiated neuroendocrine tumors. We could not confirm that finding in TNETs as we found that only 40% of atypical carcinoid tumors expressed SSTR2 while 100% of small cell carcinomas expressed that marker. However, our overall number of TNETs was low which could have at least contributed to that discrepancy.

Evidence also suggests that SSTR2 expression may be more common in early than in late tumor stages in neuroendocrine tumors. In the study by Popa et al. of gastrointestinal neuroendocrine tumors, SSTR2 expression was 100% in tumors of early stage while only 56% of advanced stage tumors expressed SSTR2 (39). Interestingly, in our study SSTR2 expression was overall more commonly seen in advanced stage tumors (stages IIIA, IVA, IVB) than in stage I tumors although there was no statistically significant difference. However, that finding may have been biased by the case distribution as carcinomas and TNET were more commonly of high stage while thymomas were of low stage in our study. In addition, most of our cases were not neuroendocrine tumors in contrast to the study by Popa et al. Unfortunately, we were not able to compare the expression of SSTR2 between low and high stage for thymic carcinomas and TNETs separately due to the relative low number of cases.

In 9 of our cases 68Ga-DOTATATE PET scans were available. The results of the 68Ga-DOTATATE PET scans appeared to correlate with the expression of the SSTR2 protein by immunohistochemistry. Indeed in 2 patients with Krenning score of 3 tumors showed strong and diffuse SSTR2 expression. A third patient with a scan of Krenning score 3 had strong SSTR2 expression in 10% of tumor cells. In contrast, all cases with Krenning score 2 and lower had no SSTR2 expression in tumor cells except one atypical carcinoid tumor in which the scan reportedly did not show any uptake but the tissue showed moderate expression of SSTR2 in 10% of tumor cells. A potential reason for that apparent discrepancy may be that standard uptake value (SUV) per voxel is used to create a PET scan in 3D. SUV is a mathematical best estimate of how much radiotracer is in each voxel at a given point in time. In the case of a 68Ga-DOTATATE PET scan the point in time is 60 minutes after injection. SUV is not a direct measure of how many tumor cells express SSTR2. Nor is SUV a measure of how many copies of SSTR2 are expressed on a given cell. SUV is a measure of both and other factors as well. SUV is a measure of radiotracer per voxel, which is likely correlated to the amount of SSTR2 expressed on cells in a voxel. Therefore, if the tumor cells expressing SSTR2 are spread out in 3D space, perhaps due to dead cells, extracellular fibrosis or other structures in the voxel, the SUV will go down, and as such the Krenning score will go down. Our findings of the correlation between 68Ga-DOTATATE PET scan and SSTR2 expression in tissue are supported by the study by Lechner et al (23) of nasopharyngeal carcinomas. In that study the authors found a significant correlation between SSTR2 expression levels and uptake of 68Ga DOTATATE suggesting that this imaging modality may have potential as a noninvasive marker to monitor SSTR2 expression and as a target for SSTR2 receptor-targeted radionuclide therapy. This was also shown in an earlier study by Miederer et al. that evaluated a variety of neuroendocrine tumors of the gastrointestinal and pancreatobiliary tract, lung, thyroid, and thymoma and confirmed that the SUV of the 68Ga-DOTATATE scan correlated with the score of SSTR2 expression in the respective tissue (40). In a study of lung neuroendocrine tumors, SSTR2 expression in tissue correlated with octreotide scintigraphy in 71% of cases (41).

In our study, age was associated with SSTR2 expression in that patients with TET that expressed SSTR2 in at least 50% of the tumor cells were significantly younger than patients with TET that expressed SSTR2 in 1-49% of tumor cells. While this appears to be a new finding it may, at least in part, be because patients with thymic carcinomas and TNETs were younger than patients with thymoma and SSTR2 was more commonly expressed in thymic carcinomas and TNETs than in thymomas. A multivariate analysis could not be performed given the relative low number of patients.

Our study has several limitations. Although this is one of the largest case series of TET, the overall number of patients who had a 68Ga-DOTATATE PET scan available was relatively small. Furthermore, a comparison group of patients with TET treated with octreotide despite a negative 68Ga-DOTATATE PET scan was not available. Given the low number of cases survival analysis was limited. Also, because of the paucity of TET, patients included in this study were recruited between 1969 and 2021, a relatively long time span during which treatment regimens may have changed. Furthermore, while antigen expression is in general relatively stable in formalin-fixed paraffin-embedded tissue, various fixatives used over time and some degradation are possibilities and could potentially account for lower or lack of expression of SSTR2 in some tumors.

CONCLUSIONS

SSTR2 expression in TET, specifically lymphoepithelial carcinomas, squamous cell carcinomas, atypical carcinoid tumors, and small cell carcinomas may be a biomarker to

identify patients who may respond to octreotide therapy. G68-DOTATATE PET scan may be useful to predict expression of SSTR2 in tissue; however, it cannot predict whether SSTR2 is expressed in tumor cells or other cells such as inflammatory cells. Larger, ideally multi-institutional studies are necessary to independently and prospectively validate our results and to correlate SSTR2 expression in TETs and/or 68Ga-DOTATATE PET scans with response to octreotide therapy.

DATA AVAILABILITY STATEMENT

The original contributions presented in the study are included in the article. Further inquiries can be directed to the corresponding author.

ETHICS STATEMENT

The studies involving human participants were reviewed and approved by Mayo Clinic Rochester Institutional Review Board. Written informed consent for participation was not required for this study in accordance with the national legislation and the institutional requirements.

AUTHOR CONTRIBUTIONS

AR, GJ, and AM contributed to the conception and design of the study. AR and SR collected patient information. AR reviewed histologic sections of all cases. GJ reviewed the DOTATATE scans. SJ performed the statistical analysis. AR wrote the first draft of the manuscript. All authors contributed to manuscript revision, read, and approved the submitted version.

FUNDING

Mayo Clinic receives funding from Novartis to support research performed by GJ. The funder was not involved in the study design, collection, analysis, interpretation of data, the writing of this article or the decision to submit it for publication.

REFERENCES

1. Roden AC, Fang W, Shen Y, Carter BW, White DB, Jenkins SM, et al. Distribution of Mediastinal Lesions Across Multi-Institutional, International, Radiology Databases. *J Thorac Oncol* (2020) 15:568–79. doi: 10.1016/j.jtho.2019.12.108
2. Roden AC, Yi ES, Cassivi SD, Jenkins SM, Garces YI, Aubry MC. Clinicopathological Features of Thymic Carcinomas and the Impact of Histopathological Agreement on Prognostical Studies. *Eur J Cardiothorac Surg* (2013) 43:1131–9. doi: 10.1093/ejcts/ezs529
3. Hishida T, Nomura S, Yano M, Asamura H, Yamashita M, Ohde Y, et al. Long-Term Outcome and Prognostic Factors of Surgically Treated Thymic Carcinoma: Results of 306 Cases From a Japanese Nationwide Database Study. *Eur J Cardiothorac Surg* (2016) 49:835–41. doi: 10.1093/ejcts/ezv239
4. Zhao Y, Gu H, Fan L, Han K, Yang J, Zhao H. Comparison of Clinical Features and Survival Between Thymic Carcinoma and Thymic Carcinoid Patients. *Eur J Cardiothorac Surg* (2017) 52:33–8. doi: 10.1093/ejcts/ezx037
5. Sakane T, Murase T, Okuda K, Saida K, Masaki A, Yamada T, et al. A Mutation Analysis of the EGFR Pathway Genes, RAS, EGFR, PIK3CA, AKT1 and BRAF, and TP53 Gene in Thymic Carcinoma and Thymoma Type a/B3. *Histopathology* (2019) 75:755–66. doi: 10.1111/his.13936
6. Bakhos CT, Salami AC, Kaiser LR, Petrov RV, Abbas AE. Thymic Neuroendocrine Tumors and Thymic Carcinoma: Demographics, Treatment, and Survival. *Innovations (Phila)* (2020) 15:468–74. doi: 10.1177/1556984520949287
7. Bohnenberger H, Strobel P. Recent Advances and Conceptual Changes in the Classification of Neuroendocrine Tumors of the Thymus. *Virchows Arch* (2021) 478:129–35. doi: 10.1007/s00428-021-03037-1
8. Radovich M, Pickering CR, Felau I, Ha G, Zhang H, Jo H, et al. The Integrated Genomic Landscape of Thymic Epithelial Tumors. *Cancer Cell* (2018) 33:244–58. doi: 10.1016/j.ccell.2018.01.003
9. Giaccone G, Kim C, Thompson J, McGuire C, Kallakury B, Chahine JJ, et al. Pembrolizumab in Patients With Thymic Carcinoma: A Single-Arm, Single-Centre, Phase 2 Study. *Lancet Oncol* (2018) 19:347–55. doi: 10.1016/S1470-2045(18)30062-7
10. Petrini I, Meltzer PS, Kim IK, Lucchi M, Park KS, Fontanini G, et al. A Specific Missense Mutation in GTF2I Occurs at High Frequency in Thymic Epithelial Tumors. *Nat Genet* (2014) 46:844–9. doi: 10.1038/ng.3016
11. Nathany S, Tripathi R, Mehta A. Gene of the Month: GTF2I. *J Clin Pathol* (2021) 74:1–4. doi: 10.1136/jclinpath-2020-207013
12. Tiseo M, Damato A, Longo L, Barbieri F, Bertolini F, Stefani A, et al. Analysis of a Panel of Druggable Gene Mutations and of ALK and PD-L1 Expression in a Series of Thymic Epithelial Tumors (TETs). *Lung Cancer* (2017) 104:24–30. doi: 10.1016/j.lungcan.2016.12.005
13. Schirosi L, Nannini N, Nicoli D, Cavazza A, Valli R, Buti S, et al. Activating C-KIT Mutations in a Subset of Thymic Carcinoma and Response to Different C-KIT Inhibitors. *Ann Oncol* (2012) 23:2409–14. doi: 10.1093/annonc/mdr626
14. Simonelli M, Zucali PA, Suter MB, Lorenzi E, Rubino L, Fatuzzo G, et al. Targeted Therapy for Thymic Epithelial Tumors: A New Horizon? Review of the Literature and Two Cases Reports. *Future Oncol* (2015) 11:1223–32. doi: 10.2217/fon.14.318
15. Aesif SW, Aubry MC, Yi ES, Kloft-Nelson SM, Jenkins SM, Spears GM, et al. Loss of P16ink4a Expression and Homozygous CDKN2A Deletion Are Associated With Worse Outcome and Younger Age in Thymic Carcinomas. *J Thorac Oncol* (2017) 12:860–71. doi: 10.1016/j.jtho.2017.01.028
16. Enkner F, Pichlhofer B, Zaharie AT, Krunic M, Holper TM, Janik S, et al. Molecular Profiling of Thymoma and Thymic Carcinoma: Genetic Differences and Potential Novel Therapeutic Targets. *Pathol Oncol Res* (2017) 23:551–64. doi: 10.1007/s12253-016-0144-8
17. Katsuya Y, Fujita Y, Horinouchi H, Ohe Y, Watanabe S, Tsuta K. Immunohistochemical Status of PD-L1 in Thymoma and Thymic Carcinoma. *Lung Cancer* (2015) 88:154–9. doi: 10.1016/j.lungcan.2015.03.003
18. Yokoyama S, Miyoshi H, Nishi T, Hashiguchi T, Mitsuoka M, Takamori S, et al. Clinicopathologic and Prognostic Implications of Programmed Death Ligand 1 Expression in Thymoma. *Ann Thorac Surg* (2016) 101:1361–9. doi: 10.1016/j.athoracsur.2015.10.044
19. Terra S, Mansfield AS, Vrana JA, Roden AC. Heterogeneity of Programmed Death-Ligand 1 Expression in Thymic Epithelial Tumours Between Initial Specimen and Synchronous or Metachronous Metastases or Recurrences. *Histopathology* (2019) 74:364–7. doi: 10.1111/his.13750
20. Sakane T, Murase T, Okuda K, Takino H, Masaki A, Oda R, et al. A Comparative Study of PD-L1 Immunohistochemical Assays With Four Reliable Antibodies in Thymic Carcinoma. *Oncotarget* (2018) 9:6993–7009. doi: 10.18632/oncotarget.24075
21. Lehman JM, Hoeksema MD, Staub J, Qian J, Harris B, Callison JC, et al. Somatostatin Receptor 2 Signaling Promotes Growth and Tumor Survival in Small-Cell Lung Cancer. *Int J Cancer* (2019) 144:1104–14. doi: 10.1002/ijc.31771

22. Lehman JM. Amassion PP: Somatostatin Receptor 2 Targeting in Small Cell Lung Carcinoma: Perspectives. *Oncotarget* (2019) 10:4727–30. doi: 10.18632/oncotarget.27107
23. Lechner M, Schartinger VH, Steele CD, Nei WL, Ooft ML, Schreiber LM, et al. Somatostatin Receptor 2 Expression in Nasopharyngeal Cancer is Induced by Epstein Barr Virus Infection: Impact on Prognosis, Imaging and Therapy. *Nat Commun* (2021) 12:117. doi: 10.1038/s41467-020-20308-8
24. Janssen I, Chen CC, Taieb D, Patronas NJ, Millo CM, Adams KT, et al. 68ga-DOTATATE PET/CT in the Localization of Head and Neck Paragangliomas Compared With Other Functional Imaging Modalities and CT/MRI. *J Nucl Med* (2016) 57:186–91. doi: 10.2967/jnumed.115.161018
25. Ivanidze J, Roytman M, Sasson A, Skafida M, Fahey TJ 3rd, Osborne JR, et al. Molecular Imaging and Therapy of Somatostatin Receptor Positive Tumors. *Clin Imaging* (2019) 56:146–54. doi: 10.1016/j.clinimag.2019.04.006
26. Boettcher AN. Somatostatin Receptor Type 2 as an Imaging and Treatment Target for Thyroid Cancer. *Radiol Imaging Cancer* (2021) 3:e219009. doi: 10.1148/rycan.2021219009
27. Stueven AK, Kayser A, Wetz C, Amthauer H, Wree A, Tacke F, et al. Somatostatin Analogues in the Treatment of Neuroendocrine Tumors: Past, Present and Future. *Int J Mol Sci* (2019) 20. doi: 10.3390/ijms20123049
28. Thakur S, Daley B, Millo C, Cochran C, Jacobson O, Lu H, et al. (177)Lu-DOTA-EB-TATE, a Radiolabeled Analogue of Somatostatin Receptor Type 2, for the Imaging and Treatment of Thyroid Cancer. *Clin Cancer Res* (2021) 27:1399–409. doi: 10.1158/1078-0432.CCR-20-3453
29. Caplin ME, Pavel M, Ruszniewski P. Lanreotide in Metastatic Enteropancreatic Neuroendocrine Tumors. *N Engl J Med* (2014) 371:1556–7. doi: 10.1056/NEJMoa1316158
30. Kirzinger L, Boy S, Marienhagen J, Schuierer G, Neu R, Ried M, et al. Octreotide LAR and Prednisone as Neoadjuvant Treatment in Patients With Primary or Locally Recurrent Unresectable Thymic Tumors: A Phase II Study. *PloS One* (2016) 11:e0168215. doi: 10.1371/journal.pone.0168215
31. Palmieri G, Montella L, Martignetti A, Muto P, Di Vizio D, De Chiara A, et al. Somatostatin Analogs and Prednisone in Advanced Refractory Thymic Tumors. *Cancer* (2002) 94:1414–20. doi: 10.1002/cncr.10374
32. Loehrer PJSr., Wang W, Johnson DH, Aisner SC, Ettinger DS. Octreotide Alone or With Prednisone in Patients With Advanced Thymoma and Thymic Carcinoma: An Eastern Cooperative Oncology Group Phase II Trial. *J Clin Oncol* (2004) 22:293–9. doi: 10.1200/JCO.2004.02.047
33. Thoracic Tumours. *WHO Classification of Tumours 5ed*. Lyon, France: International Agency for Research on Cancer (2021).
34. Amin MBAmerican Joint Committee on Cancer and American Cancer Society. *AJCC Cancer Staging Manual*. BA Mahul, SB Edge, DM Gress, LR Meyer, editors. Chicago IL: American Joint Committee on Cancer, Springer (2017).
35. Volante M, Brizzi MP, Faggiano A, La Rosa S, Rapa I, Ferrero A, et al. Somatostatin Receptor Type 2a Immunohistochemistry in Neuroendocrine Tumors: A Proposal of Scoring System Correlated With Somatostatin Receptor Scintigraphy. *Mod Pathol* (2007) 20:1172–82. doi: 10.1038/modpathol.3800954
36. Hu E, Levine J. Chemotherapy of Malignant Thymoma. Case Report and Review of the Literature. *Cancer* (1986) 57:1101–4. doi: 10.1002/1097-0142(19860315)57:6<1101::AID-CNCR2820570606>3.0.CO;2-A
37. Viswanathan K, Sadow PM. Somatostatin Receptor 2 is Highly Sensitive and Specific for Epstein-Barr Virus-Associated Nasopharyngeal Carcinoma. *Hum Pathol* (2021) 117:88–100. doi: 10.1016/j.humpath.2021.08.004
38. Shang Q, Pang Y, Meng T, Hao B, Chen H. 68ga-DOTATATE PET/CT in Primary Pulmonary Lymphoepithelioma-Like Carcinoma. *Clin Nucl Med* (2021). doi: 10.1097/RLU.0000000000003857
39. Popa O, Taban SM, Pantea S, Plopeanu AD, Barna RA, Cornianu M, et al. The New WHO Classification of Gastrointestinal Neuroendocrine Tumors and Immunohistochemical Expression of Somatostatin Receptor 2 and 5. *Exp Ther Med* (2021) 22:1179. doi: 10.3892/etm.2021.10613
40. Miederer M, Seidl S, Buck A, Scheidhauer K, Wester HJ, Schwaiger M, et al. Correlation of Immunohistopathological Expression of Somatostatin Receptor 2 With Standardised Uptake Values in 68Ga-DOTATOC PET/Ct. *Eur J Nucl Med Mol Imaging* (2009) 36:48–52. doi: 10.1007/s00259-008-0944-5
41. Righi L, Volante M, Tavaglione V, Bille A, Daniele L, Angusti T, et al. Somatostatin Receptor Tissue Distribution in Lung Neuroendocrine Tumours: A Clinicopathologic and Immunohistochemical Study of 218 'Clinically Aggressive' Cases. *Ann Oncol* (2010) 21:548–55. doi: 10.1093/annonc/mdp334

Conflict of Interest: AM reports research support from the NIH, DoD, Mark Foundation, Novartis and Verily; remuneration to his institution for participation on advisory boards for AbbVie, Astra Zeneca, BeiGene, BMS, Genentech and Janssen; travel support and payment from Shanghai Roche Pharmaceuticals Ltd.; and is a nonremunerated director of the Mesothelioma Applied Research Foundation. GJ reports that Mayo Clinic receives research funding from Novartis to support his work and that he is on the Advisory Board, Novartis.

The remaining authors declare that the research was conducted in the absence of any commercial or financial relationships that could be construed as a potential conflict of interest.

Publisher's Note: All claims expressed in this article are solely those of the authors and do not necessarily represent those of their affiliated organizations, or those of the publisher, the editors and the reviewers. Any product that may be evaluated in this article, or claim that may be made by its manufacturer, is not guaranteed or endorsed by the publisher.

Copyright © 2022 Roden, Rakshit, Johnson, Jenkins and Mansfield. This is an open-access article distributed under the terms of the Creative Commons Attribution License (CC BY). The use, distribution or reproduction in other forums is permitted, provided the original author(s) and the copyright owner(s) are credited and that the original publication in this journal is cited, in accordance with accepted academic practice. No use, distribution or reproduction is permitted which does not comply with these terms.

frontiers in Surgery

ORIGINAL RESEARCH
published: 18 February 2022
doi: 10.3389/fsurg.2022.726673

Pathological Features and Prognosis of Thymoma With or Without Myasthenia Gravis

Yunfeng Zhang, Lei Yu and Ji Ke*

Department of Thoracic Surgery, Beijing Tongren Hospital, Capital Medical University, Beijing, China

Introduction: To evaluate the different pathological and clinical characters of thymoma with and without myasthenia gravis (MG) and to determine whether the presence of MG influences the prognosis in patients with thymoma.

Methods: Four hundred and twenty-five consecutive patients operated was analyzed. A median sternotomy was used in 189 cases, and video-assisted thoracoscopic thymectomy was used in 236 cases. These patients with thymoma were subdivided into two groups: thymoma with myasthenia gravis MG ($n = 220$) and thymoma without MG ($n = 205$). All thymic epithelial tumors were classified according to the WHO histologic classification and the Masaoka clinical staging system. The result was evaluated according to the Myasthenia Gravis Foundation of America's criterion. The clinical features of the 2 test were compared between the two groups, and the survival analysis of Cox treatment effects was compared between the two groups.

Results: There were no perioperative deaths. The proportions of type A and thymic carcinoma were 0% in the group with MG and 10.7% (22/205) and 11.2% (23/205), respectively, in the group without MG. Thymic hyperplasia around the thymoma was 29.1% (64/220) in patients with MG and only 6.3% (13/205) in patients without MG ($\chi^2 = 23.63$, $P = 0.000$). The overall survival curve showed that the 5- and 10-year survival rates in the group without MG were 89.2 and 77.4%, respectively, while those in the MG group were 91.1 and 80.5%.

Conclusions: The existence of MG has little influence on the prognosis of thymomas, but it is suitable for early diagnosis and treatment. Extended thymectomy should be performed on all patients with thymoma, whether they have MG or not.

Keywords: thymoma, myasthenia gravis, prognosis, surgical options, pathological features

OPEN ACCESS

Edited by:
Hasan Fevzi Batirel, Marmara University, Turkey

Reviewed by:
Carmelina Cristina Zirafa, University Hospital of Pisa, Italy
Alper Toker, West Virginia University, United States

****Correspondence:***
Yunfeng Zhang
zhangyf_2021@21cn.com

Specialty section:
This article was submitted to Thoracic Surgery, a section of the journal Frontiers in Surgery

Received: *24 June 2021*
Accepted: *20 January 2022*
Published: *18 February 2022*

Citation:
Zhang Y, Yu L and Ke J (2022) Pathological Features and Prognosis of Thymoma With or Without Myasthenia Gravis. Front. Surg. 9:726673. doi: 10.3389/fsurg.2022.726673

INTRODUCTION

Thymoma is often accompanied by paraneoplastic syndromes, such as hyperthyroidism, pure erythrocyte aplasia anemia, MG, and endocrinopathy. MG is the most common of these. Domestic and foreign data show that the proportion of MG combined with thymoma is 11.2–29.8%, while the proportion of thymoma combined with MG is 14.9–60.3%. There are differences in clinicopathological characters between thymoma combined with MG and thymoma alone. Academic circles have had disagreements about their outcome (1, 2). We retrospectively analyzed 425 patients with thymoma who underwent surgery in our hospital from January 2003 to December 2010 and discussed their clinical characteristics.

MATERIALS AND METHODS

Study Subjects

From January 2003 to December 2010, 425 cases of thymoma were treated by thoracic surgery in Beijing Tongren Hospital, including 198 males and 227 females, aged 23 to 80, with a median age of 53. The course of disease ranged from 18 days to 4.5 years, with a median course of 9 months. Based on whether myasthenia gravis was combined, 220 patients were divided into a myasthenia gravis thymoma group (thymoma with MG group), and 205 patients were divided into a thymoma without MG group. The specific conditions of the two groups are shown in **Table 1**. Anti-acetylcholine receptor antibodies were positive in 141 patients (64.1%) in the MG group. The MG group was divided into 74 cases of type I, 43 cases of type IIa, 47 cases of type IIb, 24 cases of type IIIa, 25 cases of type IIIb, four cases of type IVa and three cases of type IVb according to the clinical classification of the American Myasthenia Gravis Foundation of America (MGFA) (3, 4). In the pre-operative MG group, 185 patients (84.1%) were treated with bromo-pyridostigmine, and 89 patients (40.5%) were treated with glucocorticoids.

Research Methods

Surgical approach: 189 patients underwent median sternotomy (5). Double-lumen endotracheal intubation was used for the operation. The patient was placed in the supine position, and a median incision was made from the upper sternal notch to the xiphoid process. The sternum was split longitudinally from bottom to top along the median line with an electric saw, and distracted by a sternal retractor to expose the mediastinal area. The bilateral phrenic nerves were clearly distinguished, the mediastinal pleura was opened, and the right inferior pole of the thymus was freed upward to the confluence of the right internal mammary vein into the superior vena cava. The right upper pole was completely removed at the angle between the superior vena cava and the intramammary vessels. The innominate vein was carefully dissected, the thymus nourishing vessel was found, and the proximal end was clipped with a titanium clip and cut off with a supersonic knife. The left lobe of the thymus was treated with the same method. The thymus and thymic tumors were completely excised, and the fat of each group of the anterior mediastinum was removed. Partial pericardiectomy or pulmonary wedge resection is necessary for tumors invading pericardium and lung tissue (see **Figure 1**).

Another 236 patients underwent enlarged thymectomy and thymoma resection by thoracoscopy (6). All patients in the thoracoscopic surgery group underwent a unilateral thoracic approach. General anesthesia/double-lumen intubation was used for the operation. The left or right approach was decided according to the location of the thymic tumor. In the right approach, the patient was placed in the left lateral decubitus position. Under the guidance of thoracoscopy after lung collapse, 1.5 cm incisions were made at the 2nd intercostal space and the 4th intercostal space of the ipsilateral axillary anterior line, respectively, as the operation hole. The mediastinal pleura was opened and the thymus was completely free from the sternal surface. The right upper pole was completely removed at the angle between the superior vena cava and internal mammary vessels. The innominate vein was carefully dissected, the thymus nourishing vessel was found, and the proximal end was clipped with a titanium clip and cut off with a supersonic knife. The left lobe of the thymus was treated in the same way. The thymus was completely excised, and the fat in each group of the anterior mediastinum was removed. Fat removal at the base of the neck was performed through a 2–3 cm transverse incision at the neck to remove fat from the pretracheal fascia (see **Table 1** for details). Extended thymectomy refers to the removal of adipose tissue and ectopic thymus in the cervical root and anterior mediastinum groups in addition to complete thymectomy (3). Unresected cases included partial tumor resection and simple biopsy.

Tumor classification, staging and treatment: All thymic tumors were classified and staged according to WHO (2004 Edition) tissue classification (7) and modified Masaoka clinical stage (8). Type A and stage I thymoma need no adjuvant treatment except an operation. Patients with type AB, B1, or stage II and III thymomas were treated with mediastinal radiotherapy. Radiotherapy and chemotherapy were started 1 month after operations for stage IV thymoma and thymic cancer. The curative effect for patients with MG was evaluated according to MGFA standards (4).

Follow-Up Method

Follow-up was completed by telephone, letter, email, and outpatient service. The follow-up time was 3, 6 months, 1, 2, 3, 5, and 10 years after the operation. The follow-up period was 7–12 years, with an average of 9.5 years. The follow-up included checking current symptoms, medication, imaging data, and blood examination.

Statistical Methods

SPSS 19.0 software was used to analyze the data. The measurement data of normal distribution was expressed with, and the comparison between groups was conducted by *t*-tests. The measurement data of non-normal distribution was expressed by M (QR), and the comparison between groups was conducted by rank–sum test. The count data were expressed by frequency and percentage, and the comparison between groups was conducted by Chi-square tests. The survival curve was compared by Cox survival analysis. The difference was statistically significant ($P < 0.05$).

RESULTS

Surgical Results

There was no intraoperative death in any patients. Among 32 patients with unresectable thymoma (12 with MG, 20 without MG), 11 patients with thymoma invading superior vena cava or pulmonary vessels, and 21 patients with pleural and pericardial metastasis. In 393 cases, the thymus and tumor were completely removed. There were 47 cases (12.0%) of thymoma invaded pericardium, 35 cases (8.9%) of lung adhesion, and 29 cases (7.4%) of left innominate vein invaded. There was no difference in patients' ICU and hospital stays between the two groups. In 75 cases (19.1%), patients had post-operative complications,

TABLE 1 | Comparison of clinicopathological features between thymoma patients with and without myasthenia gravis.

Group	Number of cases	Male/female	Age			Masaoka clinical stage (number)				Sternotomy	Thoracoscopic surgery
			>60	41~60	≤40	I	II	III	IV		
Thymoma with MG	220	98/122	56	126	38	74	90	49	7	99	121
Thymoma without MG	205	100/105	48	133	24	58	76	55	16	112	93
Chi-square value	-	1.289	1.522	1.494	1.427	2.133	1.663	1.473	1.637	1.433	1.622
P-value	-	0.621	0.389	0.474	0.376	0.372	0.528	0.445	0.531	0.421	0.489

Group	Combined hyperthyroidism	WHO Pathological Classification						Histopathology of thymus around tumor			Unresected cases
		TypeA	AB	B1	B2	B3	Thymic carcinoma	Thymic atrophy	Thymic hyperplasia	microscopic thymoma	
Thymoma with MG	52	0	49	58	67	46	0	137	64	7	12
Thymoma without MG	9	22	31	43	53	33	23	171	13	1	20
Chi-square value	12.310	16.225	3.551	2.405	1.956	1.623	18.142	—	23.630	—	4.325
P-value	0.000	0.000	0.059	0.120	0.161	0.202	0.000	—	0.000	—	0.028

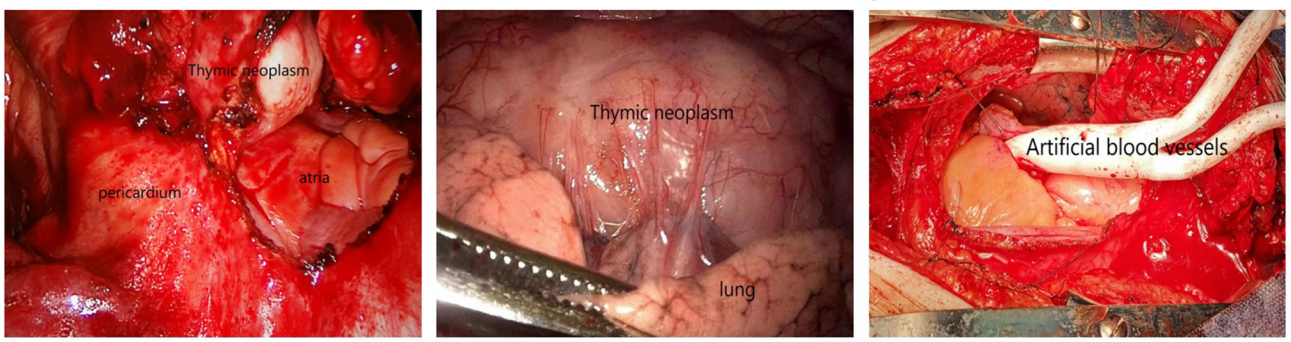

FIGURE 1 | (A) Tumor invasion of pericardium; **(B)** Tumor invasion of lung tissue; **(C)** The tumor invaded the innominate and superior vena cava, and the tumor was resected followed by artificial vascular replacement.

including 43 patients with MG who experienced myasthenic crisis, and 19 cases of pneumonia, six cases of pulmonary embolism, and seven cases of sternal incision infection (see **Table 2**).

Pathological Examination Results

The proportion of type A thymoma and thymic carcinoma in the combined group was 0%, while that in the thymoma without MG group was 10.7 and 11.2%, respectively. The results of pathological examination of thymus tissue around the tumor showed that the proportion of thymus hyperplasia was 29.1% (64/220) in the MG group and 6.3% (13/205) in the group without MG ($\chi^2 = 23.63$, $P = 0.000$). In the MG group, a small thymoma was found in seven cases around the tumor, with a maximum diameter of 2–5 mm.

Masaoka clinical staging results: in the MG group, stage III and IV thymoma accounted for 25.5% (56/220). In the group without MG, stage III and IV accounted for 34.6% (71/205) ($\chi^2 = 1.785$, $P = 0.163$).

TABLE 2 | Surgical results and complications data.

	Thymoma with MG ($n = 220$)	Thymoma without MG ($n = 205$)	*P*-value
Unresectable thymoma	12	20	0.028
Operation time (min)	112.35 ± 20.46	115.29 ± 23.75	0.171
Intensive care unit length of stay (d)	6 ± 1.5	7 ± 2.5	6.943
hospital length of stay (d)	9 ± 2.5	11 ± 3.0	4.188
Complications			
Myasthenic crisis	36	7	0.000
Pneumonia	11	8	0.584
Pulmonary embolism	3	3	0.931
Sternal incision infection	4	3	0.774

TABLE 3 | Analysis of histological and clinical types of thymomas in patients without MG.

Without MG (205)	A (22)	AB (31)	B1 (43)	B2 (53)	B3 (33)	C (23)
I (58)	16 (72.73%)	15 (48.39%)	13 (30.23%)	8 (15.09%)	6 (18.18%)	0
II (76)	6 (27.27%)	14 (45.16%)	21 (48.84%)	27 (50.94%)	8 (24.24%)	0
III (55)	0	2 (6.45%)	7 (16.28%)	13 (24.53%)	16 (48.48%)	17 (73.91%)
IV (16)	0	0	2 (4.65%)	5 (9.43%)	3 (9.09%)	6 (26.09%)
				13 + 5 (33.96%)	16 + 3(57.58%)	100%

Follow-Up Results

There were 50 patients lost to follow-up. Among 375 patients who were followed up, 208 cases were in the MG group and 167 cases in the group without MG. The overall survival curve showed that the 5- and 10-year survival rates in the group without MG were 89.2 and 77.4%, respectively, while those in the MG group were 91.1 and 80.5%. Eight patients died of non-thymoma related diseases (four of heart disease, two of kidney disease, and two of cerebral vascular disease). Within 5 years of the operation, 17 patients in the MG group died. Of these, 10 died of myasthenic crisis (three patients died of myasthenic crisis during radiotherapy, and seven patients died of recurrence and metastasis of thymoma). In the group without MG, 12 patients died. Of these, nine died from stage III or IV thymoma or thymic carcinoma.

In the MG group, the complete remission (CR) rate of myasthenia gravis was 21.6% (45/208) in the second year after the operation. The CR was increased to 31.3% (65/208) in the fifth year after the operation. In the second year after the operation, the effective rate was 75.9% (158/208), with no change in MG in 41 cases and aggravation in nine cases.

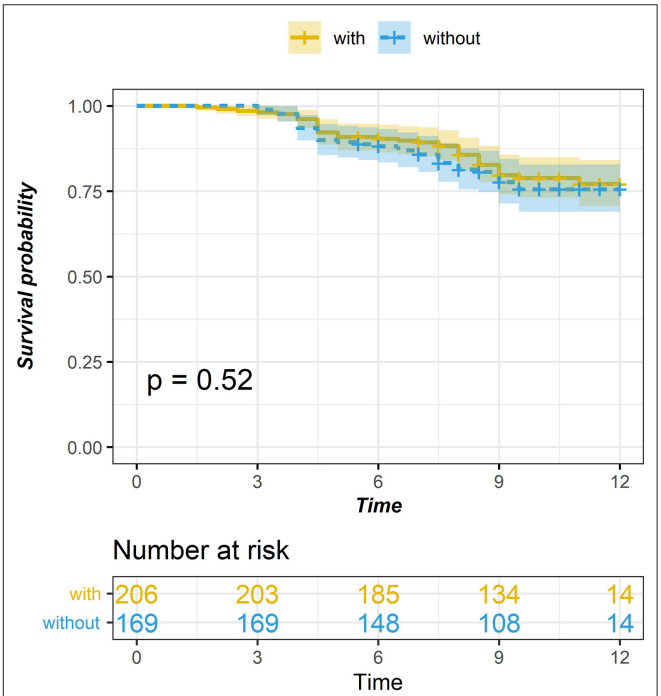

FIGURE 2 | Comparison of survival curve between thymic tumor and thymoma with myasthenia gravis ($P = 0.784$).

Correlation Between Histological Type, Clinical Stage, and Prognosis

No recurrence was found in patients with type A thymoma. Among the 183 cases with complete resection, 22 cases (10.5%) relapsed in the MG group and 20 cases (12.1%) relapsed in the group without MG. There was no significant difference between the two groups ($\chi^2 = 0.256$, $P = 0.637$). According to the analysis of thymomas in the group without MG, the proportion of stage III and IV increased with the increase of the malignant degree of thymic tumors, which was 33.96% for type B2, 57.58% for type B3 and 100% for type C (see **Table 3**). Tumor stage directly determines the survival and prognosis of patients. The 5- and 10-year survival rates of stage III and IV thymoma patients without MG were 86.23 and 68.41%, respectively, which were significantly lower than 98.56 and 89.48% of stage I and II patients ($P = 0.023$).

Through the study of the survival curves of the two groups, it is found that although the follow-up data after 5 years show that the survival time of thymoma patients without MG is slightly lower than that of thymoma patients in MG group, there is no significant difference in the long-term survival rate between the two groups, and the existence of myasthenia has no significant impact on the prognosis of thymoma patients (see **Figure 2**).

DISCUSSION

The impact of MG on the prognosis of thymoma has been the focus of debate in academia for some time. Academia has considered MG as an unfavorable prognostic factor of thymoma, which increased perioperative and post-operative mortality by inducing myasthenic crisis, and other issues. Moreover, the tumor classification has a certain impact on the occurrence of perioperative myasthenic crisis. The incidence of perioperative myasthenic crisis in type A thymoma is lower, while the incidence of type AB and B is higher (9–11). However, in recent years, some scholars believe that the occurrence of MG is conducive to early diagnosis, a high success rate of surgical resection, and a good prognosis (2, 3, 9). We retrospectively analyzed 425 thymoma patients who underwent surgery in our hospital from January 2003 to December 2010, and this should be one of the longest follow ups in the literature. The results of our study showed that the 5-year survival rate of the MG group was slightly lower than

that of the group without MG, and the 10-year survival rate and tumor recurrence rate were similar. In the MG group, 10 cases died due to myasthenia crisis, which were the aggravation of new myasthenia or the progression of original myasthenia symptoms, most of which were caused by tumor recurrence. From this, it can be seen that the long-term prognosis of thymoma patients with myasthenia was poor and the mortality was relatively high. After analysis, it was believed that the patients with myasthenia gravis were diagnosed in our hospital mostly because of the ptosis of the upper eyelids, while the patients in the group without MG were mostly treated after the occurrence of local compression or invasive symptoms (such as chest pain, cough, and even dyspnea). The patients in stage III and IV of the thymoma group without MG accounted for 34.6%, which was higher than that in the group with MG (25.5%). The number of unresected cases was also higher. We believe that thymoma combined with MG has little effect on its long-term efficacy. However, for some patients with symptoms of MG first diagnosed with thymic tumors, the tumors are at a relatively early stage, greatly improving the resection rate of tumors. The prognosis is also ideal.

In addition to the complete resection of thymic tumors, we advocate enlarged thymectomy, i.e., complete resection of thymus and removal of fat and ectopic thymus in the cervical root and anterior mediastinum groups, whether through a median sternotomy or thoracoscopic surgery (11). We believe that myasthenia gravis is not entirely thymoma-induced, and 29.1% of patients in the MG group had hyperplasia of thymic tissue around the thymoma, compared with only 6.3% in the group without MG. In some patients, the proliferation of thymic tissue around the tumor may be the real cause of MG. In addition to the presence of microthymoma in the ectopic thymus (12), thymoma resection alone or thymectomy is not conducive to the treatment of MG. In some cases, new MG occurs post-operatively (13) and may even induce myasthenic crisis post-operatively. Therefore, whether combined with MG or not, enlarged thymectomy should be the standard surgical approach for thymoma treatment.

In addition, complete thymectomy is important for long-term outcomes in patients with thymoma (14–16). Nine of the 12 deaths in the group without MG 5 years after surgery died of unresected stage IV thymoma or thymic adenocarcinoma.

When analyzing the post-operative pathological data, we also found no type A thymoma and thymic adenocarcinoma in the MG group. Domestic and foreign reports show that the incidence of type A thymoma is 0–14%, type AB is 6–42%, type B1 is 7–50%, type B2 is 24–71%, and type B3 is 25–65%, and there is almost no MG in patients with thymic cancer (8, 17–21). In this study, the proportion of type A thymoma and thymic adenocarcinoma in the group without MG was 10.7 and 11.2%, respectively, and the proportions of type B1 and B2 thymoma in the two groups were basically similar.

The combination of MG has little effect on the long-term efficacy of thymoma patients, but the presence of MG is conducive to the early diagnosis and treatment of thymoma. Surgery for thymoma with or without MG should be performed with thymoma and enlarged thymectomy. Type A thymoma and thymic adenocarcinoma are rarely associated with MG. Myasthenic crisis, stage IV thymoma, and thymic adenocarcinoma were the main causes of death in the thymoma group with MG and thymoma alone, respectively.

DATA AVAILABILITY STATEMENT

The original contributions presented in the study are included in the article/supplementary material, further inquiries can be directed to the corresponding author.

ETHICS STATEMENT

The studies involving human participants were reviewed and approved by the Ethics Committee of Beijing Tongren Hospital. The patients/participants provided their written informed consent to participate in this study.

AUTHOR CONTRIBUTIONS

YZ conceived of the study. LY participated in its design and coordination. JK helped to draft the manuscript. All authors read and approved the final manuscript.

REFERENCES

1. López-Cano M, Ponseti-Bosch JM, Espin-Basany E, Sánchez-García JL, Armengol-Carrasco M. Clinical and pathologic predictors of outcome in thymoma-associated myasthenia gravis. *Ann Thorac Surg.* (2003) 76:1643–9. doi: 10.1016/S0003-4975(03)01139-1
2. Kondo K, Monden Y. Thymoma and myasthenia gravis: a clinical study of 1,089 patients from Japan. *Ann Thorac Surg.* (2005) 79:219–24. doi: 10.1016/j.athoracsur.2004.06.090
3. Margaritora S, Cesario A, Cusumano G, Meacci E, D'Angelillo R, Bonassi S, et al. Thirty-five-year follow-up analysis of clinical and pathologic outcomes of thymoma surgery. *Ann Thorac Surg.* (2010) 89:245–52. doi: 10.1016/j.athoracsur.2009.08.074
4. Jaretzki A, III, Barohn RJ, Ernstoff RM, Kaminski HJ, Keesey JC, Penn AS, et al. Myasthenia gravis: recommendations for clinical research standards Task Force of the Medical Scientific Advisory Board of the Myasthenia Gravis Foundation of America. *Neurology.* (2000) 55:16–23. doi: 10.1212/WNL.55.1.16
5. Yu L, Wang TY, Ma Shan, et al. Comparison of mid-term and long-term efficacy of thoracoscopy and sternotomy for myasthenia gravis. *Chinese Med J.* (2007) 87:3171–3.
6. Ma S, Yu L. Zhang Y. Thoracoscopic thymectomy for myasthenia gravis. *J Thorac Cardiovasc Surg.* (2006) 22:365–6.
7. Rosai J. *Histological Typing of Tumors of the Thymus//World Health Organization International Histological Classification of Tumors[M].* 2nd ed. New York, NY, Berlin: Springer-Verlag (1999).
8. Detterbeck FC. Clinical value of the WHO classification system of thymoma. *Ann Thorac Surg.* (2006) 81:2328–34. doi: 10.1016/j.athoracsur.2005.11.067
9. Patrizio C, Marco C, Giovanni C, Bartolomei C, Mumoli N. Pseudoischemic electrocardiogram in myasthenia gravis with thymoma: reversibility after thymectomy. *Clin Cardiol.* (2009) 32:E75–8. doi: 10.1002/clc.20309

10. Okumura M, Miyoshi S, Takeuchi Y, Yoon HE, Minami M, Takeda SI, et al. Results of surgical treatment of thymomas with special reference to the involved organs. *J Thorac Cardiovasc Surg.* (1999) 117:605–13. doi: 10.1016/S0022-5223(99)70343-0
11. Wang GG, Chen C, Zheng W, Guo ZH, Zhu Y, Wu WD. Video-assisted thoracoscopic surgery for thymoma in 75 cases. *Chin J Minimally Invasive Surg.* (2013) 13:581–3.
12. Kondo K, Monden Y. Myasthenia gravis appearing after thymectomy for thymoma. *Eur J Cardiothorac Surg.* (2005) 28:22–5. doi: 10.1016/j.ejcts.2005.03.039
13. Cheuk W, Tsang WY, Chan JK. Microthymoma: definition of the entity and distinction from nodular hyperplasia of the thymic epithelium (so-called microscopic thymoma). *Am J Surg, Pathol.* (2005) 29:415–9. doi: 10.1097/01.pas.0000152130.58492.de
14. Andreas R, Xiaopan Y, James H, Antonicelli A, Ahmad U, Korst RJ, et al. Postoperative radiation therapy is associated with longer overall survival in completely resected stage II and III thymoma – an analysis of the international thymic malignancies interest group (ITMIG) retrospective database. *J Thorac Oncol.* (2016) 11:1785–92. doi: 10.1016/j.jtho.2016.06.011
15. Kondo K, Monden Y. Therapy for thymic epithelial tumors: a clinical study of 1,320 patients from Japan. *Ann Thorac Surg.* (2003) 76:878–84. doi: 10.1016/S0003-4975(03)00555-1
16. Sevtap G, Ahmet A, Nagihan I, Akgül AG, Liman ST, et al. Characterization of malignant thrombus in an invasive thymoma with intravascular growth. *J Radiol Case Rep.* (2013) 7:17–23. doi: 10.3941/jrcr.v7i2.1115
17. Kondo K, Yoshizawa K, Tsuyuguchi M, Kimura S, Sumitomo M, Morita J, et al. WHO histologic classification is a prognostic indicator in thymoma. *Ann Thorac Surg.* (2004) 77:1183–8. doi: 10.1016/j.athoracsur.2003.07.042
18. Davenport E, Malthaner RA. The role of surgery in the management of thymoma: a systematic review. *Ann Thorac Surg.* (2008) 86:673–84. doi: 10.1016/j.athoracsur.2008.03.055
19. Chalabreysse L, Roy P, Cordier JF, Loire R, Gamondes JP, Thivolet-Bejui F. Correlation of the WHO schema for the classification of thymic epithelial neoplasms with prognosis: a retrospective study of 90 tumors. *Am J Surg Pathol.* (2002) 26:1605–11. doi: 10.1097/00000478-200212000-00008
20. Okumura M, Ohta M, Tateyama H, Nakagawa K, Matsumura A, Maeda H, et al. The World Health Organization histologic classification system reflects the oncologic behavior of thymoma: a clinical study of 273 patients. *Cancer.* (2002) 94:624–32. doi: 10.1002/cncr.10226
21. Nakagawa K, Asamura H, Matsuno Y, Suzuki K, Kondo H, Maeshima A, et al. Thymoma: a clinicopathologic study based on the new World Health Organization classification. *Thorac Cardiovasc Surg.* (2003) 126:1134–40. doi: 10.1016/S0022-5223(03)00798-0

Conflict of Interest: The authors declare that the research was conducted in the absence of any commercial or financial relationships that could be construed as a potential conflict of interest.

Publisher's Note: All claims expressed in this article are solely those of the authors and do not necessarily represent those of their affiliated organizations, or those of the publisher, the editors and the reviewers. Any product that may be evaluated in this article, or claim that may be made by its manufacturer, is not guaranteed or endorsed by the publisher.

Copyright © 2022 Zhang, Yu and Ke. This is an open-access article distributed under the terms of the Creative Commons Attribution License (CC BY). The use, distribution or reproduction in other forums is permitted, provided the original author(s) and the copyright owner(s) are credited and that the original publication in this journal is cited, in accordance with accepted academic practice. No use, distribution or reproduction is permitted which does not comply with these terms.

frontiers in Surgery

ORIGINAL RESEARCH
published: 15 March 2022
doi: 10.3389/fsurg.2022.852906

Can the Ratio SUVmax of the Lesion/SUVmax of Mediastinal Tissues Guide the Choice of Surgical Access for the Resection of Thymic Epithelial Tumors?

Sotirios D. Moraitis[1,2], Apostolos C. Agrafiotis[3], Evangelia Skoura[4], Dimitrios Kalkanis[5], Dimitrios Moraitis[6], Periklis Tomos[7], Theodoros Liakakos[8] and Dimitrios Angouras[9]*

[1] Department of Joint Corps Armed Forces Cardiac Surgery, 401 Hellenic Army Hospital, Athens, Greece, [2] Department of Thoracic Surgery, Athens Naval and Veterans Hospital, Athens, Greece, [3] Department of Thoracic Surgery, Saint-Pierre University Hospital, Université Libre de Bruxelles (ULB), Brussels, Belgium, [4] Department of Nuclear Medicine, Bioiatriki, Athens, Greece, [5] Department of Nuclear Medicine, Iatropolis, Athens, Greece, [6] Department of Administration, Athens Naval and Veterans Hospital, Athens, Greece, [7] Department of Thoracic Surgery, Attikon University Hospital, Medical School, National and Kapodistrian University of Athens, Athens, Greece, [8] Department of Surgery, Laikon University Hospital, Medical School, National and Kapodistrian University of Athens, Athens, Greece, [9] Department of Cardiac Surgery, Attikon University Hospital, Medical School, National and Kapodistrian University of Athens, Athens, Greece

OPEN ACCESS

Edited by:
Marco Scarci,
San Gerardo Hospital, Italy

Reviewed by:
Masayuki Chida,
Dokkyo Medical University, Japan
Savvas Lampridis,
Guy's and St Thomas' NHS Foundation Trust, United Kingdom

****Correspondence:***
Apostolos C. Agrafiotis
apostolos.agrafiotis@stpierre-bru.be

Specialty section:
This article was submitted to Thoracic Surgery, a section of the journal Frontiers in Surgery

Received: *11 January 2022*
Accepted: *07 February 2022*
Published: *15 March 2022*

Citation:
Moraitis SD, Agrafiotis AC, Skoura E, Kalkanis D, Moraitis D, Tomos P, Liakakos T and Angouras D (2022) Can the Ratio SUVmax of the Lesion/SUVmax of Mediastinal Tissues Guide the Choice of Surgical Access for the Resection of Thymic Epithelial Tumors? Front. Surg. 9:852906. doi: 10.3389/fsurg.2022.852906

Background: There are studies showing the utility of the 18-fluorodeoxyglucose positron emission tomography (^{18}FDG PET) scan in the management of patients with thymic epithelial tumors. It seems to be a correlation between the standard uptake value (SUVmax) of thymic epithelial tumors and the histological type and the stage. This study aims to use the ratio of the SUVmax of the lesion to the SUVmax of the adjacent mediastinal tissues in order to guide the choice of the surgical access.

Methods: All patients who presented an anterior mediastinal lesion with a high suspicion of being of thymic origin were included in a prospective database. A ratio inferior to 1 could predict a benign nature and less aggressive behavior, and a minimally invasive approach was performed. A ratio superior to 1 suggested a malignant and aggressive behavior, and a median sternotomy (or a thoracotomy) was performed.

Results: There were 15 male (mean age 44.6 ± 16.26 years, range 25–73) and 15 female patients (mean age 50.1 ± 16.94 years, range 25–76). When the ratio is inferior to 1, it predicts benign disease in 80% of cases. When it is superior to 1, it predicts in half of cases advanced histological types (high risk thymomas and thymic carcinomas). On the contrary, it can quite accurately predict advanced Masaoka–Koga stages.

Conclusions: The protocol of this study is in accordance with the current literature showing the utility of ^{18}FDG PET scan in the treatment of thymic epithelial tumors. This study goes one step further since the choice of surgical access is based on the SUVmax values. The ratio SUVmax of the lesion/SUVmax of the mediastinal tissues could be a new marker, more pertinent than absolute SUVmax values.

Keywords: standard uptake value, surgical access, thymic epithelial tumors, thymoma, thymic carcinoma

INTRODUCTION

Thymic epithelial tumors consist a highly heterogeneous group of anterior mediastinal lesions. They account for 15% of all anterior mediastinal tumors (1). Except for this group of tumors, there are also benign lesions of thymic origin, such as thymolipoma, thymic cysts, and thymic hyperplasia, which are treated with surgical resection (1). Thymic cysts can be congenital or acquired, the latter carrying a greater risk to be associated with inflammatory conditions or neoplasms, such as thymoma, thymic carcinoma, and Hodgkin's lymphoma (1). On the other hand, the diagnosis of thymic hyperplasia is important for two reasons. First, it must be distinguished from thymic neoplasia, and secondly because it can be associated with autoimmune conditions, such as myasthenia gravis and rheumatoid arthritis (2). Thymomectomy plus total thymectomy (thymothymectomy) is recommended over simple thymomectomy for the surgical treatment of thymic epithelial tumors (3). The optimal surgical access is a subject of debate (4). However, it would be useful for the surgical planning to be able to predict the nature (especially in terms of invasiveness) of the lesion. There is much research during the last years concerning the utility of the 18-fluorodeoxyglucose positron emission tomography (^{18}FDG PET) scan (5–15). It seems to be a correlation between the standard uptake value (SUVmax) of thymic epithelial tumors and the histological type according to the WHO classification and the stage according to the Masaoka–Koga classification. There are also studies trying to correlate the ratio of the SUVmax of the lesion to the SUVmax of the adjacent mediastinal tissues with the invasive nature of thymic epithelial tumors. Based on those data, this study aims to use this ratio in order to guide the choice of the surgical access for the resection of these lesions.

METHODS

This is a prospective single-center study. The local ethics committee approved the study protocol (Ref: 1722/23-05-2014). From June 2014 to June 2020, all patients who presented with an anterior mediastinal lesion with a high suspicion of being of thymic origin were included in a prospective database. Patients who were considered functionally inapt to undergo surgery, patients with lesions that were considered not resectable, and patients who declined surgical treatment were excluded from the study. Informed consent was obtained from all patients. Preoperatively, all patients underwent pulmonary function tests, a cardiac ultrasound, and a chest CT scan with contrast agent injection (if no contra-indication). The presence of antibodies against the acetylcholine receptor (anti-AChR Ab) and anti-muscle-specific kinase antibodies (anti-MuSK Ab) in the plasma of patients was investigated. A chest MRI was not routinely performed. An ^{18}FDG PET scan was performed in all patients as part of the standard preoperative workup. The SUVmax of the lesion was calculated by the nuclear medicine physician, and the SUVmax of the mediastinum was by convention calculated at the level of the aortic arch. According to our protocol, a ratio inferior to 1 could predict a benign nature and less aggressive behavior of the lesion; if there was no other contra-indication or technical difficulty (e.g., a voluminous lesion), then a minimally invasive approach, such as thoracoscopic thymectomy or cervical thymectomy, was performed. On the contrary, a ratio superior to 1 could suggest a malignant and aggressive behavior; in that case, a median sternotomy (or a thoracotomy if the tumor was lateralized) was the preferred surgical access. In case of a perioperative modification of the surgical access (e.g., conversion to a full median sternotomy in case of hemorrhage, technical difficulties, or if locally invasive disease was encountered during a minimally invasive approach), the patients were analyzed in an intention-to-treat manner.

STATISTICAL ANALYSIS

The chi-square test was used for the identification of independence between two nominal variables. The Fisher criterion was applied. In case of association of two variables, the logistic regression technique was used. Logistic regression examines a depended nominal variable regarding one or more independent ones. In particular, a logistic regression model has been implemented to measure the relationship between diameter and SUVmax ratio superior to 1. A Mann–Whitney *U*-test was used as a non-parametric alternative to the independent *t*-test. The chi-square test and the logistic regression technique examined the dependency or independency among variables. IBM SPSS 23 and Microsoft Office suite (Excel) spreadsheets were used to analyze and graph the data.

RESULTS

Thirty patients were included in this protocol (mean age 47.4 ± 16.55 years, range 25–76). There were 15 male (mean age 44.6 ± 16.26 years, range 25–73) and 15 female patients (mean age 50.1 ± 16.94 years, range 25–76). Three patients (10%) suffered from myasthenia gravis. The demographic and other patients' characteristics are demonstrated in **Table 1**. In 10 patients, the ratio SUVmax of the lesion/SUVmax of the mediastinal tissues was inferior to 1 (Group 1), and in 20 patients, the ratio was superior to 1 (Group 2). The ratio distribution is demonstrated in **Figure 1**. The characteristics of each group according to the SUVmax ratio are demonstrated in **Table 2**. In the Group 1, three patients underwent a median sternotomy. In fact, two of the patients declined minimally invasive surgery and preferred a sternotomy, and the third patient presented with a lesion of 10 cm. In the whole group of 10 patients, the histopathological examination of the resected specimen revealed 8 benign lesions and 2 thymomas with the WHO classification histological type superior to B1 and Masaoka–Koga stage superior to I. In the Group 2, one patient underwent VATS (she refused a median sternotomy), and another patient underwent cervical thymectomy (she had already undergone a total thyroidectomy for thyroid cancer, and she refused another surgical access than a collar incision). In the whole group of 20 patients, the final histology was compatible with high-risk thymomas (thymomas with the WHO classification histological type superior to B1) in 8 patients. The Masaoka–Koga stage was I in 2 cases and superior

TABLE 1 | Demographics and other patients' characteristics.

Sex (M/F)	15/15
Age (mean ± SD) [range] years	(47.4 ± 16.55) [25–76]
Size (mean ± SD) [range] cm	(7.92 ± 3.41) [2.2–18]
Thymomas	14 (46.6%)
Thymic carcinomas	2 (6.6%)
Thymolipomas	3 (10%)
Thymic hyperplasia	7 (23.3%)
Thymic remnant	3 (10%)
Other	1 (3.3%)
SUVmax of the lesion (mean ± SD) [range]	(3.47 ± 2.39) [1.1–12.4]
SUVmax of mediastinal tissues (mean ± SD) [range]	(1.89 ± 0.41) [1.3–3.3]
SUVmax ratio (mean ± SD) [range]	(1.96 ± 1.62) [0.65–7.75]
WHO Classification	
A	1 (7.1%)
AB	3 (21.4%)
B1	2 (14.2%)
B2	3 (21.4%)
Mixed B1B2	1 (7.1%)
B3	–
Mixed B2B3	4 (28.5%)
Masaoka–Koga Classification	
I	2 (12.5%)
IIa	5 (31.2%)
IIb	3 (18.7%)
III	3 (18.7%)
IVa	3 (18.7%)
Surgical access	
Sternotomy	19 (63.3%)
VATS	8 (26.6%)
Thoracotomy	2 (6.6%)
Cervicotomy	1 (3.3%)
Resection margins (thymomas and thymic carcinomas)	
R0	13 (81.3%)
R1	3 (18.7%)

VATS, video-assisted thoracoscopic surgery.

TABLE 2 | Comparison of the two groups of patients according to the SUVmax ratio.

Category	Group 1 (SUVmax ratio <1)	Group 2 (SUVmax ratio >1)	*p*-value
Sex (M/F)	(7/3)	(8/12)	0.245
Age (mean ± SD) [range] years	42.6 ± 15.76 [27–73]	49.8 ± 16.8 [25–76]	0.373
Size (mean ± SD) [range] cm	(5.79 ± 2.49) [2.2–10]	(9.09 ± 3.25) [4.5–18]	0.002
Thymomas	2	12	0.058
Thymic carcinomas	0	2	0.54
Thymolipomas	3	0	0.03
Thymic hyperplasia	3	4	0.657
Thymic remnant	2	1	0.251
Other	0	1	1
WHO classification			
A	0	1	1
AB	0	3	0.532
B1	0	2	0.54
B2	1	2	1
Mixed B1B2	0	1	1
B3	0	0	–
Mixed B2B3	1	3	1
Masaoka–Koga classification			
I	0	2	0.54
IIa	1	4	0.64
IIb	1	2	1
III	0	3	0.532
IVa	0	3	0.532
Surgical access			
Sternotomy	3	16	0.005
VATS	7	1	0
Thoracotomy	0	2	0.54
Cervicotomy	0	1	1
Resection margins (thymomas and thymic carcinomas)			
R0	2	11	0.119
R1	0	3	0.532
Capsular invasion	2	13	0.02

VATS, video-assisted thoracoscopic surgery.

to I in 11 cases. As shown in **Table 2**, there are more thymomas and more advanced Masaoka–Koga stages in the SUVmax ratio >1 group; nevertheless, the small enrollment does not permit to reach statistical significance. In half of the patients of this cohort, there was a capsular invasion (15 out of 30 patients). More specifically, the 60.9% of patients operated with an open procedure presented a capsular invasion. On the contrary, only 14.3% of patients who underwent minimally invasive surgery had a capsular invasion. In the SUVmax ratio >1 group, the capsular invasion was significantly higher ($p = 0.02$). To estimate the relationship between "SUV ratio" and "presence of malignancy," the technique of logistic regression was used. The related odds ratio is 12. The conversion of odds ratio to probability reveals that the probability of presence of malignancy with ratio >1 is 92.31%. In addition, the logistic regression model revealed that if the diameter of the tumor is increased per 1 cm, then the odds ratio of presence in the Group 2 (SUVmax ratio > 1) is 1.719 higher.

DISCUSSION

There are many studies that investigated the utility of ^{18}FDG PET scan in the workup of thymic epithelial tumors in terms of diagnosis, evaluation of aggressive behavior, and response to treatment (5–15). Kumar et al. (5) stressed the possibility to differentiate low-risk (A, AB, and B1) and high-risk (B2 and B3) thymomas according to the WHO classification by using

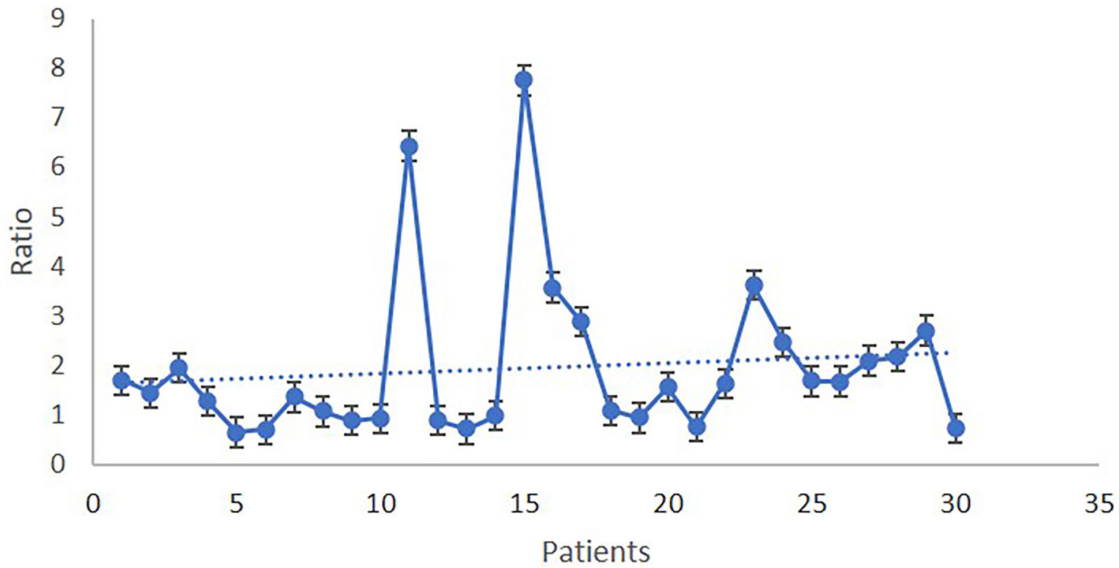

FIGURE 1 | The SUVmax of the lesion/SUVmax of mediastinal tissue ratio distribution.

the ^{18}FDG PET/CT scan. Thymomas can also be distinguished from thymic carcinomas. The studies conducted by Sung et al. (6) and Luzzi et al. (7) were in the same direction. In addition, they confirmed the opinion of El-Bawab et al. (8) concerning the contribution of ^{18}FDG PET scan to the differential diagnosis between thymomas and thymic hyperplasia. Igai et al. (9) were able to correlate the SUVmax of the tumor with the histological type, but they did not correlate the SUVmax with the stage of the disease. Similarly, Purandare et al. (14) showed that the SUVmax of thymic carcinomas was significantly higher than low-risk and high-risk thymomas. The SUVmax in patients with advanced stage disease was higher but not statistically significant compared to the early-stage disease (14). On the contrary, Fukumoto et al. (10) and Ito et al. (15) proved this correlation. Furthermore, the opinion of Ito et al. (15) is that there is a statistically significant difference in the SUVmax between thymic carcinoma and high-grade thymoma, among high-grade and low-grade thymomas, and that the ^{18}FDG PET/CT scan could predict tumor invasion into pericardium, lungs, and brachiocephalic vein (15). Watanabe et al. (16) presented that the ^{18}FDG PET scan can differentiate thymoma from thymic cancer, diffuse large B-cell lymphoma, and Hodgkin's lymphoma, whereas the SUVmax of the lesion cannot predict the histological diagnosis of thymoma (16). Terzi et al. (11) evaluated the SUVmax of the lesion, the SUVmax of the mediastinum, and the ratio of these two variables. They found that there is a correlation between this ratio and the advanced stage of the disease (11). A meta-analysis showed that SUVmax could be able to predict the WHO grade in thymic epithelial tumors (17). On the contrary, there is no robust data permitting to use FDG uptake as a predictive factor for disease stage.

To the best of our knowledge, there is no previous study that takes into consideration the values of the ^{18}FDG PET scan to guide the choice of the surgical access. The choice of the surgical access is of paramount importance, especially in case of advanced Masaoka–Koga stage, in order to achieve free surgical margins. Since there is no evidence regarding the optimal surgical access for thymic epithelial tumors (18–20), its choice should be based on tumor size, surgical expertise, and patient's preference. In the protocol presented herein, all these elements were taken into account while choosing the surgical access, justifying the derogations from the initial hypothesis. In our study when the ratio SUVmax of the lesion/SUVmax of the mediastinal tissues is inferior to 1, it seems to predict benign disease in 80% of cases. Consequently, a minimally invasive approach is privileged even if it has some limitations, as in case of a voluminous lesion. On the other hand, the choice of an open sternotomy may seem maximalist because there are some false positives in that group. Nevertheless, when the ratio is superior to 1, the probability of presence of malignancy is 92.31%, whereas it can quite accurately predict advanced Masaoka–Koga stages. It can predict in half of cases advanced histological types according to the WHO classification (high-risk thymomas and thymic carcinomas). Taking into account that nowadays all types of thymomas regardless of histological type are considered as malignant lesions (21–24) in contrast to the previous belief that A, AB, and B1 types are rather benign, then a ratio >1 in the current study predicted malignancy in 15 out of 20 cases. The

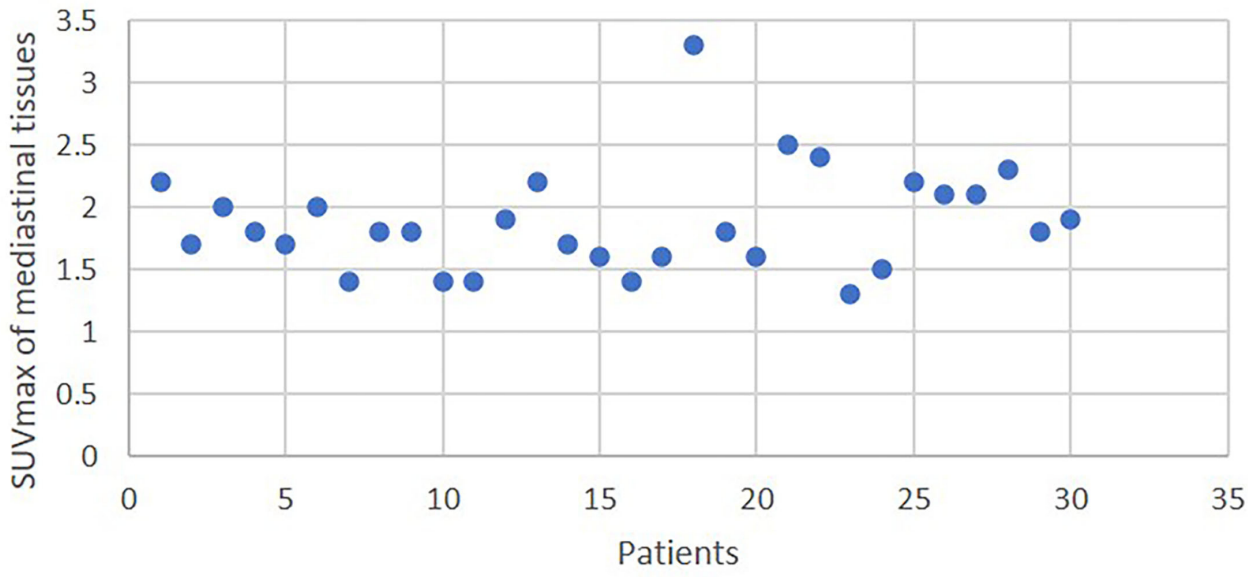

FIGURE 2 | The distribution of mediastinal tissue SUVmax.

selection of an open access procedure, based on ratio >1, led us on the percentage of 81.3% of R0 resection margins (**Table 1**). Apart from the above limitations, the most important is the fact that it is a single-center cohort with a small enrollment. Nevertheless, this protocol can be the basis for the conduction of larger multicentric studies in order to validate the usefulness of the ratio. The strong point of this study is its prospective nature. In addition, the use of the ratio rather than absolute SUVmax values could overcome the potential confounding factors related to SUVmax variations due to physiological and technical factors. Van Den Hoff et al. (24) strongly support the opinion of the use of tumor-to-blood pool ratio, instead of tumor SUV, for SUV-based approaches. In our study, the narrow range of the denominator's measurements (range of SUVmax of mediastinal tissues: 1.3–3.3) could allow us a speculation about the pertinence of the ratio, as an index (**Figure 2**).

CONCLUSIONS

Despite its small enrollment, this study predicts quite accurately the behavior of thymic epithelial tumors. The protocol of this study is in accordance with the current literature showing the utility of ^{18}FDG PET scan in the treatment of thymic epithelial tumors. This study goes one step further since the choice of surgical access is based on the SUVmax values. In particular, the ratio SUVmax of the lesion/SUVmax of the mediastinal tissues could be a new marker, more pertinent than absolute SUVmax values. Nevertheless, other parameters, such as tumor size, patient preference, experience of the operating surgeon, and local infrastructure, should be considered while planning the surgical access. Larger studies should be conducted to validate such a protocol in the highly heterogeneous environment of thymic epithelial tumors.

DATA AVAILABILITY STATEMENT

The raw data supporting the conclusions of this article will be made available by the authors, without undue reservation.

ETHICS STATEMENT

The studies involving human participants were reviewed and approved by Athens Naval and Veterans Hospital Ethics Committee (Ref: 1722/23-05-2014). The patients/participants provided their written informed consent to participate in this study.

AUTHOR CONTRIBUTIONS

SM, DA, and TL: conception and design. DM, DK, and ES: administrative support. AA and SM: provision of study materials or patients. SM, PT, DK, ES, and TL: collection and assembly of data. SM, DM, AA, and PT: data analysis and interpretation. All authors: manuscript writing and final approval of manuscript. All authors contributed to the article and approved the submitted version.

REFERENCES

1. Takeda S, Miyoshi S, Minami M, Mitsunori O, Akira M, Hikaru M. Clinical spectrum of mediastinal cysts. *Chest.* (2003) 124:125–32. doi: 10.1378/chest.124.1.125
2. Oral H, Bilgin E, Yildirim S, Onder SC, Demirkazik F, Uysal S, et al. Mediastinal mass in a patient with rheumatoid arthritis: lymphoid cystic thymic hyperplasia. *Rheumatol Adv Pract.* (2021) 5:rkab049. doi: 10.1093/rap/rkab049
3. Guerrera F, Falcoz PE, Moser B, van Raemdonck D, Bille A, Toker A, et al. Thymomectomy plus total thymectomy versus simple thymomectomy for early-stage thymoma without myasthenia gravis: a European Society of Thoracic Surgeons Thymic Working Group Study. *Eur J Cardiothorac Surg.* (2021) 60:881–7. doi: 10.1093/ejcts/ezab316
4. Suda T, Kaneda S, Hachimaru A, Tochii D, Maeda R, Tochii S, et al. Thymectomy *via* a subxiphoid approach: single-port and robot-assisted. *J Thorac Dis.* (2016) 8:S265–71. doi: 10.3978/j.issn.2072-1439.2016.02.34
5. Kumar A, Regmi SK, Dutta R, Kumar R, Gupta SD, Das P, et al. Characterization of thymic masses using 18FDG-PET-CT. *Ann Nucl Med.* (2009) 23:569–77. doi: 10.1007/s12149-009-0283-z
6. Sung YM, Lee KS, Kim BT, Choi JY, Shim YM Yi CA. 18F-FDG-PET/CT of thymic epithelial tumors: usefulness of distinguishing and staging tumor subgroups. *J Nucl Med.* (2006) 47:1628–34.
7. Luzzi K, Campione A, Gorla A, Vassallo G, Bianchi A, Biggi A, et al. Role of fluorine-fluorodeoxyglucose positron emission tomography/computed tomography in preoperative assessment of anterior mediastinal masses. *Eur J Cardiothorac Surg.* (2009) 36:475–9. doi: 10.1016/j.ejcts.2009.03.055
8. El-Bawab H, Al-Sugair AA, Rafay M, Hajjar W, Mahdy M, Al-Kattan K. Role of fluorine-18 fluorodeoxyglucose positron emission tomography in thymic pathology. *Eur J Cardiothorac Surg.* (2007) 31:731–6. doi: 10.1016/j.ejcts.2007.01.024
9. Igai H, Matsuura N, Tarumi S, Chang SS, Misaki N, Go T, et al. Usefulness of [F] fluoro-2-deoxy-D-glucose positron emission tomography for predicting the World Health Organization malignancy grade of thymic epithelial tumors. *Eur J Cardiothorac Surg.* (2011) 40:143–5. doi: 10.1016/j.ejcts.2010.09.009
10. Fukumoto K, Taniguchi T, Ishikawa Y, Kawaguchi K, Fukui T, Kato K, et al. The utility of [18F]- fluorodeoxyglucose positron emission tomography-computed tomography in thymic epithelial tumors. *Eur J Cardiothorac Surg.* (2012) 42:e152–6. doi: 10.1093/ejcts/ezs527
11. Terzi A, Bertolaccini L, Rizzardi G, Luzzi L, Bianchi A, Campione A, et al. Usefulness of 18-FDGPET/CT in the pre-treatment evaluation of thymic epithelial neoplasms. *Lung Cancer.* (2011) 74:239–43. doi: 10.1016/j.lungcan.2011.02.018
12. Thomas A, Mena E, Kurdziel K, Venzon D, Khozin S, Berman AW, et al. 18F-Fluorodeoxyglucose positron emission tomography in the management of patients with thymic epithelial tumors. *Clin Cancer Res.* (2013) 19:1487–93. doi: 10.1158/1078-0432.CCR-12-2929
13. Viti A, Terzi A, Bianchi A, Bertolaccini L. Is a positron emission tomography-computed tomography scan useful in the staging of thymic epithelial neoplasms? *Interact CardioVasc Thorac Surg.* (2014) 19:129–34. doi: 10.1093/icvts/ivu068
14. Purandare NC, Pramesh CS, Karimundackal G, Jiwnani S, Agrawal A, Shah S, et al. Thymic epithelial tumors : Can fluorodeoxyglucose positron emission tomography help in predicting histologic type and stage? *Indian J Cancer.* (2016) 53:270–3. doi: 10.4103/0019-509X.197717
15. Ito T, Suzuki H, Sakairi Y, Wada H, Nakajima T, Yoshino I. 18F-FDG-PET/CT predicts grade of malignancy and invasive potential of thymic epithelial tumors. *Gen Thorac Cardiovasc Surg.* (2021) 69:274–81. doi: 10.1007/s11748-020-01439-7
16. Watanabe T, Shimomura H, Mutoh T, Saito R, Goto R, Yamada T. et al. Positron emission tomography/computed tomography as a clinical diagnostic tool for anterior mediastinal tumors. *Surg Today.* (2019) 49:143–9. doi: 10.1007/s00595-018-1712-1
17. Treglia G, Sadeghi R, Giovanella L, Cafarotti S, Filosso P, Lococo F. Is (18)F-FDG PET useful in predicting the WHO grade of malignancy in thymic epithelial tumors? A meta-analysis. *Lung Cancer.* (2014) 86:5–13. doi: 10.1016/j.lungcan.2014.08.008
18. Buentzel J, Heinz J, Hinterthaner M, Schondube FA, Straube C, Roever C, et al. Robotic versus thoracoscopic thymectomy: the current evidence. *Int J Med Robot.* (2017) 13:e1847. doi: 10.1002/rcs.1847
19. Kang CH, Hwang Y, Lee HJ, Park IK, Kim YT. Robotic thymectomy in anterior mediastinal mass: propensity score matching study with transsternal thymectomy. *Ann Thorac Surg.* (2016) 102:895–901. doi: 10.1016/j.athoracsur.2016.03.084
20. Marulli G, Maessen J, Melfi F, Schmid TA, Keijzers M, Fanucchi O, et al. Multi-institutional European experience of robotic thymectomy for thymoma. *Ann Cardiothorac Surg.* (2016) 5:18–25. doi: 10.3978/j.issn.2225-319X.2015.08.13
21. Detterbeck FC, Parsons AM. Thymic tumors. *Ann Thorac Surg.* (2004) 77:1860–9. doi: 10.1016/j.athoracsur.2003.10.001
22. Marx A, Chan JK, Coindre JM, Detterbeck F, Girard N, Harris NL, et al. The 2015 World Health Organization Classification of Tumors of the Thymus: Continuity and Changes. *J Thorac Oncol.* (2015) 10:1383–95. doi: 10.1097/JTO.0000000000000654
23. Marx A, Ströbel P, Badve SS, Chalabreysse L, Chan JKC, Chen G, et al. ITMIG consensus statement on the use of the WHO histological classification of thymoma and thymic carcinoma: refined definitions, histological criteria and reporting. *J Thorac Oncol.* (2014) 9:596–611. doi: 10.1097/JTO.0000000000000154
24. van den Hoff J, Oehme L, Schramm G, Maus J, Lougovski A, Petr J, et al. The PET-derived tumor-to-blood standard uptake ratio (SUR) is superior to tumor SUV as a surrogate parameter of the metabolic rate of FDG. *EJNMMI Res.* (2013) 3:77. doi: 10.1186/2191-219X-3-77

Conflict of Interest: The authors declare that the research was conducted in the absence of any commercial or financial relationships that could be construed as a potential conflict of interest.

Publisher's Note: All claims expressed in this article are solely those of the authors and do not necessarily represent those of their affiliated organizations, or those of the publisher, the editors and the reviewers. Any product that may be evaluated in this article, or claim that may be made by its manufacturer, is not guaranteed or endorsed by the publisher.

Copyright © 2022 Moraitis, Agrafiotis, Skoura, Kalkanis, Moraitis, Tomos, Liakakos and Angouras. This is an open-access article distributed under the terms of the Creative Commons Attribution License (CC BY). The use, distribution or reproduction in other forums is permitted, provided the original author(s) and the copyright owner(s) are credited and that the original publication in this journal is cited, in accordance with accepted academic practice. No use, distribution or reproduction is permitted which does not comply with these terms.

frontiers | Frontiers in Oncology

REVIEW
published: 08 April 2022
doi: 10.3389/fonc.2022.808019

Thymic Carcinoma: A Review

Doaa Alqaidy[1] *and Cesar A. Moran*[2*]

[1] Department of Pathology and Laboratory Medicine, University of California San Francisco, San Francisco, CA, United States, [2] Department of Pathology, MD Anderson Cancer Center, University of Texas, Houston, TX, United States

The diagnosis of thymic carcinoma may pose significant problems not necessarily in the histopathological diagnosis but rather in assigning the thymus as specific origin. Often the tissue available for interpretation is obtained *via* a mediastinocopic biopsy, which raises two different issues -minimal tissue and lack of specific features to make a carcinoma of thymic origin. In addition, if to that conundrum we add that there is no magic immunohistochemical stain that will unequivocally lead to the interpretation of thymic carcinoma, then we are left with a true clinical-radiological-pathological correlation. In this review, we will highlight some of those challenges that diagnostic surgical pathologists may encounter in the histopathological assessment of thymic carcinoma as well as in the staging of these tumors.

Keywords: thymus, carcinoma, mediastinum, thymoma, staging

OPEN ACCESS

Edited by:
Alona Zer,
Rambam Health Care Campus, Israel

Reviewed by:
Izidor Kern,
University Clinic of Pulmonary and Allergic Diseases Golnik, Slovenia
Marco Schiavon,
University Hospital of Padua, Italy

***Correspondence:**
Cesar A. Moran
cesarmoran@mdanderson.org

Specialty section:
This article was submitted to Thoracic Oncology, a section of the journal Frontiers in Oncology

Received: *02 November 2021*
Accepted: *10 March 2022*
Published: *08 April 2022*

Citation:
Alqaidy D and Moran CA (2022) Thymic Carcinoma: A Review. Front. Oncol. 12:808019. doi: 10.3389/fonc.2022.808019

INTRODUCTION

Primary thymic carcinoma in general practice represents a small percentage of thymic epithelial neoplasms (1). Contrary to thymoma, which is much more common, and a tumor in which the histopathological features, in the majority of cases, allow for the tumor to be not only diagnosed easier but also be placed in specific anatomical area, the diagnostic features of thymic carcinoma are not specific, and its diagnosis requires complete clinical and radiological correlations.

Historically, the entity that we currently recognize as thymic carcinoma had not been acknowledged in the literature until Shimosato et al. (2) reported a series of cases in which the authors provided enough evidence to define the tumor as of arising from the mediastinal compartment. Followed that series of cases, there have been numerous other reports; however, the only two series that have reported more than 60 cases of primary thymic carcinoma are the ones presented by Suster-Rosai (3) and Moran et al. (4), which together will gather only 125 patients with thymic carcinoma and if to that we may add that at least in the Suster-Rosai series, the authors also included some neuroendocrine carcinomas, then we have the two largest series with even fewer non-neuroendocrine thymic carcinomas. Nevertheless, other series consisting of fewer cases have provide important clinical and pathological information, which over the years has expanded not only the clinical knowledge of thymic carcinoma but also has expanded the histopathological spectrum of these tumors (5).

CLINICAL FEATURES

Similar to what occurs with the histopathological features of thymic carcinoma —non-specific, the clinical features of patients with these tumors are also rather non-specific. The tumor has been described in a wide range of individuals ranging from very young to older patients, reports of thymic carcinoma in association with some autoimmune diseases or paraneoplastic syndromes including myasthenia gravis have been presented in the literature. However, we consider that those reports are likely coincidental occurrences rather than true link associations. Thymic carcinoma does not appear to have a strong association with Myasthenia Gravis or other autoimmune disease that have been reported in association with thymomas (3, 4, 6). More recently NUT carcinoma, which is another tumor that may occur in the midline appears to affect rather younger individuals. However, the morphology of the tumor is that of a poorly differentiated carcinoma, which requires FISH analysis to properly designate the tumor as NUT carcinoma (7).

The ideal clinical and radiological features of patients with thymic carcinoma should be that of a patient without any prior history of carcinoma and presenting with an anterior mediastinal mass.

In terms of survival, if we compare the two largest series of thymic carcinomas, we can see some differences. In the Suster-Rosai experience (3), the 5-years survival was recorded at 33%, while in the Weissferdt-Moran (4), it was recorded at 65%. It is possible that in the Suster-Rosai series of cases the survival may have been influenced by including neuroendocrine neoplasms, while in the Weissferdt-Moran, those tumors were excluded. Nevertheless, survival will be influenced not only by the histology of the tumor but also by the staging at the time of diagnosis.

PATHOLOGICAL FEATURES

The gross features of thymic carcinoma only rarely will provide clues of the possibility of thymic carcinoma, as the tumor may show areas of necrosis, hemorrhage, and infiltrative borders. However, those parameters are not specific for thymic carcinoma and may be seen in some cases of thymoma (8). Similarly, the tumor may also show cystic changes but once again, cystic changes are much more common in thymoma than thymic carcinoma. The gold standard to arrive at specific diagnosis is on histopathological evaluation.

The histopathological features of thymic carcinoma can be illustrated in a rather diagrammatic way taking the normal thymus as a starting point and following it down to the changes that may be seen in thymoma and further into thymic carcinoma (**Figure 1**). We consider that all those changes are part of the spectrum that thymic epithelial neoplasms. From the light microscopic point of view, the features of thymic carcinoma can be summarized based on the cellularity of the tumor or based on the growth pattern; thus, tumors can be either of the conventional type or of specific subtypes:

Conventional:

- The majority of thymic carcinomas show squamous differentiation and the degree of differentiation varies from well to poorly differentiated tumors (9–13) (**Figures 2A, B**). However, it is also important to keep in mind that all thymomas will also show squamous differentiation because the normal thymic gland also show positive staining in the normal cellularity of the thymus with markers that are commonly used to stain squamous cell carcinomas. Therefore, there is nothing specific for the diagnosis of thymic carcinoma except the presence of an anterior mediastinal mass in the setting of a patient with no other relevant clinical history of malignancy. Over the years, there has been an emphasis on certain histopathological criteria that may be used in the majority of these tumors and that includes the loss of the organotypical features and the presence of overtly cellular atypia and mitotic activity (14, 15).
- Spindle cell morphology is another unusual growth pattern that may be seen in some thymic carcinomas (16) (**Figure 3**). Here the most important consideration would be separating spindle cell thymic carcinoma from spindle cell thymoma or another spindle cell neoplasm of different lineage. However, once again the presence of marked nuclear atypia and mitotic activity will lead to the correct interpretation of thymic carcinoma, while the use of immunohistochemical stains will also be of aid if the consideration is another spindle cell neoplasm. The use of immunohistochemical markers in this particular histology will likely show similar imunophenotype as conventional thymic squamous carcinoma.
- Poorly differentiated (undifferentiated) carcinoma without any morphological or immunohistochemical differentiation (17, 18). This particular group of tumors may show considerable difficulty in diagnosis as there is a need to properly exclude metastatic disease from outside of the mediastinal compartment.
    - One important histopathological characteristic of thymic carcinoma is the presence of an inflammatory component in association with the carcinoma, more often composed of plasma cells, which is contrary to thymoma in which the presence of T-cell lymphocytes aids in the diagnosis. However, there are exceptions:
        - Micronodular thymic carcinoma with B-cell lymphoid hyperplasia (**Figure 4**) although rare, represents the counterpart of thymoma with B-cell lymphoid hyperplasia. Both tumors show similar histopathological features and it is the cytological features of the epithelial proliferation, which separates both entities (19, 20).

Subtypes:

The different subtypes that have been described in thymic carcinoma are wide and essentially the tumor may show similar characteristics as other tumors of non-thymic origin. Those growth patterns include:

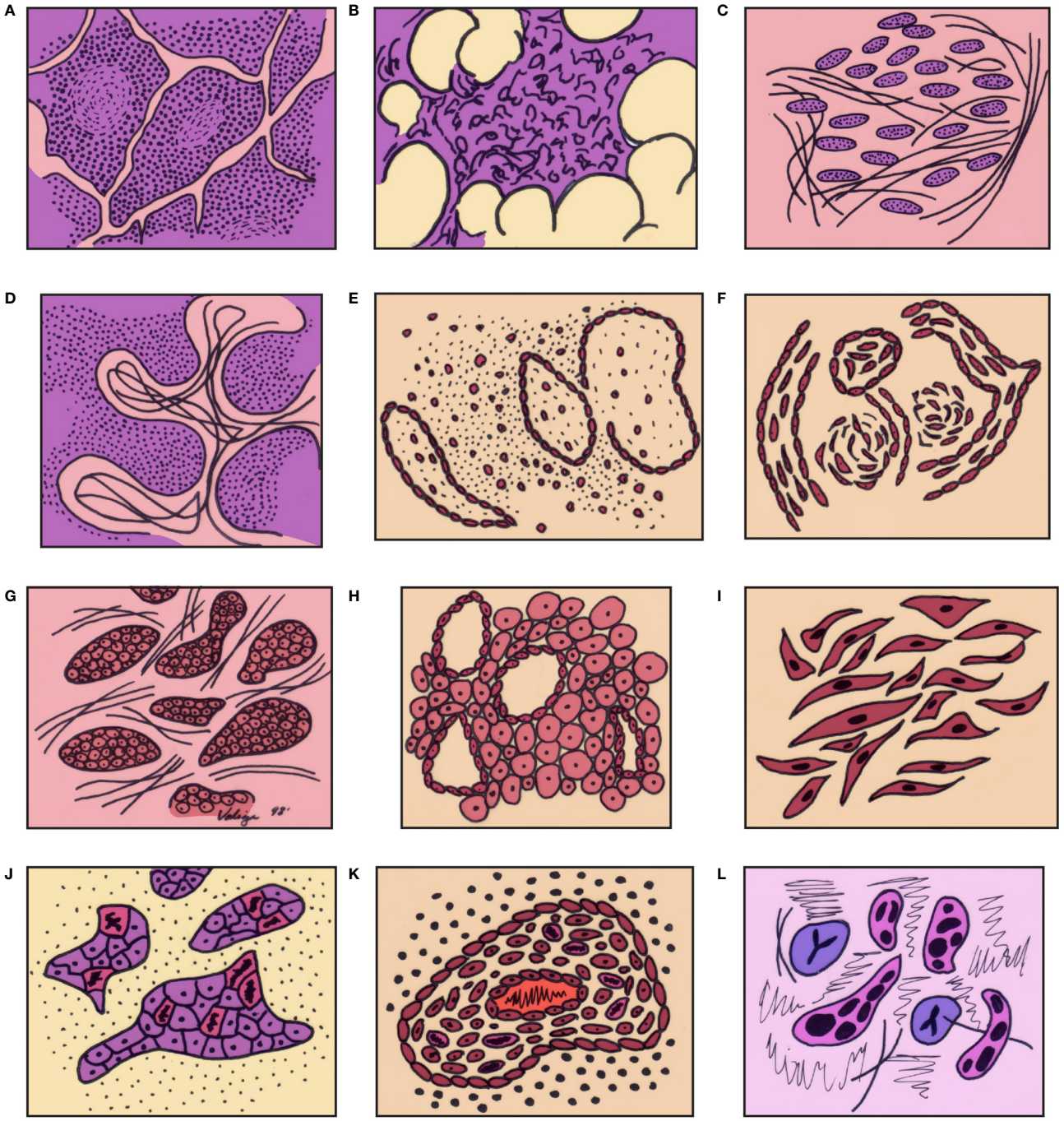

FIGURE 1 | Graphic illustration of the spectrum of differentiation of thymic epithelial neoplasms from normal thymus through high grade thymic carcinoma: **(A)** thymus in a child, **(B)** thymus in the adult, **(C)** thymus with involutional changes, **(D)** thymoma (lymphocyte rich – WHO type B1), **(E)** Thymoma (mixed cellularity – WHO type B2), **(F)** Spindle cell thymoma (WHO type A), **(G)** atypical thymoma – preservation of organotypical features, **(H)** atypical thymoma (perivascular spaces), **(I)** Atypical spindle cell thymoma, **(J)** thymic carcinoma – loss of organotypical features, **(K)** thymic carcinoma – inflammatory reaction, **(L)** thymic carcinoma – cellular atypia and mitotic activity in epithelial cells. (with permission from Dr. Moran copyright © Dr. Moran).

○ Adenocarcinoma.

■ Even though adenocarcinoma rarely occurs as primary carcinoma of the thymus, the diagnosis of these tumor may pose considerable difficulty as the majority of adenocarcinomas in the thorax are of lung origin. The tumor may show a colonic-like, papillary, and micropapillary growth patterns (**Figures 5**, **6**). In addition, the immunohistochemical profile of thymic adenocarcinoma is also rather non-specific and may be shared

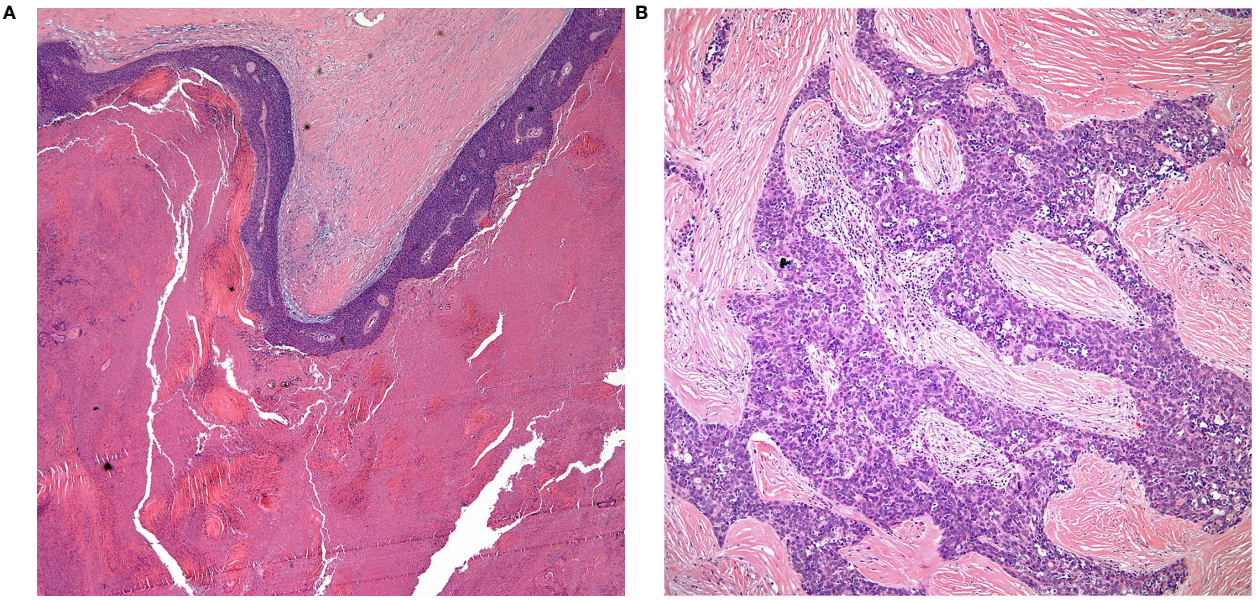

FIGURE 2 | **(A)** keratinizing squamous cell carcinoma, **(B)** thymic carcinoma with loss of organotypical features.

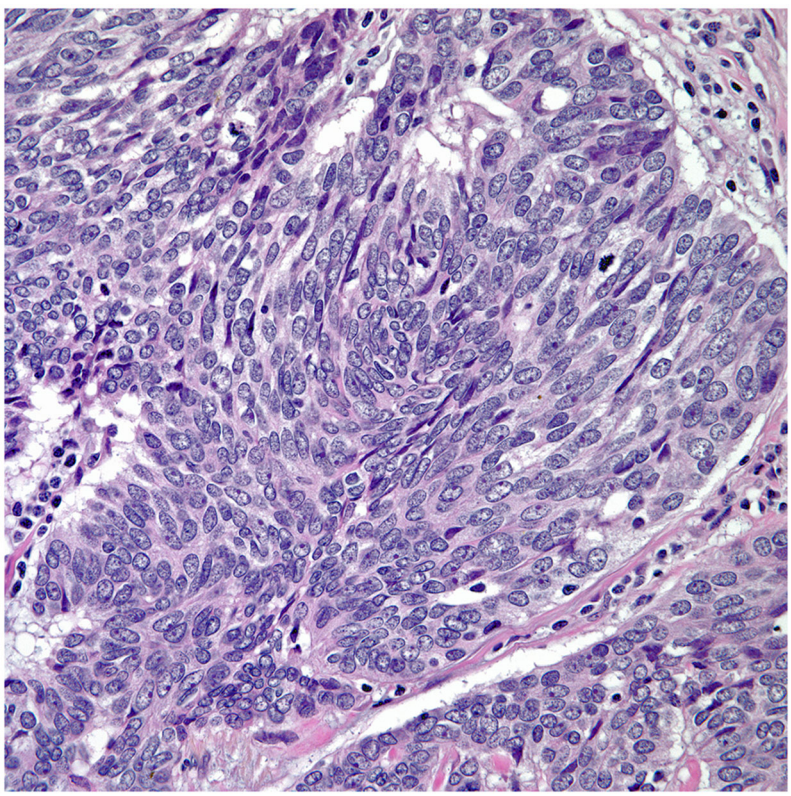

FIGURE 3 | Thymic sarcomaoitd carcinoma.

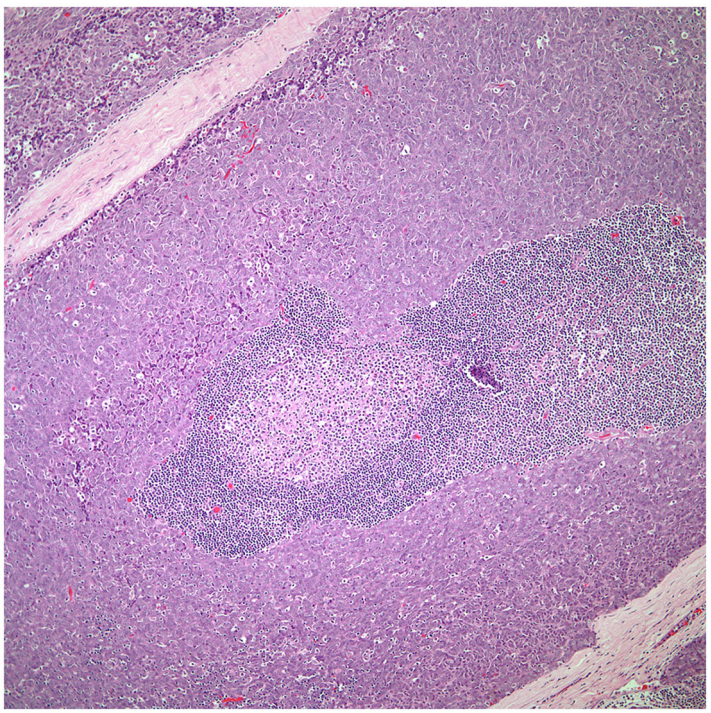

FIGURE 4 | Low power view of a micronodular thymic carcinoma with B-cell lymphoid hyperplasia, note the presence of a germinal center.

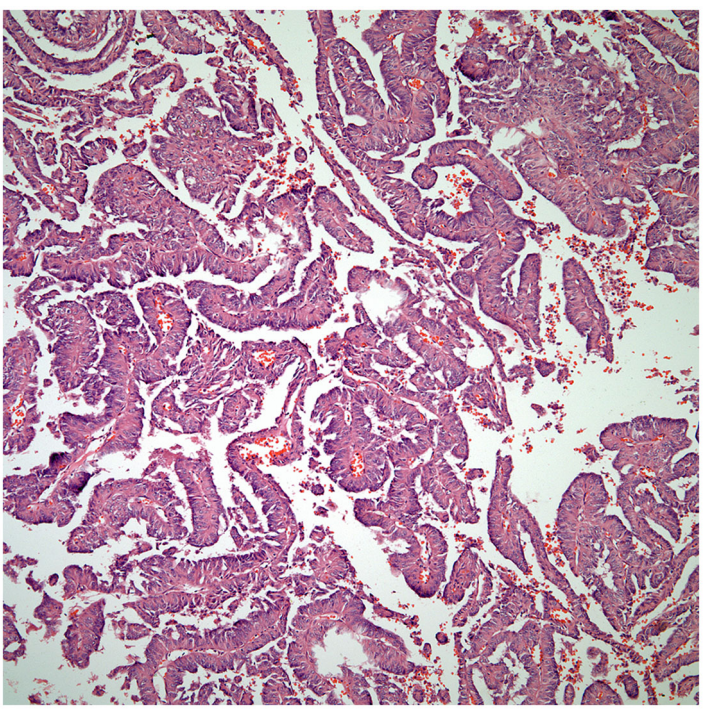

FIGURE 5 | Thymic papillary carcinoma.

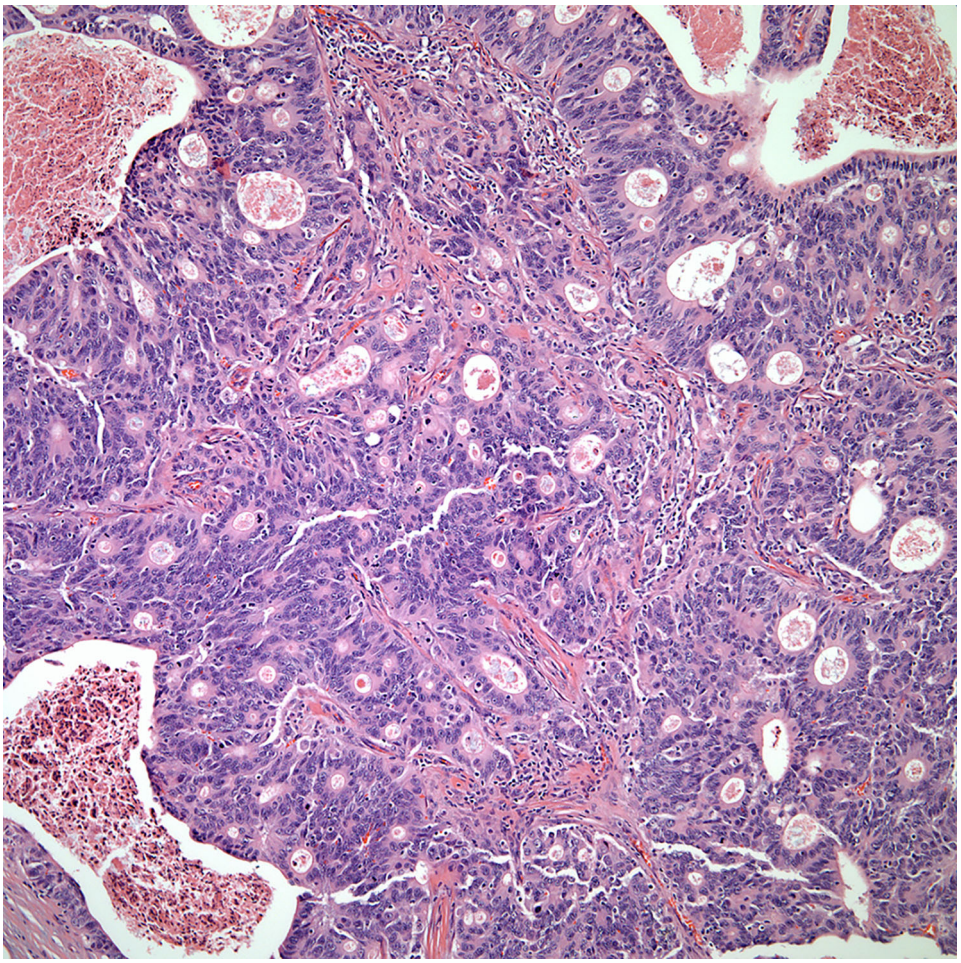

FIGURE 6 | Thymic mucinous adenocarcinoma with "colonic" features.

with other adenocarcinomas of lung or extra-thoracic origin (21–24).

○ Salivary gland type:

■ Mucoepidermoid carcinoma and to some extent basaloid carcinoma of the thymus show similar features as those described in the salivary gland (**Figures 7**, **8**). Although basaloid carcinoma does not necessarily belong to the group of salivary gland type carcinomas, some of the histopathological features mimic those of the salivary gland. In addition, both tumors may also show cystic changes and both tumors are considered of low-grade malignancy even though mucoepidermoid carcinoma may also be of high-grade histology (25–29). More important is to highlight that the immunohistochemistry of mucoepidermoid carcinoma is also of squamous differentiation and the diagnosis should be based on the presence of mucous producing cells (mucocytes) admixed with the epidermoid proliferation without keratinization. More recent the use of MAML-2 has been correlated with these tumors; however, there are only a few reports of MAML in thymic mucoepidermoid carcinomas to draw more solid conclusions. Needless to say, even though mucoepidermoid and basaloid carcinomas are the most common in this family of tumors, other tumors that have been described include adenoid cystic carcinoma and epithelial myoepithelial carcinoma. However, those two latter tumors are rare in the thymus.

IMMUNOHISTOCHEMICAL AND MOLECULAR FEATURES

One of the bigger issues in understanding the immunohistochemical properties of thymic epithelial neoplasms is the lack of understanding of the immunohistochemical features of the normal thymic gland. Essentially, the normal thymus will show positive staining for markers that are commonly employed in the assessment of squamous carcinomas. Immunostains for p40, keratin 5/6, p63 are positive in the normal thymus (epithelial cells), thymoma, and thymic carcinoma (30). Therefore, those stains have limit value in

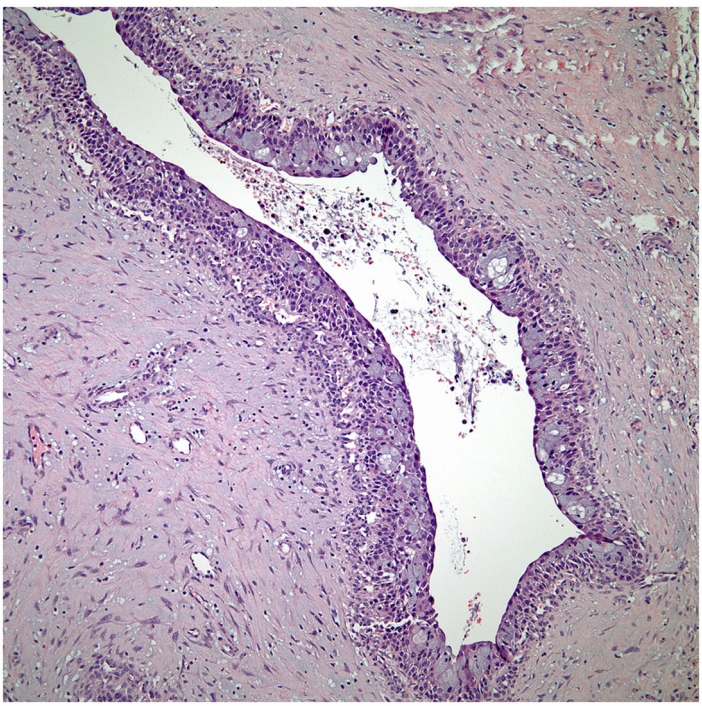

FIGURE 7 | Thymic low-grade mucoepidermoid carcinoma with cystic changes.

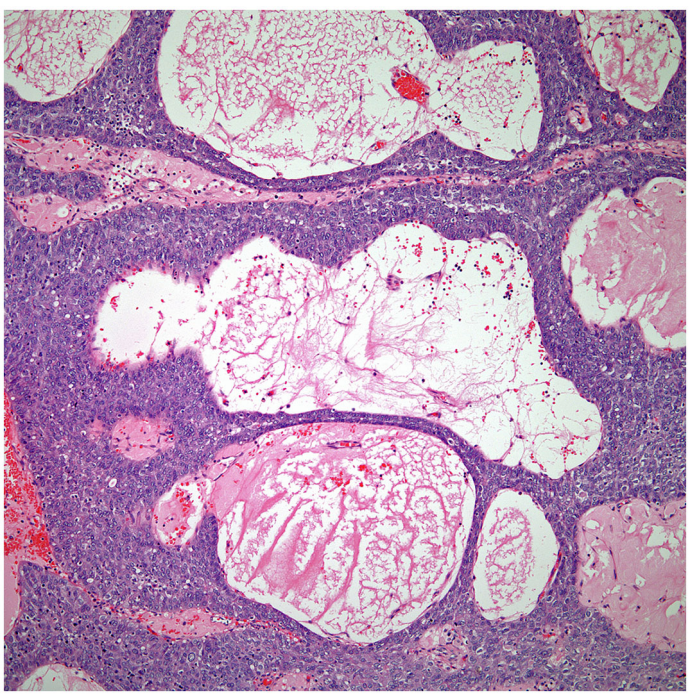

FIGURE 8 | Cystic basaloid carcinoma of the thymus.

the setting of thymic epithelial neoplasms. Although CD5 has been considered a good marker for thymic carcinoma, such marker can also show positive staining in atypical thymoma, some conventional thymomas, and other carcinomas of non-thymic origin. On the other hand, some studies on immunohistochemistry have been designed to separate atypical thymomas from thymic carcinoma and although important, as of today, there is not a single immunohistochemical stain that is specific for thymic carcinoma (31–36).

Due to the unusual occurrence of thymic carcinoma, larger studies using molecular techniques is still lacking. However, some authors have investigated the role of EGFR and HER-2, but the results have not been definitive in the role of those biomarkers (37–39).

THYMIC CARCINOMA STAGING

Unfortunately, over the years the Masaoka staging system that was proposed for thymomas has been the one used for thymic carcinoma (40). However, contrary to the controversy that exists

TABLE 1 | Suggested TNM staging system for thymic carcinoma.

T1 (Figure 9)	T2 (Figure 10)	T3 (Figure 11)
Limited to the thymic gland	*invading visceral pleura* *Lung, pericardium* *Great vessels, chest wall* *Diaphragm.*	*direct extra-thoracic tumor extension*
N0	**N1**	
Negative nodes	*positive thoracic nodes*	
M0	**M1**	
No distant metastasis	*distant metastasis*	

Groups
Stage I – T1-N0-M0.
Stage II – T2-N0-M0.
Stage III - T3-N0-M0.
Any T, N1, M0.
Any T, any N, M1.

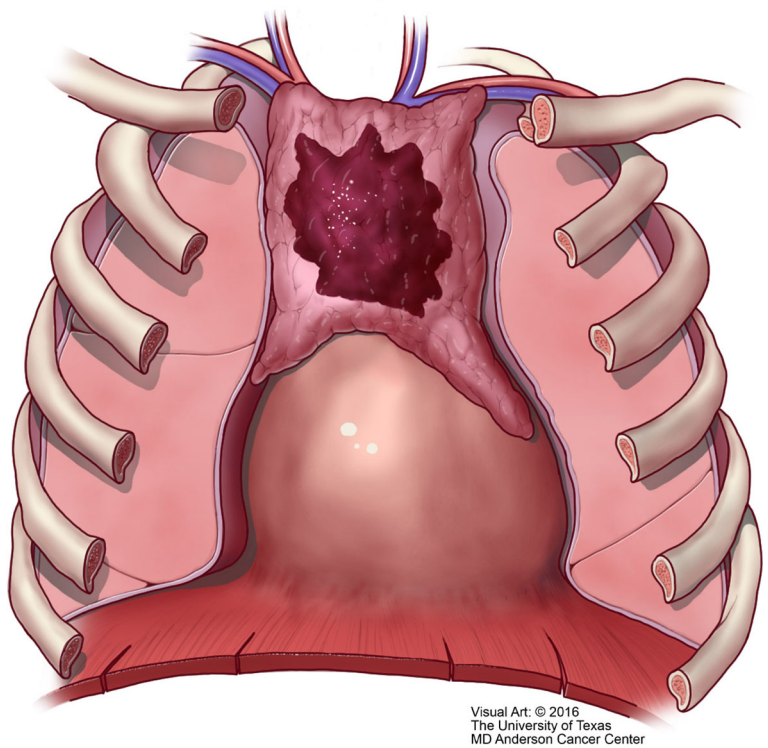

FIGURE 9 | T1 thymic carcinoma in which the tumor is limited to the mediastinal compartment.

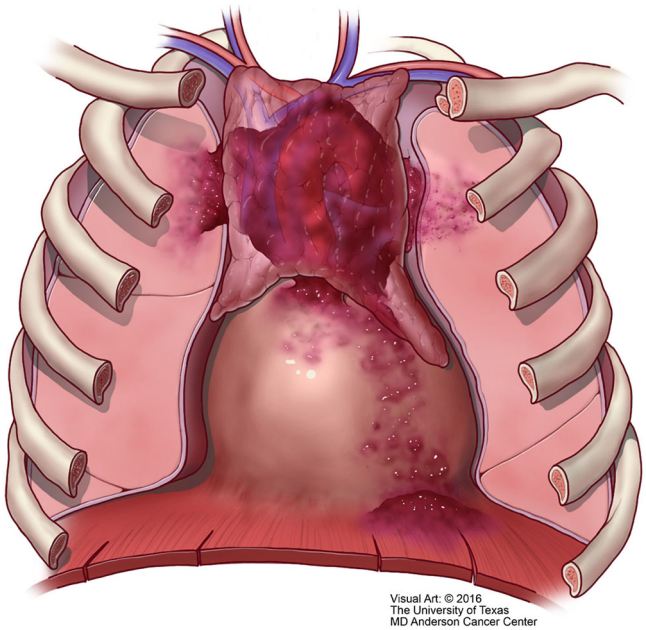

FIGURE 10 | T2 thymic carcinoma in which the tumor invades adjacent structures but within the mediastinal compartment.

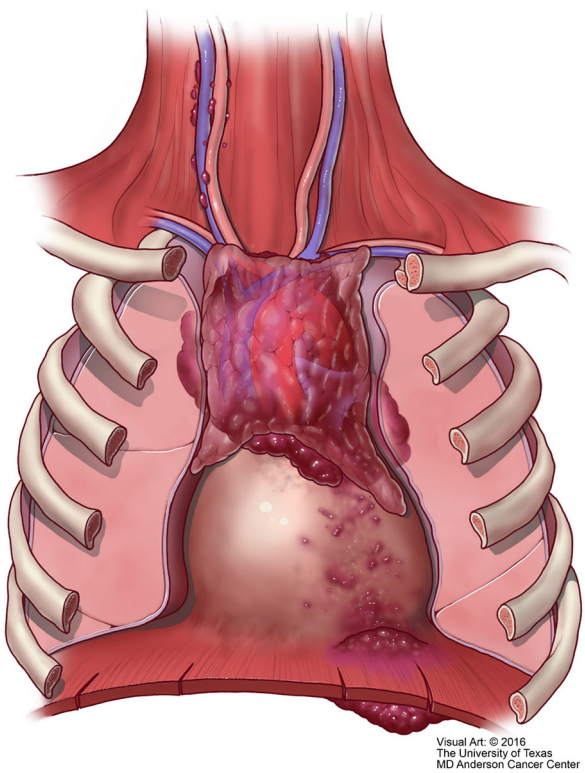

FIGURE 11 | M1 thymic carcinoma in which the tumor invades below the diaphragm or above the thoracic inlet (with permission from Dr. Moran Copyright © 2016).

whether the TNM system is applicable to thymoma, we consider that the TNM system is definitely applicable to thymic carcinoma. There is nothing new in that affirmation as there have been several studies using TNM for thymoma that have concluded that TNM is better suited for thymic carcinoma (41–43). However, the authors of the latest version of the WHO book for thoracic tumors (44) have endorsed the use of TNM for all thymic epithelial tumors. We disagree not only with the general use of TNM for all thymic epithelial neoplasm but also to some extent with the definitions in the different stages that have been proposed. Specific reviews on the topic of TNM staging for thymomas have already been presented in the literature (45). In our own experience, we have observed that lymph node metastasis to any lymph node is important in the survival of patients with thymic carcinoma and do not consider that separating lymph nodes between superficial or deep lymph nodes provides a valid statistically meaningful difference in patients with thymic carcinoma. Therefore, based on our own published experienced we have suggested a TNM staging system specifically for thymic carcinoma that is depicted in **Table 1** with the respective illustrative component (**Figures 9–11**). Such assessment has been previously illustrated in some publications and textbooks (46–48).

CONCLUSIONS

It is important to highlight that there is nothing specific in the histology of thymic carcinoma. The diagnosis requires careful clinical and radiological assessment. Because of the different growth patterns present in thymic carcinoma, the tumor may also mimic other tumors of non-thymic origin. In addition, in small mediastinoscopic biopsies, the separation between atypical thymoma and thymic carcinoma may not be easily attained. Even though the TNM system is a good approach for the staging of thymic carcinoma, we consider that the one suggested by the WHO for all thymic epithelial neoplasms is not appropriate for all these tumors. Lymph node metastasis in thymic carcinomas regardless of the location of the lymph node is an important characteristic that plays a role in the clinical outcome of these patients.

AUTHOR CONTRIBUTIONS

Both of the authors DA and CM contributed in the writing of the manuscript. All authors contributed to the article and approved the submitted version.

REFERENCES

1. Weiss GJ. Thymic Carcinoma: Current and Future Therapeutic Interventions. *Expert Opin investigational Drugs* (2010) 19(8):1007–16. doi: 10.1517/13543784.2010.504708
2. Shimosato Y, Kameya T, Nagai K, Suemasu K. Squamous Cell Carcinoma of the Thymus. An Analysis of Eight Cases. *Am J Surg Pathol* (1977) 1(2):109–21. doi: 10.1097/00000478-197706000-0002
3. Suster S, Rosai J. Thymic Carcinoma: A Cliniocopatrologic Study of 60 Cases. *Cancer* (1991) 15:1025–32. doi: 10.1002/1097-0142(19910215)67:4<1025::AID-CNCR2820670427>3.0.CO;2-F
4. Weissferdt A, Moran CA. Thymic Carcinoma, Part 1: A Clinicopathologic and Immunohistochemical Study of 65 Cases. *Am J Clin Pathol* (2012) 138 (1):103–14. doi: 10.1309/AJCP88FZTWANLRCB
5. Snover DC, Levine GD, Rosai J. Thymic Carcinoma. Five Distinctive Histological Variants. *Am J Surg Pathol* (1982) 6(5):451–70. doi: 10.1097/00000478-198207000-00007
6. Weissferdt A, Kalhor N, Bishop J, Jang SA, Ro J, Petersson F, et al. Thymoma: A Clinicoaptholgoical Correlations of 1470 Cases. *Hum Pathol* (2018) 73:7–15. doi: 10.1016/j.humpath.2017.08.018
7. French CA. NUT Carcinoma: Clinicopathologic Features, Pathogenesis, and Treatment. *Pathol Int* (2018) 68:583–95. doi: 10.1111/pin.12727
8. Moran CA, Suster S. Thymoma With Prominent Cystic and Hemorrhagic Changes and Areas of Necrosis and Infarction: A Clinicopathologic Study of 25 Cases. *Am J Surg Pathol* (2001) 25:1086–90. doi: 10.1097/00000478-200108000-00015
9. Weissferdt A, Moran CA. Thymic Carcinoma Associated With Multilocular Thymic Cyst: A Clinicopathologic Study of 7 Cases. *Am J Surg Pathol* (2011) 35(7):1074–9. doi: 10.1097/PAS.0b013e31821c7402
10. Wang L, Wang D, Qian K, Lu D, Chen L, Zhao L, et al. Thymic Adenocarcinoma Associated With Thymic Cyst: A Case Report and Review of Literature. *Int J Clin Exp Pathol* (2015) 8(5):5890.
11. Weissferdt A, Kalhor N, Moran CA. Cystic Well-Differentiated Squamous Cell Carcinoma of the Thymus: A Clinicopathological and Immunohistochemical Study of Six Cases. *Histopathology* (2016) 68(3):333–8. doi: 10.1111/his.12748
12. Dimery IW, Lee JS, Blick M, Pearson G, Spitzer G, Hong WK. Association of the Epstein-Barr Virus With Lymphoepithelioma of the Thymus. *Cancer* (1988) 61(12):2475–80. doi: 10.1002/1097-0142(19880615)61:12<2475::AID-CNCR2820611215>3.0.CO;2-5
13. Suster S, Moran CA. Thymic Carcinoma: Spectrum of Differentiation and Histologic Types. *Pathology* (1998) 30(2):111–22. doi: 10.1080/00313029800169056
14. Moran CA, Suster S. Thymic Carcinoma: Current Concepts and Histologic Features. *Hematology/oncology Clinics North America* (2008) 22(3):393–407. doi: 10.1016/j.hoc.2008.03.002
15. Ritter JH, Wick MR. Primary Carcinomas of the Thymus Gland. *Semin Diagn pathology;* (1999) 16:18–31.
16. Suster S, Moran CA. Spindle Cell Thymic Carcinoma: Clinicopathologic and Immunohistochemical Study of a Distinctive Variant of Primary Thymic Epithelial Neoplasm. *Am J Surg Pathol* (1999) 23(6):691–700. doi: 10.1097/00000478-199906000-00009
17. Nonaka D, Rodriguez J, Rollo JL, Rosai J. Undifferentiated Large Cell Carcinoma of the Thymus Associated With Castleman Disease-Like Reaction: A Distinctive Type of Thymic Neoplasm Characterized by an Indolent Behavior. *Am J Surg Pathol* (2005) 29(4):490–5. doi: 10.1097/01.pas.0000155148.45423.b5
18. Weissferdt A, Moran CA. Anaplastic Thymic Carcinoma: A Clinicopathologic and Immunohistochemical Study of 6 Cases. *Hum Pathol* (2012) 43(6):874–7. doi: 10.1016/j.humpath.2011.07.015
19. Weissferdt A, Moran CA. Micronodular Thymic Carcinoma With Lymphoid Hyperplasia: A Clinicopathological and Immunohistochemical Study of Five Cases. *Modern Pathol* (2012) 25(7):993–9. doi: 10.1038/modpathol.2012.40
20. Suister S, Moran CA. Micronodular Thymoma With Lymphoid B-Cell Hyperplasia: Clinicopathologic and Immunohistochemical Study of Eighteen Cases of a Distinctive Morphologic Variant of Thymic Epithelial Neoplasm. *Am J Surg Pathol* (1999) 23:955–62. doi: 10.1097/00000478-199908000-00014
21. Kalhor N, Moran CA. Primary Thymic Adenocarcinomas: A Clinicopathological and Immunohistochemical Study of 16 Cases With Emphasis on the Morphological Spectrum of Differentiation. *Hum Pathol* (2018) 74:73–82. doi: 10.1016/j.humpath.2018.01.011
22. Ra SH, Fishbein MC, Baruch-Oren T, Shintaku P, Apple SK, Cameron RB, et al. Mucinous Adenocarcinomas of the Thymus: Report of 2 Cases and Review of the Literature. *Am J Surg Pathol* (2007) 31(9):1330–6. doi: 10.1097/PAS.0b013e31802f72ef

23. Moser B, Schiefer AI, Janik S, Marx A, Prosch H, Pohl W, et al. Adenocarcinoma of the Thymus, Enteric Type: Report of 2 Cases, and Proposal for a Novel Subtype of Thymic Carcinoma. *Am J Surg Pathol* (2015) 39(4):541–8. doi: 10.1097/PAS.0000000000000359
24. Akiba J, Harada H, Yokoyama S, Hashiguchi T, Kawahara A, Mitsuoka M, et al. Mucinous Cystic Tumor With CK20 and CDX2 Expression of the Thymus: Is This a Benign Counterpart of Adenocarcinoma of the Thymus, Enteric Type? *Pathol Int* (2016) 66(1):29–33. doi: 10.1111/pin.12361
25. Moran CA, Suster S. Mucoepidermoid Carcinoma of the Thymus: A Clinicopathologic Study of Six Cases. *Am J Surg Pathol* (1995) 19:826–34. doi: 10.1097/00000478-199507000-00011
26. Nonaka D, Klimstra D, Rosai J. Thymic Mucoepidermoid Carcinoma: A Clinicopathologic Study of 10 Cases and Review of the Literature. *Am J Surg Pathol* (2004) 28:1526–31. doi: 10.1097/01.pas.0000137999.23780.2a
27. Weissferdt A, Kalhor A, Moran CA. Pleuromediastinal Epithelial-Myoepithelial Carcinoma: A Clinicopathologic and Immunohistochemical Study of Two Cases. *Am J Clin Pathol* (2016) 146:736–40. doi: 10.1093/ajcp/aqw199
28. Roden AC, Erickson-Johnson MR, Eunhee SY, García JJ. Analysis of MAML2 Rearrangement in Mucoepidermoid Carcinoma of the Thymus. *Hum Pathol* (2013) 44(12):2799–805. doi: 10.1016/j.humpath.2013.07.031
29. Prieto-Granada CN, Inagaki H, Mueller J. Thymic Mucoepidermoid Carcinoma: Report of a Case With CTRC1/3-MALM2 Molecular Studies. *Int J Surg Pathol* (2015) 23(4):277–83. doi: 10.1177/1066896915576959
30. Perez YE, Moran CA. The Thymus: General Concepts on Embryology, Anatomy, Histology, and Immunohistochemistry. *Semin Diagn Pathol* (2022) 39(2):86–91. doi: 10.1053/j.semdp.2021.06.003
31. Hishima T, Fukayama M, Fujisawa M, Hayashi Y, Arai K, Funata N, et al. CD5 Expression in Thymic Carcinoma. *Am J Pathol* (1994) 145(2):268.
32. Kornstein MJ, Rosai J. CD5 Labeling of Thymic Carcinomas and Other Nonlymphoid Neoplasms. *Am J Clin Pathol* (1998) 109(6):722–6. doi: 10.1093/ajcp/109.6.722
33. Tateyama H, Eimoto T, Tada T, Hattori H, Murase T, Takino H. Immunoreactivity of a New CD5 Antibody With Normal Epithelium and Malignant Tumors Including Thymic Carcinoma. *Am J Clin Pathol* (1999) 111(2):235–40. doi: 10.1093/ajcp/111.2.235
34. Nonaka D, Henley JD, Chiriboga L, Yee H. Diagnostic Utility of Thymic Epithelial Markers CD205 (DEC205) and Foxn1 in Thymic Epithelial Neoplasms. *Am J Surg Pathol* (2007) 31(7):1038–44. doi: 10.1097/PAS.0b013e31802b4917
35. Kojika M, Ishii G, Yoshida J, Nishimura M, Hishida T, Ota S-j, et al. Immunohistochemical Differential Diagnosis Between Thymic Carcinoma and Type B3 Thymoma: Diagnostic Utility of Hypoxic Marker, GLUT-1, in Thymic Epithelial Neoplasms. *Modern Pathol* (2009) 22(10):1341–50. doi: 10.1038/modpathol.2009.105
36. Hirabayashi H, Fujii Y, Sakaguchi M, Tanaka H, Yoon HE, Komoto Y, et al. P16ink4, pRB, P53 and Cyclin D1 Expression and Hypermethylation of CDKN2 Gene in Thymoma and Thymic Carcinoma. *Int J Cancer* (1997) 73 (5):639–44. doi: 10.1002/(SICI)1097-0215(19971127)73:5<639::AID-IJC5>3.0.CO;2-Y
37. Yoh K, Nishiwaki Y, Ishii G, Goto K, Kubota K, Ohmatsu H, et al. Mutational Status of EGFR and KIT in Thymoma and Thymic Carcinoma. *Lung Cancer* (2008) 62(3):316–20. doi: 10.1016/j.lungcan.2008.03.013
38. Zettl A, Ströbel P, Wagner K, Katzenberger T, Ott G, Rosenwald A, et al. Recurrent Genetic Aberrations in Thymoma and Thymic Carcinoma. *Am J Pathol* (2000) 157(1):257–66. doi: 10.1016/S0002-9440(10)64536-1
39. Girard N, Shen R, Guo T, Zakowski MF, Heguy A, Riely GJ, et al. Comprehensive Genomic Analysis Reveals Clinically Relevant Molecular Distinctions Between Thymic Carcinomas and Thymomas. *Clin Cancer Res* (2009) 15(22):6790–9. doi: 10.1158/1078-0432.CCR-09-0644
40. Masaoka A. Staging System of Thymoma. *J Thorac Oncol* (2010) 5(10):S304–S12. doi: 10.1097/JTO.0b013e3181f20c05
41. Tsuchiya R, Koga K, Matsuno Y, Mukai K, Shimosato Y. Thymic Carcinoma: Proposal for Pathological TNM and Staging. *Pathol Int* (1994) 44(7):505–12. doi: 10.1111/j.1440-1827.1994.tb02600.x
42. Blumberg D. Thymic Carcinoma: Current Staging Does Not Predict Prognosis. *J Thorac Cardiovasc Surg* (1999) 117:628–30.
43. Girard N, Mornex F, Van Houtte P, Cordier J. Thymoma and Thymic Carcinoma. In: *Management of Rare Adult Tumours*. New York, USA: Springer (2009). p. 401–13.
44. World Health Organization (WHO). Classification of Tumors. In: *Thoracic Tumours*, *5th Ed*, vol. 5. Lyon, France. (2021).
45. Moran CA. Thymoma Staging: An Analysis of the Different Schemas. *Adv Anat Pathol* (2021) 28:298–305. doi: 10.1097/PAP.0000000000000315
46. Weissferdt A, Moran CA. Thymic Carcinoma, Part 2: A Clinicopathologic Correlation of 33 Cases With a Proposed Staging System. *Am J Clin Pathol* (2012) 138(1):115–21. doi: 10.1309/AJCPLF3XAT0OHADV
47. Kalhor N, Moran C. Thymic Carcinoma. *Mediastinal Pathology Springer* (2019) . p:237–86. doi: 10.1007/978-3-319-98980-8_8
48. Kalhor N, Weissferdt A, Moran CA. Thoracic Pathology, Chapter 11. In: *Oncological Surgical Pathology*, vol. I, Chapter 11. New York, USA: Springer (2020). p. 649–50.

Conflict of Interest: The authors declare that the research was conducted in the absence of any commercial or financial relationships that could be construed as a potential conflict of interest.

Publisher's Note: All claims expressed in this article are solely those of the authors and do not necessarily represent those of their affiliated organizations, or those of the publisher, the editors and the reviewers. Any product that may be evaluated in this article, or claim that may be made by its manufacturer, is not guaranteed or endorsed by the publisher.

Copyright © 2022 Alqaidy and Moran. This is an open-access article distributed under the terms of the Creative Commons Attribution License (CC BY). The use, distribution or reproduction in other forums is permitted, provided the original author(s) and the copyright owner(s) are credited and that the original publication in this journal is cited, in accordance with accepted academic practice. No use, distribution or reproduction is permitted which does not comply with these terms.

frontiers | Frontiers in Oncology

ORIGINAL RESEARCH
published: 13 May 2022
doi: 10.3389/fonc.2022.869982

Computed Tomography-Based Radiomics for Differentiation of Thymic Epithelial Tumors and Lymphomas in Anterior Mediastinum

Wenzhang He[1†], Chunchao Xia[1†], Xiaoyi Chen[1], Jianqun Yu[1], Jing Liu[1], Huaxia Pu[1], Xue Li[1], Shengmei Liu[1], Xinyue Chen[2] and Liqing Peng[1]*

[1] Department of Radiology, West China Hospital, Sichuan University, Chengdu, China, [2] Computed Tomography (CT) Collaboration, Siemens Healthineers, Chengdu, China

OPEN ACCESS

Edited by:
Mylene Truong,
University of Texas MD Anderson Cancer Center, United States

Reviewed by:
Massimo Galia,
University of Palermo, Italy
Guolin Ma,
China-Japan Friendship Hospital, China

***Correspondence:**
Liqing Peng
pengliqing@wchscu.cn

[†]These authors have contributed equally to this work and share first authorship

Specialty section:
This article was submitted to Thoracic Oncology, a section of the journal Frontiers in Oncology

Received: 05 February 2022
Accepted: 11 April 2022
Published: 13 May 2022

Citation:
He W, Xia C, Chen X, Yu J, Liu J, Pu H, Li X, Liu S, Chen X and Peng L (2022) Computed Tomography-Based Radiomics for Differentiation of Thymic Epithelial Tumors and Lymphomas in Anterior Mediastinum. Front. Oncol. 12:869982. doi: 10.3389/fonc.2022.869982

Objective: To investigate the differential diagnostic performance of computed tomography (CT)-based radiomics in thymic epithelial tumors (TETs) and lymphomas in anterior mediastinum.

Methods: There were 149 patients with TETs and 93 patients with lymphomas enrolled. These patients were assigned to a training set (n = 171) and an external validation set (n = 71). Dedicated radiomics prototype software was used to segment lesions on preoperative chest enhanced CT images and extract features. The multivariable logistic regression algorithm was used to construct three models according to clinico-radiologic features, radiomics features, and combined features, respectively. Performance of the three models was compared by using the area under the receiver operating characteristic curves (AUCs). Decision curve analysis was used to evaluate clinical utility of the three models.

Results: For clinico-radiologic model, radiomics signature model, and combined model, the AUCs were 0.860, 0.965, 0.975 and 0.843, 0.961, 0.955 in the training cohort and the test cohort, respectively (all $P<0.05$). The accuracies of each model were 0.836, 0.895, 0.918 and 0.845, 0.901, 0.859 in the two cohorts, respectively (all $P<0.05$). Compared with the clinico-radiologic model, better diagnostic performances were found in the radiomics signature model and the combined model.

Conclusions: Radiomics signature model and combined model exhibit outstanding and comparable differential diagnostic performances between TETs and lymphomas. The CT-based radiomics analysis might serve as an effective tool for accurately differentiating TETs from lymphomas before treatment.

Keywords: radiomics, thymic epithelial tumors, lymphoma, anterior mediastinum, computed tomography

INTRODUCTION

Thymic epithelial tumors (TETs), including thymomas and thymic carcinomas, are derived from thymic epithelial cells and are relatively rare mediastinal tumors (1). Lymphoma is divided into Hodgkin's lymphoma and non-Hodgkin's lymphoma (2). It is a serious malignant tumor derived from the lymphatic system, accounting for 3.2% of newly diagnosed neoplasms and 2.9% of cancer-specific mortality in China in 2018 (3). The difference is that anterior mediastinum is not a common primary site of lymphoma, but a common site of TETs (4).

For TETs, even the well-differentiated thymoma subtypes are considered to be malignant tumors with indolent growth, they also show potential for local invasion, pleural dissemination, and even distant metastasis. Therefore, once TETs are detected, surgical treatment is the mainstay treatment, and radiotherapy, chemotherapy, and other adjuvant treatments are usually supplements depending on final pathology and clinical stage according to relating treatment guidelines (5, 6). On the contrary, radiotherapy and chemotherapy are the first-line options for the treatment of lymphoma while surgical treatment is not recommended according to treatment guidelines for malignant lymphoma in 2021 in China (2, 7).

TETs and lymphomas in anterior mediastinum usually manifest as soft-tissue masses or nodules with similar imaging features (8). In clinical practice, based on typical clinical manifestations and traditional imaging findings, such as with or without myasthenia gravis, age of onset, lymphadenopathy, and imaging features, partial patients could be accurately diagnosed (9). However, the preoperative accurate diagnosis of the two types of neoplasms is usually influenced by the overlap of clinical and radiologic manifestations, the heterogeneity of disease manifestations and difficulty to obtain pathological tissues due to the complexity of the anterior mediastinum. Based on previous computed tomography (CT)-based routine preoperative examinations, although preoperative biopsy is recommended, non-essential or non-therapeutic thymectomy is not uncommon for patients with anterior mediastinal space-occupying lesions (4, 6).

Therefore, it is of great value to distinguish TETs and lymphomas non-invasively before management. Recently, radiomics with machine learning algorithms to mine high-dimensional invisible and interpretable image information into objective and quantitative mathematical data has been an established tool in the differential diagnosis of nodules/masses, prediction of tumor pathological subtypes, evaluation of disease sensitivity to treatment (10–14). According to the literature, there were only a few radiomics-based studies on anterior mediastinal diseases, especially TETs (11, 15). Some previous studies have verified that radiomics could be used for the grading of TETs and the diagnosis of partial anterior mediastinal nodules or masses (11, 15, 16). CT is commonly used in the diagnosis of chest diseases. Compared with traditional CT examination and clinical data, radiomics features extracted from CT images could provide more diagnostic information. Therefore, patients of lymphoma with atypical clinical and radiologic manifestations may avoid unnecessary surgery and receive effective treatment earlier.

Thus, we aimed to investigate the differential diagnostic performance of CT-based radiomics in thymic epithelial tumors (TETs) and lymphomas in anterior mediastinum.

MATERIALS AND METHODS

Subjects

The ethics committee of the participating center approved the study. The need for informed patient consent was waived because of the retrospective nature of the analysis and the use of anonymized data.

An author collected hospitalized patients diagnosed with TETs (including thymoma, thymic carcinoma) and lymphoma within the time range of October 2008 to March 2021 from the information management department of West China Hospital. A total of 852 patients were found, of which 332 had TETs and 520 had lymphomas. The author queried the patient's pathological data from the Electronic Medical Records and searched for patients' chest enhanced computed tomography (CECT) images in DICOM format in the Picture Archiving and Communication System, and the time of CT examination was within 30 days before the patient's pathological samples were obtained. Pathological results came from thoracentesis, lymphadenectomy, or postoperative tissue. Then pathologically confirmed patients with CECT images had 195 with lymphomas and 222 with TETs.

Each enrolled patient met the following exclusion criteria. The exclusion criteria included : 1) age<16 years old, 2) with intervention before CECT examination, 3) history of malignancy or concomitant malignancy, 4) inadequate clinical data, 5) TETs with completely cystic components, and 6) inadequate image quality. Consequently, 242 patients, including 149 patients with TETs and 93 patients with lymphomas, consisted of study cohorts. The patient selection workflow is shown in **Figure 1**. Subtype distribution of two tumors is shown in **Figure 2**.

Clinico-Radiologic Characteristics

For TETs patients and lymphoma patients, the characteristic of P<0.10 difference between the two groups would be further used for univariate logistic regression analysis. The univariate analysis results are shown in **Tables 1** and **2**. **Table 2** showed the clinical characteristics, including clinical manifestations, symptoms, and laboratory examination results. Clinical manifestations and symptoms were collected from the first hospitalization record in the Hospital Information System by one author. Myasthenia gravis and autoimmune diseases were counted separately. In addition, autoimmune diseases including myasthenia gravis, systemic lupus erythematosus, ankylosing spondylitis, and so on, were related to thymoma (17). The laboratory results came from once test obtained before the treatment and within 3 days of the CT examination.

In PACS, two radiologists (with 5 years and 10 years of experience with chest CT, respectively) worked together to analyze radiological characteristics, including morphological

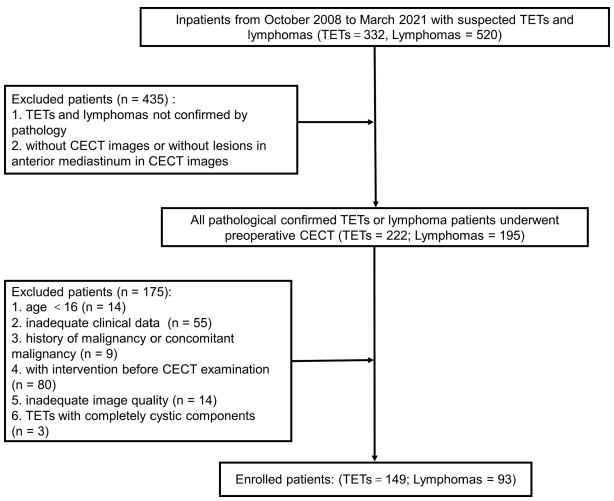

FIGURE 1 | The patient selection workflow. TETs, thymic epithelial tumors; CECT, chest enhanced computed tomography.

related features and some quantifiable features, with the naked eye in the Picture Archiving and Communication System. When there was an inconsistency, the two radiologists would reach an agreement through discussion. Normalized enhancement value (NEV) was calculated as NEV = EV*lesion*/EV*aorta*, where EV*lesion* and EV*aorta* are the CT value difference before and after enhancement in the largest cross-section of the lesion and in the lumen of the ascending aorta at the same cross-section. The CT images used to extract radiomics features and to analysis by the naked eye came from the same CT examination. When more than once CT examination was available for radiological analysis, we selected the last CT examination before surgery or biopsy.

Chest Enhanced CT Scan

Before CECT images collection, a total of 80–120 mL (1.5 mL/kg) of iodinated contrast agent was injected *via* the antecubital vein at a flow rate of 4 mL/s. CECT scans were obtained at 40 sec after injection of contrast media. All the CECT images were acquired by standard institutional procedure protocols and stored in DICOM format. Related parameters are shown in **Table 3**. In all patients, CT images were acquired in the supine position at full inspiration.

ROI Acquisition and Radiomics Feature Extraction

The CECT images in DICOM format from selected patients were segmented by using "Radiomics" (Syngo. *via* Frontier, Vision 1.0.0, Siemens, Germany), a dedicated prototype software, and this program employs an embedded 3D-printing technique in a semi-automatic manner to label the preoperative soft tissue. The overall procedures of this analysis scheme were composed of two major steps: first, tumor segmentation was conducted manually; and thereafter, texture features were calculated automatically. The manual segmentation of neoplasms in the anterior mediastinum was performed independently by a chest radiologist. The region of interest (ROI) was depicted around the border of each tumor (**Figure 3**). After segmenting a 3-dimensional volume of interest (3D-VOI), texture features were automatically calculated and extracted. In addition, another chest radiologist segmented 30 cases including 15 pathologically proven TETs and 15 lymphomas randomly selected from all samples to evaluate the inter-operator variability. Features with intraclass correlation coefficient value higher than 0.8 were considered stable and used for model construction. The definition included the following criteria : 1) calcification, hemorrhage, liquefaction, necrosis, and blood vessels within the lesion with the largest diameter <2 mm in the tumor were regarded as components of the lesion, and will be included ; 2) the soft-tissue boundary avoided surrounding fat, metal stents, blood, and other structures ; 3) to eliminate partial volume effect, the outline boundary was ≤1 mm of the lesion, and the first and last layers of the lesion were removed.

Before performing features calculations, "Radiomics" automatically resampled the 3D-VOI to a pixel pitch of 1.0 mm in three anatomical directions to reduce the impact of pixel size and thickness. In the original VOIs, different filters would be applied, such as the Laplacian of Gaussian filtering, wavelet filtering, nonlinear intensity transformation, and others. Finally, 1226 radiomics features were as follows : 1) 17 shape and

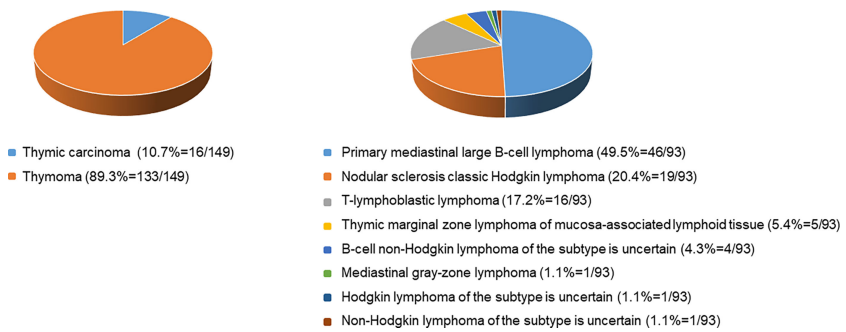

FIGURE 2 | Subtype distribution of thymic epithelial tumors and lymphomas.

TABLE 1 | Estimated risk of radiologic characteristics by univariate logistic regression analysis.

Variables	TETs	Lymphomas	Estimated risk	*P* valve
Max diameter (cm)	5.2 ± 2.4	9.7 ± 3.0	1.87(1.61-2.22)	<0.001
Location				
0, central	130 (87.2)	76 (81.7)	1.53(0.74-	0.200
1, peripheral	19 (12.8)	17 (18.3)	3.13)	
Morphology				
0, regular	48 (32.2)	12 (12.9)	3.21(1.64-	0.001
1, irregular	101 (67.8)	81 (87.1)	6.69)	
Fat gap				
0, present	43 (28.9)	7 (7.5)	4.98(2.26-	<0.001
1, absent	106 (71.1)	86 (92.5)	12.60)	
Small vessel				
0, absent	93 (62.4)	8 (8.6)	17.6 (8.38-	<0.001
1, present	56 (37.6)	85 (91.4)	42.00)	
Pericardial effusion				
0, absent	138 (92.6)	31 (33.3)	25.1 (12.30-	<0.001
1, present	11 (7.4)	62 (66.7)	55.60)	
Pleural effusion				
0, absent	135 (90.6)	53 (57.0)	7.28 (3.74-	<0.001
1, present	14 (9.4)	40 (43.0)	14.90)	
Necrosis				
0, absent	91 (61.1)	23 (24.7)	4.78 (2.72-	<0.001
1, present	58 (38.9)	70 (75.3)	8.62)	
Density uniformity				
0, uniform	56 (37.6)	16 (17.2)	2.90 (1.57-	<0.001
1, nonuniform	93 (62.4)	77 (82.8)	5.59)	
Boundary clarity				
0, clear	114 (76.5)	19 (20.4)	12.7 (6.88-	<0.001
1, vague	35 (23.5)	74 (79.6)	24.40)	
CT value (HU)	45.6 ± 11.4	42.2 ± 9.3	0.97 (0.94-0.99)	0.019
NEV	0.119 ± 0.079	0.088 ± 0.055	0.00 (0.00-0.05)	0.001

Max diameter, The longest diameter in the largest cross-section of the tumor; Location, Peripheral is defined as more than 2/3 of the tumor volume is located on one side of the mid-sternal line; Morphology, Lesions with round, oval, or rectangular shape are defined as regular morphology; Fat gap, Fat gaps between the nodules/masses and the ascending aorta or main pulmonary artery; Small vessel, Continuous blood pool enhancement on the chest enhanced CT image; Pericardial effusion (Pleural effusion), CT images show pericardial (pleural) thickening, pericardial (pleural) effusion, or both; Boundary clarity, Existing fuzzy boundary between the tumor and the surrounding structures, which is defined as unclear boundary; NEV, Normalized enhancement value.

size features, 2) 18 first-order features, 3) 65 texture features, 4) 1116 high-order features and features that have undergone multiple mathematical transformations (wavelet, square, square root, logarithm, and exponents decompositions of first-order statistics and texture features), were extracted from the original and post-processed 3D-VOI of every patient.

Feature Selection and Model Building

All patients were first splitted into training cohort and test cohort with a ratio of 7:3 by using the stratified random sampling technique: 171 patients (mean age, 43.2 ± 14.8 years; TETs, 105 cases; lymphoma, 66 cases) were allocated into the training cohort; 71 patients (mean age, 42.7 ± 15.7 years; TETs, 44 cases; lymphoma, 27 cases) were allocated into the test cohort. Training cohort was used to train the model based on the least absolute shrinkage and selection operator regression model with tuned parameter of lambda. Since there was a class imbalance that might affect the model tuning, synthetic minority over-sampling technique was applied to the training cohorts before formal model training. The lambda was tuned across multiple values between 0.01-0.2 and the optimum value was decided when the model gained the highest AUC by 5 repeats 10-fold cross-validation. In addition, this performance of optimal setting was also recorded. Next, the feature importance ranking list was derived based on this least absolute shrinkage and selection operator model. Appropriate number of features were selected on this order of importance to simplify the radiomics multivariate logistic regression model, based on acceptable performance relative to the optimal setting.

Regarding the clinical and radiologic features, univariate logistic regression was applied. In addition, features with statistical significance (P<0.05) were selected. The features enrolled in the radiomics and clinico-radiologic model were the candidates for the combined model. Similarly, those features with no statistical significance (P≥0.05) in the combined model were removed to ease the redundancy of the model.

The performance of the model according to receiver operator curves (ROC) was evaluated in training and independent test cohorts, respectively. Besides the diagnostic performance-related statistics by these two cohorts regarding sensitivity, specificity,

TABLE 2 | Estimated risk of clinical characteristics by univariate logistic regression analysis.

Variables	TETs	Lymphomas	Estimated risk	*P* valve
Age (years)	50.2 ± 12.4	31.2 ± 10.0	0.88 (0.85-0.91)	<0.001
Sex				
0, male	73 ± 49.0	42 ± 45.2	1.17 (0.69-1.97)	0.600
1, female	76 ± 51.0	51 ± 54.8		
Chest pain				
0, absent	121 (81.2)	60 (64.5)	2.38 (1.32-4.32)	0.004
1, present	28 (18.8)	33 (35.5)		
Respiratory symptom				
0, absent	105 (70.5)	31 (33.3)	5.10 (2.93-9.07)	<0.001
1, present	44 (29.5)	62 (66.7)		
B symptom				
0, absent	132 (88.6)	77 (82.8)	1.61(0.77-3.39)	0.200
1, present	17 (11.4)	16 (17.2)		
Lymphadenopathy				
0, absent	148 (99.3)	76 (81.7)	33.1(6.61-602.00)	<0.001
1, present	1 (0.7)	17 (18.3)		
Myasthenia gravis				
0, absent	110 (73.8)	92 (98.9)	0.03 (0.00-0.15)	<0.001
1, present	39 (26.2)	1 (1.1)		
Autoimmune disease				
0, absent	106 (71.1)	91 (97.8)	0.05 (0.01-0.18)	<0.001
1, present	43 (28.9)	2 (2.2)		
Red blood cell count ($\times10^{12}$/L)	4.6 ± 0.7	4.6 ± 0.6	0.93 (0.61-1.42)	0.700
Leukocyte count ($\times10^{9}$/L)	6.5 ± 2.6	14.9 ± 43.7	1.00 (0.99-1.00)	0.056
Lymphocyte count ($\times10^{9}$/L)	1.8 ± 0.7	1.3 ± 1.1	0.39 (0.25-0.59)	<0.001
Platelet count ($\times10^{9}$/L)	187.8 ± 70.0	290.0 ± 123.3	1.01 (1.01-1.02)	<0.001
Lactate dehydrogenase (IU/L)	163.5 ± 40.2	437.0 ± 385.2	1.02 (1.02-1.03)	<0.001

B symptoms is defined as the patient manifests at least one of the following three symptoms: 1) unexplained fever >38℃, 2) night sweats , 3) weight loss more than 10% within 6 months respiratory symptom including cough, wheezing, expectoration, chest tightness, and hemoptysis; lymphadenopathy, lymphadenopathy at physical examination.

and accuracy were illustrated using a confusion matrix. Finally, decision curve analysis was used to evaluate clinical utility of the three models in the training cohort. The workflow of this study is shown in **Figure 3**.

Statistical Analysis

All statistical analyses were performed using R software (version 1.1.453) and SPSS (version 26, SPSS Chicago, IL). Qualitative variables were presented as frequencies. Normally distributed variables were shown as the mean ± SD (standard deviation). Between TETs and lymphomas (two groups), the clinico-radiologic characteristics were compared by using the chi-square test or Fisher's exact test for categorical variables and independent t-test or the Mann-Whitney U test for continuous variables. $P<0.05$ indicated statistical difference. Univariate logistic regression analysis was performed for those parameters that showed $P<0.10$ when compared between two groups. The results of univariate logistic regression analysis are shown as OR (95% CI) and *P* value in **Tables 1** and **2**. Inter-operator variability of the radiomics features was assessed with ICC. Interclass correlation coefficient (≦0.40, poor agreement; 0.41–0.60, moderate agreement; 0.61–0.80, good agreement; and>0.80, excellent agreement). The ROCs of the radiomics model in the two cohorts were compared with the DeLong test to evaluate whether overfitting occurred. Decision curve analysis was performed to determine the clinical usefulness of the three

TABLE 3 | Computed tomography image acquisition parameters.

Manufacturers	Image extent (pixels)	Voxel space (mm)	Slice thickness (mm)	Voltage (kV)	Tube current (mA)
SIEMENS, n=144	512×512	Mean ± SD	0.7, n= 2; 1.0, n=2	80, n= 2	Mean ± SD
PHILIPS, n=65		0.707 ± 0.077	2.0, n=1; 2.5, n=1	100, n= 70	278.6 ± 100.8
UIH, n=12		Median 0.702	5.0, n=220; 7.0, n=5	120, n=168	Median 267
GE, n=21		Range	7.5, n=1; 8.0, n=9	140, n=2	Range
		0.539-0.973			79-649

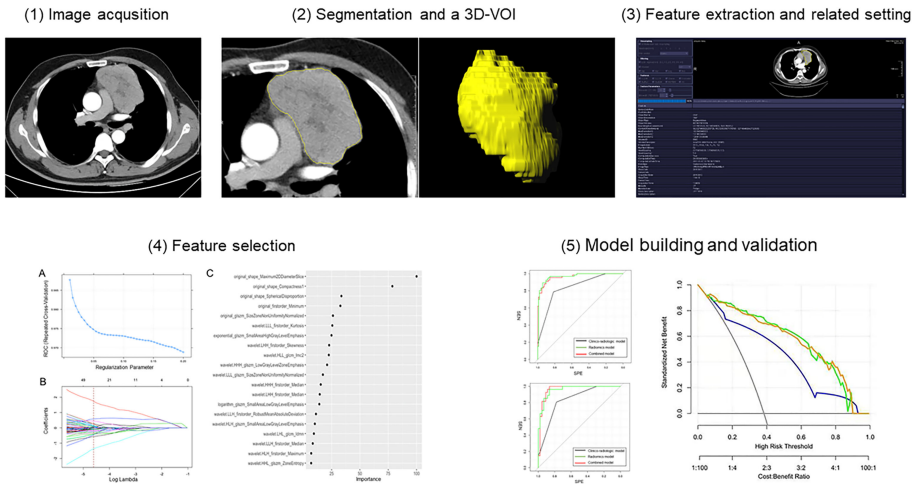

FIGURE 3 | Workflow diagram of radiomics analysis. 3D-VOI, 3-dimensional volume of interest.

models by calculating the net benefits at different threshold probabilities in the whole cohort. The net benefit is equivalent to the proportion of net true positives in brief.

RESULTS

Basic Clinico-Radiologic Characteristics

Of the 242 patients, 149 patients were diagnosed with TETs and 93 patients with lymphomas. Compared with patients with lymphoma, patients with TETs had a later age of onset (P<0.001) and showed less chest pain (P=0.004), respiratory symptoms (P<0.001), and lymphadenopathy (P<0.001). Regarding gender distribution and B symptoms, no significant differences were found between the two groups (P=0.600, 0.200, respectively). In laboratory tests, compared with lymphoma patients, TETs patients had higher lymphocyte counts (P<0.001), lower platelet counts (P<0.001), and lower lactate dehydrogenase (P<0.001), while red blood cell counts and white cell counts showed no significant difference (P=0.700, P=0.056, respectively). Details of the demographical data and clinical characteristics of the training and test cohorts are summarized in **Table 2**.

For comparison of the radiologic features in TETs and lymphoma, there was no significant difference about location distribution between the two groups (P=0.200). The TETs group had a smaller tumor diameter than the lymphoma group (P<0.001), but higher CT value and NEV (P<0.001, P=0.001, respectively). Compared with the lymphoma group, more obvious fat gap between the lesion and big vessels (pulmonary trunk and ascending aorta), less pleural and pericardial effusion existed in the TETs group (all P<0.001). Less necrosis, better density uniformity, and clearer boundary of lesions were found in the TETs group (all P<0.001) than the lymphoma group. More comprehensive information is listed in **Table 1**.

Model Building

Among 242 patients in our study, 171 patients were allocated into the training cohort, while 71 patients were in the test cohort. A total of 385 radiomics features were shown to be stable (good and excellent agreement), including 17 shape and size features, 13 first-order features, 34 texture features, and 321 high-order features and features that have undergone multiple mathematical transformations. After SMOTE, the training cohort was up-sampled to the number of 462 with a class ratio of 264:198 for TETs:lymphoma. An AUC of 0.981 (95% CI: 0.971–0.991) suggested that there was no significant affect toward the model tuning from the imbalance between the patient groups in our study. After the tuning process, the optima Lambda was set to be 0.01 for our dataset. The mean AUC for each lambda tuned with our resample by 5-repeated 10-fold cross-validation is shown in **Figure 4A**. In addition, the optimal AUC was reached beyond 0.9. For each tuned lambda, the coefficients of the features are shown in **Figure 4B**. Moreover, the importance ranking list based on the model is shown in **Figure 4C**.

In our study, the regression model with the top 5 features on the order of importance gave us acceptance AUC relative to the optimal setting. Moreover, these five radiomics features by 3D texture analysis in original images included three shape-related features, one first order related feature, and one feature about gray level size zone matrix (GLSZM). Three shape-related features included maximum 2D diameter slice, compactness 1, and spherical disproportion. Minimum as a first-order feature represented minimum eigenvalue and size zone nonuniformity normalized was a feature calculated from GLSZM. Three clinico-radiologic characteristics, including lymphadenopathy (+/-), myasthenia gravis (+/-), and pericardial effusion (+/-), constituted the clinico-radiologic model. For the final combined model, all the features in the radiomics and clinico-radiologic models were enrolled except lymphadenopathy (+/-) which was removed as redundant.

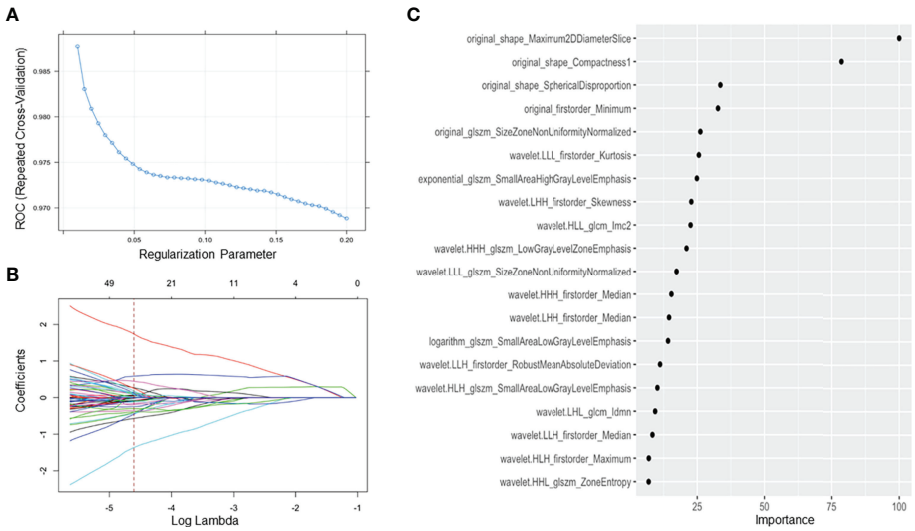

FIGURE 4 | Feature selection using the least absolute shrinkage and selection operator regression method. **(A)** The tuned parameter (λ) in the LASSO model was selected *via* 5 repeats 10-fold cross-validation based on minimum criteria. The dotted blue curve indicates the average binominal deviance values for each model with a given λ. The λ value was set as 0.01 in this study; **(B)** the dotted vertical line was plotted at the selected λ value, resulting in 20 radiomics features; **(C)** sorting the importance of radiomics features, and the top 5 features were included in our model.

Model Validation and Comparison

The ROC results of three models are shown in **Table 4** and **Figure 5**. The performance of the radiomics model was good in the training group with an AUC of 0.965 (95% CI: 0.941-0.990). The classification accuracy, sensitivity, and specificity were 89.5%, 83.3%, and 93.3%, respectively. Good performance was also observed in the test group with AUC being 0.961 (95% CI: 0.917–1.00). The accuracy, sensitivity, and specificity were 90.1%, 92.6%, and 88.6%, respectively. For the clinico-radiologic model, all performance metrics were lower than that of the radiomics model excluding specificity. The AUCs were 0.860 (95% CI: 0.808–0.913) and 0.843 (95% CI: 0.759–0.928) in the training group and test group, respectively. The classification accuracies were 83.6% and 84.5% in the 2 groups, respectively.

In the combined model, AUCs in the training group and independent test group were 0.975 (95% CI: 0.956-0.995) and 0.955 (95% CI: 0.915-0.996), respectively; while the classification accuracies were 89.5% and 90.1%, respectively. In addition, the combined model showed comparative diagnostic performance to radiomics signature model. The performance of the radiomics model and the combined model were both significantly higher than that of the clinical model.

Furthermore, decision curve analysis demonstrated that the combined model and radiomics signature model would offer net benefits over the "TETs-all", "lymphoma-all", and the clinico-radiologic model within a certain range of threshold (5%–90% for combined model; 10%–87% for radiomics signature model) in the training cohort (**Figure 6**). Moreover, the combined model and the radiomics signature model showed comparable net benefits.

DISCUSSION

Due to the differences in therapeutic approaches, accurate diagnosis of TETs and lymphomas before treatment is of great significance for clinical decision (6, 18). CT is a routine examination for chest diseases including mediastinal lesions and lung diseases. Nevertheless, imaging methods such as CT

TABLE 4 | Differentiation performance of clinico-radiologic model, radiomics model, and combined model in the training and test cohorts.

Variables	Training cohort				Test cohort			
	AUC	ACC (%)	SEN (%)	SPE (%)	AUC	ACC (%)	SEN (%)	SPE (%)
Clinico-radiologic model	0.860 (95% CI: 0.808-0.913)	83.6	71.2	91.4	0.843 (95% CI: 0.759-0.923)	84.5	70.4	93.2
Radiomics model	0.965 (95% CI: 0.941-0.990)	89.5	83.3	93.3	0.961(95% CI: 0.917-1.000)	90.1	92.6	88.6
Combined model	0.975 (95% CI: 0.956-0.995)	91.8	89.4	93.3	0.955(95% CI: 0.915-0.996)	85.9	81.5	88.6

AUC, area under the summary receiver operating characteristic curve; ACC, accuracy; SEN, sensitivity; SPE, specificity; CI, confidence interval.

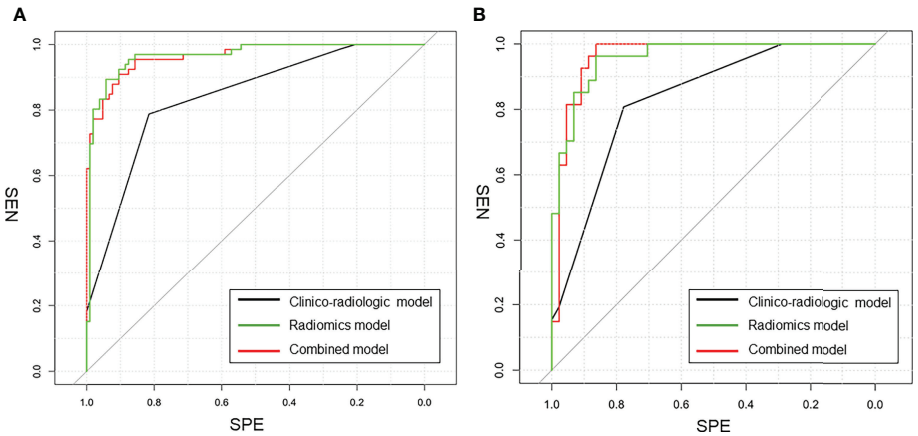

FIGURE 5 | The comparison of ROC curves in this study. **(A)** in the training cohort. AUC = 0.975 for the combined model, 0.860 for the clinico-radiologic model, and 0.965 for the radiomics model; **(B)** in the external validation cohort. AUC = 0.955 for the combined model, 0.843 for the clinico-radiologic model, and 0.961 for the radiomics model.

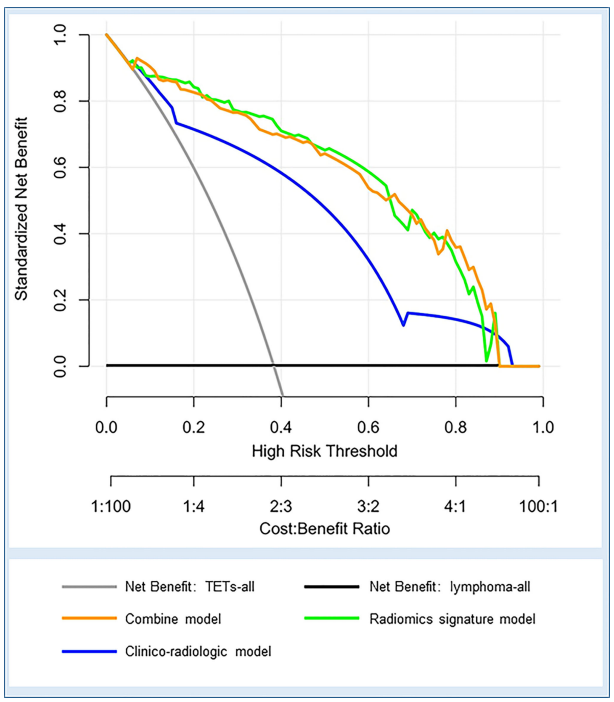

FIGURE 6 | Decision curve analysis for the three models in the whole cohort. The net benefit vs. the threshold probability is plotted. The x-axis shows the threshold probability. The y-axis shows the net benefit. A model is only clinically useful if it has a higher net benefit than the default diagnosis of TETs-all and lymphoma-all. The two curves (orange and green curves) indicate that the combined model and the radiomics signature model are superior to the diagnosis of TETs-all (gray line), the diagnosis of lymphoma-all (black line), and the clinico-radiologic model (blue curve) within a threshold probability of 5%-90% (orange curve) and 10%-87% (green curve).

and magnetic resonance imaging are still challenging in accurate diagnosis of mediastinal masses in clinical practice. Tomiyama et al. (19) reported that for neoplasms in anterior mediastinum, the diagnostic accuracies of CT and MRI for thymoma, thymic carcinoma, and lymphoma were 83%, 13%, 55% and 84%, 13%, 43%, respectively. In the study of Ackman et al. (4), unnecessary or non-therapeutic thymectomy accounted for 43.8% (70/160) of the 160 thymectomy cases including lymphomas (54.3%, 38/70), thymic bed cysts (24.3%, 17/70), and other lesions. The unclear preoperative diagnosis in some patients has led to many unnecessary surgical treatments. Recently, newly emerged radiomics showed potential in accurate differentiation of different space-occupying lesions before treatment using the texture feature analysis. Kayi Cangir et al. (20) revealed that radiomic signature using the k-nearest neighbor classier based on enhanced CT had excellent efficacy for discriminating low- vs. high-risk thymoma groups with an AUC of 0.943 in the validation cohort. As CT is more widely used and it serves as the standard-of-care imaging tool for pre-treatment evaluation of anterior mediastinal diseases, it is more convenient and effective to construct radiomics models using features extracted from routinely obtained contrast CT images. In our study, we developed and validated CT-based radiomics models for non-invasive differentiation of TETs and lymphomas. Our results showed that the AUCs of the radiomic model based on enhanced CT in the training and test cohorts for TETs and lymphomas differentiation were outstanding (0.965 and 0.961, respectively). In addition, this model, with the accuracies of 89.5% and 90.1% in training and test cohorts, respectively, is superior to traditional CT in distinguishing the two sorts of tumors. A study by Kirienko et al. (16) described that a radiomic model to differentiate TETs and lymphomas based on non-enhanced chest CT showed AUCs of 0.93 and 0.84 in the training and test cohorts, respectively. The accuracies of their model in the

training cohort and test cohort were 91.3% and 76.9%, respectively, and it was also better than conventional CT in distinguishing TETs and lymphomas. Compared with the study by Kirienko et al. (16), our study had better results with higher AUCs in two cohorts and better stability between the training cohort and the test cohort, which may be explained by that our study had a larger sample size and the radiomics features were extracted from contrast-enhanced CT images. It is worth noting that a significant enhancement difference between TETs and lymphomas was found in our study, which is consistent with the results of some previous studies (21, 22). Significant blood supply differences exist between the two sorts of tumors. At the fine scale, texture features extracted from the enhanced CT images might represent the distribution of contrast media in the extracellular space between intra- and extravascular (23). Thus, radiomics signature from enhanced CT may be more effective in showing the internal heterogeneity between TETs and lymphoma. In addition, in the study by Huet et al. (24), for the differentiation of high-risk TETs and low-risk TETs, the enhanced CT-based radiomics model using the random forest machine learning classifier achieved an AUC of 0.81, which was better than the AUC of 0.61 by non-enhanced CT-based radiomics model. For tumors at other sites, radiomics from enhanced CT showed excellent performances in assessment of colorectal cancer heterogeneity and differentiation of benign and malignant gallbladder polypoid lesions (22, 24).

Furthermore, based on the obvious enhancement difference between TETs and lymphomas, different techniques were also used to explore the differential value between the two types of tumors. In previous studies, triple-phase CT spectral imaging and contrast-enhanced ultrasound imaging had been used in differentiating thymic neoplasms and lymphomas with the best AUCs of 0.875 and 0.668, respectively (21, 22). In the study by Sakai et al. (25),the accuracy for differentiating thymoma and non-thymoma by dynamic magnetic resonance imaging was 81%. In our study, the radiomics model based on enhanced CT with a best AUC of 0.961 and accuracy of 90.1% had a better differentiation efficacy than the studies above. Compared with imaging features on spectral CT, contrast-enhanced ultrasound, and dynamic magnetic resonance imaging, radiomics signature from contrast enhanced CT also showed superior differential performance between TETs and lymphoma (21, 22, 25). In addition, ^{18}F-FDG PET-CT and whole-body MRI could assess the patients' general condition, which were meaningful to anterior mediastinal primary lymphomas with multiple systemic involvement. It is well known that PET-CT is used for pre-treatment staging, treatment efficacy evaluation, and post-treatment follow-up in patients with lymphoma (26, 27). Further, Lei et al. (28) explored the performance of metabolism parameters, including SUVmean, SUVmax, TLG, and MTV, of ^{18}F-FDG PET-CT for distinguishing TETs from lymphomas. The performance of the study of Lei et al. (28) with best AUC of 0.767 and best accuracy of 72.8% in SUVmax and SUVmin, respectively, was inferior to ours. In general, lymphomas have higher FDG uptake than TETs (28). However, the lower metabolic activity of indolent lymphomas and the markedly different metabolic activity associated with the grade of TETs may be accountable for the unsatisfactory results of metabolic parameters for the differentiation of the two kinds of tumors (27, 29–31). Regrettably, there was no whole-body MRI study in this topic. In addition, whole-body MRI with advantages in whole-body scanning may perform better than chest MRI. Radiomics signature may be related to some of the biological behavior of the tumors as it is able to mine more image information invisible to the naked eyes and objectively quantify the features. These features may be well associated with heterogeneity of the lesion itself (32, 33). Additionally, no extra-cost is needed for the patients.

In terms of clinical factors, lymphadenopathy (–) and myasthenia gravis (+) included in our model revealed a higher risk of patients with TETs than with lymphoma, which was consistent with previous research (16). The top three clinico-radiologic features in the ranking list based on this model with optimal lambda contained myasthenia gravis rather than autoimmune disease. For malignant tumors, pericardial effusion can be caused by pericardial involvement even in patients without symptoms or with atypical symptoms (34). The most common causes of pericardial effusion caused by tumor involvement were lung cancer, breast cancer, and hematologic tumors such as leukemia, Hodgkin's lymphoma, and non-Hodgkin's lymphoma (35). However, pericardial effusion occurred when thymic malignancies invaded the pericardium, but this was uncommon, even if the primary lesion was often in the anterior mediastinum (23). In our study, lymphomas were mainly non-inert growth types as shown in **Figure 2**. In addition, the larger the lymphoma was, the more likely concomitant of local and systemic symptoms such as chest pain, respiratory symptoms, and B symptoms, which may be related to the lymphoma's greater growth capacity and aggressiveness to surrounding tissues (**Table 2**).

In addition, we further established a combined model based on radiomics features and clinico-radiologic characteristics. Compared with the radiomics signature model, the combined model did not show a significant improvement in discriminative efficacy, which yielded AUCs of 0.975 and 0.955, and accuracies of 91.8% and 85.9% in the training and test cohorts, respectively. The superior performance of the combined model in this study may be attributed to the inclusion of radiomics signature, which contain many quantitative features, especially parameters not easy to be obtained through simple visual analysis or conventional imaging tools. Both the radiomics features model and the combined model in the current study had outstanding and comparable performance in distinguishing TETs and lymphomas and can provide a net benefit superior to the diagnosis of "TETs-all", the diagnosis of "lymphoma-all", and the clinico-radiologic model in the decision curve.

There were several limitations in our study. First, selection bias maybe came from the research nature, a retrospective study from a single center. Second, this study included patients over a longer period; thus, the images were collected from CT scanners of different vendors; however, a good result proved the generalization ability of this radiomics signature model.

Finally, the imbalance between groups may affect model tuning. However, the synthetic minority over-sampling technique used in the training group found that the ROC of the model was 0.981 (95% CI: 0.971–0.991) and the imbalance between groups did not affect the model performance.

CONCLUSION

The radiomics signature model and combined model exhibit outstanding and comparable differential diagnostic performances between TETs and lymphomas. The CT-based radiomics analysis might serve as an effective tool for accurate differentiating TETs from lymphomas before treatment in clinical practice.

DATA AVAILABILITY STATEMENT

The original contributions presented in the study are included in the article/supplementary material. Further inquiries can be directed to the corresponding author.

AUTHOR CONTRIBUTIONS

WH, CX, and LP: study design. WH and CX: data collection. WH and CX: data processing. All authors: manuscript writing. All authors: manuscript revision. All authors: final approval of manuscript. All authors contributed to the article and approved the submitted version.

FUNDING

This work was supported by the National Natural Science Foundation of China (No. 81601462) and the Key Research & Development Project of Science and Technology of Sichuan Province (No. 2021YFS0142).

ACKNOWLEDGMENTS

We are grateful to Siemens Healthineers for technical support.

REFERENCES

1. Marx A, Chan JK, Coindre JM, Detterbeck F, Girard N, Harris NL, et al. The 2015 World Health Organization Classification of Tumors of the Thymus: Continuity and Changes. *J Thorac Oncol* (2015) 10(10):1383–95. doi: 10.1097/JTO.0000000000000654
2. Matasar MJ, Zelenetz AD. Overview of Lymphoma Diagnosis and Management. *Radiol Clin North Am* (2008) 46(2):175–98, vii. doi: 10.1016/j.rcl.2008.03.005
3. Liu W, Liu J, Song Y, Zeng X, Wang X, Mi L, et al. Burden of Lymphoma in China, 2006–2016: An Analysis of the Global Burden of Disease Study 2016. *J Hematol Oncol* (2019) 12(1):115. doi: 10.1186/s13045-019-0785-7
4. Ackman JB, Verzosa S, Kovach AE, Louissaint A Jr., Lanuti M, Wright CD, et al. High Rate of Unnecessary Thymectomy and Its Cause. Can Computed Tomography Distinguish Thymoma, Lymphoma, Thymic Hyperplasia, and Thymic Cysts? *Eur J Radiol* (2015) 84(3):524–33. doi: 10.1016/j.ejrad.2014.11.042
5. Conforti F, Pala L, Giaccone G, De Pas T. Thymic Epithelial Tumors: From Biology to Treatment. *Cancer Treat Rev* (2020) 86:102014. doi: 10.1016/j.ctrv.2020.102014
6. Imbimbo M, Ottaviano M, Vitali M, Fabbri A, Leuzzi G, Fiore M, et al. Best Practices for the Management of Thymic Epithelial Tumors: A Position Paper by the Italian Collaborative Group for ThYmic MalignanciEs (TYME). *Cancer Treat Rev* (2018) 71:76–87. doi: 10.1016/j.ctrv.2018.10.001
7. Zhu J, Ma J. Union for China Lymphoma Investigators of Chinese Society of Clinical O: Chinese Society of Clinical Oncology (CSCO) Diagnosis and Treatment Guidelines for Malignant Lymphoma 2021 (English Version). *Chin J Cancer Res* (2021) 33(3):289–301. doi: 10.21147/j.issn.1000-9604.2021.03.01
8. Priola AM, Priola SM, Cardinale L, Cataldi A, Fava C. The Anterior Mediastinum: Diseases. *Radiol Med* (2006) 111(3):312–42. doi: 10.1007/s11547-006-0032-5
9. Takahashi K, Al-Janabi NJ. Computed Tomography and Magnetic Resonance Imaging of Mediastinal Tumors. *J Magn Reson Imaging* (2010) 32(6):1325–39. doi: 10.1002/jmri.22377
10. Liu Z, Wang S, Dong D, Wei J, Fang C, Zhou X, et al. The Applications of Radiomics in Precision Diagnosis and Treatment of Oncology: Opportunities and Challenges. *Theranostics* (2019) 9(5):1303–22. doi: 10.7150/thno.30309
11. Yasaka K, Akai H, Abe O, Ohtomo K, Kiryu S. Quantitative Computed Tomography Texture Analyses for Anterior Mediastinal Masses: Differentiation Between Solid Masses and Cysts. *Eur J Radiol* (2018) 100:85–91. doi: 10.1016/j.ejrad.2018.01.017
12. Feng Z, Rong P, Cao P, Zhou Q, Zhu W, Yan Z, et al. Machine Learning-Based Quantitative Texture Analysis of CT Images of Small Renal Masses: Differentiation of Angiomyolipoma Without Visible Fat From Renal Cell Carcinoma. *Eur Radiol* (2018) 28(4):1625–33. doi: 10.1007/s00330-017-5118-z
13. Cardillo G, Carleo F, Giunti R, Lopergolo MG, Salvadori L, De Massimi AR, et al. Predictors of Survival in Patients With Locally Advanced Thymoma and Thymic Carcinoma (Masaoka Stages III and IVa). *Eur J Cardiothorac Surg* (2010) 37(4):819–23. doi: 10.1016/j.ejcts.2009.11.001
14. Chae HD, Park CM, Park SJ, Lee SM, Kim KG, Goo JM. Computerized Texture Analysis of Persistent Part-Solid Ground-Glass Nodules: Differentiation of Preinvasive Lesions From Invasive Pulmonary Adenocarcinomas. *Radiology* (2014) 273(1):285–93. doi: 10.1148/radiol.14132187
15. Liu J, Yin P, Wang S, Liu T, Sun C, Hong N. CT-Based Radiomics Signatures for Predicting the Risk Categorization of Thymic Epithelial Tumors. *Front Oncol* (2021) 11:628534. doi: 10.3389/fonc.2021.628534
16. Kirienko M, Ninatti G, Cozzi L, Voulaz E, Gennaro N, Barajon I, et al. Computed Tomography (CT)-Derived Radiomic Features Differentiate Prevascular Mediastinum Masses as Thymic Neoplasms Versus Lymphomas. *Radiol Med* (2020) 125(10):951–60. doi: 10.1007/s11547-020-01188-w
17. Weissferdt A, Kalhor N, Bishop JA, Jang SJ, Ro J, Petersson F, et al. Thymoma: A Clinicopathological Correlation of 1470 Cases. *Hum Pathol* (2018) 73:7–15. doi: 10.1016/j.humpath.2017.08.018
18. Duwe BV, Sterman DH, Musani AI. Tumors of the Mediastinum. *Chest* (2005) 128(4):2893–909. doi: 10.1378/chest.128.4.2893
19. Tomiyama N, Honda O, Tsubamoto M, Inoue A, Sumikawa H, Kuriyama K, et al. Anterior Mediastinal Tumors: Diagnostic Accuracy of CT and MRI. *Eur J Radiol* (2009) 69(2):280–8. doi: 10.1016/j.ejrad.2007.10.002
20. Kayi Cangir A, Orhan K, Kahya Y, Ozakinci H, Kazak BB, Konuk Balci BM, et al. CT Imaging-Based Machine Learning Model: A Potential Modality for Predicting Low-Risk and High-Risk Groups of Thymoma: "Impact of Surgical Modality Choice". *World J Surg Oncol* (2021) 19(1):147. doi: 10.1186/s12957-021-02259-6
21. Xie Y, Zhang S, Liu J, Liang X, Zhang X, Zhang Y, et al. Value of CT Spectral Imaging in the Differential Diagnosis of Thymoma and Mediastinal Lymphoma. *Br J Radiol (2019)* (1095) 92:20180598. doi: 10.1259/bjr.20180598
22. Kong J, Fu JJ, Yang W, Sun Y, Wang S, Bai J, et al. Contrast-Enhanced Ultrasound Features of Mediastinal Lymphomas and Thymic Epithelial Tumors. *J Clin Ultrasound* (2020) 48(1):19–28. doi: 10.1002/jcu.22782
23. Ng F, Ganeshan B, Kozarski R, Miles KA, Goh V. Assessment of Primary Colorectal Cancer Heterogeneity by Using Whole-Tumor Texture Analysis: Contrast-Enhanced CT Texture as a Biomarker of 5-Year Survival. *Radiology* (2013) 266(1):177–84. doi: 10.1148/radiol.12120254

24. Hu J, Zhao Y, Li M, Liu Y, Wang F, Weng Q, et al. Machine-Learning-Based Computed Tomography Radiomic Analysis for Histologic Subtype Classification of Thymic Epithelial Tumours. *Eur J Radiol* (2020) 126:108929. doi: 10.1016/j.ejrad.2020.108929
25. Sakai S, Murayama S, Soeda H, Matsuo Y, Ono M, Masuda K. Differential Diagnosis Between Thymoma and non-Thymoma by Dynamic MR Imaging. *Acta Radiol* (2002) 43(3):262–8. doi: 10.1080/j.1600-0455.2002.430306.x
26. Albano D, Micci G, Patti C, Midiri F, Albano S, Lo Re G, et al. Whole-Body Magnetic Resonance Imaging: Current Role in Patients With Lymphoma. *Diagnostics (Basel)* (2021) 11(6):1007. doi: 10.3390/diagnostics11061007
27. Milgrom SA, Rechner L, Berthelsen A. The Optimal Use of PET/CT in the Management of Lymphoma Patients. *Br J Radiol (2021)* (1127) 94:20210470. doi: 10.1259/bjr.20210470
28. Zhu L, Li X, Wang J, Fu Q, Liu J, Ma W, et al. Value of Metabolic Parameters in Distinguishing Primary Mediastinal Lymphomas From Thymic Epithelial Tumors. *Cancer Biol Med* (2020) 17(2):468–77. doi: 10.20892/j.issn.2095-3941.2019.0428
29. Lee J, Cho YS, Kim J, Shim YM, Lee KH, Choi JY. Prognostic Significance of Metabolic Parameters by (18)F-FDG PET/CT in Thymic Epithelial Tumors. *Cancers (Basel)* (2021) 13(4):712. doi: 10.3390/cancers13040712
30. Nakagawa K, Takahashi S, Endo M, Ohde Y, Kurihara H, Terauchi T. Can (18)F-FDG PET Predict the Grade of Malignancy in Thymic Epithelial Tumors? An Evaluation of Only Resected Tumors. *Cancer Manag Res* (2017) 9:761–8. doi: 10.2147/CMAR.S146522
31. Lee HS, Oh JS, Park YS, Jang SJ, Choi IS, Ryu JS. Differentiating the Grades of Thymic Epithelial Tumor Malignancy Using Textural Features of Intratumoral Heterogeneity via (18)F-FDG PET/CT. *Ann Nucl Med* (2016) 30(4):309–19. doi: 10.1007/s12149-016-1062-2
32. Davey A, van Herk M, Faivre-Finn C, Mistry H, McWilliam A. Is Tumour Sphericity an Important Prognostic Factor in Patients With Lung Cancer? *Radiother Oncol* (2020) 143:73–80. doi: 10.1016/j.radonc.2019.08.003
33. Apostolova I, Rogasch J, Buchert R, Wertzel H, Achenbach HJ, Schreiber J, et al. Quantitative Assessment of the Asphericity of Pretherapeutic FDG Uptake as an Independent Predictor of Outcome in NSCLC. *BMC Cancer* (2014) 14:896. doi: 10.1186/1471-2407-14-896
34. Shepherd FA. Malignant Pericardial Effusion. *Curr Opin Oncol* (1997) 9 (2):170–4. doi: 10.1097/00001622-199703000-00011
35. Chiles C, Woodard PK, Gutierrez FR, Link KM. Metastatic Involvement of the Heart and Pericardium: CT and MR Imaging. *Radiographics* (2001) 21 (2):439–49. doi: 10.1148/radiographics.21.2.g01mr15439

Conflict of Interest: Author XinC was employed by the company Siemens Healthineers.

The remaining authors declare that the research was conducted in the absence of any commercial or financial relationships that could be construed as a potential conflict of interest.

Publisher's Note: All claims expressed in this article are solely those of the authors and do not necessarily represent those of their affiliated organizations, or those of the publisher, the editors and the reviewers. Any product that may be evaluated in this article, or claim that may be made by its manufacturer, is not guaranteed or endorsed by the publisher.

Copyright © 2022 He, Xia, Chen, Yu, Liu, Pu, Li, Liu, Chen and Peng. This is an open-access article distributed under the terms of the Creative Commons Attribution License (CC BY). The use, distribution or reproduction in other forums is permitted, provided the original author(s) and the copyright owner(s) are credited and that the original publication in this journal is cited, in accordance with accepted academic practice. No use, distribution or reproduction is permitted which does not comply with these terms.

frontiers | Frontiers in Oncology

ORIGINAL RESEARCH
published: 06 June 2022
doi: 10.3389/fonc.2022.847957

The Studies of Prognostic Factors and the Genetic Polymorphism of Methylenetetrahydrofolate Reductase C667T in Thymic Epithelial Tumors

Miaolong Yan[1,2†], Jiayuan Wu[2†], Min Xue[2,3], Juanfen Mo[2], Li Zheng[2], Jun Zhang[4], Zhenzhen Gao[5*] and Yi Bao[2,5*]*

[1] The Fourth School of Clinical Medicine, Zhejiang Chinese Medical University, Hangzhou, China, [2] The Key Laboratory, The Second Affiliated Hospital of Jiaxing University, Jiaxing, China, [3] Graduate School, Bengbu Medical College, Bengbu, China, [4] The Department of Thoracic Surgery, The Second Affiliated Hospital of Jiaxing University, Jiaxing, China, [5] The Department of Oncology, The Second Affiliated Hospital of Jiaxing University, Jiaxing, China

OPEN ACCESS

Edited by:
Cesar Moran, University of Texas MD Anderson Cancer Center, United States

Reviewed by:
Anja Roden, Mayo Clinic, United States
Jelena Stojsic, University of Belgrade, Serbia

***Correspondence:**
Yi Bao
ybao2011@zjxu.edu.cn
Zhenzhen Gao
sophiever0112@163.com
Jun Zhang
18967383559@189.cn

†These authors have contributed equally to this work

Specialty section:
This article was submitted to Surgical Oncology, a section of the journal Frontiers in Oncology

Received: *03 January 2022*
Accepted: *11 May 2022*
Published: *06 June 2022*

Citation:
Yan M, Wu J, Xue M, Mo J, Zheng L, Zhang J, Gao Z and Bao Y (2022) The Studies of Prognostic Factors and the Genetic Polymorphism of Methylenetetrahydrofolate Reductase C667T in Thymic Epithelial Tumors. Front. Oncol. 12:847957. doi: 10.3389/fonc.2022.847957

Objective: To describe the clinical features of a cohort of patients with thymic epithelial tumors (TETs) and to analyze their prognostic factors. In particular, we investigated the correlation between the genetic polymorphism of methylenetetrahydrofolate reductase (*MTHFR*) C667T and the incidence of TETs.

Methods: Pathological records were reviewed from the database of the Second Affiliated Hospital of Jiaxing University, from January 2010 to December 2020, and 84 patients with TETs were recruited for this study. Univariate and multivariate analyses were performed to determine the prognostic factors. The genetic polymorphism of *MTHFR* C667T was examined in the patients with TETs and in a group of healthy individuals. The correlation between *MTHFR* transcriptional levels and methylation was analyzed using The Cancer Genome Atlas (TCGA) thymoma dataset from the cBioPortal platform.

Results: Kaplan–Meier univariate survival analysis showed that sex, age, the maximum tumor diameter, surgery, chemotherapy, radiotherapy, WHO histological classification, Masaoka–Koga stage, and 8th UICC/AJCC TNM staging, were statistically significantly correlated with the prognosis of patients with TETs. The Masaoka–Koga stage and 8th UICC/AJCC TNM staging were strongly correlated with each other in this study (r=0.925, P<0.001). Cox multivariate survival analysis showed that the maximum tumor diameter, Masaoka–Koga stage, and 8th UICC/AJCC TNM staging were independent prognostic factors affecting the overall survival (OS) of patients with TETs (P<0.05). The *MTHFR* C667T genotype (χ^2 = 7.987, P=0.018) and allele distribution (χ^2 = 5.750, P=0.016) were significantly different between the patients and healthy controls. CT heterozygous and TT homozygous genotypes at this *MTHFR* polymorphism significantly increased the risk of TETs (odds ratio [OR] =4.721, P=0.008). Kaplan–Meier univariate survival analysis showed that there was no correlation between different genotypes and the prognosis

of TETs (CC versus CT + TT, χ^2 =0.003, *P*=0.959). Finally, a negative correlation between the transcriptional and methylation levels of *MTHFR* was observed in the TCGA thymoma dataset (*r*=-0.24, *P*=0.010).

Conclusions: The Masaoka–Koga stage, 8th UICC/AJCC TNM staging, and maximum tumor diameter were independent prognostic factors for TETs. Reduced methylation levels of *MTHFR* and particular polymorphic variants may contribute to the susceptibility to developing TETs.

Keywords: thymic epithelial tumors, Masaoka–Koga Stage, 8th UICC/AJCC TNM staging, *MTHFR* polymorphism, methylation

INTRODUCTION

Thymic epithelial tumors (TETs), including thymoma and thymic carcinoma (TC), are derived from thymic epithelial cells and lymphocytes of the thymus. The thymus is the site of maturation for T cells and plays an integral role involving in adaptive immunity. Thymoma is associated with autoimmune-related syndromes including myasthenia gravis (MG), pure erythrocyte hypoplasia, and hypogammaglobulinemia (1, 2). The 5-year survival rates for thymomas and TCs have been reported to be approximately 78% and 40%, respectively (3).

According to the 2015 World Health Organization (WHO) classifications, TETs are classified into six categories: type A, AB, B1, B2, and B3 thymoma and TC, based on the morphology of tumor cells and the number of non-neoplastic lymphocytes (4). Thymomas are divided into two groups: low-risk thymomas (A, AB, and B1) and high-risk thymomas (B2 and B3). The Masaoka–Koga stage is widely adopted for the classification of TETs into stages I, II, III, and IV, based on the degree of tumor cell invasion (5). In addition to the Masaoka–Koga stage, the 8th UICC/AJCC TNM classification is also used in clinical TET staging. This describes not only the degree of tumor invasion but also the tumor spread and lymphatic infiltration (6).

Patients with low-risk thymomas rarely experience recurrence after a complete resection (7), but nevertheless, thymomas are considered as malignant tumors (8). TC is further divided into several subtypes, including squamous cell carcinoma, basaloid carcinoma, mucoepidermoid carcinoma, lymphoepithelioma-like carcinoma, and clear cell carcinoma (9). Most patients with relatively low-risk thymomas are asymptomatic. Conversely, invasive subtypes of thymomas and TCs exhibit aggressive behaviors by invading adjacent structures such as the pleura and pericardium.

Although surgical resection is usually accepted as a primary therapeutic strategy in a curative setting, adjuvant chemotherapy and/or radiotherapy is used in some patients who are at a high risk of recurrence to prolong survival (8, 10).

Currently, the etiology of TETs remains largely unknown. A point mutation in the gene encoding *MTHFR*, which is located on chromosome 1p36.3, is associated with several malignancies, including colon cancer, gastric cancer, lung cancer, esophageal squamous cell carcinoma, breast cancer, and gynecological cancer (11–18). *MTHFR* is a critical enzyme involved in the folate metabolism pathway and DNA methylation and synthesis (19). The *MTHFR* C677T, a cytosine (C) to a thymine (T) substitution at position 677, which changes an alanine to a valine, leads to impaired folate binding and reduced *MTHFR* activity (20, 21). MTHFR deficiency may result in insufficient DNA methylation and genetic instability and may promote the development of malignancies (22).

To explore the correlation between the *MTHFR* C677T polymorphism and TETs, the distribution of this single-nucleotide polymorphism was examined in TET patients and healthy controls in this study. Additionally, the correlation between *MTHFR* methylation and *MTHFR* transcriptional levels was also investigated using The Cancer Genome Atlas (TCGA) database of TETs. A decreased *MTHFR* expression can lead to dysregulated folic acid metabolism, resulting in abnormal DNA methylation and nucleotide synthesis, which may be involved in the susceptibility to develop TETs.

MATERIALS AND METHODS

Study Subjects

We retrospectively analyzed 84 cases of TETs (56 cases of thymoma and 28 cases of TC) who were diagnosed by pathological examination from January 2010 to December 2020 and were treated in the Second Affiliated Hospital of Jiaxing University. Clinical data were recorded and retrieved from the electronic database of the hospital. The present study was approved by the Ethics Committee of the Second Affiliated Hospital of Jiaxing University (Ethical Code number: LWSC041), and written informed consent was obtained from all patients.

Detection of *MTHFR* Gene Polymorphism and Bioinformatics Study

Among these 84 patients, blood samples were obtained from only 33 cases, which were used to detect *MTHFR* gene polymorphism in this study. Samples were collected from 21 men and 11 women, ranging from 32 to 74 years old between January 2015 and January 2018. A total of 72 healthy individuals (38 men and 34 women) ranging from 51 to 75 years old were recruited as controls. Genomic DNA was extracted from peripheral venous blood (2 ml) using a commercial kit

according to the manufacturer's instructions (BaiO Technology Co, Ltd., Shanghai, China). The DNA purity (A260/A280 ratio) was determined by using a NanoDrop spectrophotometer (Thermo Fisher Scientific, Waltham, MA, USA). The chips that can detect *MTHFR* gene C667T polymorphism were purchased from Shanghai BaiO Company and hybridized by using a BaiO biochip hybridization instrument (BaiO Technology Co., Ltd., China). Data were recorded by a BaiO biochip reader and were analyzed by using a BaiO analysis software (BaiO Technology Co., Ltd., China).

The *MTHFR* transcriptional expression data (123 patients with TETs) from the TCGA database were obtained from the cbioportal platform (http://www.cbioportal.org). Clinical data showed that among these 123 patients with TETs, 64 (52.0%) cases were men and 59 (48.0%) cases were women, with a median age of 60.5 years. Thymectomy was performed in all patients, 41 of whom underwent postoperative radiotherapy and 6 of whom underwent postoperative chemotherapy. The correlation between the mRNA levels of MTHFR and its methylation was analyzed in this platform.

Treatments

Surgical resection was performed in 76 patients in this retrospective study. The complete resection rate was 77.6%. Among them, 5 patients with incomplete surgical resection underwent multiple therapies. Among a total of 84 patients, 10 patients with thymoma and 22 patients with TC were treated by platinum-based chemotherapy with an average of 4 cycles. A total of 3 patients with thymoma and 6 patients with TC received postoperative adjuvant radiotherapy. The dose of radiotherapy was approximately 54 Gy (1.8 ~ 2.0 Gy/f).

Follow-Up

The follow-up time was from the time of pathological diagnosis to the death or last follow-up time of the patients, recorded every month. The contents of follow-up included the progression of the disease, stability of the disease, death of the patient, and so on. Overall survival (OS) is defined as the time of the first diagnosis to death. The cut-off time of the study was 2020-12-31.

Statistical Analysis

All statistical analyses were performed by using Statistical Package for the Social Sciences (SPSS), version 25.0 (IBM Inc., Chicago, IL, USA). Log-rank analysis was used for the comparisons between the different factors affecting prognosis. Multivariate analysis for OS was performed using a Cox proportional hazards model. All significant variables in the univariate analysis including sex, age, smoking status, maximum tumor diameter, chemotherapy, radiotherapy, WHO histological classification, Masaoka–Koga stage, 8th UICC/AJCC TNM staging, and clinical symptoms were used in the multivariate analysis. The Kaplan–Meier survival rate was calculated and drawn by the SPSS software. The chi-square test was used to compare the *MTHFR* C667T genotype and allele distribution between patients with TETs and healthy controls. Logistic regression analysis was used to analyze the correlation between different genotypes *MTHFR* C667T and TET susceptibility. Spearman correlation analysis was performed to analyze the correlations of the mRNA levels of *MTHFR* expression and its methylation by using the TCGA database. $P<0.05$ was considered to be statistically significant.

RESULTS

Patient Characteristics

In total, 84 patients diagnosed with thymomas (n=56) and TCs (n=28) who met predefined criteria were recruited in this study. General characteristics were listed in **Table 1**. The study consisted of 51 (60.7%) men and 33 (39.3%) women, with a median age of 58 years (range 22–88 years). In addition, 31 cases were asymptomatic at the first visit, 21 cases complained of chest pain or chest distress, 11 cases had respiratory symptoms (including cough and pulmonary infection), and 12 cases had MG. A total of 9 cases were accompanied by other clinical symptoms, such as lumbago and trauma. At the end of follow-up time on December 31, 2020, 19 patients with TETs were deceased, including 4 patients with thymomas and 15 patients with TCs.

Analysis of Prognostic Factors of TETs

The median follow-up period was 36 months. The 5-year survival rate of patients with TETs was 71.9% (**Figure 1**). Univariate analysis showed that sex (P = 0.005), age (P = 0.019), the maximum tumor diameter (P < 0.001), surgery (P <

TABLE 1 | The characteristics of all the cases recruited in the study (n = 84).

Sex (male)	51 (60.7%)
Age (years)	58 [22,88]
Follow-up duration (months)	36 [1,126]
Medium tumor diameter (cm)	5 [1.1,14.5]
Smoking status	21 (25.0%)
Surgery	76 (90.5%)
Chemotherapy	32 (38.1%)
Radiotherapy	9 (10.7%)
WHO histological classification	
Low-risk thymomas (A/AB/B1)	34 (40.5%)
High-risk thymomas (B2/B3)	22 (26.2%)
Thymic carcinomas (TCs)	28 (33.3%)
Masaoka–Koga stage	
I	23 (27.4%)
II	24 (28.6%)
III	15 (17.8%)
IV	22 (26.2%)
8th UICC/AJCC TNM staging	
I	43 (51.2%)
II	4 (2.8%)
III	15 (17.8%)
IV	22 (26.2%)
Clinical symptoms	
Asymptomatic	31 (36.9%)
Respiratory symptoms	11 (13.1%)
Chest pain/chest distress	21 (25.0%)
Myasthenia gravis	12 (14.3%)
Other symptoms	9 (10.7%)

Respiratory symptoms: cough, pneumonia.
Other symptoms: lumbago, trauma, gout, dizziness, lymphedema.

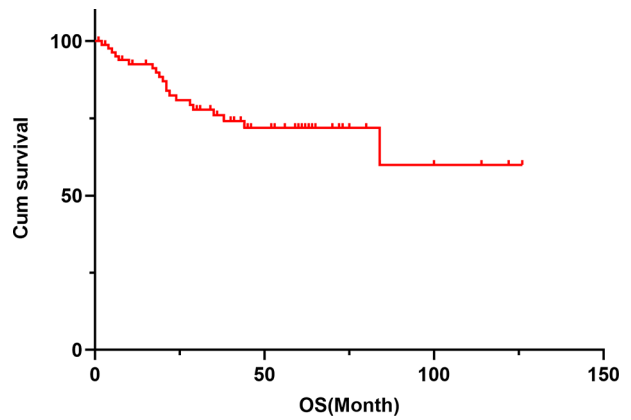

FIGURE 1 | The cumulative survival curve of patients with TETs. The 1-year survival rate was 92.6%, the 3-year survival rate was 76.0%, and the 5-year survival rate was 71.9% in patients with TETs.

0.001), chemotherapy (P < 0.001), radiotherapy (P = 0.001), WHO histological classification (P < 0.001), Masaoka–Koga stage (P < 0.001), and 8th UICC/AJCC TNM staging TNM stage (P < 0.001) were associated with TET prognosis (**Table 2**). Other variables, including clinical symptoms and the smoking status, were not associated to prognosis. Among these factors, male sex, older age (>58 years old), the maximum tumor diameter (>5 cm), no surgery, no chemotherapy, no radiotherapy, a higher grade of WHO histological classification and advanced tumor stage (both the Masaoka–Koga stage and the 8th UICC/AJCC TNM staging) were correlated with poor prognosis. The survival curves of different variables are shown in **Figure 2**: sex (A), age (B), the maximum tumor diameter (C), surgery (D), chemotherapy I, radiotherapy (F), WHO histological classification (G), Masaoka–Koga stage (H), and 8th UICC/AJCC TNM staging (I). The Masaoka–Koga stage and 8th UICC/AJCC TNM staging were strongly correlated with each other in this study (r=0.925, P<0.001). These univariate analysis data were used to establish a subsequent multivariate Cox proportional hazards regression model on the basis of the Masaoka–Koga stage and UICC/AJCC TNM staging. The results showed that the maximum tumor diameter (P = 0.040, hazard ratio [*HR*]: 3.623, *95%CI*: 1.058~12.403 on the basis of Masaoka–Kaga stage; P = 0.045, *HR*:3.629, *95%CI*: 1.027~12.822 on the basis of UICC/AJCC TNM staging), Masaoka–Koga stage (P = 0.008, HR: 5.513, 95%*CI*: 1.564~19.434), and 8th UICC/AJCC TNM staging (P = 0.007, *HR*: 8.476, *95%CI*:1.815~39.596) were identified as independent prognostic factors of patients with TETs (**Tables 3**, **4**).The 5-year survival rates of TET patients with Masaoka–Koga stage I, II, III, and IV were 100%, 95.8%, 78.6%, and 20.5%, respectively (**Figure 2H**). The 5-year survival rates for UICC/AJCC TNM stages I, II, III, and IV were 100%, 100%, 73.3%, and 20.5%, respectively (**Figure 2I**).

TABLE 2 | Univariate analyses of overall survival for 84 patients with TETs.

Clinical factors	χ^2	*P*
Sex		
Female		
Male	7.748	.005
Age (years)		
≤58		
>58	5.460	.019
Maximum tumor diameter (cm)		
≤5		
>5	13.561	.000
Smoking status	1.802	.180
Surgery	13.025	.000
Chemotherapy	19.522	.000
Radiotherapy	10.887	.001
WHO histological classification	24.157	.000
Low-risk thymomas/high-risk thymomas/TCs		
Masaoka–Koga stage	55.816	.000
I/II/III/IV		
8th UICC/AJCC TNM staging	57.096	.000
I/II/III/IV		
Clinical symptoms	5.238	.264
Asymptomatic		
Respiratory symptoms		
Chest pain/chest distress		
Myasthenia gravis		
Other symptoms		

MTHFR C667T Genotypes in Patients With TETs

MTHFR polymorphism in healthy individuals and patients with TETs was further investigated in this study. The results of the chi-square test showed that the genotype (χ^2 = 7.987, P = 0.018) and allele distribution (χ^2 = 5.750, P = 0.016) statistically significantly differed between patients and healthy controls (**Table 5**). In logistic regression analysis, heterozygous and homozygous genotypes (CT+TT) showed higher TET susceptibility (odds ratio [*OR*] = 4.721, P = 0.008, **Table 6**). The analysis also revealed that, compared to the T allele, the presence of the *MTHFR* C allele at this position was adversely associated with the incidence of TETs (T vs. C: *OR* = 2.067, *95% CI*: 1.136–3.758, P = 0.017, **Table 6**). Kaplan–Meier univariate survival analysis was further conducted, and data showed that there was no correlation between different genotypes and the prognosis of TETs (CC vs. CT + TT, χ^2 = 0.003, P = 0.959, **Figure 3**).

Correlation of mRNA and Methylation Levels of *MTHFR* in Patients With TETs

Using the gene expression profiles of TETs from the TCGA database, a negative correlation was observed between *MTHFR* mRNA levels and their methylation by using Spearman correlation analysis (r= -0.24, P = 0.010, **Figure 4**).

DISCUSSION

Basic Features

In the present study, the median age of the patients at the time of TET diagnosis was 58 years. Using univariate analysis, we observed that the patients with TETs who were older than 58

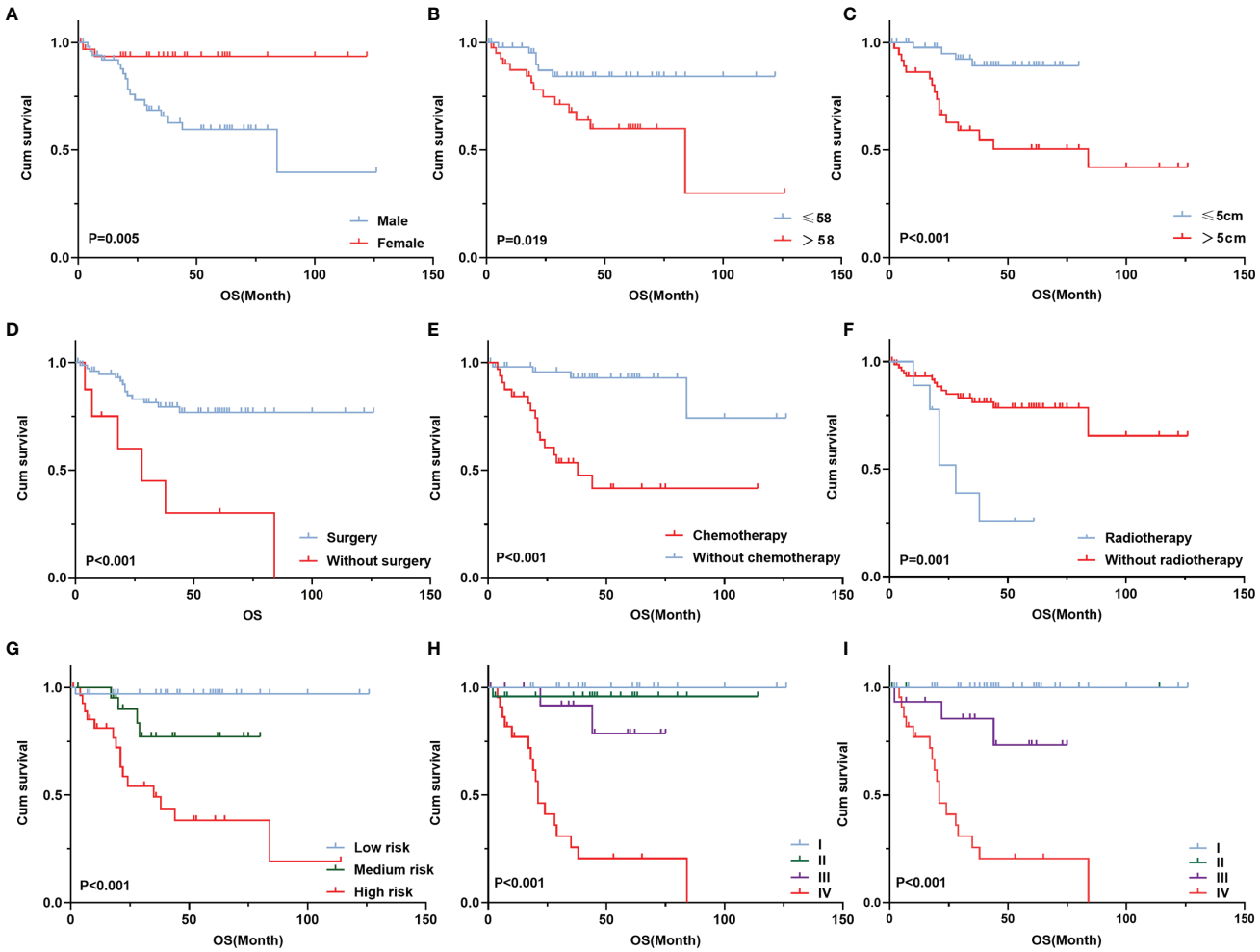

FIGURE 2 | Survival curve of different prognostic factors of 84 patients with TETs. Cumulative survival according to completion of sex **(A)**, age **(B)**, maximum tumor diameter **(C)**, surgery **(D)**, chemotherapy **(E)**, radiotherapy **(F)**, WHO histological classification **(G)**, Masaoka–Koga stage **(H)**, and 8th UICC/AJCC TNM staging **(I)**.

TABLE 3 | Multivariate analyses of overall survival for 84 patients with TETs (I).

Clinical factors	HR	95%CI	*P*
Sex			
Female			
Male	1.557	.246-9.836	.638
Age (years)			
≤58			
>58	1.460	.460-4.549	.514
Maximum tumor diameter (cm)			
≤5			
>5	3.623	1.058-12.403	.040
Surgery	1.360	.387-4.784	.632
Chemotherapy	2.160	.550-8.487	.270
Radiotherapy	1.061	.332-3.386	.921
WHO histological classification	1.261	.453-3.508	.657
Low-risk thymomas/high-risk thymomas/TCs			
Masaoka–Koga stage	5.513	1.564-19.434	.008
I/II/III/IV			

TABLE 4 | Multivariate analyses of overall survival for 84 patients with TETs (II).

Clinical factors	HR	95%CI	*P*
Sex			
Female			
Male	2.075	.307-14.023	.454
Age (years)			
≤58			
>58	1.333	.416-4.268	.628
Maximum tumor diameter (cm)			
≤5			
>5	3.629	1.027-12.822	.045
Surgery	1.463	.414-5.179	.555
Chemotherapy	1.980	.502-7.818	.330
Radiotherapy	1.032	.332-3.306	.957
WHO histological classification	1.127	.393-3.233	.824
Low-risk thymomas/high-risk thymomas/TCs			
8th UICC/AJCC TNM staging	8.476	1.815-39.596	.007
I/II/III/IV			

years or were men had a poor prognosis. As shown in **Figure 1**, the OS of the TET patients gradually decreased with an increase in age. These data were supported by the results of a previous study suggesting that young patients with thymoma have a better performance status and less comorbidities and have a better prognosis than older patients (23). Liu et al. reported similar results in patients with thymoma but not in patients with TC (24). In our study, we analyzed thymoma and TC as a single group, and found that age tended to be a prognostic factor. Sex was not identified as a predictive factor in several studies (25, 26); however, in our study, we observed a worse prognosis in male patients with TETs than in their female counterparts. We consider this to be due to the majority of TC patients in our cohort being men with a reduced survival time.

A tumor diameter greater than 5 cm was observed to be an independent prognostic value of TETs in our study, resulting in a poor prognosis. This conclusion was supported by another study, which showed that the tumor diameter is an independent prognostic factor and may even be an indication for surgical treatment (27). Based on the study by Okumura et al., a tumor diameter ≥5 cm was suggested to be an independent risk factor, which was consistent with our findings (28).

Most patients in our cohort were asymptomatic, which may be related to the improved auxiliary inspection technologies and health awareness in our population. The association between autoimmune diseases (ADs) and thymoma has been well established, particularly MG, which has been accompanied in 20%–25% of thymoma patients based on a previous report (29). In our cohort, approximately 22.9% of thymomas were complicated by MG, but only 7% of TC patients had MG. A further analysis of our data showed that MG did not affect the prognosis of TETs, which was inconsistent with previous studies showing that MG is not an independent or direct prognostic factor of TETs, but it may be helpful in an earlier diagnosis of TETs, leading to a better prognosis (30, 31). However, controversial data showed that patients with MG symptoms had a worse prognosis than patients without MG symptoms (32). The relative small numbers of each cohort due to the low incidence of TETs may contribute to the variance. In addition, the data may present a confounding bias as they were generated from a single center lacking external verification, and therefore, multicenter studies may be needed to draw a comprehensive conclusion.

WHO Histological Classification

In our study, the cut-off time was 2020-12-31, and therefore, the 2015 WHO histological classification system was used in this study. Our results demonstrated that this classification was associated with the OS of TET patients, but was not an independent prognostic factor by Cox multivariate survival analysis, which was consistent with previous studies (33, 34). An increased WHO histological grade showed more malignant behavior and was associated with a poor prognosis (33). We also reviewed our data using the new 2021 WHO histological classification and observed no change in our results because

TABLE 5 | The chi-square test of *MTHFR* C667T genotypes and allele distribution.

Group	Genotype			Allele		χ^2	*P*
	CC Case (%)	CT Case (%)	TT Case (%)	C Case (%)	T Case (%)		
Controls	29(40.3)	35(48.6)	8(11.1)	93(64.6)	51(35.4)	7.987	.018[a]
Patients	4(12.5)	22(68.7)	6(18.8)	30(46.9)	34(53.1)	5.750	.016[b]

[a]*Compared MTHFR C667T genotype distribution in patients with TETs and healthy controls.*
[b]*Compared MTHFR C667T allele distribution in patients with TETs and healthy controls.*

TABLE 6 | Correlation analysis between *MTHFR* C667T genotypes and TET susceptibility.

Variable	OR (95%CI)	*P*
CT/CC	4.557 (1.409-14.735)	.011
TT/CC	2.332 (1.108-4.906)	.026
CT+TT/CC	4.721 (1.497-14.889)	.008
T/C	2.067 (1.136-3.758)	.017

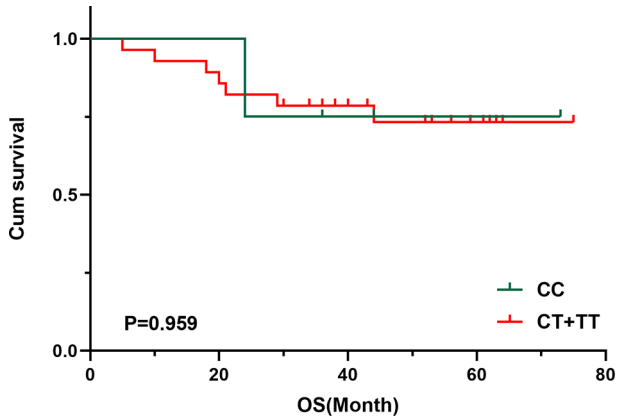

FIGURE 3 | Survival curve of *MTHFR* C667T polymorphism of 33 patients with TETs. Cumulative survival according to *MTHFR* C667T polymorphism.

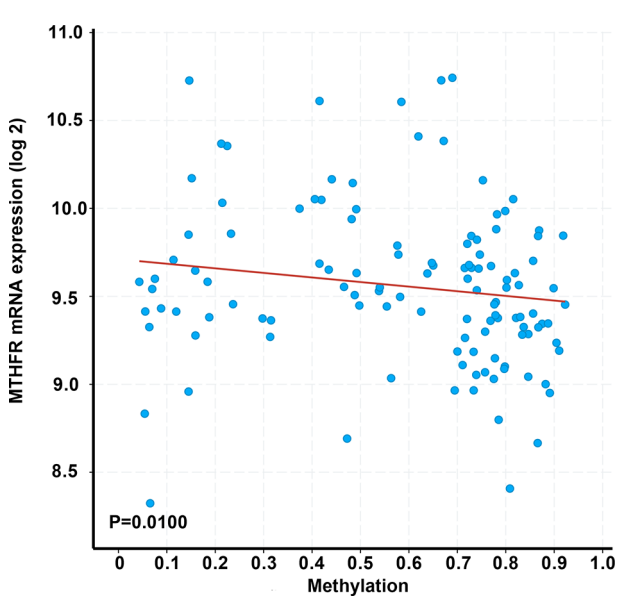

FIGURE 4 | Correlation between *MTHFR* transcriptional levels and its methylation in 123 patients with TETs. Correlations were estimated using Spearman's bivariate correlation coefficient (*r*= -0.24), with a p-value <0.05 considered as statistically significant.

the new classification system did not affect our data on the pathological diagnosis of TETs (35).

Masaoka–Koga Stage and 8th UICC/AJCC TNM Staging

The Masaoka–Koga stage was established by Masoka in a retrospective analysis of 93 patients with TETs and was further modified by Koga in 1994 (36, 37). Many studies have shown that the Masaoka–Koga stage is a prognostic factor for predicting the survival time of TETs (38–40). In addition to the Masaoka–Koga stage, the 8th UICC/AJCC TNM staging for TET patients is also used in clinical practice. In our study, both the Masaoka–Koga and the 8th UICC/AJCC TNM staging served as independent prognostic factors for TETs as supported by published literatures (41, 42).

Treatment

Thymectomy is the first choice of treatment advocated for all patients with TETs and has been shown to be an independent prognostic factor. According to Okereke et al. (43), early-stage thymoma and even advanced TETs with pleural metastasis can benefit from surgical resection (44). In our study, although there was only a correlation in the univariate analysis, the data suggested that most patients who have undergone surgery have a good prognosis. Chemotherapy is not recommended for patients who have undergone complete thymoma resection at an early stage (45). Advanced TETs are prone to invading adjacent tissues and organs, resulting in difficulties associated with incomplete resection. Postoperative adjuvant chemotherapy is recommended in patients with advanced TET to reduce the regional recurrence and distant metastasis (46). Therefore, these patients are likely to benefit from cisplatin-based chemotherapy (47). In our study, the patients with TETs, and apparently those with advanced disease, appeared to benefit from chemotherapy, especially in advanced patients. In addition to chemotherapy, radiotherapy has been proposed to improve the survival of patients with advanced TETs (48). Better outcomes have been observed in patients with TETs receiving postoperative radiotherapy (PORT) than in those who only underwent surgery (48). In our study, patients with TC who were treated with PORT showed remarkable local control with mild toxicities. For patients with advanced TETs, particularly TC patients, it may be valuable to explore novel treatment strategies, such as immunotherapy.

MTHFR C677T Genotypes and Methylation Under TET Patients

Evidence from previous studies implicates the gene encoding the folate-metabolizing enzyme MTHFR in cancer, such as gastric cancer and colorectal cancer (CRC) (49, 50). Our study demonstrates the increased risk of TETs in individuals with heterozygous or homozygous T genotypes (CT+TT) at the C667 polymorphism. Patients with TETs are likely to have CT and TT genotypes, but no correlation was observed between the genetic alteration and prognosis of TETs. According to published data from a meta-analysis of 5,423 CRC patients with CT+TT at the

MTHFR C667T polymorphism, no prognostic association was observed with either the CC or CT+TT genotypes at the *MTHFR* C667T polymorphism (50). Another study concluded that the *MTHFR* C677T polymorphism is unlikely to be a prognostic factor for esophagogastric cancer (51). These data were consistent with our findings. However, interestingly, data indicated that the *MTHFR* C667T polymorphism affected the prognosis of patients with CRC who were treated with chemotherapeutic drugs including pemetrexed and 5-fluorouracil (52, 53), suggesting that the impaired the folic acid metabolic pathway may affect the sensitivity to chemotherapy drugs and consequent prognostic events.

MTHFR C677T polymorphisms decrease the enzyme activity of the *MTHFR* enzyme as compared to the wild type and are associated with DNA hypomethylation (54, 55). This can lead to an increased expression of oncogenes, increased DNA chain breaks, and impaired DNA repair (56). *MTHFR* methylation levels were negatively correlated with the mRNA level of MTHFR using the data derived from the TCGA database. Aberrant DNA methylation may be the etiology and molecular pathogenesis of malignancies including TETs. Chen et al. reported that the degree of hypomethylation was associated with increased disease severity in TETs (1).

CONCLUSIONS

Taken together, in our 84 cases, the maximum tumor diameter (>5 cm), high Masaoka–Koga stage, and 8th UICC/AJCC TNM staging served as independent poor prognostic factors. The decreased methylation of *MTHFR* and increased *MTHFR* C677T genotype (CT+TT) may contribute to the susceptibility to develop TETs.

DATA AVAILABILITY STATEMENT

The original contributions presented in the study are included in the article/supplementary material. Further inquiries can be directed to the corresponding authors.

ETHICS STATEMENT

The studies involving human participants were reviewed and approved by The ethic committee of the Second Affiliated Hospital of Jiaxing University. The patients/participants provided their written informed consent to participate in this study.

AUTHOR CONTRIBUTIONS

MY performed partial clinical data collection, analyses, and manuscript writing. JW performed partial experiments and data analyses. MX, JM, and LZ performed literature reviews and partial data analyses. JZ collected the clinical data of patients with TETs. ZG mentored MY clinical data collection and analyses. YB designed the study and revised the manuscript. All authors read and approved the final manuscript.

FUNDING

This work was supported by the Health Bureau of Zhejiang Province (Grant no. 2020KY952), and the Science and Technology Bureau of Jiaxing (Grant no. 2018AY32007 and 2021AY30019).

REFERENCES

1. Chen C, Yin N, Yin B, Lu Q. DNA Methylation in Thoracic Neoplasms. *Cancer Lett* (2011) 301(1):7–16. doi: 10.1016/j.canlet.2010.10.017
2. Vaziri M, Rad K. Synchronous Thymoma and Oligodendroglioma: A Rare Association. *Int J Surg Case Rep* (2016) 21:95–8. doi: 10.1016/j.ijscr.2016.02.029
3. Kurihara N, Saito H, Nanjo H, Konno H, Atari M, Saito Y, et al. Thymic Carcinoma With Myasthenia Gravis: Two Case Reports. *Int J Surg Case Rep* (2016) 27:110–2. doi: 10.1016/j.ijscr.2016.08.010
4. Janik S, Bekos C, Hacker P, Raunegger T, Schiefer AI, Mullauer L, et al. Follistatin Impacts Tumor Angiogenesis and Outcome in Thymic Epithelial Tumors. *Sci Rep* (2019) 9(1):17359. doi: 10.1038/s41598-019-53671-8
5. Sato Y, Yanagawa M, Hata A, Enchi Y, Kikuchi N, Honda O, et al. Volumetric Analysis of the Thymic Epithelial Tumors: Correlation of Tumor Volume With the WHO Classification and Masaoka Staging. *J Thorac Dis* (2018) 10 (10):5822–32. doi: 10.21037/jtd.2018.09.133
6. Carter BW, Benveniste MF, Madan R, Godoy MC, Groot PM, Truong MT, et al. IASLC/ITMIG Staging System and Lymph Node Map for Thymic Epithelial Neoplasms. *Radiographics* (2017) 37(3):758–76. doi: 10.1148/rg.2017160096
7. Wang X, Sun W, Liang H, Mao X, Lu Z. Radiomics Signatures of Computed Tomography Imaging for Predicting Risk Categorization and Clinical Stage of Thymomas. *BioMed Res Int* (2019) 2019:3616852. doi: 10.1155/2019/3616852
8. Liu L, Lu F, Pang P, Shao G. Can Computed Tomography-Based Radiomics Potentially Discriminate Between Anterior Mediastinal Cysts and Type B1 and B2 Thymomas? *BioMed Eng Online* (2020) 19(1):89. doi: 10.1186/s12938-020-00833-9
9. Yang X, Zhao K, Li C, Yang Y, Guo C, Pu Y, et al. Thymic Squamous Cell Carcinoma: A Population-Based Surveillance, Epidemiology, and End Result Analysis. *Front Oncol* (2020) 10:592023. doi: 10.3389/fonc.2020.592023
10. Masaoka A, Yamakawa Y, Niwa H, Fukai I, Saito Y, Tokudome S, et al. Thymectomy and Malignancy. *Eur J Cardiothorac Surg* (1994) 8(5):251–3. doi: 10.1016/1010-7940(94)90155-4
11. Yuan JM, Lu SC, Van Den Berg D, Govindarajan S, Zhang ZQ, Mato JM, et al. Genetic Polymorphisms in the Methylenetetrahydrofolate Reductase and Thymidylate Synthase Genes and Risk of Hepatocellular Carcinoma. *Hepatology* (2007) 46(3):749–58. doi: 10.1002/hep.21735
12. Zhang W, Press OA, Haiman CA, Yang DY, Gordon MA, Fazzone W, et al. Association of Methylenetetrahydrofolate Reductase Gene Polymorphisms and Sex-Specific Survival in Patients With Metastatic Colon Cancer. *J Clin Oncol* (2007) 25(24):3726–31. doi: 10.1200/JCO.2007.11.4710
13. Xue HC, Wang JM, Xu B, Guo GP, Hua ZL, Zhou Q, et al. [Correlation of Aberrant Methylation of MGMT Gene to MTHFR C677T Genetic Polymorphisms in Esophageal Squamous Cell Carcinoma]. *Ai Zheng* (2008) 27(12):1256–62.
14. Liew SC, Gupta ED. Methylenetetrahydrofolate Reductase (MTHFR) C677T Polymorphism: Epidemiology, Metabolism and the Associated Diseases. *Eur J Med Genet* (2015) 58(1):1–10. doi: 10.1016/j.ejmg.2014.10.004

15. Ding H, Wang Y, Chen Y, Liu C, Qiu H, Kang M, et al. Methylenetetrahydrofolate Reductase Tagging Polymorphisms Are Associated With Risk of Non-Small Cell Lung Cancer in Eastern Chinese Han Population. *Oncotarget* (2017) 8(66):110326–36. doi: 10.18632/oncotarget.22887
16. Amirfallah A, Kocal GC, Unal OU, Ellidokuz H, Oztop I, Basbinar Y. DPYD, TYMS and MTHFR Genes Polymorphism Frequencies in a Series of Turkish Colorectal Cancer Patients. *J Pers Med* (2018) 8(4):1. doi: 10.3390/jpm8040045
17. Dong Y, Yi X, Yujie Z, Huixia Z, Yan C. Relationship Between the Methylation of Folic Acid Metabolism-Related Genes and the Incidence and Prognosis of Esophageal Cancer Among Ethnic Kazakhs. *J Cancer* (2018) 9(16):2865–75. doi: 10.7150/jca.25270
18. Meneses-Sanchez P, Garcia-Hernandez SC, Porchia LM, Perez-Fuentes R, Torres-Rasgado E, Del Angel Soto A, et al. C677T and A1298C Methylenetetrahydrofolate Reductase Polymorphisms and Breast Cancer Susceptibility Among Latinos: A Meta-Analysis. *Breast Cancer* (2019) 26 (5):602–11. doi: 10.1007/s12282-019-00961-8
19. Gatarek P, Rosiak A, Borowczyk K, Glowacki R, Kaluzna-Czaplinska J. Higher Levels of Low Molecular Weight Sulfur Compounds and Homocysteine Thiolactone in the Urine of Autistic Children. *Molecules* (2020) 25(4):973. doi: 10.3390/molecules25040973
20. Wu X, Yang K, Tang X, Sa Y, Zhou R, Liu J, et al. Folate Metabolism Gene Polymorphisms MTHFR C677T and A1298C and Risk for Preeclampsia: A Meta-Analysis. *J Assist Reprod Genet* (2015) 32(5):797–805. doi: 10.1007/s10815-014-0408-8
21. Karatoprak E, Sozen G, Yilmaz K, Ozer I. Interictal Epileptiform Discharges on Electroencephalography in Children With Methylenetetrahydrofolate Reductase (MTHFR) Polymorphisms. *Neurol Sci* (2020) 41(3):631–6. doi: 10.1007/s10072-019-04119-4
22. Lewinska A, Adamczyk-Grochala J, Deregowska A, Wnuk M. Sulforaphane-Induced Cell Cycle Arrest and Senescence Are Accompanied by DNA Hypomethylation and Changes in microRNA Profile in Breast Cancer Cells. *Theranostics* (2017) 7(14):3461–77. doi: 10.7150/thno.20657
23. Bian D, Zhou F, Yang W, Zhang K, Chen L, Jiang G, et al. Thymoma Size Significantly Affects the Survival, Metastasis and Effectiveness of Adjuvant Therapies: A Population Based Study. *Oncotarget* (2018) 9(15):12273–83. doi: 10.18632/oncotarget.24315
24. Liu M, Wang C, Gao L, Lv C, Fu X. Clinical Significance of Age at Diagnosis Among Patients With Thymic Epithelial Tumors: A Population-Based Study. *Aging (Albany NY)* (2020) 12(6):4815–21. doi: 10.18632/aging.102897
25. Song Z, Jin X, Zhang Y. Treatment and Prognosis of Type B2 Thymoma. *World J Surg Oncol* (2014) 12:291. doi: 10.1186/1477-7819-12-291
26. Zhao M, Yin J, Yang X, Jiang T, Lu T, Huang Y, et al. Nomogram to Predict Thymoma Prognosis: A Population-Based Study of 1312 Cases. *Thorac Cancer* (2019) 10(5):1167–75. doi: 10.1111/1759-7714.13059
27. Wright CD, Wain JC, Wong DR, Donahue DM, Gaissert HA, Grillo HC, et al. Predictors of Recurrence in Thymic Tumors: Importance of Invasion, World Health Organization Histology, and Size. *J Thorac Cardiovasc Surg* (2005) 130 (5):1413–21. doi: 10.1016/j.jtcvs.2005.07.026
28. Okumura M, Yoshino I, Yano M, Watanabe SI, Tsuboi M, Yoshida K, et al. Tumour Size Determines Both Recurrence-Free Survival and Disease-Specific Survival After Surgical Treatment for Thymoma. *Eur J Cardiothorac Surg* (2019) 56(1):174–81. doi: 10.1093/ejcts/ezz001
29. Kondo K, Monden Y. Thymoma and Myasthenia Gravis: A Clinical Study of 1,089 Patients From Japan. *Ann Thorac Surg* (2005) 79(1):219–24. doi: 10.1016/j.athoracsur.2004.06.090
30. Li W, Miao Z, Liu X, Zhang Q, Sun L, Li P, et al. Thymic Carcinoma Patients With Myasthenia Gravis Exhibit Better Prognoses. *Int J Clin Oncol* (2016) 21 (1):75–80. doi: 10.1007/s10147-015-0862-z
31. Zhai Y, Wei Y, Hui Z, Gao Y, Luo Y, Zhou Z, et al. Myasthenia Gravis Is Not an Independent Prognostic Factor of Thymoma: Results of a Propensity Score Matching Trial of 470 Patients. *Front Oncol* (2020) 10:583489. doi: 10.3389/fonc.2020.583489
32. Zhang Z, Cui Y, Jia R, Xue L, Liang H. Myasthenia Gravis in Patients With Thymoma Affects Survival Rate Following Extended Thymectomy. *Oncol Lett* (2016) 11(6):4177–82. doi: 10.3892/ol.2016.4528
33. Rena O, Papalia E, Maggi G, Oliaro A, Ruffini E, Filosso P, et al. World Health Organization Histologic Classification: An Independent Prognostic Factor in Resected Thymomas. *Lung Cancer* (2005) 50(1):59–66. doi: 10.1016/j.lungcan.2005.05.009
34. Knetki-Wroblewska M, Kowalski DM, Olszyna-Serementa M, Krzakowski M, Szolkowska M. Thymic Epithelial Tumors: Do We Know All the Prognostic Factors? *Thorac Cancer* (2021) 12(3):339–48. doi: 10.1111/1759-7714.13750
35. Marx A, Chan JKC, Chalabreysse L, Dacic S, Detterbeck F, French CA, et al. The 2021 WHO Classification of Tumors of the Thymus and Mediastinum: What Is New in Thymic Epithelial, Germ Cell, and Mesenchymal Tumors? *J Thorac Oncol* (2022) 17(2):200–13. doi: 10.1016/j.jtho.2021.10.010
36. Masaoka A, Monden Y, Nakahara K, Tanioka T. Follow-Up Study of Thymomas With Special Reference to Their Clinical Stages. *Cancer* (1981) 48(11):2485–92. doi: 10.1002/1097-0142(19811201)48:11<2485::aid-cncr2820481123>3.0.co;2-r
37. Koga K, Matsuno Y, Noguchi M, Mukai K, Asamura H, Goya T, et al. A Review of 79 Thymomas: Modification of Staging System and Reappraisal of Conventional Division Into Invasive and Non-Invasive Thymoma. *Pathol Int* (1994) 44(5):359–67. doi: 10.1111/j.1440-1827.1994.tb02936.x
38. Bernard C, Frih H, Pasquet F, Kerever S, Jamilloux Y, Tronc F, et al. Thymoma Associated With Autoimmune Diseases: 85 Cases and Literature Review. *Autoimmun Rev* (2016) 15(1):82–92. doi: 10.1016/j.autrev.2015.09.005
39. Jackson MW, Palma DA, Camidge DR, Jones BL, Robin TP, Sher DJ, et al. The Impact of Postoperative Radiotherapy for Thymoma and Thymic Carcinoma. *J Thorac Oncol* (2017) 12(4):734–44. doi: 10.1016/j.jtho.2017.01.002
40. Minami K, Jimbo N, Tanaka Y, Uchida T, Okamoto T, Shimizu N, et al. Fibrous Bands Associated With Higher Masaoka Stage and Poor Recurrence-Free Survival in Patients With Thymoma. *Thorac Cancer* (2021) 12(3):349–56. doi: 10.1111/1759-7714.13755
41. Tian W, Sun Y, Wu Q, Jiao P, Ma C, Yu H, et al. Surgical Outcomes of 215 Patients With Thymic Epithelial Tumors: A Single-Center Experience. *Thorac Cancer* (2020) 11(7):1840–7. doi: 10.1111/1759-7714.13464
42. Smith A, Cavalli C, Harling L, Harrison-Phipps K, Routledge T, Pilling J, et al. Impact of the TNM Staging System for Thymoma. *Mediastinum* (2021) 5:32. doi: 10.21037/med-21-24
43. Okereke IC, Kesler KA, Morad MH, Mi D, Rieger KM, Birdas TJ, et al. Prognostic Indicators After Surgery for Thymoma. *Ann Thorac Surg* (2010) 89 (4):1071–9. doi: 10.1016/j.athoracsur.2010.01.026
44. Yuan ZY, Gao SG, Mu JW, Xue Q, Mao YS, Wang DL, et al. Long-Term Outcomes of 307 Patients After Complete Thymoma Resection. *Chin J Cancer* (2017) 36(1):46. doi: 10.1186/s40880-017-0213-8
45. Sakai M, Onuki T, Inagaki M, Yamaoka M, Kitazawa S, Kobayashi K, et al. Early-Stage Thymic Carcinoma: Is Adjuvant Therapy Required? *J Thorac Dis* (2013) 5(2):161–4. doi: 10.3978/j.issn.2072-1439.2013.01.06
46. Wei ML, Kang D, Gu L, Qiu M, Zhengyin L, Mu Y. Chemotherapy for Thymic Carcinoma and Advanced Thymoma in Adults. *Cochrane Database Syst Rev* (2013) 8):CD008588. doi: 10.1002/14651858.CD008588.pub2
47. Song Z, Yu X, Zhang Y. Chemotherapy and Prognosis in Advanced Thymic Carcinoma Patients. *Clinics (Sao Paulo)* (2015) 70(12):775–80. doi: 10.6061/clinics/2015(12)03
48. Rimner A, Yao X, Huang J, Antonicelli A, Ahmad U, Korst RJ, et al. Postoperative Radiation Therapy Is Associated With Longer Overall Survival in Completely Resected Stage II and III Thymoma-An Analysis of the International Thymic Malignancies Interest Group Retrospective Database. *J Thorac Oncol* (2016) 11(10):1785–92. doi: 10.1016/j.jtho.2016.06.011
49. Keld R, Thian M, Hau C, Sajid J, Kumar N, Ang Y. Polymorphisms of MTHFR and Susceptibility to Oesophageal Adenocarcinoma in a Caucasian United Kingdom Population. *World J Gastroenterol* (2014) 20(34):12212–6. doi: 10.3748/wjg.v20.i34.12212
50. Chen XL, Wang YM, Zhao F, Chen Z, Yang X, Sun C, et al. Methylenetetrahydrofolate Reductase Polymorphisms and Colorectal Cancer Prognosis: A Meta-Analysis. *J Gene Med* (2019) 21(9):e3114. doi: 10.1002/jgm.3114
51. Blank S, Rachakonda S, Keller G, Weichert W, Lordick F, Langer R, et al. A Retrospective Comparative Exploratory Study on Two Methylentetrahydrofolate Reductase (MTHFR) Polymorphisms in

Esophagogastric Cancer: The A1298C MTHFR Polymorphism Is an Independent Prognostic Factor Only in Neoadjuvantly Treated Gastric Cancer Patients. *BMC Cancer* (2014) 14:58. doi: 10.1186/1471-2407-14-58
52. Tiseo M, Giovannetti E, Tibaldi C, Camerini A, Di Costanzo F, Barbieri F, et al. Pharmacogenetic Study of Patients With Advanced non-Small Cell Lung Cancer (NSCLC) Treated With Second-Line Pemetrexed or Pemetrexed-Carboplatin. *Lung Cancer* (2012) 78(1):92–9. doi: 10.1016/j.lungcan.2012.07.009
53. Yeh CC, Lai CY, Chang SN, Hsieh LL, Tang R, Sung FC, et al. Polymorphisms of MTHFR C677T and A1298C Associated With Survival in Patients With Colorectal Cancer Treated With 5-Fluorouracil-Based Chemotherapy. *Int J Clin Oncol* (2017) 22(3):484–93. doi: 10.1007/s10147-016-1080-z
54. Izmirli M. A Literature Review of MTHFR (C677T and A1298C Polymorphisms) and Cancer Risk. *Mol Biol Rep* (2013) 40(1):625–37. doi: 10.1007/s11033-012-2101-2
55. Amenyah SD, McMahon A, Ward M, Deane J, McNulty H, Hughes CF, et al. Riboflavin Supplementation Alters Global and Gene-Specific DNA Methylation in Adults With the MTHFR 677 TT Genotype. *Biochimie* (2020) 173:17–26. doi: 10.1016/j.biochi.2020.04.007
56. Kumar A, Rao A, Bhavani S, Newberg JY, Murphy RF. Automated Analysis of Immunohistochemistry Images Identifies Candidate Location Biomarkers for Cancers. *Proc Natl Acad Sci USA* (2014) 111(51):18249–54. doi: 10.1073/pnas.1415120112

Conflict of Interest: The authors declare that the research was conducted in the absence of any commercial or financial relationships that could be construed as a potential conflict of interest.

Publisher's Note: All claims expressed in this article are solely those of the authors and do not necessarily represent those of their affiliated organizations, or those of the publisher, the editors and the reviewers. Any product that may be evaluated in this article, or claim that may be made by its manufacturer, is not guaranteed or endorsed by the publisher.

Copyright © 2022 Yan, Wu, Xue, Mo, Zheng, Zhang, Gao and Bao. This is an open-access article distributed under the terms of the Creative Commons Attribution License (CC BY). The use, distribution or reproduction in other forums is permitted, provided the original author(s) and the copyright owner(s) are credited and that the original publication in this journal is cited, in accordance with accepted academic practice. No use, distribution or reproduction is permitted which does not comply with these terms.

frontiers | Frontiers in Oncology

SYSTEMATIC REVIEW
published: 24 June 2022
doi: 10.3389/fonc.2022.881553

Thymomas With Intravascular and Intracardiac Growth

Andrea Valeria Arrossi[1]*, *Josephine K. Dermawan*[2], *Michael Bolen*[3] and *Daniel Raymond*[4]

[1] Department of Pathology, Robert J. (R.J) Tomsich Pathology and Laboratory Medicine Institute, Cleveland Clinic, Cleveland, OH, United States, [2] Department of Pathology, Memorial Sloan Kettering Cancer Center, New York, NY, United States, [3] Imaging Institute, Cardiovascular and Thoracic Radiology, Cleveland Clinic, Cleveland, OH, United States, [4] Department of Thoracic Surgery, Cleveland Clinic, Cleveland, OH, United States

Thymomas are derived from the epithelial component of the thymus and constitute the most common tumor of the anterior mediastinum. These neoplasms are considered malignant for their potential for invasion and metastases. Several histopathologic subclassification schemes have been proposed over the years, however, correlation of histotypes with prognosis remains controversial. In contrast, studies invariably have shown that staging and resection status correlate with oncologic behavior and disease outcomes. In this regard, several staging systems have been presented, though transcapsular invasion and degree of involvement of adjacent anatomic structures are common denominators of all schemes. Involvement of the great vessels and heart most commonly results from direct invasion, which may lead to unusual clinical presentations such as superior vena cava syndrome. Moreover, intravascular and intracardiac growth with or without direct mural invasion rarely occurs. We provide an overview of thymomas with intravascular and intracardiac involvement.

Keywords: invasive thymoma, staging, intravascular growth, superior vena cava syndrome, intravascular growth pattern

OPEN ACCESS

Edited by:
Cesar Moran,
University of Texas MD Anderson Cancer Center, United States

Reviewed by:
Niccolò Daddi,
University of Bologna, Italy
Michael Ried,
University Hospital Regensburg, Germany

***Correspondence:**
Andrea Valeria Arrossi
arrossa@ccf.org

Specialty section:
This article was submitted to Thoracic Oncology, a section of the journal Frontiers in Oncology

Received: *22 February 2022*
Accepted: *05 May 2022*
Published: *24 June 2022*

Citation:
Arrossi AV, Dermawan JK, Bolen M and Raymond D (2022) Thymomas With Intravascular and Intracardiac Growth. Front. Oncol. 12:881553. doi: 10.3389/fonc.2022.881553

INTRODUCTION

Thymomas are malignant neoplasms derived from the epithelial component of the thymus. While they constitute the most common malignancy primary to the mediastinum, thymomas are rare, with a reported age standardized rate of 0.15 to 0.19/100,000 (1).

Given the complex histologic morphology and architecture of the normal thymus, thymomas are histologically characterized by their morphologic heterogeneity and have remained difficult to categorize by conventional histologic findings. Similarly, while treatment modalities, oncologic behavior, and disease outcomes are delineated by the clinical and pathologic staging, this parameter did not escape from the thymoma controversies in the literature.

Notably, disparity and lack of granularity amongst the current staging systems creates some challenges in the studies of locally advanced thymomas with vascular or cardiac involvement. In the Masaoka-Koga staging system (2) these tumors would classify as stage III. However, there is no differentiation in stage based on organ involvement type thus innominate vein (InV) involvement (often resectable) and direct myocardial involvement (often unresectable) are staged similarly (**Table 1**). The latest version of the TNM staging system does provide greater clarity. Macroscopic invasion into

TABLE 1 | Masaoka-Koga Stage.

I	Grossly and microscopically completely encapsulated
II	a. Microscopic transcapsular invasion b. Macroscopic capsular invasion into thymic or surrounding fatty tissue or grossly adherent to but not breaking through, mediastinal pleura or pericardium
III	Macroscopic invasion of neighboring organs pericardium, great vessels, or lung
IV	a. Pleural or pericardial dissemination b. Lymphatic or hematogenous metastasis

neighboring organs has been further differentiated in the T classification (3). The T3 group includes invasion into adjacent structures that are typically considered resectable and include InV, superior vena cava (SVC), chest wall, phrenic nerve, and extracardiac pulmonary vessels. On the other hand, T4 includes invasion into structures that are classically not considered resectable and include aorta, arch vessels, main pulmonary artery, myocardium, trachea or esophagus (**Table 2**). However, with advances in cardiac and great vessel surgery, paradigms are evolving with respect to determination of resectability. For example, focal great vessel involvement is no longer necessarily considered a formidable challenge.

Invasion of the great vessels, particularly InV and SVC, is not uncommon in advanced thymomas, however, in most cases, stage III (Masaoka-Koga) or T3 (TNM system) result from invasion of extravascular structures, i.e. lung and/or pericardium (4–8). Furthermore, 2 patterns of vascular invasion may be found. Vessels may be involved by contiguous extension (**Figure 1** Left), or, rarely, by downstream endoluminal growth into the large vessels and heart (**Figure 1** Right).

In this report, we summarize the cases in the English medical literature that provide detail of thymic tumors with intravascular/thrombotic growth protruding into the SVC, its tributaries, and heart, without evidence of contiguous extension through their walls. Our purpose is to highlight this unusual pattern of vascular invasion and generate the base for the identification and further evaluation of these cases.

DESIGN

A search of thymomas with vascular involvement was performed in the PubMed database (National Medical Library) using the following search terms: "thymoma" and "vascular" and/or each of the terms "intravascular", and/or "superior vena cava", "innominate vein", "brachiocephalic vein", "atrium", "cardiac", "heart", "intracardiac", "thrombosis".

All pertinent articles in the English language medical literature were reviewed. Only those studies with confirmed endovascular growth as the pattern of vascular involvement (**Figure 1** Left) were included. Articles referring to cases with vascular involvement resulting from adjacent contiguous invasion, or without detailed data regarding the pattern of vascular invasion were excluded (4–7, 9–21).

The clinical, radiographic, and surgical data were gathered and tabulated for each publication.

TABLE 2 | TNM Stage.

T1	a. Encapsulated or unencapsulated with or without extension into mediastinal fat b. Extension into mediastinal pleura
T2	Pericardium
T3	Lung, InV, SVC, chest wall, phrenic nerve, hilar extrapericardial pulmonary vessels
T4	Aorta, arch vessels, main pulmonary artery, myocardium, trachea, or esophagus

InV, Innominate vein; SVC, Superior vena cava.

RESULTS

Thirty-five publications of patients with confirmed radiographic and/or surgical description of intravascular/intracardiac spread of thymoma without evidence of direct connection were found after thorough review of the numerous articles from the English medical literature. Each publication reported 1 patient with these characteristics (22–55).

The detailed results are shown in **Table 3**. In summary, there were a total of 34 patients (17 females and 15 males, gender not available in 2 cases) with an average age of 58 years old. Twenty-six cases (87%) presented with swelling of the veins of the face, neck, upper extremities, and/or chest wall, characteristic of SVC syndrome, 7 of them associated with dyspnea. SVC syndrome was not present in 5 (17%) patients, 1 was an incidental finding during cardiac surgery, and 4 presented with dizziness and cough, abdominal pain and distension, ptosis, pain and weight loss, ptosis, and chest discomfort respectively. The patient with ptosis was the only one with evidence of myasthenia gravis. Clinical presentation was not provided in 4 patients.

Patients received a wide range of diagnostic imaging studies, with all but 5 having either magnetic resonance imaging (MRI) and/or computed tomography (CT) imaging performed as part of the evaluation. All 5 patients who did not undergo CT or MRI were evaluated in 1997 or earlier and had echocardiography or catheter-based venography. By imaging studies, invasion of the SVC was seen in 28 (85%) patients, 21 of whom with involvement of the right atrium (RA) and 15 with involvement of SVC tributaries, mostly InV. Vascular invasion was not detected radiographically in 1 patient. Radiographic data was not available in 2 patients. Both intraoperative and imaging data were provided in 27 cases. Of those, concordant findings were present in 20 cases and in 7 cases, 1 or more involved vessels were encountered intraoperatively.

The average size of the thymomas (available in 23 cases) was 8.9 cm, ranging from 3 to 16 cm. The histologic type was reported in 27 cases: WHO types A in 3, AB in 5, B1 in 2, and B2 and B3 in 5. Two cases were reported as epithelial-predominant, 'mixed" in 1, "type II" in 1, and lymphoepithelial in 1.

DISCUSSION

Thymomas are the most common primary tumor occurring in the anterior mediastinum, with an annual incidence 0.15 to 0.19/

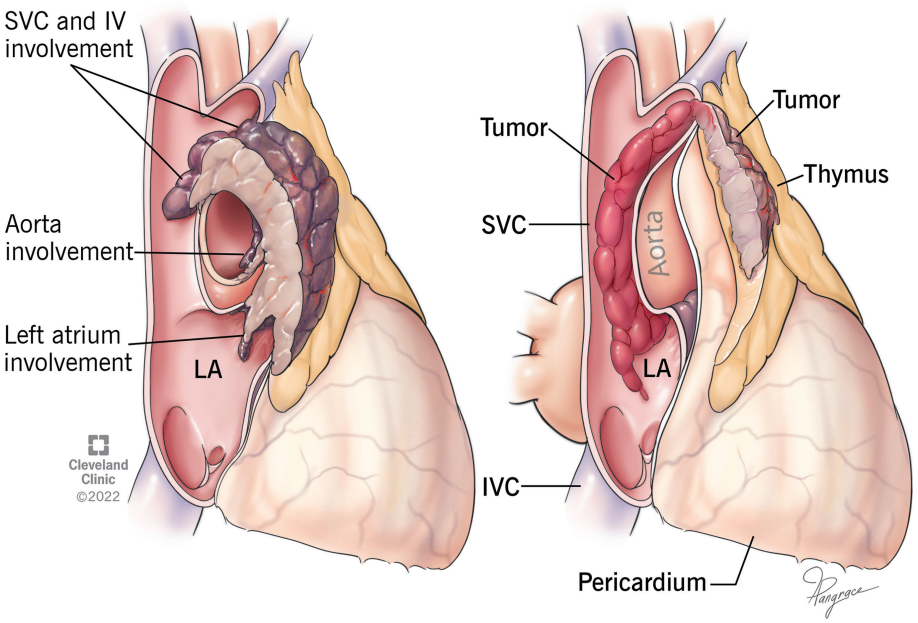

FIGURE 1 | Drawing of 2 different types of vascular invasion. Left: Thymoma invades superior vena cava (SVC), innominate vein (IV), aorta, and left atrium (LA) by contiguous infiltration. Right: Thymoma shows a single point of wall invasion into the vessel with intravascular downstream extension into SVC and LA without contiguous involvement.

100,000 (1). All age groups are affected, but most commonly they occur in middle-aged adults (40-50 years). Patients may present with symptoms due to mass effect, autoimmune or paraneoplastic syndromes or metastases, and in a subset of patients, thymomas are found incidentally during thoracic imaging. Autoimmune or paraneoplastic symptoms are most commonly, but are not limited to, neuromuscular disorders (myasthenia gravis), immunodeficiency disorders (hypogammaglobulinemia), or hematologic diseases (pure cell aplasia, hemolytic anemia).

Once a diagnosis is made, a multidisciplinary treatment approach with clinicians experienced with thymoma/thymic carcinoma is vital. Tumor type, stage, extent of invasiveness, potential phrenic nerve involvement, and the physiologic status of the patient are all essential considerations when determining the appropriate multi-modal treatment plan. In the circumstance of potential vascular or cardiac involvement, surgery may still play a role in the patient management depending on degree and location of involvement.

At the time of presentation, most tumors (65%) are Masaoka-Koga stage I or II, 25% are stage III, and around 10% are stage IV (8). Half of all presentations have invasion into surrounding structures but remain candidates for multimodal therapy including surgical resection. This emphasizes the importance of multidisciplinary management. Unfortunately, the Masaoka-Koga staging system makes no differentiation in stage based on organ involvement type thus innominate vein involvement (often resectable) and direct myocardial involvement (often unresectable) are staged similarly (**Table 1**). This is better reflected in the latest version of the TNM staging system, in which invasion of mediastinal organs is further divided into T3 (invasion or lung, InV, SVC, phrenic nerve, chest wall or extrapericardial pulmonary arteries) and T4 (invasion of aorta, arch vessels, intrapericardial pulmonary artery, myocardium, trachea and/or esophagus) (**Table 2**) (3).

We present a review of thymoma cases reported in the English medical literature that demonstrated vascular invasion through endovascular and intracardiac growth not associated with contiguous extension from the main mass (**Figure 1**). SVC syndrome was the most common presentation of these patients. In most cases, imaging studies were able to demonstrate endovascular growth with good correlation with the intraoperative findings. These cases are staged as Masaoka-Koga III or TNM system T3, however they have an unusual unifying component, the intravascular extension of tumor. It is hypothesized that thymomas enter the great veins through small vessels, such as the thymic veins, or focal transmural invasion, analogous to other angioinvasive malignancies such as renal cell carcinoma, leading to its growth along the venous stream down into the larger veins and atrium. Protrusion of the tumor into the thymic veins was noted intraoperatively in some of the cases in this review.

The WHO classification is currently the primary scheme used for the histologic typification of thymomas (56). Types A, AB, B1, B2, and B3 are divided based on cell morphology and progressive loss of the background population of immature thymic lymphocytes. While the prognosis of thymomas is mainly dependent on stage and resection status, Weiss et al. showed that recurrence rate was correlated with the WHO histotypes but

TABLE 3 | Patient characteristics and tumor details.

Year	Ref	Age	Gender	Clinical presentation (as described)	MG	Imaging studies	Imaging studies: vessels involved	Intraoperative vessels involved	Imaging: other organs	Intraoperative: oher organs	Largest size (cm)	Histologic type
1978	22	70	F	dyspnea, face swelling, hoarseness	No	SVC cavogram	InV, SVC	InV, SVC	N/A	none	16	LE
1979	23	39	M	SVC syndrome	No	angiography	SVC	SVC	none	none	N/A	N/A
1989	24	80	F	swollen neck veins, pleural effusion	No	echocardiography, angiography	SVC, RA	surgery not performed	N/A	N/A	N/A	spindle cell
1990	25	38	M	abdominal pain, weight loss	No	echocardiography	SVC, RA, RV	SVC, RA, RV	none	pericardium	9	N/A
1990	26	50	M	Neck and chest venous distension, face swelling	No	CT, SVC cavogram	SVC	SVC	N/A	N/A	10	EP
1992	28	65	f	dizziness, cough, anorexia	No	echocardiography, transesophageal US	SVC, RA	SVC, RA	none	none	N/A	N/A
1992	27	72	M	swelling of the face and exertional dyspnea	No	CT, SVC cavogram	SVC	InV, SVC, RA	pericardial efussion	pericardium, RUL, LUL	15.5	EP
1993	29	56	M	face and upper extremity edema	No	US, CT, MRI, SVC cavogram	SVC, RA	SVC, RA	N/A	pericardium	4	EP
1994	39	37	M	SOB, edema upper limb, hemoptysis, cardiac tamponade	No	CT, echocardiogram	SVC	SVC	pericardium, RML, chest wall	pericardium, RML, chest wall	N/A	N/A
1997	31	52	F	neck swelling	No	transthoracic 2-dimensional echocardiography	InV, SVC, RA	InV, SVC, RA	none	none	15	N/A
1999	32	74	M	eyelid ptosis, myasthenia gravis	Yes	CT	N/A	InV	none	sternothyroid and sternohyoid muscles	5.2	EP
1999	33	44	M	facial, upper extremity edema, hoarseness,	No	CT, echocardiogram, venography, gallium scintigraphy	InV, SVC, RA	InV, azygous ven, SVC, RA	none	pericardium, LUL, RUL, RML, right phrenic nerve	N/A	N/A
2004	34	64	N/A	anterior chest discomfort	No	CT	InV, SVC	InV, SVC	pericardial effusion	pericardium, RUL	16	B2
2006	35	56	F	swelling of face and upper extremities	No	CT, MRI, echocardiogram	InV, SVC, RA	InV, SVC, RA	N/A	LUL, tumor implant in diaphragm	N/A	AB
2007	36	71	F	lethargy, facial edema	No	CT, MRI	InV, SVC	InV, SVC	none	left phrenic nerve	6	AB
2007	37	48	M	face and the right upper extremity	No	CT, echocardiography, venocavogram	InV, SVC and RA	InV, SVC, LBCV, RA	none	pericardium, RUL, RML, right phrenic nerve	N/A	AB
2007	38	86	M	N/A	N/A	MDCT angiography	InV, SVC, RA	no surgery	N/A	N/A	N/A	N/A
2008	39	50	F	dyspnea, enlargement of chest vessels	No	CT, cardiac MRI	SVC, RA	N/A	N/A	right side of the sternum.	13	N/A
2009	40	53	M	face and upper extremity edema.	No	CT	InV, SVC, right atrium	InV, SVC, RA, tricuspid valve, RV	none	right lung hilum, right phrenic nerve, pericardium	10	AB
2010	41	40	N/A	swelling of the face and the left upper extremity	No	CT, echocardiogram	InV, SVC, RA	InV, SVC, RA	pericardial effusion	none	14	B3
2012	42	53	F	SVC syndrome	No	CT, echocardiography	SVC, RA	InV, SVC, RA	N/A	right phrenic nerve	8	N/A
2012	43	69	M	swelling of the face and bilateral upper extremities	No	CT, MRI	InV, SVC, jugular and subclavian veins	InV, SVC, jugular, subclavian veins	N/A	pericardium	N/A	AB
2013	44	44	F	facial and left upper limb edema	No	CT, PET CT, echocardiogram	InV, SVC, RA	InV, SVC, RA	N/A	pericardium	5.2	B3

(Continued)

TABLE 3 | Continued

Year	Ref	Age	Gender	Clinical presentation (as described)	MG	Imaging studies	Imaging studies: vessels involved	Intraoperative vessels involved	Imaging: other organs	Intraoperative: oher organs	Largest size (cm)	Histologic type
2013	46	39	F	facial edema and dyspnea	No	CT, PET-CT	InV, SVC and right atrium	ImV, SVC, RA	none	none	N/A	B2
2013	47	53	F	severe dyspnea and facial oedema	No	NCCT, CCT, MRI	InV, SVC, RA	no data	N/A	N/A	N/A	B3
2013	45	74	M	SVC syndrome	No	CT, MRI, angiography	InV, SVC, RA	no surgery	N/A	N/A	6	B2
2014	48	54	M	N/A	N/A	CT, MRI	SVC, azygos vein, RA	InV, SVC, azygos vein, RA	N/A	none	3	B3
2016	49	57	F	facial swelling	No	CT, CT angiography	InV, SVC	InV, SVC	N/A	N/A	3.5	B2
2016	50	74	F	Face and upper extremity swelling, chest wall, jugular veins distention	No	echocardiogram, cardiovascular MRI	SVC, RA	InV, SVC, RA	none	RUL, pericardium, right phrenic nerve	9.9	B1
2018	51	84	F	N/A	No	CT, PET/CT	none seen	InV, *via* thymic vein	metastases bilateral lungs		4.4	A
2019	52	50	F	N/A	No	CT, echocardiogram	InV, SVC, RA	InV, SVC, RA	pericardial effusion	IVC	5	B3
2019	53	39	F	facial and upper limb swelling	No	CT, MRI	InV	InV, SVC	pericardium	lung, pericardium	7.9	B1
2020	55	63	F	exertional dyspnea, and upper limb and facial edema	No	N/A	N/A	InV, SVC	none	mediastinal pleura, pericardium, RUL, LUL	12	B2
2020	54	76	M	incidental, cardiac surgery	No	CT, MRI	InV, SVC, RA	N/A		N/A	6.5	A

CT, Computed tomography; EP, Epithelial predominant; InV, Innominate vein; LE, lymphoepithelial; LUL, Left upper lobe; MG, Myasthenia gravis; MRI, Magnetic resonance studies; PET, Positron emission tomography; RA, Right atrium; RML, Right middle lobe; RUL, right upper lobe; RV, Right ventricle; SVC, Superior vena cava.
N/A, not applicable.

not overall survival (57). However, the relevance of the pathologic classification as a prognostic indicator for recurrence and overall survival has been the subject of numerous studies, with discrepant results. Furthermore, several other histologic schemes have been proposed in the literature, and the controversy regarding which one is the most reproducible, applicable to, and reflective of clinical behavior is ongoing.

Histologic data was available in 25 cases and included 14 cases B2 and B3 (3 older cases classified as epithelial predominant were converted to B3 in this review). Surprisingly, types A, AB, and B1 grouped together were reported at frequencies comparable to types B2 and B3.

Imaging plays a central role in the diagnosis and staging of thymomas. Thymomas typically present in an anterior mediastinal location, arising from one side of the thymus with well-defined margins, smooth or lobulated contours, and locations varying from thoracic inlet to cardiophrenic angle (58). Use of intravenous contrast is indicated whenever feasible, as this allows for improved assessment of vascular involvement, as well as enhancement characterization of the mass. Vascular invasion is suggested by alteration of vessel lumen contour, encasement or obliteration of vessel, or soft tissue intravascular extension, which may also extend to pericardium or cardiac chambers (59). Use of ECG synchronized imaging, either by CT or MRI may allow for improved delineation of cardiac involvement.

Involvement of the mediastinal vessels, in particular InV and/or SVC, is not uncommon in locally advanced thymomas (about 15%), however, lung and pericardium are the most frequently involved organs in Masaoka-Koga stage III or TNM T3 tumors (4–8). The impact on tumor behavior of vascular involvement remains unclear, however, recurrence rates tend to be higher, and disease-free survival shorter, in cases with invasion of the great vessels compared to those without (4, 6, 7). More so, almost no studies evaluate the significance of differentiating specific vessel involvement. In this regard, in a study of clinicopathologic correlation of 250 thymoma cases by Moran et al. the InV was stratified separately from the other great vessels and heart as stage IIA and stage IIC respectively. This stratification did not result statistically significant, however, the number of cases in the study was low, with only 56 tumors stage IIA and 2 tumors stage IIC. Nonetheless, these groups were still included in the proposed staging system. The authors manifest that such stratification is important for the possibility of advances in surgical techniques, additional therapy, and future larger studies. (**Table 4**) (60). For instance, extended involvement of the surrounding anatomic structures (Masaoka stage III or TNM

TABLE 4 | Moran Stage.

0	Encapsulated tumor
I	Invasive tumor into perithymic adipose tissue
II	Direct invasion
	A. InV, mediastinal pleura, lung
	B. Pericardium
	C. Great vessels (aorta, SVC), heart
III	Metastatic disease
	A. Intrathoracic structures, diaphragm, LNs
	B. Extrathoracic invasion

InV, Innominate vein; SVC, Superior vena cava; LNs, Lymph nodes.

system T3) makes radical surgery unfeasible in up to 30% to 40% of invasive thymomas and thymic carcinomas grouped together (20). Involvement of the InV, however, can be addressed with simple vein resection with or without reconstruction, and involvement of the SVC can be addressed surgically in certain circumstances although cardiopulmonary bypass may be necessary. Thus, there is likely significantly variability in the determination of resectability based on surgeon and center level experience.

Notably, Moran et al. also recognized that vascular invasion in thymomas may follow 2 different patterns, either direct wrapping/extension into the vascular wall, or spread within the vessel itself, as the cases reviewed in this article. Whether staging should be different for these tumors is uncertain. The significance of specific vessel differentiation in the stratification of staging systems, and the pattern of vascular involvement would need to be elucidated.

Limitations

In this study, we present cases of thymoma with intravascular/thrombotic pattern of vascular invasion based on a review of the literature. We excluded the cases that presented vascular invasion by contiguity, as well as those we deemed confusing or ambiguous. However, we recognize that our study is based on a retrospective literature review, and as such, accuracy of the data might be difficult to assess in some cases, especially older reports, which constitutes the main limitation of our study. Nonetheless, we believe that our study could set the base for the identification of these cases and development of future studies to delineate their significance.

CONCLUSION

We provide a descriptive analysis of thymoma cases with vascular invasion resulting from downstream polypoid and/or thrombotic intravascular growth detected with imaging studies and/or intraoperatively. intravascular spread is rare among thymomas, regardless of histologic type or staging, and may create uncertainties regarding management. We acknowledge that precise assessment of the incidence of this phenomenon is challenging due to the ambiguity in defining the pattern of vascular invasion in most studies. Importantly, vital to the most appropriate intra-operative planning and perioperative support in managing patients with thymomas is an ongoing, multidisciplinary evaluation, appropriate physiologic assessment of the patient, and precise staging.

DATA AVAILABILITY STATEMENT

The raw data supporting the conclusions of this article will be made available by the authors, without undue reservation.

AUTHOR CONTRIBUTIONS

AA contributed to conception and design of the study, literature search using the MedHub database, extraction of data from the literature, and writing the first draft of the manuscript. JD, MB, and DR wrote sections of the manuscript. All authors contributed to manuscript revision, read, and approved the submitted version.

REFERENCES

1. Hsu C-H, Chan JK, Yin C-H, Lee C-C, Chern C-U, Liao C-I. Trends in the Incidence of Thymoma, Thymic Carcinoma, and Thymic Neuroendocrine Tumor in the United States. *PloS One* (2019) 14(12):e0227197. doi: 10.1371/journal.pone.0227197
2. Koga K, Matsuno Y, Noguchi M, Mukai K, Asamura H, Goya T, et al. A Review of 79 Thymomas: Modification of Staging System and Reappraisal of Conventional Division Into Invasive and non-Invasive Thymoma. *Pathol Int* (1994) 44(5):359–67. doi: 10.1111/j.1440-1827.1994.tb02936.x
3. Detterbeck FC, Stratton K, Giroux D, Asamura H, Crowley J, Falkson C, et al. The IASLC/ITMIG Thymic Epithelial Tumors Staging Project: Proposal for an Evidence-Based Stage Classification System for the Forthcoming (8th) Edition of the TNM Classification of Malignant Tumors. *J Thorac Oncol Off Publ Int Assoc Study Lung Cancer* (2014) 9(9 Suppl 2):S65–72. doi: 10.1097/JTO.0000000000000290
4. Okumura M, Miyoshi S, Takeuchi Y, Yoon H-E, Minami M, Takeda S-I, et al. Results of Surgical Treatment of Thymomas With Special Reference to the Involved Organs. *J Thorac Cardiovasc Surg* (1999) 117(3):605–12. doi: 10.1016/S0022-5223(99)70343-0
5. Wright CD, Wain JC, Wong DR, Donahue DM, Gaissert HA, Grillo HC, et al. Predictors of Recurrence in Thymic Tumors: Importance of Invasion, World Health Organization Histology, and Size. *J Thorac Cardiovasc Surg* (2005) 130(5):1413–21. doi: 10.1016/j.jtcvs.2005.07.026
6. Utsumi T, Shiono H, Matsumura A, Maeda H, Ohta M, Tada H, et al. Stage III Thymoma: Relationship of Local Invasion to Recurrence. *J Thorac Cardiovasc Surg* (2008) 136(6):1481–5. doi: 10.1016/j.jtcvs.2008.05.012
7. Comacchio GM, Dell'Amore A, Marino MC, Russo MD, Schiavon M, Mammana M, et al. Vascular Involvement in Thymic Epithelial Tumors: Surgical and Oncological Outcomes. *Cancers* (2021) 13(13):3355. doi: 10.3390/cancers13133355
8. Detterbeck FC, Zeeshan A. Thymoma: Current Diagnosis and Treatment. *Chin Med J (Engl)* (2013) 126(11):2186–91. doi: 10.3760/cma.j.issn.0366-6999.20130177
9. Dartevelle P, Chapelier A, Navajas M, Levasseur P, Rojas A, Khalife J, et al. Replacement of the Superior Vena Cava With Polytetrafluoroethylene Grafts Combined With Resection of Mediastinal-Pulmonary Malignant Tumors. *J Thorac Cardiovasc Surg* (1987) 94(3):361–6. doi: 10.1016/S0022-5223(19)36248-8
10. Freedberg. The Evaluation of MRI in the Evaluation of Intracardiac Tumors Diagnosed by Ecocardiography. *Circulation* (1988) 77:96. doi: 10.1161/01.CIR.77.1.96
11. Dartevelle PG, Chapelier AR, Pastorino U, Corbi P, Lenot B, Cerrina J, et al. Long-Term Follow-Up After Prosthetic Replacement of the Superior Vena Cava Combined With Resection of Mediastinal-Pulmonary Malignant Tumors. *J Thorac Cardiovasc Surg* (1991) 102(2):259–65. doi: 10.1016/S0022-5223(19)36558-4

12. Shimizu N, Moriyama S, Aoe M. The Surgical Treatment of Invasive Thymoma. *J Thorac Cardiovasc Surg* Vol. 103. (1992). pp. 414–20. doi: 10.1016/S0022-5223(19)34979-7
13. Yagi K, Hirata T, Fukuse T, Yokomise H, Inui K, Ike O, et al. Surgical Treatment for Invasive Thymoma, Especially When the Superior Vena Cava is Invaded. *Ann Thorac Surg* (1996) 61(2):521–4. doi: 10.1016/0003-4975(95)00983-3
14. Bacha EA, Chapelier AR, Macchiarini P, Fadel E, Dartevelle PG. Surgery for Invasive Primary Mediastinal Tumors. *Ann Thorac Surg* (1998) 66(1):234–9. doi: 10.1016/S0003-4975(98)00350-6
15. Lanuti M, De Delva PE, Gaissert HA, Wright CD, Wain JC, Allan JS, et al. Review of Superior Vena Cava Resection in the Management of Benign Disease and Pulmonary or Mediastinal Malignancies. *Ann Thorac Surg* (2009) 88(2):392–7. doi: 10.1016/j.athoracsur.2009.04.068
16. Marulli G, Lucchi M, Margaritora S, Cardillo G, Mussi A, Cusumano G, et al. Surgical Treatment of Stage III Thymic Tumors: A Multi-Institutional Review From Four Italian Centers☆. *Eur J Cardiothorac Surg* (2011) 39(3):e1–7. doi: 10.1016/j.ejcts.2010.11.026
17. De Giacomo T, Patella M, Mazzesi G, Venuta F. Successful Resection of Thymoma Directly Invading the Right Atrium Under Cardiopulmonary Bypass. *Eur J Cardiothorac Surg* (2015) 48(2):332–3. doi: 10.1093/ejcts/ezu376
18. Dai W, Dong J, Zhang H, Yang X, Li Q. Superior Vena Cava Replacement Combined With Venovenous Shunt for Lung Cancer and Thymoma: A Case Series. *J Thorac Dis* (2018) 10(1):363–70. doi: 10.21037/jtd.2017.12.130
19. Maurizi G, Poggi C, D'Andrilli A, Vanni C, Ciccone AM, Ibrahim M, et al. Superior Vena Cava Replacement for Thymic Malignancies. *Ann Thorac Surg* (2019) 107(2):386–92. doi: 10.1016/j.athoracsur.2018.08.060
20. Bertolaccini L, Prisciandaro E, Galetta D, Casiraghi M, Guarize J, Petrella F, et al. Outcomes and Safety Analysis in Superior Vena Cava Resection for Extended Thymic Epithelial Tumors. *Ann Thorac Surg* (2021) 112(1):271–7. doi: 10.1016/j.athoracsur.2020.07.069
21. Okereke OU, Nzewi OC, Chikwendu VC, Odigwe E, Onuigbo WB. Radical Excision of Invasive Thymoma With Intracardiac Extension. *J Cardiovasc Surg (Torino)* (1994) 35(4):355–8.
22. Arai T, Inagaki K, Hata E, Hirata M, Onoue Y, Morimoto K. Reconstruction of the Superior Vena Cava in a Patient With a Thymoma. *Chest* (1978) 73(2):230–1. doi: 10.1378/chest.73.2.230
23. Tanabe T, Kubo Y, Hashimoto M, Sugie S. Patch Angioplasty of the Superior Vena Caval Obstruction (Case Reports With Long Follow-Up Results). *J Cardiovasc Surg (Torino)* (1979) 20(5):519–22.
24. Korobkin M, Gasano VA. Intracaval and Intracardiac Extension of Malignant Thymoma: CT Diagnosis. *J Comput Assist Tomogr* (1989) 13(2):348–50. doi: 10.1097/00004728-198903000-00035
25. Airan. Malignant Thymoma Presenting Intracardiac Tumor and SVC Obstruction. *Ann Thorac Surg* (1990) 50:989–91. doi: 10.1016/0003-4975(90)91143-Y
26. Chiou GTJ, Chen C-L, Wei J, Hwang W-S. Reconstruction of Superior Vena Cava in Invasive Thymoma. *Chest* (1990) 97(2):502–3. doi: 10.1378/chest.97.2.502
27. Yokoi K, Miyazawa N, Mori K, Saito Y, Tominaga K, Imura G, et al. Invasive Thymoma With Intracaval Growth Into the Right Atrium. *Ann Thorac Surg* (1992) 9(53):507–9.
28. Missault L, Duprez D, De Buyzere M, Cambier B, Adang L, Clement D. Right Atrial Invasive Thymoma With Protrusion Through the Tricuspid Valve. *Eur Heart J* (1992) 13(12):1726–7. doi: 10.1093/oxfordjournals.eurheartj.a060132
29. Futami S, Yamasaki T, Minami R, Matsuba K, Inoue K, Nishimoto S, et al. Intracaval and Intracardiac Extension of Malignant Thymoma. *Intern Med* (1993) 32(3):257–60. doi: 10.2169/internalmedicine.32.257
30. Dib H, Friedman B, Khouli H. Malignant Thymoma*A Complicated Triad of SVC Syndrome, Cardiac Tamponade, and DIC. *Chest* (1993) 105:941–2. doi: 10.1378/chest.105.3.941
31. Filippone G, Savona I, Tomasello V, Guzzetta P, Zarcone N, Agate V. Radical Excision of Invasive Thymoma With Intracaval and Intracardial Extension: A Successful Case Report. *J Cardiovasc Surg (Torino)* (1997) 38(5):547–9.
32. Nomori H, Horio H, Morinaga S, Suemasu K. Minimally Invasive Thymoma With Extensive Intravascular Growth. *Jpn J Clin Oncol* (1999) 29(12):630–2. doi: 10.1093/jjco/29.12.630
33. Minato N, Rikitake K, Ohnishi H, Takarabe K, Ishida H. Invasive Thymoma With Intracaval Growth Extending and Directly Invading the Right Atrium. *J Cardiovasc Surg (Torino)* (1999) 40(6):915–7.
34. Terada Y, Ono N, Noguchi T, Kamakari K, Kitano M. A Case of Thymoma Protruding Into the Superior Vena Cava Through the Thymic Vein. *Ann Thorac Surg* (2004) 77(3):1088–90. doi: 10.1016/S0003-4975(03)01172-X
35. Ichimura H, Usui S, Okazaki H, Konishi T, Osaka M, Jikuya T, et al. Excision After Chemoradiotherapy of Invasive Thymoma Extending Into the Right Atrium: Report of a Case. *Surg Today* (2006) 36(6):534–7. doi: 10.1007/s00595-006-3188-7
36. Konstantinov IE, Saxena P, Koniuszko M, Ghosh S, Low VHS, Khor TS, et al. Superior Vena Cava Obstruction by Tumour Thrombus in Invasive Thymoma: Diagnosis and Surgical Management. *Heart Lung Circ* (2007) 16(6):462–4. doi: 10.1016/j.hlc.2006.08.010
37. Shudo Y, Takahashi T, Ohta M, Ikeda N, Matsue H, Taniguchi K. Radical Operation for Invasive Thymoma With Intracaval, Intracardiac, and Lung Invasion. *J Card Surg* (2007) 22(4):330–2. doi: 10.1111/j.1540-8191.2007.00417.x
38. Alladin M, Bozlar U, Turba UC, Kron IL, Ahmed H, Hagspiel KD. Mediastinal Thymoma Invading the Superior Vena Cava and the Right Atrium. *Acta Cardiol* (2007) (5):517–8. doi: 10.2143/AC.62.5.2023417
39. Dursun M, Sarvar S, Cekrezi B, Kaba E, Bakir B, Toker A. Cardiac Metastasis From Invasive Thymoma *Via* the Superior Vena Cava: Cardiac MRI Findings. *Cardiovasc Intervent Radiol* (2008) 31(S2):209–12. doi: 10.1007/s00270-007-9146-y
40. Amirghofran H, Emaminia A, Rayatpisheh S, Malek-Hosseini S, Attaran Y, et al. Intracardiac Invasive Thymoma Presenting as Superior Vena Cava Syndrome. *Ann Thorac Surg* (2009) 87:1616–8. doi: 10.1016/j.athoracsur.2008.09.052
41. Li W, Chen X, Lv X, Guo X, Yang Y, Ni Y, et al. Resection of an Invasive Thymoma Extending Into the Superior Vena Cava and Right Atrium. *J Card Surg* (2010) 25(5):515–7. doi: 10.1111/j.1540-8191.2010.01036.x
42. Toker A, Tireli E, Tanju S, Kaya S. Transcaval Invasion of Right Atrium by Thymoma: Resection *via* Transient Cava-Pulmonary Shunt. *Eur J Cardiothorac Surg* (2012) 41(5):1175–7. doi: 10.1093/ejcts/ezr261
43. Tsutsui S, Ashizawa K, Tagawa T, Nagayasu T, Hayashi T, Uetani M. Invasive Thymoma With Venous Intraluminal Extension: CT and MRI Findings. *Clin Imaging* (2012) 36(6):854–7. doi: 10.1016/j.clinimag.2012.01.033
44. Rizzardi G, Arena V, Passera E, Bortolotti L. Radical Surgery in an Unusual Case of Thymoma With Intraluminal Growth Into the Superior Vena Cava and Right Atrium. *Interact Cardiovasc Thorac Surg* (2013) 17(6):1054–5. doi: 10.1093/icvts/ivt397
45. Kurata A, Saji H, Ikeda N, Kuroda M. Intracaval and Intracardiac Extension of Invasive Thymoma Complicated by Superior and Inferior Vena Cava Syndrome: Intracardiac Extension of Thymoma. *Pathol Int* (2013) 63(1):56–62. doi: 10.1111/pin.12023
46. Kim HJ, Cho SY, Cho WH, Lee DH, Lim DH, Seo PW, et al. An Unusual Case of Superior Vena Cava Syndrome Caused by the Intravascular Invasion of an Invasive Thymoma. *Tuberc Respir Dis* (2013) 75(5):210–3. doi: 10.4046/trd.2013.75.5.210
47. Gümüstas S, Akça A, Inan N, Akgül AG, Liman ST. Characterization of Malignant Thrombus in an Invasive Thymoma With Intravascular Growth. *J Radiol Case Rep* (2013) 7(2):17–23. doi: 10.3941/jrcr.v7i2.1115
48. Melloni G, Bandiera A, Castiglioni A, Zannini P. Thymoma With Intravascular Extension Into the Right Atrium. *Eur J Cardiothorac Surg* (2014) 45(4):e126–6. doi: 10.1093/ejcts/ezt618
49. Ohata K, Yoshimura T, Matsubara Y, Yasuhara Y, Terada Y. Invasive Thymoma Protruding Into the Superior Vena Cava Through the Thymic Vein. *Ann Thorac Cardiovasc Surg* (2016) 22(2):122–4. doi: 10.5761/atcs.cr.15-00149
50. Afzal A, Wong I, Korniyenko A, Ivanov A, Worku B, Gulkarov I. Superior Vena Cava Syndrome From an Invasive Thymoma With Transcaval Invasion to the Right Atrium. *J Surg Case Rep* (2016) 2016(4):rjw044. doi: 10.1093/jscr/rjw044
51. Kawakita N, Kondo K, Toba H, Yoneda A, Takizawa H, Tangoku A. A Case of Atypical Type A Thymoma With Vascular Invasion and Lung Metastasis. *Gen Thorac Cardiovasc Surg* (2018) 66(4):239–42. doi: 10.1007/s11748-017-0794-9
52. Yang T, Hui R, Wu Q, Tian J, Chen H. An Invasive Thymoma Extending Into the Superior Vena Cava and Right Atrium. *Ann Transl Med* (2019) 7(18):498. doi: 10.21037/atm.2019.08.59

53. Sena A, Ferreira R, Gonçalves J, Nobre Â. Surgical Treatment of an Advanced Stage Thymoma in a Good's Syndrome Patient - Case Report. *Rev Port Cir Cardiotorac Vasc* (2019) 26(4):269–71.
54. Singh N, Nand P, Alison P. Complex Redo Surgery to Treat a Large Thymoma Invading the Right Atrium. *J Card Surg* (2020) 35(6):1368–70. doi: 10.1111/jocs.14571
55. Shen W, Cao Y, Wang X, Zhang P, Zhou Q. Invasive Thymoma With Intravascular Growth Into the Great Veins and Right Atrium: A Case Report. *Thorac Cancer* (2020) 11(5):1326–9. doi: 10.1111/1759-7714.13242
56. WHO Classification of Tumours Editorial Board. Tumours of the Thymus, Thymoma. In: *WHO Classification of Tumours Thoracic Tumours, 5th ed*, vol. 5. Lyon, France: International Agency for Research on Cancer (2021). p. 319–49.
57. Weis C-A, Yao X, Deng Y, Detterbeck FC, Marino M, Nicholson AG, et al. The Impact of Thymoma Histotype on Prognosis in a Worldwide Database. *J Thorac Oncol* (2015) 10(2):367–72. doi: 10.1097/JTO.0000000000000393
58. Benveniste MFK, Rosado-de-Christenson ML, Sabloff BS, Moran CA, Swisher SG, Marom EM. Role of Imaging in the Diagnosis, Staging, and Treatment of Thymoma. *RadioGraphics* (2011) 31(7):1847–61. doi: 10.1148/rg.317115505
59. Rosado-de-Christenson ML, Strollo DC, Marom EM. Imaging of Thymic Epithelial Neoplasms. *Hematol Oncol Clin North Am* (2008) 22(3):409–31. doi: 10.1016/j.hoc.2008.03.011
60. Moran CA, Walsh G, Suster S, Kaiser L. A Clinicopathologic Correlation of 250 Cases With a Proposed Staging System With Emphasis on Pathologic Assessment. *Am J Clin Pathol* (2012) 137:451–61. doi: 10.1309/AJCP36ALGUZWOSEA

Conflict of Interest: The authors declare that the research was conducted in the absence of any commercial or financial relationships that could be construed as a potential conflict of interest.

Publisher's Note: All claims expressed in this article are solely those of the authors and do not necessarily represent those of their affiliated organizations, or those of the publisher, the editors and the reviewers. Any product that may be evaluated in this article, or claim that may be made by its manufacturer, is not guaranteed or endorsed by the publisher.

Copyright © 2022 Arrossi, Dermawan, Bolen and Raymond. This is an open-access article distributed under the terms of the Creative Commons Attribution License (CC BY). The use, distribution or reproduction in other forums is permitted, provided the original author(s) and the copyright owner(s) are credited and that the original publication in this journal is cited, in accordance with accepted academic practice. No use, distribution or reproduction is permitted which does not comply with these terms.

frontiers | Frontiers in Oncology

ORIGINAL RESEARCH
published: 08 July 2022
doi: 10.3389/fonc.2022.869253

Development and Validation of a CT-Based Radiomics Nomogram in Patients With Anterior Mediastinal Mass: Individualized Options for Preoperative Patients

Zhou Zhou[1†], *Yanjuan Qu*[1†], *Yurong Zhou*[1], *Binchen Wang*[1], *Weidong Hu*[2] *and Yiyuan Cao*[1*]

[1] Department of Radiology, Zhongnan Hospital of Wuhan University, Wuhan, China, [2] Department of Thoracic Surgery, Zhongnan Hospital of Wuhan University, Wuhan, China

OPEN ACCESS

Edited by:
Mylene Truong,
University of Texas MD Anderson Cancer Center, United States

Reviewed by:
Marta Bogowicz,
Maastro Clinic, Netherlands,
Güntuğ Batıhan,
SBU Dr. Suat Seren Chest Diseases and Surgery Training and Research Hospital, Turkey

***Correspondence:**
Yiyuan Cao
33738829@qq.com

[†]These authors have contributed equally to this work and share first authorship

Specialty section:
This article was submitted to Thoracic Oncology, a section of the journal Frontiers in Oncology

Received: 04 February 2022
Accepted: 09 June 2022
Published: 08 July 2022

Citation:
Zhou Z, Qu Y, Zhou Y, Wang B, Hu W and Cao Y (2022) Development and Validation of a CT-Based Radiomics Nomogram in Patients With Anterior Mediastinal Mass: Individualized Options for Preoperative Patients. Front. Oncol. 12:869253. doi: 10.3389/fonc.2022.869253

Background: To improve the preoperative diagnostic accuracy and reduce the non-therapeutic thymectomy rate, we established a comprehensive predictive nomogram based on radiomics data and computed tomography (CT) features and further explored its potential use in clinical decision-making for anterior mediastinal masses (AMMs).

Methods: A total of 280 patients, including 280 with unenhanced CT (UECT) and 241 with contrast-enhanced CT (CECT) scans, all of whom had undergone thymectomy for AMM with confirmed histopathology, were enrolled in this study. A total of 1,288 radiomics features were extracted from each labeled mass. The least absolute shrinkage and selection operator model was used to select the optimal radiomics features in the training set to construct the radscore. Multivariate logistic regression analysis was conducted to establish a combined clinical radiographic radscore model, and an individualized prediction nomogram was developed.

Results: In the UECT dataset, radscore and the UECT ratio were selected for the nomogram. The combined model achieved higher accuracy (AUC: 0.870) than the clinical model (AUC: 0.752) for the prediction of therapeutic thymectomy probability. In the CECT dataset, the clinical and combined models achieved higher accuracy (AUC: 0.851 and 0.836, respectively) than the radscore model (AUC: 0.618) for the prediction of therapeutic thymectomy probability.

Conclusions: In patients who underwent UECT only, a nomogram integrating the radscore and the UECT ratio achieved good accuracy in predicting therapeutic thymectomy in AMMs. However, the use of radiomics in patients with CECT scans did not improve prediction performance; therefore, a clinical model is recommended.

Keywords: anterior mediastinal mass, radiomics, nomogram, thymectomy, computed tomography

INTRODUCTION

Mediastinal masses are uncommon compared to masses in the lungs. The prevalence of mediastinal masses ranges from 0.73% to 0.9%, taking reference from a population-based cohort study (1) and two lung cancer screening studies (2, 3). The masses most commonly occur in the anterior mediastinum, accounting for 50%–69.8% of all mediastinal masses (4, 5). Anterior mediastinal masses (AMMs) include a wide range of pathological entities, varying from benign cysts to neoplasms (benign and malignant) (6, 7). Therefore, they often pose a diagnostic challenge for clinicians (8).

Surgical excision is one of the most common treatments for AMMs (9), which may not necessarily be appropriate. The overall non-therapeutic thymectomy rate ranges from 22% to 68%, as it had been reported in the literature (10, 11), and is often due to diagnostic inaccuracies. For example, masses that did not warrant surgical intervention were misdiagnosed as thymomas (10). Thus, a definitive diagnosis is crucial for better preoperative counseling, appropriate treatment decisions, and follow-up management.

Biopsy of AMMs is an invasive approach to obtain tissue before surgical intervention and treatment for histopathological analysis (12, 13). However, not all patients are eligible for biopsy given the presence of certain comorbidities as well as lesion size and location (8, 14). On the other hand, there are also cases where direct surgical resection can be performed based only on imaging and clinical features, bypassing the superfluous step of biopsy (8). Imaging examination, as a non-invasive approach, is indispensable for preoperative workup and is essential for the differential diagnosis, staging, and follow-up monitoring of AMMs (15). CT is universally available for routine preoperative preparation and remains the current modality of choice. Nevertheless, the average diagnostic accuracy only ranged from 35% to 78% when radiologists provided the diagnosis based on their understanding and judgment of demographic and CT imaging features (5, 16, 17). The discriminating ability for malignant germ cell tumors (35%), thymic carcinomas (38%), and cysts (46%) is not satisfactory (5). Thus, there is an urgent need to improve the radiological diagnostic accuracy of AMMs to reduce the chances of unnecessary surgery for individuals who are unlikely to benefit from it.

Radiomics is an emerging translational field of research aimed at extracting features, more than those observed by radiologists, from radiological images for clinical decision-making (18). Most radiomics studies investigated thymic epithelial tumors (TETs) (19–21), the most prevalent primary tumor in the anterior mediastinum that accounts for 47% of the total mediastinal tumors (22). Quantitative radiomics analysis based on CT, MRI, and PET/CT has been conducted and has shown good diagnostic performance in differentiating tumor subtypes, staging, invasiveness, and risk categorization in TETs (19, 21, 23, 24). However, there is no empirical evidence proving that CT-based radiomics analysis would be beneficial for reducing the non-therapeutic thymectomy rate in AMMs. As such, this is an interesting problem that requires further investigation.

In this study, we sought to evaluate the potential value of CT-based radiomics features by establishing a comprehensive predictive nomogram that aims to improve preoperative diagnostic accuracy and reduce the non-therapeutic thymectomy rate. We also investigated the radiomics features extracted using different CT imaging techniques, including unenhanced CT (UECT) and contrast-enhanced CT (CECT), and explored their potential use in the clinical decision-making regarding AMMs.

MATERIALS AND METHODS

Patient Selection

This retrospective, single-center study was approved by our institutional ethics committee (no. 2022048 K), which waived the need for informed consent. The workflow diagram of the analysis is shown in **Figure 1**.

We searched the electronic medical record system of our hospital for patients (n = 695) who underwent surgical resection of suspected mediastinal masses at our institution from January 2017 to April 2021. The inclusion criteria were as follows: 1) AMM, 2) underwent UECT and/or CECT within 1 month before surgery, and 3) available clinical data and surgical records. The exclusion criteria were as follows: 1) previous treatment or biopsy before the CT scan, 2) low-dose lung cancer screening or lung nodule follow-up CT scan protocols, 3) poor image quality due to severe respiratory motion artifacts or other reasons, 4) incomplete UECT data, and 5) hyperthyroidism or myasthenia gravis. AMM was defined as any mass no less than 5 mm in the short-axis diameter that was located in the anterior mediastinum as defined by the International Thymic Malignancy Interest Group (25, 26). The center method was used for defining the mass center on axial CT images and further locating the theoretical site of mass origin (25, 26). When multiple masses were present in a single patient, they were evaluated separately.

In total, 280 patients with 280 UECT and 241 CECT scans were enrolled in this retrospective study. Clinical information, including age, sex, body mass index (BMI), and pathological diagnosis of all cases, was obtained from our institutional medical record system. The median time from the preoperative CT scan to surgery was 7.5 days (interquartile range, IQR: 3–10) in UECT and 6 days (IQR: 3–9) on CECT.

Pathological Analysis

Surgical resection generally refers to total thymectomy or total thymectomy with partial en bloc resection of adjacent structures when complete resection is necessary. The procedures included open thoracotomy, mediastinoscopy, or robot-assisted mediastinoscopy. All resected specimens were formalin-fixed and hematoxylin–eosin-stained according to standard procedures. The pathological diagnosis was independently performed by two pathologists who were blinded to the radiological diagnosis. The diagnosis was made and reported according to the classification criteria issued in the 4th edition of the WHO classification of tumors of the thymus in 2015 (27).

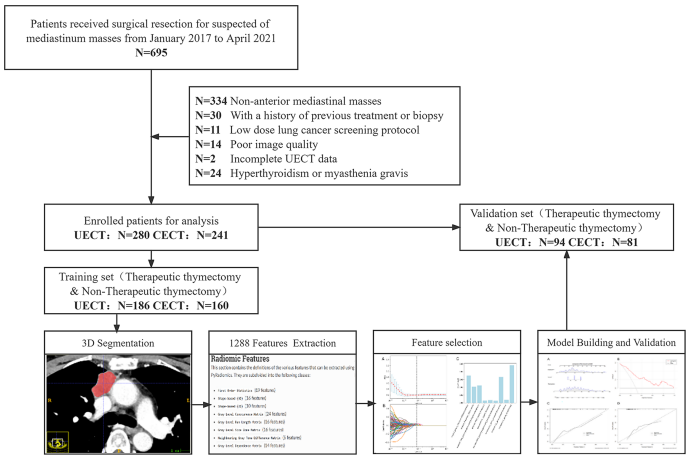

FIGURE 1 | Flowchart of the patient recruitment pathway. The flowchart shows how the study population has been selected and its retrospective manner. *N*, number; UECT, unenhanced computed tomography; CECT, contrast-enhanced computed tomography.

Image Acquisition

CT imaging was performed using one of four 64-slice multidetector CT scan machines (Philips Brilliance CT 64; Philips Medical Systems, Eindhoven, Netherlands), Philips IQon spectral CT (Philips Medical Systems, Eindhoven, Netherlands), GE Discovery CT750 HD (GE Medical Systems, Waukesha, USA), and Somatom Definition Flash (Siemens Healthineers, Erlangen, Germany). Detailed acquisition and reconstruction protocol specifications are provided in **Supplementary Material 1**. All CT scans were performed over the entire thorax, in the supine position, at the end of the inspiratory phase. CECT was obtained 60 s after contrast agent administration. The contrast agent (Omnipaque 350, GE Healthcare, Waukesha, USA) was intravenously administered at a dose of 1.5 ml/kg body weight and a rate of 3.0 ml/s *via* a power injector, followed by a 20.0-ml saline flush.

Mass Analysis and Segmentation

Location (unilateral or bilateral), size (maximum axial diameter), shape (regular, irregular), boundary (clear, indistinct), mediastinal fatty line (preserved, infiltrate), fatty component (absence, presence), calcification (absence, presence), pericardial effusion (absence, presence), pleural effusion (absence, presence), and enhancement homogeneity (homogeneous, inhomogeneous) were verified by two radiologists (YZ and ZZ, both with 6 years of experience in thoracic imaging diagnosis) who were blinded to the pathological diagnosis. Subsequently, two attenuation-to-background ratios were calculated for each mass:

$$\text{UECT ratio} = \frac{\text{AMM attenuation}_{\text{UECT}}}{\text{Pectoralis major attenuation}_{\text{UECT}}}$$

$$\text{CECT ratio} = \frac{\text{AMM attenuation}_{\text{UECT}} - \text{AMM attenuation}_{\text{CECT}}}{\text{Pectoralis major attenuation}_{\text{UECT}} - \text{Pectoralis major attenuation}_{\text{CECT}}}$$

All CT findings were evaluated based on the mediastinal window setting on the transverse plain CT scan section (window width, 300 HU; window level, 30 HU).

The included masses were independently segmented by two radiologists (YZ and ZZ) using the open-source image processing software ITK-SNAP 3.8.0 (www.itksnap.org) (28). A three-dimensional mask, defined as the delineation around the mass border for every CT axial plane, was delineated manually. The original digital imaging in communications in medicine format and the segmentation mask were exported directly into neuroimaging informatics technology initiative (NIfTI) format after the above segmentation process.

Radiomics Feature Extraction

Referring to the recommended standardized radiomics analysis workflow (18), segmentation data were analyzed using Pyradiomics (version 3.0.1 https://pyradiomics.readthedocs.io/) in Python (version 3.7 https://www.python.org/) to extract the radiomics features (29). The NIfTI format data were resampled into 1.0 × 1.0 × 1.0-mm^3 voxels using a nearest-neighbor algorithm. In total, 1,288 radiomics features were extracted, and the specific classifications were as follows: 1) first-order statistics and filter-based features (n = 252), 2) shape (n = 14), 3) gray level co-occurrence matrix and filter-based features (n = 308), 4) gray level run length matrix and filter-based features (n = 224), 5) gray level size zone matrix and filter-based features (n = 224), 6) gray level dependence matrix and filter-based features (n = 196), and 7) neighboring gray tone difference matrix and filter-based features (n = 70). All extracted radiomics features are listed in **Supplementary Material 2**. In addition to the shape features, all the features were computed on the original image or on a Gaussian- or wavelet-filtered image. Most features were defined in compliance with the imaging biomarker standardization initiative. The bin size in our analysis is 25.

Radiomics Feature Selection and Predictive Model Building

The CECT and UECT datasets were randomly divided into training and validation sets in a ratio of 2:1. The median padding method was used to fill in missing values and replace outliers, after which the standardized data were subsequently used for statistical analyses. Radiomics features from the training set were selected using the Mann–Whitney test or independent Student's *t*-test when results achieved $p < 0.05$. The selected features were further filtered using least absolute shrinkage and selection operator (LASSO) with 10-fold cross-validation. Clinical and radiographic features were analyzed using the Mann–Whitney test, independent Student's *t*-test, or chi-square test when appropriate. Countable data were analyzed with the chi-square test, data that fit the normal distribution were analyzed with the independent Student's *t*-test, and data that did not fit the normal distribution were analyzed using the Mann–Whitney test.

The receiver operating characteristic (ROC) curve was used to evaluate the predictive performance of the radscore (radiomics feature) model, clinical model (clinical and radiographic features), and combined model (clinical + radscore model) in the training and validation sets. The Youden index was calculated, and the score at the maximum Youden index was taken as the cutoff value. An individualized prediction nomogram was constructed.

Statistical Analysis

The intraclass correlation coefficient (ICC) was used to assess interobserver agreement during the segmentation process. Features with an ICC greater than 0.90 were retained for further statistical analysis. LASSO, Mann–Whitney test, independent Student's *t*-test, chi-square test, and multivariate logistic analyses were performed to select the clinical, radiographic, and radiomics features. *p*-value was adjusted for multiple comparisons in the radiomics feature selection step as false discovery rate (FDR)-corrected *q*-value with a significance level of 0.05. Other statistical tests were two-sided with a significance level of 0.05. All statistical analyses were performed using the R software (version 4.0.5 https://www.r-project.org/) with "readr," "irr," "rms," "foreign," "Matrix," "Hmisc," "rmda," "ggprism," "ggDCA," "ggplot2," "ggsci," "glmnet," "fdrtool," and "regplot" packages.

RESULTS

Clinical and Radiographic Features

A total of 280 patients with 280 UECT and 241 CECT scans were recruited for this study. The pathological characteristics of the patients are shown in **Table 1**. Around 92.14% (258/280) of the masses were completely resected. The non-therapeutic thymectomy rates were 51.07% (143/280) and 48.55% (117/241) in the UECT and CECT datasets, respectively.

In the UECT dataset, diameter, shape, boundary, mediastinal fatty line, and UECT ratio showed a statistically significant difference ($p < 0.05$) between the non-therapeutic thymectomy and therapeutic thymectomy groups in both the training and validation sets, while sex, pleural effusion, and calcification exhibited evident differences in either the training or validation set (**Table 2**).

TABLE 1 | Pathology characteristics of patients in UECT and CECT.

Diagnoses	UECT (*n* = 280)	NECT (*n* = 241)
Therapeutic thymectomy		
WHO type A thymoma	8	7
WHO type AB thymoma	23	20
WHO type B1 thymoma	12	10
WHO type B2 thymoma	22	22
WHO type B3 thymoma	14	13
Thymic carcinoma	22	22
Lymphoma	4	4
Small cell carcinoma	4	2
Atypical carcinoid	2	2
Castleman's disease	3	2
Sarcomatoid carcinoma	3	3
Metastatic lymphoma node	2	2
Thyroid carcinoma	1	1
Seminoma	3	2
Yolk sac tumor	2	2
Teratoma	10	9
Aggressive fibromatosis	1	1
Solitary fibrous tumor	1	0
Total	137	124
Non-therapeutic thymectomy		
Cyst	110	89
Thymic hyperplasia	15	13
Hemangioma	5	3
Tuberculosis	5	4
Sarcoidosis	3	3
Eutopic thyroid	1	1
Lymphoma node	1	1
Fibrosing mediastinitis	3	3
Total	143	117

Data are the number of masses. UECT, unenhanced computed tomography; CECT, contrast-enhanced computed tomography; WHO, World Health Organization.

Furthermore, multivariate analysis revealed significant differences in diameter, calcification, and UECT ratio. These three features were subsequently selected to establish the UECT clinical model.

Calculation formula

$$= -3.333043 + 0.025668 \times \text{diameter} + 1.008648 \times \text{calcification} + 2.825093 \times \text{UECT ratio}$$

The area under the curve (AUC) of the clinical model was 0.814 (95% CI, 0.751–0.867; threshold: 0.06431; sensitivity: 79.12%; specificity: 72.63%) in the training set and 0.752 (95% CI, 0.653–0.836; threshold: 0.02138; sensitivity: 69.57%; specificity: 70.83%) in the validation set (**Figure 2**).

In the CECT dataset, diameter, shape, mediastinal fatty line, homogeneity, and UECT ratio showed statistical differences ($p < 0.05$) between the non-therapeutic thymectomy and therapeutic thymectomy groups in both the training and validation sets, while boundary, sex, pleural effusion, and calcification exhibited evident differences in either the training

TABLE 2 | The clinical and radiographic features in the training and validation sets of UECT.

Characteristics	Training set (*n* = 186)			Validation set (*n* = 94)		
	Therapeutic thymectomy (*n* = 91)	Non-therapeutic thymectomy (*n* = 95)	*p*-value	Therapeutic thymectomy (*n* = 46)	Non-therapeutic thymectomy (*n* = 48)	*p*-value
Age, years	56.5 (46.1, 63.5)	53.4 (45.7, 60.6)	0.181	57.4 (47.1, 64.7)	57.0 (49.2, 64.9)	0.464
Gender			**0.006**			0.833
Female	41 (39.8%)	62 (60.2%)		24 (52.2%)	24 (50.0%)	
Male	50 (60.2%)	33 (39.8%)		22 (47.8%)	24 (50.0%)	
BMI, kg/m^2	22.4 (20.7, 24.3)	23.1 (21.2, 25.2)	0.300	22.3 (20.6, 24.1)	22.7 (20.1, 25.5)	0.560
Diameter, mm	54.3 (39.0, 70.6)	36.0 (23.0, 54.7)	**<0.001**	52.2 (35.8, 69.8)	24.0 (18.8, 46.9)	**<0.001**
UECT ratio	0.86 (0.73, 0.95)	0.57 (0.24, 0.84)	**<0.001**	0.81 (0.63, 0.92)	0.61 (0.29, 0.86)	**0.008**
Location			0.464			0.064
Unilateral	43 (47.3%)	50 (52.6%)		19 (41.3%)	30 (62.5%)	
Bilateral	48 (52.8%)	45 (47.4%)		27 (58.7%)	18 (37.5%)	
Shape			**<0.001**			**0.016**
Regular	65 (71.4%)	88 (92.6%)		33 (71.7%)	44 (91.7%)	
Irregular	26 (28.6%)	7 (7.4%)		13 (28.3%)	4 (8.3%)	
Boundary			**0.013**			**0.026**
Clear	78 (85.7%)	92 (96.8%)		37 (80.4%)	46 (95.8%)	
Indistinct	13 (14.3%)	3 (3.2%)		9 (19.6%)	2 (4.2%)	
Mediastinal fatty line			**<0.001**			**0.001**
Preserve	70 (76.9%)	93 (97.9%)		32 (69.6%)	47 (97.9%)	
Infiltrate	21 (23.1%)	2 (2.1%)		14 (30.4%)	1 (2.1%)	
Fatty component			0.604			0.481
Absence	86 (94.5%)	88 (92.6%)		41 (89.1%)	45 (93.7%)	
Presence	5 (5.5%)	7 (7.4%)		5 (10.9%)	3 (6.3%)	
Calcification			**0.018**			0.165
Absence	61 (67.0%)	81 (85.3%)		36 (78.3%)	43 (89.6%)	
Present	30 (33.0%)	14 (14.7%)		10 (21.7%)	5 (10.4%)	
Pleural effusion			0.242			**0.005**
Absence	86 (94.5%)	93 (97.9%)		39 (84.78%)	48 (100.0%)	
Present	5 (5.5%)	2 (2.1%)		7 (15.22%)	0(0.0%)	
Pericardial effusion			0.983			0.113
Absence	87 (95.6%)	95 (100.0%)		43 (93.5%)	48 (100.0%)	
Presence	4 (4.4%)	0 (0.0%)		3 (6.5%)	0 (0.0%)	

Enumeration data are the number of masses with percentage in parentheses, and measurement data are expressed as median and interquartile range (IQR). Bold p-values <0.05. BMI, body mass index; UECT, unenhanced computed tomography.

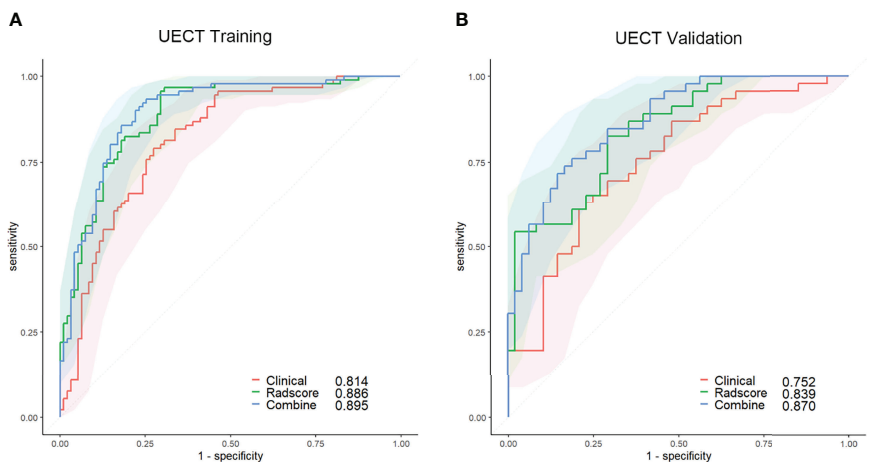

FIGURE 2 | ROC curves of the clinical (red lines), radscore (green lines), and combined (blue lines) models in the training set **(A)** and validation set **(B)** of the UECT model. The shaded areas represent the confidence intervals of the ROC curves. UECT, unenhanced computed tomography; ROC, receiver operating characteristic.

TABLE 3 | The clinical and radiographic features in the training and validation sets of CECT.

Characteristics	Training set (*n* = 160)			Validation set (*n* = 81)		
	Therapeutic thymectomy (*n* = 82)	Non-therapeutic thymectomy (*n* = 78)	*p*-value	Therapeutic thymectomy (*n* = 42)	Non-therapeutic thymectomy (*n* = 39)	*p*-value
Age, years	56.3 (45.6, 63.3)	53.0 (45.5, 62.2)	0.428	57.7 (41.8, 63.9)	53.2 (45.5, 60.6)	0.643
Gender			0.192			**0.036**
Female	41 (50.0%)	47 (60.3%)		15 (35.7%)	23 (59.0%)	
Male	41 (50.0%)	31 (39.7%)		27 (64.3%)	16 (41.0%)	
BMI, kg/m^2	22.6 (20.8, 24.4)	23.1 (21.2, 25.5)	0.407	22.2 (20.6, 23.8)	23.3 (21.4, 24.9)	0.050
Diameter, mm	55.9 (41.4, 71.4)	32.5 (22.3, 58.8)	**<0.001**	53.5 (37.2, 68.5)	27.8 (19.6, 45.1)	**<0.001**
UECT ratio	0.84 (0.71, 0.94)	0.63 (0.29, 0.86)	**<0.001**	0.81 (0.63, 0.93)	0.47 (0.24, 0.81)	**<0.001**
CECT ratio	4.22 (1.94, 9.82)	1.28 (0.28, 4.23)	0.180	4.09 (1.47, 9.39)	0.83 (0.27, 2.29)	0.263
Location			0.160			0.429
Unilateral	34 (41.5%)	37 (47.4%)		20 (47.6%)	22 (56.4%)	
Bilateral	48 (58.5%)	41 (52.6%)		22 (52.4%)	17 (43.6%)	
Shape			**0.003**			**<0.001**
Regular	60 (73.2%)	71 (91.0%)		27 (64.3%)	37 (94.87%)	
Irregular	22 (26.8%)	7 (9.0%)		15 (35.7%)	2 (5.13%)	
Boundary			**0.005**			0.058
Clear	67 (81.7%)	75 (96.2%)		35 (83.3%)	38 (97.4%)	
Indistinct	15 (18.3%)	3 (3.85%)		7 (16.7%)	1 (2.6%)	
Mediastinal fatty line			**<0.001**			**<0.001**
Preserve	62 (75.6%)	76 (97.4%)		29 (69.1%)	38 (97.4%)	
Infiltrate	20 (24.4%)	2 (2.6%)		13 (30.9%)	1 (2.6%)	
Fatty component			0.766			0.093
Absence	75 (91.5%)	73 (93.6%)		39 (92.9%)	35 (89.7%)	
Presence	7 (8.5%)	5 (6.4%)		3 (7.1%)	4 (10.3%)	
Calcification			**0.020**			0.145
Absence	54 (65.9%)	64 (82.1%)		32 (76.2%)	35 (89.7%)	
Present	28 (34.1%)	14 (17.9%)		10 (23.8%)	4 (10.3%)	
Pleural effusion			**<0.001**			1.000
Absence	71 (86.6%)	78 (100.0%)		41 (97.6%)	39 (100.0%)	
Present	11 (13.4%)	0 (0.0%)		1 (2.4%)	0(0.0%)	
Pericardial effusion			0.059			0.494
Absence	77 (93.9%)	78 (100.0%)		40 (95.2%)	39 (100.0%)	
Present	5 (6.1%)	0 (0.0%)		2 (4.8%)	0(0.0%)	
Homogeneity			**<0.001**			**<0.001**
Homogeneous	25 (30.5%)	65 (83.3%)		19 (45.2%)	35 (89.7%)	
Inhomogeneous	57 (69.5%)	13 (16.7%)		23 (54.8%)	4 (10.3%)	

Enumeration data are the number of masses with percentage in parentheses, and measurement data are expressed as median and interquartile range (IQR). Bold p-values <0.05. BMI, body mass index; CECT, contrast-enhanced computed tomography.

or validation set (**Table 3**). Multivariate analysis revealed significant differences in diameter, UECT ratio, and homogeneity. These three features were subsequently selected to establish a clinical CECT model.

Calculation formula

$$= -3.6322 + 0.01939 \times \text{diameter} - 1.77731 \times \text{homogeneity} - 2.35451 \times \text{UECT ratio}$$

The AUC of the clinical model was 0.852 (95% CI, 0.793–0.911; threshold: −0.92923; sensitivity: 90.24%; specificity: 67.95%) in the training set and 0.851 (95% CI, 0.769–0.933; threshold: −1.62975; sensitivity: 97.62%; specificity: 61.54%) in the validation set (**Figure 3**).

Radiomics Feature Selection

In the UECT dataset, 587 features with good agreement (ICC > 0.90) were selected for further reduction (**Supplementary Material 3**). A total of 564 features were removed due to lack of statistical difference in the Mann–Whitney test, and 20 features were removed due to high correlation with other features in LASSO selection, with four features remaining (**Supplementary Material 4; Figure 4**). Consequently, the selected features were subjected to a radscore model:

$$\begin{aligned}\text{Calculation formula} = {} & -0.206691567 + 0.394716773 \times \\ & \text{wavelet . HLH \_ glrlm \_ RunEntropy} \\ & +0.003935499 \\ & \times \text{log . sigma.5.0.mm.3D \_ glszm \_ SmallAreaHighGrayLevelEmphasis} \\ & +0.014854691 \times \text{log . sigma.1.0.mm.3D \_ glcm \_ JointAverage} \\ & - 5.008866283 \\ & \times \text{original \_ shape \_ SurfaceVolumeRatio}\end{aligned}$$

The AUC of the radscore model was 0.886 (95% CI, 0.831–0.928; threshold: 0.40102; sensitivity: 96.70%; specificity: 69.47%) in the training set and 0.839 (95% CI, 0.749–0.907; threshold:

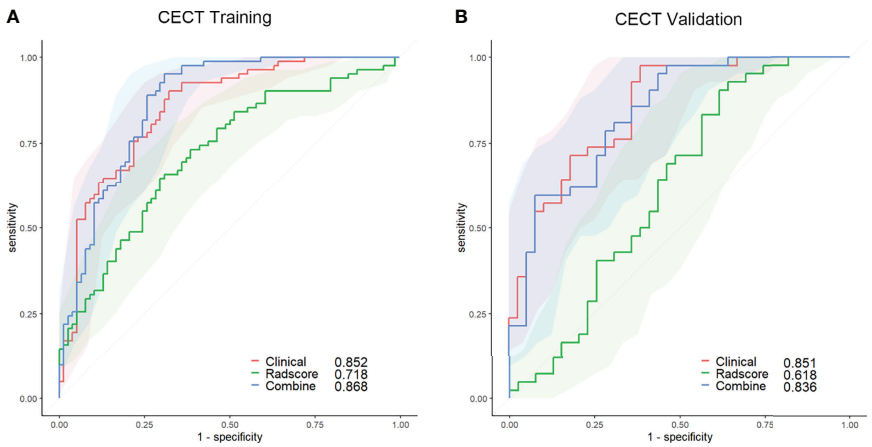

FIGURE 3 | ROC curves of the clinical (red lines), radscore (green lines), and combined (blue lines) models in the training set **(A)** and validation set **(B)** of the CECT model. The shaded areas represent the confidence intervals of the ROC curves. CECT, contrast-enhanced computed tomography; ROC, receiver operating characteristic.

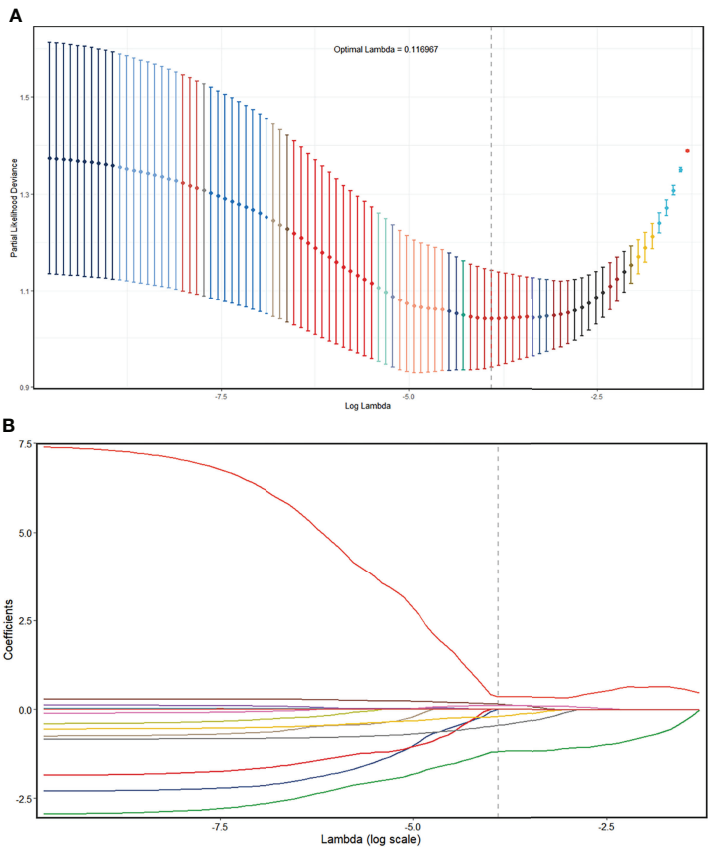

FIGURE 4 | Radiomics feature selection using the LASSO regression model in the UECT model. **(A)** The partial likelihood deviance from the LASSO regression cross-validation procedure was plotted against log(λ). The optimal λ value of 0.116967 was selected. **(B)** LASSO coefficient profiles of the radiomics features. As the tuning parameter (λ) increased using 10-fold cross-validation, more coefficients tended to approach 0 and the optimal non-zero coefficients were generated, which yielded a set of the optimal radiomics features. LASSO, least absolute shrinkage and selection operator; UECT, unenhanced computed tomography.

0.47809; sensitivity: 82.61%; specificity: 70.83%) in the validation set (**Figure 2**).

In the CECT dataset, 846 features with good agreement (ICC > 0.90) were selected for further reduction (**Supplementary Material 3**). A total of 712 features were removed due to lack of statistical difference in the Mann–Whitney test, and 129 features were removed due to their high correlation with other features, with five remaining features (**Supplementary Material 5; Figure 5**). Consequently, the selected features were subjected to a radscore model:

$$\begin{aligned}\text{Calculation formula} = {} & -4.67265 + 0.000380729 \\ & \times \text{wavelet . HHL \_ glrlm \_ LongRunHighGrayLevelEmphasis} + 4.73167 \\ & \times \text{log . sigma.4.0.mm.3D \_ glcm \_ Idmn} - 15.76711 \times \text{wavelet . HLL \_ ngtdm \_ Contrast} \\ & -0.1337031 \times \text{log . sigma.5.0.mm.3D \_ gldm \_ LowGrayLevelEmphasis} \\ & +0.01050467 \times \text{log . sigma.2.0.mm.3D \_ glcm \_ JointAverage}\end{aligned}$$

The AUC of the radscore model was 0.718 (95% CI, 0.639–0.797; threshold: 0.07717; sensitivity: 64.63%; specificity: 70.51%) in the training set and 0.618 (95% CI, 0.492–0.745; threshold: −0.02176; sensitivity: 90.48%; specificity: 38.46%) in the validation set (**Figure 3**).

Construction of the Prediction Nomogram and Clinical Utility

In the UECT dataset, diameter, calcification, and UECT ratio were incorporated into the multivariate logistic analysis to develop a prediction nomogram (**Figure 6**). As a result, the UECT ratio and radscore were selected as independent predictors of therapeutic thymectomy.

$$\begin{aligned}\text{Calculation formula} \\ = -4.52179 + 1.78133 \times \text{UECT ratio} + 7.75105 \times \text{Radscore}\end{aligned}$$

The calibration curve of the nomogram for predicting the probability of AMM suitable for therapeutic thymectomy demonstrated an acceptable agreement between prediction and

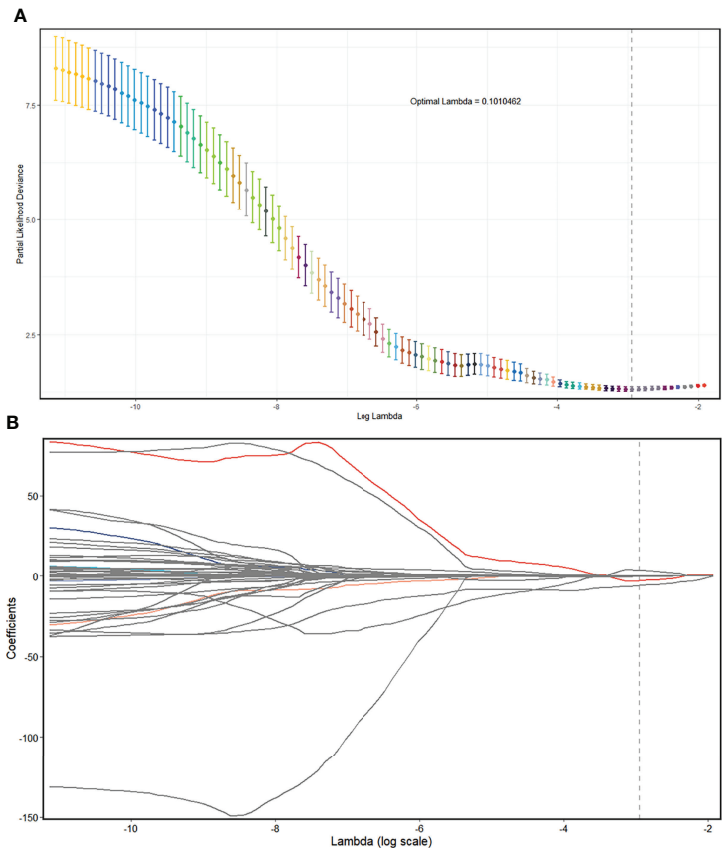

FIGURE 5 | Radiomics feature selection using the LASSO regression model in the CECT model. **(A)** The partial likelihood deviance from the LASSO regression cross-validation procedure was plotted against log(λ). The optimal λ value of 0.1010462 was selected. **(B)** LASSO coefficient profiles of the radiomics features. As the tuning parameter (λ) increased using 10-fold cross-validation, more coefficients tended to approach 0 and the optimal non-zero coefficients were generated, which yielded a set of the optimal radiomics features. LASSO, least absolute shrinkage and selection operator; CECT, contrast-enhanced computed tomography.

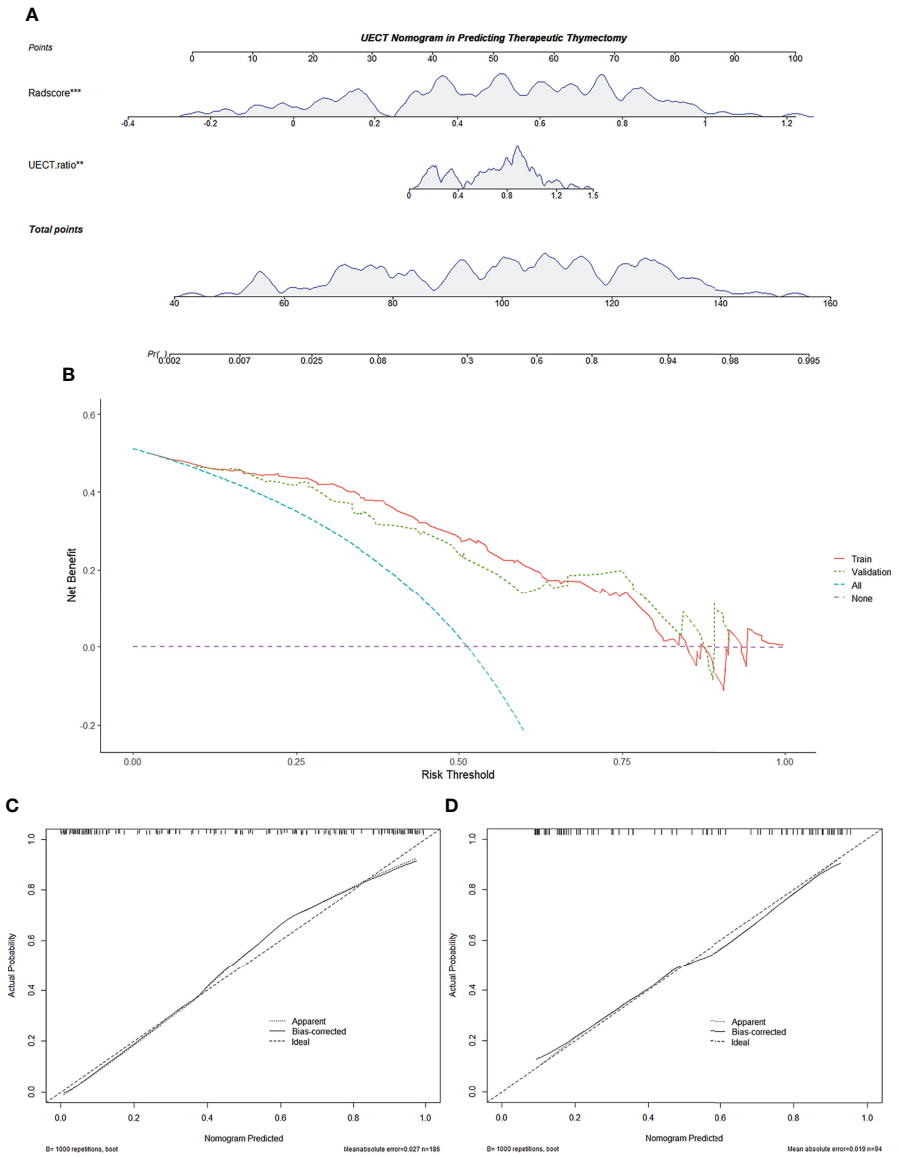

FIGURE 6 | Radiomics-based nomogram was developed in the training set for the UECT model. **(A)** Radscore and the UECT ratio were incorporated. **(B)** Decision curve of the nomogram. The *y*-axis represents the net benefit. The *x*-axis represents the threshold probability. The red line represents the radiomics-based nomogram of the training set. The green line represents the radiomics-based nomogram of the validation set. The blue line represents the assumption that all AMMs are fit for therapeutic thymectomy. The violet line represents the assumption that all AMMs are not fit for therapeutic thymectomy. The decision curve demonstrates that if the threshold probability is >5%, using the nomogram for therapeutic thymectomy adds more benefit than predicting either all or no patients. **(C)** Calibration curve of the radiomics-based nomogram in the training set. **(D)** Calibration curve of the radiomics-based nomogram in the validation set. The 45-degree lines represent perfect predictions. The black dotted lines represent the predictive performance of the nomogram. A closer fit to the 45-degree line represents a better prediction. AMM, anterior mediastinal mass; UECT, unenhanced computed tomography.

observation in the training and validation sets (**Figure 6**). The AUC of the combined model was 0.895 (95% CI, 0.842–0.935; threshold: 0.15017; sensitivity: 93.41%; specificity: 74.74%) in the training set and 0.870 (95% CI, 0.784–0.930; threshold: 0.61539; sensitivity: 76.09%; specificity: 81.25%) in the validation set (**Figure 2**). The decision curve analysis of the nomogram is presented in **Figure 6**.

The radscore and the combined model achieved a higher accuracy (AUC: 0.886 and 0.895, respectively) than the clinical model (AUC: 0.814) for the prediction of therapeutic

thymectomy probability among patients with AMMs in the UECT training set (Delong test; $p = 0.019$ and 0.001, respectively). A difference was observed only between the combined and clinical models in the validation set ($p = 0.005$).

In the CECT dataset, the UECT ratio and homogeneity were incorporated with the radscore into the multivariate logistic analysis and were selected for developing the prediction nomogram:

Calculation formula

$$= -2.6841 + 2.2589 \times \text{UECT ratio} + 2.2589 \times \text{homogeneity} + 3.3255 \times \text{Radscore}$$

The calibration curve of the nomogram for predicting the probability of AMM suitable for therapeutic thymectomy demonstrated an acceptable agreement between prediction and observation in the training and validation sets. The AUC of the combined model was 0.868 (95% CI, 0.805–0.916; threshold: −0.83458; sensitivity: 95.12%; specificity: 69.13%) in the training set and 0.836 (95% CI, 0.738–0.909; threshold: 0.71154; sensitivity: 59.52%; specificity: 95.31%) in the validation set (**Figure 3**).

The clinical and combined models achieved a higher accuracy (AUC: 0.852 and 0.868, respectively) than the radscore model (AUC: 0.718) for the prediction of therapeutic thymectomy probability among patients with AMMs in the CECT training set (Delong test; $p < 0.001$ and 0.004, respectively). Similar results were obtained for the validation set.

DISCUSSION

In this retrospective study, we developed and validated two radiomic nomograms for preoperative AMMs. The nomogram demonstrated an individualized selection of AMMs, which could help in screening patients who required surgical intervention.

For chest UECT-identified AMMs, follow-up diagnosis was always based on radiological features on CECT or MRI, and clinicians tended to choose surgical intervention as the first management strategy. The non-therapeutic thymectomy rate was as high as 51.07% (143/280) in our study, which is in line with previous studies (22%–68%) (10, 11). Unlike in previous studies (10), lymphoma was assigned to the therapeutic thymectomy group in our study. We considered that routine follow-up may not be justified for this disease since therapeutic thymectomy could help determine the pathological diagnosis, which is essential for subsequent treatments. There has been increased awareness of non-therapeutic thymectomy cases, and a more accurate preoperative diagnosis contributes to avoiding them.

In the current study, we mainly focused on UECT and CECT, which are the most common imaging examinations in routine preoperative preparation. Usually, in cases of renal insufficiency, CECT may be replaced with MRI or saved with only UECT. The value of the UECT clinical model was limited according to the AUC (training: 0.814, validation: 0.752), whereas the CECT clinical model was found to be acceptable (AUC, training: 0.852, validation: 0.851). In our study, patients who were suitable for surgical resection presented with larger diameters and larger UECT ratios and were inhomogeneous. Diameter is a readily accessible observable metric for the clinical diagnosis of AMMs, and this finding is consistent with that of a previous study (30). Previous studies have mostly focused on distinguishing between benign and malignant AMMs (30, 31). In our study, the therapeutic thymectomy group consisted mostly of malignant masses, which may explain the diameter result. In previous studies, benign masses had lower attenuation than malignant masses (16, 31). To reduce the risk of bias, attenuation was substituted by the UECT ratio in our study; therefore, our results also fit well with previous studies on this aspect. Cysts (76.1%, 89/117) were the most common low attenuation masses in the non-therapeutic thymectomy group, which might be the reason why we found the UECT ratio larger in the therapeutic thymectomy group. Mass enhancement patterns are typically associated with necrosis, cystic changes, and heterogeneity. TETs formed the largest proportion, approximately 75.8% (94/124), of the therapeutic thymectomy group. The inhomogeneity rate of TETs was approximately 67% versus 0% for cysts, as reported in the literature (10). The different disease distributions likely resulted in different radiological characteristics. We also explored other possible reasons for these silent radiological features. Unilateral location, lobulation, and fewer fatty components are commonly used to identify TETs (10, 16). However, all three features failed to achieve statistical significance in this study. As such, these results may be attributed to our grouping method. Teratomas, which occur in a central location, are oval or rounded, contain a fatty component, and require surgical intervention because of the risk of developing malignant change. It was also categorized into the therapeutic thymectomy group. This may partially explain the negative results obtained.

To construct the radiomics-based radscore, we screened 1,288 candidate radiomics features on both the UECT and CECT datasets. Radiomics analyses yielded results that differed from those of the clinical models. The UECT radscore model (AUC: training: 0.886, validation: 0.839) was more effective than the CECT score model (AUC: training: 0.718, validation: 0.618). There are some controversies regarding the diagnostic efficacy of UECT and CECT radiomics modeling. Yasaka et al. (32) studied solid AMMs and cysts using quantitative CT texture analyses and found that CECT (AUC: 0.983) was more effective than UECT (AUC: 0.780). Similar results were obtained in a study by Wang et al. that focused on risk categorization and clinical staging of thymomas (33). However, our results are similar to those of Sui et al., who showed that the radiomics features of UECT performed better than those of CECT in the prediction of anterior mediastinal lesion risk grading (34). This discrepancy could have been caused by a grouping bias. Another possible explanation is that the biological heterogeneity within the tumor that can be characterized by radiomics is confounded by contrast material (35). SurfaceVolumeRatio is one of the four target features selected and used to construct the UECT radscore model. It had a lower

median value in the therapeutic thymectomy group, indicating that masses tended to have a more compact shape in this group. JointAverage had a higher median value in the therapeutic thymectomy group, reflecting mass attenuation. RunEntropy and SmallAreaHighGrayLevelEmphasis were utilized to evaluate heterogeneity, which resulted in higher median values in the therapeutic thymectomy group. This suggests that the heterogeneity of masses in this group was more apparent.

A comparison of the predictive power of the clinical, radscore, and combined models was performed in our study. In the UECT dataset, the predictive performance of the combined model (AUC: 0.870) was higher than that of the clinical model (AUC: 0.754; $p = 0.005$). Although there was no significant difference between the clinical and radscore models (AUC: 0.839; $p = 0.093$), the AUC of the radscore model was higher. This implies that incorporating the radscore to develop a combined model may improve the predictive performance for the therapeutic thymectomy ratio compared to using the UECT clinical model only. Therefore, we adopted a nomogram that presented quantitative differences, which is more accessible than the calculation formula. The nomogram combining radscore and UECT ratio demonstrated satisfactory calibration and discrimination in the training and validation sets. This finding offers the potential for application in patients with renal failure or contrast allergies. In the CECT dataset, the predictive performance of the combined model (AUC: 0.836) and the clinical model (AUC: 0.851) was higher than that of the radscore model (AUC: 0.618; $p = 0.002$ and <0.001, respectively). This result could provide some hints that assessing the CECT qualitative and quantitative features such as UECT ratio, diameter, and enhancement homogeneity could reduce the unnecessary non-therapeutic thymectomy rate in AMMs. Comparing the UECT combined model (AUC: 0.870) to the CECT clinical model (AUC: 0.851), we see that their performance is very similar. In this case, expert-based lesion quantification on CECT is probably more efficient and faster than expert-based lesion quantification on UECT plus target delineation and radiomics calculation.

Several limitations of this pilot study must be acknowledged. First, this was a retrospective study in which only surgically resected AMMs were included, and patient selection bias was inevitable. Second, our study was subject to the inherent limitations of any single-center study, without external validation. Third, the technical parameters and scan protocols for the CT examinations were not consistent. Although resampling-based approaches have been adopted to address this problem, the potential influence of radiomic stability should still be considered. Another point of concern was that the CT imaging evaluations of both UECT and CECT groups were done based on the UECT scans, except for enhancement homogeneity and CECT ratio; therefore, we recommend that all patients require a UECT scan. In addition, the distribution of the pathological types of AMMs was uneven, and the number of TETs and cysts was relatively large. This might have affected the stability of the model. Finally, image processing algorithms and segmentation process techniques are bottlenecks of radiomics applications, which are time-consuming and highly prone to artificial error. This may restrict the further clinical application of these techniques, and there remains a need to develop a more reliable and robust segmentation tool.

CONCLUSION

In patients who underwent UECT scan only, a nomogram model integrating the radscore and UECT ratio achieved good accuracy in predicting therapeutic thymectomy probability in AMMs. Nevertheless, the use of radiomics as a clinical biomarker in CECT scans did not improve the predictive performance of the model. A clinical model consisting of the diameter, UECT ratio, and homogeneity may be helpful and more practical in finding an appropriate solution for the management of AMMs. The individualized model may avoid blind follow-ups and high non-therapeutic thymectomy rates.

DATA AVAILABILITY STATEMENT

The raw data supporting the conclusions of this article will be made available by the authors, without undue reservation.

AUTHOR CONTRIBUTIONS

Conceptualization: YC and WH. Methodology: YC and YZ. Software: ZZ and BW. Validation: YZ, YC, and ZZ. Formal analysis: ZZ and BW. Investigation: YQ. Data curation: ZZ and YQ. Writing—original draft preparation: ZZ. Writing—review and editing: ZZ, YZ, and YC. Visualization: ZZ. Supervision: YC. Project administration: YC. Funding acquisition: YC. All authors have read and agreed to the published version of the manuscript.

FUNDING

This work was supported by the Zhongnan Hospital of Wuhan University (znpy2019038).

SUPPLEMENTARY MATERIAL

The Supplementary Material for this article can be found online at: https://www.frontiersin.org/articles/10.3389/fonc.2022.869253/full#supplementary-material

REFERENCES

1. Araki T, Nishino M, Gao W, Dupuis J, Washko GR, Hunninghake GM, et al. Anterior Mediastinal Masses in the Framingham Heart Study: Prevalence and CT Image Characteristics. *Eur J Radiol Open* (2015) 2:26–31. doi: 10.1016/j.ejro.2014.12.003
2. Yoon SH, Choi SH, Kang CH, Goo JM. Incidental Anterior Mediastinal Nodular Lesions on Chest CT in Asymptomatic Subjects. *J Thorac Oncol* (2018) 13(3):359–66. doi: 10.1016/j.jtho.2017.11.124
3. Henschke CI, Lee I-J, Wu N, Farooqi A, Khan A, Yankelevitz D, et al. CT Screening for Lung Cancer:Prevalence and Incidence of Mediastinal Masses. *Radiology* (2006) 239(2):586–90. doi: 10.1148/radiol.2392050261
4. Roden AC, Fang W, Shen Y, Carter BW, White DB, Jenkins SM, et al. Distribution of Mediastinal Lesions Across Multi-Institutional, International, Radiology Databases. *J Thorac Oncol* (2020) 15(4):568–79. doi: 10.1016/j.jtho.2019.12.108
5. Tomiyama N, Honda O, Tsubamoto M, Inoue A, Sumikawa H, Kuriyama K, et al. Anterior Mediastinal Tumors: Diagnostic Accuracy of CT and MRI. *Eur J Radiol* (2009) 69(2):280–8. doi: 10.1016/j.ejrad.2007.10.002
6. Fan L, Wang Y, Zhou Y, Li Q, Yang W, Wang S, et al. Lung Cancer Screening With Low-Dose CT: Baseline Screening Results in Shanghai. *Acad Radiol* (2019) 26(10):1283–91. doi: 10.1016/j.acra.2018.12.002
7. Nakazono T, Yamaguchi K, Egashira R, Mizuguchi M, Irie H. Anterior Mediastinal Lesions: CT and MRI Features and Differential Diagnosis. *Japan J Radiol* (2021) 39(2):101–17. doi: 10.1007/s11604-020-01031-2
8. Ghigna M-R, Thomas de Montpreville V. Mediastinal Tumours and Pseudo-Tumours: A Comprehensive Review With Emphasis on Multidisciplinary Approach. *Eur Respir Rev* (2021) 30(162):200309. doi: 10.1183/16000617.0309-2020
9. Voulaz E, Veronesi G, Infante M, Cariboni U, Testori A, Novellis P, et al. Radical Thymectomy Versus Conservative Thymomectomy in the Surgical Treatment of Thymic Malignancies. *J Thorac Dis* (2018) 10(7):4127–36. doi: 10.21037/jtd.2018.06.04
10. Ackman JB, Verzosa S, Kovach AE, Louissaint A, Lanuti M, Wright CD, et al. High Rate of Unnecessary Thymectomy and its Cause. Can Computed Tomography Distinguish Thymoma, Lymphoma, Thymic Hyperplasia, and Thymic Cysts? *Eur J Radiol* (2015) 84(3):524–33. doi: 10.1016/j.ejrad.2014.11.042
11. Kent MS, Wang T, Gangadharan SP, Whyte RI. What is the Prevalence of a "Nontherapeutic" Thymectomy? *Ann Thorac Surg* (2014) 97(1):276–82. doi: 10.1016/j.athoracsur.2013.07.121
12. Lee HN, Yun SJ, Kim JI, Ryu C-W. Diagnostic Outcome and Safety of CT-Guided Core Needle Biopsy for Mediastinal Masses: A Systematic Review and Meta-Analysis. *Eur Radiol* (2020) 30(1):588–99. doi: 10.1007/s00330-019-06377-4
13. Iguchi T, Hiraki T, Matsui Y, Fujiwara H, Sakurai J, Masaoka Y, et al. CT Fluoroscopy-Guided Core Needle Biopsy of Anterior Mediastinal Masses. *Diagn Intervention Imaging* (2018) 99(2):91–7. doi: 10.1016/j.diii.2017.10.007
14. Petranovic M, Gilman MD, Muniappan A, Hasserjian RP, Digumarthy SR, Muse VV, et al. Diagnostic Yield of CT-Guided Percutaneous Transthoracic Needle Biopsy for Diagnosis of Anterior Mediastinal Masses. *Am J Roentgenol* (2015) 205(4):774–9. doi: 10.2214/AJR.15.14442
15. Ackman JB, Chung JH, Walker CM, Bang TJ, Carter BW, Hobbs SB, et al. ACR Appropriateness Criteria® Imaging of Mediastinal Masses. *J Am Coll Radiol* (2021) 18(5):S37–51. doi: 10.1016/j.jacr.2021.01.007
16. Hammer MM, Miskin N, Madan R, Hunsaker AR. Predictive Features for Anterior Mediastinal Mass Diagnoses. *J Comput Assist Tomogr* (2019) 43(1):98–103. doi: 10.1097/RCT.0000000000000782
17. Nam JG, Goo JM, Park CM, Lee H-J, Lee CH, Yoon SH. Age- and Gender-Specific Disease Distribution and the Diagnostic Accuracy of CT for Resected Anterior Mediastinal Lesions. *Thorac Cancer* (2019) 10(6):1378–87. doi: 10.1111/1759-7714.13081
18. Rizzo S, Botta F, Raimondi S, Origgi D, Fanciullo C, Morganti AG, et al. Radiomics: The Facts and the Challenges of Image Analysis. *Eur Radiol Exp* (2018) 2(1):36. doi: 10.1186/s41747-018-0068-z
19. Xiao G, Rong W-C, Hu Y-C, Shi Z-Q, Yang Y, Ren J-L, et al. MRI Radiomics Analysis for Predicting the Pathologic Classification and TNM Staging of Thymic Epithelial Tumors: A Pilot Study. *Am J Roentgenol* (2019) 214(2):328–40. doi: 10.2214/AJR.19.21696
20. Liu J, Yin P, Wang S, Liu T, Sun C, Hong N. CT-Based Radiomics Signatures for Predicting the Risk Categorization of Thymic Epithelial Tumors. *Front Oncol* (2021) 11:628534(165). doi: 10.3389/fonc.2021.628534
21. Hu J, Zhao Y, Li M, Liu Y, Wang F, Weng Q, et al. Machine-Learning-Based Computed Tomography Radiomic Analysis for Histologic Subtype Classification of Thymic Epithelial Tumours. *Eur J Radiol* (2020) 126:108929. doi: 10.1016/j.ejrad.2020.108929
22. Fujii Y. Published Guidelines for Management of Thymoma. *Thorac Surg Clin* (2011) 21(1):125–9. doi: 10.1016/j.thorsurg.2010.08.002
23. Shen Q, Shan Y, Xu W, Hu G, Chen W, Feng Z, et al. Risk Stratification of Thymic Epithelial Tumors by Using a Nomogram Combined With Radiomic Features and TNM Staging. *Eur Radiol* (2021) 31(1):423–35. doi: 10.1007/s00330-020-07100-4
24. Milgrom SA, Elhalawani H, Lee J, Wang Q, Mohamed ASR, Dabaja BS, et al. A PET Radiomics Model to Predict Refractory Mediastinal Hodgkin Lymphoma. *Sci Rep* (2019) 9(1):1322. doi: 10.1038/s41598-018-37197-z
25. Carter BW, Tomiyama N, Bhora FY, Rosado de Christenson ML, Nakajima J, Boiselle PM, et al. A Modern Definition of Mediastinal Compartments. *J Thorac Oncol* (2014) 9(9):S97–S101. doi: 10.1097/JTO.0000000000000292
26. Carter BW, Benveniste MF, Madan R, Godoy MC, de Groot PM, Truong MT, et al. ITMIG Classification of Mediastinal Compartments and Multidisciplinary Approach to Mediastinal Masses. *RadioGraphics* (2017) 37(2):413–36. doi: 10.1148/rg.2017160095
27. Travis WD, Brambilla E, Nicholson AG, Yatabe Y, Austin JHM, Beasley MB, et al. The 2015 World Health Organization Classification of Lung Tumors: Impact of Genetic, Clinical and Radiologic Advances Since the 2004 Classification. *J Thorac Oncol* (2015) 10(9):1243–60. doi: 10.1097/JTO.0000000000000630
28. Yushkevich PA, Piven J, Hazlett HC, Smith RG, Ho S, Gee JC, et al. User-Guided 3D Active Contour Segmentation of Anatomical Structures: Significantly Improved Efficiency and Reliability. *NeuroImage* (2006) 31(3):1116–28. doi: 10.1016/j.neuroimage.2006.01.015
29. van Griethuysen JJM, Fedorov A, Parmar C, Hosny A, Aucoin N, Narayan V, et al. Computational Radiomics System to Decode the Radiographic Phenotype. *Cancer Res* (2017) 77(21):e104. doi: 10.1158/0008-5472.CAN-17-0339
30. McErlean A, Huang J, Zabor EC, Moskowitz CS, Ginsberg MS. Distinguishing Benign Thymic Lesions From Early-Stage Thymic Malignancies on Computed Tomography. *J Thorac Oncol* (2013) 8(7):967–73. doi: 10.1097/JTO.0b013e3182904bc2
31. Araki T, Sholl LM, Gerbaudo VH, Hatabu H, Nishino M. Intrathymic Cyst: Clinical and Radiological Features in Surgically Resected Cases. *Clin Radiol* (2014) 69(7):732–8. doi: 10.1016/j.crad.2014.03.002
32. Yasaka K, Akai H, Abe O, Ohtomo K, Kiryu S. Quantitative Computed Tomography Texture Analyses for Anterior Mediastinal Masses: Differentiation Between Solid Masses and Cysts. *Eur J Radiol* (2018) 100:85–91. doi: 10.1016/j.ejrad.2018.01.017
33. Wang X, Sun W, Liang H, Mao X, Lu Z. Radiomics Signatures of Computed Tomography Imaging for Predicting Risk Categorization and Clinical Stage of Thymomas. *BioMed Res Int* (2019) 2019:3616852. doi: 10.1155/2019/3616852
34. Sui H, Liu L, Li X, Zuo P, Cui J, Mo Z. CT-Based Radiomics Features Analysis for Predicting the Risk of Anterior Mediastinal Lesions. *J Thorac Dis* (2019) 11(5):1809–18. doi: 10.21037/jtd.2019.05.32
35. He L, Huang Y, Ma Z, Liang C, Liang C, Liu Z. Effects of Contrast-Enhancement, Reconstruction Slice Thickness and Convolution Kernel on the Diagnostic Performance of Radiomics Signature in Solitary Pulmonary Nodule. *Sci Rep* (2016) 6(1):34921. doi: 10.1038/srep34921

Conflict of Interest: The authors declare that the research was conducted in the absence of any commercial or financial relationships that could be construed as a potential conflict of interest.

Publisher's Note: All claims expressed in this article are solely those of the authors and do not necessarily represent those of their affiliated organizations, or those of the publisher, the editors and the reviewers. Any product that may be evaluated in this article, or claim that may be made by its manufacturer, is not guaranteed or endorsed by the publisher.

Copyright © 2022 Zhou, Qu, Zhou, Wang, Hu and Cao. This is an open-access article distributed under the terms of the Creative Commons Attribution License (CC BY). The use, distribution or reproduction in other forums is permitted, provided the original author(s) and the copyright owner(s) are credited and that the original publication in this journal is cited, in accordance with accepted academic practice. No use, distribution or reproduction is permitted which does not comply with these terms.

frontiers | Frontiers in Oncology

TYPE Clinical Trial
PUBLISHED 18 October 2022
DOI 10.3389/fonc.2022.891383

Check for updates

OPEN ACCESS

EDITED BY
Marco Lucchi,
University of Pisa, Italy

REVIEWED BY
Giuseppe Giaccone,
Cornell University, United States
Paolo Mendogni,
IRCCS Ca 'Granda Foundation
Maggiore Policlinico Hospital, Italy

*CORRESPONDENCE
Patrick J. Loehrer Sr
ploehrer@iu.edu

SPECIALTY SECTION
This article was submitted to Thoracic Oncology, a section of the journal Frontiers in Oncology

RECEIVED 07 March 2022
ACCEPTED 05 August 2022
PUBLISHED 18 October 2022

CITATION
Abu Zaid MI, Radovich M, Althouse S, Liu H, Spittler AJ, Solzak J, Badve S and Loehrer PJ Sr (2022) A phase II study of buparlisib in relapsed or refractory thymomas.
Front. Oncol. 12:891383.
doi: 10.3389/fonc.2022.891383

COPYRIGHT
© 2022 Abu Zaid, Radovich, Althouse, Liu, Spittler, Solzak, Badve and Loehrer. This is an open-access article distributed under the terms of the Creative Commons Attribution License (CC BY). The use, distribution or reproduction in other forums is permitted, provided the original author(s) and the copyright owner(s) are credited and that the original publication in this journal is cited, in accordance with accepted academic practice. No use, distribution or reproduction is permitted which does not comply with these terms.

A phase II study of buparlisib in relapsed or refractory thymomas

Mohammad I. Abu Zaid[1], Milan Radovich[2], Sandra Althouse[1], Hao Liu[1], Aaron J. Spittler[1], Jeffrey Solzak[2], Sunil Badve[3] and Patrick J. Loehrer Sr[1]*

[1]Department of Medicine, Indiana University Melvin and Bren Simon Comprehensive Cancer Center, Indianapolis, IN, United States, [2]Caris Life Science, Dallas, TX, United States, [3]Department of Biostatistics, Emory University, Atlanta, GA, United States

Purpose: To investigate the efficacy and safety of buparlisib, an oral pan-PI3K inhibitor, in relapsed or refractory thymomas.

Methods: This was a single center, single arm, open label phase II trial of buparlisib in patients with recurrent thymoma who have progressed after at least one prior line of treatment. The primary endpoint was objective response rate (complete response [CR] + partial response [PR]). Secondary endpoints included toxicity; progression free survival (PFS); overall survival (OS); disease control rate (DCR), i.e., the percentage of patients who achieve either PR or CR or stable disease [SD] for at least 4 months.

Results: Between 10/13/2014 and 1/18/2017, 14 patients with stage IV disease were enrolled. Median age was 58y (23–74). 71% were females and 71% white. All patients had WHO B2 (29%) or B3 (71%) thymoma. Patients received buparlisib for a median of 4.5m (2–33). At a median follow up of 16.6m (2.4–31.3), onr patients (7%) achieved a PR. DCR was 50%. Median PFS was 11.1m (95% CI 2.9 – 18.8). Median OS, updated as of March, 2021 was 22.5m (10.7–31.3). Most common grade 3-4 adverse events related to buparlisib were dyspnea (21%), rash (14%), elevated transaminases (14%), cough (7%), pneumonitis (7%), anxiety (7%), fatigue (7%) and hyperglycemia (7%). Reasons for treatment discontinuation included progression of disease (n= 5), rash (n=4), pulmonary toxicity (n=3), sinusitis (n=1), and disseminated toxoplasmosis plus autoimmune cholangitis (n=1). As of 3/2021, 8 patients have died, 7 due to disease progression and 1 due to central nervous system toxoplasmosis and autoimmune cholangitis.

Conclusion: Buparlisib showed modest activity in patients with relapsed or refractory thymomas. Further investigation of PI3K pathway targeted therapy in thymoma is warranted. (clinicaltrials.gov ID: NCT02220855).

Clinical trial registration: clinicaltrials.gov, identifier (NCT02220855)

KEYWORDS

buparlisib, PI3Kinase inhibitor, thymoma, thymic epithelial tumors, phosphoinositide-3-kinase/Akt (PI3K/Akt) pathway

Introduction

Thymic malignancies are rare but represent the most common tumors in the anterior mediastinum (1). Thymic epithelial tumors (TET) originate from the epithelial cells within the thymus and are histologically classified into WHO types A, AB, B1, B2, B3 thymoma, and thymic carcinoma. Whereas types A, AB and B1 thymomas have a better prognosis than the other histologies, all of these tumors are felt to be malignant and thus capable of producing metastasis and death. Management is multidisciplinary in nature with complete surgical resection the primary means for long-term survival.

In the setting of advanced thymoma or thymic carcinoma, the chance of cure is remote, and systemic therapy is typically employed with or without radiation therapy. Evidence-based guidelines favor combination chemotherapy regimens in the first line, usually containing a platin agent and some combination of doxorubicin, cyclophosphamide, paclitaxel, or etoposide (2–4). Unfortunately, given the rarity of the disease, there have been few prospective trials of systemic therapy in the advanced or metastatic settings. Using platin-based combination chemotherapy, response rates in first line therapy for locally advanced or metastatic disease are good are over 50% as reported in multiple phase II studies but few produce durable remissions (5).

As such, the vast majority of patients with locally advanced or metastatic thymic malignancies ultimately fail initial therapy and therefore require second-line therapy. Few agents have been investigated for these patients with variable rates of response (10-20%) which are rarely durable. Examples of these agents include: octreotide ± prednisone, imatinib, pemetrexed, belinostat, gefitinib, everolimus and interleukin-2 (5). There is a clear need for better therapies, especially those that can target specific mutations (6).

Given the infrequency of these tumors, the use of established tumor cell lines has been invaluable to evaluate potential new targets for therapeutic trials. One of these targets is the phosphoinositide-3-kinase/Akt (PI3K/Akt) pathway. Prior published data from our group demonstrated that a subset of thymomas activate the PI3K pathway through upregulation of a large microRNA cluster on Chromosome 19 (7). We have also demonstrated that the majority of thymomas have an active pathway as evidenced by elevated phospho-AKT compared to normal tissues (7). Albertobello and colleagues demonstrated that a mutation in the gene, PIK3R2 (that encodes a regulatory subunit of PI3K) and other PI3K subunit genes were found in a newly established thymic carcinoma (MP57) cell line, where inhibition of PI3K with GDC-0941 resulted in anti-tumor activity (8). Another independent group also observed an activated PI3K pathway at the protein level in thymoma tissues (9). Further support of targeting the PI3K pathway comes from a Phase II trial in thymoma patients with the mTOR inhibitor, everolimus. This demonstrated a disease control rate in 30 of 32 (93.8%, 95% CI, 79.2% to 99.2%) including three (9.4%) PRs (10).

Supported by this preclinical data, we initiated a Phase II trial of the oral pan-PI3K inhibitor, buparlisib, in patients with advanced thymoma (clinicaltrials.gov ID: NCT02220855). Buparlisib has potent inhibitory activity of all PI3K isoforms: alpha, beta, gamma, and delta. The primary objective of this trial was to evaluate the objective response rate, with secondary objectives being progression free survival, duration of response, toxicity, and overall survival.

Methods

Trial design and patient selection

We initiated a single-arm, Phase II trial of the oral pan-PI3K inhibitor, buparlisib, in patients with relapsed or refractory thymomas. The primary endpoint was objective response rate (ORR), with secondary endpoints of progression free survival (PFS), overall survival (OS), disease control rate (DCR), and toxicity evaluation. An exploratory objective to evaluate

molecular markers of response was also planned. Eligible patients must have had with histologically confirmed thymoma (WHO Type A, AB, B1, B2, B3) with least one prior line of platinum-based chemotherapy (unless refused or not tolerated). Patients with thymic carcinoma (WHO Type TC) were excluded. Patients must have measurable disease, adequate bone marrow function (ANC _1.5 x 10^9/L, platelets _100,000 x 10^9/L, Hb >9 g/dl), liver function tests (ALT and AST WNL or ¾3 x ULN if liver metastases present, bilirubin WNL or ¾1.5 x ULN if liver metastasis present) and serum creatinine ¾ 1.5 x ULN. Patients with concurrent severe and/or uncontrolled concomitant medical conditions (e.g. cardiac, diabetic, gastrointestinal or pulmonary dysfunction). Pulmonary function tests including measures of predicted lung volumes and DLco were performed only for those patients in whom pulmonary dysfunction was suspected. Patients who were on chronic oral corticosteroids or immunosuppressive agents were not eligible. Buparlisib (also known as BKM120) was administered orally at 100mg QD for two or more months until disease progression or unacceptable toxicity. The study was initially designed to treat patients until disease progression or unacceptable toxicity for a maximum of one year. The study was amended later to allow treatment beyond one year for those with continued benefit from treatment.

Statistical design

The primary endpoint of the study was objective response rate (CR+PR) according to RECIST 1.1 criteria for buparlisib monotherapy in patients with advanced thymomas. The sample size was calculated based on the objective response rate. A two-stage Simon's Minimax design was used to test the null hypothesis of 10% objective response rate (p_0 = 0.10) versus a clinically meaningful response rate of 30% (p_1 = 0.30) with a two-sided alpha = 0.10 and a power of 90%. The first stage of the study was planned to enroll 16 evaluable patients with thymoma. If ¾ 1 of the 16 patients demonstrated an objective response, then no further patients would be accrued. If two or more of the first 16 patients have a response, then accrual would continue until 25 evaluable patients would be treated. If there are 2 to 4 patients with a response in the total of 25 evaluable patients, then the objective response rate would be considered as uninterestingly low, while if there are 5 or more patients of the 25 who have a response, then the study therapy would be considered as clinically sufficient to warrant further study in a phase IIb or III trial. Under the null hypothesis (10% response rate), the probability of early termination in this cohort is estimated to be 52%. The sponsor prematurely terminated the study due to discontinuation of the investigational drug program. Prior to this, a total of 14 patients are included for efficacy and safety analyses.

Data analysis

Demographic and disease characteristics were summarized using descriptive statistics. As the study was discontinued by an external reason that was completely independent of the observed data, the primary outcome of objective response rate was calculated with 95% confidence interval without adjustment to the two-stage nature of the study design. Survival curves were estimated using the Kaplan-Meier method, with 95% confidence interval calculated using Greenwood's method. Progression Free Survival was defined as the time from study start until progression or death, with censoring at last follow-up. Overall survival was defined as the time from the study start to documented death, with censoring at last follow-up.

Molecular analysis

Whole exome sequencing

This trial was able to capture 10 matched pairs of tumor and peripheral blood. The concentration and quality of gDNA was assessed using Agilent 4200 TapeStation. A DNA Integrity Number (DIN) of five or higher was required to pass quality control. One hundred nanograms of DNA per patient sample were used to prepare single-indexed cDNA libraries using SureSelectXTHS Human All Exon V6 (Agilent). The resulting libraries were assessed for their quantity and size distribution using Qubit 2.0 (Life Technologies) and Agilent 2100 Bioanalyzer. Libraries pooled at 200pM were utilized for clustering amplification using HiSeq 3000/4000 PE cluster kit and sequenced with 2x75bp paired-end configuration on the HiSeq 4000 (Illumina) using HiSeq 3000/4000 PE SBS kit. A Phred Q-score was used to measure the quality of sequencing with more than 90% of the reads reaching Q30 (99.9% base call accuracy).

The sequencing data was first assessed using FastQC (Babraham Bioinformatics, Cambridge, UK) for quality control. The sequenced libraries were mapped to the human genome (UCSC hg38) using BWA MEM aligner in an alternate contig aware (alt-aware) manner followed by post alt-processing step with BWA kit. The PCR duplicates were marked using PICARD Mark Duplicates. The coverage across target regions was assessed using PICARD Collect Alignment Summary Metrics and Collect Hs Metrics. Quality control of sequencing and mapping results was summarized using MultiQC. Base quality score recalibration (BQSR) was performed using GATK Base Recalibrator and Print Reads to generate analysis-ready BAM files. GATK Mutect2 was used to generate somatic variant VCF files and Ingenuity Variant Analysis (Qiagen) was used to visualize variants. For copy number analysis, variants were called using CODEX2 (11). Standard quality control was used comparing matched patient samples.

RT-PCR

RNA from 14 patients was isolated using Allprep DNA/RNA FFPE kit (Qiagen #80234). cDNA conversion was then performed using High Capacity RNA-to-cDNA kit at 1ug per patient (Thermo Fisher Scientific). MicroRNA experiments were run on 7900HT Fast Real-Time PCR system and expression was observed using TaqMan Gene Expression Mastermix and miRNAs 519d, 517a, and RNU48 as the endogenous (Thermo Fisher Scientific Assay ID: 47897_mir, 479485_mir, and 001006 respectively). Analysis was achieved using Sequence Detection System version 2.4 and RQ manager (Thermo Fisher Scientific)

Results

Baseline characteristics

The patients characteristics are illustrated in Table 1. This trial enrolled a total of 14 patients with relapsed or refractory thymomas. The median age was 58 years (23 – 74) with 71% being females. All patients had stage IVa (pleural metastasis) or IVb (other metastatic sites) disease. The patients were heavily pretreated with a median of 3.5 prior regimens (range 0-8) and the majority had prior radiation therapy.

TABLE 1 Subjects characteristics at time of enrollment to the study.

Characteristic	Value (n=14)
Age, median in years (range)	57.8 (23.0-74.5)
Gender, n (%)	
Female	10 (71%)
Male	4 (29%)
WHO histological subclassification, n (%)	
B2	4 (29%)
B3	10 (71%)
Masaoka Staging, n (%)	
IVa	6 (43%)
IVb	8 (57%)
Presence of paraneoplastic syndromes, n (%)	
Yes (myasthenia gravis (MG)-2; pure red cell aplasia plus MG-1; hypogammaglobulinemia-1)	4 (29%)
No	10 (71%)
ECOG performance status, n (%)	
0	14 (100%)
Prior therapies	
History of prior surgery	12 (86%)
History of prior radiation therapy	8 (57%)
Number of prior chemotherapy regimens, median (range)*	3.5 (0-8)
Prior platinum-based chemotherapy*	13 (93%)

ECOG, Eastern Cooperative Oncology Group; WHO, World Health Organization.
*one patient refused initial standard cisplatin therapy.

Adverse events

All reported toxicities related to buparlisib are listed in Table 2. The grade 3-4 adverse events were dyspnea (21%), rash (14%), elevated transaminases (14%), cough (7%), pneumonitis (7%), anxiety (7%), fatigue (7%) and hyperglycemia (7%). One patient developed documented pneumonitis which resolved with corticosteroids but was removed from study. No patient had irreversible pulmonary fibrosis.

Efficacy results

Patients received buparlisib for a median of 4.5 months (2 – 33). At a median follow up of 35.8 months (range 6.3 – 58.6 month), 1 out 14 patients (7.1% with 95% CI, 2%-42.8%) achieved a PR. DCR was 50%. The median progression-free survival (PFS) was 11.1 months (95% CI 2.9 – 18.8). As demonstrated in the waterfall plot shown in Figure 1, the majority of patients had some degree of regression with this agent. As of March, 2021, eight patients have died, seven due to disease progression and one due to central nervous system toxoplasmosis and autoimmune cholangitis. The median OS with the updated data was 40.0 months (95% CI, 28.3 – not reached) with the overall survival curve in Figure 2.

Molecular analysis of the C19MC cluster and exome-sequencing

In our previous studies, it was found that thymomas types A and A/B revealed a microRNA cluster on chr19q13.42 that was significantly overexpressed. With thymoma WHO subtypes being ambiguous, microRNAs 519d and 517a from this cluster were tested to evaluate activation status among the patients in this trial who have responded versus those that had progressive disease. In all patients that were tested, both mir519d and mir517a were observed to have little to no expression at the RNA level that would indicate that a patient may have been incorrectly subtyped pathologically (Figure 3).

Whole exome sequencing

Ten patients with matched tumor and blood samples were sequenced to observe any genomic variants that may explain the responses to buparlisib seen in two of the patients. Looking at SNVs we found no significant alterations that would explain sensitivity to PI3K inhibition. Further observation of copy number variation found a single amplification in PIK3CD in

10.3389/fonc.2022.891383

TABLE 2 Treatment Related Adverse Events.

	Grade of toxicities								
AE Term	**1**	**2**	**3**	**4**	**5**	**Total**	**% Total**	**Grade 3-5**	**% Grade 3-5**
Fatigue	8	2	1	0	0	11	79	1	7
Anorexia	8	2	0	0	0	10	71	0	0
Pruritus	6	4	0	0	0	10	71	0	0
Rash acneiform	3	4	1	0	0	8	57	1	7
Rash maculo-papular	0	1	1	0	0	2	14	1	7
Anxiety	3	3	1	0	0	7	50	1	7
Cough	2	3	1	0	0	6	43	1	7
Nausea	6	0	0	0	0	6	43	0	0
Dyspnea	1	1	3	0	0	5	36	3	21
Pneumonitis	0	4	1	0	0	5	36	1	7
Tremor	5	0	0	0	0	5	36	0	0
Depression	2	1	0	0	0	3	21	0	0
Dysgeusia	2	1	0	0	0	3	21	0	0
Hyperglycemia	2	0	1	0	0	3	21	1	7
Insomnia	2	1	0	0	0	3	21	0	0
Musculoskeletal and connective tissue disorder	3	0	0	0	0	3	21	0	0
Alopecia	2	0	0	0	0	2	14	0	0
Diarrhea	1	1	0	0	0	2	14	0	0
Dizziness	1	1	0	0	0	2	14	0	0
Dyspepsia	1	1	0	0	0	2	14	0	0
Endocrine disorders - Other, specify	1	1	0	0	0	2	14	0	0
Mucositis oral	1	1	0	0	0	2	14	0	0
Skin and subcutaneous tissue disorders - Other, specify	2	0	0	0	0	2	14	0	0
Vomiting	2	0	0	0	0	2	14	0	0
Weight loss	1	1	0	0	0	2	14	0	0
Non-cardiac chest pain	1	1	0	0	0	2	14	0	0
Alanine aminotransferase increased	0	0	0	1	0	1	7	1	7
Aspartate aminotransferase increased	0	0	0	1	0	1	7	1	7
Confusion	1	0	0	0	0	1	7	0	0
Constipation	1	0	0	0	0	1	7	0	0
Fever	0	1	0	0	0	1	7	0	0
Gastrointestinal disorders - Other, specify	1	0	0	0	0	1	7	0	0
Headache	1	0	0	0	0	1	7	0	0
Hypokalemia	1	0	0	0	0	1	7	0	0
Infections and infestations - Other, specify	0	1	0	0	0	1	7	0	0
Pain in extremity	0	1	0	0	0	1	7	0	0
Platelet count decreased	1	0	0	0	0	1	7	0	0
Psychiatric disorders - Other, specify	1	0	0	0	0	1	7	0	0
Respiratory, thoracic, and mediastinal disorders - Other, specify	0	0	1	0	0	1	7	1	7
Sinusitis	0	1	0	0	0	1	7	0	0
Skin infection	0	1	0	0	0	1	7	0	0
Edema limbs	0	1	0	0	0	1	7	0	0
Bronchial infection	0	1	0	0	0	1	7	0	0

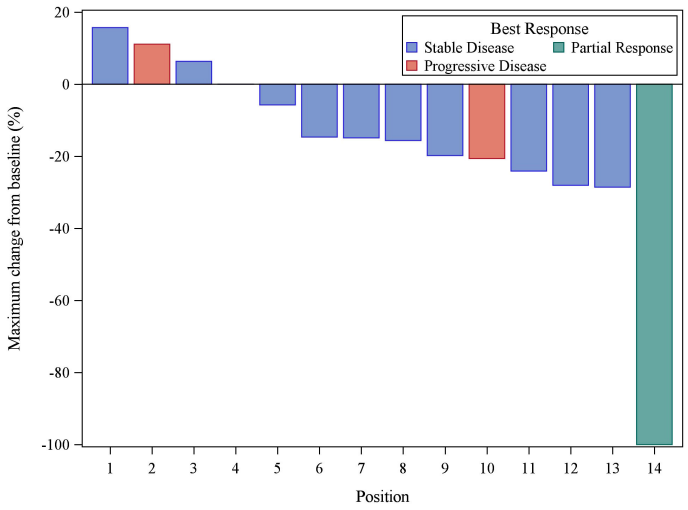

FIGURE 1
Waterfall plot of the 14 evaluable patients treated with buparlisib demonstrating best response of target lesions by RECIST criteria. One PR result was unconfirmed by follow-up scan (taken off study for toxicity).

patient. This however did not meet the criteria of significance and could be described as an aneuploidy. Here we have found no significant genomic markers of response for buparlisib.

Discussion

Therapeutic options for patients with recurrent TETs are limited. Whereas systemic cisplatin-based chemotherapy commonly produces remissions in previously untreated patients, most targeted agents have limited impact in previously treated disease. These include agents such as pemetrexed, sunitinib, cixutumumab and pembrolizumab (5, 12) with objective response rates between 6- 23%. In one of the largest prospective trials evaluating the mTOR inhibitor, everolimus, in recurrent TET (thymoma and thymic carcinoma), five partial and one complete responses were noted in 51 patients (CR + PR =12%) with 3 partial responses occurring in the 32 patients with thymoma (10). This current trial is the first proof of principle study that prospectively

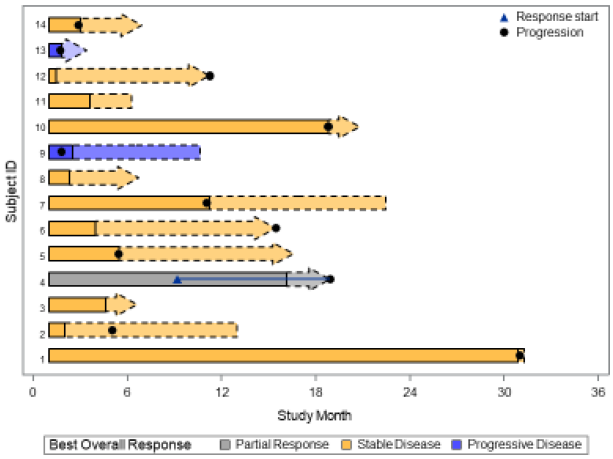

FIGURE 2
Swimmer plot of the 14 evaluable patients treated with buparlisib.

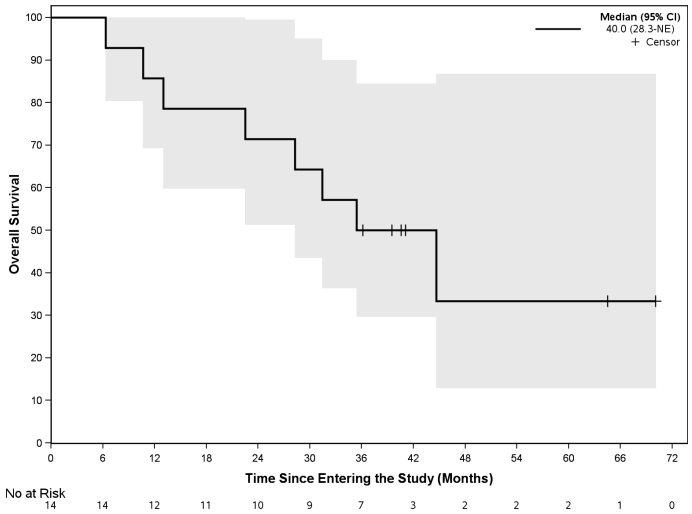

FIGURE 3
Kaplan-Meier survival curve of all evaluable patients.

evaluated a PI3K inhibitor in thymoma. This trial clearly demonstrates clinical activity with buparsilib in patients with recurrent thymoma.

The rationale for evaluating this targeted therapeutic approach is based upon strong preclinical data. A unique microRNA cluster on chromosome 19 (C19MC) has been identified that is highly overexpressed in a significant subset of thymomas primarily comprised of the A and A/B subtype (7). We subsequently validated this observation in additional 35 thymomas by qPCR (7). This cluster is normally silent in adult tissues, with normal expression restricted to embryonic development. MicroRNAs within the C19MC cluster, miR-517 and miR-519d, have been previously demonstrated to inhibit key proteins in the PI3K/AKT pathway. Namely, PTEN, a negative regulator of AKT, and p21, a cell cycle arrest protein (13). In addition, gene expression analysis reveals over-expression of PIK3CA (aka PI3K p110), the canonical activator of AKT.To confirm, we performed a quantitative ELISA on a validation set of 35 thymomas for phospho-AKT (Ser 473), and demonstrate that C19MC positive thymomas have significantly higher levels of phospho-AKT compared to C19MC negative thymomas which in-turn has higher levels than adjacent normal tissue. Similarly, mutations of PI3K have also been observed in a new thymic carcinoma cell line, (MP57) (8).

These data demonstrate that TETs have the potential to have sensitivity to PI3K inhibition, in particular those that are positive for C19MC. We further tested a variety of PI3K, AKT, and mTOR inhibitors in our thymoma cell line (IU-TAB-1) and found significant activity for several of these agents (Figure 4). The serine-threonine kinase mammalian target of rapamycin (mTOR) is a key component of the PI3K/AKT/mTOR intracellular axis. Several investigators suggest that the PI3K/AKT network plays an important role in thymoma growth as mentioned above and may sensitize cells thymic epithelial tumors (TET) to mTOR inhibition (8, 14). This study confirmed that targeted blockage of the PI3k/AKT pathway has merit in advanced thymoma.

One of the limitations of this study was that all of the patients entered on the trial had WHO type B2 and B3 thymoma, whereas the molecular features suggest that the PI3K/AKT pathway may be especially important for WHO type A and AB thymoma. As the frequency of recurrent metastatic disease is more common in B2 and B3 thymoma, patients with type A, AB and B1 histology still develop recurrent metastatic disease but were not seen on this study. Another limitation was that the study was terminated early when the sponsoring company determined that they would no longer pursue this drug because of toxicities seen in other concurrent and previous trials. We did observe toxicity (notably dermatologic and pulmonary) that led to early discontinuation in several patients. Patients with thymoma have a high incidence of autoimmune disorders and altered immune systems making them more susceptible to opportunistic infections. In this series, one patient who was on study for 31 months developed autoimmune cholangitis and was started on corticosteroids, but died from disseminated CNS toxoplasmosis (documented by autopsy) many years after first contracting this disease. This patient was not neutropenic at the time of his diagnosis but died within one month of discontinuing study drug.

Early discontinuation was required in over half of the treated patients. Nonetheless, the results from this trial, demonstrate activity in thymoma among 14 patients treated on trial. All but

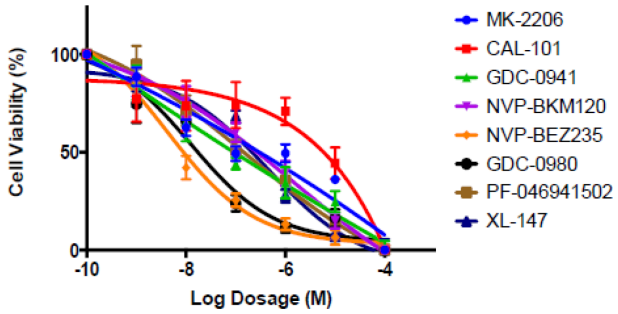

FIGURE 4
The thymoma cell line, IU-TAB-1 with increasing dosages of PI3K, AKT and dual PI3K/mTOR inhibitors. Cells were treated for 72 hours, and cell viability was assessed. The data demonstrates marked sensitivity of the cell lines to these inhibitors including Buparlisib (NVP BKM120)

five of the 14 eligible patients had some degree of regression while on therapy. Since initiation of this trial, three PIK3CA inhibitors have been approved by the FDA including, copanlisib (for refractory lymphoma); duvelisib (for refractory CLL and follicular B-cell lymphoma); and alpelisib (for refractory breast cancer) (15–17). Non-infectious pneumonitis and severe cutaneous reactions were noted to occur in ¾5-10% of treated patients. This trial provides evidence to support further evaluation of the targeting of PI3K/Akt pathway with novel and less toxic agents in patients with advanced thymoma.

Data availability statement

The datasets used in this study are not publicly available due to privacy concerns. Requests to access the dataset can be directed to the corresponding author.

Ethics statement

This study was reviewed and approved by Indiana University IRB. The patients/participants provided their written informed consent to participate in this study.

Author contributions

MA – Protocol design, manuscript composition and review. MR - Protocol design, manuscript composition and review. SA – Data collection and manuscript review. HL - Statistical review and manuscript review. AS - Data collection, manuscript composition and review. JS - Laboratory analysis, manuscript composition and review. SB - Pathology review, manuscript composition and review. PL - Protocol design, analysis, manuscript composition and review. All authors contributed to the article and approved the submitted version.

Funding

This work was supported by the National Cancer Institute Award CA082709. The authors also declare that this study received funding from Novartis in the form of the investigational drug. The funder was not involved in the study design, collection, analysis, interpretation of data, the writing of this article or the decision to submit it for publication.

Conflict of interest

Authors MR and JS were employed by the company Caris Life Science.

The remaining authors declare that the research was conducted in the absence of any commercial or financial relationships that could be construed as a potential conflict of interest.

Publisher's note

All claims expressed in this article are solely those of the authors and do not necessarily represent those of their affiliated organizations, or those of the publisher, the editors and the reviewers. Any product that may be evaluated in this article, or claim that may be made by its manufacturer, is not guaranteed or endorsed by the publisher.

References

1. Tomaszek S, Wigle DA, Keshavjee S, Fischer S. Thymomas: Review of current clinical practice. *Ann Thorac Surg* (2009) 87:1973–80. doi: 10.1016/j.athoracsur.2008.12.095

2. Giaccone G, Ardizzoni A, Kirkpatrick A, Clerico M, Sahmoud T, van Zandijk N, et al. Cisplatin and etoposide combination chemotherapy for locally advanced or metastatic thymoma. A phase II study of the European organization for research and treatment of cancer lung cancer cooperative group. *J Clin Oncol* (1996) 14:814–20. doi: 10.1200/JCO.1996.14.3.814

3. Loehrer PJ Sr., Jiroutek M, Aisner S, Aisner J, Green M, Thomas CR, et al. Combined etoposide, ifosfamide, and cisplatin in the treatment of patients with advanced thymoma and thymic carcinoma: An intergroup trial. *Cancer* (2001) 91:2010–5. doi: 10.1002/1097-0142(20010601)91:11<2010::AID-CNCR1226>3.0.CO;2-2

4. Lemma GL, Lee JW, Aisner SC, Langer CG, Tester WJ, Johnson DH, et al. Phase II study of carboplatin and paclitaxel in advanced thymoma and thymic carcinoma. *J Clin Oncol* (2011) 29:2060–5. doi: 10.1200/JCO.2010.32.9607

5. Berghmans T, Durieux Y, Holbrechts S, Jungels C, Lafitte JJ, Meert AP, et al. Systemic treatments for thymoma and thymic carcinoma: A systemic review. *Lung Cancer* (2018) 126:25–31. doi: 10.1016/j.lungcan.2018.10.018

6. Rajan A, Giaccone G. Targeted therapy for advanced thymic tumors. *J Thorac Oncol* (2010) 5:S361– 4. doi: 10.1097/JTO.0b013e3181f21114

7. Radovich M, Solzak JP, Hancock BA, Conces ML, Atale R, Porter RF, et al. A large microRNA cluster on chromosome 19 is a transcriptional hallmark of WHO type a and AB thymomas. *Br J Cancer* (2016) 114:477–84. doi: 10.1038/bjc.2015.425

8. Alberobello AT, Wang Y, Beerkens FJ, Conforti F, McCutcheon JN, Rao G, et al. PI3K as a potential therapeutic target in thymic epithelial tumors. *J Thorac Oncol* (2016) 11:1345–56. doi: 10.1016/j.jtho.2016.04.013

9. Maury JM, Merveilleux du Vignaux C, Drevet G, Zarza V, Chalabreysse L, Maisse C, et al. Activation of the mTOR/ akt pathway in thymic epithelial cells derived from thymomas. *PLoS One* (2019) 14:e0197655. doi: 10.1371/journal.pone.0197655

10. Zucali PA, De Pas TM, Palmieri G, Favaretto A, Chella A, Tiseo M, et al. Phase II study of everolimus in patients with thymoma and thymic carcinoma previously treated with cisplatin-based chemotherapy. *J Clin Oncol* (2018) 36:342–9. doi: 10.1200/JCO.2017.74.4078

11. Jiang Y, Wang R, Urrutia E, Anastopoulos IN, Nathanson KL, Zhang NR, et al. CODEX2: Full-spectrum copy number variation detection by high-throughput DNA sequencing. *Genome Biol* (2018) 19:202. doi: 10.1186/s13059-018-1578-y

12. Gbolahan OB, Porter RF, Salter JT, Yiannoutsos C, Burns M, Chiorean EG, et al. A phase II study of pemetrexed in patients with recurrent thymoma and thymic carcinoma. *J Thorac Oncol* (2018) 13:1940–48. doi: 10.1016/j.jtho.2018.07.094

13. Fornari F, Milazzo M, Chieco P, Negrini M, Marasco E, Capranico G, et al. In hepatocellular carcinoma miR-519d is up-regulated by p53 and DNA hypomethylation and targets CDKN1A/p21, PTEN, AKT3 and TIMP2. *J Pathol* (2012) 227:275–85. doi: 10.1002/path.3995

14. Zucali PA, Petrini I, Lorenzi E, Merino M, Cao L, Di Tommaso L, et al. Insulin-like growth factor-1 receptor and phosphorylated AKT-serine 473 expression in 132 resected thymomas and thymic carcinomas. *Cancer* (2010) 116:4686–95. doi: 10.1002/cncr.25367

15. Markham A. Copanlisib: First global approval. *Drugs* (2017) 77:2057–62. doi: 10.1007/s40265-017-0838-6

16. Blair HA. Duvelisib: First global approval. *Drugs* (2018) 78:1847–53. doi: 10.1007/s40265-018-1013-4

17. Markham A. Apelisib: First global approval. *Drugs* (2019) 79:1249–53. doi: 10.1007/s40265-019-01161-6

Frontiers in Oncology

Advances knowledge of carcinogenesis and tumor progression for better treatment and management

The third most-cited oncology journal, which highlights research in carcinogenesis and tumor progression, bridging the gap between basic research and applications to imrpove diagnosis, therapeutics and management strategies.

Discover the latest Research Topics

See more →

Frontiers

Avenue du Tribunal-Fédéral 34
1005 Lausanne, Switzerland
frontiersin.org

Contact us

+41 (0)21 510 17 00
frontiersin.org/about/contact